PATHWAY, GENETIC AND PROCESS ENGINEERING OF MICROBES FOR BIOPOLYMER SYNTHESIS

EDITED BY: Ignacio Poblete-Castro, Bernd Rehm and Bruce Ramsay
PUBLISHED IN: Frontiers in Bioengineering and Biotechnology

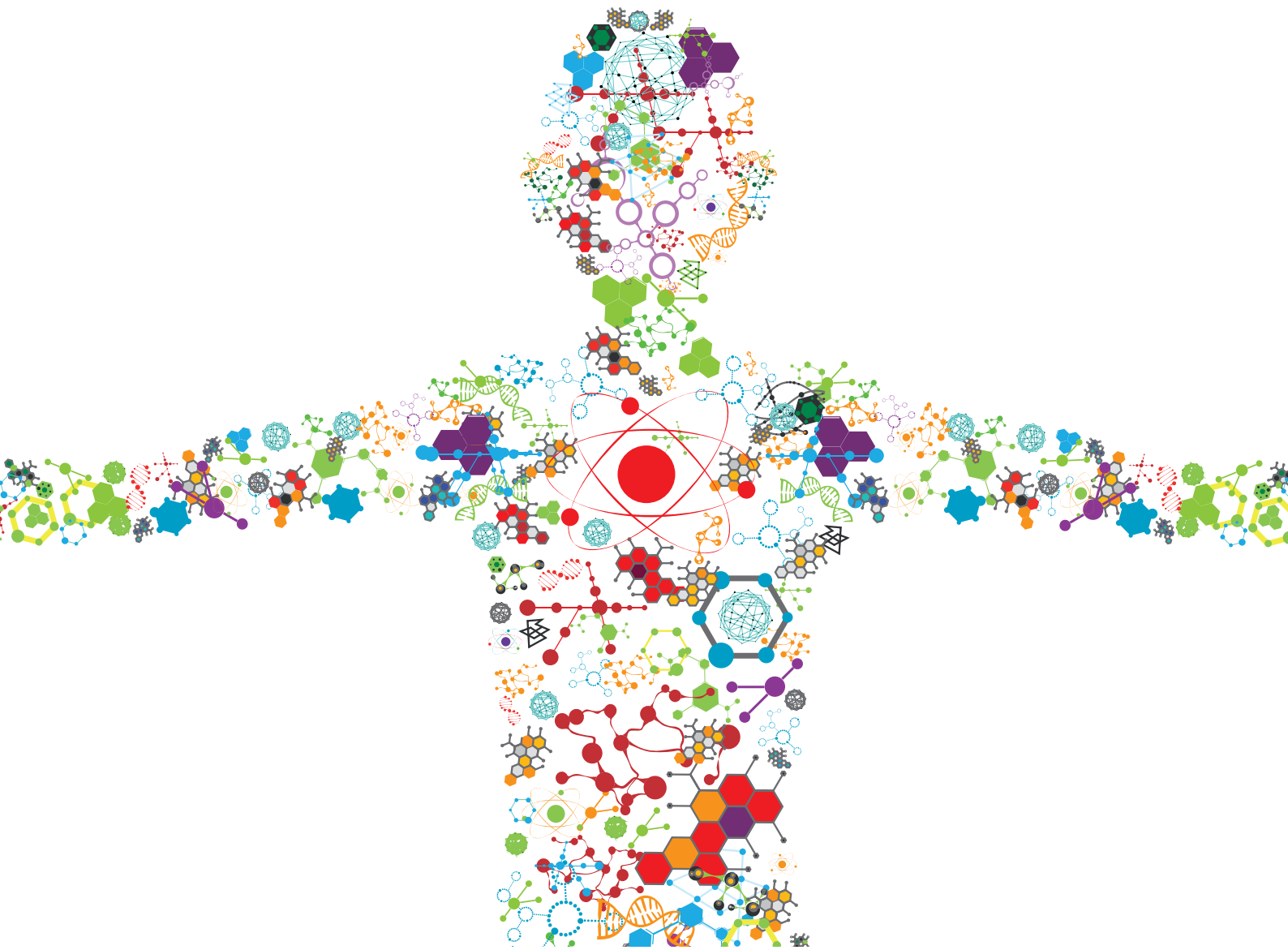

frontiers Research Topics

ISSN 1664-8714
ISBN 978-2-88966-461-0
DOI 10.3389/978-2-88966-461-0

About Frontiers

Frontiers is more than just an open-access publisher of scholarly articles: it is a pioneering approach to the world of academia, radically improving the way scholarly research is managed. The grand vision of Frontiers is a world where all people have an equal opportunity to seek, share and generate knowledge. Frontiers provides immediate and permanent online open access to all its publications, but this alone is not enough to realize our grand goals.

Frontiers Journal Series

The Frontiers Journal Series is a multi-tier and interdisciplinary set of open-access, online journals, promising a paradigm shift from the current review, selection and dissemination processes in academic publishing. All Frontiers journals are driven by researchers for researchers; therefore, they constitute a service to the scholarly community. At the same time, the Frontiers Journal Series operates on a revolutionary invention, the tiered publishing system, initially addressing specific communities of scholars, and gradually climbing up to broader public understanding, thus serving the interests of the lay society, too.

Dedication to Quality

Each Frontiers article is a landmark of the highest quality, thanks to genuinely collaborative interactions between authors and review editors, who include some of the world's best academicians. Research must be certified by peers before entering a stream of knowledge that may eventually reach the public - and shape society; therefore, Frontiers only applies the most rigorous and unbiased reviews.
Frontiers revolutionizes research publishing by freely delivering the most outstanding research, evaluated with no bias from both the academic and social point of view. By applying the most advanced information technologies, Frontiers is catapulting scholarly publishing into a new generation.

What are Frontiers Research Topics?

Frontiers Research Topics are very popular trademarks of the Frontiers Journals Series: they are collections of at least ten articles, all centered on a particular subject. With their unique mix of varied contributions from Original Research to Review Articles, Frontiers Research Topics unify the most influential researchers, the latest key findings and historical advances in a hot research area! Find out more on how to host your own Frontiers Research Topic or contribute to one as an author by contacting the Frontiers Editorial Office: frontiersin.org/about/contact

PATHWAY, GENETIC AND PROCESS ENGINEERING OF MICROBES FOR BIOPOLYMER SYNTHESIS

Topic Editors:
Ignacio Poblete-Castro, Andres Bello University, Chile
Bernd Rehm, Griffith University, Australia
Bruce Ramsay, Queen's University, Canada

Professor Bruce Ramsay holds a patent for a method of synthesising medium chain length polyhydroxyalkanoate. All other Guest Editors declare no competing interests with regards to the Research Topic subject.

Citation: Poblete-Castro, I., Rehm, B., Ramsay, B., eds. (2021). Pathway, Genetic and Process Engineering of Microbes for Biopolymer Synthesis. Lausanne: Frontiers Media SA. doi: 10.3389/978-2-88966-461-0

Table of Contents

frontiers in Bioengineering and Biotechnology

EDITORIAL
published: 23 December 2020
doi: 10.3389/fbioe.2020.618383

Editorial: Pathway, Genetic and Process Engineering of Microbes for Biopolymer Synthesis

Ignacio Poblete-Castro[1]*, *Bruce A. Ramsay*[2] *and Bernd H. A. Rehm*[3]

[1] Biosystems Engineering Lab, Faculty of Life Sciences, Center for Bioinformatics and Integrative Biology, Universidad Andres Bello, Santiago, Chile, [2] Chemical Engineering Department, Queen's University, Kingston, ON, Canada, [3] Centre for Cell Factories and Biopolymers, Griffith Institute for Drug Discovery, Griffith University, Nathan, QLD, Australia

Keywords: polyhydroxyalkanoates, alginates, succinic and lactic acid, metabolic engineering, epothilone, poly(γ-glutamic acid) (γ-PGA), cell autolysis, (R)-3-hydroxy fatty acids

Editorial on the Research Topic

Pathway, Genetic and Process Engineering of Microbes for Biopolymer Synthesis

OPEN ACCESS

Edited and reviewed by:
Georg M. Guebitz,
University of Natural Resources and Life Sciences Vienna, Austria

***Correspondence:**
Ignacio Poblete-Castro
ignacio.poblete@unab.cl

Specialty section:
This article was submitted to Industrial Biotechnology, a section of the journal Frontiers in Bioengineering and Biotechnology

Received: *16 October 2020*
Accepted: *30 November 2020*
Published: *23 December 2020*

Citation:
Poblete-Castro I, Ramsay BA and Rehm BHA (2020) Editorial: Pathway, Genetic and Process Engineering of Microbes for Biopolymer Synthesis. Front. Bioeng. Biotechnol. 8:618383. doi: 10.3389/fbioe.2020.618383

Together with the climate crisis, the heavy accumulation in oceans and soils of persistent pollutants, like polycyclic aromatics hydrocarbons and synthetic plastics, are the main drivers to impact nature and threaten human survival. It is particularly striking that most industrial polymers still originate from petrochemical sources—nearly 99% of the overall worldwide production. The result is materials that remain intact for centuries once deposited in the environment. Relying on non-renewable fossil chemicals limits our ability to establish a circular economy that promises to curb current emissions and contribute moderately to the global carbon cycle without surpassing its carrying capacity.

For decades, commercial biopolymers have also been produced by microbial fermentation since nature has endowed many bacteria from urban sites to extreme environments (Orellana-Saez et al., 2019) with the enzymatic machinery to assemble these macromolecules. Despite the rapid pace of innovation, microbial biopolymers are still expensive to synthesize because the generally oxygen-intensive fermentation processes, downstream processing, and carbon feedstock cost boost production expenses (Oliveira et al., 2020). The biopolymers must additionally possess specific mechanical and physical properties to be processed industrially into products with a variety of applications (Moradali and Rehm, 2020).

Beyond their initial use as raw materials for packaging and films, biopolymers are finding new applications in biomedicine serving as drug nanocarriers, wound dressings, and tissue engineering materials along with usages as pharmaceutical coatings. The most profitable biopolymers are the family of polypeptides. Particularly, polyketides (PKs) have lured special attention in the clinical sector as they are efficient anticancer drugs and exhibit biological activity (antibiotics) against resistant bacteria and fungi. The food industry also employs biopolymers as thickeners and stabilizer agents. Moreover, water treatment and remediation technologies benefit from biopolymer physicochemical features as they act as dye removers and flocculation agents. Combining bacterial genome engineering with optimized cultivation modes in bioreactor enables the biosynthesis

of tailor-made macromolecules from renewable carbon substrates and waste streams that meet technical requirements essential for medical and environmental applications. Together these strategies promise to accelerate the design of cost-effective processes that can compete against the classical petrochemical route.

This special issue sought to gather original studies and review papers covering the rational engineering of the gene repertory of microbes, synthetic bacterial consortia, and bioprocess optimization for efficient biopolymer production. Researchers across the globe poured efforts into the microbial synthesis of poly(3-hydroxyalkanoates) (PHAs), poly(γ-glutamic acid) (γ-PGA), epothilone, extracellular hydroxyalkanoic acids, alginates, and the starting building blocks succinate and D-lactate.

Two research groups studied bacteria of the *Bacillus* genus specialized in producing the versatile polyamide, poly(γ-glutamic acid). Wang et al. expanded the range of molecular weights ($6.82{\cdot}10^4$ to $1.78{\cdot}10^6$ Da) of the biosynthesized γ-PGA by modulating the expression of the poly(γ-glutamic acid) depolymerase in *B. licheniformis* via promoter and signal peptide engineering. In another study, Halmschlag et al. investigated the metabolome profile of *B. subtilis* with altered rates of γ-PGA synthesis, using different promoters and induction degrees. They showed that if glutamate was not added to the culture, *B. subtilis* increased the phosphoenolpyruvate concentration while producing high levels of the biopolymer. They postulated that a reduction of the growth rate and diverting carbon fluxes toward glutamine synthesis could enhance γ-PGA production in *B. subtilis*.

The bacteria-derived anticancer compound epothilone is one of the most effective drugs against breast cancer with tolerable side effects. To improve epothilone synthesis in *Sorangium cellulosum*, Ye et al. targeted suitable promoters for overexpressing epothilone biosynthetic genes. This strategy yielded high-expression of the *epoA*, epoC, and epoK genes by inducing the P3 promoter contained in both a TALE-VP64 and dCas9-VP64 vectors, reaching elevated amounts of epothilone B and D.

Many articles evolved around PHAs synthesis. First, Velázquez-Sánchez et al. reviewed the importance of altering the regulatory circuits governing PHA accumulation in well-established host producers for modulating physicochemical properties and biopolymer yields. Similarly, Godard et al. applied a multi-omic approach to decipher the molecular mechanism behind the osmotic-stress adaptation of *Bacillus megaterium* that triggers enhanced synthesis of poly(3-hydroxybutyrate) (PHB). NADPH's oversupply, accompanied by an altered abundance of enzymes and genes belonging to central carbon metabolism, increased acetyl-CoA flux toward PHB synthesis. Engineering the industrial host *Escherichia coli*, Li et al. successfully produced high levels of PHB optimizing the ribosome binding site sequences of several genes attaining 85% of the cell dry mass (CDM) as PHB. Process optimization is another means to increase biopolymer productivity. Oliveira-Filho et al. utilized xylose, a promising 5-carbon sugar derived from hemicellulose, for fed-batch PHB production in *Burkholderia sacchari* under nitrogen or phosphorus limitation, resulting in both cases in a yield of 0.37 (gPHB $g_{xylose^{-1}}$).

Novel strategies for downstream processing of intracellular biopolymers are essential for decreasing the production costs. Delving into this topic, Yañez et al. present the latest advances of metabolically engineered strains and process setup for secreting *R*-3-hydroxy fatty acids and cell disruption for PHA release. On the same subject, an original study by Poblete-Castro et al. rationally engineered *Pseudomonas putida*, a native medium-chain length PHA producer, to alter the cell's osmotic state overexpressing the major porin enzymes along with inactivating the inner membrane enzyme MscL. When the engineered *P. putida* was given an osmotic upshift and then a rapid passage to a hypotonic condition, the cells suffered membrane disruption (95% of the population) after 3 h and displayed a PHA recovery of 94%.

Synthetic bacterial consortia are sustainable paths to produce PHAs from low-cost feedstocks. Taking advantage of the CO_2 conversion ability of *Synechococcus elongatus,* Hobmeier et al. grew this cyanobacterium autotrophically to secrete sucrose in a first stage and subsequently form PHA in Δ*nasT P. putida*, unable to consume nitrate and harnessed with genes necessary for sucrose catabolism, finally amassing 14.8% of CDM as PHA from CO_2.

Another important microbial biopolymer is alginate, which finds uses in the pharmaceutical and food industry. Constructing a transposon insertion mutant library, Mærk et al. screened for regulatory and metabolic genes involved in impaired alginate production in *Azotobacter vinelandii*. Genes belonging to the peptidoglycan, the TCA cycle, and vitamin biosynthesis appear to be crucial for assembling these macromolecules, while the addition of succinate or lysine improved alginate yields.

Finally, two engineered *E. coli* strains, each specialized in the degradation of xylose and glucose, produced the bioplastic precursor monomers succinate and D-lactate simultaneously. Flores et al. demonstrated that by co-culturing these cell factories in a defined population ratio, the bacterial community produced 88 g L^{-1} D-lactate and 84 g L^{-1} succinate.

Together, the studies published in this Research Topic reveal the ongoing efforts to obtain tailored biopolymers for various applications via fine-tuning gene expression and the host strains' pathway operation. Many challenges remain, especially in attaining maximal biopolymer production performance of engineered cell factories during fermentation in bioreactors with the desired monomer composition and physical properties.

AUTHOR CONTRIBUTIONS

IP-C conceived the idea of the Research Topic and served as editor. BAR and BHRA served as editor. All author contributed to the editorial and approved the submitted version.

REFERENCES

Moradali, M. F., and Rehm, B. H. A. (2020). Bacterial biopolymers: from pathogenesis to advanced materials. *Nat. Rev. Microbiol.* 18, 195–210. doi: 10.1038/s41579-019-0313-3

Oliveira, G. H. D., Zaiat, M., Rodrigues, J. A. D., Ramsay, J. A., and Ramsay, B. A. (2020) Towards the production of mcl-PHA with enriched dominant monomer content: process development for the sugarcane biorefinery context. *J. Polym. Environ.* 28, 844–853. doi: 10.1007/s10924-019-01637-2

Orellana-Saez, M., Pacheco, N., Costa, J. I., Mendez, K. N., Miossec, M. J., Meneses, C., et al. (2019) In-depth genomic and phenotypic characterization of the antarctic psychrotolerant strain Pseudomonas sp. MPC6 reveals unique metabolic features, plasticity, and biotechnological potential. *Front. Microbiol.* 10:1154. doi: 10.3389/fmicb.2019.01154

Conflict of Interest: BAR holds a patent for a method of synthesizing medium chain length polyhydroxyalkanoate.

The remaining authors declare that the research was conducted in the absence of any commercial or financial relationships that could be construed as a potential conflict of interest.

frontiers in Bioengineering and Biotechnology

ORIGINAL RESEARCH
published: 26 November 2019
doi: 10.3389/fbioe.2019.00334

An Easy and Efficient Strategy for the Enhancement of Epothilone Production Mediated by TALE-TF and CRISPR/dcas9 Systems in *Sorangium cellulosum*

Wei Ye†, *Taomei Liu*†, *Muzi Zhu*, *Weimin Zhang**, *Zilei Huang*, *Saini Li*, *Haohua Li*, *Yali Kong* and *Yuchan Chen*

State Key Laboratory of Applied Microbiology Southern China, Guangdong Provincial Key Laboratory of Microbial Culture Collection and Application, Guangdong Open Laboratory of Applied Microbiology, Guangdong Institute of Microbiology, Guangdong Academy of Sciences, Guangzhou, China

OPEN ACCESS

Edited by:
Bernd Rehm,
Griffith University, Australia

Reviewed by:
Bo Zhang,
Zhejiang University of Technology, China
Fengjie Cui,
Jiangsu University, China

***Correspondence:**
Weimin Zhang
wmzhang@gdim.cn

†*These authors have contributed equally to this work*

Specialty section:
This article was submitted to Industrial Biotechnology, a section of the journal Frontiers in Bioengineering and Biotechnology

Received: *26 June 2019*
Accepted: *30 October 2019*
Published: *26 November 2019*

Citation:
Ye W, Liu T, Zhu M, Zhang W, Huang Z, Li S, Li H, Kong Y and Chen Y (2019) An Easy and Efficient Strategy for the Enhancement of Epothilone Production Mediated by TALE-TF and CRISPR/dcas9 Systems in Sorangium cellulosum. Front. Bioeng. Biotechnol. 7:334. doi: 10.3389/fbioe.2019.00334

Epothilones are a kind of macrolides with strong cytotoxicity toward cancer cells and relatively lower side effects compared with taxol. Epothilone B derivate ixabepilone has been used for the clinical treatment of advanced breast cancer. However, the low yield of epothilones and the difficulty in the genetic manipulation of *Sorangium cellulosum* limited their wider application. Transcription activator-like effectors-Trancriptional factor (TALE-TF)-VP64 and clustered regularly interspaced short palindromic repeats (CRISPR)/dCas9-VP64 have been demonstrated as effective systems for the transcriptional improvement. In this study, a promoter for the epothilone biosynthesis cluster was obtained and the function has been verified. The TALE-TF-VP64 and CRISPR/dcas9-VP64 target P3 promoter were electroporated into *S. cellulosum* strain So ce M4, and the transcriptional levels of epothilone biosynthesis-related genes were significantly upregulated. The yield of epothilone B was improved by 2.89- and 1.53-fold by the introduction of recombinant TALE-TF-VP64-P3 and dCas9-VP64-P3 elements into So ce M4, respectively. The epothilone D yield was also improved by 1.12- and 2.18-fold in recombinant dCas9-So ce M4 and TALE-VP64 strains, respectively. The transcriptional regulation mechanism of TALE-TF-VP64 and the competition mechanism with endogenous transcriptional factor were investigated by electrophoretic mobility shift assay (EMSA) and chromatin immunoprecipitation (ChIP), demonstrating the combination of the P3 promoter and TALE-TF element and the competition between TALE-TF and endogenous transcriptional protein. This is the first report on the transcriptional regulation of the epothilone biosynthetic gene cluster in *S. cellulosum* using the TALE-TF and dCas9-VP64 systems, and the regulatory mechanism of the TALE-TF system for epothilone biosynthesis in *S. cellulosum* was also firstly revealed, thus shedding light on the metabolic engineering of *S. cellulosum* to improve epothilone yields substantially and promoting the application of epothilones in the biomedical industry.

Keywords: *Sorangium cellulosum*, TALE-TF, CRISPR/dCas9 activation, epothilones, regulatory mechanism

INTRODUCTION

Epothilones are 16-member macrolides with strong anticancer activity and produced by *Sorangium cellulosum*. Epothilones show stronger anticancer effects, broader spectrum of antitumor activity, simpler structure, lower side effects, and much better water solubility than the popular anticancer drug taxol (Bollag et al., 1995; Gerth et al., 1996; Höfle et al., 1996). Taxol yield has fallen sharply because *Taxus* has become increasingly rare, and the high cost of producing taxol through total synthesis has expanded the demand for alternative drugs. Epothilone B derivate ixabepilone has been approved in the clinical treatment of advanced breast cancer, and epothilone B and epothilone D and their derivatives show great potential in cancer treatment, especially for patients with taxane-resistant metastatic breast cancer (Roché et al., 2007; Thomas et al., 2007; Sparano et al., 2010). Epothilones have been considered an ideal substitute for taxol. However, epothilone yield remains low because of the difficulty in genetically manipulating *S. cellulosum* and the cytotoxicity of epothilones during the heterologous expression of epothilone biosynthesis cluster. The low yield of epothilones has limited their application in cancer treatment, and methods for enhancing epothilone yield and optimizing cultivation conditions are limited and random (Ye et al., 2016). Epothilone biosynthesis genes have been successively expressed in some bacteria, including *Myxococcus xanthus* and *Burkholderiales* sp. However, the improvement of epothilone yield through the heterologous expression of epothilone biosynthetic gene clusters is limited because of the toxicity of epothilone toward heterologous hosts. Epothilone yield in native host *S. cellulosum* is usually higher than heterologous hosts because of the high tolerance of *S. cellulosum* to the cytotoxicity of epothilones. Therefore, *S. cellulosum* is the best candidate for the expression of epothilone biosynthetic gene cluster. The scarcity of a genetic manipulation system for *S. cellulosum* impedes progress in the genetic engineering of epothilone biosynthesis in *S. cellulosum*. The transcription enhancement of epothilone biosynthetic cluster is an effective approach for improving epothilone yield. However, there are still few reports on the epothilone yield improvement in *S. cellulosum* by transcriptional activation approaches. Hence, improving epothilone yield by genetically engineering *S. cellulosum* through the transcriptional enhancement of epothilone biosynthetic cluster is urgent.

The epothilone biosynthesis cluster of *S. cellulosum* is a 56-kb gene cluster (Julien et al., 2000; Molnár et al., 2000). Different approaches have been adopted to enhance epothilone yield. Gong et al. (2007) fused the proplasts of different epothilone-producing strains to enhance epothilone B yield to 45.2 mg/L. Meng et al. (2010) improved epothilone B yield in *S. cellulosum* strain ATCC15384 from 5 to 9 mg/L by optimizing fermentation conditions. The biosynthetic cluster of epothilones was identified and heterologously expressed in *Streptomyces coelicolor*, and epothilones A and B were produced with very low yield (Tang et al., 2000). The whole gene cluster of *S. cellulosum* So0157-2 including the promoter sequence was inserted into *M. xanthus* by transposition insertion (Han et al., 2013; Zhu et al., 2015). Epothilone biosynthetic cluster was expressed in *M. xanthus*, and the *epoK* gene, which is responsible for the transformation of epothilone D to epothilone B, was disrupted for the increase of epothilone D yield to 20 mg/L (Julien and Shah, 2002). The CRISPR/Cas9 system is an effective tool for the specific regulation of gene expression levels (Alessandro et al., 2014). CRISPR/dCas9 technology was employed in *M. xanthus* to improve the transcription of heterologously expressed biosynthetic genes for the production of epothilones, and the yield of epothilone B was significantly improved (Peng et al., 2018). The promoters and transcriptional regulatory proteins of epothilone biosynthesis cluster have been investigated. The different promoters of epothilone biosynthetic clusters from *S. cellulosum* were identified and found to have high similarity but very different activities; thus, these promoters are important targets for the regulation of epothilone biosynthesis (Zhu et al., 2013). Proteins binding to the promoters of epothilone biosynthetic clusters were isolated from *S. cellulosum* strain So 0157-2, and their functions were verified by electrophoretic mobility shift assay (EMSA). Transcription activator-like effectors (TALEs) are DNA-binding proteins with high specificity and derived from *Xanthomonas* sp. (Joung and Sander, 2013). A TALE could be combined with transcriptional activation factor (TALE-TF) including VP64 to enhance the transcription level of target genes. The TALE-TF (Perez-Pinera et al., 2013; Hu et al., 2014; Uhde-stone et al., 2014) and CRISPR/dCas9 system (Gao et al., 2013; Qi et al., 2013; Chavez et al., 2015) have been widely used in the enhancement of target genes in mammalian cells. In this study, the promoter P3 of the epothilone biosynthetic cluster in *S. cellulosum* strain So ce M4 was cloned, and the function was validated by detecting luciferase activity. Recombinant TALE-TF and CRISPR/dCas9 elements targeting the P3 promoter were introduced into *S. cellulosum* strain So ce M4 for the upregulation of the transcriptional levels of epothilone biosynthetic genes and enhancement of epothilone yields. This study was the first report on the transcriptional regulation of epothilone biosynthetic cluster in *S. cellulosum* strain through the TALE-TF technology and CRISPR/dCas9 systems, and this is also the first investigation on the transcriptional mechanism of epothilone biosynthetic gene cluster that employs TALE-TF elements by using EMSA and chromatin immunoprecipitation (ChIP) in *S. cellulosum*; hence, this study is of significance for the epothilone yield improvement in *S. cellulosum* So ce M4 by transcriptional regulation approaches. Our investigation provided the molecular clues for the future transcriptional regulation of epothilone biosynthesis in *S. cellulosum* to improve the biosynthesis efficiency of epothilones in *S. cellulosum,* thereby expanding the application of epothilones in cancer treatment.

Abbreviations: CHIP, Chromatin immunoprecipitation; CRISPR, Clustered regularly interspaced short palindromic repeats; ECL, Enhanced chemiluminescence; EMSA, Electrophoretic mobility shift assay; LC-MS, Liquid chromatograph-mass spectrometer; TALE-TF, Transcription activator-like effectors-Trancriptional factor.

MATERIALS AND METHODS

Materials

S. cellulosum strain So ce M4 (accession no. GQ845309) was isolated from the soil of Xinyi City, Guangdong Province. A FastTALE^{TM} assembly kit including the Ptalen R36 vector was

purchased from Sidansai (Shanghai, China). PLX-sgRNA and dCas9-VP64 were purchased from addgene (USA). *S. cellulosum* was cultured in a G52 medium, and the growth temperature was 28°C.

Amplification and Identification of the P3 Promoter

The P3 promoter was amplified with primers P3 F: TGGCGT CGGGCGCGGGGTCG and P3 R: CCACTCGACCCCGCGC CCGAC to amplify the promoter for epothilone biosynthesis in So ce M4, and the genomic DNAs of So ce M4, So ce M1, and So ce M6 were used as templates. The P3 promoter was then ligated into the pMD18-T vector, and the positive clone was selected with an LB plate containing 100 μg/ml ampicillin and then sequenced. The P3 promoter and pgpd promoter were inserted into the pGL3-Basic vector by using restriction sites *Xho*I and *Hin*dIII to initiate the luciferase expression. The recombinant vectors pGL3-P3, pGL3-pgpd, and pGL3-Basic were transformed into the BL21 (DE3) strain. The bacteria were collected and sonicated, and the supernatants after centrifugation under 8,000 rpm for 10 min were collected and then incubated with luciferin agent for 5 min in equal volume following the instructions of Bright-Lumi^{TM}. Firefly Luciferase Reporter Gene Assay Kit (Beyotime, Shanghai, China), and the fluorescence intensities of different supernatants with luciferin agent were detected by an RF-5301PC fluorophotometer (SHIMADZU, Japan).

Construction of Plasmids and Mutants

The primers used for the construction of plasmids are listed in **Table S1**. The TALE module targeting the core sequences of the P3 promoter was constructed with the FastTALE^{TM} assembly kit (SIDANSAI, Shanghai, China). The pgpd promoter in the Ptalen R36 (SIDANSAI, Shanghai, China) vector was replaced with the P43 promoter after being digested with restriction enzymes *Asc*I and *Spe*I (Fermentas, ME, USA). The P3 promoter is suitable for *S. cellulosum*. The VP64 element was inserted into the Ptalen R36 vector to replace the *Fok*I element by using the restriction enzyme sites *BamH*I and *Sac*I (Fermentas, ME, USA). The P43 promoter and gRNA sequence targeting sequence in the core sequence of the P3 promoter were fused together by fusing PCR using Prime STAR Max Mix (Takara, Japan); then, the fused fragment was inserted into the pLX-sgRNA vector employing restriction sites *Xho*I and *Nhe*I.

Introduction of Recombinant TALE-TF Element and dCas9 System

The So ce M4 strain was cultured in a G52 medium for 12 h, and the cells were collected by centrifugation at 8,000 rpm and 4°C. The pellets were washed with ice-cold sterilized water twice to prepare So ce M4 competent cells. The recombinant TALE-TF and dCas9-VP64+PLX-sgRNA vectors were electroporated into the competent cells of So ce M4 under 2.0 KV in a 2.0-cm cuvette. The G52 medium was added for the recovery of So ce M4 competent cells. A G52 plate with 50 μg/ml kanamycin and G52 medium with 100 μg/ml ampicillin were used for the selection of the positive clone containing recombinant TALE-TF element and recombinant dCas9-VP64+PLX-sgRNA vectors, respectively. The genomic DNAs of recombinant So ce M4 clones were extracted using the Genomic DNA extraction kit (Tiangen, Beijing, China) and then used as templates; the primers colE F and colE R were used to amplify colE replicon in Ptalen R36 vector to ensure the introduction of recombinant TALE-TF vector. Primers f1F and f1R, and P43 F and P43 R (**Table S1**) were used to demonstrate the successful introduction of PLx-sgRNA and pcDNA-dCas9-VP64 vectors.

The total RNAs of the recombinant strain containing TALE-TF element (TALE-So ce M4) and dCas9-VP64 vector (dCas9-So ce M4) were extracted, and the cDNAs were obtained with a 5× all-in-one reverse transcription mix (Abm, Canada). Then, qRT-PCR was performed by using the primers listed in **Table S2** and qRT-PCR mix (Abm, Canada), together with QuantStudio 7 Flex Real-Time PCR System (Thermo Fisher, USA) to detect the relative expression levels of epothilone biosynthetic genes, and GAPDH was used as a reference gene. The qRT-PCR products were identified by using 1% agarose gel.

Yield Evaluation of Native and Recombinant So ce M4 Strains

Epothilones B and D (Aladin, Shanghai, China) standard at 100, 75, 50, 25, and 10 mg/L were used in the evaluation of epothilones B and D yields in the native and recombinant So ce M4 strains. The native and recombinant So ce M4 strains were inoculated into a G52 medium and cultivated at 28°C. Then, 5% XAD-16 macroporous resin (Amberlite, USA) and 3 mM sodium propionate (Sigma, USA) were added after 3 days of cultivation. After 7 days of cultivation, the resin was eluted using 80% methanol, and the eluent was concentrated to 2 ml with rotary evaporators (EYELA, USA) at 50°C. Then, 10 μl of the concentrated solution and epothilone standards were loaded onto a liquid chromatograph-mass spectrometer (Agilent 6430, USA). The abundances of the ion peaks of epothilones B (508.2, 530.2) and D (492.3, 514.3) were calculated for the evaluation of the yields of epothilones B and D in the native and recombinant So ce M4 strains.

ChIP Assay of Recombinant TALE-So ce M4 Strain

The ChIP assay of TALE-So ce M4 strain was performed with a ChIP assay kit (Beyotime, China). TALE-So ce M4 strain was cultivated for 24 h at 28°C and 200 rpm and then incubated at 37°C for 10 min. Then, 1% formaldehyde was added for the cross-linking of the target protein and genome DNA. After 3 days of cultivation, glycine solution was added, and PBS containing 1 mM PMSF was added to wash the *S. cellulosum* cells. The So ce M4 cells were collected after centrifugation at 8,000 rpm at 4°C. The SDS lysis buffer was added to the lysis So ce M4 cells, and then the samples were sonicated on ice. The supernatant was collected after centrifugation at 12,000 *g* and then eluted with a ChIP dilution buffer. Thereafter, 70 μl of protein A+G agarose/sperm DNA was added and incubated at 4°C for 30 min. Anti-FLAG mouse monoclonal antibody (Abcam, USA) with dilution of 1:2,000 was added and incubated at 4°C overnight. Then, 60 μl of protein A+G agarose/sperm DNA was added to

pull down the primary antibody-TALE protein-DNA complex. The supernatant was removed cautiously after centrifugation, and the precipitate was washed and finally eluted with an elution buffer (1% SDS, 0.1 M $NaHCO_3$). The eluate was used as the template, and primer P3 F was used to amplify the desired fragment. The loading buffer was added to the eluate. SDS-PAGE and Western blot analysis using the anti-FLAG antibody were performed to confirm the successful immune precipitation of recombinant TALE protein in the So ce M4 strain.

Acquisition of Native Regulatory Protein and Recombinant TALE Protein

The core sequence of the P3 promoter was prepared through annealing and then labeled with biotin with a biotin-labeling kit (Beyotime, Beijing, China). The total protein of the native and TALE So ce M4 cells were extracted with a protein extraction kit (Invitrogen, USA). The biotin-labeled P3 promoter with a volume of 10 μl was immobilized on streptavidin beads (Biomag, Wuxi, China), and 10 μl of the extracted proteins was added and incubated at 37°C for 1 h. Then, 50 μl of 95% deionized formamide containing 10 mM EDTA was added to elute the P3 promoter regulatory protein complex.

The recombinant TALE-VP64 vector targeting ATCTTGTGATTCCCCT in the core sequence of the P3 promoter was transformed into BL21(DE3) competent cells and cultivated in an LB medium overnight at 37°C, and the supernatant was collected after sonication. The supernatant was added into FLAG tag magnetic beads and incubated at 37°C for 1 h, and 10 mM glycine solution (pH 2.5) was added to elute the recombinant TALE-VP64 protein. The protein in the elution buffer was identified by SDS-PAGE and Western blot analysis.

EMSA Assay

The core (5′-TGCGATCTTGTGATTCCCCTTCTGATCT TTAAAATTTCCCGATCCCCCAT-3′) and non-core sequences (TGCGATCTTGTGATTCCCCTTCTGATCTTTAAAATTTC CCGATCC) were labeled with biotin by using the biotin-labeling kit (Beyotime, Beijing, China). The biotin-11-dUTP was added to the 3′ end of the target sequence by using terminal deoxynucleotidyl transferase and incubating at 37°C for 30 min. The sense and antisense strands were incubated at 95°C for 2 min and then cooled to room temperature. The biotin-labeled P3 core and non-core sequences were incubated with recombinant TALE-TF protein and native transcriptional factor P3*Fis* protein at 25°C for 10 min, respectively. The competition EMSA shift experiment was performed by incubating the biotin-labeled probe with P3*Fis* protein and recombinant TALE-VP64-P3 protein together, and the probe without the addition of protein was used as the negative control. A gel-shift buffer was added and identified by using the EMSA gel and then transferred onto nylon membrane under 380 mA for 30 min. Then, the membrane

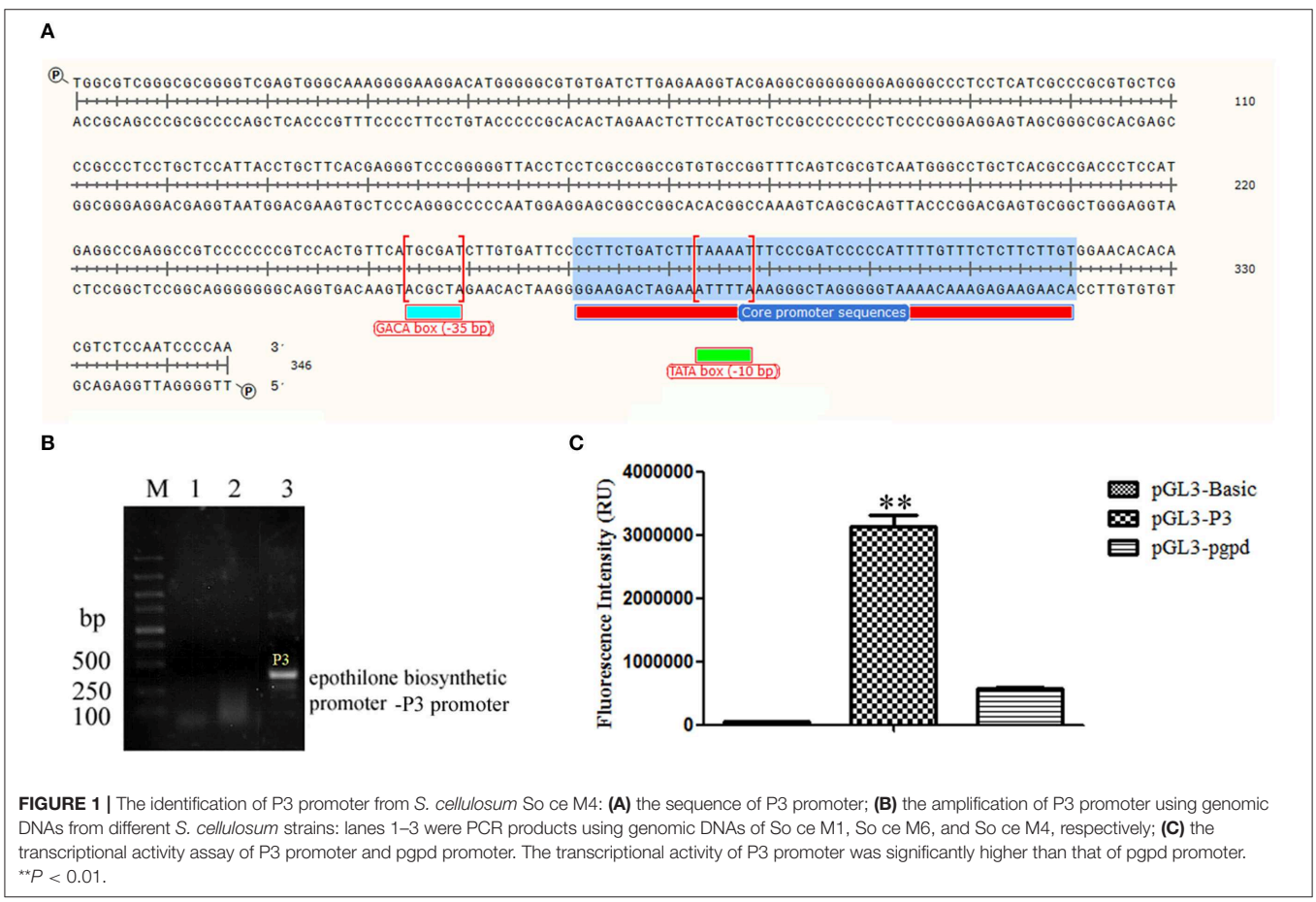

FIGURE 1 | The identification of P3 promoter from *S. cellulosum* So ce M4: **(A)** the sequence of P3 promoter; **(B)** the amplification of P3 promoter using genomic DNAs from different *S. cellulosum* strains: lanes 1–3 were PCR products using genomic DNAs of So ce M1, So ce M6, and So ce M4, respectively; **(C)** the transcriptional activity assay of P3 promoter and pgpd promoter. The transcriptional activity of P3 promoter was significantly higher than that of pgpd promoter. $^{**}P < 0.01$.

was fixed by using a UV-light cross-linker and blocked with 5% non-fat milk for 30 min at room temperature. The membrane was incubated with biotin antibody (1:5,000) for 40 min at room temperature. The membrane was washed, and the bands were visualized by adding enhanced chemiluminescence substrate according to the instruction of the manufacturers.

RESULTS

Identification of Epothilone Biosynthetic Promoter in So ce M4

The upper primer 5′-TGGCGTCGGGCGCGGGG-3′ and down primer 5′-TTGGGGATTGGAGACG-3′ were used to amplify the epothilone biosynthetic promoter-P3 promoter with a length of 346 bp. The promoter was located at the upstream of the *epoA* gene, the first gene of the epothilone gene cluster. The core region was predicted at 250–299 bp, the sequence of TAAAAT at the core region of P3 (279–284 bp) was considered TATA box at the −10 bp region, and the sequence of TGCGAT was considered the GACA box of the P3 promoter (**Figure 1A**). The P3 promoter was then inserted into vector pGL3-basic to initiate the expression of luciferase. The pgpd promoter was also inserted into pGL3-basic as a reference. The supernatant was obtained after the sonication of recombinant BL21 (DE3) strain harboring plasmid pGL3-P3. The fluorescence photometer was used to detect fluorescence intensity. As shown in **Figure 1B**, the fluorescence intensity of the recombinant strain containing PGL3-P3 was remarkably higher than that in strains harboring the vectors pGL3-basic and pGL3-pgpd. The results provided strong evidence of the function of the P3 promoter in the epothilone biosynthetic cluster of *S. cellulosum* So ce M4 (**Figure 1C**).

Construction and Introduction of Recombinant Plasmid

The core sequence of the P3 promoter was predicted as TGCGATCTTGTGATTCCCCTTCTGATCTTTAAAATTT CCCGATCCCCCAT (http://www.fruitfly.org/seq_tools/promoter.html), and the TALE module targeting sequence ATCTTGTGATTCCCCT was constructed using a fast TALEN assembly kit (SiDansai Biotechnology Ltd. Shanghai). Then, the TALE module was inserted into the vector containing VP64 and FLAG tag (**Figure S1**). Then, the CMV promoter was replaced by the P43 promoter, which is suitable for *S. cellulosum* So ce M4 (**Figure 2A**). Then, the P43 promoter was inserted into the pLX-sgRNA and pcDNA-dCas9-VP64 vectors (**Figure 2B**). The DNA targeting ATCTTGTGATTCCCCT was inserted into the pLX-sgRNA vector. The restriction sites *Xho*I and *Nhe*I were introduced to the P43 promoter and sgRNA scaffold assembled with the target sequence, and then digested and ligated into the pLX-sgRNA vector (**Figure S1**). The recombinant TALE-VP64-P3 vector and pcDNA-P43-dCas9-VP64+pLX-sgRNA-P3 were electroporated into *S. cellulosum* So ce M4 cells. Then, the positive clone was selected using the G52 plate containing kanamycin and G52 plate containing ampicillin, respectively.

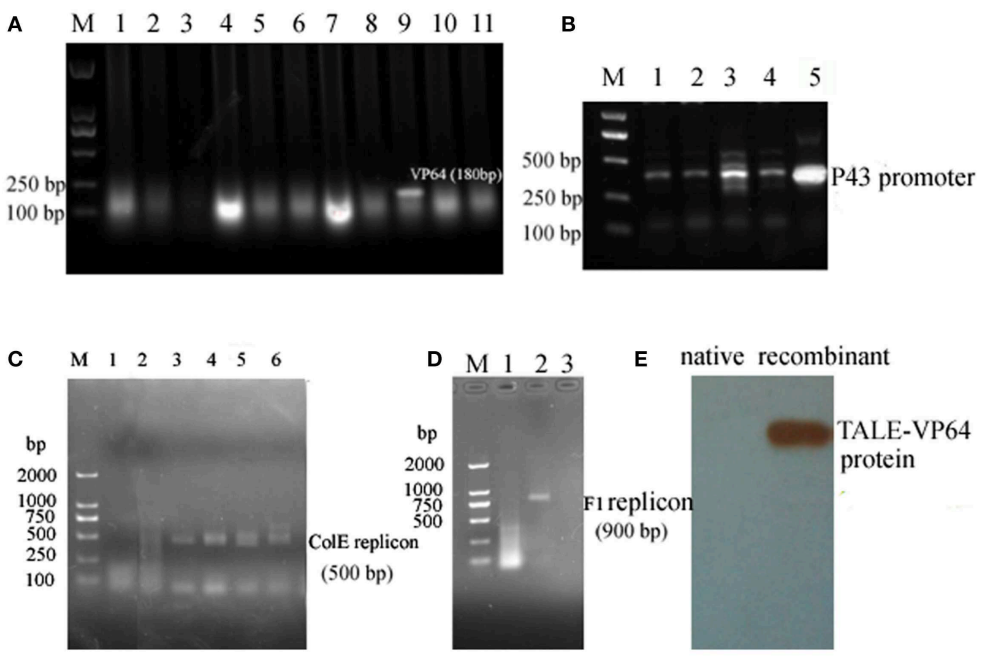

FIGURE 2 | The construction and introduction of recombinant TALE-VP64 and dCas9-VP64 elements: **(A)** the insertion of VP64 element: M. DNA Marker; lanes 1–11 were colony PCR products, lane 9 was the positive clone; **(B)** the insertion of P43 promoter into TALE-VP64 vector and pLX-sgRNA, lanes 1–4 were colony PCR using different colonies as template, lane 5 was positive control; **(C)** the confirmation of the introduction of TALE-VP64-P3 into So ce M4, lane 1 was the native So ce M4, lanes 2–6 were colony PCR products; **(D)** the confirmation of the introduction of dCas9-VP64-P3 into So ce M4: lane 1 was the native So ce M4, lanes 2 and 3 were colony PCR products; **(E)** the confirmation of the introduction of TALE-VP64-P3 vector by Western blot, anti-FLAG antibody was used as a primary antibody.

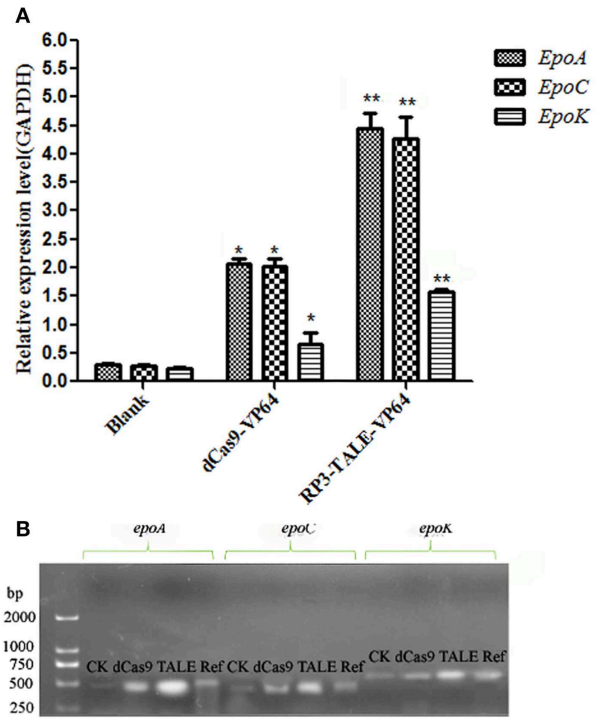

FIGURE 3 | The expression levels of epothilone-biosynthesis-related genes in *S. cellulosum* So ce M4: **(A)** qRT-PCR analysis; **(B)** the agarose gel electrophoresis of qRT-PCR products. CK means qRT-PCR products using cDNA of the native So ce M4 as a template, ref means the qRT-PCR results of GAPDH gene, which was used as a reference gene. dCas9, TALE refer to qRT-PCR products using cDNAs of the dCas9-So ce M4 and TALE-So ce M4 recombinant strains, respectively. *indicates $P < 0.05$, **indicates $P < 0.01$.

The successful amplification of ColE1 (**Figure 2C**) and f1 replicons (**Figure 2D**) confirmed the successful introduction of recombinant TALE-VP64 and dCas9-VP64 vector into *S. cellulosum* So ce M4. The total proteins of native and TALE-So ce M4 were extracted, and the anti-FLAG antibody was used to detect the recombinant protein. The band with a molecular weight of 100 kDa confirmed the expression of recombinant TALE protein in TALE-So ce M4, which was detected in native So ce M4 (**Figure 2E**).

Expression of Genes Related to Epothilone Biosynthesis in So ce M4

The total RNAs of the native and recombinant So ce M4 strains were extracted, and the cDNAs were obtained and used as templates to detect the expression levels of epothilone biosynthesis genes, including *epoA*, *epoC*, and *epoK*. The results indicated that the expression level of *epoA* in the recombinant So ce strain containing TALE-VP64 elements (TALE-So ce M4) was ∼14.89 ± 2.36-fold of that in the native So ce M4 strain. The expression level of *epoA* in the recombinant So ce strain containing dCas9-VP64 (dCas9-So ce M4) was ∼6.95 ± 0.38-fold of that in the native So ce M4 strain (**Figure 3A**). The qRT-PCR products were detected by electrophoresis (**Figure 3B**). The strongest bands corresponding to *epoA*, *epoC*, and *epoK* were detected in the TALE-So ce M4 strain, and the weakest was detected in the native So ce M4. The remarkably much higher expression level of epothilone biosynthesis-related genes in the recombinant So ce M4 strains as compared with that in the original So ce M4 strains suggested that the introduction of TALE-TF and dCas9-VP64 can upregulate the biosynthesis of epothilones in So ce M4 strains.

Improvement in the Epothilone Yields of the Recombinant So ce M4 Strains

The secondary products of the So ce M4 strains were extracted by using methanol and detected by HPLC-MS. The extract ion chromatographs of epothilones B and D in different So ce M4 strains were acquired. The abundance of epothilone B peaks (508.3, 530.3, and 546.3; **Figure S2**) and epothilone D peaks (492.2 and 514.2; **Figure S3**) were calculated for the evaluation of epothilones B and D yields in the So ce M4 strains. When epothilones B and D were used as references, the epothilone B yields in native, dCas9-, and TALE-So ce M4 were 7.64 ± 1.18, 19.33 ± 1.56, and 29.72 ± 2.66 mg/L, respectively. The introduction of dCas9-VP64 and TALE-VP64 elements into the So ce M4 strain improved epothilone B yield by 1.53- and 2.89-fold, respectively. The epothilone D yields in the native, dCas9-, and TALE-So ce M4 were 4.35 ± 0.16, 9.22 ± 1.32, and 13.83 ± 1.67 mg/L, respectively (**Figure 4**). The TALE-TF element and dCas9-VP64 element improved the epothilone D yield in So ce M4 1.12- and 2.18-fold, respectively. The lower increase in epothilone D yield as compared with that in epothilone B is due to the increased expression level of *epoF* in the dCas9- and TALE-So ce M4 strains, which are responsible for the conversion of epothilone D into epothilone B.

ChIP Assay of Recombinant TALE-So ce M4 Strain

The anti-FLAG primary antibody was used to pull down the recombinant TALE-protein and combined DNA complex. The molecular weight of the obtained protein was ∼110 kDa, as estimated by SDS-PAGE (**Figure 5A**). The result of the Western blot using the anti-FLAG antibody indicated that the obtained band was the TALE-P3 protein, which was not obtained in the native So ce M4 strain. The obtained protein-DNA complex was used as the template (**Figure 5B**), P3 F was used as the primer, and a fragment with a length of 350 bp approximately corresponding to the P3 promoter was detected (**Figure 5C**). The sequencing result confirmed that the obtained fragment was the P3 promoter, demonstrating the combination of recombinant TALE-P3 protein and the P3 promoter in the recombinant TALE-So ce M4 strain.

Acquisition of Native Regulatory Protein and Recombinant TALE Protein

The total protein of the So ce M4 stains was extracted at a concentration of 4.15 mg/ml, and the core sequence of the P3 promoter was labeled with biotin. Thus, the native regulatory protein was pulled down by the P3 promoter. The SDS-PAGE

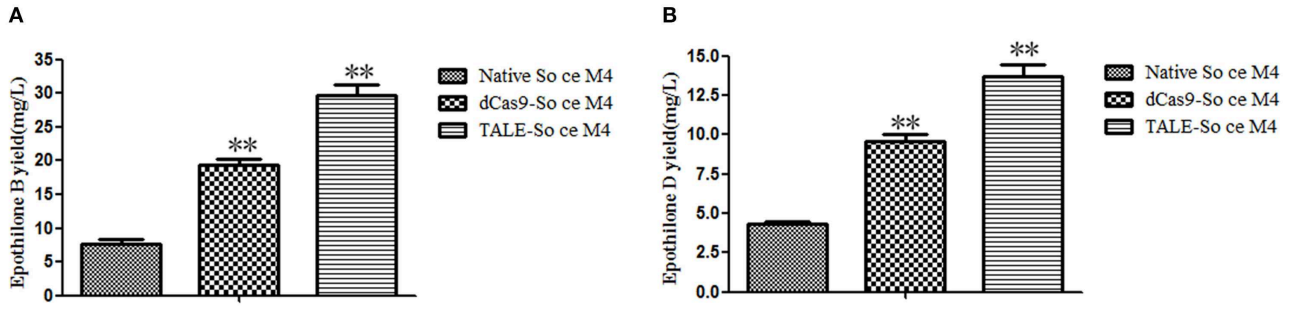

FIGURE 4 | The epothilone yields in different So ce M4 strains: **(A)** epothilone B yields in different So ce M4 strains; **(B)** epothilone D yields in different So ce M4 strains. **indicates $P < 0.01$.

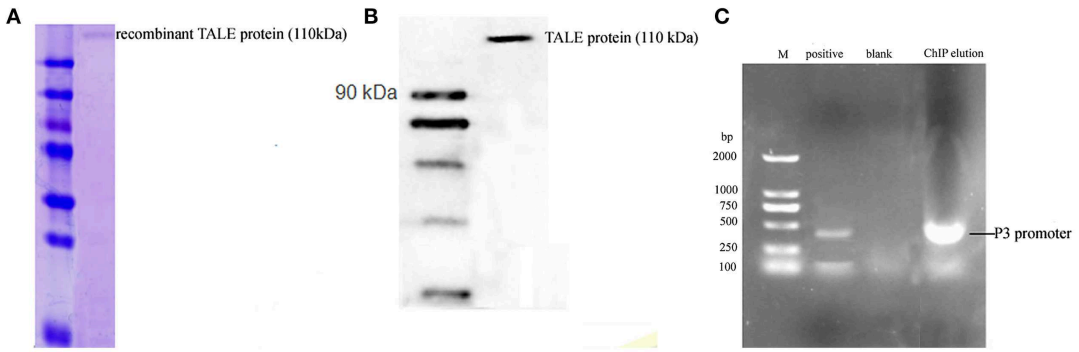

FIGURE 5 | The ChIP assay of *S. cellulosum* So ce M4 containing recombinant TALE-VP64 vector: **(A)** the SDS-PAGE analysis of ChIP eluate; **(B)** the Western blot analysis of ChIP eluate; **(C)** the verification of the presence of P3 promoter in ChIP eluate: M. DNA marker, lanes 1–3 were positive control, blank control, and PCR product using ChIP eluate as a template.

results suggested that the obtained regulatory protein was ∼38.0 kDa (**Figure 6A**), and the protein sequencing results showed that the protein sequence matched with an uncharacterized protein in *S. cellulosum* strain So ce 56. The part of digested peptide identified with a shotgun mass spectrometer matched a kind of Fis family transcriptional regulator in the *S. cellulosum* strain So0157-2. This regulator is responsible for the modulation of epothilone biosynthesis in So0157-2. This finding indicated that the obtained protein is a novel kind of regulatory protein for epothilone biosynthesis in So ce M4 strains and named P3*Fis* protein (**Figure 6B**). The TALE-VP64 element targeting P3 promoter was introduced into the BL21 (DE3) strain, and the recombinant TALE protein was expressed under the P43 constitutive promoter. The P3 promoter was labeled with biotin, and streptomycin affinity beads were used to purify the recombinant TALE-VP64 protein with molecular weight of ∼110 kDa, and the acquirement of recombinant TALE-VP64 protein was demonstrated via Western blot analysis using the anti-FLAG primary antibody.

EMSA Assay of the P3 Promoter and Regulatory Proteins

The core sequence of the P3 promoter and other sequences with length of 50 bp (TGGCGTCGGGCGCGGGGTCGAGTGG GCAAAGGGGAAGGACATGGGGGCGT) were labeled with biotin, and the labeled sequences without protein addition was used as a control, as shown in **Figure 7**. The most remarkable shift was obtained after the addition of the recombinant TALE-TF protein into the P3 core sequence, and a weak shift was observed after the addition of the native regulatory protein. The shift observed after the addition of the mixture of native regulatory protein and recombinant TALE-TF was weaker than that observed after the addition of the regulatory protein alone, suggesting the competitive inhibition of native regulatory protein and recombinant TALE-VP64 protein during the combination of regulatory proteins with the P3 promoter. However, no shift was observed upon the addition of both regulatory proteins into the labeled non-core sequence of the P3 promoter, indicating that the binding sequence of the recombinant TALE-VP64 protein and native regulatory protein was the core sequence of the P3 promoter TGCGATCTTGTGATTCCCCTTCTGAT CTTTAAAATTTCCCGATCCCCCAT.

DISCUSSION

The P3 promoter for epothilone biosynthetic cluster in *S. cellulosum* strain So ce M4 strain was firstly identified. Then, the recombinant TALE-TF element and CRISPR-dCas9-VP64 element targeting the core sequence of the P3 promoter were transformed into the So ce M4 strain

A

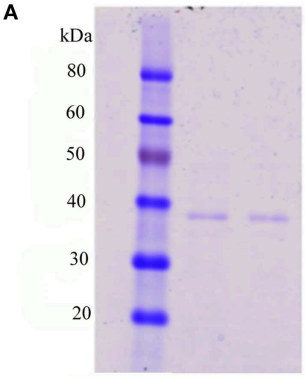

native regulatroy protein (38 kDa)

B

Accession	Score	Protein description
AoA150T0D7	32	Fis family transcriptional regulator OS=*Sorangium cellulosum*

A0A150SMK3_SORCE **Score:** 39 **Matches:** 5(1) **Sequences:** 3(1) **emPAI:** 0.06

Transcriptional regulator OS=Sorangium cellulosum GN=BE17_31545 PE=4 SV=1

Check to include this hit in error tolerant search or archive report

Query	Observed	Mr(expt)	Mr(calc)	ppm	Miss	Score	Expect	Rank	Unique	Peptide
641	410.7216	819.4287	819.4239	5.86	0	39	0.0062	2		R.VGAFEAAR.G
642	410.7219	819.4293	819.4239	6.59	0	(11)	4	8		R.VGAFEAAR.G
2003	476.7451	951.4756	951.4774	-1.93	0	4	9.5	2		K.NGTTLSGFR.V
7049	472.5729	1414.6970	1414.7052	-5.80	1	9	5	6	U	R.DGKEGSSPALEGLR.D
7050	472.5738	1414.6995	1414.7052	-4.06	1	(3)	20	10	U	R.DGKEGSSPALEGLR.D

FIGURE 6 | The acquisition of native regulatory protein P3*Fis* in *S. cellulosum* So ce M4: **(A)** the SDS-PAGE analysis of native regulatory protein obtained by P3 probe; **(B)** the amino acid sequencing of native regulatory protein.

for the upregulation of the expression levels of epothilone-biosynthesis-related genes and the improvement of the yields of epothilones B and D. The combination of the recombinant TALE-VP64 element with the P3 promoter *in vivo* and *in vitro* was confirmed by ChIP and EMSA assays, and the binding sequences of the P3 promoter were demonstrated. The native regulatory protein for epothilone biosynthesis in So ce M4 strain was pulled down by using the P3 promoter as the probe, and the competitive inhibition mechanism was demonstrated. The CRISPR/dCas9-VP64 system had been employed in the metabolic engineering of *M. xanthus* (Peng et al., 2018). However, the CRISPR/dCas9 system has not been used in the genetic engineering of *S. cellulosum*, let alone the TALE-TF technology. This study was the first report on the epothilone improvement in *S. cellulosum* strain by using the TALE-TF and CRISPR-dCas9 systems. The regulatory mechanism of TALE-TF elements for epothilone biosynthesis and its competitive effect with native regulatory protein in the *S. cellulosum* strain were also firstly illustrated, thus providing the molecular clues for the further regulation of epothilone biosynthesis in other *S. cellulosum* strains. Hence, this study is of significance and novelty with regard to the improvement of epothilone production in *S. cellulosum* by genetic engineering approaches, especially transcriptional activation.

The epothilones are potent anticancer drugs that bind to tubulin and inhibit the disassembly of microtubules (Bian et al., 2017). The epothilone B derivative ixabepilone has been approved for use in the treatment of breast and ovarian cancer patients, showing remarkable curative effect compared with taxol (Roché et al., 2007; Thomas et al., 2007; Sparano et al., 2010). However, the high cost of ixabepilone due to its complex production procedure limits its clinical application (Sparano et al., 2010). Thus, different approaches have been adopted to improve epothilone production. However, the difficulty in the genetic manipulation of *S. cellulosum*, the unclear genetic information for each *S. cellulosum* strain, and the lack of recognition for epothilone biosynthesis promoter and regulatory proteins impedes the progress of epothilone yield improvement in *S. cellulosum* (Ye et al., 2016). The 440-bp upstream sequence of the epothilone biosynthetic gene cluster from different *S. cellulosum* strains was cloned and identified, and the results indicated that the sequences of different promoters showed high similarity, whereas the transcriptional activities of these promoters remarkably vary probably because of the presence of stem-loop structures in the promoter sequences (Zhu et al.,

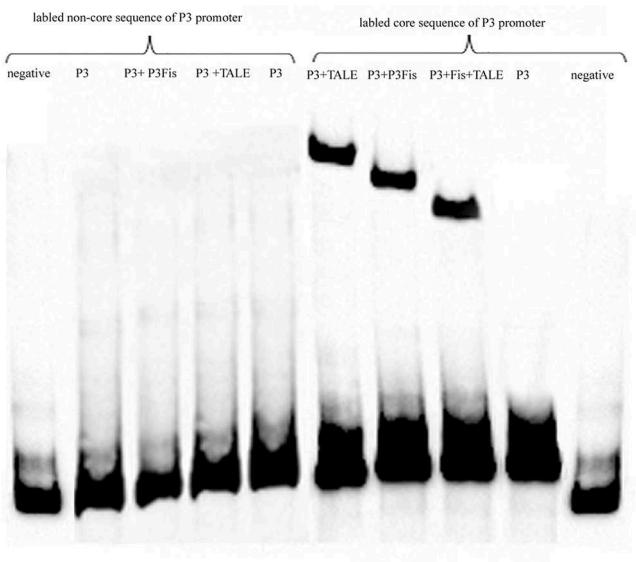

FIGURE 7 | The EMSA assay of native regulatory protein P3*Fis* and recombinant TALE-VP64 protein using biotin labeled core sequences of P3 promoter as probe. The non-core sequences of P3 promoter with the same length was also labeled as a control.

2013). Different primers were designed to obtain promoters for epothilone biosynthesis in So ce M4, and several sequences were obtained. However, only the essential elements for promoter were found in the P3 promoter, and only the P3 promoter showed strong transcriptional activity. The complete genome of the epothilone-producing strain *S. cellulosum* So0157-2 was sequenced (Schneiker et al., 2007; Han et al., 2013; Bian et al., 2017), the Fis family regulatory protein was identified (Schneiker et al., 2007; Zhu et al., 2012), and the binding activity of this regulatory protein epothilone biosynthesis promoter was confirmed by EMSA assay *in vitro*. The binding activity of Etf1 with epothilone biosynthesis promoter was demonstrated by the co-expression of Etf1 and the promoter ligated with reporter gene EGFP. However, the binding activity of the regulatory protein and promoter has not been confirmed in the So0157-2 strain because of the difficulty in genetically manipulating this strain. Meanwhile, the *in vitro* binding activity of the recombinant regulatory protein TALE-VP64-P3 with epothilone biosynthesis promoter in the *S. cellulosum* So ce M4 strain was firstly confirmed by ChIP assay.

Given that the cell behavior of *S. cellulosum* is complex, leading to increases in the levels of metabolic and regulatory factors and high variability of metabolites and genetic information, genetically manipulating *S. cellulosum* is difficult (Dworkin, 1983; Julien and Shah, 2002). Thus, many researchers have focused on the heterologous expression of the epothilone biosynthetic gene cluster in *M. xanthus* strains. However, the highest yield of epothilone B in recombinant *M. xanthus* strain was <5 mg/L because of the cytotoxicity of epothilones. The disruption of the *epoK* gene in the *M. xanthus* strain can improve the epothilone D yield to 20 mg/L (Julien and Shah, 2002; Bian et al., 2017; Peng et al., 2018). The CRISPR/dCas9 system was introduced into the *M. xanthus* strain, thus improving epothilone B yield 2-fold to 15 mg/L. The epothilone B yield in the *S. cellulosum* strain was higher than 50 mg/L (Gong et al., 2007), indicating that *S. cellulosum* is the optimal candidate host for the production of epothilones. The dcas9 fused with Cuω and the sgRNA targeting sequences with different spacers to the epothilone gene cluster were co-transformed into *M. xanthus*. The results displayed that the sgRNA-targeting spacers of 200 bp at the upstream of the start codon of *epoA* can achieve the highest improvement in epothilone B yield (Peng et al., 2018). Different transcription factors were fused with dCas9 to improve the expression levels of *epoA*, *B*, *C*, *D*, *E*, *F*, and *P* genes in *M. xanthus*, and the expression levels of *epoA* and *epoP* were improved ∼8- and 12-fold, respectively. The epothilones A and B yields in *M. xanthus* were improved by <2-fold by the CRISPR/dCas9 system, which was less than that the TALE-TF system used in *S. cellulosum* in our study. The results were in accordance with our investigation on *epo* gene expression levels and epothilones yields. Some epothilone biosynthetic genes, which were located far from the P3 promoter, also showed high expression levels; for instance, the expression level of the *epoK* gene in the TALE-So ce M4 was ∼7.09 ± 1.25-fold of that in the native So ce M4 strain, which may be due to the presence of other promoters in epothilone biosynthesis gene cluster of *S. cellulosum* So ce M4 besides P3 promoter. The production of epothilones was positive related to the expression levels of various epothilone biosynthetic genes. The low expression levels of some epothilone biosynthetic genes as compared with the expression level of *epoA* and the limited supply of precursors including propanyl COA in the fermentation liquid resulted in low increment in epothilone yield relative to that of the epothilone biosynthetic genes.

The 5′ end of the P3 promoter in *S. cellulosum* was at ∼-440 bp, and the core sequence was ∼-250 bp. Thus, the core sequence of the P3 promoter was ∼200 bp upstream of the epothilone biosynthetic gene cluster in So ce M4. Thus, the approaches using TALE-VP64 and dCas9-VP64 activators targeting the core sequence of the P3 promoter were effective in improving epothilone B yield in the So ce M4 strain. The introduction of recombinant TALE-VP64 protein and dCas9-VP64 improved epothilone B yield 2.89- and 1.53-fold, respectively. The higher increased increment of epothilone B yield by the transformation of the recombinant TALE-TF element into the So ce M4 strain compared with that of the CRISPR-dCas9 elements was probably due to the increased binding activity and specificity of TALE elements with the core sequence of the P3 promoter relative to those of the sgRNA sequence. It was also reported that protein-DNA binding showed higher affinity and specificity than DNA-DNA binding (Ashworth and Baker, 2009).

CONCLUSIONS

In this study, a novel promoter P3 for the epothilone biosynthesis in *S. cellulosum* So ce M4 was acquired, and

the transcriptional activity was also verified. The TALE-TF technology and CRISPR/dCas9 technology were firstly used to enhance the biosynthetic efficiency of the epothilone biosynthetic gene cluster, and the introduction of dCas9-VP64 and TALE-VP64 elements into the So ce M4 strain improved epothilone B and epothilone D yields by 1.53- and 2.89-fold and 1.12- and 2.18-fold, respectively. The transcriptional regulatory mechanism of TALE-TF elements and the competitive inhibitory effect with novel native regulatory protein P3*Fis* were revealed by EMSA and ChIP analysis. This is the first report on the transcriptional regulation of the epothilone biosynthetic gene cluster in *S. cellulosum* using the TALE-TF and dCas9-VP64 systems, as well as the regulatory mechanism of the TALE-TF system in *S. cellulosum*. Our investigation would open a new avenue for the yield improvement of anticancer drug epothilones in the native host *S. cellulosum* by transcription activation approaches, thus promoting the applications of epothilones and their derivatives in the biomedical industry.

DATA AVAILABILITY STATEMENT

The datasets generated for this study are available on request to the corresponding author and **Supplementary Materials**.

AUTHOR CONTRIBUTIONS

WY and WZ designed the experiments. WY, TL, MZ, ZH, YK, YC, and SL conducted experiments. SL and HL provided materials. WY, TL, and WZ analyzed data. WY wrote the manuscript, which was revised by WZ. WZ directed the research.

FUNDING

Financial support for this research was provided by the National Natural Science Foundation of China (31500037), the Natural Science Foundation of Guangdong Province (2019A1515011829, 2019A1515011702), the Science and Technology Planning Project of Guangdong Province (2016A020222022), and the GDAS' Project of Science and Technology Development (2019GDASYL-0105003).

SUPPLEMENTARY MATERIAL

The Supplementary Material for this article can be found online at: https://www.frontiersin.org/articles/10.3389/fbioe.2019.00334/full#supplementary-material

Figure S1 | The activation of epothilone biosynthetic cluster using TALE-VP64 and dCas9-VP64 system in *S. cellulosum* So ce M4.

Figure S2 | The detection of epothilone B yields in different So ce M4 strains by LC-MS: **(A)** epothilone standard; **(B)** native So ce M4; **(C)** RP3-So ce M4; **(D)** dCas9-So ce M4. The MS peak of 508.3 was corresponding to epothilone B, and the peak of 508.3 was extracted from the chromatography of different So ce M4 strains.

Figure S3 | The detection of epothilone D yields in different So ce M4 strains by LC-MS: **(A)** epothilone standard; **(B)** native So ce M4; **(C)** RP3- So ce M4; **(D)** dCas9-So ce M4. The MS peak of 492.2 was corresponding to epothilone B, and the peak of 492.2 was extracted from the chromatography of different So ce M4 strains.

Table S1 | Primers used for the construction of recombinant TALE-TF vector and dCas9-VP64 vectors.

Table S2 | Primers used for the qRT-PCR of genes related to the epothilone biosynthesis in *S. cellulosum* So ce M4.

REFERENCES

Alessandro, L., Dennis, S., and Carlo, M. C. (2014). Synthetic RNAs for gene regulation: design principles and computational tools. *Front. Bioeng. Biotechnol.* 2:65. doi: 10.3389/fbioe.2014.00065

Ashworth, J., and Baker, D. (2009). Assessment of the optimization of affinity and specificity at protein-DNA interfaces. *Nucleic Acids Res.* 37:e73. doi: 10.1093/nar/gkp242

Bian, X., Tang, B., Yu, Y., Tu, Q., Gross, F., Wang, H., et al. (2017). Heterologous production and yields improvement of epothilones in *Burkholderiales* strain DSM 7029. *ACS Chem. Biol.* 12, 1805–1812. doi: 10.1021/acschembio.7b00097

Bollag, D. M., McQueney, P. A., Zhu, J., Hensens, O., Koupal, L., Liesch, J., et al. (1995). Epothilones, a new class of microtubule-stabilizing agents with a taxol-like mechanism of action. *Cancer Res.* 55, 2325–2333.

Chavez, A., Scheiman, J., Vora, S., Pruitt, B. W., Tuttle, M. P. R., Iyer, E., et al. (2015). Highly efficient Cas9-mediated transcriptional programming. *Nat. Methods* 12, 326–328. doi: 10.1038/nmeth.3312

Dworkin, M. (1983). Tactic behavior of *Myxococcus xanthus*. *J. Baeteriol.* 154, 452–459.

Gao, X., Tsang, J. C., Gaba, F., Wu, D., Lu, L., and Liu, P. (2013). Comparison of TALE designer transcription factors and the CRISPR/dCas9 in regulation of gene expression by targeting enhancers. *Nucleic Acids Res.* 42:e155. doi: 10.1093/nar/gku836

Gerth, K., Bedorf, N., Hofle, G., Irschik, H., and Reichenbach, H. (1996). Epothilons A and B: antifungal and cytotoxic compounds from *Sorangium cellulosum* (Myxobacteria). Production, physico-chemical and biological properties. *J. Antibiot.* 49, 560–563. doi: 10.7164/antibiotics.49.560

Gong, G. L., Sun, X., Liu, X. L., Hu, W., Cao, W. R., Liu, H., et al. (2007). Mutation and a high-throughput screening method for improving the production of Epothilones of *Sorangium*. *J. Ind. Microbiol. Biotechnol.* 34, 615–623. doi: 10.1007/s10295-007-0236-2

Han, K., Li, Z. F., Peng, R., Zhu, L. P., Zhou, T., Wang, L. G., et al. (2013). Extraordinary expansion of a *Sorangium cellulosum* genome from an alkaline milieu. *Sci. Rep.* 3:2101. doi: 10.1038/srep02101

Höfle, G., Bedorf, N., Steinmetz, H., Schomburg, D., Gerth, K., and Reichenbach, H. (1996). Epothilone A and B-novel 16-membered macrolides with cytotoxic activity: isolation, crystal structure, and conformation in solution. *Angew. Chem. Int. Ed.* 35, 1567–1569. doi: 10.1002/anie.199615671

Hu, J., Lei, Y., Wong, W. K., Liu, S., Lee, K. C., He, X., et al. (2014). Direct activation of human and mouse Oct4 genes using engineered TALE and Cas9 transcription factors. *Nucleic Acids Res.* 42, 4375–4390. doi: 10.1093/nar/gku109

Joung, J. K., and Sander, J. D. (2013). TALENs: a widely applicable technology for targeted genome editing. *Nat. Rev. Mol. Cell Bio.* 14, 49–55. doi: 10.1038/nrm3486

Julien, B., and Shah, S. (2002). Heterologous expression of epothilone biosynthetic genes in *Myxococcus xanthus*. *Antimicro. Agent Ahemothe.* 46, 2772–2778. doi: 10.1128/AAC.46.9.2772-2778.2002

Julien, B., Shah, S., Ziermann, R., Goldman, R., Katz, L., and Khosla, C. (2000). Isolation and characterization of the epothilone biosynthetic gene cluster from *Sorangium cellulosum*. *Gene* 249, 153–160. doi: 10.1016/S0378-1119(00)00149-9

Meng, F. X., Li, Y. X., Guo, W. L., Lu, J. H., Du, L. N., and Teng, L. R. (2010). Optimization of fermentation medium for epothilones production with sequential statistical approach. *Chem. Res. Chin. Univ.* 26, 86–91.

Molnár, I., Schupp, T., Ono, M., Zirkle, R., Milnamow, M., Nowak-Thompson, B., et al. (2000). The biosynthetic gene cluster for the microtubule-stabilizing agents epothilones A and B from *Sorangium cellulosum* So ce90. *Chem. Biol.* 7, 97–109. doi: 10.1016/S1074-5521(00)00075-2

Peng, R., Wang, Y., Feng, W. W., Yue, X. J., Chen, J. H., Hu, X. Z., et al. (2018). CRISPR/dCas9-mediated transcriptional improvement of the biosynthetic gene cluster for the epothilone production in *Myxococcus xanthus*. *Microb. Cell Fact.* 17:15. doi: 10.1186/s12934-018-0867-1

Perez-Pinera, P., Ousterout, D. G., Brunger, J. M., Farin, A. M., Glass, K. A., Guilak, F., et al. (2013). Synergistic and tunable human gene activation by combinations of synthetic transcription factors. *Nat. Methods* 10, 239–242. doi: 10.1038/nmeth.2361

Qi, L. S., Larson, M. H., Gilbert, L. A., Doudna, J. A., Weissman, J. S., Arkin, A. P., et al. (2013). Repurposing CRISPR as an RNA-guided platform for sequence-specific control of gene expression. *Cell* 152, 1173–1183. doi: 10.1016/j.cell.2013.02.022

Roché, H., Yelle, L., Cognetti, F., Mauriac, L., Bunnell, C., Sparano, J., et al. (2007). Phase II clinical trial of ixabepilone (BMS-247550), an epothilone B analog, as first-line therapy in patients with metastatic breast cancer previously treated with anthracycline chemotherapy. *J. Clin. Oncol.* 25, 3415–3420. doi: 10.1200/JCO.2006.09.7535

Schneiker, S., Schneiker, S., Perlova, O., Kaiser, O., Gerth, K., Alici, A., et al. (2007). Complete genome sequence of the myxobacterium *Sorangium cellulosum*. *Nat. Biotechnol.* 25, 1281–1289. doi: 10.1038/nbt1354

Sparano, J. A., Vrdoljak, E., Rixe, O., Xu, B., Manikhas, A., Medina, C., et al. (2010). Randomized phase III trial of ixabepilone plus capecitabine versus capecitabine in patients with metastatic breast cancer previously treated with an anthracycline and a taxane. *J. Clin. Oncol.* 28, 3256–3263. doi: 10.1200/JCO.2009.24.4244

Tang, L., Shah, S., Chung, L., Carney, J., Katz, L., Khosla, C., et al. (2000). Cloning and heterologous expression of the epothilone gene cluster. *Science* 287, 640–642. doi: 10.1126/science.287.5453.640

Thomas, E., Tabernero, J., Fornier, M., Conté, P., Fumoleau, P., Lluch, A., et al. (2007). Phase II clinical trial of ixabepilone (BMS-247550), an epothilone B analog, in patients with taxane-resistant metastatic breast cancer. *J. Clin. Oncol.* 25, 3399–3406. doi: 10.1200/JCO.2006.08.9102

Uhde-stone, C., Cheung, E., and Lu, B. (2014). TALE activators regulate gene expression in a position- and strand-dependent manner in mammalian cells. *Biochem. Biophy. Res. Com.* 443, 1189–1194. doi: 10.1016/j.bbrc.2013.12.111

Ye, W., Zhang, W. M., Chen, Y. C., Li, H. H., Li, S., Pan, Q., et al. (2016). A new approach for improving epothilone B yield in *Sorangium cellulosum* by the introduction of *vgb epoF* genes. *J. Ind. Microbiol. Biotechnol.* 43, 641–650. doi: 10.1007/s10295-016-1735-9

Zhu, L. P., Han, L., Li, S. G., and Li, Y. Z. (2012). Novel characters of myxobacterial modular natural product assembly lines. *Prog. Biochem. Biophys.* 39, 525–539. doi: 10.3724/SP.J.1206.2011.00325

Zhu, L. P., Li, Z. F., Sun, X., Li, S. G., and Li, Y. Z. (2013). Characteristics and activity analysis of epothilone operon promoters from *Sorangium cellulosum* strains in *Escherichia coli*. *Appl. Microbiol. Biotechnol.* 97, 6857–6866. doi: 10.1007/s00253-013-4830-0

Zhu, L. P., Yue, X. J., Han, K., Li, Z. F., Zheng, L. S., Yi, X. N., et al. (2015). Allopatric integrations selectively change host transcriptomes, leading to varied expression efficiencies of exotic genes in *Myxococcus xanthus*. *Microb. Cell. Fact.* 14:105. doi: 10.1186/s12934-015-0294-5

Conflict of Interest: The authors declare that the research was conducted in the absence of any commercial or financial relationships that could be construed as a potential conflict of interest.

frontiers in Bioengineering and Biotechnology

ORIGINAL RESEARCH
published: 08 January 2020
doi: 10.3389/fbioe.2019.00416

Investigating Nutrient Limitation Role on Improvement of Growth and Poly(3-Hydroxybutyrate) Accumulation by *Burkholderia sacchari* LMG 19450 From Xylose as the Sole Carbon Source

*Edmar R. Oliveira-Filho, Jefferson G. P. Silva, Matheus Arjona de Macedo, Marilda K. Taciro, José Gregório C. Gomez and Luiziana F. Silva**

Department of Microbiology, Institute of Biomedical Sciences, University of São Paulo, São Paulo, Brazil

OPEN ACCESS

Edited by:
Ignacio Poblete-Castro, Andres Bello University, Chile

Reviewed by:
Martin Koller, University of Graz, Austria
Justyna Mozejko-Ciesielska, University of Warmia and Mazury in Olsztyn, Poland

***Correspondence:**
Luiziana F. Silva
lukneif@.usp.br

Specialty section:
This article was submitted to Industrial Biotechnology, a section of the journal Frontiers in Bioengineering and Biotechnology

Received: *07 October 2019*
Accepted: *29 November 2019*
Published: *08 January 2020*

Citation:
Oliveira-Filho ER, Silva JGP, de Macedo MA, Taciro MK, Gomez JGC and Silva LF (2020) Investigating Nutrient Limitation Role on Improvement of Growth and Poly(3-Hydroxybutyrate) Accumulation by Burkholderia sacchari LMG 19450 From Xylose as the Sole Carbon Source. Front. Bioeng. Biotechnol. 7:416. doi: 10.3389/fbioe.2019.00416

Burkholderia sacchari LMG19450, a non-model organism and a promising microbial platform, was studied to determine nutrient limitation impact on poly(3-hydroxybutyrate) [P(3HB)] production and bacterial growth from xylose, a major hemicellulosic residue. Nitrogen and phosphorus limitations have been studied in a number of cases to enhance PHA accumulation, but not combining xylose and *B. sacchari*. Within this strategy, it was sought to understand how to control PHA production and even modulate monomer composition. Nitrogen-limited and phosphorus-limited fed-batch experiments in bioreactors were performed to evaluate each one's influence on cell growth and poly(3-hydroxybutyrate) production. The mineral medium composition was defined based on yields calculated from typical results so that nitrogen was available during phosphorus limitation and residual phosphorus was available when limiting nitrogen. Sets of experiments were performed so as to promote cell growth in the first stage (supplied with initial xylose 15 g/L), followed by an accumulation phase, where N or P was the limiting nutrient when xylose was fed in pulses to avoid concentrations lower than 5 g/L. N-limited fed-batch specific cell growth (around 0.19 1/h) and substrate consumption (around 0.24 1/h) rates were higher when compared to phosphorus-limited ones. Xylose to PHA yield was similar in both conditions [0.37 $g_{P(3HB)}/g_{xyl}$]. We also described *pst* gene cluster in *B. sacchari*, responsible for high-affinity phosphate uptake. Obtained phosphorus to biomass yields might evidence polyphosphate accumulation. Results were compared with studies with *B. sacchari* and other PHA-producing microorganisms. Since it is the first report of the mentioned kinetic parameters for LMG 19450 growing on xylose solely, our results open exciting perspectives to develop an efficient bioprocess strategy with increased P(3HB) production from xylose or xylose-rich substrates.

Keywords: xylose, *Burkholderia sacchari*, poly(3-hydroxybutyrate), bioreactors, biopolymers

INTRODUCTION

Polyhydroxyalkanoates (PHA) are biopolyesters naturally produced and accumulated as intracellular granules by many Eubacteria and Archaea strains under unbalanced growth conditions (Lee, 1996; Koller et al., 2017). Considered as biocompatible and fully biodegradable (Keshavarz and Roy, 2010), these biopolymers are proposed as a valuable biomaterial presenting promising biomedical applications (Zhang et al., 2018). Although it has interesting characteristics, PHA production is still too expensive due to the prices of carbon sources, which represents up to 50% of the final production costs (Choi and Lee, 1997). This is one of the main obstacles in effectively introducing these biopolymers in the market.

The use of agroindustrial by-products as carbon feedstocks has been a strategy to produce PHA and other bioproducts in integrated biorefineries (Perlack, 2005; Silva et al., 2014; Aslan et al., 2016; Wang et al., 2018). Xylose, the second most abundant sugar in nature (Lachke, 2002), emerges as an exciting agricultural by-product to be explored as an inexpensive carbon source to produce PHA (Silva et al., 2014; Jiang et al., 2016). In Brazil, 633×10^6 tons of sugarcane were processed in the 2017/2018 harvest (https://www.conab.gov.br/info-agro/safras/cana/boletim-da-safra-de-cana-de-acucar), representing 177×10^6 tons of bagasse (Pessoa et al., 1997), part of which is burned to generate energy in the sugar and ethanol mills (Nonato et al., 2001). If submitted to an efficient hydrolysis treatment, as described by Paiva et al. (2009), this amount of bagasse would represent up to 430×10^5 tons of xylose available to be converted into value-added bioproducts.

Since the present federal legislation in Brazil aims to gradually eliminate the burning step performed previously to harvest, more sugarcane residues are expected to be available to other industrial applications (Silva et al., 2014). In addition, the production of second-generation ethanol is still not feasible, considering that hemicellulosic sugars are still poorly fermented by ethanologenic yeasts and bagasse pretreatment high costs (dos Santos et al., 2016).

Among a diversity of PHA$^+$ bacterial strains, *Burkholderia sacchari* LFM101 LMG19450^T (Brämer et al., 2001; Alexandrino et al., 2015) stands out for its ability to produce poly(3-hydroxybutyrate) [P(3HB)] from sucrose (Gomez et al., 1996, 1997). *B. sacchari* also metabolizes other carbohydrates: xylose, glucose, and arabinose (Brämer et al., 2001; Silva et al., 2004). Conveniently, *B. sacchari* is capable of incorporating other short- and medium-chain monomers as 3-hydroxyvalerate (3HV), 4-hydroxybutyrate (4HB), and 3-hydroxyhexanoate (3HHx) in the nascent polymeric chain, when supplied with co-substrates (Mendonça et al., 2014; Miranda De Sousa Dias et al., 2017).

One of the requirements for expressive PHA accumulation is carbon source excess combined with limitation of nutrients, such as nitrogen, phosphorus, iron, sulfur, magnesium, potassium, or oxygen (Schlegel et al., 1961). Therefore, the study of different nutritional limitations is an important factor to increase PHA concentration and content, as each nutrient limiting condition might have different effects on cell metabolism, growth, and PHA production. According to each strain, the best performance on polymer accumulation can be associated to one specific nutrient and must be determined to improve process of production.

Albeit important, there are only a few studies with phosphorus limitation as condition for PHA production available (Tu et al., 2019), most of which focused on PHA production from activated sludge (Chinwetkitvanich et al., 2004; Rodgers and Wu, 2010; Wen et al., 2010; Cavaillé et al., 2013; Tu et al., 2019). *Pseudomonas putida*, the model organism for medium-chain-length PHA production, was evaluated under different phosphorus limitation conditions, at various cultivations times, achieving increased PHA productivity, content, and concentration (Lee et al., 2000). Also, the initial phosphate concentration in *Ralstonia eutropha* fed-batch was shown as critical to achieve higher P(3HB) productivity and concentration values (Ryu et al., 1997). *Haloferax mediterranei* PHA production capacity was also evaluated under phosphorus limitation revealing promising results (Lillo and Rodriguez-Valera, 1990; Melanie et al., 2018).

An important factor to be considered when studying PHA production under phosphorus limitation is the fact that a previous study suggested that *B. sacchari* probably accumulates inorganic polyphosphate (Gomez et al., 1997). Polyphosphate accumulation in bacteria has been described to happen under several stress conditions, such as low pH, osmotic stress, or nutrient limitations, and might have various physiological functions: energy source, reservoir for phosphorus, among others (Kornberg et al., 1999). Additionally, some studies show that PHA and polyphosphate metabolism (production and utilization) are particularly linked, as evidenced by PHA depolymerase or polyphosphate kinase mutant strains of *R. eutropha* H16 (Tumlirsch et al., 2015) and *P. putida* KT2440 (Casey et al., 2013), which have differential PHA and polyphosphate production profiles.

In this work, the effects of nitrogen or phosphorus limitations in *B. sacchari* LFM101 growth and PHA biosynthesis using xylose as the sole source of carbon were evaluated. Also, the genes related to phosphorus consumption and polyphosphate were annotated in *B. sacchari* genome sequence. Results presented herein will be useful for the improvement of PHA homo- and copolymers production from xylose or xylose-rich agroindustrial by-products using *B. sacchari*, a promising microbial cell factory for bioproduction of value-added bioproducts, in the context of an integrated biorefinery (Nonato et al., 2001).

MATERIALS AND METHODS

Microorganisms and Culture Media

B. sacchari LFM101 LMG19450^T, recently reclassified as *Paraburkholderia sacchari* (Sawana et al., 2014), was used in this study as a platform for the production of PHA from xylose.

Lysogeny Broth (LB) (NaCl, 5 g/L; tryptone, 10 g/L; and yeast extract, 5 g/L) was used to grow *B. sacchari*. Seed cultures for fed-batch experiments were grown on mineral salts medium (MM1) with xylose as the sole carbon source (15 g/L). MM1 composition is detailed in **Table 1**. Flasks were incubated in a rotary shaker for 20 h at 30°C and 150 rpm.

TABLE 1 | Composition of the media used in this work.

Component	MM1	MM2 (N limited)	MM3 (P limited)
Medium composition (g/L)			
Na_2HPO_4	3.50	–	–
KH_2PO_4	1.50	0.87	0.21
$(NH_4)_2SO_4$	3.00	2.91	11.63
$MgSO{\cdot}7H_2O$	0.20	0.31	0.31
$CaCl_2{\cdot}2H_2O$	0.01	0.01	0.01
Ammonium citrate iron	0.06	0.06	0.06
NaCl	–	1.00	1.00
Trace elements solution	1 ml/L	2 ml/L	2 ml/L

Changes between MM2 and MM3 are in gray.
Trace elements solution composition was: H_3BO_3 (0.30 g/L); $CoCl_2{\cdot}6H_2O$ (0.20 g/L); $ZnSO_4{\cdot}7H_2O$ (0.10 g/L); $MnCl_2{\cdot}4H_2O$ (0.03 g/L); $NaMoO_4{\cdot}2H_2O$ (0.03 g/L); $NiCl_2{\cdot}6H_2O$ (0.02 g/L); $CuSO_4{\cdot}5H_2O$ (0.01 g/L).

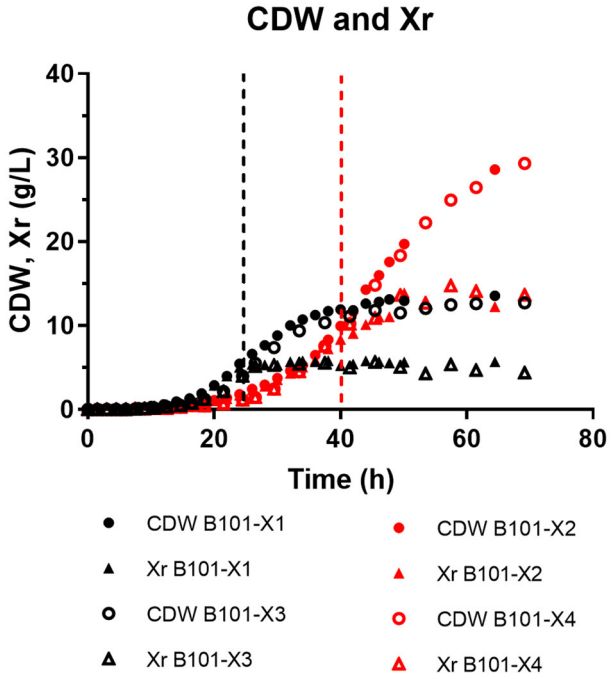

FIGURE 1 | Cell dry weight (CDW) and residual biomass (Xr) (both in g/L) obtained for each fed-batch cultivation. B101-X1 and B101-X3 refer to experiments under nitrogen limitation (black dots/lines), while B101-X2 and B101-X4 refer to experiments under phosphorus limitation (red dots/lines).

Fed-batch/bioreactor experiments were carried out in two different mineral salts media: MM2 and MM3. MM2 composition was adapted to limit nitrogen availability and MM3 was adapted to limit phosphorus availability. Both media are detailed in **Table 1**. Xylose was sterilized separately and aseptically added to the culture media; the final concentration used was 15–20 g/L, which was sufficient for cell growth until the start of P(3HB) accumulation phase considering previously obtained yield data (Guamán et al., 2018).

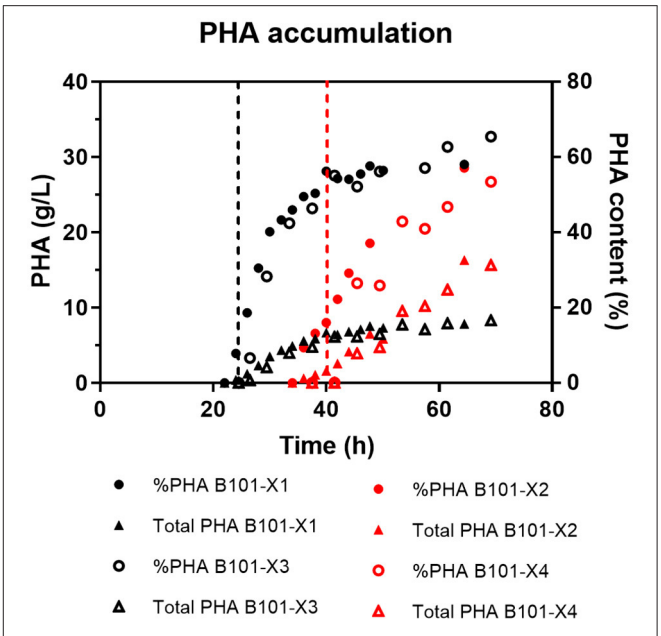

FIGURE 2 | PHA (g/L, left y-axis) and content (%, right y-axis) obtained for each fed-batch cultivation. B101-X1 and B101-X3 refer to experiments under nitrogen limitation (black dots/lines), while B101-X2 and B101-X4 refer to experiments under phosphorus limitation (red dots/lines). Black dashed lines mark the start of the accumulation phase under nitrogen limitation, while red dashed lines mark the start of the accumulation phase under phosphorus limitation.

Culture Conditions

Fed-Batch Cultivations

For bioreactor assays, *B. sacchari* LFM101 was pre-incubated for 24 h at 30°C and 150 rpm in 1-L Erlenmeyer flasks with 200 ml of MM1 containing xylose (15 g/L). Two sets of fed-batch experiments were performed in two identical bioreactors (Applikon Biotechnology Inc., Delft, Netherlands) using a working volume of 3 L, at 30°C for up to 70 h. The first set was B101-X1 (nitrogen limitation) and B101-X2 (phosphorus limitation). The second set was a replica for each condition: B101-X3 (nitrogen limitation) and B101-X4 (phosphorus limitation).

The pH was set at 7.00 ± 0.05 and controlled by automatic addition of NaOH (1 M) or H_2SO_4 (1 M). Dissolved oxygen was maintained above 40% of saturation by varying the agitation speed. Two different mineral media were used in fed-batch experiments, as described above.

Culture samples were harvested periodically to measure cell dry weight (CDW); xylose, nitrogen, and phosphorus concentration; P(3HB) content; and residual biomass [Xr = CDW – P(3HB) in g/L].

Gene Annotation

The genome sequence of *B. sacchari* (Alexandrino et al., 2015), privately available at RAST server (Aziz et al., 2008), was analyzed regarding the presence of genes related to phosphorus consumption, namely, the *pst*

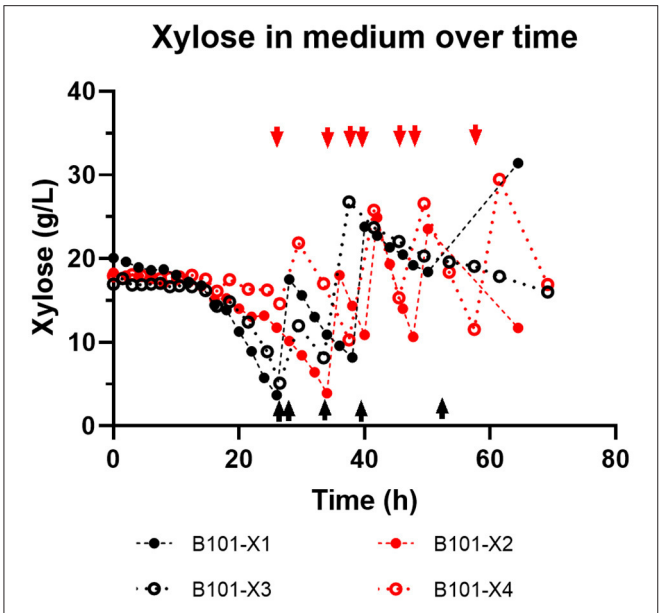

FIGURE 3 | Xylose concentration (g/L) in medium over time obtained for each fed-batch cultivation. B101-X1 and B101-X3 refer to experiments under nitrogen limitation (black dots/lines), while B101-X2 and B101-X4 refer to experiments under phosphorus limitation (red dots/lines). Black dashed lines mark the start of the accumulation phase under nitrogen limitation, while red dashed lines mark the start of the accumulation phase under phosphorus limitation. Arrows indicate feeding instants.

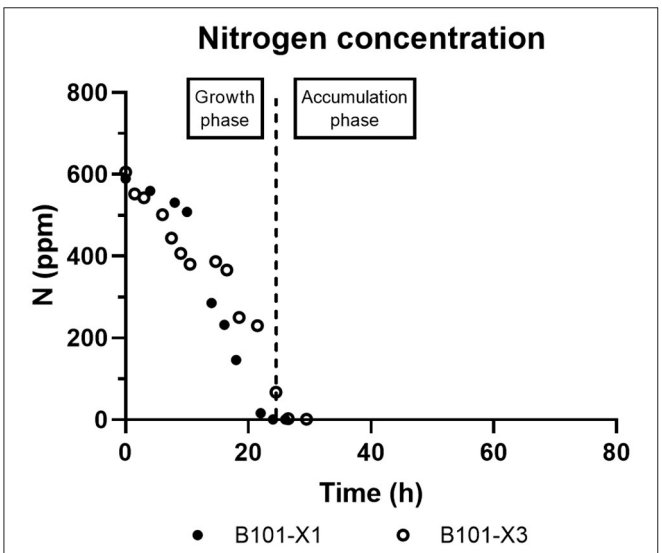

FIGURE 4 | B101-X1 and B101-X3 nitrogen concentration over time.

operon, and polyphosphate kinase genes. BLAST tool (Altschul et al., 1990) was used to confirm annotation and to compare protein sequences with *Escherichia coli*. Promoter sequences were predicted using Softberry BPROM (Solovyev and Salamov, 2011).

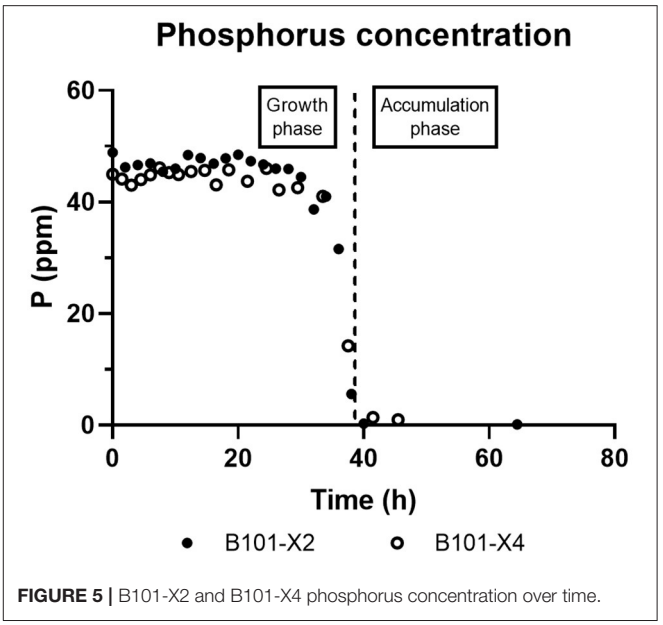

FIGURE 5 | B101-X2 and B101-X4 phosphorus concentration over time.

Analytical Methods

Biomass Concentration

The cells from 10 ml of culture were harvested by centrifugation at 10,600 *g* and lyophilized in microtubes. Dry biomass was weighed using an Adventurer® Analytical balance (OHAUS, Parsippany, New Jersey, USA) and expressed as CDW (cell dry weight in grams per liter).

Xylose Determination

Xylose concentration was determined by HPLC. Samples were injected into an Ultimate 3000 HPLC (Thermo Fisher Scientific Inc., Waltham, MA, USA) equipped with an Aminex-HPX-87H (Bio-Rad Laboratories Inc., Hercules, California, USA). Separation occurred at 40°C with H_2SO_4 solution (5 mM) at a flow rate of 0.6 ml/min. The standard curve was constructed using D(+)xylose solutions (Merck KGaA, Darmstadt, Germany). A refractive index detector, Shodex RI-101 (Shodex, Munich, Germany), was applied for peak detection.

Ammonium Concentration

The ammonium concentration was determined with an ion-selective electrode. After alkalinization of the sample, a High Performance Ammonia Ion Selective Electrode Orion 9512HPBNWP (Thermo Fisher Scientific Inc., Waltham, MA, USA) coupled to an Orion™ 4-Star Plus pH/ISE Benchtop Multiparameter Meter (Thermo Fisher Scientific Inc., Waltham, MA, USA) was used to measure the ammonia gas formed. Ammonium amount was calculated from a $(NH_4)_2SO_4$ standard curve containing up to 500 ppm of N.

Phosphorus determination

Phosphorus concentration was determined using the ascorbic acid colorimetric method (adapted from Rice et al., 2012). Briefly, a volume of reactive solution [20% (v/v) H_2SO_4 6N, 20% (v/v) of ammonium molybdate 2.5% (w/v), and 20% (v/v) ascorbic acid

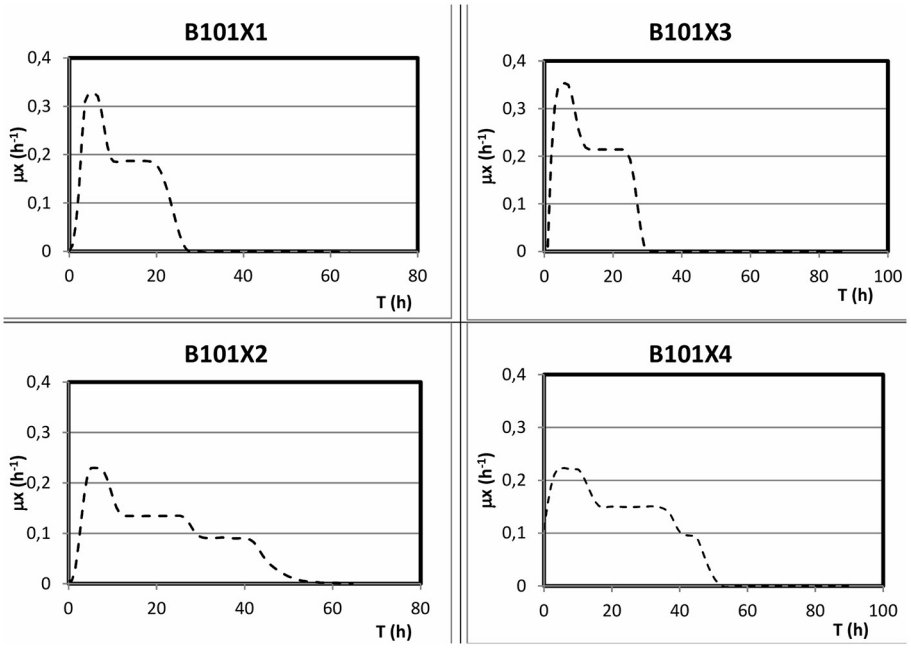

FIGURE 6 | Representation of the obtained μ in different culture media.

10% (w/v)] was added to an equal volume of supernatant samples. After incubation at 37°C for 1 h, absorbance was read at 820 nm.

Poly(3-hydroxybutyrate) Content Measurement

Ten milligrams of freeze-dried cells was propanolyzed (Riis and Mai, 1988). P(3HB) content was determined as described previously (Gomez et al., 1996) with an Agilent 7890A GC System (Agilent Technologies, Santa Clara, California, USA) equipped with an HP1 capillary column after sample split (1:10). Nitrogen (1.0 ml/min) was used as the carrier gas. Injector and flame ionization detector temperature were 250 and 300°C, respectively. The oven was programmed to maintain the temperature at 100°C for 1 min and then increase the temperature at a rate of 8°C /min up to 210°C, which was maintained for 15 min. Benzoic acid was used as the internal standard (Sigma-Aldrich, Saint Louis, Missouri, USA). P(3HB-*co*-3HV) (Sigma-Aldrich, Saint Louis, Missouri, USA) and medium-chain-length (C6–C12) PHA produced by *P. putida* ATCC 29347 from different fatty acids or by *Pseudomonas* sp. LFM046 from glucose were used as external standards.

RESULTS

Growth Phase

In all experiments, P(3HB) accumulation was not detected during the growth phase (**Figures 1**, **2**). B101-X1 and B101-X3 are replicas of nitrogen limitation condition, while B101-X2 and B101-X4 are replicas of phosphorus limitation condition. Xylose concentration in medium over time for each fed-batch is presented in **Figure 3**. Regarding nitrogen-limited fed-batches (B101-X1 and B101-X3), P(3HB) accumulation started after 24–26 h of cultivation when nitrogen concentration was almost depleted (2–12 mg/L) (**Figures 2**, **4**). In these fed-batches, phosphorus quantification revealed that this nutrient was not limited during all the cultivation, although it was consumed after nitrogen depletion. Nitrogen to residual biomass yield ($Y_{Xr/N}$) was calculated, representing around 7.5 (g/g).

Regarding phosphorus-limited experiments (B101-X2 and B101-X4), nitrogen quantification revealed that this nutrient was not limited during cultivation, as planned. Phosphorus concentration started to decrease after 20 h of batch, with phosphorus to residual biomass yield ($Y_{Xr/P}$) around 80 g/g. P(3HB) accumulation started around 40 h of cultivation (**Figure 2**), when phosphorus concentration was *circa* 31 mg/L, indicating that this is the limiting concentration for *B. sacchari*. Phosphorus depletion was observed right after P(3HB) accumulation started (**Figures 2**, **5**). Growth profiles were obtained, from which kinetic parameters were calculated. The variation profile of μ during the growth phase is represented in **Figure 6**.

Poly(3-hydroxybutyrate) Accumulation Phase

Gas chromatography of the propyl-esters from samples was compared to chromatograms obtained from different standards ranging from 3HB to 3HDd (including unsaturated monomers). Only 3HB was detected (**Supplementary Figure 1**).

PHA accumulation phase started when cell growth stopped due to nitrogen (B101-X1 and B101-X3) (**Figures 1**, **2**, **4**) or phosphorus limitation (B101-X2 and B101-X4) (**Figures 1**, **2**, **5**). In this phase, acetyl-CoA generated from xylose metabolism

TABLE 2 | Residual biomass yield from nitrogen or phosphorus (g/g) [$Y_{Xr/E}$] from the tested conditions.

Yield	Mean value ± Standard deviation
$Y_{Xr/N}$	7.63 ± 0.16
$Y_{Xr/P}$	80

TABLE 3 | Summary of data obtained in fed-batch experiments using *Burkholderia sacchari* LFM101, supplying xylose as the sole carbon source under different nutrient limitations to PHA accumulation.

Limitation	Parameters		
	CDW (g/L)	P(3HB) (%)	Volumetric productivity (g/L·h)
Nitrogen	13.10 ± 0.57	61.70 ± 5.23	0.12 ± 0.00
Phosphorus	29.25 ± 0.90	55.25 ± 2.62	0.24 ± 0.01

CDW: cell dry weight (g/L); P(3HB): polymer content of CDW (% of CDW).

TABLE 4 | P(3HB) yields from xylose (g/g) [$Y_{P(3HB)/xyl}$] and specific P(3HB) production rates (1/h) [q_P] from the tested conditions.

Limitation	Phase 1	Phase 2
$Y_{P(3HB)/xyl}$ (g/g)		
Nitrogen	0.38 ± 0.00 (24–34 h)	0.28 ± 0.01 (34–48 h)
Phosphorus	0.36 ± 0.01 (40–69 h)	–
q_P (1/h)		
Nitrogen	0.09 ± 0.01 (24–34 h)	0.03 ± 0.01 (34–49.5 h)
Phosphorus	0.04 ± 0.00 (40–69 h)	–

Nitrogen limited fed-batches presented two phases of biopolymer accumulation, while phosphorus-limited ones presented only one during all the experimental time. Each phase also presents a different q_P. The time intervals of each phase are indicated in parentheses.

was routed to PHA biosynthesis. Data obtained in two sets of experiments were used to calculate pseudo-stoichiometric and kinetic parameters of growth and PHA accumulation phases. These values are presented in **Tables 2**–**4**.

Two-phases of P(3HB) production were observed in nitrogen-limited experiments (**Figure 2**), phase 1 from 23 to 34 h and phase 2 from 34 to 49 h. This was reflected by xylose to P(3HB) yields [$Y_{P(3HB)/xyl}$] and specific rates of P(3HB) production (q_P). In phosphorus-limited experiments, a single phase of P(3HB) production was observed during the entire experiment course (**Figure 2**), with a single $Y_{P(3HB)/xyl}$ and q_P.

High-Affinity Inorganic Phosphate Transport and Polyphosphate Production Encoding Genes

B. sacchari genome was browsed using SEED viewer online tool (Overbeek et al., 2014). **Table 5** lists the gene sequences found, as well as the encoded protein, its length, and identity to *E. coli* protein.

Regarding the operon arrangement, *pstS*, *pstC*, *pstA*, and *pstB* are arranged as an operon, as a simple promoter was predicted upstream *pstS*. Another promoter sequence was predicted upstream of *phoU* (inside *pstB* coding sequence), forming a *phoUB* operon. Finally, regulatory sequence *phoR* possesses its own promoter sequence. Interestingly, *ppk* and *ppx* genes were located downstream of *phoR* sequence. A close *in silico* examination revealed an rpoD17 binding site in *phoUB* and *ppx* putative promoter sequences and an rpoD16 binding site in *ppk* putative promoter sequence.

TABLE 5 | Features of *B. sacchari* inorganic phosphate transport and polyphosphate production genes and protein identity to *E. coli* homologs.

Gene	Encoded protein	Identity[a] (%)	Protein length (aa)
pstS	Phosphate-binding protein	62	343
pstC	Phosphate transport system permease protein	75	328
pstA	Phosphate transport system permease protein	74	298
pstB	Phosphate import ATP-binding protein	82	278
phoU	Phosphate-specific transport system accessory protein	48	234
phoB	Phosphate regulon transcriptional regulatory protein	58	233
phoR	Phosphate regulon sensor protein	37	437
ppk1	Polyphosphate kinase 1	36	706
ppk2	Polyphosphate kinase 2	62	375
ppx	Exopolyphosphatase	41	515

[a] *Identity with E. coli homologs.*

Figure 7 represents the arrangement of the cluster composed by *pst* genes plus *ppk* and *ppx*. A gene encoding for polyphosphate kinase 2 (EC 2.7.4.1) was also annotated, although located at a different genomic loci.

DISCUSSION

Growth Phase

A few bacterial strains are considered as efficient regarding growth on xylose, the most abundant sugar in hemicellulosic residues (Li et al., 2017). The study of different experimental conditions to convert xylose into fine chemicals is of great interest in order to define new perspectives to design and establish efficient bioprocess techniques. Phosphorus-limited experiments achieved higher CDW and biomass when compared to nitrogen-limited experiments.

From the obtained μ values, we can infer two (nitrogen limitation) or three (phosphorus limitation) different specific growth rates (**Figure 6**). In nitrogen-limitation condition (B101-X1 and X3), maximum specific growth rates were maintained for up to 6 h of cultivation around 0.34 1/h. After this period, μ decreased to values (around 0.20 1/h) that were maintained until the end of the growth phase. On the other hand, maximum specific growth rates in phosphorus limitation condition (B101-X2 and X4) reached 0.22 1/h, shifting to 0.14 1/h in the second growth phase and then finally to 0.09 1/h until the end of growth.

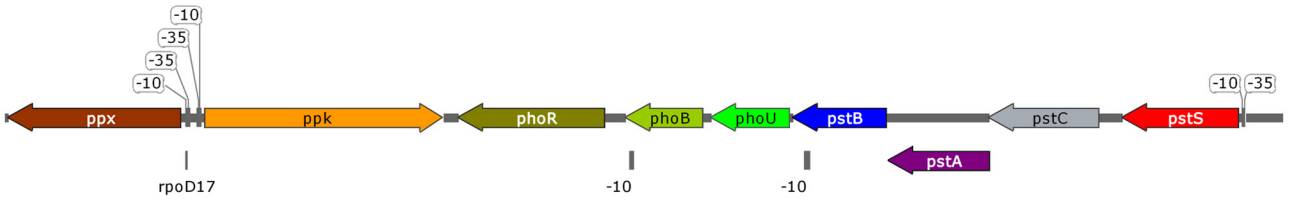

FIGURE 7 | Scheme of *B. sacchari* LFM101 high-affinity phosphate consumption and polyphosphate production gene cluster.

It is important to notice that the second phase was longer under higher concentrations of phosphorus (B101-X1 and X3).

In a different study, when cultivated under lower phosphorus concentration, *B. sacchari* growth rate was 0.15 1/h (Guamán et al., 2018), lower than the herein obtained under higher phosphorus concentrations (B101-X1 and -X3), which suggests that phosphorus concentration was limiting growth.

In nitrogen-limited experiments, residual biomass yield from nitrogen was around 7.5 g/g, close to what was obtained for *B. sacchari* in a previous study by Rocha and co-authors (7.25 g/g) (Rocha et al., 2008). Also for the same strain, a similar yield value was cited by Gomez and co-authors (6.62 g/g) (Gomez et al., 1997). This $Y_{Xr/N}$ value is similar to that obtained for *E. coli*, 8.00 (g/g) (Egli, 2015). $Y_{Xr/N}$ values from 5 to 8 g/g were reported for *P. putida* IPT046 in bioreactor cultivations under different conditions of dissolved oxygen and nitrogen amounts (Diniz et al., 2004). Since *B. sacchari* is not able to fix nitrogen (Martínez-Aguilar et al., 2008), we can assume that this nutrient is used mainly for nucleic acids and protein biosynthesis.

Regarding phosphorus concentration in P-limited cultivations, KH_2PO_4 amount in the initial batch was calculated to achieve a residual CDW of 5 g/L, considering a $Y_{Xr/P}$ value of 40 g/g (Taciro, 2008). As these conditions rendered an Xr value around 10 g/L (2-fold increase when compared to the expected value), we can assume that $Y_{Xr/P}$ for *B. sacchari* is around 80 g/g, similar to what was previously obtained for *B. sacchari* supplied with sucrose, around 82 g/g (Gomez et al., 1997). The obtained $Y_{Xr/P}$ is considerably higher when compared to *E. coli*, 33 g/g (Egli, 2015). Taciro (2008) mentions $Y_{Xr/P}$ values from chemostats of 30–40 g/g under phosphorus limitation and 20–30 g/g under nitrogen limitation conditions for *P. putida* IPT046. Considering those $Y_{Xr/P}$ values for *E. coli* and *Pseudomonas*, *B. sacchari* biomass composition presents lower phosphorus amounts. Also, as phosphorus is a significant component of nucleic acids, it should be noted that *B. sacchari* genome size is 7.2 Mb (Alexandrino et al., 2015), *E. coli* K-12 MG1655 genome size is 4.6 Mb (Blattner et al., 1997), and *Pseudomonas* LFM046 genome size is 6.0 Mb (Cardinali-Rezende et al., 2015). In addition, phospholipids are also important components synthesized from phosphorus.

Interestingly, phosphorus-limited experiments presented residual biomass production (Xr) during the accumulation phase (**Figure 1**), even after phosphorus depletion in the culture media, albeit severely reduced when compared to Xr increase during the growth phase. We suggest that the polyphosphate produced during the growth phase was then degraded and sustained Xr increase after phosphorus depletion in the culture media. Also, phosphorus consumption after nitrogen depletion in nitrogen-limited experiments strongly suggests that *B. sacchari* accumulates polyphosphate, similar to what was found previously by Gomez et al. (1997). Nevertheless, it is also important to mention that the seed culture was grown in a phosphorus-rich medium (MM1), probably using *pit*-mediated transport, a phosphate low-affinity transport system. Cells that were grown with P-limitation may already have a higher adaptation requirement at first, i.e., activation of the *pst*-mediated transport system.

B. sacchari Phosphate Transport and Polyphosphate Metabolism Gene Cluster

Genome analysis revealed that a complete *pst* locus is present in *B. sacchari* genome, together with *ppk1* and *ppx* located downstream of *pst* locus. *ppk2* gene was located elsewhere in the chromosome. A similar gene arrangement was found in *Burkholderia xenovorans* LB400, *Ralstonia solanacearum* GMI1000, *Burkholderia ambifaria* AMMD, and *R. eutropha* JMP134 (genome sequences available for comparison at RAST server). A similar operon organization (number and location of gene promoters, i.e., regulation) was described in *Pseudomonas aeruginosa* (Munévar et al., 2017). These genes are part of the PHO regulon, regulated by the concentration of phosphate in the medium (Santos-Beneit, 2015). Phosphate uptake in *E. coli* occurs following two kinetically different systems: high-affinity (Pst) and low-affinity (Pit) systems (Medveczky and Rosenberg, 1971; Willsky and Malamy, 1976). The Pst system is active in phosphorus-limiting conditions and, as such, is of greatest interest to our study. The Pst system is a conventional ABC transporter, in which PstS binds to extracellular phosphate, PstA and PstC are permeases that channel phosphate through the periplasmic space (Webb et al., 1992), and PstB binds to ATP, which is the energy source for the transport (Chan and Torriani, 1996). This transport system was previously reported in a *Burkholderia* strain (Ruiz-Lozano and Bonfante, 1999). Regarding *phoB* and *phoR* gene products, PhoB and PhoR are part of a two-component system that regulates PHO gene expression. PhoR sensor kinase autophosphorylates and phosphorylates PhoB in low-phosphate concentration. PhoB-P then promotes the expression of PHO genes (Santos-Beneit, 2015). Under phosphate excess, regulator protein PhoU is known to repress PHO genes expression via dephosphorylation of PhoB-P.

Putative promoter sequences were identified for *ppk1*, *ppk2*, and *ppx*, the central genes in polyphosphate formation (*ppk1* and *ppx*) and degradation (*ppk2* and *ppx*). As found in *P. aeruginosa*, *ppk1* and *ppx* are adjacent and in opposite directions (Zago et al., 1999), suggesting a differential expression regulation. Ppk1 protein is involved in the formation of polymer from ATP, while Ppk2 encoding gene, which was annotated in a different genomic *loci*, is typically found in *P. aeruginosa* and associated with the synthesis/degradation of polyphosphate from/to GTP or ATP (Zhang et al., 2002). Ppx degrades polyphosphate into orthophosphate, and its encoding sequence was first described in *E. coli* forming an operon with *ppk1* protein (Akiyama et al., 1993). We identified a putative promoter sequence in *B. sacchari*'s *ppx*, which indicates differential regulation.

Together, the increased $Y_{Xr/P}$ (higher to what has been presented in the literature) and genomic evidence suggests that *B. sacchari* accumulates polyphosphate granules, as firstly suggested by Gomez and co-workers (Gomez et al., 1997).

Poly(3-hydroxybutyrate) Accumulation Phase

P(3HB) contents were similar in both tested conditions (55–61% of cell dry weight), comparable to what was reported in previous studies using *R. eutropha* (Kim et al., 1994; Ryu et al., 1997).

Nitrogen limitation yielded approximately equal P(3HB) content (7.8 g/L). In contrast, phosphorus limitation yielded higher P(3HB) amount (*ca*. 16 g/L). This reflected in the volumetric productivity of P(3HB) in this strategy [0.25 gP(3HB)/L·h], which can be attributed to higher cell growth sustained by greater levels of nitrogen in MM3.

Under nitrogen limitation, two different biopolymer accumulation phases were observed. The first one presented a $Y_{P(3HB)/xyl}$ (0.38 g/g) representing 79% of the maximum theoretical value (0.48 g/g), calculated considering that 6 mol of xylose is converted to 5 mol of 3HB. The second accumulation phase yield (0.275 g/g) represents 57% of the maximum theoretical value.

In comparison, phosphorus-limited experiments presented a single accumulation phase during the experiment time. The obtained $Y_{P(3HB)/xyl}$ value, 0.36 g/g, corresponds to 74% of the maximum theoretical value. Although only one phase was observed, these cultivations required longer time to start P(3HB) accumulation, suggesting that longer experiments could clarify the accumulation profile of *B. sacchari* in this condition.

Nitrogen is used by bacterial cells to synthesize nucleic acids and proteins, while phosphorus is converted to nucleic acids and phospholipids. We can note that in the accumulation phase, q_P values are 1-fold reduced in phosphorus-limited experiments when compared to nitrogen limitation condition.

Although under phosphorus limitation conditions *B. sacchari* achieved higher P(3HB) production in g/L, P(3HB) production required more time, almost 20 h, to achieve an equal P(3HB) content [%P(3HB)] when compared to the nitrogen limitation condition. A similar situation was described in a study investigating the effect of phosphorus limitation on PHA production by activated sludge biomass (Chinwetkitvanich et al., 2004). The phosphorus consumption of *B. sacchari* showed that this nutrient was substantially consumed after 20 h of cultivation, reaching depletion shortly after this period. The same profile was reported by Ryu and co-workers when studying PHA accumulation by *R. eutropha* (Ryu et al., 1997).

In this study, P(3HB), the most-studied PHA, was produced from xylose. P(3HB) characteristics include high crystallinity, stiffness, and brittleness. *B. sacchari* is also capable of incorporating other monomers as 3HV (Silva et al., 2002), 3HHx (Mendonça et al., 2017), and 4HB (Cesário et al., 2014; Miranda De Sousa Dias et al., 2017) when adequate co-substrates are supplied; therefore, studies combining xylose and co-substrates feeding may benefit from the results here presented, contributing to reduce costs of production by using xylose from hemicellulosic residues.

CONCLUSIONS

This work describes, for the first time to our knowledge, the effects of two different nutritional limitations on the growth and P(3HB) accumulation by the non-model *bacterium B. sacchari* from xylose solely. Higher μ_{max} were observed under nitrogen-limiting conditions, indicating that an increased phosphorus concentration is a defining factor to achieve higher growth rates on xylose. Although phosphorus limitation (nitrogen excess) resulted in higher CDW, and thus higher P(3HB) concentration, in g/L, the biopolymer accumulation phase started 20 h after nitrogen limitation conditions. To avoid this delay, the seed cultures could be previously adapted to diminished phosphorus concentrations. Further transcriptomics studies, including PHO regulon expression assessment, would contribute to elucidate the metabolic pathways responsible for the observed physiological phenomenon. Since *B. sacchari* is considered as a promising microbial cell factory for the biotechnological production of PHA and xylitol (Raposo et al., 2017), this work may contribute to the establishment of cheaper and sustainable production of polyhydroxybutyrate from agroindustrial by-products. Considering the context of integrating PHA production to a sugar and ethanol biorefinery, the use of xylose, not really fermented by ethanologenic yeasts, can represent an important step toward sustainability of the process. Results presented here contribute to the knowledge on the conditions appropriate do promote the best efficiency in converting xylose to P(3HB) in this model.

DATA AVAILABILITY STATEMENT

The datasets generated for this study are available on request to the corresponding author.

AUTHOR CONTRIBUTIONS

LS, JG, and MT jointly conceived and supervised the study. EO-F and JS performed the experiments. EO-F and MM prepared the initial version of this manuscript. All authors analyzed the data, read, improved, and approved the final manuscript.

FUNDING

This work was supported by the National Council for Scientific and Technological Development CNPq–Brazil (140321/2017-9 EO-F Ph.D. Scholarship) and São Paulo Research Foundation (FAPESP 2016/00842-0, awarded to LS). This study was financed in part by the Coordenação de Aperfeiçoamento de Pessoal de Nível Superior–Brasil (CAPES)–Finance Code 001: JS and MM Scholarships. JG (309134/2015-3) and LS (308306/2015-5) were grateful to CNPq–Brazil for their technological development productivity fellowships.

SUPPLEMENTARY MATERIAL

The Supplementary Material for this article can be found online at: https://www.frontiersin.org/articles/10.3389/fbioe.2019.00416/full#supplementary-material

REFERENCES

Akiyama, M., Crooke, E., and Kornberg, A. (1993). An exopolyphosphatase of *Escherichia coli*. The enzyme and its *ppx* gene in a polyphosphate operon. *J. Biol. Chem.* 268, 633–639.

Alexandrino, P. M. R., Mendonça, T. T., Guamán Bautista, L. P., Cherix, J., Lozano-Sakalauskas, G. C., Fujita, A., et al. (2015). Draft genome sequence of the polyhydroxyalkanoate-producing bacterium *Burkholderia sacchari* LMG 19450 isolated from Brazilian sugarcane plantation soil. *Genome Announc.* 3:e00313-15. doi: 10.1128/genomeA.00313-15

Altschul, S. F., Gish, W., Miller, W., Myers, E. W., and Lipman, D. J. (1990). Basic local alignment search tool. *J. Mol. Biol.* 215, 403–410. doi: 10.1016/S0022-2836(05)80360-2

Aslan, A. K. H. N., Ali, M. D. M., Morad, N. A., and Tamunaidu, P. (2016). Polyhydroxyalkanoates production from waste biomass. *IOP Conf. Ser. Earth Environ. Sci.* 36:012040. doi: 10.1088/1755-1315/36/1/012040

Aziz, R. K., Bartels, D., Best, A. A., DeJongh, M., Disz, T., Edwards, R. A., et al. (2008). The RAST Server: rapid annotations using subsystems technology. *BMC Genomics* 9:75. doi: 10.1186/1471-2164-9-75

Blattner, F. R., Plunkett, G., Bloch, C. A., Perna, N. T., Burland, V., Riley, M., et al. (1997). The complete genome sequence of *Escherichia coli* K-12. *Science* 277, 1453–1462. doi: 10.1126/science.277.5331.1453

Brämer, C. O., Vandamme, P., da Silva, L. F., Gomez, J. G., and Steinbüchel, A. (2001). Polyhydroxyalkanoate-accumulating bacterium isolated from soil of a sugar-cane plantation in Brazil. *Int. J. Syst. Evol. Microbiol.* 51, 1709–1713. doi: 10.1099/00207713-51-5-1709

Cardinali-Rezende, J., Alexandrino, P. M. R., de Nahat, R. A. T. P. S., Sant'Ana, D. P. V., Silva, L. F., Gomez, J. G. C., et al. (2015). Draft genome sequence of Pseudomonas sp. strain LFM046, a producer of medium-chain-length polyhydroxyalkanoate. *Genome Announc.* 3, 45–46.

Casey, W. T., Nikodinovic-Runic, J., Fonseca Garcia, P., Guzik, M. W., McGrath, J. W., Quinn, J. P., et al. (2013). The effect of polyphosphate kinase gene deletion on polyhydroxyalkanoate accumulation and carbon metabolism in *Pseudomonas putida* KT2440. *Environ. Microbiol. Rep.* 5, 740–746. doi: 10.1111/1758-2229.12076

Cavaillé, L., Grousseau, E., Pocquet, M., Lepeuple, A.-S., Uribelarrea, J.-L., Hernandez-Raquet, G., et al. (2013). Polyhydroxybutyrate production by direct use of waste activated sludge in phosphorus-limited fed-batch culture. *Bioresour. Technol.* 149, 301–309. doi: 10.1016/j.biortech.2013.09.044

Cesário, M. T., Raposo, R. S., M. D. de Almeida, M. C., van Keulen, F., Ferreira, B. S., Tole, J. P., et al. (2014). Production of poly(3-hydroxybutyrate-co-4-hydroxybutyrate) by *Burkholderia sacchari* using wheat straw hydrolysates and gamma-butyrolactone. *Int. J. Biol. Macromol.* 71, 59–67. doi: 10.1016/j.ijbiomac.2014.04.054

Chan, F. Y., and Torriani, A. (1996). PstB protein of the phosphate-specific transport system of *Escherichia coli* is an ATPase. *J. Bacteriol.* 178, 3974–3977. doi: 10.1128/jb.178.13.3974-3977.1996

Chinwetkitvanich, S., Randall, C. W., and Panswad, T. (2004). Effects of phosphorus limitation and temperature on PHA production in activated sludge. *Water Sci. Technol.* 50, 135–143. doi: 10.2166/wst.2004.0507

Choi, J., and Lee, S. Y. (1997). Process analysis and economic evaluation for Poly(3-hydroxybutyrate) production by fermentation. *Bioprocess Eng.* 17, 335–342. doi: 10.1007/s004490050394

Diniz, S. C., Taciro, M. K., Gomez, J. G. C., and da Cruz Pradella, J. G. (2004). High-cell-density cultivation of *Pseudomonas putida* IPT 046 and medium-chain-length polyhydroxyalkanoate production from sugarcane carbohydrates. *Appl. Biochem. Biotechnol.* 119, 51–70. doi: 10.1385/abab:119:1:51

dos Santos, L. V., de Barros Grassi, M. C., Gallardo, J. C. M., Pirolla, R. A. S., Calderón, L. L., de Carvalho-Netto, O. V., et al. (2016). Second-generation ethanol: the need is becoming a reality. *Ind. Biotechnol.* 12, 40–57. doi: 10.1089/ind.2015.0017

Egli, T. (2015). Microbial growth and physiology: a call for better craftsmanship. *Front. Microbiol.* 6:287. doi: 10.3389/fmicb.2015.00287

Gomez, J. G. C., Fontolan, V., Alli, R. C., Rodrigues, M. F. A., Netto, C. L., Silva, L. F., et al. (1997). Production of P3HB-*co*-3HV by soil isolated bacteria able to use sucrose. *Rev. Microbiol.* 28, 43–48.

Gomez, J. G. C., Rodrigues, M. F. A., Alli, R. C. P., Torres, B. B., Netto, C. L. B., Oliveira, M. S., et al. (1996). Evaluation of soil gram-negative bacteria yielding polyhydroxyalkanoic acids from carbohydrates and propionic acid. *Appl. Microbiol. Biotechnol.* 45, 785–791. doi: 10.1007/s002530050763

Guamán, L. P., Oliveira-Filho, E. R., Barba-Ostria, C., Gomez, J. G. C., Taciro, M. K., and da Silva, L. F. (2018). *xylA* and *xylB* overexpression as a successful strategy for improving xylose utilization and poly-3-hydroxybutyrate production in *Burkholderia sacchari*. *J. Ind. Microbiol. Biotechnol.* 45, 165–173. doi: 10.1007/s10295-018-2007-7

Jiang, G., Hill, D. J., Kowalczuk, M., Johnston, B., Adamus, G., Irorere, V., et al. (2016). Carbon sources for polyhydroxyalkanoates and an integrated biorefinery. *Int. J. Mol. Sci.* 17:1157. doi: 10.3390/ijms17071157

Keshavarz, T., and Roy, I. (2010). Polyhydroxyalkanoates: bioplastics with a green agenda. *Curr. Opin. Microbiol.* 13, 321–326. doi: 10.1016/j.mib.2010.02.006

Kim, B. S., Lee, S. C., Lee, S. Y., Chang, H. N., Chang, Y. K., and Woo, S. I. (1994). Production of poly(3-hydroxybutyric acid) by fed-batch culture of *Alcaligenes eutrophus* with glucose concentration control. *Biotechnol. Bioeng.* 43, 892–898. doi: 10.1002/bit.260430908

Koller, M., Maršálek, L., de Sousa Dias, M. M., and Braunegg, G. (2017). Producing microbial polyhydroxyalkanoate (PHA) biopolyesters in a sustainable manner. *N. Biotechnol.* 37, 24–38. doi: 10.1016/j.nbt.2016.05.001

Kornberg, A., Rao, N. N., and Ault-Riché, D. (1999). Inorganic polyphosphate: a molecule of many functions. *Annu. Rev. Biochem.* 68, 89–125. doi: 10.1146/annurev.biochem.68.1.89

Lachke, A. (2002). Biofuel from D-xylose — The second most abundant sugar. *Reson.* 7, 50–58. doi: 10.1007/BF02836736

Lee, S. Y. (1996). Bacterial polyhydroxyalkanoates. *Biotechnol. Bioeng.* 49, 1–14. doi: 10.1002/(SICI)1097-0290(19960105)49:1<1::AID-BIT1>3.0.CO;2-P

Lee, S. Y., Wong, H. H., Choi, J., Lee, S. H., Lee, S. C., and Han, C. S. (2000). Production of medium-chain-length polyhydroxyalkanoates by high-cell-density cultivation of *Pseudomonas putida* under phosphorus limitation. *Biotechnol. Bioeng.* 68, 466–470. doi: 10.1002/(SICI)1097-0290(20000520)68:4<466::AID-BIT12>3.0.CO;2-T

Li, J., Wang, C., Yang, G., Sun, Z., Guo, H., Shao, K., et al. (2017). Molecular mechanism of environmental d-xylose perception by a XylFII-LytS complex in bacteria. *Proc. Natl. Acad. Sci. U.S.A.* 114, 8235–8240. doi: 10.1073/pnas.1620183114

Lillo, J. G., and Rodriguez-Valera, F. (1990). Effects of culture conditions on poly(beta-hydroxybutyric acid) production by *Haloferax mediterranei*. *Appl. Environ. Microbiol.* 56, 2517–2521.

Martínez-Aguilar, L., Díaz, R., Peña-Cabriales, J. J., Estrada-de Los Santos, P., Dunn, M. F., and Caballero-Mellado, J. (2008). Multichromosomal genome structure and confirmation of diazotrophy in novel plant-associated *Burkholderia* species. *Appl. Environ. Microbiol.* 74, 4574–4579. doi: 10.1128/AEM.00201-08

Medveczky, N., and Rosenberg, H. (1971). Phosphate transport in *Escherichia coli*. *Biochim. Biophys. Acta Biomembr.* 241, 494–506. doi: 10.1016/0005-2736(71)90048-4

Melanie, S., Winterburn, J. B., and Devianto, H. (2018). Production of biopolymer polyhydroxyalkanoates (PHA) by extreme halophilic marine archaea *Haloferax mediterranei* in medium with varying phosphorus concentration. *J.Eng.Technol.Sci.* 50, 255–271. doi: 10.5614/j.eng.technol.sci.2017.50.2.7

Mendonça, T. T., Gomez, J. G. C., Buffoni, E., Sánchez Rodriguez, R. J., Schripsema, J., Lopes, M. S. G., et al. (2014). Exploring the potential of *Burkholderia sacchari* to produce polyhydroxyalkanoates. *J. Appl. Microbiol.* 116, 815–829. doi: 10.1111/jam.12406

Mendonça, T. T., Tavares, R. R., Cespedes, L. G., Sánchez-Rodriguez, R. J., Schripsema, J., Taciro, M. K., et al. (2017). Combining molecular and bioprocess techniques to produce poly(3-hydroxybutyrate-*co*-3-hydroxyhexanoate) with controlled monomer composition by *Burkholderia sacchari*. *Int. J. Biol. Macromol.* 98, 654–663. doi: 10.1016/j.ijbiomac.2017.02.013

Miranda De Sousa Dias, M., Koller, M., Puppi, D., Morelli, A., Chiellini, F., and Braunegg, G. (2017). Fed-batch synthesis of poly(3-hydroxybutyrate) and poly(3-hydroxybutyrate-*co*-4-hydroxybutyrate) from sucrose and 4-hydroxybutyrate precursors by *Burkholderia sacchari* strain DSM 17165. *Bioengineering* 4:36. doi: 10.3390/bioengineering4020036

Munévar, N. F. V., de Almeida, L. G., and Spira, B. (2017). Differential regulation of polyphosphate genes in *Pseudomonas aeruginosa*. *Mol. Genet. Genomics* 292, 105–116. doi: 10.1007/s00438-016-1259-z

Nonato, R. V., Mantelatto, P. E., and Rossell, C. E. (2001). Integrated production of biodegradable plastic, sugar and ethanol. *Appl. Microbiol. Biotechnol.* 57, 1–5. doi: 10.1007/s002530100732

Overbeek, R., Olson, R., Pusch, G. D., Olsen, G. J., Davis, J. J., Disz, T., et al. (2014). The SEED and the Rapid Annotation of microbial genomes using Subsystems Technology (RAST). *Nucleic Acids Res.* 42, D206–D214. doi: 10.1093/nar/gkt1226

Paiva, J. E., de Maldonade, I. R., and Scamparini, A. R. P. (2009). Xylose production from sugarcane bagasse by surface response methodology. *Rev. Bras. Eng. Agríc. Ambient.* 13, 75–80. doi: 10.1590/S1415-43662009000100011

Perlack, R. D. (2005). *Biomass as Feedstock for a Bioenergy and Bioproducts Industry: The Technical Feasability of a Billion-Ton Annual Supply*. doi: 10.2172/885984

Pessoa, A., Jr., Mancilha, I. M., and Sato, S. (1997). Acid hydrolysis of hemicellulose from sugarcane bagasse. *Braz. J. Chem. Eng.* 14. doi: 10.1590/S0104-66321997000300014

Raposo, R. S., de Almeida, M. C., de Oliveira, M. D., da Fonseca, M. M., and Cesário, M. T. (2017). A *Burkholderia sacchari* cell factory: production of poly-3-hydroxybutyrate, xylitol and xylonic acid from xylose-rich sugar mixtures. *N. Biotechnol.* 34, 12–22. doi: 10.1016/j.nbt.2016.10.001

Rice, E. W., Baird, R. B., Eaton, A. D., and Clesceri, L. S. (eds.). (2012). *Standard Methods For The Examination Of Water And Wastewater*, *22nd Edn*. Denver, CO: American Water Works Association.

Riis, V., and Mai, W. (1988). Gas chromatographic determination of poly-β-hydroxybutyric acid in microbial biomass after hydrochloric acid propanolysis. *J. Chromatogr. A* 445, 285–289. doi: 10.1016/S0021-9673(01)84535-0

Rocha, R. C. S., da Silva, L. F., Taciro, M. K., and Pradella, J. G. C. (2008). Production of poly(3-hydroxybutyrate-*co*-3-hydroxyvalerate) P(3HB-*co*-3HV) with a broad range of 3HV content at high yields by *Burkholderia sacchari* IPT 189. *World J. Microbiol. Biotechnol.* 24, 427–431. doi: 10.1007/s11274-007-9480-x

Rodgers, M., and Wu, G. (2010). Production of polyhydroxybutyrate by activated sludge performing enhanced biological phosphorus removal. *Bioresour. Technol.* 101, 1049–1053. doi: 10.1016/j.biortech.2009.08.107

Ruiz-Lozano, J. M., and Bonfante, P. (1999). Identification of a putative P-transporter operon in the genome of a *Burkholderia* strain living inside the arbuscular mycorrhizal fungus Gigaspora margarita. *J. Bacteriol.* 181, 4106–4109.

Ryu, H. W., Hahn, S. K., Chang, Y. K., and Chang, H. N. (1997). Production of poly(3-hydroxybutyrate) by high cell density fed-batch culture of *Alcaligenes eutrophus* with phosphate limitation. *Biotechnol. Bioeng.* 55, 28–32. doi: 10.1002/(SICI)1097-0290(19970705)55:1<28::AID-BIT4>3.0.CO;2-Z

Santos-Beneit, F. (2015). The Pho regulon: a huge regulatory network in bacteria. *Front. Microbiol.* 6:402. doi: 10.3389/fmicb.2015.00402

Sawana, A., Adeolu, M., and Gupta, R. S. (2014). Molecular signatures and phylogenomic analysis of the genus *Burkholderia*: proposal for division of this genus into the emended genus *Burkholderia* containing pathogenic organisms and a new genus *Paraburkholderia* gen. nov. harboring environmental species. *Front. Genet.* 5:429. doi: 10.3389/fgene.2014.00429

Schlegel, H. G., Gottschalk, G., and Von Bartha, R. (1961). Formation and utilization of poly-β-hydroxybutyric acid by Knallgas bacteria (*Hydrogenomonas*). *Nature* 191, 463–465. doi: 10.1038/191463a0

Silva, L. F., Gomez, J. G. C., Taciro, M. K., Ramos, M. E. M., Carter, J. M., and Pradella, J. G. C. (2002). *Brazilian Patent PI 0207356-0 B1 Processo de Produção de PHB e seu Copolímero PHB-co-HV a Partir de Hidrolisados de Bagaço de Cana-de-Açúcar*. Rio de Janeiro: INPI-Brasil.

Silva, L. F., Taciro, M. K., Michelin Ramos, M. E., Carter, J. M., Pradella, J. G. C., and Gomez, J. G. C. (2004). Poly-3-hydroxybutyrate (P3HB) production by bacteria from xylose, glucose and sugarcane bagasse hydrolysate. *J. Ind. Microbiol. Biotechnol.* 31, 245–254. doi: 10.1007/s10295-004-0136-7

Silva, L. F., Taciro, M. K., Raicher, G., Piccoli, R. A. M., Mendonça, T. T., Lopes, M. S. G., et al. (2014). Perspectives on the production of polyhydroxyalkanoates in biorefineries associated with the production of sugar and ethanol. *Int. J. Biol. Macromol.* 71, 2–7. doi: 10.1016/j.ijbiomac.2014.06.065

Solovyev, V., and Salamov, A. (2011). "Automatic annotation of microbial genomes and metagenomic sequences," in *Metagenomics and its Applications in Agriculture, Biomedicine and Environmental Studies*, ed R. W. Li (Hauppauge, NY: Nova Science Publishers, Inc.), 61–78. Available online at: https://www.researchgate.net/publication/259450599_V_Solovyev_A_Salamov_2011_Automatic_Annotation_of_Microbial_Genomes_and_Metagenomic_Sequences_In_Metagenomics_and_its_Applications_in_Agriculture_Biomedicine_and_Environmental_Studies_Ed_RW_Li_Nova_Sc (accessed March 21, 2018).

Taciro, M. K. (2008). *Processo Contínuo de Produção de Polihidroxialcanoatos de Cadeia Média (PHAmcl) Sob Limitaçao Múltipla de Nutrientes* (Doctoral thesis), Universidade de São Paulo, São Paulo, Brazil.

Tu, W., Zhang, D., and Wang, H. (2019). Polyhydroxyalkanoates (PHA) production from fermented thermal-hydrolyzed sludge by mixed microbial cultures: the link between phosphorus and PHA yields. *Waste Manage.* 96, 149–157. doi: 10.1016/j.wasman.2019.07.021

Tumlirsch, T., Sznajder, A., and Jendrossek, D. (2015). Formation of polyphosphate by polyphosphate kinases and its relationship to poly(3-hydroxybutyrate) accumulation in *Ralstonia eutropha* strain H16. *Appl. Environ. Microbiol.* 81, 8277–8293. doi: 10.1128/AEM.02279-15

Wang, J., Shen, X., Lin, Y., Chen, Z., Yang, Y., Yuan, Q., et al. (2018). Investigation of the synergetic effect of xylose metabolic pathways on the production of glutaric acid. *ACS Synth. Biol.* 7, 24–29. doi: 10.1021/acssynbio.7b00271

Webb, D. C., Rosenberg, H., and Cox, G. B. (1992). Mutational analysis of the *Escherichia coli* phosphate-specific transport system, a member of the traffic ATPase (or ABC) family of membrane transporters. A role for proline residues in transmembrane helices. *J. Biol. Chem.* 267, 24661–24668.

Wen, Q., Chen, Z., Tian, T., and Chen, W. (2010). Effects of phosphorus and nitrogen limitation on PHA production in activated sludge. *J. Environ. Sci.* 22, 1602–1607. doi: 10.1016/s1001-0742(09)60295-3

Willsky, G. R., and Malamy, M. H. (1976). Control of the synthesis of alkaline phosphatase and the phosphate-binding protein in *Escherichia coli*. *J. Bacteriol.* 127, 595–609.

Zago, A., Chugani, S., and Chakrabarty, A. M. (1999). Cloning and characterization of polyphosphate kinase and exopolyphosphatase genes from *Pseudomonas aeruginosa* 8830. *Appl. Environ. Microbiol.* 65, 2065–2071.

Zhang, H., Ishige, K., and Kornberg, A. (2002). A polyphosphate kinase (PPK2) widely conserved in bacteria. *Proc. Natl. Acad. Sci. U.S.A.* 99, 16678–16683. doi: 10.1073/pnas.262655199

Zhang, J., Shishatskaya, E. I., Volova, T. G., da Silva, L. F., and Chen, G.-Q. (2018). Polyhydroxyalkanoates (PHA) for therapeutic applications. *Mater. Sci. Eng. C Mater. Biol. Appl.* 86, 144–150. doi: 10.1016/j.msec.2017.12.035

Conflict of Interest: The authors declare that the research was conducted in the absence of any commercial or financial relationships that could be construed as a potential conflict of interest.

frontiers in Bioengineering and Biotechnology

ORIGINAL RESEARCH
published: 17 January 2020
doi: 10.3389/fbioe.2019.00475

Identification of Regulatory Genes and Metabolic Processes Important for Alginate Biosynthesis in *Azotobacter vinelandii* by Screening of a Transposon Insertion Mutant Library

Mali Mærk[1†], Øyvind M. Jakobsen[2†], Håvard Sletta[2], Geir Klinkenberg[2], Anne Tøndervik[2], Trond E. Ellingsen[2], Svein Valla[1‡] and Helga Ertesvåg[1]*

[1] Department of Biotechnology and Food Science, Norwegian University of Science and Technology, Trondheim, Norway, [2] SINTEF Industry, Trondheim, Norway

Azotobacter vinelandii produces the biopolymer alginate, which has a wide range of industrial and pharmaceutical applications. A random transposon insertion mutant library was constructed from *A. vinelandii* ATCC12518Tc in order to identify genes and pathways affecting alginate biosynthesis, and about 4,000 mutant strains were screened for altered alginate production. One mutant, containing a *mucA* disruption, displayed an elevated alginate production level, and several mutants with decreased or abolished alginate production were identified. The regulatory proteins AlgW and AmrZ seem to be required for alginate production in *A. vinelandii*, similarly to *Pseudomonas aeruginosa*. An *algB* mutation did however not affect alginate yield in *A. vinelandii* although its *P. aeruginosa* homolog is needed for full alginate production. Inactivation of the fructose phosphoenolpyruvate phosphotransferase system protein FruA resulted in a mutant that did not produce alginate when cultivated in media containing various carbon sources, indicating that this system could have a role in regulation of alginate biosynthesis. Furthermore, impaired or abolished alginate production was observed for strains with disruptions of genes involved in peptidoglycan biosynthesis/recycling and biosynthesis of purines, isoprenoids, TCA cycle intermediates, and various vitamins, suggesting that sufficient access to some of these compounds is important for alginate production. This hypothesis was verified by showing that addition of thiamine, succinate or a mixture of lysine, methionine and diaminopimelate increases alginate yield in the non-mutagenized strain. These results might be used in development of optimized alginate production media or in genetic engineering of *A. vinelandii* strains for alginate bioproduction.

Keywords: alginate, *Azotobacter vinelandii*, *amrZ*, *fruA*, *algB*, medium supplements

OPEN ACCESS

Edited by:
Bruce Ramsay,
Queen's University, Canada

Reviewed by:
Alvaro Diaz,
Pontificia Universidad Católica de Valparaíso, Chile
Mlguel Castañeda,
Meritorious Autonomous University of Puebla, Mexico

****Correspondence:***
Helga Ertesvåg
helga.ertesvag@ntnu.no

†Present address:
Mali Mærk,
PHARMAQ AS, Overhalla, Norway
Øyvind M. Jakobsen,
NTNU Social Research, Trondheim, Norway

‡Deceased

Specialty section:
This article was submitted to Industrial Biotechnology, a section of the journal Frontiers in Bioengineering and Biotechnology

Received: *07 October 2019*
Accepted: *23 December 2019*
Published: *17 January 2020*

Citation:
Mærk M, Jakobsen ØM, Sletta H, Klinkenberg G, Tøndervik A, Ellingsen TE, Valla S and Ertesvåg H (2020) Identification of Regulatory Genes and Metabolic Processes Important for Alginate Biosynthesis in Azotobacter vinelandii by Screening of a Transposon Insertion Mutant Library. Front. Bioeng. Biotechnol. 7:475. doi: 10.3389/fbioe.2019.00475

INTRODUCTION

Alginate is the collective term for a family of linear polysaccharides consisting of varying amounts of β-D-mannuronic acid (M) and α-L-guluronic acid (G) (Haug et al., 1966). In nature alginates are produced by brown seaweeds and by several bacteria in the genera *Pseudomonas* and *Azotobacter*, among them the soil bacterium *A. vinelandii* (Gorin and Spencer, 1966). Bacterial alginate is produced as an exopolysaccharide, and the biosynthetic apparatus is similar in both genera (Ertesvåg, 2015). However, *A. vinelandii* produces alginate constitutively, while biosynthesis is activated only under certain environmental conditions in *Pseudomonas* spp.

Alginates are commercially important biopolymers with a wide range of industrial and technological applications (Skjåk-Bræk et al., 2015). All commercial alginate production is currently based on extraction from brown algae, which yields complex mixtures of alginates with regard to both chain composition and molecular weight (Andersen et al., 2012). The bulk alginates used in for example food and cosmetic industry can be acquired at prices as low as 5 USD per kilogram, while pharmaceutical or medical grade alginates with defined molecular weights and M/G profiles, and thus more defined material properties, cost about 100 USD per gram (NovaMatrix web catalog prices, September 2019). New pharmaceutical and medical applications are being developed, and this increases the demand for high-end alginates. Because engineered bacteria have the potential for *in vivo* production of homogeneous alginates with specialized compositions (Remminghorst and Rehm, 2006), there is considerable interest in microbial bioproduction of these polymers. Furthermore, as most current applications rely on the gelling properties of G-blocks (stretches of consecutive G residues) (Andersen et al., 2012), *A. vinelandii* is an attractive candidate for strain engineering due to its innate ability to introduce G-blocks in the alginate chains (Ertesvåg et al., 1995; Svanem et al., 1999). No strains producing G-block alginates have been identified among the *Pseudomonas* species studied so far.

In order to optimize bacterial production processes, it is important to understand how alginate biosynthesis is regulated as well as elucidate which other metabolic aspects have an influence on production levels. The precursor for the alginate monomers is fructose 6-phosphate, so alginate biosynthesis is closely connected to the central carbohydrate metabolism of the cells (Maleki et al., 2015, 2017; Ertesvåg et al., 2017). Alginate production is furthermore an energy demanding process and is tightly controlled by a complex network of regulators which also influence other cellular processes (Urtuvia et al., 2017). The state of several cellular processes can therefore be expected to affect the biosynthesis of alginate. So far, the regulatory network controlling alginate biosynthesis has mainly been studied in *P. aeruginosa*. Regulatory differences between *P. aeruginosa* and *A. vinelandii* have already been observed (Núñez et al., 1999; López-Pliego et al., 2018), demonstrating a need for further investigations of these mechanisms in the latter organism. In addition, previous investigations of *A. vinelandii* have mainly been directed toward gene disruptions or environmental factors leading to an increase in alginate biosynthesis (Núñez et al., 2013; Ahumada-Manuel et al., 2017; Quiroz-Rocha et al., 2017). Identification of genes and processes which influence alginate biosynthesis negatively is however equally important in order to achieve a better understanding of limiting factors, which is a central issue when industrial production purposes are considered.

The aim of this study was to investigate factors affecting alginate biosynthesis in *A. vinelandii* by screening of a transposon insertion library of strain ATCC12518Tc, a tetracycline-resistant derivative of ATCC12518. The genome of *A. vinelandii* DJ, also a derivative of ATCC12518, has been sequenced (Setubal et al., 2009), thus greatly simplifying identification of the affected genes in transposon insertion mutants with interesting phenotypes. We have previously screened a *Pseudomonas fluorescens* transposon library (Ertesvåg et al., 2017), and an additional aim of the current study was to compare the results from the two bacteria in order to detect similarities and differences between the two genera.

MATERIALS AND METHODS

General Cultivation of Bacteria

The bacterial strains and plasmids used in this work are described in **Table 1**. *Escherichia coli* strains were routinely grown in LB broth (10 g/l tryptone, 5 g/l yeast extract, 5 g/l NaCl) or on LB agar at 37°C. *A. vinelandii* strains were routinely grown in liquid Burk's medium (BM) or RA1 medium (Gimmestad et al., 2006) supplemented with 3.0 ml/l TMS1 (Wentzel et al., 2012) or on BM or RA1 agar at 30°C. The media contained 20 g/l of the relevant carbon source unless stated otherwise. Biotin (1.6 μM), lysine (0.5 mM), methionine (0.6 mM), diaminopimelate (0.2 mM), adenine (0.8 mM), thiamine (2 μM), pyridoxine (5 μM), pyridoxal (5 μM), or succinate (30 mM) were added in some experiments. Antibiotics were present in the following concentrations when used in cultivations: ampicillin 200 μg/ml, tetracycline 15 μg/ml, spectinomycin 20 μg/ml, apramycin 25 μg/ml (*A. vinelandii*) or 50 μg/ml (*E. coli*), kanamycin 2 μg/ml (*A. vinelandii*) or 50 μg/ml (*E. coli*).

Standard Procedures

Plasmid isolations, enzymatic DNA manipulations and agarose gel electrophoresis were performed according to Sambrook and Russell (2001). Transformation and conjugation was performed as described earlier (Gimmestad et al., 2009). Pwo SuperYield DNA Polymerase (Roche Diagnostics) or Q5 polymerase (New England Laboratories) was used to amplify DNA from *A. vinelandii*. The QIAquick Gel Extraction Kit and QIAquick PCR Purification Kit (QIAGEN) were used for DNA purifications from gel electrophoresis and enzymatic reactions, respectively. Chromosomal DNA was isolated from *A. vinelandii* strains using the PurElute™ Bacterial Genomic Kit (EdgeBio). Cells were washed with 0.9% NaCl, 10 mM EDTA (pH 8.0) prior to DNA isolation in order to remove extracellular alginate. DNA sequencing was performed using the BigDye® Terminator v1.1 Cycle Sequencing Kit (Applied Biosystems). Transposon insertion sites were identified using primers that are complementary to the ends of the inserted fragment, and genomic DNA isolated from each mutant as the template, thus

TABLE 1 | Bacterial strains and plasmids used in this work.

Strain or plasmid	Description	References
STRAINS		
Escherichia coli		
S17.1	RP4 2-Tc::Mu-Km::*Tn7pro, res, mod*	Simon et al., 1983
S17.1 (λpir)	λ*pir* (for replication of oriR6K-plasmids) *recA, thi pro hsdR-M*$^+$ RP4 2-Tc::Mu-Km::*Tn7*Tp^r Sm^r	de Lorenzo et al., 1993
Azotobacter vinelandii		
ATCC12518	Alginate producing wild type strain.	ATCC
ATCC12518Tc	Derivative of ATCC12518 where the *tetAR* genes from pLit28Tc are inserted in one of the four homologous transposase genes *Avin09530*, *Avin31560*, *Avin36480,* and *Avin49630*. (Exact location not determined because these homologs differ in only 1 bp.) Tc^r	This work
PLASMIDS		
pCAM140	Delivery vector of mini-Tn5. Ap^r, Sp^r	Wilson et al., 1995
pLit28Tc	ColE1. Tc^r, Ap^r	Bakkevig et al., 2005
pKD21	Tn5-based mini-transposon vector encoding luciferase controlled by a mutant Pm-promoter. Km^r.	Bakkevig et al., 2005
pIB11	RK2 based expression vector using the inducible *Pm*-XylS promoter system. Km^r.	Bakke et al., 2009
pHE206	Derivative of pLit28Tc containing a 1.0 kb KpnI-HindIII restricted PCR fragment encoding the 3′ end of the putative transposase gene *Avin31560* downstream of *tetR*. Tc^r, Ap^r	This work
pHE208	Derivative of pHE206 containing a 1.5 kb SpeI-XhoI restricted PCR fragment encoding the 5′ end of *Avin31560* and the upstream *ispB*-like gene upstream of *tetA*, resulting in a gene replacement vector containing *Avin31560* disrupted by insertion of the *tetA-tetR* genes. Tc^r, Ap^r	This work
pMH13	Derivative of pKD21 containing wild type Pm-promoter. *neo* replaced by apramycin resistance gene. Am^r	This work
pHE319	Derivative of pMH13 in which the luciferase gene was replaced by a 1.9 kb PCR-fragment encoding *dxs-1*. Am^r	This work
pHE536	Derivative of pIB11 where a 1.2 kb PCR fragment encoding *algW* replaced *bla*. Km^r.	This work
pHE537	Derivative of pIB11 where a 0.4 kb PCR fragment encoding *amrZ* replaced *bla*. Km^r.	This work
pHE542	Derivative of pIB11 where a 2.0 kb PCR fragment encoding *fruA* replaced *bla*. Km^r.	This work

allowing direct sequencing of the genomic regions flanking the insertion. Primer sequences for PCR and sequencing are available upon request.

Construction of a Transposon Insertion Mutant Library

The mini-Tn5 transposon delivery vector pCAM140 which encodes a spectinomycin resistance gene flanked by transcriptional terminators to avoid read-through from the transposon (Wilson et al., 1995) was introduced to *A. vinelandii* ATCC12518Tc by conjugation. Mating was performed at 30°C on LB agar and transconjugants were selected on RA1 agar containing tetracycline and spectinomycin. Selection plates also contained alginate lyase AlgL (6.5 mU/cm^2) (Ertesvåg et al., 1998); the enzyme was applied to the plates before spreading the cells in order to reduce the colony mucoidicity of alginate-producing transconjugants. Transconjugant colonies were picked using a Genetix Q-Pix2 robotic colony picker and transferred to 96-well microtiter plates containing 110 µl liquid 0.5x RA1 medium ($CaCl_2 \cdot 2H_2O$ and MOPS concentrations as for 1x medium, and 10 g/l fructose) with tetracycline and spectinomycin. *A. vinelandii* insertion mutants are known to sometimes contain copies of both mutant and wild-type alleles, so to eliminate wild-type chromosome copies the transconjugants were grown by repeated transfers in selective media. All liquid and microtiter plate handling were performed by a Beckman Coulter Core robotic equipped with a Beckma Coulter NXP liquid handling unit.

Alginate Analyses

Culture samples (diluted in 0.2 M NaCl when necessary to reduce viscosity) were centrifuged to remove bacterial cells, and the alginates in the cell-free supernatants were deacetylated by mild alkaline treatment as described previously (Ertesvåg and Skjåk-Bræk, 1999). The alginate content in the deacetylated samples was determined enzymatically as described earlier (Østgaard, 1992; Maleki et al., 2015). Samples for alginate quantification were collected from transconjugants cultivated in 96-well microtiter plates with 110 µl selective 0.5x RA1 medium in each well. Mutants displaying a potential increase or decrease in alginate production were verified by assessing alginate production in triplicate cultures in 96-deepwell plates with 600 µl selective 0.2x RA1 medium in each well, or in 250 ml shake flask with 30 ml 0.5x RA1 medium. In all experiments, *A. vinelandii* ATCC12518Tc was included as a reference. The reference strain displayed similar alginate production and growth characteristics in deepwell plates and in shake flasks. The final alginate production and cell densities reported in this study are based on measurements of extracellular alginate concentration (described above) and OD_{660} respectively, sampled in stationary phase.

For qualitative analyses of complemented strains, 1 ml culture was centrifuged, NaCl was added to the supernatant (0.1 M) and the alginate was precipitated with an equal amount of isopropanol. Only alginate-producing strains produce a pellet in this assay. The mutant strain, or mutant strain with an empty vector (pIB11), was always used as a control.

Fermentations

Fermentations of *A. vinelandii* strains were performed as described by Steigedal et al. (2008) except that the inoculum was cultivated in two steps in 0.5x RA1 medium in shake flasks.

The first culture was cultivated until visible growth, followed by inoculating 3% into fresh medium for the second stage inoculum, which was then cultivated over night before being transferred, 3%, to 3 l Applikon fermentors with 1 l of 0.5x PM1 containing the following ingredients per liter: fructose (50 g), peptone (4.75 g), $MgSO_4 \cdot 7H_2O$ (0.3 g), KH_2PO_4 (65 mg), K_2HPO_4 (16 mg), NaCl (0.2 g), $CaCl_2 \cdot 2H_2O$ (0.29 g), $FeSO_4 \cdot 7H_2O$ (20 mg), and Clerol FBA622 (antifoam, 0.5 g). The fermentations were performed at 30°C. pH was adjusted to 7.2 from start and controlled at this pH by addition of NaOH. The dissolved oxygen was controlled to 10% of saturation by automatic control of the stirrer speed. Aeration rate in the culture medium in fermentors was initially 0.25 vvm (l_{gas}/l_{liquid} per minute) and was increased up to 1.0 vvm when required for maintaining dissolved oxygen without exceeding the maximum stirrer speed of the fermentor (2,000 rpm).

RESULTS

Construction and Screening of the Transposon Insertion Mutant Library

In order to obtain an unbiased transposon insertion library allowing for auxotrophic mutants, the strains have to be maintained on a rich medium. This required insertion of a resistance marker into the *A. vinelandii* ATCC12518 strain, to allow for counter selection of *E. coli* after conjugation. Using the gene replacement vector pHE208, we therefore constructed a tetracycline resistant derivative of ATCC12518, designated ATCC12518Tc, in which a putative transposase gene is disrupted by insertion of the *tetA-tetR* genes (**Table 1**). Strain ATCC12518Tc produced 8.3 (±0.9) g/l alginate in batch fermentations, which is about 70% of that observed for the wild type. The reason for this reduction is not known. The production level is however still sufficient to allow for identification of mutants with lowered alginate production, and the decrease could potentially be beneficial for identification of mutants with increased production. A transposon insertion library of ∼4,000 transconjugants was made from *A. vinelandii* ATCC12518Tc as described in the Materials and Methods section.

The mutant strains from the library were cultivated in 96-well microtiter plates and screened with regard to alginate production levels compared to the reference strain ATCC12518Tc (see Materials and Methods section). Mutants that failed to grow (∼1,000 mutants) were disregarded. Among the viable mutants, the screen identified 56 mutants with potentially increased alginate production (>125% alginate concentration relative to the reference strain) and 241 mutants with potentially lowered alginate production (<50% relative to the reference).

Verification of Mutants With Altered Alginate Production Levels

Selected mutants with potentially altered alginate production were recultivated in triplicates in deepwell plates and/or shake flasks (see Materials and Methods section) for verification of the initial screening results. A total of 17 mutants with potentially increased alginate production and 109 mutants with potentially lowered alginate production were chosen for verification experiments. Using the same criteria as above, an increase or decrease in alginate production relative to the reference strain was affirmed for 2 and 68 of these candidates, respectively. The verified mutants showing increased or decreased alginate production are hereafter referred to as up-mutants and down-mutants, respectively, and their alginate production and growth levels relative to the reference strain is given in **Table 2**. Several of the mutant strains were observed to aggregate in liquid culture. Thus, growth measured as OD_{660} could not always be considered a reliable measure and is therefore not discussed in more detail. It should however be noted that for one of the up-mutants, with a transposon insertion in *pgm-2*, the apparent increase in alginate yield is most likely caused by an increased cell density in the cultures (**Table 2**).

Validation of the Verification Process by Batch Fermentation Trials

To further confirm the alginate phenotypes observed in the verification experiments, fermentations were performed for 12 of the down-mutants and one up-mutant (36C11) in order to obtain growth and alginate production data under highly controllable conditions. Very low or no alginate production (<10% relative to the reference strain) was confirmed for 10 of the down-mutants (27H10, 33A03, 20A04, 22B07, 08E05, 20A06, 36F10, 22G07, 39H08, and 21C03), while the remaining two were shown to produce 67% (03E03) and 35% alginate (45G12) compared to the reference strain. Batch fermentation of the up-mutant 36C11 confirmed a significant increase in alginate production; 180% relative to ATCC12518Tc. The general agreement between the fermentation results and the alginate production levels observed in deepwell plates indicate that verification experiments with triplicate deepwell plate cultivations can be regarded as a reliable method for evaluating large numbers of *A. vinelandii* strains with regard to alginate production.

Identification of Disrupted Genes in Mutants With Altered Alginate Production

The transposon insertion points were identified in the genomes of the verified up- and down-mutants (**Table 2**) by determining the chromosomal DNA sequences flanking the transposons and performing BLAST (Altschul et al., 1997) searches against the *A. vinelandii* DJ genome (Setubal et al., 2009). The affected genes include genes involved in metabolism, transport, translation and gene regulation (**Table 2**). For 11 of the mutants in **Table 2**, the affected genes were annotated as hypothetical. Ten of the mutants have insertions in structural genes directly involved in alginate biosynthesis (*algD*, *algK*, *algJ*, *algI*, and *algA*) (Rehm et al., 1996), and show the expected *alg*$^-$ phenotype. For further investigations of selected mutants, we chose to focus on some of the genes with known or putative regulatory functions. Moreover, in an earlier study on the alginate-producing mutant of *P. fluorescens*, it was reported that inactivation of many genes in the central metabolism resulted in lower alginate production. We therefore wanted to investigate whether this appeared to be the case for *A. vinelandii* as well.

TABLE 2 | *A. vinelandii* transposon insertion mutants displaying altered alginate production levels.

Metabolic category	Strain	GeneID for inactivated gene	Gene name	Gene product	Relative growth	Relative alginate production
Reference strain	ATCC12518Tc				1.0	1.0
Mutants with lowered alginate production (deepwell plate cultivations)						
Aromatic compounds	33F08	Avin08040		Aromatic acid decarboxylase	0.7	0.1
Biosynthesis of cofactors	27H10	Avin05990	*bioF*	8-amino-7-oxononanoate synthase	0.8	0.1
	33A03	Avin07870	*dxs-1*	1-deoxy-D-xylulose 5-phosphate synthase	0.6	0.0
Cell envelope	03E03	Avin05370		Lipopolysaccharide biosynthesis protein	0.6	0.1
	03G10	Avin15980		Glycosyl transferase	0.7	0.4
	30F06	Avin26720		OmpA/MotB domain protein	0.7	0.0
Cellular processes	14B06	Avin45390	*hslU*	Heat shock protein	0.7	0.3
	20A04	Avin12950	*algW*	Htr-like protease	0.7	0.0
	22B07	Avin27920	*flhB*	Flagellar biosynthetic protein	0.7	0.1
	25H12	Avin35740		Conjugation protein	0.9	0.3
	37D04	Avin41270		Peptidase M48	0.7	0.0
Central intermediary metabolism	13E05	Avin31330		Alkanesulfonate monooxygenase	0.7	0.3
	29D11	Avin18740		Acetyl CoA hydrolase/transferase	0.6	0.1
	31H08	Avin25610		TauD/TfdA dioxygenase family protein	0.7	0.0
	26B04	Avin08860 and/or Avin08880		Phenol hydroxylase subunit (DmpK) and/or sigma54-dependent activator protein	0.7	0.2
DNA metabolism	15B03	Avin20500		Phage integrase	1.0	0.1
	27D11	Avin52330		Type III restriction enzyme Res subunit	0.7	0.2
Energy metabolism	08B10	Avin21890		Monooxygenase	0.9	0.3
	08E05	Avin12210	*fruA*	Fructose PTS IIBC	0.6	0.0
	20A06	Avin29770	*sucA*	2-oxoglutarate dehydrogenase E1 component	0.8	0.0
	22H06	Avin28560	*nuoN*	Proton-translocating NADH-quinone oxidoreductase	0.6	0.1
	36F10	Avin26020	*gcvP2*	Glycine dehydrogenase	0.4	0.2
Extracellular polysaccharides	10B06	Avin10970	*algD*	GDP-mannose 6-dehydrogenase	0.7	0.1
	12B08	Avin10970	*algD*	GDP-mannose 6-dehydrogenase	0.5	0.1
	25G08	Avin10970	*algD*	GDP-mannose 6-dehydrogenase	0.8	0.1
	43G02	Avin10970	*algD*	GDP-mannose 6-dehydrogenase	0.8	0.1
	10E01	Avin10860	*algA*	Mannose 1-phosphate guanylyltransferase/mannose 6-phosphate isomerase	0.8	0.2
	12G04	Avin10940	*algK*	Alginate biosynthesis protein	0.6	0.0
	19H12	Avin10930	*algJ*	Alginate biosynthesis protein	0.7	0.1
	29H08	Avin10930	*algJ*	Alginate biosynthesis protein	0.7	0.1
	21F06	Avin10890	*algI*	Alginate O-acetyl transferase	0.9	0.1
	35G10	Avin10890	*algI*	Alginate O-acetyl transferase	0.7	0.1
Hypothetical	13F07	Avin31830		Hypothetical protein	0.8	0.3
	15E07	Avin09340		Hypothetical protein	0.5	0.1
	15H03	Avin41170		Hypothetical protein	0.9	0.1
	24A04	Avin36260		Hypothetical protein	0.6	0.1
	24F09	Avin28850		Hypothetical protein	0.6	0.1
	26C02	Avin11200		Membrane protein	0.7	0.2
	26D10	Avin39360		Hypothetical protein	0.7	0.1
	31G08	Avin33410		Hypothetical protein	0.8	0.1
	32E09	Avin34870		Hypothetical protein	0.9	0.1
	36A03	Avin16680/−20990		Hypothetical protein	1.0	0.1
	39D11	Avin43510		Hypothetical protein	0.7	0.1
Lipids	07B03	Avin29550	*arsB*	Type III PKS	0.6	0.0
	10E09	Avin13550		Enoyl-CoA hydratase/isomerase	0.9	0.1

(Continued)

TABLE 2 | Continued

Metabolic category	Strain	GeneID for inactivated gene	Gene name	Gene product	Relative growth	Relative alginate production
Other	16H06	Avin21160		Enterobactin domain protein	0.7	0.1
	29F10	Avin05960		Aminoglycoside phosphotransferase	0.8	0.3
	31H01	Avin32770		Metallophosphoesterase	0.6	0.2
	32B04	Avin25650		NRPS: amino acid adenylation	0.5	0.1
Purines and pyrimidines	22G07	Avin39660	*purL*	Phosphoribosylformyl-glycinamidine synthase	0.8	0.0
	32A11	Avin02510		Thymidylate kinase	0.7	0.1
Regulatory functions	09D06	Avin34410	*amrZ*	Alginate and motility regulator Z DNA binding protein	0.8	0.0
	22F02	Avin34410	*amrZ*	Alginate and motility regulator Z DNA binding protein	0.8	0.0
	39H08	Avin34410	*amrZ*	Alginate and motility regulator Z DNA binding protein	0.7	0.2
	21A12	Avin18010	*dctB*	C4-dicarboxylate transport sensory histidine protein kinase	0.6	0.1
	21C03	Avin13880		Transcriptional regulatory protein	1.0	0.1
	31F07	Avin10390		LysR family regulatory protein	0.8	0.1
	39C09	Avin38020		Transcriptional regulator	0.7	0.1
	42G12	Avin32720		Response regulator	0.9	0.4
	49G12	Avin18640		Sensory histidine protein kinase	0.7	0.1
Translation	43C11	Avin23730		Modification methylase	0.7	0.1
Transport and binding proteins	01A04	Avin14160		ABC transporter component	0.6	0.1
	10D12	Avin12330		TonB-dependent siderophore receptor	0.6	0.1
	27D02	Avin40960		ABC transporter component	0.5	0.0
	28A08	Avin14340		Acriflavin resistance protein	0.9	0.1
	28D07	Avin47130		TonB-dependent receptor	0.7	0.2
	38D10	Avin19760		Phosphonate ABC transporter	0.5	0.1
Transposon	40A06	Avin09580/-10840/-15010/-23940/-33330/-36160/-49850		Transposase	0.6	0.1
Mutants with increased alginate production (shake flask cultivations)						
Energy metabolism	39G08	Avin27440	*pgm-2*	2,3-bisphosphoglycerate-independent phosphoglycerate mutase	1.4	1.3
Transcription	36C11	Avin13700	*mucA*	Sigma factor AlgU negative regulatory protein	0.7	1.7

Alginate production and cell growth (OD_{660}) as observed in deepwell plate or shake flask cultivations, given as fractions normalized relative to that of the reference strain ATCC12518Tc. (Defined as 1.0 for the reference strain, which had an average growth of OD660 and an average alginate production of 7 g/l). The results shown are average values based on triplicate cultivations. The inactivated gene, identified by insertion point sequencing, is given for each mutant. Sequencing also showed that none of the mutants with insertions in the same gene have the same insertion point, and thus result from independent insertion events. Known or putative gene names, gene products and metabolic categories were retrieved from the A. vinelandii DJ genome database (Setubal et al., 2009). See text for discussion of specific mutants.

Transposon Insertions in Regulatory Genes Presumed to Be Involved in Alginate Biosynthesis

The regulation of alginate biosynthesis has mostly been studied in *P. aeruginosa* (reviewed in Hay et al., 2014; Urtuvia et al., 2017). The phenotypes of *A. vinelandii* mutants found to have insertions in such genes are therefore discussed taking *P. aeruginosa* strains with disruptions in homologous genes into consideration. One mutant was found to have the transposon inserted in the known *A. vinelandii* alginate regulatory gene *mucA*, and five mutants had insertions in homologs of alginate regulatory genes known from *P. aeruginosa*: *algW, amrZ* (three independent mutants), and *algB*. These mutants are described below. The gene context of the genes discussed below are shown in **Supplementary Figure S1**. In addition, several other genes putatively involved in transcription regulation were identified in the screen (**Table 2**), but since their targets are unknown, they were not studied further.

MucA is an anti-sigma factor that represses sigma factor AlgU, which is needed for expression of alginate biosynthetic gene *algD* (and possibly other alginate biosynthetic genes). *A. vinelandii mucA* mutants have previously been shown to display increased alginate production (Martínez-Salazar et al., 1996; Núñez et al., 2000). As could be expected, this is also the case for the *mucA*::TnCAM140 mutant identified in this work.

The protease AlgW has been shown to be required for activation of alginate biosynthesis in *P. aeruginosa*, by degrading MucA in a MucE-dependent manner (Wood et al., 2006; Qiu et al., 2007; Cezairliyan and Sauer, 2009). The *algW*::TnCAM140 mutant identified in this work does not produce alginate, which indicates that the *A. vinelandii* AlgW homolog has a function similar to the *P. aeruginosa* protease even though there is no *mucE* homolog in *A. vinelandii* (Setubal et al., 2009). However, when complemented with *algW* encoded on plasmid pHE536, the alginate production was not restored.

An *algB*::TnCAM140 mutant was identified among the mutants with lowered alginate production in the initial screen, but further evaluations showed that the production level of this mutant is actually comparable to that of the reference strain. The two-component response regulator AlgB is required for alginate production in *P. aeruginosa* (Goldberg and Ohman, 1987; Goldberg and Dahnke, 1992; Wozniak and Ohman, 1994) where it positively regulates expression of biosynthetic genes by direct binding to P*algD* (Leech et al., 2008). Our results thus indicate that the role of the AlgB homolog in *A. vinelandii* differs from that of *P. aeruginosa* AlgB. PCR on chromosomal DNA from the transposon mutant confirmed the absence of wild type copies of the *algB* gene. Thus, it appears that AlgB is not required for alginate production in *A. vinelandii*.

AmrZ (AlgZ) is a DNA binding protein required for transcription from P*algD* in *P. aeruginosa* (Baynham et al., 1999), and has also been shown to negatively regulate motility in both *P. aeruginosa* and *P. fluorescens* via FleQ (Baynham et al., 2006; Tart et al., 2006; Martínez-Granero et al., 2012). Expression of *P. aeruginosa amrZ* is controlled by the sigma factor AlgU (AlgT) (Wozniak et al., 2003). AlgU negatively regulates motility in *A. vinelandii* as well, but via CydR and FlhDC instead of AmrZ and FleQ (León and Espín, 2008). An *amrZ* mutant has not previously been described in *Azotobacter*. The alginate production in our *amrZ*::TnCAM140 mutant was restored by complementation using plasmid pHE537, which encodes *amrZ*. This confirms that AmrZ is necessary for alginate production in *A. vinelandii*, like it is in *P. aeruginosa*.

A *fruA* Transposon Insertion Abolishes Alginate Production in *A. vinelandii*

Alginate production was absent in a mutant with the transposon insertion in an *E. coli fruA* homolog. Complementation with plasmid pHE542 encoding *fruA* restored the strain's ability to produce alginate (data not shown), demonstrating that the observed phenotype was indeed caused by the *fruA* disruption. As FruA is a part of the fructose phosphoenolpyruvate phosphotransferase system (PTS) (Prior and Kornberg, 1988), the lack of alginate synthesis could simply be caused by limited carbon uptake, since fructose was used as the carbon source in cultivations. The *fruA*::TnCAM140 mutant was therefore evaluated in media containing other carbon sources, but still did not produce alginate when fructose was replaced with glucose, glycerol or sucrose (data not shown).

Mutations in Genes Encoding Proteins Involved in Biosynthesis of Vitamins, Cofactors and Biosynthetic Precursors Affect Alginate Production Levels

Transposon insertions in genes involved in isoprenoid, purine and thiamine biosynthesis resulted in decreased alginate production in *A. vinelandii*, and the same has previously been observed for *P. fluorescens* (**Figure 1**). Several other *A. vinelandii* mutants shown to produce very little or no alginate have transposon insertions in genes involved in the biosynthesis of cofactors (vitamins) or central metabolic precursors (**Table 2**). Selected mutants in these categories are described below.

1-deoxy-D-xylulose-5-phosphate synthase (Dxs) synthesizes the common precursor for thiamine, pyridoxine, and isoprenoid biosynthesis (Sprenger et al., 1997). An *A. vinelandii dxs-1* mutant identified in our screen was found to produce no or very low amounts of alginate. *A. vinelandii* has two nearly identical *dxs* genes, but the phenotype of the *dxs-1* mutant indicates that the expression of *dxs-2* alone is not sufficient for alginate production. Production was restored by cloning wt *dxs-1* on a transposon and transferring it back to the *dxs-1*::TnCAM140 mutant (data not shown), thus confirming that *dxs-1* is required for alginate production in *A. vinelandii*. Cultivating the *dxs-1*::TnCAM140 mutant with pyridoxine, pyridoxal or thiamine added to the growth medium did however not restore alginate production (data not shown).

The phosphoribosylformylglycinamidine synthase PurL is involved in *de novo* biosynthesis of purines (Sampei and Mizobuchi, 1989). A *purL* mutation abolished alginate production in both *A. vinelandii* (this study) and *P. fluorescens* (Ertesvåg et al., 2017). For *P. fluorescens* this was also observed for several additional mutants where genes involved in either *de novo* or salvage pathways for purine synthesis were disrupted (**Figure 1**). Some of these *P. fluorescens* mutants were complemented, and complementation was shown to restore alginate biosynthesis (Ertesvåg et al., 2017).

PurL is also involved in biosynthesis of thiamine, as thiamine is derived from the purine biosynthesis intermediate 5-amino-1-(5-phospho-D-ribosyl)imidazole (AIR) (Begley et al., 1999). Thiamine is an essential cofactor for a variety of enzymes, several of which play important roles in carbohydrate metabolism. Due to the central roles of purines and thiamine, *A. vinelandii* cells that do not synthesize these compounds would be expected to be unable to grow in the media used in this study. *A. vinelandii* insertion mutants are however known to sometimes contain copies of both mutant and wild-type alleles. This was shown to be the case for the *purL*::TnCAM140 mutant, which explains how the strain was still able to grow normally.

Likewise, a low-alginate-producing *bioF*::TnCAM140 mutant was shown to retain wild-type alleles. A genetically pure *bioF* mutant would not be expected to grow in unsupplemented media, as BioF is an 8-amino-7-oxononanoate synthase involved in the synthesis of biotin, a cofactor required for cellular growth (Marquet et al., 2001).

Our results also revealed that alginate production was abolished in an *A. vinelandii sucA*::TnCAM140 mutant. SucA

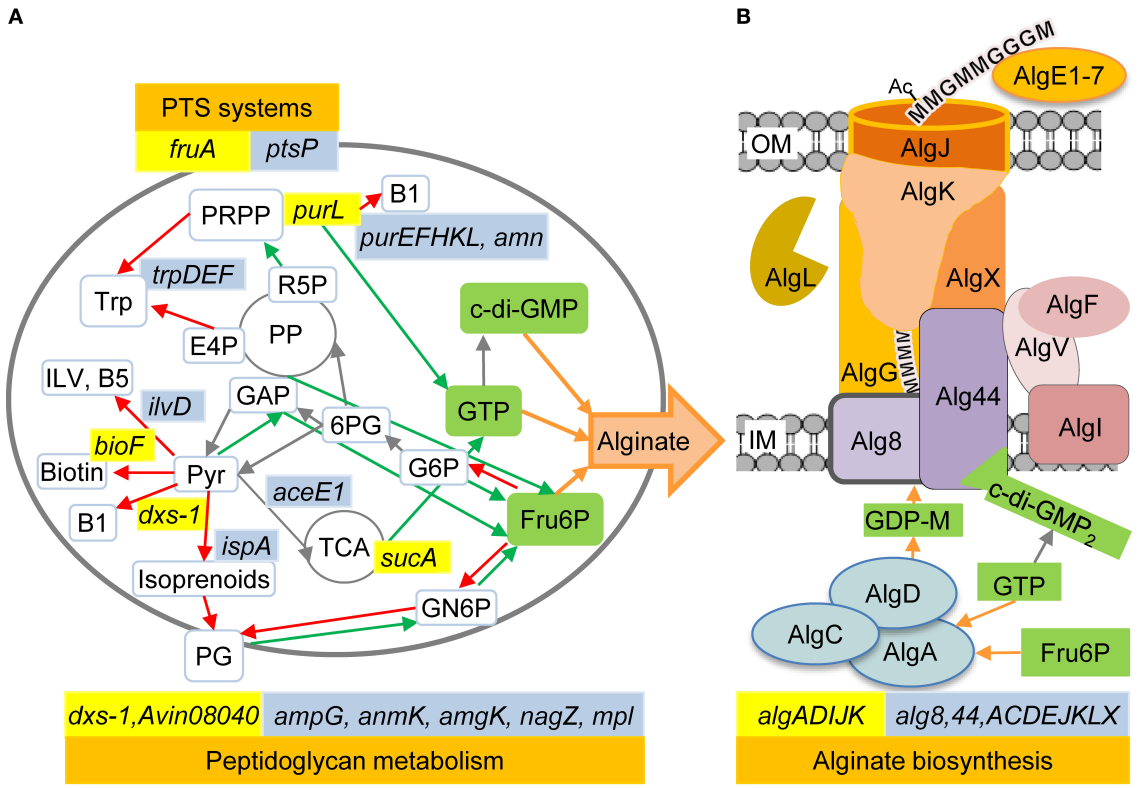

FIGURE 1 | The relationship between alginate biosynthesis and the cellular metabolism in *A. vinelandii* and *P. fluorescens*. **(A)** A simplified model of the cell's metabolism highlighting the processes identified in the present study as being important for full alginate biosynthesis levels. **(B)** The proteins and metabolites directly needed for alginate biosynthesis (adapted from Ertesvåg et al., 2017). *A. vinelandii* genes discussed in the current paper are highlighted in yellow, while the previously identified *P. fluorescens* genes are highlighted in blue. In *P. fluorescens*, the AlgJ homolog is named AlgE, while the AlgV homolog is named AlgJ. Red arrows indicate pathways competing with accumulation of the three metabolites Fru6P, GTP, and c-di-GMP, which are essential for alginate biosynthesis, while green arrows indicate pathways that would increase the synthesis of one of these three metabolites. Each arrow may represent several enzymatic steps. OM, Outer membrane; IM, Inner membrane; 6PG, 6-Phosphogluconate; Ac, Acetyl; B1, Thiamine; B5, Pantothenate; E4P, Erythrose 4-phosphate; G, Guluronic acid residue; GN6P, Glucosamine 6-phosphate; G6P, Glucose 6-phosphate; ILV, Isoleucine Leucine Valine; M, Mannuronic acid residue; PG, Peptidoglycan; PP, Pentose-phosphate cycle; PRPP, Phosphoribosyl pyrophosphate; Pyr, Pyruvate; R5P, Ribose 5-phosphate; TCA, Tricarboxylic acid cycle; Trp, Tryptophan.

is part of the 2-oxoglutarate dehydrogenase complex, which catalyzes the irreversible conversion of 2-oxoglutarate to succinyl-CoA in the tricarboxylic acid (TCA) cycle. In addition to being an intermediate in the TCA cycle, succinyl-CoA is a precursor for several important biomolecules. Inactivation of *sucA* would be expected to reduce growth rate (Yu et al., 2006), but PCR showed that the *sucA* mutant, like the *purL* and *bioF* mutants, has retained both disrupted and wild-type alleles, which can explain why growth was unimpaired (**Table 2**).

Alginate Production Is Limited by Access to Key Metabolites in *A. vinelandii*

As mentioned earlier, *A. vinelandii* has multiple copies of its chromosome and will use this to retain wild type copies of genes necessary to maintain an adequate growth rate even if the inactivated version is selected for by an antibiotic. As described above, the *purL, bioF,* and *sucA* mutants all contained wild type copies of their chromosomes in addition to chromosomes where the gene was inactivated by the transposon. Such mutants may easily revert to the wild type, and any analyses of growth or alginate production would be hampered by perceivable fluctuations of the relative copy-number of each chromosome between different cells in the population. Moreover, complementation results of such mutants are not easily interpreted, since any perceived wild-type phenotype theoretically could be caused by a high copy-number of the wild type chromosome rather than by the complementing plasmid.

Still, the phenotypes of the *dxs-1*, *purL, bioF,* and *sucA* mutants indicate that a lack of essential vitamins or other key metabolites negatively affects *A. vinelandii* alginate production, even when growth is only mildly affected or not affected at all. If this is the case, it is also possible that insufficient access to such compounds is a limiting factor for alginate biosynthesis in the reference strain.

In light of this, we settled on an alternative approach to further assess the impact of these mutations. We hypothesized that sufficient availability of compounds like succinate, biotin, thiamine, or purines could be necessary for alginate biosynthesis, and thus also be a limiting factor for alginate biosynthesis in the reference strain. To investigate this, strain ATCC12518Tc was

TABLE 3 | Growth medium combinations used for cultivation experiments to assess nutrient supplements.

Growth medium	Carbon source	Additional nutrient supplement(s)
RA1	Fructose	None
RA1	Fructose	Succinate
RA1	Fructose	Pyridoxine (vitamin B6)
RA1	Fructose	Pyridoxal (vitamin B6)
RA1	Fructose	Thiamine (vitamin B1)
RA1	Fructose	Thiamine and pyridoxine
RA1	Fructose	Thiamine and pyridoxal
RA1	Fructose	Adenine
RA1	Fructose	Lysine, methionine and diaminopimelate
RA1	Fructose	Biotin (vitamin B7)

cultivated in RA1 medium with different supplements: succinate, the four vitamins pyridoxal, pyridoxine, thiamine and biotin, the purine adenine, and a mixture of the three amino acids diaminopimelate, lysine, and methionine (**Table 3**). The amino acids were chosen due to their dependence on the succinate-derivative succinyl CoA for biosynthesis. While this is true for diaminopimelate and lysine; in *A. vinelandii* methionine biosynthesis is catalyzed by MetX instead of MetA, and probably utilizes acetyl-CoA and not succinyl-CoA as an acyl-donor (Ferla and Patrick, 2014).

The cultivation results showed that while cell growth was not significantly affected by any of the added nutrients (**Figure 2A**), addition of succinate, thiamine or a mixture of lysine, methionine, and diaminopimelate increased the amount of measured alginate in the cultures by ∼40% (**Figure 2B**). The observed effect of succinate supplementation could be due to the added carbon, since ∼5 g/l was added to the medium (in addition to the main carbon source; 20 g/l fructose), but cell growth did not increase relative to the reference. The effect of the amino acid supplement could also be related to the role of diaminopimelate as a precursor in peptidoglycan biosynthesis (Mengin-Lecreulx et al., 1996), as there appears to be a connection between peptidoglycan metabolism and alginate biosynthesis (**Figure 1**). Thus, the availability of thiamine and possibly TCA cycle intermediates appears to be limiting for alginate production in *A. vinelandii*.

DISCUSSION

The presented screen had limited coverage, since several genes known to be necessary for alginate biosynthesis were not identified (confer **Figure 1B**). Still, genes not previously known to be required for alginate production were identified as necessary, the most interesting of which may be *fruA*. The scarcity of mutants with a reproducible increase in alginate production could reflect the fact that the reference strain, ATCC12518Tc, produces quite large amounts of the polysaccharide, so there might be fewer single gene mutations that will have a pronounced positive effect on production levels. The current study focused on two groups of genes; genes with assumed regulatory functions and genes connected to central metabolism.

Mutations in Regulatory Genes

Alginate production is dependent on the RpoE-like sigma factor AlgU. MucA is an anti-sigma factor, which sequesters AlgU. A *mucA* mutant was identified in the present study, and as could be expected, this mutant showed an increase in alginate production levels. In *P. aeruginosa,* release of AlgU is controlled by a proteolytic cascade similar to the activation of RpoE in *E. coli*, and AlgW is needed for the first proteolytic cleavage (Delgado et al., 2018). A non-alginate producing *algW* mutant was identified in the present study but could not be complemented by plasmid pHE536. More studies on the role of AlgW and other proteases in *A. vinelandii* are needed in order to elucidate the proteolytic cascade for AlgU activation in this organism.

While the two-component response regulator AlgB is necessary for alginate production in *P. aeruginosa*, our study indicates that this is not the case in *A. vinelandii*. A possible explanation would be that the mutant expresses a truncated AlgB protein which has retained sufficient function to carry out its role in alginate synthesis. This is however not very likely, since the transposon insertion splits the gene almost evenly in half, and a specific amino acid in the C-terminal end has previously been shown to be necessary for the binding of AlgB to P*algD* in *P. aeruginosa* (Ma et al., 1998; Leech et al., 2008). The AlgB proteins from *P. aeruginosa* PAO1 and *A. vinelandii* DJ are of equal length and share 75% sequence identity.

In *P. aeruginosa* the cognate histidine kinase of AlgB is KinB, but AlgB phosphorylation is not needed for its role in alginate production (Ma et al., 1998). KinB has recently been shown to be a negative regulator of alginate biosynthesis in this organism, as AlgW-dependent proteolysis of MucA does not occur in the presence of KinB (Damron et al., 2009). However, no histidine kinase gene is found in the vicinity of *algB* in *A. vinelandii*, and a homology search of the *A. vinelandii* DJ genome revealed that it does not encode a KinB homolog. The phenotype of our mutant and the absence of a KinB homolog indicate that the *algB* gene may not have a role in the regulation of alginate biosynthesis in *A. vinelandii.*

AmrZ was originally identified as a positive regulator for alginate biosynthesis in *P. aeruginosa* (Baynham and Wozniak, 1996). The protein was later found to also act as a positive or negative regulator for several other genes, that encode proteins involved in motility, polysaccharide biosynthesis, iron homeostasis, c-di-GMP production etc., in various species of *Pseudomonas* (See Martínez-Granero et al., 2014; Prada-Ramírez et al., 2016; Hou et al., 2019, and references therein). Interestingly, the effect of AmrZ differs between species; while a *P. aeruginosa amrZ* mutant had an increased level of c-di-GMP (Hou et al., 2019), a *P. fluorescens amrZ* mutant displayed severely reduced levels (Muriel et al., 2018). The effect on motility is also species dependent, from severe defects to hypermotility (Baltrus et al., 2018). The present study shows that *amrZ* is necessary for alginate production in *A. vinelandii.* AmrZ has not previously been studied in *A. vinelandii*, and given

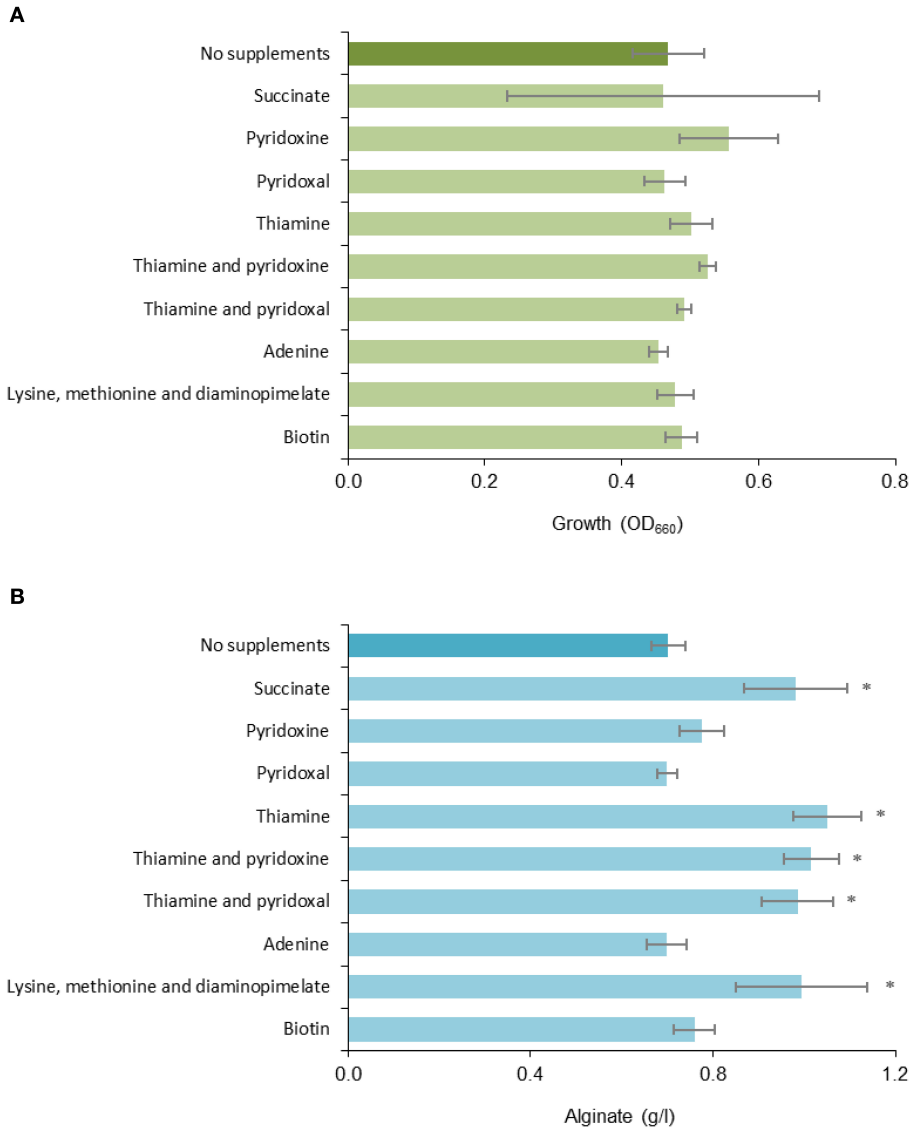

FIGURE 2 | Effect of different media supplements on **(A)** growth and **(B)** alginate production. Triplicate cultures of *A. vinelandii* ATCC12518Tc was grown in deepwell plates containing RA1 with TMS1, fructose and different supplements for 48 h before sampling. Cultures without supplements were included as a reference. Error bars represent one standard deviation. *denotes a statistically significant increase in alginate concentration relative to the reference ($p \leq 0.05$).

the pleiotropic effects of its homolog in *Pseudomonas* spp., it would be interesting to further investigate the role of AmrZ in *A. vinelandii*.

FruA Is Necessary for Alginate Biosynthesis

Our growth studies showed that FruA is necessary for alginate production on several carbon sources, also those that do not require this protein for uptake. Many carbohydrate PTS systems have regulatory roles besides their function in sugar uptake and phosphorylation (reviewed in Deutscher et al., 2006), which is another possible explanation for the absence of alginate production in this mutant. Similarly to *P. putida* (Velázquez et al., 2007), *A. vinelandii* encodes two PTS systems; FruA-FruB (PTS^{Fru}) and PtsO-PtsN-PtsP (PTS^{Ntr}). The latter is not involved in carbohydrate uptake, but is believed to be involved in coordinating nitrogen and carbon metabolism in several bacteria and has been shown to affect various metabolic processes (reviewed in Deutscher et al., 2006). Furthermore, cross-talk between the PTS^{Fru} and PTS^{Ntr} systems has been demonstrated in *P. putida* (Pflüger-Grau et al., 2011). In *A. vinelandii*, the PTS^{Ntr} system has been shown to be involved in regulation of polyhydroxybutyrate and alkylresorcinol synthesis (Segura and Espín, 1998; Noguez et al., 2008; Muriel-Millán et al., 2015). As these studies were carried out on derivatives of the *A. vinelandii* UW strain, which does not produce alginate, it is not known whether PTS^{Ntr} mutations also have an effect on alginate

synthesis. However, the screening of a *P. fluorescens* transposon insertion library (**Figure 1**) revealed that inactivation of *ptsP* does affect alginate production negatively in this strain. Thus, our results indicate that the *A. vinelandii* PTS^{Fru} system could have a role in regulation of alginate biosynthesis, possibly via interaction with the PTS^{Ntr} system.

Alginate Biosynthesis Seems to Be Regulated by the Metabolic Status of the Cell

Our earlier studies in *P. fluorescens* indicated that even in a *mucA* mutant, alginate biosynthesis does not start immediately after the first alginate biosynthetic complexes have been assembled (Maleki et al., 2016). Moreover, both the *P. fluorescens* transposon insertion study (Ertesvåg et al., 2017) and studies focusing on the synthesis of fructose 6-phosphate (Maleki et al., 2015, 2017) clearly indicated that the cells prioritize growth and survival over alginate production. The present study indicates that the same is true for *A. vinelandii*.

Some of the mutants identified in our screen had insertions in genes encoding proteins homologous to or in the same metabolic pathways as proteins identified and confirmed as relevant for alginate biosynthesis in the *P. fluorescens* screen (**Figure 1**). Even if many of these *A. vinelandii* mutants were not complemented, the concurrence makes it more plausible that the observed phenotypes are due to the introduced mutations.

A. vinelandii Avin08040 and an *mpl* homolog appear to form an operon, with *Avin08040* located upstream of *mpl*. The transposon insertion in *Avin08040* resulted in decreased alginate production, and a slight decrease has also been observed for a *P. fluorescens mpl* mutant (Ertesvåg et al., 2017). The murein peptide ligase Mpl is involved in the recycling of cell wall peptidoglycan (Mengin-Lecreulx et al., 1996), a process where degradation products from peptidoglycan can be used to resynthesize more peptidoglycan or be utilized as an energy source (Park and Uehara, 2008). *Avin08040* encodes a probable aromatic acid decarboxylase of unknown function, but the observed phenotype of this mutant could result from polar effects on *mpl* expression; a defect in peptidoglycan recycling would impose a drain on fructose-6-phosphate, making less available for alginate biosynthesis. It is also possible that Avin08040 plays a hitherto unknown role in utilization of peptidoglycan degradation products.

Results obtained in the current study show that *dxs-1* is necessary for alginate biosynthesis in *A. vinelandii*. Negative impact on alginate production has also been reported for a *P. fluorescens ispA* mutant (Ertesvåg et al., 2017). For *P. fluorescens* this could be due to a polar effect on *dxs* expression, as these genes are part of the *xseB-ispA-dxs* gene cluster encoding exodeoxyribonuclease VII small subunit, geranyl transferase (isoprenoid biosynthesis), and 1-deoxy-D-xylulose-5-phosphate synthase (thiamine, pyridoxine, and isoprenoid biosynthesis). *P. fluorescens* has one such cluster (Winsor et al., 2016) while the *A. vinelandii* genome contains two nearly identical copies (Setubal et al., 2009). The two *A. vinelandii* Dxs proteins are identical except for one Pro to Ala substitution, but according to our results the bacterium does not produce alginate when only *dxs-2* is intact. Alginate production was restored by complementation with wt *dxs-1*, but not by addition of pyridoxine, pyridoxal or thiamine to the growth medium. This suggests that the role of Dxs-1 in alginate biosynthesis could be related to its role in isoprenoid biosynthesis, or to some yet unknown function of this protein.

We were unable to isolate pure mutants with insertions in the *sucA, purl,* and *bioF* genes. Still, in light of the results from *P. fluorescens*, the phenotype of the *A. vinelandii purL* mutant was as expected and demonstrates that *A. vinelandii* mutants can exhibit changed alginate phenotypes even if the mutant strain is not genetically pure. Based on the expected deficiencies in the identified metabolic mutants, cultivation of the parent strain was performed with addition of selected medium supplements (**Table 3**). The results (**Figure 2**) show that adding thiamine, succinate or a mixture of lysine, methionine, and diaminopimelate resulted in increased alginate biosynthesis for the wild type strain. There is no obvious connection between thiamine or succinate levels and alginate biosynthesis, but both compounds are essential for several central metabolic processes. A deficiency can thus be expected to cause suboptimal performance of the cellular metabolism, which could render the cell unable to carry out certain energy-demanding secondary processes, such as biosynthesis of exopolysaccharides.

Furthermore, it was recently shown that *A. vinelandii* cells cultivated using succinate as the sole carbon source produce more alginate and also show differential expression of sRNA genes belonging to the GacS/A-Rsm regulatory system (affects *algD* expression) compared to cells cultivated with glucose or fructose (López-Pliego et al., 2018). Interestingly, succinate, methionine, diaminopimelate and lysine have been shown to lower the thiamine requirement in *Salmonella typhimurium,* probably by reducing the need for succinyl-CoA synthase (Enos-Berlage and Downs, 1997). Since thiamine biosynthesis is competing with purine biosynthesis for precursors, this is an indirect link to alginate biosynthesis (**Figure 1**). Succinyl CoA is also a precursor for protein succinylation, and such posttranslational modification is used to fine-tune the metabolism (Yang et al., 2015). In addition to proteins involved in TCA and gluconeogenesis, four proteins necessary for alginate biosynthesis, namely AlgU, MucB, AlgR, and AlgC, were found to be succinylated in *P. aeruginosa* (Gaviard et al., 2018).

CONCLUSIONS

Screening of the described *A. vinelandii* transposon mutant library identified only one strain, a *mucA*::TnCAM140 mutant, which produces significantly more alginate per cell than the reference strain. Several gene disruptions resulting in decreased or abolished alginate production were however identified, including genes not previously known to affect alginate biosynthesis. The data also provided new insights regarding alginate regulatory genes in *A. vinelandii* and the cellular

processes and metabolites that influence alginate synthesis in this organism. Finally, analyses of the data resulted in the identification of nutrients that limit alginate production in the reference strain, which would not have been easily found using metabolic modeling. The results obtained in the present study will be valuable both for development of alginate bioproduction media and for genetic engineering of *A. vinelandii* toward optimization of alginate production and yield.

DATA AVAILABILITY STATEMENT

All relevant data is contained within the manuscript.

AUTHOR CONTRIBUTIONS

MM, HS, TE, SV, and HE participated in the design of the study. MM, ØJ, HS, GK, and AT performed the experiments. MM and HE reviewed bioinformatic information and literature on relevant genes and drafted the manuscript. All authors read and approved the manuscript.

FUNDING

This work was supported by the Research Council of Norway and FMC Biopolymers. Open access publication was supported by NTNU's publishing fund.

ACKNOWLEDGMENTS

The authors thank Tone Haugen and Vu To for assisting with cultivations, fermentations, and alginate assays and Margit Dagsdatter Haugsnes for constructing the transposon vector pMH13.

SUPPLEMENTARY MATERIAL

The Supplementary Material for this article can be found online at: https://www.frontiersin.org/article/10.3389/fbioe.2019.00475/full#supplementary-material

Supplementary Figure S1 | Gene context of the genes discussed in the Paper: The discussed genes are shown as blue arrows, neighboring genes as red arrows, and the transposon insertions by bars. The genes are sorted by their mutation identifier.

REFERENCES

Ahumada-Manuel, C. L., Guzmán, J., Peña, C., Quiroz-Rocha, E., Espín, G., and Núñez, C. (2017). The signaling protein MucG negatively affects the production and the molecular mass of alginate in *Azotobacter vinelandii*. *Appl. Microbiol. Biotechnol.* 101, 1521–1534. doi: 10.1007/s00253-016-7931-8

Altschul, S. F., Madden, T. L., Schaffer, A. A., Zhang, J., Zhang, Z., Miller, W., et al. (1997). Gapped BLAST and PSI-BLAST: a new generation of protein database search programs. *Nucleic Acids Res.* 25, 3389–3402. doi: 10.1093/nar/25.17.3389

Andersen, T., Strand, B. L., Formo, K., Alsberg, E., and Christensen, B. E. (2012). Alginates as biomaterials in tissue engineering. *Carbohydr. Chem.* 37, 227–258. doi: 10.1039/9781849732765-00227

Bakke, I., Berg, L., Aune, T. E., Brautaset, T., Sletta, H., Tøndervik, A., et al. (2009). Random mutagenesis of the *Pm* promoter as a powerful strategy for improvement of recombinant-gene expression. *Appl. Environ. Microbiol.* 75, 2002–2011. doi: 10.1128/AEM.02315-08

Bakkevig, K., Sletta, H., Gimmestad, M., Aune, R., Ertesvåg, H., Degnes, K., et al. (2005). Role of the *Pseudomonas fluorescens* alginate lyase (AlgL) in clearing the periplasm of alginates not exported to the extracellular environment. *J. Bacteriol.* 187, 8375–8384. doi: 10.1128/JB.187.24.8375-8384.2005

Baltrus, D. A., Dougherty, K., Diaz, B., and Murillo, R. (2018). Evolutionary plasticity of AmrZ regulation in *Pseudomonas*. *mSphere* 3. doi: 10.1128/mSphere.00132-18

Baynham, P. J., Brown, A. L., Hall, L. L., and Wozniak, D. J. (1999). *Pseudomonas aeruginosa AlgZ*, a ribbon-helix-helix DNA-binding protein, is essential for alginate synthesis and *algD* transcriptional activation. *Mol. Microbiol.* 33, 1069–1080. doi: 10.1046/j.1365-2958.1999.01550.x

Baynham, P. J., Ramsey, D. M., Gvozdyev, B. V., Cordonnier, E. M., and Wozniak, D. J. (2006). The *Pseudomonas aeruginosa* ribbon-helix-helix DNA-binding protein AlgZ (AmrZ) controls twitching motility and biogenesis of type IV pili. *J. Bacteriol.* 188, 132–140. doi: 10.1128/JB.188.1.132-140.2006

Baynham, P. J., and Wozniak, D. J. (1996). Identification and characterization of AlgZ, an AlgT-dependent DNA-binding protein required for *Pseudomonas aeruginosa algD* transcription. *Mol. Microbiol.* 22, 97–108. doi: 10.1111/j.1365-2958.1996.tb02659.x

Begley, T. P., Downs, D. M., Ealick, S. E., McLafferty, F. W., Van Loon, A. P. G. M., Taylor, S., et al. (1999). Thiamin biosynthesis in prokaryotes. *Arch. Microbiol.* 171, 293–300. doi: 10.1007/s002030050713

Cezairliyan, B. O., and Sauer, R. T. (2009). Control of *Pseudomonas aeruginosa* AlgW protease cleavage of MucA by peptide signals and MucB. *Mol. Microbiol.* 72, 368–379. doi: 10.1111/j.1365-2958.2009.06654.x

Damron, F. H., Qiu, D., and Yu, H. D. (2009). The *Pseudomonas aeruginosa* sensor kinase KinB negatively controls alginate production through AlgW-dependent MucA proteolysis. *J. Bacteriol.* 191, 2285–2295. doi: 10.1128/JB.01490-08

de Lorenzo, V., Cases, I., Herrero, M., and Timmis, K. N. (1993). Early and late response of TOL promoters to pathway inducers: identification of postexponential promoters in *Pseudomonas putida* with *lacZ-tet* bicistronic reporters. *J. Bacteriol.* 175, 6902–6907. doi: 10.1128/jb.175.21.6902-6907.1993

Delgado, C., Florez, L., Lollett, I., Lopez, C., Kangeyan, S., Kumari, H., et al. and Mathee, K. (2018). *Pseudomonas aeruginosa* regulated intramembrane proteolysis: protease MucP can overcome mutations in the AlgO periplasmic protease to restore alginate production in nonmucoid revertants. *J. Bacteriol.* 200:e00215-18. doi: 10.1128/JB.00215-18

Deutscher, J., Francke, C., and Postma, P. W. (2006). How phosphotransferase system-related protein phosphorylation regulates carbohydrate metabolism in bacteria. *Microbiol. Mol. Biol. Rev.* 70, 939–1031. doi: 10.1128/MMBR.00024-06

Enos-Berlage, J. L., and Downs, D. M. (1997). Mutations in *sdh* (succinate dehydrogenase genes) alter the thiamine requirement of *Salmonella typhimurium*. *J. Bacteriol.* 179, 3989–3996. doi: 10.1128/jb.179.12.3989-3996.1997

Ertesvåg, H. (2015). Alginate-modifying enzymes: biological roles and biotechnological uses. *Front. Microbiol.* 6:523. doi: 10.3389/fmicb.2015.00523

Ertesvåg, H., Erlien, F., Skjåk-Bræk, G., Rehm, B. H., and Valla, S. (1998). Biochemical properties and substrate specificities of a recombinantly produced *Azotobacter vinelandii* alginate lyase. *J. Bacteriol.* 180, 3779–3784.

Ertesvåg, H., Høidal, H. K., Hals, I., K., Rian, A., Doseth, B., and Valla, S. (1995). A family of modular type mannuronan C-5-epimerase genes controls alginate structure in *Azotobacter vinelandii*. *Mol. Microbiol.* 16, 719–731. doi: 10.1111/j.1365-2958.1995.tb02433.x

Ertesvåg, H., and Skjåk-Bræk, G. (1999). "Modification of alginate using mannuronan C-5-epimerases," in *Methods in Biotechnology 10, Carbohydrate Biotechnology Protocols,* ed C. Bucke (Totowa, NJ: Humana Press Inc.), 71–78. doi: 10.1007/978-1-59259-261-6_6

Ertesvåg, H., Sletta, H., Senneset, M., Sun, Y. Q., Klinkenberg, G., Konradsen, T. A., et al. (2017). Identification of genes affecting alginate biosynthesis in

Pseudomonas fluorescens by screening a transposon insertion library. *BMC Genomics* 18:11. doi: 10.1186/s12864-016-3467-7

Ferla, M. P., and Patrick, W. M. (2014). Bacterial methionine biosynthesis. *Microbiology* 160, 1571–1584. doi: 10.1099/mic.0.077826-0

Gaviard, C., Broutin, I., Cosette, P., Dé, E., Jouenne, T., and Hardouin, J. (2018). Lysine succinylation and acetylation in *Pseudomonas aeruginosa*. *J. Proteome Res*. 17, 2449–2459. doi: 10.1021/acs.jproteome.8b00210

Gimmestad, M., Ertesvåg, H., Heggeset, T. M. B., Aarstad, O., Svanem, B. I. G., and Valla, S. (2009). Characterization of three new *Azotobacter vinelandii* alginate lyases, one of which is involved in cyst germination. *J. Bacteriol*. 191, 4845–4853. doi: 10.1128/JB.00455-09

Gimmestad, M., Steigedal, M., Ertesvåg, H., Moreno, S., Christensen, B. E., Espín, G., et al. (2006). Identification and characterization of an *Azotobacter vinelandii* Type I secretion system responsible for export of the AlgE-type mannuronan C5-epimerases. *J. Bacteriol*. 188, 5551–5560. doi: 10.1128/JB.00236-06

Goldberg, J. B., and Dahnke, T. (1992). *Pseudomonas aeruginosa* AlgB, which modulates the expression of alginate, is a member of the NtrC subclass of prokaryotic regulators. *Mol. Microbiol.* 6, 59–66. doi: 10.1111/j.1365-2958.1992.tb00837.x

Goldberg, J. B., and Ohman, D. E. (1987). Construction and characterization of *Pseudomonas aeruginosa algB* mutants: role of *algB* in high-level production of alginate. *J. Bacteriol.* 169, 1593–1602. doi: 10.1128/jb.169.4.1593-1602.1987

Gorin, P., and Spencer, J. F. (1966). Exocellular alginic acid from *Azotobacter vinelandii*. *Can. J. Chem*. 44, 993–998. doi: 10.1139/v66-147

Haug, A., Larsen, B., and Smidsrød, O. (1966). A study of the constitution of alginic acid by partial acid hydrolysis. *Acta Chem. Scand.* 20, 183–190. doi: 10.3891/acta.chem.scand.20-0183

Hay, I. D., Wang, Y., Moradali, M. F., Rehman, Z. U., and Rehm, B. H. (2014). Genetics and regulation of bacterial alginate production. *Environ. Microbiol*. 16, 2997–3011. doi: 10.1111/1462-2920.12389

Hou, L. L., Debru, A., Chen, Q. Q., Bao, Q. Y., and Li, K. W. (2019). AmrZ regulates swarming motility through cyclic di-GMP-dependent motility inhibition and controlling pel polysaccharide production in *Pseudomonas aeruginosa* PA14. *Front. Microbiol*. 10:1847. doi: 10.3389/fmicb.2019.01847

Leech, A. J., Sprinkle, A., Wood, L., Wozniak, D. J., and Ohman, D. E. (2008). The NtrC family regulator AlgB, which controls alginate biosynthesis in mucoid *Pseudomonas aeruginosa*, binds directly to the *algD* promoter. *J. Bacteriol*. 190, 581–589. doi: 10.1128/JB.01307-07

León, R., and Espín, G. (2008). *flhDC*, but not *fleQ*, regulates flagella biogenesis in *Azotobacter vinelandii*, and is under AlgU and CydR negative control. *Microbiology* 154, 1719–1728. doi: 10.1099/mic.0.2008/017665-0

López-Pliego, L., García-Ramírez, L., Cruz-Gómez, E. A., Domínguez-Ojeda, P., López-Pastrana, A., Fuentes-Ramírez, L. E., et al. (2018). Transcriptional study of the RsmZ-sRNAs and their relationship to the biosynthesis of alginate and alkylresorcinols in *Azotobacter vinelandii*. *Mol. Biotechnol.* 60, 670–680. doi: 10.1007/s12033-018-0102-7

Ma, S., Selvaraj, U., Ohman, D. E., Quarless, R., Hassett, D. J., and Wozniak, D. J. (1998). Phosphorylation-independent activity of the response regulators AlgB and AlgR in promoting alginate biosynthesis in mucoid *Pseudomonas aeruginosa*. *J. Bacteriol.* 180, 956–968.

Maleki, S., Almaas, E., Zotchev, S. B., Valla, S., and Ertesvåg, H. (2016). Alginate biosynthesis factories in *Pseudomonas fluorescens*: localization and correlation with alginate production level. *Appl. Environ. Microbiol*. 82, 2027–2036. doi: 10.1128/AEM.03114-15

Maleki, S., Hrudikova, R., Zotchev, S. B., and Ertesvåg, H. (2017). Identification of a new phosphatase enzyme potentially involved in sugar-phosphate stress response in *Pseudomonas fluorescens*. *Appl. Environ. Microbiol.* 83:e02361–e02316. doi: 10.1128/AEM.02361-16

Maleki, S., Mærk, M., Valla, S., and Ertesvåg, H. (2015). Mutational analyses of glucose dehydrogenase and glucose-6-phosphate dehydrogenase genes in *Pseudomonas fluorescens* reveal their effects on growth and alginate production. *Appl. Environ. Microbiol*. 81, 3349–3356. doi: 10.1128/AEM.03653-14

Marquet, A., Bui, B. T., and Florentin, D. (2001). Biosynthesis of biotin and lipoic acid. *Vitam. Horm*. 61, 51–101. doi: 10.1016/S0083-6729(01)61002-1

Martínez-Granero, F., Navazo, A., Barahona, E., Redondo-Nieto, M., Rivilla, R., and Martín, M. (2012). The Gac-Rsm and SadB signal transduction pathways converge on AlgU to downregulate motility in *Pseudomonas fluorescens*. *PLoS ONE* 7:e31765. doi: 10.1371/journal.pone.0031765

Martínez-Granero, F., Redondo-Nieto, M., Vesga, P., Martín, M., and Rivilla, R. (2014). AmrZ is a global transcriptional regulator implicated in iron uptake and environmental adaption in *P. fluorescens* F113. *BMC Genomics* 15:237. doi: 10.1186/1471-2164-15-237

Martínez-Salazar, J. M., Moreno, S., Nájera, R., Boucher, J. C., Espín, G., Soberón-Chávez, G., et al. (1996). Characterization of the genes coding for the putative sigma factor AlgU and its regulators MucA, MucB, MucC, and MucD in *Azotobacter vinelandii* and evaluation of their roles in alginate biosynthesis. *J. Bacteriol*. 178, 1800–1808. doi: 10.1128/jb.178.7.1800-1808.1996

Mengin-Lecreulx, D., van Heijenoort, J., and Park, J. T. (1996). Identification of the *mpl* gene encoding UDP-N-acetylmuramate: L-alanyl-gamma-D-glutamyl-meso-diaminopimelate ligase in *Escherichia coli* and its role in recycling of cell wall peptidoglycan. *J. Bacteriol.* 178, 5347–5352. doi: 10.1128/jb.178.18.5347-5352.1996

Muriel, C., Arrebola, E., Redondo-Nieto, M., Martínez-Granero, F., Jalvo, B., Pfeilmeier, S., et al. (2018). AmrZ is a major determinant of c-di-GMP levels in *Pseudomonas fluorescens* F113. *Sci. Rep.* 8:1979. doi: 10.1038/s41598-018-20419-9

Muriel-Millán, L. F., Moreno, S., Romero, Y., Bedoya-Peréz, L. P., Castañeda, M., Segura, D., et al. (2015). The unphosphorylated EIIA(Ntr) protein represses the synthesis of alkylresorcinols in *Azotobacter vinelandii*. *PLoS ONE* 10:e0117184. doi: 10.1371/journal.pone.0117184

Noguez, R., Segura, D., Moreno, S., Hernandez, A., Juarez, K., and Espín, G. (2008). Enzyme I NPr, NPr and IIA Ntr are involved in regulation of the poly-beta-hydroxybutyrate biosynthetic genes in *Azotobacter vinelandii*. *J. Mol. Microbiol. Biotechnol.* 15, 244–254. doi: 10.1159/000108658

Núñez, C., Leon, R., Guzman, J., Espín, G., and Soberon-Chavez, G. (2000). Role of *Azotobacter vinelandii mucA* and *mucC* gene products in alginate production. *J. Bacteriol*. 182, 6550–6556. doi: 10.1128/JB.182.23.6550-6556.2000

Núñez, C., Moreno, S., Soberon-Chavez, G., and Espín, G. (1999). The *Azotobacter vinelandii* response regulator AlgR is essential for cyst formation. *J. Bacteriol*. 181, 141–148.

Núñez, C., Peña, C., Kloeckner, W., Hernández-Eligio, A., Bogachev, A. V., Moreno, S., et al. (2013). Alginate synthesis in *Azotobacter vinelandi*i is increased by reducing the intracellular production of ubiquinone. *Appl. Microbiol. Biotechnol.* 97, 2503–2512. doi: 10.1007/s00253-012-4329-0

Østgaard, K. (1992). Enzymatic microassay for the determination and characterization of alginates. *Carbohydr. Polym*. 19, 51–59. doi: 10.1016/0144-8617(92)90054-T

Park, J. T., and Uehara, T. (2008). How bacteria consume their own exoskeletons (turnover and recycling of cell wall peptidoglycan). *Microbiol. Mol. Biol. Rev*. 72, 211–227. doi: 10.1128/MMBR.00027-07

Pflüger-Grau, K., Chavarría, M., and de Lorenzo, V. (2011). The interplay of the EIIA(Ntr) component of the nitrogen-related phosphotransferase system (PTS(Ntr)) of *Pseudomonas putida* with pyruvate dehydrogenase. *Biochim. Biophys. Acta* 1810, 995–1005. doi: 10.1016/j.bbagen.2011.01.002

Prada-Ramírez, H. A., Pérez-Mendoza, D., Felipe, A., Martínez-Granero, F., Rivilla, R., Sanjuán, J., et al. (2016). AmrZ regulates cellulose production in *Pseudomonas syringae* pv. tomato DC3000. *Mol. Microbiol*. 99, 960–977. doi: 10.1111/mmi.13278

Prior, T. I., and Kornberg, H. L. (1988). Nucleotide sequence of *fruA*, the gene specifying enzyme II^{fru} of the phosphoenolpyruvate-dependent sugar phosphotransferase system in *Escherichia coli* K12. *J. Gen. Microbiol.* 134, 2757–2768. doi: 10.1099/00221287-134-10-2757

Qiu, D., Eisinger, V. M., Rowen, D. W., and Yu, H. D. (2007). Regulated proteolysis controls mucoid conversion in *Pseudomonas aeruginosa*. *Proc. Natl. Acad. Sci. U.S.A.* 104, 8107–8112. doi: 10.1073/pnas.0702660104

Quiroz-Rocha, E., Bonilla-Badía, F., Garcia-Aguílar, V., López-Pliego, L., Serrano-Román, J., Cocotl-Yañez, M., et al. (2017). Two-component system CbrA/CbrB controls alginate production in *Azotobacter vinelandii*. *Microbiology* 163, 1105–1115. doi: 10.1099/mic.0.000457

Rehm, B. H., Ertesvåg, H., and Valla, S. (1996). A new *Azotobacter vinelandii* mannuronan C-5-epimerase gene (*algG*) is part of an *alg* gene cluster physically organized in a manner similar to that in *Pseudomonas aeruginosa*. *J. Bacteriol*. 178, 5884–5889. doi: 10.1128/jb.178.20.5884-5889.1996

Remminghorst, U., and Rehm, B. H. (2006). Bacterial alginates: from biosynthesis to applications. *Biotechnol. Lett*. 28, 1701–1712. doi: 10.1007/s10529-006-9156-x

Sambrook, J., and Russell, D. W. (2001). *Molecular Cloning: A Laboratory Manual*. New York, NY: Cold Spring Harbor Laboratory Press.

Sampei, G., and Mizobuchi, K. (1989). The organization of the *purL* gene encoding 5'-phosphoribosylformylglycinamide amidotransferase of *Escherichia coli*. *J. Biol. Chem.* 264, 21230–21238.

Segura, D., and Espín, G. (1998). Mutational inactivation of a gene homologous to *Escherichia coli ptsP* affects poly-beta-hydroxybutyrate accumulation and nitrogen fixation in *Azotobacter vinelandii*. *J. Bacteriol.* 180, 4790–4798.

Setubal, J. C., dos Santos, P., Goldman, B. S., Ertesvåg, H., Espín, G., Rubio, L. M., et al. and Wood, D. (2009). The genome sequence of *Azotobacter vinelandii*, an obligate aerobe specialized to support diverse anaerobic metabolic processes. *J. Bacteriol.* 191, 4534–4545. doi: 10.1128/JB.00504-09

Simon, R., Priefer, U., and Pühler, A. (1983). A broad host range mobilization system for *in vivo* genetic engineering: transposon mutagenesis in Gram negative bacteria. *Biotechnology* 1, 784–791. doi: 10.1038/nbt1183-784

Skjåk-Bræk, G., Donati, I., and Paoletti, S. (2015). "Alginate hydrogels: properties and applications," in *Polysaccharide Hydrogels: Characterization and Biomedical Applications,* eds P. Matricardi, F. Alhaique, and T. Coviello (Boca Raton, FL: Pan Stanford Publishing Pte Ltd), 449–498. doi: 10.1201/b19751-14

Sprenger, G. A., Schorken, U., Wiegert, T., Grolle, S., de Graaf, A. A., Taylor, S. V., et al. (1997). Identification of a thiamin-dependent synthase in *Escherichia coli* required for the formation of the 1-deoxy-D-xylulose 5-phosphate precursor to isoprenoids, thiamin, and pyridoxol. *Proc. Natl. Acad. Sci. U.S.A.* 94, 12857–12862. doi: 10.1073/pnas.94.24.12857

Steigedal, M., Sletta, H., Moreno, S., Mærk, M., Christensen, B. E., Bjerkan, T., et al. (2008). The *Azotobacter vinelandii* AlgE mannuronan C-5-epimerase family is essential for the *in vivo* control of alginate monomer composition and for functional cyst formation. *Environ. Microbiol.* 10, 1760–1770. doi: 10.1111/j.1462-2920.2008.01597.x

Svanem, B. I. G., Skjåk-Bræk, G., Ertesvåg, H., and Valla, S. (1999). Cloning and expression of three new *Azotobacter vinelandii* genes closely related to a previously described gene family encoding mannuronan C-5-epimerases. *J. Bacteriol.* 181, 68–77.

Tart, A. H., Blanks, M. J., and Wozniak, D. J. (2006). The AlgT-dependent transcriptional regulator AmrZ (AlgZ) inhibits flagellum biosynthesis in mucoid, nonmotile *Pseudomonas aeruginosa* cystic fibrosis isolates. *J. Bacteriol.* 188, 6483–6489. doi: 10.1128/JB.00636-06

Urtuvia, V., Maturana, N., Acevedo, F., Peña, C., and Díaz-Barrera, A. (2017). Bacterial alginate production: an overview of its biosynthesis and potential industrial production. *World J. Microbiol. Biotechnol.* 33:198. doi: 10.1007/s11274-017-2363-x

Velázquez, F., Pflüger, K., Cases, I., De Eugenio, L. I., and de Lorenzo, V. (2007). The phosphotransferase system formed by PtsP, PtsO, and PtsN proteins controls production of polyhydroxyalkanoates in *Pseudomonas putida*. *J. Bacteriol.* 189, 4529–4533. doi: 10.1128/JB.00033-07

Wentzel, A., Bruheim, P., Øverby, A., Jakobsen, Ø. M., Sletta, H., Omara, W. A., et al. (2012). Optimized submerged batch fermentation strategy for systems scale studies of metabolic switching in *Streptomyces coelicolor* A3(2). *BMC Syst. Biol.* 6:59. doi: 10.1186/1752-0509-6-59

Wilson, K. J., Sessitsch, A., Corbo, J. C., Giller, K. E., Akkermans, A. D., and Jefferson, R. A. (1995). Beta-Glucuronidase (GUS) transposons for ecological and genetic studies of Rhizobia and other Gram-negative bacteria. *Microbiology* 141, 1691–1705. doi: 10.1099/13500872-141-7-1691

Winsor, G. L., Griffiths, E. J., Lo, R., Dhillon, B. K., Shay, J. A., and Brinkman, F. S. (2016). Enhanced annotations and features for comparing thousands of *Pseudomonas* genomes in the Pseudomonas genome database. *Nucleic Acids Res.* 44, D646–D653. doi: 10.1093/nar/gkv1227

Wood, L. F., Leech, A. J., and Ohman, D. E. (2006). Cell wall-inhibitory antibiotics activate the alginate biosynthesis operon in *Pseudomonas aeruginosa*: roles of sigma (AlgT) and the AlgW and Prc proteases. *Mol. Microbiol.* 62, 412–426. doi: 10.1111/j.1365-2958.2006.05390.x

Wozniak, D. J., and Ohman, D. E. (1994). Transcriptional analysis of the *Pseudomonas aeruginosa* genes *algR*, *algB*, and *algD* reveals a hierarchy of alginate gene expression which is modulated by algT. *J. Bacteriol.* 176, 6007–6014. doi: 10.1128/jb.176.19.6007-6014.1994

Wozniak, D. J., Sprinkle, A. B., and Baynham, P. J. (2003). Control of *Pseudomonas aeruginosa algZ* expression by the alternative sigma factor AlgT. *J. Bacteriol.* 185, 7297–7300. doi: 10.1128/JB.185.24.7297-7300.2003

Yang, M. K., Wang, Y., Chen, Y., Cheng, Z. Y., Gu, J., Deng, J. Y., et al. (2015). Succinylome analysis reveals the involvement of lysine succinylation in metabolism in pathogenic *Mycobacterium tuberculosis*. *Mol. Cell. Proteomics* 14, 796–811. doi: 10.1074/mcp.M114.045922

Yu, B. J., Sung, B. H., Lee, J. Y., Son, S. H., Kim, M. S., and Kim, S. C. (2006). *sucAB* and *sucCD* are mutually essential genes in Escherichia coli. *FEMS Microbiol. Lett.* 254, 245–250. doi: 10.1111/j.1574-6968.2005.00026.x

Conflict of Interest: The authors ØJ, HS, GK, AT, and TE were employed by the Research Foundation SINTEF Industry.

All authors declare that the research was conducted in the absence of any commercial or financial relationships that could be construed as a potential conflict of interest.

frontiers in Bioengineering and Biotechnology

ORIGINAL RESEARCH
published: 30 January 2020
doi: 10.3389/fbioe.2020.00038

Identification of Key Metabolites in Poly-γ-Glutamic Acid Production by Tuning γ-PGA Synthetase Expression

*Birthe Halmschlag[1], Sastia P. Putri[2], Eiichiro Fukusaki[2] and Lars M. Blank[1]**

[1] Institute of Applied Microbiology-iAMB, Aachen Biology and Biotechnology-ABBt, RWTH Aachen University, Aachen, Germany, [2] Department of Biotechnology, Graduate School of Engineering, Osaka University, Osaka, Japan

Poly-γ-glutamic acid (γ-PGA) production is commonly achieved using glycerol, citrate, and L-glutamic acid as substrates. The constitutive expression of the γ-PGA synthetase enabled γ-PGA production with *Bacillus subtilis* from glucose only. The precursors for γ-PGA synthesis, D- and L-glutamate, are ubiquitous metabolites. Hence, the metabolic flux toward γ-PGA directly depends on the concentration and activity of the synthetase and thereby on its expression. To identify pathway bottlenecks and important metabolites that are highly correlated with γ-PGA production from glucose, we engineered *B. subtilis* strains with varying γ-PGA synthesis rates. To alter the rate of γ-PGA synthesis, the expression level was controlled by two approaches: (1) Using promoter variants from the constitutive promoter P_{veg} and (2) Varying induction strength of the xylose inducible promoter P_{xyl}. The variation in the metabolism caused by γ-PGA production was investigated using metabolome analysis. The xylose-induction strategy revealed that the γ-PGA production rate increased the total fluxes through metabolism indicating a driven by demand adaption of the metabolism. Metabolic bottlenecks during γ-PGA from glucose were identified by generation of a model that correlates γ-PGA production rate with intracellular metabolite levels. The generated model indicates the correlation of certain metabolites such as phosphoenolpyruvate with γ-PGA production. The identified metabolites are targets for strain improvement to achieve high level γ-PGA production from glucose.

Keywords: biopolymer, *Bacillus subtilis*, natto, metabolomics, natural product

OPEN ACCESS

Edited by:
Bernd Rehm,
Griffith University, Australia

Reviewed by:
Zhongyu You,
Jiaxing University, China
Jin-feng Zhang,
Huaiyin Institute of Technology, China

****Correspondence:***
Lars M. Blank
lars.blank@rwth-aachen.de

Specialty section:
This article was submitted to Industrial Biotechnology, a section of the journal Frontiers in Bioengineering and Biotechnology

Received: *04 October 2019*
Accepted: *16 January 2020*
Published: *30 January 2020*

Citation:
Halmschlag B, Putri SP, Fukusaki E and Blank LM (2020) Identification of Key Metabolites in Poly-γ-Glutamic Acid Production by Tuning γ-PGA Synthetase Expression. Front. Bioeng. Biotechnol. 8:38. doi: 10.3389/fbioe.2020.00038

INTRODUCTION

Poly-γ-glutamic acid (γ-PGA) is an anionic, biodegradable, non-toxic polymer composed of D- and L-glutamic acid units linked by γ-glutamyl bonds. γ-PGA production with *Bacillus subtilis* is mainly known from *B. subtilis* (natto) in the production of natto, a traditional Japanese dish. But *B. subtilis* has also been considered as a promising organism for industrial production of γ-PGA. In case of glutamate-independent production of γ-PGA, *B. subtilis* C1 has been used with glucose and citrate as substrates resulting in a maximal titer of 21.4 g L^{-1} γ-PGA (Shih et al., 2005). Higher γ-PGA titers have been achieved by process optimization. The use of several substrates for γ-PGA production and different process strategies like fed-batch cultivations have been reported (Ogawa et al., 1997; Yoon et al., 2000). Mostly wild-type γ-PGA producers like *B. subtilis* (natto) (Ogawa et al., 1997) and *Bacillus licheniformis* ATCC9945 (Cromwick et al., 1996) have been used for the

production focusing rather on process optimization than on metabolic engineering strategies to achieve a more efficient production. In order to find metabolic engineering targets to enhance γ-PGA production, a genetically easily amenable host organism is favorable.

The synthesis of γ-PGA is catalyzed by an enzyme complex, the γ-PGA synthetase, which is encoded by the *pgs* operon. The operon consists of four genes: *pgsB, pgsC, pgsA*, and *pgsE*. Moreover, one hydrolyzing enzyme, the γ-PGA depolymerase is encoded by a gene located directly downstream of the *pgs* genes. The expression of *pgs* genes is both sufficient and necessary to achieve γ-PGA production in *B. subtilis* (Urushibata et al., 2002). The expression in *B. subtilis* 168 can be achieved by either deleting the mutations in the *degU* and the *swrA* gene encoding for the expression regulator DegU and the swarming motility factor, respectively (Ohsawa et al., 2009), or by controlling the expression from an alternative promoter (Urushibata et al., 2002).

During γ-PGA production, glutamate is a central metabolite. Glutamate is used as cell wall constituent in its D-enantiomeric form, as amino acid for protein synthesis in its L-form and finally, for γ-PGA production in both forms. Taking into account that glutamate also plays an important role in linking carbon and nitrogen metabolism, its production and turnover has to be carefully regulated. Hence, the overproduction of γ-PGA can be seen as metabolic burden for the cells. Therefore, it is important to clarify the influence of the γ-PGA synthetase amount, which can be controlled by the promoter strength, as well as the influence of γ-PGA overproduction on the metabolism. In many cases the gene expression is only evaluated at the points of knockout or overexpression, but the whole range of effects can only be explained by specifically tuning the gene expression (Alper et al., 2005). To fine tune gene expression, promoter libraries for pro- and eukaryotic promoters have been created (Jensen and Hammer, 1998; Blazeck and Alper, 2013; Redden et al., 2015). The promoter located upstream of the vegetative genes (P_{veg}) is known as a strong promoter of *B. subtilis*. Based on this promoter, a promoter library harboring changes in the −10 region of the promoter has been created (Guiziou et al., 2016). For these promoter variants, the activity of the promoter was even increased. In the case of γ-PGA production, it might also be of interest to use weaker promoters in order not to increase the demand on glutamate too excessively. For the development of a promoter library, the exact activity of a promoter variant can be tested based on the expression of a reporter gene. The use of the Green Fluorescing Protein (GFP) as reporter allows for the selection of promoter variants based on the measured fluorescence (Chalfie et al., 1994). The *gfpmut3* gene encodes a stable variant of GFP (Cormack et al., 1996). Besides promoter libraries, the expression of specific genes may also be controlled by the use of an inducible promoter. The *B. subtilis* xylose promoter (P_{xyl}) is transcriptionally repressed by XylR and induced by xylose (Gärtner et al., 1988). Hence, the strength of gene expression can be controlled by P_{xyl} and varying inducer concentrations.

Recent advances in the design of whole-cell biocatalysts focus on rational approaches (Kuhn et al., 2010). The integration of omics data strongly supports the biocatalyst development (Joyce and Palsson, 2006; Tyo et al., 2007). Especially the field of metabolomics is widely used to guide metabolic engineering efforts (Putri et al., 2013). The fine-tuning of gene expression by promoter strength enables the control of metabolic flux on the most fundamental level. Metabolome analysis of strains with varying flux can be used to identify key metabolites in production strains. The identified metabolites offer targets for metabolic engineering in order to cure metabolic bottlenecks of producer strains and thereby increase the production by targeted strain design.

In this study, we investigated the metabolic response of *B. subtilis* in dependence of *pgs* expression. The laboratory strain *B. subtilis* 168 has been reported as favorable γ-PGA production host due to its natural competence and well-investigated genetics and physiology (Halmschlag et al., 2019). Two alternative promoters were used, the constitutive P_{veg} and variants thereof and the inducible P_{xyl} promoter. In depth metabolome analysis revealed strong responses of metabolism to γ-PGA production, while homeostasis for glutamate. The results can guide targeted strain design efforts for the intensified production of γ-PGA.

MATERIALS AND METHODS

Reagents

D-Glucose, L-glutamic acid, NH_4Cl, K_2HPO_4, $MgSO_4 \times 7H_2O$, $CaCl_2 \times 2H_2O$, $MnSO_4 \times H_2O$, $FeCl_3 \times 6H_2O$, $ZnSO_4 \times 7H_2O$, Na_2-EDTA, $CuSO_4 \times 5H_2O$ and $CoCl_2 \times 6H_2O$ were purchased from Carl Roth GmbH + Co., KG (Karlsruhe, Germany). LC/MS-grade ultra-pure water, HPLC-grade chloroform, acetic acid, H_2SO_4 and NH_4HCO_3 were purchased from Wako Pure Chemical Industries, Ltd. (Osaka, Japan). 10-Camphorsulfonic acid and tributylamine were purchased from SigmaAldrich (St. Louis, MO, United States).

Strains, Plasmids and Growth Conditions

The bacterial strains and plasmids used and created in this study are listed in **Table 1**. All cloning steps were carried out in Escherichia *coli* DH5α. The recombinase positive *E. coli* strain JM101 was used to obtain plasmids for the transformation of *B. subtilis*. The strain *B. subtilis* Δspo (Halmschlag et al., 2019) was used for the development of the promoter library and as production host for γ-PGA production.

For plasmid construction and counter selection, all strains were cultivated at 37°C in LB medium containing 100 μg/mL spectinomycin or 0.5% (w/v) mannose when required. For γ-PGA production and metabolome analysis, the *B. subtilis* strains were grown in glucose minimal medium.

Pgs Expression Induction With Xylose

For the use of xylose as inducing agent, the *xylAB* genes encoding the xylose isomerase and xylulokinase were deleted in the background of strain *B. subtilis* Δspo. The thereby obtained strain is not capable of metabolizing xylose. Subsequently, the native P_{xyl} promoter was integrated into the genome of *B. subtilis* Δspo Δ*xylAB* upstream of the *pgs* operon. For that

TABLE 1 | Strains and plasmids used in this study.

Strain	Genotype/properties	Reference/source
Strains		
E. coli DH5α	*fhuA2* Δ (*argF-lacZ*)U169 *phoA glnV*44 Φ80 Δ(*lacZ*)M15 *gyrA*96 *recA*1 *relA*1 *endA*1 thi-1 hsdR17	Meselson and Yuan, 1968
E. coli JM101	*glnV*44 thi-1 Δ(*lac-proAB*) F′ [*lacI*^{q}*ZΔM15 traD*36 *proAB*$^+$]	Messing et al., 1981
B. subtilis IIG-Bs2	ΔSPβ Δ*skin* ΔPBSX ΔproΦ1 Δ*pks*:CmR, ΔproΦ3 *trp* + Δ*manPA*:*erm* Δ*bpr* Δ*sigG* Δ*sigE* Δ*spoGA*	Wenzel and Altenbuchner, 2015
B. subtilis Δspo	Δ*bpr* Δ*sigG* Δ*sigE* Δ*spoGA*	Halmschlag et al., 2019
B. subtilis ΔxylAB	Δ*bpr* Δ*sigG* Δ*sigE* Δ*spoGA*Δ*xylAB*	This study
B. subtilis PG1	P$_{veg}$-pgs	This study
B. subtilis PG16 (PV35.1)	Δ*bpr* Δ*sigG* Δ*sigE* Δ*spoGA* PV35.1-pgs	Halmschlag et al., 2020
B. subtilis (PV35.3)	Δ*bpr* Δ*sigG* Δ*sigE* Δ*spoGA* PV35.3-pgs	This study
B. subtilis (PV35.26)	Δ*bpr* Δ*sigG* Δ*sigE* Δ*spoGA* PV35.26-pgs	This study
B. subtilis PG10	Δ*xylAB* Δ*bpr* Δ*sigG* Δ*sigE* Δ*spoGA* Pxyl-pgs	Halmschlag et al., 2019
Plasmids		
pJOE-8739	Backbone for markerless counterselection system	Wenzel and Altenbuchner, 2015
pBS-20	Backbone for promoter library integration into *amyE* locus	This study
pBS-21	Template for promoter library construction, *amyE*_up-P$_{veg}$-*gfpmut3-amyE*_down	This study
pBS-21-PV35.01	PV35.01-*gfpmut3* promoter integration into *amyE* locus	This study
pBS-21-PV35.03	PV35.03-*gfpmut3* promoter integration into *amyE* locus	This study
pBS-21-PV35.01	PV35.26-*gfpmut3* promoter integration into *amyE* locus	This study
pRJ-8-PV35.01	PV35.01 promoter integration upstream of *pgs*	This study
pRJ-8-PV35.03	PV35.03 promoter integration upstream of *pgs*	This study
pRJ-8-PV35.26	PV35.26 promoter integration upstream of *pgs*	This study

purpose the plasmid pBs-02 was generated. The plasmid contains the backbone of pJOE8739 linearized with primers BS-25/26 (**Supplementary Table S1**), P$_{xyl}$ amplified with BS-09/10 and two integration sites up- and downstream of the native promoter P$_{pgs}$ that were amplified with the primer pairs TS1_fwd/TS1_rev and TS2_fwd/TS2_rev. The created strain expressing *pgs* under control of the xylose-inducible promoter Pxyl was designated as *B. subtilis* PG10.

Promoter Library Construction

The reporter gene *gfpmut3* was amplified from plasmid pBSMul1-gfpmut3 with primer pair BS-111/BS-112. A part of the *amyE* locus was amplified with BS-113/-114 to be used as homologous sequence for integration. For the assembly of plasmid pBS-21, the vector backbone pBs-20 was linearized with BS-25/-26. The backbone includes a spectinomycin resistance gene (*SpcR*), an origin of replication for *E. coli*, the *rop* gene with regulator function for replication and the second part of the *amyE* locus for homologous recombination into the *B. subtilis* genome. The native promoter P$_{veg}$ was amplified from genomic *B. subtilis* DNA using the primers BS-109 and BS-110. The promoter fragment was fused with the *gfpmut3* gene, the *amyE* upstream, and the pBs-20 based backbone by DNA HiFi Assembly (NEB, Frankfurt am Main, Germany). The thereby constructed plasmid pBs-21 was used as template to amplify two fragments, one containing the first homologous part (*amyE*-front) and the spectinomycin resistance gene (*SpcR*) and the other one containing the promoter, *gfp* gene and the second homologous part (*amyE*-back). The two fragments were amplified using the primer pairs BS-115/-116 and BS-117b/118, respectively. The primer BS-117b was a degenerated primer containing the NNN sequence to vary the −35 box sequence of the promoter. After fusion of the fragments by PCR and cloning into the pJET vector, *Bacillus* was transformed with the plasmids including promoter variants.

Determination of Promoter Activity

The *B. subtilis* colonies with varying promoter sequences were analyzed with respect to the promoter activity using the BioLector (m2p-labs, Baesweiler, Germany). The biomass was measured at 620 nm extinction/emission at gain 50. The fluorescence of GFP was detected with 488 nm extinction and 520 nm emission at gain 70. All colonies were analyzed in triplicates and the promoter activity was calculated as mean of the slope calculated as quotient of increase in fluorescence and increase in biomass during the exponential phase.

Integration of Promoter Variants for *pgs* Operon

The promoter sequence information was obtained by sequencing (Eurofins, Ebersberg, Germany). The observed sequences were introduced into pRJ-8 variants by amplification of the complete plasmid using specific primers (BS-180, BS-193, and BS-182 for variant PV35.1, PV35.3, and PV35.26, respectively) with mismatches in the promoter region. The thereby created linear plasmids were phosphorylated with T4 polynucleotide kinase (NEB, Frankfurt am Main, Germany) for 30 min at 37°C and subsequently ligated with T4 ligase (NEB, Frankfurt am Main, Germany). First, *E. coli* DH5α was transformed with these plasmids. The plasmids were purified and the promoter sequences were determined. Second, *B. subtilis* was transformed with those three plasmids. Successfully transformed colonies

were selected on LB agar plates containing spectinomycin. The correct integration was checked by PCR and sequencing.

Cultivation for γ-PGA and Metabolite Analysis

For the cultivation of *B. subtilis* glucose was used as sole carbon source in a minimal salt medium for the main cultures. The minimal medium contained per liter: 20 g glucose, 7 g NH_4Cl, 0.5 g $MgSO_4$, 0.15 g $CaCl_2$, 0.1 g $MnSO_4$, 0.04 g $FeCl_3$, and 1 mL of a trace element solution. The trace element solution [modified trace element solution after: (Wenzel et al., 2011)] contained per liter: 0.54 g $ZnSO_4$*7 H_2O, 30.15 g Na_2-EDTA, 0.48 g $CuSO_4$*5 H_2O and 0.54 g $CoCl_2$*6 H_2O. The medium was buffered using 0.1 M potassium phosphate buffer at pH 7. All media components were sterilized by autoclaving for 20 min at 121°C except for the trace element solution, which was sterile filtered. For xylose induction of *pgs* expression with *B. subtilis* PG10, xylose was added in concentrations of 0, 1, 5, 10, 15, 25, 40, 50, 80, 100, and 200 mM. The first pre-culture in LB medium was inoculated from a glycerol stock. The LB medium contained 10 g L^{-1} tryptone, 5 g L^{-1} yeast extract, and 10 g L^{-1} NaCl at pH 7.4. A second pre-culture in glucose minimal medium was inoculated with cells from the LB medium and grown overnight. The main cultures were inoculated to an OD_{600} of 0.05 from pre-culture. The cultivations were carried out in 250 mL Erlenmeyer flasks filled with 25 mL medium. The cultures were incubated on a rotary shaker (Bio-Shaker BR-3000LF, Taitec, Saitama, Japan) at 37°C, 200 rpm, 25 mm shaking diameter. All cultivations were performed in triplicates whereas the reported data represents the mean. The cell growth was monitored by OD_{600} measurements of samples taken from the shake flasks using the GeneQuant 100 spectrophotometer (GE Healthcare United Kingdom, Ltd., Buckinghamshire, United Kingdom). Additionally, the cell growth was monitored online with the Cell Growth Quantifier (CGQ; Aquila Biolabs, Baesweiler, Germany). The biomass concentration is given as cell dry weight (CDW) calculated from the OD_{600} using the correlation equation CDW [g L^{-1}] = 0.5381*OD_{600} + 0.0074.

Analysis of γ-PGA

The production of γ-PGA was analyzed with a cetyltrimethylammonium bromide (CTAB) assay. To purify γ-PGA, the culture broth was centrifuged for 30 min (10,000*g*, 4°C) to separate the cells. The double amount of ethanol was added to 15 mL of supernatant containing γ-PGA to precipitate the γ-PGA (1:2 ratio, sample:ethanol). The solution was incubated at 4°C overnight. By centrifugation for 10 min at 4°C and 10,000*g*, the precipitated γ-PGA was recovered as a pellet. The pellet was resuspended in 1 mL distilled water. The addition of 100 μL 0.07 M CTAB in 2% (w/v) NaOH to 100 μL of γ-PGA sample led to the precipitation of the γ-PGA/CTAB complex resulting in an increased turbidity that was measured in a plate reader (Synergy Mx plate reader, BioTek Instruments, Inc., Winooski, United States) at 400 nm. A calibration curve using a 1 MDa γ-PGA standard [(Henkel AG & Co., KGaA, Düsseldorf, Germany] was used to calculated the γ-PGA concentration in the culture broth. γ-PGA samples were diluted for the CTAB assay to reach the linear range of the assay up to 0.1 g/L γ-PGA (equaling a turbidity of <0.5).

Sample Preparation for Metabolome Analysis

A sample volume which satisfies the equation sampling volume (mL) *OD_{600} = 5 was filtered with a PVDF filter (pore size 0.45 mm; Merck Millipore, Burlington, NJ, United States) using vacuum. The filter was washed with the doubled amount of 300 mM NH_4HCO_3 (1:2 ratio, sample: NH_4HCO_3). Subsequently, the metabolism was quenched by soaking the filter in liquid N_2. The filter was transferred to a 2 mL sample tube and was stored at −80°C until metabolite extraction. To extract the metabolites, 1.875 mL of extraction solvent (1:2:2 ratio, H_2O:MeOH:chloroform, including 7 nM 10-camphorsulfonic acid as internal standard) was added to the sample tube including the filter. After vortexing, the sample tube was centrifuged at 16,000 *g* for 3 min at 4°C. 350 μL of the supernatant were transferred to a 1.5 mL sampling tube, concentrated by vacuum centrifugation for 2 h and freeze dried overnight. The pellet was stored at −80°C until analyzed by LC-MS.

Ion-Pair-LC/MS/MS Analysis

The dried sample is resuspended in 50 μL ultra-pure water and is transferred into a conical glass vial. The Ion-pair-liquid chromatography coupled with tandem mass spectrometry (LC/MS/MS) analysis was performed using a Shimadzu Nexera UHPLC system coupled with an LCMS 8030 Plus device (Shimadzu Co., Kyoto, Japan). The system was equipped with a PE capped CERI L-column 2ODS column (2.1 mm × 150 mm, particle size 3 mm, Chemicals Evaluation and Research Institute, Tokyo, Japan). As mobile phase a gradient of a mixture of solvent A and B is used, where solvent A is 10 mM tributylamine and 15 mM acetate in ultra-pure water and solvent B is pure methanol. The flow rate was set to 0.2 mL min^{-1}. For gradient elution of metabolites, starting from 0% concentration of solvent B, the concentration of B was increased to 15% after 1 min with a gradient of 30% min^{-1}, hold for 1.5 min, increased to 50% within 5 min and subsequently increased to 100% within 2 min. The 100% solvent B concentration was held for 1.5 min, decreased to 0% from 11.5 min on and held at this concentration for 8.5 min. The column oven temperature was set to 45°C. The MS parameters were as follows: probe position, þ1.5 mm; desolvation line temperature, 250°C; drying gas flow, 15 L/min; heat block temperature, 400°C; and nebulized gas flow, 2 L/min. As a Quality Control (QC) sample, 2 μL of each analyzed sample of a batch were pooled into a vial. For each sample (including the QC sample), 3 μL were injected to the ion-pair-LC/MS/MS for metabolite analysis.

Data Processing and Analysis

The calculation of the peak area was carried out using MRMPROBS ver. 2.38 and manual inspection of the chromatogram was conducted. The data was normalized

according to the peak area of the internal standard, 10-camphorsulfonic acid. SIMCA 13 (Umetrics, Umeå, Sweden) was used for principal component analysis (PCA) and partial least squares projection to latent structures (PLS) analysis.

RESULTS

To identify metabolites that are highly correlated with γ-PGA production from glucose in *B. subtilis*, intracellular metabolite measurements for strains with varying γ-PGA synthesis rates were carried out. The variation in γ-PGA synthesis rate was achieved by two approaches. First, the expression of the γ-PGA synthetase was controlled by constitutive promoters of different strengths. The promoter strength was determined by fluorescence measurements using *gfp* as reporter gene. Second, the inducible P_{xyl} promoter naturally controlling the *xylAB* operon of *B. subtilis* for xylose utilization was employed. The increase in expression of the xylose promoter correlates positively with the xylose concentration in the medium.

Integration of Promoter Variants for *pgs* Genes and γ-PGA Production

For the promoter library approach, three newly identified promoter variants based on the P_{veg} promoter were successfully integrated upstream of the *pgs* genes to control the expression of γ-PGA synthetase and subsequently to vary the γ-PGA production rate. The variants were constructed by changing the -35 box sequence of the P_{veg} promoter (TTGACA). The promoter variants differ from the original P_{veg} promoter in one or two positions. For variant PV35.01 (AAGACA), two positions were varied. The large deviation from the consensus sequence resulted in only 10% of the original activity. The change of G to T in the third position decreased the activity by 50 percent in variant PV35.3. Variant PV35.26 (GTGACA) exhibits an increased activity of 120% compared to the original promoter.

Growth of the created strains was tested by online growth measurements (CGQ) to observe possible influence of higher γ-PGA synthetase expression rates. As shown in **Figure 1**, the growth curves did not differ significantly. Independent from the promoter activity for *pgs*, all strains grew to comparably high optical densities.

The titer of γ-PGA production as analyzed by the CTAB assay (**Figure 2B**) increased with an increasing promoter activity, determined in the BioLector assay (**Figure 2A**). Hence, the γ-PGA synthesis rate increases with the activity of the promoter controlling the γ-PGA synthetase expression.

Metabolome Analysis to Reveal Key Metabolites

The created strains harboring newly generated promoter sequences with different strength were subjected to metabolome analysis to reveal key metabolites that are most correlated with γ-PGA synthesis. For metabolome analysis according to previous studies (Mitsunaga et al., 2016; Fathima et al., 2018), 93 metabolites were detected that are part of the central carbon metabolism including pentose phosphate pathway (PPP), tricarboxylic acid cycle (TCA), and glycolysis intermediates as well as amino acids and nucleotides. The samples were taken after 8 h during exponential growth. The differing γ-PGA concentrations for the tested strains at this time point demonstrate varying γ-PGA synthesis rates. The metabolome data were subjected to partial least square (PLS) analysis (**Figure 3**). The horizontal separation corresponds to the increasing γ-PGA production from left (low value for PC1) to right (high value for PC1) with R^2 and Q^2 of 0.98 and 0.87, respectively. Metabolites that exhibit loading values higher than 0.1, are shown in **Figure 3D**. Here, negative values correspond to metabolites decreasing with increasing γ-PGA production and metabolites with positive values are increased for higher γ-PGA synthesis rates.

The metabolites with high loading value originate from various metabolic pathways. The most striking loading data for metabolites from the central carbon metabolism is the data for ribose-5-phosphate (R5P), pyruvate, and dihydroxyacetone phosphate (DHAP) with negative values as well as acetyl-CoA with a positive value. Notably, the direct precursors for γ-PGA, glutamate and 2-oxoglutarate hardly change in concentration (loading values of 0.098 and 0.032, respectively). Homeostasis of these metabolites might be explained with their prominent functions in carbon and nitrogen metabolism. While other amino acids such as phenylalanine are increased other amino acids such as serine are lower concentrated during increased γ-PGA production. Serine and R5P are two metabolites which are directly derived from glycolysis intermediates, 3-phosphoglycerate and glucose-6-phosphate (G6P), respectively. The decrease in the metabolite concentrations of serine and R5P can therefore be explained by the higher demand for carbon flux through glycolysis toward the TCA cycle and glutamate. The higher flux toward glutamate is also displayed in the decreased synthesis of precursors for secondary metabolites

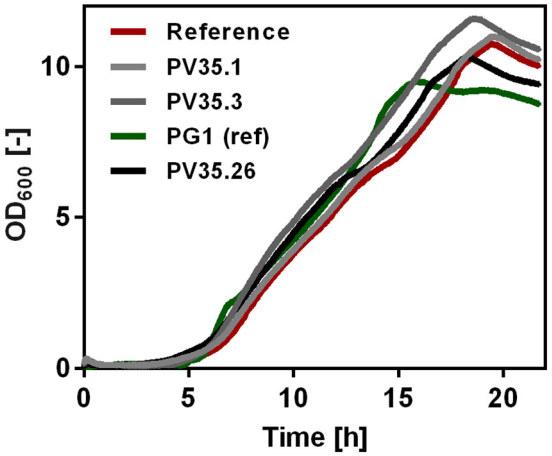

FIGURE 1 | Growth of non-γ-PGA producing *Bacillus subtilis* (reference) and γ-PGA producing *B. subtilis* PV35.1, PV35.3, PG1, and PV35.26. The optical density was determined using the Cell Growth Quantifier (CGQ, Aquila Biolabs, Baesweiler, Germany). The mean of triplicates is shown without standard deviation.

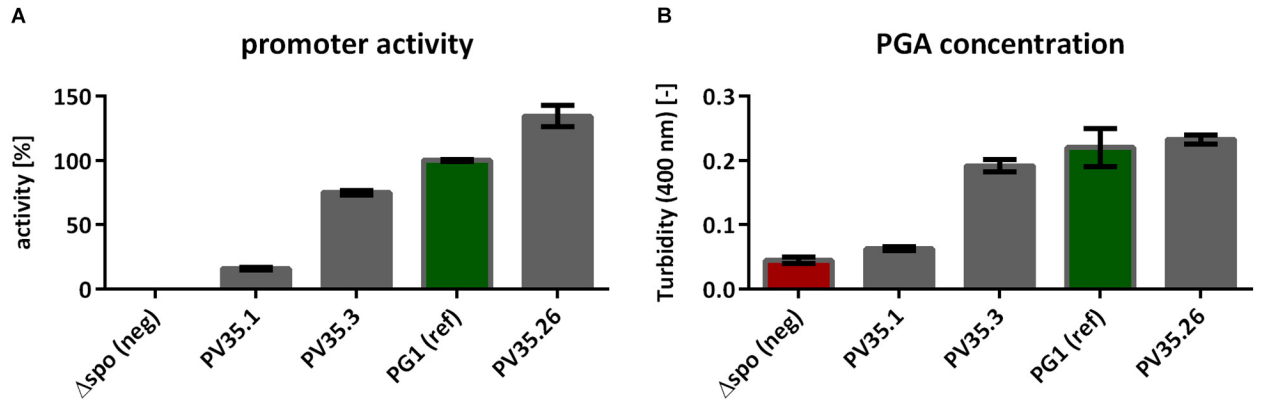

FIGURE 2 | CTAB Assay to determine the γ-PGA concentration based on the measured turbidity. The strains tested were the non-γ-PGA producing negative control *B. subtilis* Δspo and the created strains PV35.1, PV35.3, and PV35.26 with different promoter activities for the *pgs* genes **(A)**. The γ-PGA production was determined during the exponential growth phase (after 9 h, compare **Figure 1**) using the CTAB assay **(B)**. The promoter activity was calculated from the slope between fluorescence and biomass as determined by the BioLector. The error bars represent the standard deviation.

such as xanthosine 5′-phosphate (XMP). Contrary to the XMP concentration, the acetyl-CoA concentration increases with higher promoter activity. As it was shown for the comparison of a non-γ-PGA producer and a γ-PGA-producer *B. subtilis* PG1, the TCA activity is limiting the precursor supply for γ-PGA production. Meyer et al., demonstrated that citrate synthase, aconitase, and malate dehydrogenase form a protein complex catalyzing sequential reactions of the TCA cycle (Meyer et al., 2011). Additionally, the 2-oxoglutarate dehydrogenase complex and the glutamate synthase are affected by these protein-protein interactions (Meyer et al., 2011). The concentration of succinyl-CoA increases for increasing γ-PGA synthesis rates. With regard to the interaction of TCA cycle enzymes, the higher flux toward 2-oxoglutarate and glutamate likely additionally results in increased succinyl-CoA concentrations. Hence, the metabolome data suggests an increased TCA cycle activity yet being a limiting step for higher γ-PGA production from glucose as sole carbon source. The decreased concentration of R5P for higher promoter activity is surprising with respect to the glucose-6-phosphate dehydrogenase reaction, which is known as main reaction for the supply of NADPH. NADPH is used as cofactor for glutamate synthesis. Therefore, a higher demand for glutamate under γ-PGA producing conditions also results in a higher demand for NADPH. Here, the high positive loading values for both NAD^+ and $NADP^+$ are remarkable, too. Since the applied metabolite extraction method is not suitable for investigating the redox status of the cells, the increasing NAD^+ concentrations are likely due to a higher demand for NAD(P)H for increasing glutamate *de novo* synthesis.

Inducible Promoter

Besides controlling the synthetase expression using a promoter library, the expression was also altered using an inducible promoter. The xylose-inducible promoter P_{xyl} controlling the expression of the *xylAB* operon in *B. subtilis* was cloned to control *pgs* expression in *B. subtilis* PG10. The xylose promoter in *B. subtilis* PG10 contained the binding site for the xylose regulator XylR, but not the binding site for catabolite repression via CcpA. These features enabled the induction of the promoter by xylose addition and prevented the repression during growth on glucose. Moreover, the *xylAB* operon was deleted to ensure that xylose is only used as inducer and not as substrate for cell growth. In *B. subtilis*, xylose is imported via the L-arabinose permease encoded by *araE*. The *araE* expression is reported to be arabinose induced and glucose repressed (Sa Nogueira and Ramos, 1997). However, *B. subtilis* Δspo that was used to create the strains in this study grows on xylose without addition of arabinose. Hence, the xylose uptake of the strains used in this study was shown not to depend on arabinose availability. As expected, γ-PGA production increased with increasing xylose concentration (**Figure 4**). Comparable to the promoter library, a higher synthetase concentration leads to a higher γ-PGA production rate. Controls were the non-γ-PGA producing *B. subtilis* Δspo as well as the *B. subtilis* Δ*xylAB* used to create PG10, which cannot grow on xylose. In comparison to the promoter library approach, *B. subtilis* PG10 exhibits a lower growth rate (0.43 h^{-1} compared to 0.59 h^{-1}). Moreover, the γ-PGA production rate at full induction is higher for the xylose inducible promoter compared to the production rate of the strongest promoter from the library. The determined γ-PGA titers were used to correlate the xylose concentration with γ-PGA production (**Figure 4**). A logarithmic dependency between the γ-PGA production as represented by the turbidity and the inducer concentration was determined. Since saturation of the production rate was observed for xylose concentrations higher than approximately 100 mM, further concentrations ranging from 0 mM to 50 mM were used for the metabolome analysis to create more variation in the production rate.

For metabolome analysis, intracellular metabolites for 13 conditions (*B. subtilis* Δ*xylAB* with 0 and 200 mM xylose as controls, *B. subtilis* PG10 with 0, 1, 5, 10, 15, 25, 40, 50, 80, 100, and 200 mM xylose) were analyzed. For each strain and condition, the intracellular concentration of 77 metabolites

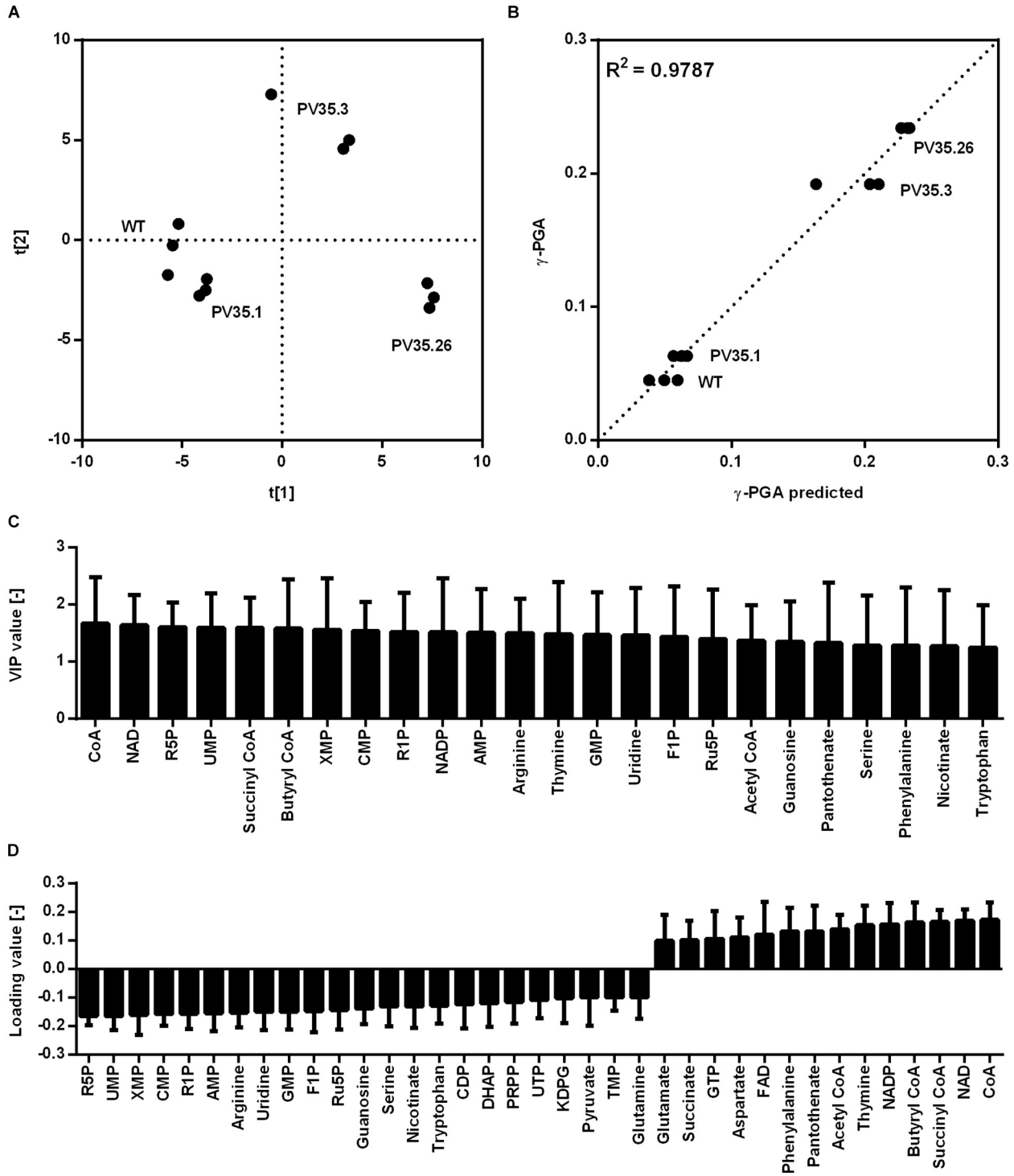

FIGURE 3 | Partial least squares projection to latent structures (PLS) analysis for γ-PGA producing strains based on a promoter library. The analysis was carried out for the non-γ-PGA producing reference (WT) and strains with newly generated promoters PV35.1, PV35.3, and PV35.26 controlling *pgs* expression. Biological triplicates for each strain were cultivated in glucose minimal medium. Samples for analysis were taken during the exponential phase (9 h). The separation according to the metabolom analysis **(A)**, the observed versus predicted γ-PGA values **(B)**,the VIP values **(C)**, and loading values **(D)** for metabolites highly connected to γ-PGA production are shown. The loading data for metabolites with loading values >0.1 are shown whereas negative values correspond to metabolites decreasing with increasing γ-PGA production and metabolites with positive values are increased for higher γ-PGA. ADP, adenosine 5′-diphosphate; AICAR 5′-phosphoribosyl-5-amino-4-imidazolecarboxamide; AMP, adenosine 5′-monophosphate; DHAP, dihydroxyacetone phosphate; G6P, glucose-6-phosphate; KDPG, 2-Keto-3-deoxy-6-phosphogluconate; IMP, Inosine 5′-monophosphate; MEP, methylerythritol 4-phosphate; PRPP, 5-phospho-alpha-D-ribose 1-diphosphate; R1P, ribose-1-phosphate; R5P, ribose-5-phosphate; SBP, sedoheptulose 1,7-bisphosphate; UDP-Glc, uridine 5′-diphosphate-glucose; XMP, xanthosine 5′-phosphate.

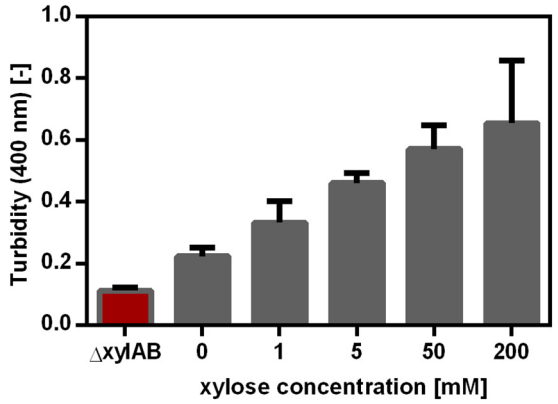

FIGURE 4 | γ-PGA synthesis as a function of xylose concentration for *B. subtilis* PG10. The γ-PGA concentration was determined by the CTAB Assay and is shown as the turbidity at 400 nm. The strains tested were the non-γ-PGA producing negative control *B. subtilis* Δ*xylAB* and *B. subtilis* PG10 with five different xylose concentrations as inducer for *pgs* gene expression. The γ-PGA production was determined during the exponential growth phase (after 9 h, compare **Figure 1**) for biological triplicates. The error bars represent the standard deviation.

was determined. The γ-PGA production was calculated based on the correlation between turbidity and xylose concentration obtained from **Figure 4**. Based on the obtained values for γ-PGA production under the investigated cultivation conditions, a PLS analysis was carried out (**Figure 5A**). The PLS analysis resulted in a model with R^2 of 0.92 and Q^2 of 0.87 (see **Figure 5B**). The samples were separated in t[1] according to the γ-PGA production rate.

Analogously to the promoter library, metabolites with varying concentrations for differing γ-PGA production rates could be identified (**Figure 5**). The metabolite concentrations with loading values higher than 0 increase with an increasing production rate. Comparing the two approaches for controlling the γ-PGA production rate, the promoter library and the xylose induction, the identified metabolites with high loading values partly differ. This fact is most likely caused by differences in growth rates and γ-PGA production rates for both approaches. Differences in metabolic demand (Koebmann et al., 2005) result in changes of metabolic fluxes and, hence, in metabolite concentrations. Changes in flux distribution have also been observed due to differing pH of the growth media and a negative correlation between acetoin and 2,3-butandiol and γ-PGA production was reported (Zhu et al., 2013). Regardless of the differences between the two approaches, several amino acids exhibit increased concentrations in both approaches. Especially phenylalanine increased with increasing promoter strength as well as increasing inducer concentration.

Further, for the xylose induction approach mostly metabolites that accumulate for higher γ-PGA production rates were identified. In this approach, the increase in γ-PGA production rate is interconnected with a slight increase in growth rate (**Figure 6**). Here, phosphoenolpyruvate (PEP) is the metabolite exhibiting the highest correlation with γ-PGA production. The PEP concentration follows the increasing trend of both γ-PGA production rate and growth rate for increasing xylose induction strength. Besides PEP, further intermediates of the central carbon metabolism increase simultaneously with the γ-PGA production rate. Several metabolites originating from glycolysis, pentose phosphate pathway and TCA cycle like G6P, R5P and 2-oxoglutarate belong to the group of metabolites with high loading values. Hence, the increased metabolite concentrations are likely due to an increased overall carbon flux and not directly due to the γ-PGA production rate. However, the higher γ-PGA production rate with increasing xylose concentration increases the demand for a higher flux through the metabolism resulting in higher glucose uptake rates as indicated by the increasing G6P concentrations. Among the metabolites that are negatively related to the higher γ-PGA production rate, glutamine is the most striking one. Since glutamine is a substrate for *de novo* synthesis of glutamate from glucose, its concentration is strongly connected to the demand for glutamate. The increasing demand for glutamate with higher γ-PGA production also influences the proline and NADP concentrations as indicated by the loading values of these metabolites. Succinate is a further metabolite indicating the changes in glutamate demand since the carbon flux at the 2-oxoglutarate branch point can either be directed toward glutamate or succinate. The obtained positive loading value for succinate indicates an increase of the concentration with increasing xylose induction. However, the absolute loading value is low emphasizing a weaker connection of the succinate concentration to the γ-PGA production rate. The comparison of concentrations for 2-oxoglutarate, succinate and glutamate (**Figure 7**) demonstrates the connection. First, the effect of higher overall carbon fluxes can also be seen for these metabolite concentrations. The concentrations of these metabolites increase to a certain extent with higher xylose concentration. While 2-oxoglutarate is increasing for xylose concentrations up to 50 mM, the glutamate and succinate concentrations are already decreasing from 25 and 10 mM on. Therefore, the positive loading value for succinate is mostly reasoned in the small concentration for the reference and increasing concentration for low xylose concentrations up to 10 mM. Additionally, the concentrations of the three metabolites at the 2-oxoglutarate branch point reflect the increasing carbon flux to glutamate for stronger induction. This effect is emphasized by the fact that succinate starts decreasing for weaker induction than glutamate. The metabolite measurement results match the increasing growth rate and γ-PGA production rate for the xylose induction approach suggesting higher metabolic fluxes caused by the demand for glutamate for γ-PGA production.

DISCUSSION

Poly-γ-glutamic acid production with glucose as sole carbon source requires strong flux rerouting in the metabolic network of *B. subtilis*. We studied the metabolic consequences of γ-PGA production using metabolome analysis of the newly generated strains. Several studies reported an increase of γ-PGA titer by the addition of exogenous glutamate (Lin et al., 2016), suggesting *de*

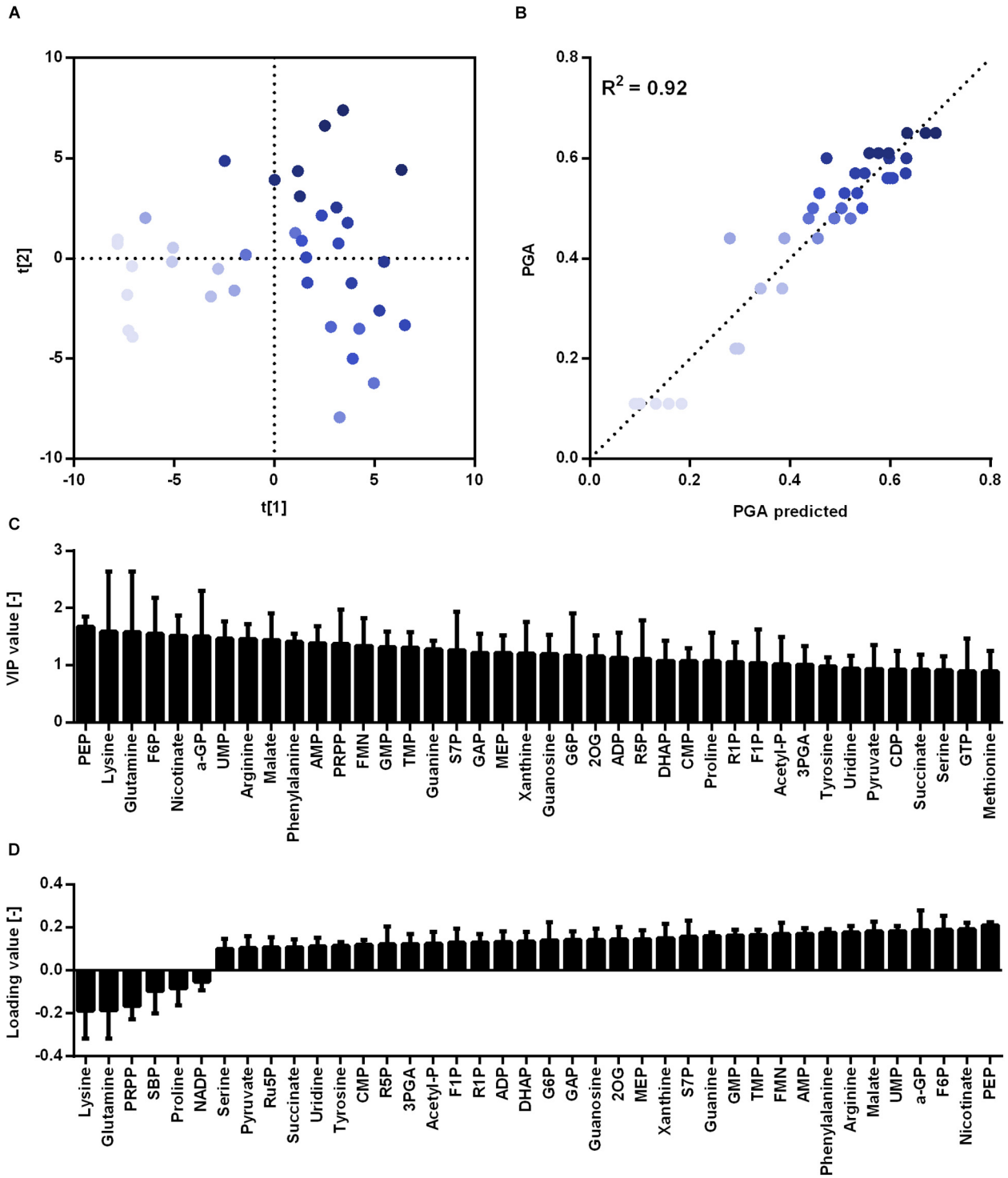

FIGURE 5 | Partial least squares projection to latent structures (PLS) analysis for non-γ-PGA producing *B. subtilis* ΔxylAB and γ-PGA producing *B. subtilis* PG10 with different strength of xylose induction. The separation according to the metabolome analysis **(A)**, the observed versus predicted γ-PGA values **(B)**, the VIP values **(C)** and loading data **(D)** for metabolites highly connected to γ-PGA production rate in xylose induction experiments are shown for different cultivation conditions with varying γ-PGA production rates (*B. subtilis* Δxyl with 0 and 200 mM xylose as controls, *B. subtilis* PG10 with 0, 1, 5, 10, 15, 25, 40, 50, 80, 100, and 200 mM xylose). The intensity of the blue color increases with increasing γ-PGA production rate. ADP: adenosine 5′-diphosphate; AICAR: 5′-phosphoribosyl-5-amino-4-imidazolecarboxamide, AMP: adenosine 5′-monophosphate, G6P: glucose-6-phosphate, IMP: inosine 5′-monophosphate, MEP: methyerythritol 4-phosphate, PRPP: 5-phospho-alpha-D-ribose 1-diphosphate, R1P: ribose-1-phosphate, R5P: ribose-5-phosphate, SBP: sedoheptulose 1,7-bisphosphate, UDP-Glc: uridine 5′-diphosphate-glucose, XMP: xanthosine 5′-phosphate.

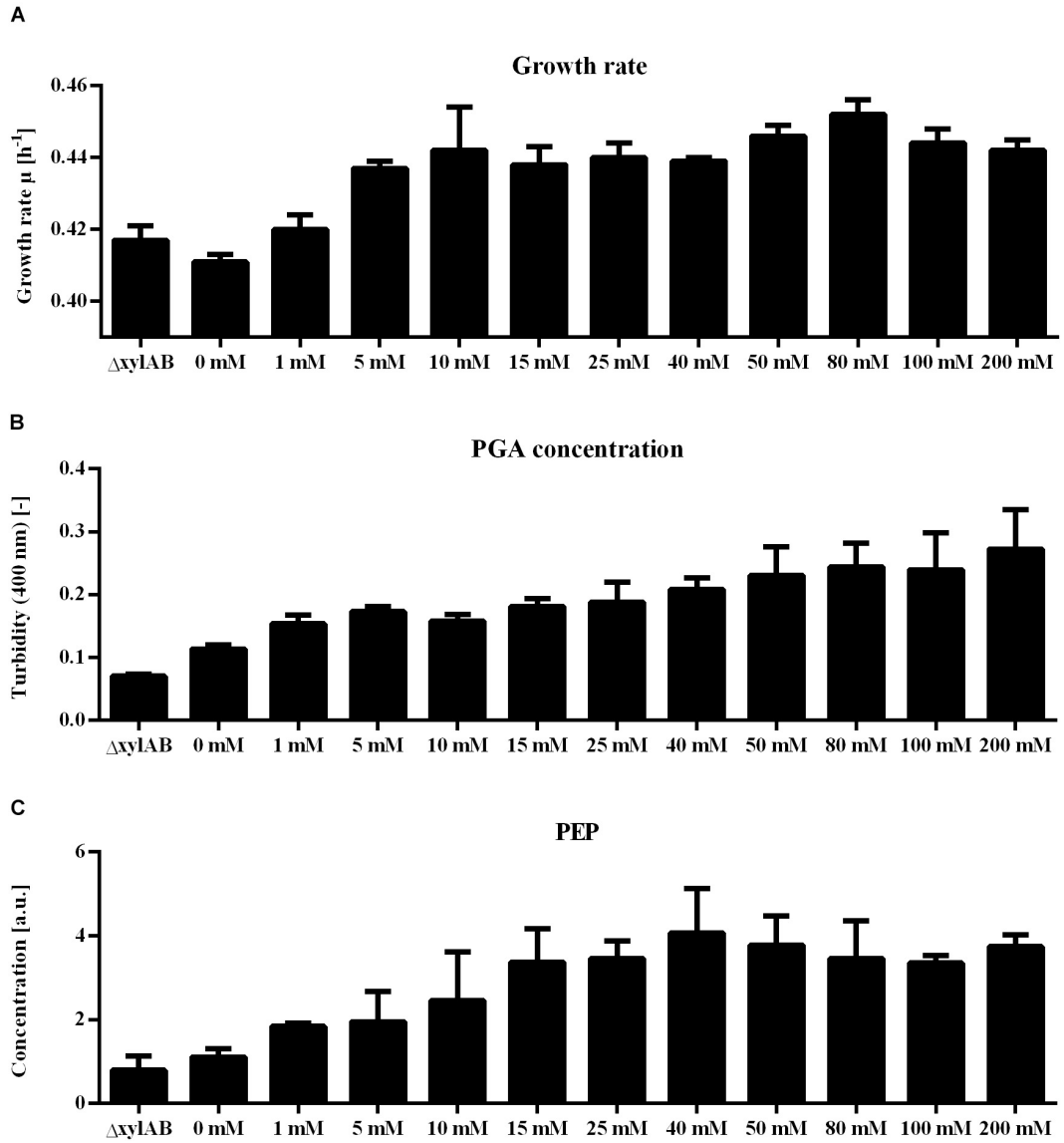

FIGURE 6 | Phenotypic analysis of non-γ-PGA producing *B. subtilis* ΔxylAB and γ-PGA producing *B. subtilis* PG10 with different strength of xylose induction. The analysis of growth rates **(A)**, γ-PGA production **(B)** and intracellular phosphoenolpyruvate (PEP) concentration **(C)** are shown for different cultivation conditions with varying γ-PGA production rates (*B. subtilis* Δxyl with 0 mM xylose as control, *B. subtilis* PG10 with 0, 1, 5, 10, 15, 25, 40, 50, 80, 100, and 200 mM xylose).

novo glutamate synthesis as bottleneck for γ-PGA production. Yao et al. (2010) investigated the origin of carbon in γ-PGA using 13C-labeled glucose and L-glutamate as carbon sources for a *B. subtilis* producer. Maximal 9% of the γ-PGA was derived from glucose. For the efficient use of glucose as sole carbon source, the metabolic bottlenecks limiting γ-PGA production need to be determined. Here, *B. subtilis* strains with varying γ-PGA production rates were subjected to metabolome analysis to identify possible bottlenecks.

The strength of γ-PGA synthetase expression was varied by two approaches: a library of constitutive promoters with differing expression strength and a xylose-inducible promoter that allowed titrating of expression strength. Notably, as the growth rate and PGA synthesis rate of *B. subtilis* differed between the different approaches, the metabolome analyses differed. Several metabolites like R5P were positively correlated during xylose induction while negatively correlated with increasing constitutive *pgs* expression using the promoter library. Especially the concentration of R5P was previously shown to increase with increasing growth rate as the RNA synthesis rate correlates positively with the growth rate. In eukaryotic cells, the intracellular R5P concentration was reported to influence the rate of *de novo* purine synthesis (Pilz et al., 1984). A higher synthesis rate of purine is interconnected with a higher growth rate since the RNA synthesis rate increases with the growth rate. Even the rate of glycolysis is partially controlled by the R5P concentration

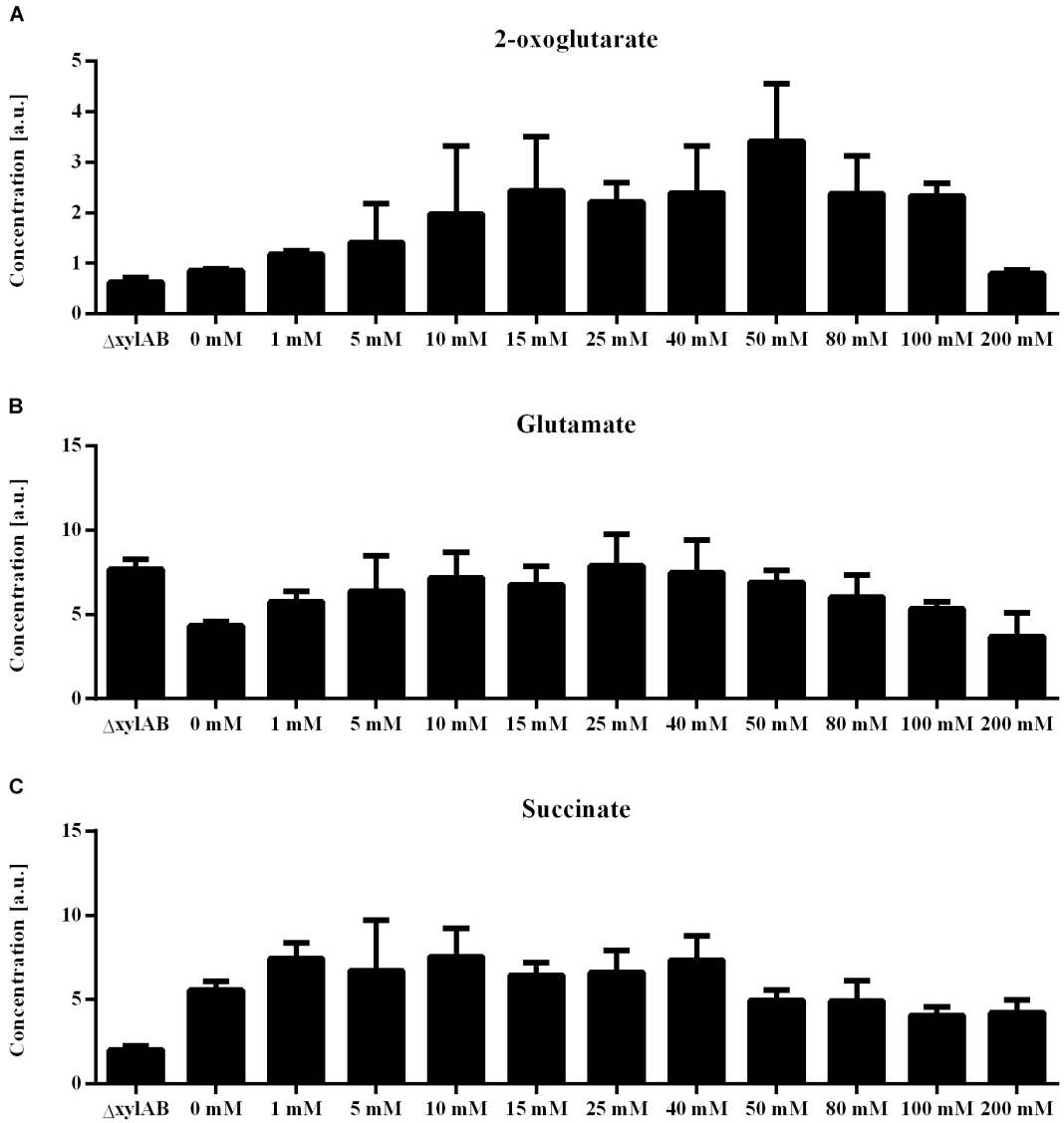

FIGURE 7 | Metabolite concentrations for non-γ-PGA producing *B. subtilis* ΔxylAB and γ-PGA producing *B. subtilis* PG10 with different strength of xylose induction for metabolite extraction during the exponential growth phase. The intracellular concentrations of 2-oxoglutarate **(A)**, glutamate **(B)**, and succinate **(C)** are given for different cultivation conditions with varying γ-PGA production rates (*B. subtilis* Δxyl with 0, and 200 mM xylose as controls, *B. subtilis* PG10 with 0, 1, 5, 10, 15, 25, 40, 50, 80, 100, and 200 mM xylose).

via the activity of pyruvate kinase in *B. licheniformis* (Tanaka et al., 1995) and *E. coli* (Waygood et al., 1975). The enzyme is activated by high R5P concentrations resulting in a higher flux through glycolysis when R5P accumulates (Sakai et al., 1986). Influencing the flux through glycolysis and the growth rate, the increasing R5P concentrations observed for higher inducer concentrations is in line with the suggestion of increasing overall fluxes. Notably, the growth rate is concurrently increasing with the γ-PGA production rate (**Figure 6**). The increasing demand for glutamate results in a higher total carbon flux. A higher growth rate is mostly connected with a higher glucose uptake rate as reflected by the increasing G6P concentrations for higher xylose induction. This positive correlation between metabolite concentration and γ-PGA production rate was not unique for R5P. These results suggest that metabolism is reacting on the increased demand for glutamate by increasing overall flux. However, besides the γ-PGA production rate the growth rate is also increasing. Based on these results, a higher γ-PGA production using this chassis might be achieved by limiting the growth rate, while maintaining or even further increasing the rate of γ-PGA production.

For the promoter library, the γ-PGA titers were lower compared to the values obtained from the xylose inducible promoter. Also, with increasing expression and hence increasing PGA production the growth rate did not differ. For the constitutive promoters, the changes in metabolite concentrations

can be solely attributed to the change in γ-PGA production. Besides the already discussed R5P further metabolites like serine and DHAP exhibited negative loading values, indicating a negative correlation of metabolite concentration and PGA production. Like R5P, serine is also known to allosterically control the pyruvate kinase activity (Amelio et al., 2014). The decreasing concentrations of both serine and R5P might therefore lead to a decreasing flux through glycolysis. However, acetyl-CoA is accumulating at higher γ-PGA production rates (**Figure 3C**). Acetyl-CoA is a substrate of the citrate synthase encoded by *citZ* (Fletchner and Hanson, 1969). The accumulation of acetyl-CoA suggests that the activity of the citrate synthase is limiting glutamate synthesis. Regardless of the γ-PGA production rate, the glutamate concentration was detected to be constant. In *B. subtilis*, the glutamate concentration is controlled by six regulator proteins (Sonenshein, 2007). As glutamate is a key metabolite in the carbon and nitrogen metabolism of the cell, the homeostatic glutamate concentration is beneficial for the cell. But the higher demand for glutamate is reflected in changes of metabolite concentrations that are not necessarily precursors for glutamate synthesis.

The metabolome analysis revealed that many nucleotides and intermediates of the purine metabolism are inversely related to the γ-PGA synthesis rate. In bacteria, nucleotides are known to participate in cell signaling and regulation as second messengers (Kalia et al., 2013). Moreover, the mentioned nucleotides are precursors for the synthesis of secondary metabolites. *B. subtilis* is especially known for industrial production of riboflavin (Perkins et al., 1999). The decreasing concentrations of intermediates from the purine pathway might therefore also be caused by the higher demand for carbon flux toward glutamate instead of other cellular products. Further direction of the carbon flux for γ-PGA synthesis might be achieved by limiting the ability of the strain to produce metabolites derived from purine metabolism.

The amino acids arginine, glutamine and proline are derived from glutamate, and therefore their synthesis is competing with γ-PGA production. The constant glutamate level during higher glutamate consumption resulted in decreased concentrations of the amino acids derived from glutamate. While arginine decreases for the promoter library approach, proline and glutamine have been determined as metabolites with negative loading values for the inducible promoter approach. But these three amino acids are involved in different regulatory systems. The global regulator of nitrogen metabolism in *B. subtilis*, TnrA, senses nitrogen availability based on the level of glutamine. TnrA forms a complex with the glutamine synthetase (Wray et al., 1996, 2001). It represses the glutamate synthase and glutamine synthetase genes. Hence, the decreasing glutamine concentration enables a higher glutamate synthase activity. During the conversion of arginine to glutamate, ornithine is formed as an intermediate. High ornithine concentrations activate the RocR protein (Belitsky and Sonenshein, 1999). In the *B. subtilis* genome the glutamate dehydrogenase *rocG* is located upstream of the *rocABC* operon which is involved in arginine-ornithine-proline metabolism (Gardan et al., 1997). The *rocG* gene is co-regulated with the *rocABC* operon by binding of the RocR regulator. Hence, RocR increases the glutamate dehydrogenase expression. This enzyme converts glutamate to 2-oxoglutarate. For higher γ-PGA production with the inducible promoter, arginine and proline exhibit reduced concentrations. These decreasing concentrations most likely also result in decreased ornithine concentrations since ornithine is an intermediate in arginine and proline synthesis. As a result of decreased ornithine concentrations, the glutamate dehydrogenase activity decreases. The decreased glutamate dehydrogenase activity limits the decrease in glutamate concentration even for higher γ-PGA production rates.

Glutamate *de novo* synthesis requires NADPH as a cofactor of glutamate synthase. The main NADPH supplying reactions are found in the pentose phosphate pathway (Zamboni et al., 2004). Metabolite analysis revealed higher concentrations for $NAD(P)^+$ with increasing γ-PGA production rate for strains with the constitutive promoter. While the analysis method does not detect the actual redox status in the cell, the increasing total concentration of $NAD(P)^+$/NAD(P)H points out the enhanced demand for redox equivalents for the production of γ-PGA.

Succinyl-CoA exhibits a highly positive loading value for the promoter library approach. In the TCA cycle, 2-oxoglutarate is converted to succinyl-CoA by the 2-oxoglutarate dehydrogenase. The increasing glutamate consumption requires a higher flux from glucose to 2-oxoglutarate. Since the branch point of 2-oxoglutarate and its conversion to glutamate is tightly regulated, the increasing succinyl-CoA concentration is likely caused by increasing fluxes to 2-oxoglutarate that are not completely directed to glutamate but also to succinyl-CoA.

High titer γ-PGA production mostly involves a mixture of carbon sources like glycerol, citrate, and glutamate as provided in medium E commonly used for γ-PGA production (Leonard et al., 1958). γ-PGA production cost can be reduced by utilization of glucose as sole carbon source. However, in *B. licheniformis* metabolome analysis revealed the limitation of γ-PGA synthetase expression when glucose is used as carbon source instead of glycerol (Mitsunaga et al., 2016). In this study, the γ-PGA synthesis was independent from the native expression regulation by integration of a constitutive and inducible promoter. Aiming at an inexpensive γ-PGA production, the provided information will be used to guide metabolic engineering for improved γ-PGA production from glucose as sole carbon source in further studies.

DATA AVAILABILITY STATEMENT

All datasets generated for this study are included in the article/**Supplementary Material**.

AUTHOR CONTRIBUTIONS

BH and LB conceived and designed the study. SP and EF contributed to the design and data analysis of metabolomics experiments. BH performed the experiments and drafted the manuscript. LB, SP, and EF revised the manuscript and approved the final manuscript.

FUNDING

This work was funded by the Deutsche Forschungsgemeinschaft (DFG) within the International Research Training Group 1628, "Selectivity in Chemo- and Biocatalysis (SeleCa)."

SUPPLEMENTARY MATERIAL

The Supplementary Material for this article can be found online at: https://www.frontiersin.org/articles/10.3389/fbioe.2020.00038/full#supplementary-material

REFERENCES

Alper, H., Fischer, C., Nevoigt, E., and Stephanopoulos, G. N. (2005). Tuning genetic control through promoter engineering. *Proc. Natl. Acad. Sci. U.S.A.* 102, 12678–12683. doi: 10.1073/pnas.0504604102

Amelio, I., Cutruzzola, F., Antonov, A., Agostini, M., and Melino, G. (2014). Serine and glycine metabolism in cancer. *Trends Biochem. Sci.* 39, 191–198.

Belitsky, B. R., and Sonenshein, A. L. (1999). An enhancer element located downstream of the major glutamate dehydrogenase gene of *Bacillus subtilis*. *Proc. Natl. Acad. Sci. U.S.A.* 96, 10290–10295. doi: 10.1073/pnas.96.18.10290

Blazeck, J., and Alper, H. (2013). Promoter engineering: recent advances in controlling transcription at the most fundamental level. *Biotechnol. J.* 8, 46–58. doi: 10.1002/biot.201200120

Chalfie, M., Tu, Y., Euskirchen, G., Ward, W. W., and Prasher, D. (1994). Green fluorescent protein as a marker for gene expression. *Science* 263, 802–805. doi: 10.1126/science.8303295

Cormack, B. P., Valdivia, R. H., and Falkow, S. (1996). FACS-optimized mutants of the green fluorescent protein (GFP). *Gene* 173, 33–38. doi: 10.1016/0378-1119(95)00685-0

Cromwick, A. M., Birrer, G. A., and Gross, R. A. (1996). Effects of pH and aeration on γ-poly(glutamic acid) formation by *Bacillus licheniformis* in controlled batch fermentor cultures. *Biotechnol. Bioeng.* 50, 222–227. doi: 10.1002/(sici)1097-0290(19960420)50:2<222::aid-bit10>3.0.co;2-p

Fathima, A. M., Chuang, D., Lavina, W. A., Liao, J., Putri, S. P., and Fukusaki, E. (2018). Iterative cycle of widely targeted metabolic profiling for the improvement of 1-butanol titer and productivity in *Synechococcus elongatus*. *Biotechnol. Biofuels* 11:188. doi: 10.1186/s13068-018-1187-8

Fletchner, V. R., and Hanson, R. S. (1969). Coarse and fine control of citrate synthase from *Bacillus subtilis*. *Biochim. Biophys. Acta* 184, 252–262. doi: 10.1016/0304-4165(69)90027-0

Gardan, R., Rapoport, G., and Debarbouille, M. (1997). Role of the transcriptional activator RocR in the arginine-degradation pathway of *Bacillus subtilis*. *Mol. Microbiol.* 24, 825–837. doi: 10.1046/j.1365-2958.1997.3881754.x

Gärtner, D., Geissendörfer, M., and Hillen, W. (1988). Expression of the *Bacillus subtilis* xyl operon is repressed at the level of transcription and is induced by xylose. *J. Bacteriol.* 170, 3102–3109. doi: 10.1128/jb.170.7.3102-3109.1988

Guiziou, S., Sauveplane, V., Chang, H. J., Clerte, C., Declerck, N., Jules, M., et al. (2016). A part toolbox to tune genetic expression in *Bacillus subtilis*. *Nucleic Acids Res.* 44, 7495–7508. doi: 10.1093/nar/gkw624

Halmschlag, B., Hoffmann, K., Hanke, R., Putri, S. P., Fukusaki, E., Büchs, J., et al. (2020). Comparison of isomerase and Weimberg pathway for γ-PGA production from xylose by engineered *Bacillus subtilis*. *Front. Bioeng. Biotechnol.* 7:476. doi: 10.3389/fbioe.2019.00476

Halmschlag, B., Steurer, X., Putri, S. P., Fukusaki, E., and Blank, L. M. (2019). Tailor-made poly-gamma-glutamic acid production. *Metab. Eng.* 55, 239–248. doi: 10.1016/j.ymben.2019.07.009

Jensen, P. R., and Hammer, K. (1998). Artificial promoters for metabolic optimization. *Biotechnol. Bioeng.* 58, 191–195. doi: 10.1002/(sici)1097-0290(19980420)58:2/3<191::aid-bit11>3.0.co;2-g

Joyce, A. R., and Palsson, B. O. (2006). The model organism as a system: integrating 'omics' data sets. *Nat. Rev. Mol. Cell Biol.* 7, 198–210. doi: 10.1038/nrm1857

Kalia, D., Merey, G., Nakayama, S., Zheng, Y., Zhou, J., Luo, Y., et al. (2013). Nucleotide, c-di-GMP, c-di-AMP, cGMP, cAMP, (p)ppGpp signaling in bacteria and implications in pathogenesis. *Chem. Soc. Rev.* 42, 305–341. doi: 10.1039/c2cs35206k

Koebmann, B., Solem, C., and Jensen, P. R. (2005). Control analysis as a tool to understand the formation of the las operon in *Lactococcus lactis*. *FEBS J.* 272, 2292–2303. doi: 10.1111/j.1742-4658.2005.04656.x

Kuhn, D., Blank, L. M., Schmid, A., and Bühler, B. (2010). Systems biotechnology - rational whole-cell biocatalyst and bioprocess design. *Eng. Life Sci.* 10, 384–397. doi: 10.1002/elsc.201000009

Leonard, C. G., Housewright, R. D., and Thorne, C. B. (1958). Effects of some metallic ions on glutamyl polypeptide synthesis by *Bacillus subtilis*. *J. Bacteriol.* 76, 499–503. doi: 10.1128/jb.76.5.499-503.1958

Lin, B., Li, Z., Zhang, H., Wu, J., and Luo, M. (2016). Cloning and expression of the gamma-polyglutamic acid synthetase gene pgsBCA in *Bacillus subtilis* WB600. *Biomed Res. Int.* 2016:3073949. doi: 10.1155/2016/3073949

Meselson, M., and Yuan, R. (1968). DNA restriction enzyme from *E. coli*. *Nature* 217, 1110–1114. doi: 10.1038/2171110a0

Messing, J., Crea, R., and Seeburg, P. H. (1981). A system for shotgun DNA sequencing. *Nucleic Acids Res.* 9, 309–321.

Meyer, F. M., Gerwig, J., Hammer, E., Herzberg, C., Commichau, F. M., Volker, U., et al. (2011). Physical interactions between tricarboxylic acid cycle enzymes in *Bacillus subtilis*: evidence for a metabolon. *Metab. Eng.* 13, 18–27. doi: 10.1016/j.ymben.2010.10.001

Mitsunaga, H., Meissner, L., Palmen, T., Bamba, T., Büchs, J., and Fukusaki, E. (2016). Metabolome analysis reveals the effect of carbon catabolite control on the poly(γ-glutamic acid) biosynthesis of *Bacillus licheniformis* ATCC 9945. *J. Biosci. Bioeng.* 121, 413–419. doi: 10.1016/j.jbiosc.2015.08.012

Ogawa, Y., Yamaguchi, F., Yuasa, K., and Tahara, Y. (1997). Efficient production of γ-polyglutamic acid by *Bacillus subtilis* (natto) in jar fermenters. *Biosci. Biotechnol. Biochem.* 61, 1684–1687. doi: 10.1271/bbb.61.1684

Ohsawa, T., Tsukahara, K., and Ogura, M. (2009). *Bacillus subtilis* response regulator DegU is a direct activator of pgsB transcription involved in gamma-poly-glutamic acid synthesis. *Biosci. Biotechnol. Biochem.* 73, 2096–2102. doi: 10.1271/bbb.90341

Perkins, J. B., Sloma, A., Hermann, T., Theriault, K., Zachgo, E., Erdenberger, T., et al. (1999). Genetic engineering of *Bacillus subtilis* for the commercial production of riboflavin. *J. Ind. Microbiol. Biotechnol.* 22, 8–18. doi: 10.1038/sj.jim.2900587

Pilz, R., Willis, R., and Boss, G. (1984). The influence of ribose 5-phosphate availability on purine synthesis of cultured human lymphoblasts and mitogen-stimulated lymphocytes. *J. Biol. Chem.* 259, 2927–2935.

Putri, S. P., Nakayama, Y., Matsuda, F., Uchikata, T., Kobayashi, S., Matsubara, A., et al. (2013). Current metabolomics: practical applications. *J. Biosci. Bioeng.* 115, 579–589. doi: 10.1016/j.jbiosc.2012.12.007

Redden, H., Morse, N., and Alper, H. S. (2015). The synthetic biology toolbox for tuning gene expression in yeast. *FEMS Yeast Res.* 15, 1–10.

Sa Nogueira, I., and Ramos, S. S. (1997). Cloning, functional analysis, and transcriptional regulation of the *Bacillus subtilis* araE gene involved in L-arabinose utilization. *J. Bacteriol.* 179, 7705–7711. doi: 10.1128/jb.179.24.7705-7711.1997

Sakai, H., Suzuki, K., and Imahori, K. (1986). Purification and properties of pyruvate kinase from *Bacillus stearothermophilus*. *J. Biochem.* 99, 1157–1167. doi: 10.1093/oxfordjournals.jbchem.a135579

Shih, I.-L., Wu, P.-J., and Shieh, C.-J. (2005). Microbial production of a poly(γ-glutamic acid) derivative by *Bacillus subtilis*. *Process Biochem.* 40, 2827–2832. doi: 10.1016/j.procbio.2004.12.009

Sonenshein, A. L. (2007). Control of key metabolic intersections in *Bacillus subtilis*. *Nat. Rev. Microbiol.* 5, 917–927. doi: 10.1038/nrmicro1772

Tanaka, K., Sakai, H., Ohta, T., and Matsuzawa, H. (1995). Molecular cloning of the genes for pyruvate kinase of two bacilli, *Bacillus psychrophilus* and *Bacillus licheniformis*, and comparison of the properties of the enzymes produced in *Escherichia coli*. *Biosci. Biotechnol. Biochem.* 59, 1536–1542. doi: 10.1271/bbb.59.1536

Tyo, K. E., Alper, H. S., and Stephanopoulos, G. N. (2007). Expanding the metabolic engineering toolbox: more options to engineer cells. *Trends Biotechnol.* 25, 132–137. doi: 10.1016/j.tibtech.2007.01.003

Urushibata, Y., Tokuyama, S., and Tahara, Y. (2002). Difference in transcription levels of cap genes for γ-polyglutamic acid production between *Bacillus subtilis* IF0 16449 and Marburg 168. *J. Biosci. Bioeng.* 93, 252–254. doi: 10.1016/s1389-1723(02)80024-x

Waygood, E. B., Rayman, M. K., and Sanwal, B. D. (1975). The control of pyruvate kinases of *Escherichia coli*. II. Effectors and regulatory properties of the enzyme activated by ribose 5-phosphate. *Chem. J. Biochem. Cell Biol.* 53, 444–454. doi: 10.1139/o75-061

Wenzel, M., and Altenbuchner, J. (2015). Development of a markerless gene deletion system for *Bacillus subtilis* based on the mannose phosphoenolpyruvate-dependent phosphotransferase system. *Microbiology* 161, 1942–1949. doi: 10.1099/mic.0.000150

Wenzel, M., Muller, A., Siemann-Herzberg, M., and Altenbuchner, J. (2011). Self-inducible *Bacillus subtilis* expression system for reliable and inexpensive protein production by high-cell-density fermentation. *Appl. Environ. Microbiol.* 77, 6419–6425. doi: 10.1128/AEM.05219-11

Wray, L. V. J., Ferson, A. E., Rohrer, K., and Fisher, S. H. (1996). TnrA, a transcription factor required for global nitrogen regulation in *Bacillus subtilis*. *Proc. Natl. Acad. Sci. U.S.A.* 93, 8841–8845. doi: 10.1073/pnas.93.17.8841

Wray, L. V. J., Zalieckas, J. M., and Fisher, S. H. (2001). *Bacillus subtilis* glutamine synthetase controls gene expression through a protein–protein interaction with transcription factor TnrA. *Cell* 107, 427–435. doi: 10.1016/s0092-8674(01)00572-4

Yao, J., Xu, H., Shi, N., Cao, X., Feng, X., Li, S., et al. (2010). Analysis of carbon metabolism and improvement of gamma-polyglutamic acid production from *Bacillus subtilis* NX-2. *Appl. Biochem. Biotechnol.* 160, 2332–2341. doi: 10.1007/s12010-009-8798-2

Yoon, S. H., Do, J. H., Lee, S. Y., and Chang, H. N. (2000). Production of poly-γ-glutamic acid by fed-batch culture of *Bacillus licheniformis*. *Biotechnol. Lett.* 22, 585–588.

Zamboni, N., Fischer, E., Laudert, D., Aymerich, S., Hohmann, H. P., and Sauer, U. (2004). The *Bacillus subtilis* yqjI gene encodes the NADP+-dependent 6-P-gluconate dehydrogenase in the pentose phosphate pathway. *J. Bacteriol.* 186, 4528–4534. doi: 10.1128/jb.186.14.4528-4534.2004

Zhu, F., Cai, J., Wu, X., Huang, J., Huang, L., Zhu, J., et al. (2013). The main byproducts and metabolic flux profiling of gamma-PGA-producing strain *B. subtilis* ZJU-7 under different pH values. *J. Biotechnol.* 164, 67–74. doi: 10.1016/j.jbiotec.2012.12.009

Conflict of Interest: The authors declare that the research was conducted in the absence of any commercial or financial relationships that could be construed as a potential conflict of interest.

frontiers in Bioengineering and Biotechnology

ORIGINAL RESEARCH
published: 21 February 2020
doi: 10.3389/fbioe.2020.00047

Metabolic Rearrangements Causing Elevated Proline and Polyhydroxybutyrate Accumulation During the Osmotic Adaptation Response of *Bacillus megaterium*

*Thibault Godard[1], Daniela Zühlke[2], Georg Richter[1], Melanie Wall[1], Manfred Rohde[3], Katharina Riedel[2], Ignacio Poblete-Castro[4], Rainer Krull[1,5,6] and Rebekka Biedendieck[5,7]**

[1] Institute of Biochemical Engineering, Technische Universität Braunschweig, Braunschweig, Germany, [2] Institute of Microbiology, Universität Greifswald, Greifswald, Germany, [3] Central Facility for Microscopy, Helmholtz Centre for Infection Research, Braunschweig, Germany, [4] Biosystems Engineering Laboratory, Center for Bioinformatics and Integrative Biology, Faculty of Life Sciences, Universidad Andres Bello, Santiago, Chile, [5] Braunschweig Integrated Centre of Systems Biology (BRICS), Technische Universität Braunschweig, Braunschweig, Germany, [6] Center of Pharmaceutical Engineering (PVZ), Technische Universität Braunschweig, Braunschweig, Germany, [7] Institute of Microbiology, Technische Universität Braunschweig, Braunschweig, Germany

OPEN ACCESS

Edited by:
Zhi-Qiang Liu, Zhejiang University of Technology, China

Reviewed by:
Trevor Carlos Charles, University of Waterloo, Canada
Rashmi Chandra, University of Waterloo, Canada
Kun Niu, Zhejiang University of Technology, China

***Correspondence:**
Rebekka Biedendieck
r.biedendieck@tu-braunschweig.de

Specialty section:
This article was submitted to Industrial Biotechnology, a section of the journal Frontiers in Bioengineering and Biotechnology

Received: *05 October 2019*
Accepted: *21 January 2020*
Published: *21 February 2020*

Citation:
Godard T, Zühlke D, Richter G, Wall M, Rohde M, Riedel K, Poblete-Castro I, Krull R and Biedendieck R (2020) Metabolic Rearrangements Causing Elevated Proline and Polyhydroxybutyrate Accumulation During the Osmotic Adaptation Response of Bacillus megaterium. Front. Bioeng. Biotechnol. 8:47. doi: 10.3389/fbioe.2020.00047

For many years now, *Bacillus megaterium* serves as a microbial workhorse for the high-level production of recombinant proteins in the g/L-scale. However, efficient and stable production processes require the knowledge of the molecular adaptation strategies of the host organism to establish optimal environmental conditions. Here, we interrogated the osmotic stress response of *B. megaterium* using transcriptome, proteome, metabolome, and fluxome analyses. An initial transient adaptation consisted of potassium import and glutamate counterion synthesis. The massive synthesis of the compatible solute proline constituted the second longterm adaptation process. Several stress response enzymes involved in iron scavenging and reactive oxygen species (ROS) fighting proteins showed higher levels under prolonged osmotic stress induced by 1.8 M NaCl. At the same time, the downregulation of the expression of genes of the upper part of glycolysis resulted in the activation of the pentose phosphate pathway (PPP), generating an oversupply of NADPH. The increased production of lactate accompanied by the reduction of acetate secretion partially compensate for the unbalanced ($NADH/NAD^+$) ratio. Besides, the tricarboxylic acid cycle (TCA) mainly supplies the produced NADH, as indicated by the higher mRNA and protein levels of involved enzymes, and further confirmed by ^{13}C flux analyses. As a consequence of the metabolic flux toward acetyl-CoA and the generation of an excess of NADPH, *B. megaterium* redirected the produced acetyl-CoA toward the polyhydroxybutyrate (PHB) biosynthetic pathway accumulating around 30% of the cell dry weight (CDW) as PHB. This direct relation between osmotic stress and intracellular PHB content has been evidenced for the first time, thus opening new avenues for synthesizing this valuable biopolymer using varying salt concentrations under non-limiting nutrient conditions.

Keywords: *Bacillus megaterium*, osmotic stress adaptation, transcriptomics, proteomics, flux analysis, proline, polyhydroxybutyrate (PHB)

INTRODUCTION

Bacillus megaterium is a big rod-shaped Gram-positive soil bacterium that has been used industrially for decades and whose product portfolio is continuously growing. It includes enzymes such as α- and β-amylases, penicillin G acylase, xylanase, hydrolases, glycosyltransferases, and cytochrome monooxygenases (Vary et al., 2007; Korneli et al., 2013; Lakowitz et al., 2017; Mayer et al., 2019). The bacterium displays several important biotechnological features such as its non-pathogenic character, broad substrate spectrum, high plasmid stability, and high secretion capacity for proteins. The development of efficient expression vectors has driven the emergence of *B. megaterium* as a significant industrial workhorse for recombinant protein production (Rygus and Hillen, 1991; Biedendieck et al., 2007b; Stammen et al., 2010; Biedendieck, 2016). Nevertheless, the limited knowledge of its metabolic adaptation strategies still restricts the detection of corresponding bottlenecks during protein production. However, the recent sequencing of the complete genome of different *B. megaterium* strains and the fast development of related omics-techniques have laid the foundations for an in-depth analysis from gene expression to metabolic fluxes, and opened up new possibilities toward its rational genetic engineering (Biedendieck et al., 2011; Eppinger et al., 2011; Liu et al., 2011; Johnson et al., 2015; Freedman et al., 2018).

Fluctuation in water potential is one of the typical issues with whom bacterial cells have to cope in both their natural environment, during drought and rainy periods, and in industrial bioreactors in which fed substrate, expected product and side-product concentrations are particularly high (Schweder et al., 1999). In the latter case, increased medium osmolarity generates a substantial water efflux from cells, which eventually leads to a reduction of overall bacterial performance through cell dehydration and related impaired metabolism and growth (Korber et al., 1996; Kempf and Bremer, 1998). As water is essential for almost every cellular process from gene translation to protein folding processing, bacteria must be able to restore the cellular water homeostasis in order to survive swiftly. One meaningful way to reduce osmolarity gradients and maintain a suitable cell volume relies on active import, production, and secretion of diverse osmolytes (Kempf and Bremer, 1998; Hoffmann and Bremer, 2017).

Under hyperosmotic stress, bacteria of *Bacillus* species require a variety of molecular and metabolic adjustments for survival. Many studies have described that in *Bacillus subtilis*, *Bacillus cereus*, and *Bacillus licheniformis* adaptation to ionic hyperosmotic stress is a two-step process during which cells first transiently import potassium ions quickly as an initial emergency response to a fast osmotic up-shock before replacing these ions ultimately by organic compounds such as sugars, amino acids, polyols and their derivatives such as betaine and ectoine that do not interfere with cellular physiology and biochemistry. Intracellular accumulation of these compounds, known as compatible solutes or osmoprotectants, to molar concentrations enables water retention and turgor maintenance indispensable for proper cell function during salt stress. The cells either import these compounds or synthesize them *de novo*. Besides their role in compensating osmolarity gradients, they also undertake protecting, stabilizing and catalyzing functions, that make them attractive for industrial applications in fields such as cosmetics, health care and biotechnology (Gröger and Wilken, 2001; Graf et al., 2008; Takagi, 2008; Oren, 2010; Hoffmann et al., 2013; Hoffmann and Bremer, 2017). The global response to salt stress in *Bacillus* species additionally involves various other biological processes such as cell wall modification, iron metabolism and redox balancing (Steil et al., 2003; Höper et al., 2006; den Besten et al., 2009; Hahne et al., 2010; Schroeter et al., 2013).

Here, we studied the impact of osmotic stress on the metabolism of the wild-type *B. megaterium* DSM319 during unlimited growth. The metabolic response of this strain to sustained salt stress (up to 1.8 M NaCl) was characterized combining whole-genome expression, intracellular proteome analyses, intra- and extracellular metabolomics as well as *in vivo* fluxomics of the central carbon metabolism, which together explains the underlying mechanism toward elevated proline and polyhydroxybutyrate content in *B. megaterium* cell.

Abbreviations: 6PG, 6-phosphoglycerate; CDW, cell dry weight; CoA, Coenzyme A; HCPC, hierarchical clustering on principal components; GC-MS, gas chromatography/mass spectrometry; HPLC, high performance liquid chromatography; LC-IMS, liquid chromatography ion mobility spectrometry; MS, mass spectrometry/spectrometer; PCA, principal component analysis; PHA, polyhydroxyalkanoate; PHB, polyhydroxybutyrate; PPP, pentose phosphate pathway; ROS, reactive oxygen species; Ru5P, ribulose-5-phosphate; UPLC, ultra-high performance liquid chromatography.

MATERIALS AND METHODS

Bacterial Strain and Growth Conditions

The wild type strain *B. megaterium* DSM319 used for all experiments was obtained from the German collection of microorganisms and cell cultures (DSMZ, Braunschweig, Germany). Cells were stepwise adapted to each cultivation condition and glycerol stocks (20% v/v) were prepared and stored at −80°C.

For pre-cultures and main cultures, a modified M9 minimal medium derived from Harwood and Cutting (1990) was used containing 5 g L^{-1} of glucose, 1 g L^{-1} of NH_4Cl, 3 g L^{-1} of KH_2PO_4, 500 mg L^{-1} NaCl, 6.7 g L^{-1} of Na_2HPO_4, 1 mg L^{-1} of $MnCl_2{\cdot}4\ H_2O$, 1.7 mg L^{-1} of $ZnCl_2$, 430 μg L^{-1} of $CuCl_2{\cdot}2\ H_2O$, 328 μg L^{-1} of $CoCl_2$, 600 μg L^{-1} of $NaMoO_4{\cdot}2\ H_2O$, 11.1 mg L^{-1} of $CaCl_2$, 30 mg L^{-1} of 3,4-DHB, 13.5 mg L^{-1} of $FeCl_3$ and 120 mg L^{-1} of $MgSO_4$. In addition to the 8.6 mM NaCl present in the M9 medium, up to 1.8 M of NaCl were additionally supplemented to this medium where indicated. For labeling experiments, unlabeled glucose was replaced by 99% 1-^{13}C-glucose or a mixture of 50% U-^{12}C/50% U-^{13}C glucose (Cambridge Isotope Laboratories Inc., Andover, MA, United States) for both the pre-cultures and main cultures, thus ensuring a biomass labeling grade superior to 99.5%. All cultivations were performed at 37°C and at least in triplicates ($n = 3$) as indicated in **Supplementary Material**.

Transcriptome Analysis

RNA extraction and purification were carried out following the protocols proposed by Biedendieck et al. (2011). The RNA concentration was subsequently determined with a NanoDrop (Peqlab Biotechnologie GmbH, Erlangen, Germany) and RNA integrity was assayed using a Bioanalyzer (Agilent Technologies, Böblingen, Germany) according to the manufacturer's instruction. Microarrays were prepared with RNA originating from 4 biological replicates (n = 4), whose RNA integrity number (RIN) were equal to or greater than 9, and designed for dual labeling. First, RNA from reference and evaluated condition were labeled with two different dyes using the "USL Fluorescent labeling kit" according the supplied instructions (Kreatech, Amsterdam, Netherlands). Dye incorporation rate was determined with the NanoDrop. Subsequently, 300 ng of labeled RNA from both conditions were mixed and RNA was further processed using the "Gene Expression Hybridization Kit" (Agilent technologies, Waldbronn, Germany). Then, samples were loaded on an Agilent microarray slide (8 × 15 K custom made) comprising 2–3 60 bp DNA probes for each gene of *B. megaterium* and hybridization took place for 17 h at 65°C and 10 min^{-1} in a hybridization oven (Agilent Technologies, Waldbronn, Germany). Finally, slides were washed with the gene expression wash buffer kit (Agilent Technologies, Waldbronn, Germany) and scanned using the Agilent C scanner associated to its proprietary software Agilent Scan Control 8.4.1 and Feature Extraction 10.7.3.1. Generated data were post-processed in R with Bioconductor for statistical analysis, including an estimation of measurement relevance using analysis of variance (ANOVA) and eliminating aberrant values from the analysis (adjusted p-values > 0.05). All complete experimental data sets were deposited in the GEO database with the accession number GSE110712.

Proteome Analysis

For proteome analysis, cells were collected in the mid-exponential phase and washed with TE-Buffer (10 mM TRIS, 1 mM EDTA, pH 8). Intracellular proteins were then extracted by mechanical cell disruption (3 × 1 min, 6.5 $m{\cdot}s^{-1}$, 4°C, FastPrep® -24, MP Biomedical, Santa Ana, CA, United States) using soda-lime glass beads (20% v/v, 0.038-0.045 mm, Worf Glaskugeln GmbH, Mainz, Germany) and protein concentration was determined (Roti® Nanoquant, Carl Roth GmbH, Karlsruhe, Germany). Prior to measurement by LC-IMS^E, protein extracts were digested with trypsin (Promega, Madison, WI, États-Unis) as described previously (Muntel et al., 2012) and peptide solution was then desalted by stage tip purification using a standard protocol (Rappsilber et al., 2007). For absolute quantification, the peptide mix was spiked with tryptic yeast alcohol dehydrogenase (Waters, Milford, MA, United States) at a final concentration of 50 fmol μL^{-1}.

Peptide separation, identification and quantification were completed using a NanoACQUITY^{TM} UPLC^{TM}-system (Waters, Milford, MA, United States) coupled to a Synapt-G2 mass spectrometer (Waters, Milford, MA, United States). Samples were loaded at a flow rate of 0.3 μL min^{-1} onto an analytical column (nanoACQUITY^{TM} UPLC^{TM} column, BEH130 C18, 1.7 μm, 75 μm/200 mm, Waters, Milford, MA, United States) and separation of peptides for IMS^E was achieved using a 90 min gradient from 5% to 26% buffer B (0.1% acetic acid in acetonitrile). All MS^E analyses were performed as previously described (Muntel et al., 2014), except that the collision energy was alternated between 4 eV in the precursor ion trace and a ramp of 25–45 eV for fragment ion trace. In addition, wave velocity was ramped from 1,000 to 400 m s^{-1} and wave height was set to 40 V.

Collected LC-IMS^E data were imported in the ProteinLynx Global Server 2.5.3-Software (PLGS, Waters, Milford, MA, United States) and further processed with the Apex3D-Algorithmus setting parameters as follows: chromatographic peak width and MS TOF resolution were set to automatic, lock mass charge 2 set to 785.8426 Da/e with a lock mass window of 0.25 Da, low and elevated energy threshold were set at 200.0 and 20.0 counts, respectively, and intensity limit at 750 counts.

Peptide sequence identification was performed with the "ion accounting" algorithm using a randomized Uniprot *B. megaterium* DSM319 database (Version August 2011) comprising all employed laboratory contaminants and the sequence of yeast alcohol dehydrogenase (ADH1 – 10,286 entries). Next criteria were set for positive protein identification: 1 fragment ion matched per peptide, 5 fragment ions matched per protein, 1 peptide matched per protein, 2 missed cleavage allowed, primary digest reagent: trypsin, fixed modification: carbamidomethylation C (+57.0215), variable modifications: deamidation N, Q (+0.9840), oxidation M (+15.9949), pyrrolidone N-TERM (-27.9949). The protein false discovery rate was set to 5%. Only 2 peptide identifications were considered for final analysis. Subsequently, MS data were corrected for detector saturation effects as described earlier (Zühlke et al., 2016).

To ensure statistical relevance, the data were strictly filtered in that only proteins found in at least 2 of 3 biological replicates per time point and 2 of 3 of the corresponding technical replicates were selected for quantification, thus reducing FDR on protein level to less than 0.3%. Finally, determined concentrations were averaged over technical replicates and submitted to a Student's t-test ($p < 0.01$) to estimate the significance of detected modifications of protein concentrations. The mass spectrometry proteomics data have been deposited to the ProteomeXchange Consortium via the PRIDE (Perez-Riverol et al., 2019) partner repository with the dataset identifier PXD015605.

Metabolome Analysis

Intracellular metabolites from the central carbon metabolism were separated by ion exclusion chromatography using a liquid chromatography system (LC, Agilent 1290, Agilent Technologies, Waldbronn, Germany) equipped with a reverse phase column (VisionHT C18 HL, 100 mm × 2 mm I.D., 1.5 μm, Grace, Columbia, MD, United States) and quantified with a triple quadrupole mass spectrometer (QTRAP 5500, AB Sciex, Darmstadt, Germany) equipped with a TurboIonSpray

source. Ten μL of sample were injected to the column and metabolite separation was performed at 50°C using a mixture of 6 mM of aqueous tributylamine solution (Eluent A, adjusted to pH 6.2 with acetic acid) and aqueous acetonitrile solution (50% v/v) supplemented with 6 mM of tributylamine (Eluent B, adjusted to pH 6.2 with acetic acid) as mobile phase. Composition of this mobile phase was gradually varied along the measurement. Separated compounds were introduced at a flow rate of 350 μL min^{-1} into the mass spectrometer (MS) via the turbo ionspray source and detection was completed by multiple reaction monitoring with the MS operating in its negative ionization mode. Besides, the MS was run in unit resolution to achieve the best possible selectivity and sensitivity. Regarding the other key MS-parameters, the entrance potential was set at −10 V, the dwell time was fixed at 5 ms for all transitions, the auxiliary gas temperature was adjusted to 550°C and the source dependent parameters were set to: ionspray voltage −4500 V, nebulizer gas (GS1) auxiliary gas (GS2), curtain gas (CUR) and collision gas CAD 60, 60, 35 medium, respectively.

Intracellular amino acids were extracted from samples taken along the exponential phase and quantified by HPLC as described before (Kromer et al., 2005; Korneli et al., 2012). Using the same extraction protocol, intracellular potassium could be quantified with a Dionex-ICS 2000 HPLC system (Thermo Fischer Scientific, Waltham, MA, United States) equipped with a Dionex IonPac CS16 cation-exchange column (3 × 250 mm, Thermo Fischer Scientific, Waltham, MA, United States) and a Dionex CERS 500 suppressor (2 mm, Thermo Fischer Scientific, Waltham, MA, United States).

For the quantification of extracellular organic acids, a Hitachi Elite Lachrom HPLC (Krefeld, Germany) equipped with an Aminex HPX 87 H column (Biorad, Hercules, CA, United States) as stationary phase and 12 mM H_2SO_4 with a constant flow of 0.5 mL min^{-1} as mobile phase was used. The detection was achieved at 210 nm and 45°C with an UV detector (Hitachi, Tokyo, Japan).

Metabolic Flux Analysis

Calculations of metabolic fluxes in *B. megaterium* were performed in Matlab 7.2 (The Mathworks, Natick, MA, United States) using the open source software OpenFLUX (Quek et al., 2009) and based on the determination of steady state ^{13}C labeling of proteinogenic amino acids, substrate uptake, product formation rates and precursor demands for biomass formation. Metabolic reaction network used for simulation was constructed based on previous flux analysis studies and greatly refined using the KEGG and Metacyc databases and genomic data (Fürch et al., 2007; Eppinger et al., 2011). The final model comprises all major central pathways such as glycolysis, pentose phosphate pathway (PPP), tricarboxylic acid (TCA) and anaplerotic reactions but also pathways specific to PHB and proline biosynthesis. Moreover, incorporated precursor demands were corrected using the macromolecular compositions of cells specifically determined for this purpose under each condition (Fürch et al., 2007).

For the determination of mass isotopomer distributions, cells were hydrolyzed (6 M HCl, 105°C, 22 h), lyophilized and submitted for analysis by GC-MS of the tert-butyl-dimethylsilyl-derivatives of the amino acids (Wittmann, 2002; Wittmann et al., 2002). The GC-MS system (Agilent 7890A and MSD 5979C, Agilent Technologies, Waldbronn Germany) was run with 1 mL min^{-1} of helium as carrier gas and equipped with an HP5MS capillary column (5% phenyl-methyl-siloxane diphenypolysiloxane, 30 m × 250 μm) and a triple quadrupole detector. The temperature gradient for separation was set to 120°C for 2 min, 8°C min^{-1} up to 200°C and 10°C min^{-1} until 325°C were reached. Ionization energy was set to 70 eV and inlet, interface and quadrupole temperatures were 250, 280, and 230°C, respectively (Wittmann, 2002). Isotopic steady state was confirmed by measuring amino acid labeling patterns of cells at different cell concentrations ($OD_{600\ nm}$ = 2, 4 and 6) and measured ^{13}C labeling patterns were automatically corrected for natural isotopes by applying correction matrices (van Winden et al., 2002). Fluxes were finally estimated through minimization of the sum of the weighted least square residuals between measured and simulated mass isotopomer distributions and confidence intervals of 95% for these fluxes were subsequently determined using a Monte-Carlo computational algorithm (Yang et al., 2005; Antoniewicz et al., 2006).

Characterization of Poly Hydroxy Acids (PHA)

Methanolysis of lyophilized cell dry mass (5 mg) was placed in sealed tubes containing 2 mL methanol, 2 mL chloroform, 15% (v/v) H_2SO_4 and 0.5 mg mL^{-1} 3-methylbenzoic acid. The tubes were incubated at 100°C for 4 h. After cooling down to room temperature, 1 mL of ultrapure water was mixed with the reaction solution and vigorously stirred for 1 min with a vortex. The mixture was then transferred to a 15 mL reaction tube and centrifuged for 10 min at 6000 *g*. The lower part of the biphasic solution, containing the methyl esters of the biopolymer, was separated and analyzed via gas chromatography coupled to mass spectrometry (YL6900, Young Instruments, South Korea) using the methodology previously described by Pacheco et al. (2019). Once the retention time of the peaks were contrasted with the standards poly(3-hydrobutyrate) obtained from Sigma-Aldrich, their chemical structures were characterized based on the resulting mass compatibility (NIST 17 Mass Spectral library).

Intracellular Concentration of Polyhydroxybutyrate (PHB)

Determination of intracellular polyhydroxybutyrate (PHB) content was carried out as described previously (Huang and Reusch, 1996). Briefly, intracellular PHB was first turned into crotonic acid by complete cells hydrolysis with 1 mL of 2 M NaOH (30 min, 99°C) and cell debris were discarded by centrifugation (13200 min^{-1}, 5 min, Microcentrifuge 5415R, Eppendorf AG, Hamburg, Germany). Subsequently, supernatants were neutralized with 1 mL of 2 M HCl and crotonic acid concentrations were finally quantified by HPLC

measurement using the same system as for organic acids and calibration levels from 50 to 500 mg L^{-1} PHB obtained by hydrolysis of pure PHB granules.

Field Emission Scanning Electron Microscopy

Field emission scanning electron microscopy of *B. megaterium* cells grown in the absence and presence of 1 M of NaCl were performed as described before (Biedendieck et al., 2007a).

Statistical Analysis

To spot elements significantly involved in response and adaptation to osmotic stress, transcriptome and proteome data were statistically analyzed with R using packages Venneuler (Wilkinson and Urbanek, 2011) for construction of Venn diagrams and FactoMineR (Lê et al., 2008) for principal component analysis (PCA) analysis and hierarchical clustering on principal components (HCPC). Furthermore, packages gplots (Warnes et al., 2014) and mixOmics (Dejean et al., 2011) were used for heatmap construction and hierarchical clustering on gene from the extended central carbon metabolism using Euclidean distance and complete linkage as measure of distance and dissimilarity, respectively. For flux analysis, the data were visualized using the tool VANTED (Junker et al., 2006) equipped with the FluxMap add-on (Rohn et al., 2012) and obtained flux maps were subsequently refined in Inkskape. Functional analysis of genes and corresponding regulons were inferred from MegaBac v9[1] and BacillusRegNet (Misirli et al., 2014) databases by comparison with information obtained from literature and the SubtiWiki database for *B. subtilis* (Mäder et al., 2012).

RESULTS

Physiological Impact of Ionic Osmotic Stress in *Bacillus megaterium*

To assess the impact of osmotic stress on the physiology of *B. megaterium* strain DSM319, the growth parameters and product yields for organic acids were determined in shaking-flask experiments in minimal medium with various NaCl concentrations ranging from zero to 1.8 M (**Table 1**). Next, to get a more in-depth insight into the molecular response at the level of the transcriptome, intracellular proteome and metabolome during the exponential growth phase ($OD_{600\ nm}$ = 5), microarrays, LC-IMS^E and HPLC-measurements were conducted. Obtained data were integrated to deduce general adaptation strategies.

A direct correlation between the increasing amount of NaCl and a reduction in the specific growth rate (μ_{max}) and the resulting biomass yield ($Y_{X/S}$) was observed (**Table 1**). The cells showed a reduced μ_{max} and $Y_{X/S}$ of around 5-fold and 40%, respectively, at 1.8 M NaCl. This condition also significantly affected the redox state of the cells, provoking an enhanced production of pyruvate (3.1-fold) and lactate (8.6-fold). On the contrary, up to 10.8-fold and 13.4-fold decreased levels of the organic acids, succinate and oxoglutarate, were found (**Table 1**).

The combined multi-omic approach performed here demonstrates that the osmotic stress impacts the metabolism of *B. megaterium* far beyond the central carbon metabolism and that gene expression and protein abundances require specific adaptations to deal with these life-threatening conditions (see below). Based on the extent of the alteration of gene expression, a distinction can be made between response to mild (≤0.6 M NaCl) and severe (>0.6 M NaCl) salt stress (**Figure 1**). Only 43 genes had their expression significantly modified at 0.6 M NaCl, while more than 300 genes were differently expressed at higher NaCl concentration. Among them, 212 genes common to both 1.2 and 1.8 M NaCl were identified. Despite a restricted modification of gene expression, 139 proteins had already significantly altered concentrations under mild salt stress (**Figure 1**). This number then increased proportionally to the supplemented salt concentration, reaching 375 proteins at 1.8 M NaCl and revealing a large core set of 60 proteins systematically more produced in the presence of salt.

The Initial Adaptation to High Salt Conditions Is Mediated by Glutamate and Potassium Accumulation

Glutamate was the most abundant metabolite in *B. megaterium* under standard conditions with a yield of 450 μmol g_{CDW}^{-1} (**Figure 2**). Together with glutamine, it is a central metabolite linking carbon and nitrogen metabolism and a major precursor for the *de novo* synthesis of proline (**Figure 3**) (Brill et al., 2011a; Gunka and Commichau, 2012). Consequently, the cell must control their intracellular pools very tightly under osmotic stress. While the glutamine pool increased concomitantly with proline titers, the intracellular glutamate pool reached its maximum at 0.6 M NaCl and gradually returned to its initial value at 1.2 M NaCl, matching the profile of intracellular potassium perfectly and revealing the two-sided nature of adaptation to salt stress (**Figure 2**).

At moderate NaCl-concentrations (≤0.6 M NaCl), cells seem to use glutamate as counterion to imported potassium for an initial adjusting turgor pressure. Its intracellular concentration was accordingly increased (McLaggan et al., 1994; Epstein, 2003). In *B. megaterium*, potassium import could be performed by the conserved uptake systems KtrAB and KtrCD as described for *B. subtilis* (**Figure 3**). However, the expression of the corresponding genes was not significantly modified (Holtmann et al., 2003). At NaCl concentrations higher than 0.6 M, the increased potassium import was replaced by proline synthesis, probably because higher potassium concentrations are cytotoxic. Accordingly, the glutamate and potassium pools were progressively reduced reaching the initial value (0 M NaCl) at NaCl concentrations of 1.2 M. Responding to the now significantly increased demand for proline, intracellular concentration of glutamate increased again slightly at 1.8 M NaCl (**Figure 2**). These results suggested

[1]http://www.megabac.tu-bs.de

TABLE 1 | Physiological data for *B. megaterium* DSM319 growing in M9 minimal medium supplemented with different concentrations of NaCl (0, 0.3, 0.6, 0.9, 1.2 and 1.8 M).

Parameter	Unit	0 M	0.3 M	0.6 M	0.9 M	1.2 M	1.8 M
μ	h^{-1}	1.19 ± 0.02	0.88 ± 0.01	0.69 ± 0.01	0.57 ± 0.01	0.39 ± 0.00	0.24 ± 0.00
$Y_{X/S}$	$g_{CDW} \cdot mol^{-1}$	83.1 ± 1.1	77.2 ± 0.9	74.6 ± 1.1	70.7 ± 1.3	67.3 ± 0.9	58.7 ± 0.7
q_s	$mmol \cdot g_{CDW}^{-1} \cdot h^{-1}$	14.4 ± 0.3	11.5 ± 0.2	9.3 ± 0.2	8.0 ± 0.2	5.8 ± 0.1	4.0 ± 0.1
$Y_{Acetate/S}$	$mmol \cdot mol^{-1}$	**669 ± 21**	526 ± 24	490 ± 19	422 ± 41	346 ± 26	253 ± 22
$Y_{Pyruvate/S}$	$mmol \cdot mol^{-1}$	6.4 ± 0.3	7.6 ± 0.4	2.9 ± 0.1	1.7 ± 0.1	2.2 ± 0.2	**20.1 ± 1.6**
$Y_{Lactate/S}$	$mmol \cdot mol^{-1}$	4.4 ± 0.3	3.6 ± 0.2	8.3 ± 0.4	15.0 ± 0.6	20.3 ± 0.6	**37.7 ± 2.0**
$Y_{Succinate/S}$	$mmol \cdot mol^{-1}$	**62.6 ± 3.2**	22.7 ± 1.0	14.7 ± 0.7	13.4 ± 0.6	10.0 ± 0.4	5.8 ± 0.6
$Y_{Oxoglutarate/S}$	$mmol \cdot mol^{-1}$	**9.7 ± 0.4**	2.3 ± 0.1	1.3 ± 0.1	0.7 ± 0.1	1.2 ± 0.1	1.6 ± 0.1
Adenylate energy charge (AEC)		0.8336	n.d.	0.7659	n.d.	0.8612	n.d.
$NADH/NAD^+$		0.0079	n.d.	0.0260	n.d.	0.0191	n.d.
$NADPH/NADP^+$		0.5162	n.d.	0.4330	n.d.	1.0551	n.d.

Bold numbers indicate maximal yield observed for each measured organic acids. n.d., not determined.

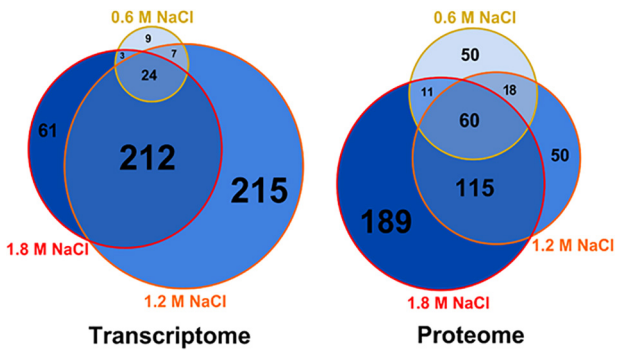

FIGURE 1 | Weighed Venn diagrams of the number of transcripts and proteins whose concentration was significantly altered in *B. megaterium* growing in M9 minimal medium with 0.6, 1.2 and 1.8 M NaCl, respectively. A gene or a transcript was considered significantly regulated when its concentration was either 1.75-fold higher or lower compared to 0 M NaCl. Gene expression was determined by microarray analysis and intracellular proteins were identified and quantified by proteome analysis using LC-IMS^E.

that accumulation of potassium plays a central role in short-term response and is also crucial for long-term adaptation of moderate halotolerant bacteria under mild salt stress (Whatmore et al., 1990).

The Second Adaptation Process to High Salt Conditions Is Based on the Synthesis of the Compatible Solute Proline

Intracellular concentrations of several amino acids, in particular of the compatible solute proline, gradually augmented with medium osmolarity. The cells strongly enhanced their proline production rates with increasing NaCl concentration and it accumulated intracellularly to yields of over 2.2 mmol g_{CDW}^{-1} at 1.8 M NaCl (**Figure 2** and **Supplementary Figure 1**). Furthermore, genes involved in the production of glycine betaine showed a 3-fold stronger expression (*gbsA* and *gbsB*). Except for *ousA* 3-fold overexpression, transcription of genes encoding osmoprotectant transporters (*opuAA* to *AC*, *opuD*) was not modified under hypertonic conditions (**Supplementary Table 1** and **Figure 3**) (Steil et al., 2003).

As further highlighted by the hierarchical clustering performed on the expression of genes belonging to the extended central carbon metabolism, rerouting of carbon fluxes toward proline synthesis under osmotic stress was fostered by altered expression of key gene modules. The transcriptome data enabled discrimination between two sets of genes involved in the proline synthesis from glutamate. Although both sets of genes encode the identical three enzymes, namely glutamate-5-kinase (*proB*, *proJ*), glutamate-5-semialdehyde dehydrogenase (*proA*, *proA**) and pyrroline-5-carboxylate reductase (*proI*, *proH*), their regulation differed significantly. Whereas expression of *proH-proJ-proA** was found 4- and 10-fold enhanced at 0.6 and 1.2 M NaCl, respectively, the expression of *proB*, *proA* and *proI* was up to 3-fold reduced (**Supplementary Figure 2**). As protein concentrations of ProA and ProA* behaved in the same way (**Supplementary Tables 1**, **2**), these results suggest that *proHJA** encodes the biosynthetic route for the unbridled synthesis of proline as an osmoprotectant, while *proBA* and *proI* seem to be responsible for the anabolic proline production, obviously negatively regulated by the product proline. Under severe osmotic stress, proline biosynthesis was furthermore promoted by the 2- to 5-fold reduced expression of genes from the arginine, amino sugar, purine and pyrimidine metabolisms, which resulted in low levels of the corresponding enzymes and moderated consumption of glutamate and glutamine for these metabolic purposes (**Supplementary Figure 2**).

Moreover, 2- to 5-fold increased expression of genes encoding the proline transporter OpuE (Bmd_1401) and two enzymes converting proline back to glutamate, the 1-pyrroline-5-carboxylate dehydrogenase (PutC) and proline oxidase (PutB), suggests that cells tightly control their proline intracellular pool and actively recycle this compound to avoid carbon wastage (**Figure 3** and **Supplementary Table 1**). In addition, the concentration of D-amino-acid transaminase (Dat) was increased by 5-fold under hypertonic conditions and

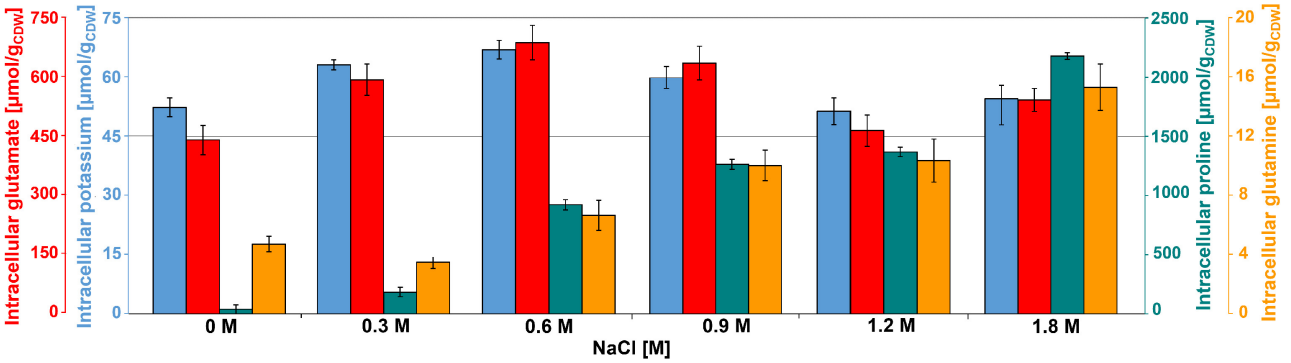

FIGURE 2 | Intracellular concentration of potassium (•), glutamate (•), glutamine (•), and proline (•) for cultivations of *B. megaterium* DSM319 in M9 minimal medium supplemented with different NaCl concentrations.

certainly improved the supply of the precursor glutamate from alanine (**Supplementary Table 2**).

Rearrangement of the Central Metabolism During Osmotic Stress Changes the Redox State of the Cell and Supplies Precursor for Protein Synthesis

To get a better insight into implications of osmotic stress on the central metabolism, we determined the carbon flux distribution by measuring the ^{13}C-labeling of proteogenic amino acids from tracer experiments with ^{13}C-glucose as substrate in the presence of up to 1.8 M NaCl (**Supplementary Tables 3–5**). We accounted for condition-specific precursor demands required for flux calculations derived from macromolecular compositions determined at 0, 0.6 and 1.2 M NaCl, respectively. They were subsequently extrapolated from these values for other NaCl concentrations (**Supplementary Figure 3** and **Supplementary Table 6**).

Results from flux analyses showed that *B. megaterium* metabolized glucose using both glycolysis and the pentose phosphate pathway (PPP) under all studied conditions (**Figures 4**, **5**). Besides, phosphoenolpyruvate carboxylase (PepC), an enzyme absent in most other *Bacillus* species, was preferred to pyruvate carboxylase (PycA) for replenishing the tricarboxylic acid (TCA) cycle. However, the coexistence of both enzymes certainly provides *B. megaterium* with enhanced flexibility to cope with a wide range of substrates and environmental conditions as proposed for *Corynebacterium glutamicum* (Sauer and Eikmanns, 2005).

Genes encoding proteins involved in balancing the redox state such as the pyruvate oxidase Pox (*bmd_1131*) were found overexpressed (2.5-fold), correlating well with similar observations made for the proteome of cells exposed to at least 1.2 M NaCl (**Figure 6**). Hence, the Pox enzyme might participate in the reduction of the NADH-to-NAD$^+$ ratio by circumventing the utilization of NAD$^+$ dependent pyruvate dehydrogenase Pdh for the conversion of pyruvate to acetyl-CoA whose concentration indeed tended to diminish at the mRNA and protein levels under high salt condition (**Figure 6**).

Since the *pox* gene showed no difference in expression at 0.6 M NaCl despite the already increased NADH-to-NAD$^+$ ratio, activation of the Pox route seems only indirectly related to the cellular redox state. Coming from the Pox route, the main pathway affected by severe osmotic stress in *B. megaterium* involves the TCA cycle. The expression of the gene encoding acetyl-CoA synthase (*acsA*) displayed a 2.6-fold increase, most likely to ensure efficient redirection of the produced acetate toward the TCA cycle (**Figure 6** and **Supplementary Table 1**) (Li et al., 2006; Kohlstedt et al., 2014). It was shown that *B. megaterium* accumulates extracellularly acetate by secretion during cultivations without re-import (Hollmann and Deckwer, 2004). Hence, it seems again that cells tend to avoid carbon wastage through secretion and instead convert acetate into acetyl-CoA to meet the physiological constraints imposed by osmotic stress.

Comparison of the flux distributions in non-stressed cells with that in cells exposed to mild ($\leq$ 0.6 M NaCl) and cells exposed to severe osmotic stress (>0.6 M NaCl), respectively, revealed a intensification of relative fluxes through the TCA cycle with increasing salt concentration (**Figure 5**). The absolute flux slightly decreased (**Figure 6**). Further, a rerouting of carbon from 2-oxoglutarate toward glutamate and proline synthesis was observed (**Figure 5**). Moreover, the precursor drain for the synthesis of biomass compounds, organic and amino acids upstream and downstream from the 2-oxoglutarate node significantly decreased with increasing salt concentration. In particular, carbon fueling the TCA cycle was preferentially recycled to oxaloacetate by malate dehydrogenase and reincorporated into the cycle, explaining the observed flux repartition at the anaplerotic node. Overall, the fluxes around this node showed no alteration despite the increased utilization of 2-oxoglutarate for proline biosynthesis.

Similarly, relative flux through the PPP intensified proportionally to the imposed osmotic burden and exceeded by far the anabolic demand, resulting in a strengthened carbon feeding back to glycolysis intermediates. Since three moles of NADPH are necessary to synthesize one mole of proline from 2-oxoglutarate, this marked increase of PPP fluxes certainly provided cells with the reducing power required for

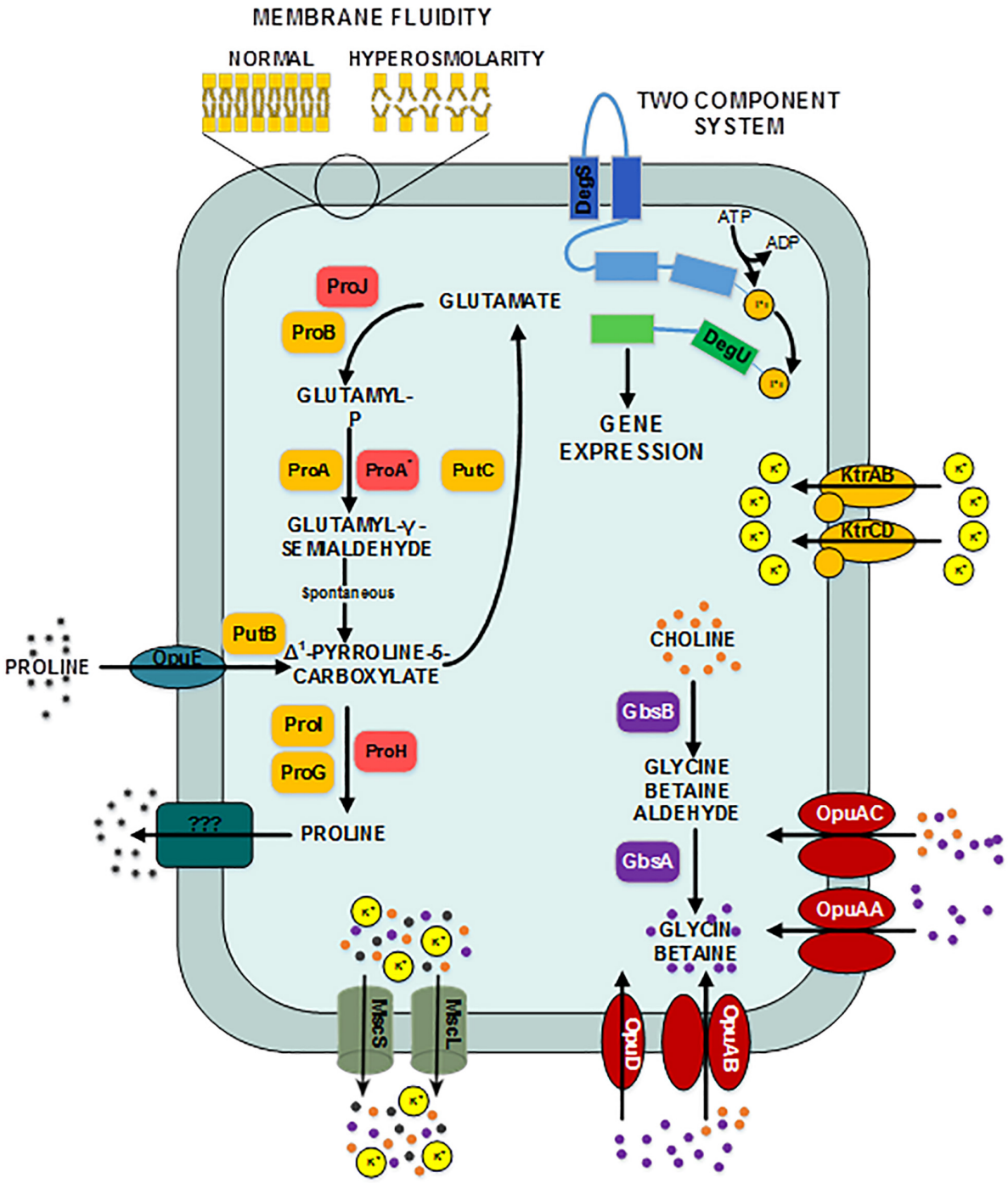

FIGURE 3 | Provisional synthetic overview of the osmotic stress response in *B. megaterium* inferred from genetic context and comparison with *B. subtilis* and *B. licheniformis* – Depending on their function, proteins have been attributed different font colors: light red for synthesis of proline as an osmoprotectant, orange for proline synthesis and utilization for biosynthetic purposes, purple for synthesis of glycin betaine from choline, red for choline and glycin betain transporters, dark turquoise for proline transporters, gray for mechanosensitive channels MscS and mscL, olive green for potassium transporters, dark pine green for unknown proline exporter, dark blue for the input domain of the sensing histidine kinase, light blue for the transmitter domain of the histidine kinase, dark green for the receiver domain of the sensing histidine kinase and light green for the output domain of the response regulator. **DegS:** two-component sensor histidine kinase, **DegU:** two-component response regulator, **GbsA:** glycine betaine-aldehyde dehydrogenase, **GbsB:** choline dehydrogenase, **KtrAB:** high affinity potassium transporter KtrA-KtrB, **KtrCD:** low affinity potassium transporter KtrC-KtrD, **MscL:** large conductance mechanosensitive channel protein, **MscS:** small conductance mechanosensitive channel protein, **ProA:** glutamate-5-semialdehyde dehydrogenase, **ProA***: glutamate-5-semialdehyde dehydrogenase **ProB:** glutamate 5-kinase, **ProG:** 1-pyrroline-5-carboxylate dehydrogenase, **ProH:** pyrroline-5-carboxylate reductase, **ProI:** pyrroline-5-carboxylate reductase, **ProJ:** glutamate-5-kinase, **PutB:** proline dehydrogenase, **Opu:** glycine betaine ABC transporter, **OpuAB:** glycine betaine ABC transporter, **OpuD:** glycine betaine transporter.

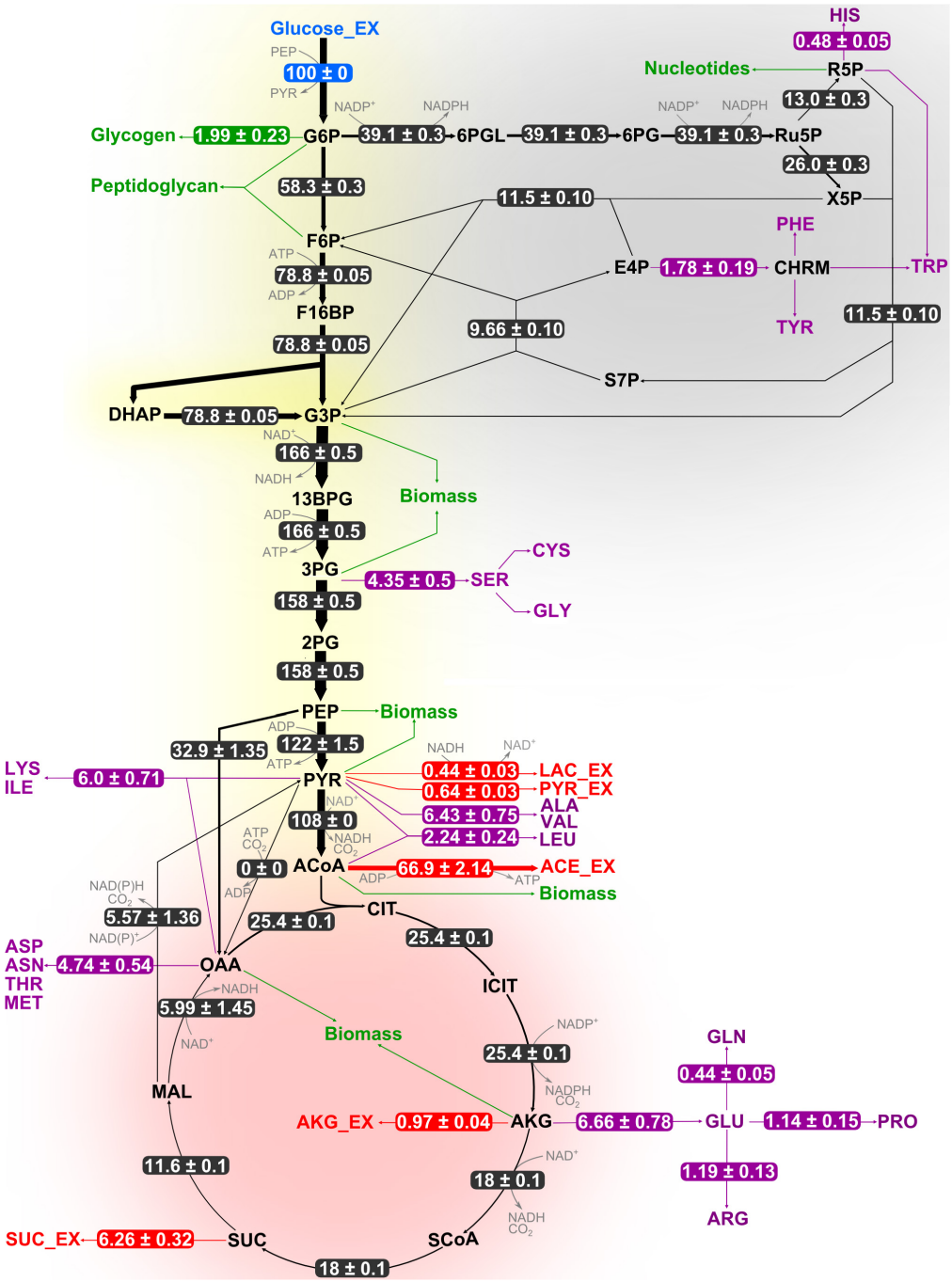

FIGURE 4 | Flux distribution within the central carbon metabolism of *B. megaterium* DSM319 growing at 37°C in M9 minimal medium. Fluxes were determined combining labeling data sets from experiments with 100% 1-^{13}C glucose and with a mixture of 50% U-^{12}C/50% U-^{13}C glucose, respectively. They are given as relative values (%) after normalization with the glucose uptake rate. Fluxes to amino acids (purple) and secretion of organic acids (red) are issued from measurements and were not simulated. Green arrows represent precursor withdrawal for the synthesis of biomass compounds.

this conversion. Together with the reduced CO_2 fixation by phosphoenolpyruvate carboxylase, these combined increases of fluxes through the TCA cycle and PPP also resulted in an up to 70% stronger CO_2 release, which partly explains the observed reduction of biomass yield under osmotic stress (**Table 1** and **Figure 5**). In contrast, relative fluxes through glycolysis remained approximately constant and admittedly participated in maintaining a high energy level even under stressful conditions, as indicated by the measured adenylate energy charge (**Table 1** and **Figure 5**).

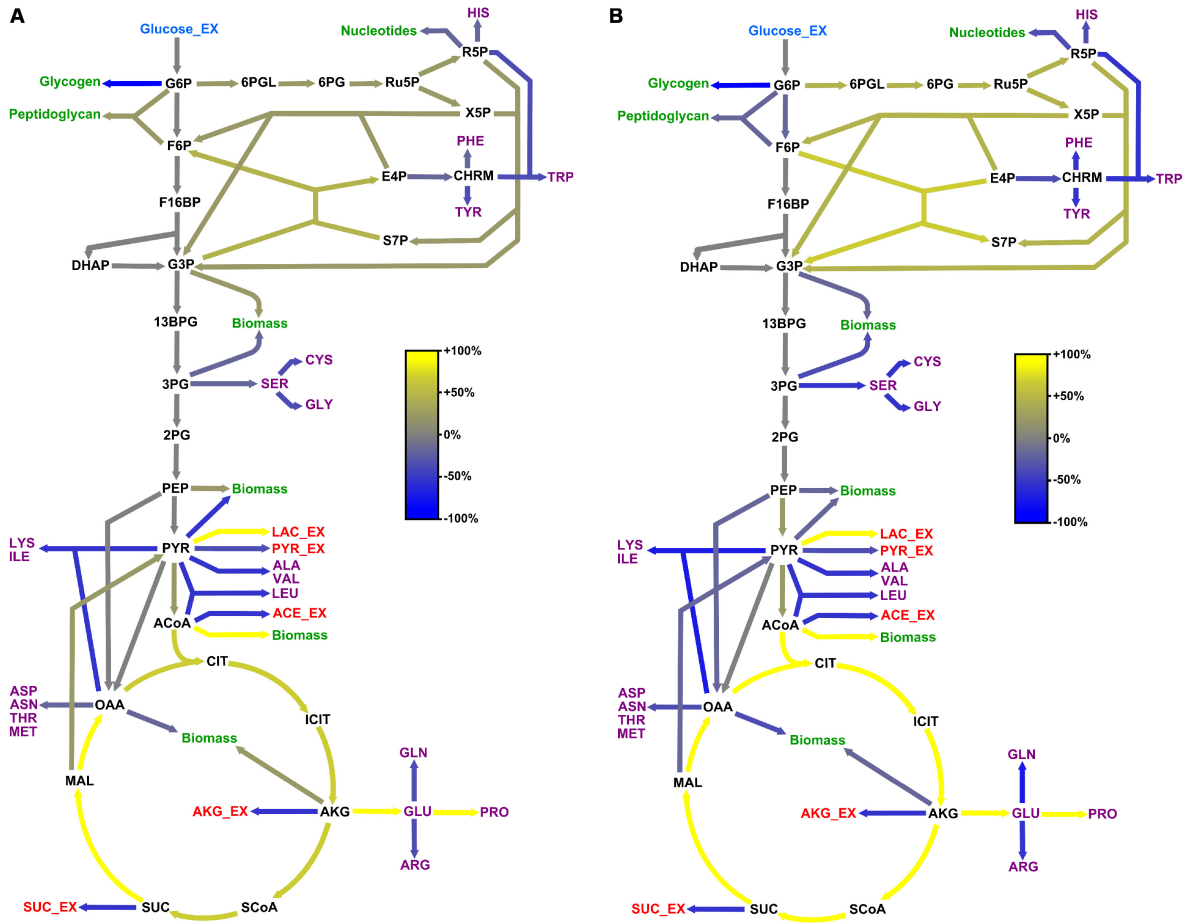

FIGURE 5 | Adaptation of carbon core metabolism to changing osmolarity. Change (%) in relative flux distribution in cells growing with 0.6 M **(A)** and 1.2 M NaCl **(B)** compared to cells growing at 37°C in standard M9 minimal medium (compare **Figure 4**).

Regarding the large carbon flux from glycolysis to proline biosynthesis, expression of several genes belonging to the TCA cycle and anaplerotic node was up to 3-fold higher in stressed cells (**Figure 6**). Concentrations of corresponding proteins were only slightly higher and cannot account alone for the massive rerouting observed, mainly because salt could also induce loss of enzyme activity (Kohlstedt et al., 2014). On the contrary, despite a 2.6-fold reduction of absolute glycolytic flux, the pools from oxaloacetic acid to 2-oxoglutarate grew more prominent with increasing salt concentration and indeed drove this rerouting which enabled the conservation of a similar TCA absolute flux (**Figure 7**). Similarly, mRNA and protein levels from the PPP did not significantly change under osmotic stress, and enhanced flux diversion may be achieved at the level of metabolites as well. As a matter fact, concentration of 6-phosphoglycerate (6PG) also increased gradually while that of ribulose-5-phosphate (Ru5P) progressively diminished with increasing salt concentration, thus reducing the mass-action ratio of the reaction catalyzed by phosphogluconate dehydrogenase (GND) and favoring 6PG conversion (**Figure 7**) (Hess and Brand, 1965).

Gene expression, enzyme concentrations and metabolic fluxes downstream of 2-oxoglutarate were not significantly changed under osmotic stress in *B. megaterium* except for the *odhA* and *odhB* genes, whose expression was higher (**Figure 7** and **Supplementary Tables 1**, **2**) while *fumC* and the corresponding enzyme fumarate hydratase (FumC) were found to be up to 3-fold reduced at severe salt. Consistent with results in *B. subtilis* and *B. licheniformis*, expression of genes encoding glutamate synthase (*gltA*, *gltB*) and concentration of these proteins were also up to 2-fold reduced despite the increased glutamate demand for proline synthesis (Schroeter et al., 2013). These three enzymes seem stress-sensitive and, given their vital metabolic functions, they are probably replaced by isoenzymes under stressful conditions.

Induction of the General *sigB*-Mediated Stress Response by High Salt Conditions

When cells were cultured at NaCl concentrations higher than 0.6 M, expression of the σ^B-operon (*rsbV*, *rsbW*, *rsbX*, *sigB*) was only up to 1.8-fold higher, while the abundance of several of its products increased up to 3-fold, suggesting the sustained activation of the general stress response under acute salt stress. In accordance with this conclusion, predicted members of the SigB-regulon (*bmd_1994*, *bmd_1557*, *bmd_1546*, *bmd_1131*,

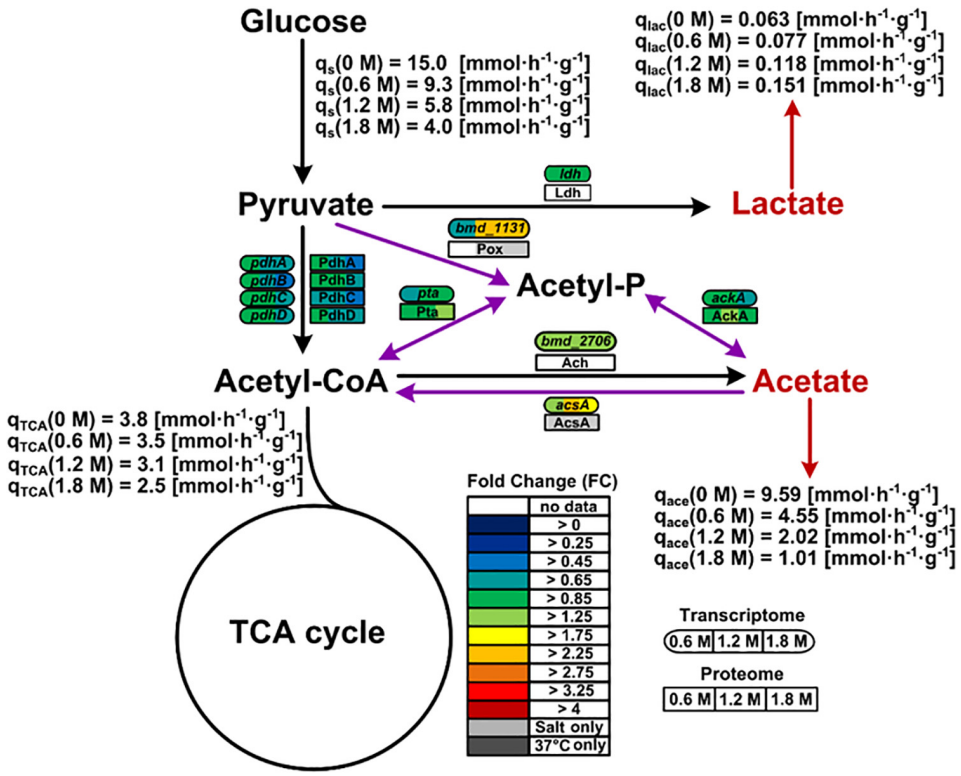

FIGURE 6 | Pox route and overflow metabolism in *B. megaterium* DSM319 growing in M9 minimal medium supplemented with different NaCl concentrations. Purple arrows correspond to reactions of the Pox route while red arrows indicate organic acid secretions. Gene expression was determined by microarray analysis using purified RNA samples obtained from four biological replicates. Intracellular proteins were identified and quantified by proteome analysis using LC-IMS^E for cells originating from three biological replicates. Values are indicated as fold change compared to expression in cells grown at 37°C in M9 minimal medium without additional NaCl supplementation. Metabolites were quantified by mass spectroscopy. **Ach:** acetyl-CoA hydrolase; **AckA:** acetate kinase; **AcsA:** acetyl-CoA synthetase; **Ldh:** lactate dehydrogenase; **Pdh:** pyruvate dehydrogenase; **Pox:** pyruvate oxidase; **Pta:** phosphate acetyltransferase.

bmd_1041, *dps*, *bmd_5086*, *bmd_3493*, *bmd_3215, gbsB, gbsA*) were between 2.2- and 12-fold more strongly expressed and concentration of the corresponding proteins up to 57-fold higher (**Supplementary Figure 4** and **Supplementary Tables 1**, **2**) (Hecker and Völker, 2001; Höper et al., 2006; Hahne et al., 2010; Misirli et al., 2014). Similarly, the concentration of the regulator of the peroxide regulon PerR was 2.6- and 4.6-fold increased at 1.2 M and 1.8 M NaCl, respectively, confirming the production of reactive oxygen species (ROS) under these conditions. The increased production of NADH dehydrogenase YutJ (BMD_4957), iron-binding protein Dps (BMD_4857), 2-cys peroxiredoxin (BMD_0990), redox regulator Rex (BMD_0255), several cytochromes P450 (BMD_1855, BMD_2035, BMD_3874) as well as the up to 4-fold induction of the gene encoding a manganese catalase (*bmd_3215*) provides further evidence that the cells produced these proteins to fight oxidative damages (**Figure 8** – Cluster 6, **Supplementary Figure 4** and **Supplementary Table 2**) (Lewis, 2002; Ishikawa et al., 2003; Rhee et al., 2005; Gyan et al., 2006; Ying, 2008).

Interestingly, concentrations of several flavodoxins (BMD_3384, BMD_3385, BMD_3911) were increased up to 6.6-fold at concentrations above 0.6 M NaCl and electron transfer flavoproteins EtfA and EtfB were even produced explicitly under these conditions. Flavodoxins have already been reported to replace ferredoxins and participate in repair activities during iron starvation and oxidative stress (Pomposiello et al., 2001; Giro et al., 2006; Tognetti et al., 2006; Zurbriggen et al., 2007). Indeed, ferredoxin functions seem to be compromised under stressful conditions because the Fe–S cluster they bear as a prosthetic group gets damaged by diverse reactive species (Singh et al., 2014). In this regard, expression of genes involved in synthesis and reparation of Fe-S clusters (*sufB*, *iscU*, *sufS*, *sufD*, *sufC*) showed upregulation by around 2-fold and concentrations of their products were accordingly higher under severe salt stress (**Supplementary Tables 1**, **2**) (Höper et al., 2006). Surprisingly despite the catalytic role of iron in ROS generation, transcription of numerous genes encoding proteins involved in iron acquisition such as siderophores (*bmd_4048*, *bmd_4051*, *bmd_4052*) and ferrichromes (*fhuD*, *fhuC*, *yclQ*, *yclP*, *yclO*, *yclN*, *yusV*, *yfhA*, *yfiZ*, *yfiY*) were among the most overexpressed (up to 15-fold) and their products display an up to 12-fold abundance increase at concentrations above 0.6 M NaCl (**Figure 8**, Cluster 6 and **Supplementary Figure 4**) (Galaris and Pantopoulos, 2008). Together with the increased production of flavodoxins, this result tends to confirm that high-salinity is also causing iron scavenging in *B. megaterium*, as

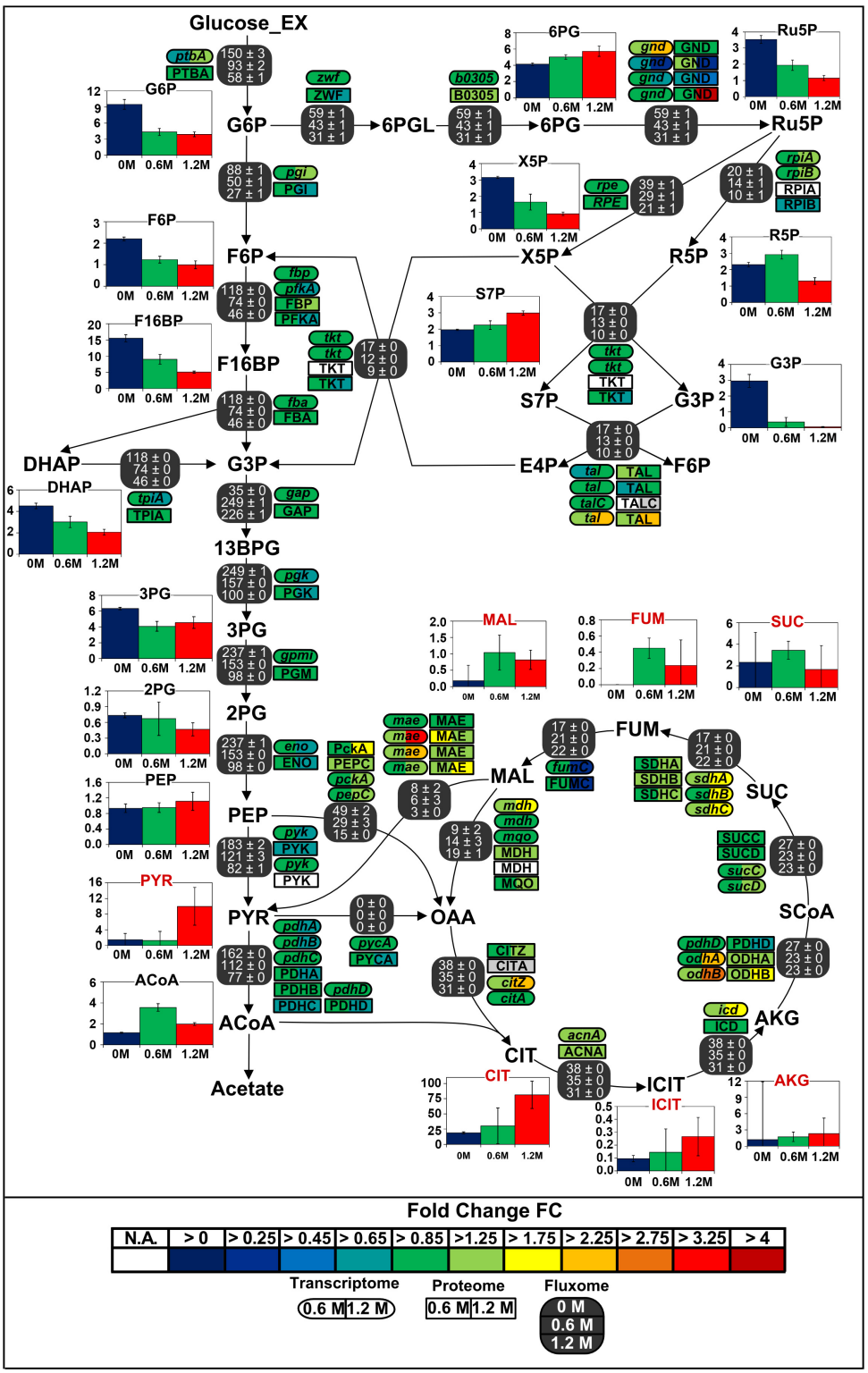

FIGURE 7 | Integrated view of the response of the central carbon metabolism of *B. megaterium* DSM319 to ionic osmotic stress. Transcriptome and proteome data are indicated as the determined fold change compared to cultivation in minimal medium without NaCl supplementation. Gene expression was determined by microarray analysis using purified RNA samples obtained from four biological replicates. Intracellular proteins were identified and quantified by proteome analysis using LC-IMS^E for cells originating from three replicates. Bar plots represent intracellular metabolite concentrations in μmol g_{CDW}^{-1}. Intracellular metabolite concentrations were determined by LC-MS/MS using a differential method, i.e., subtracting extracellular metabolite concentration from the global metabolite concentration.

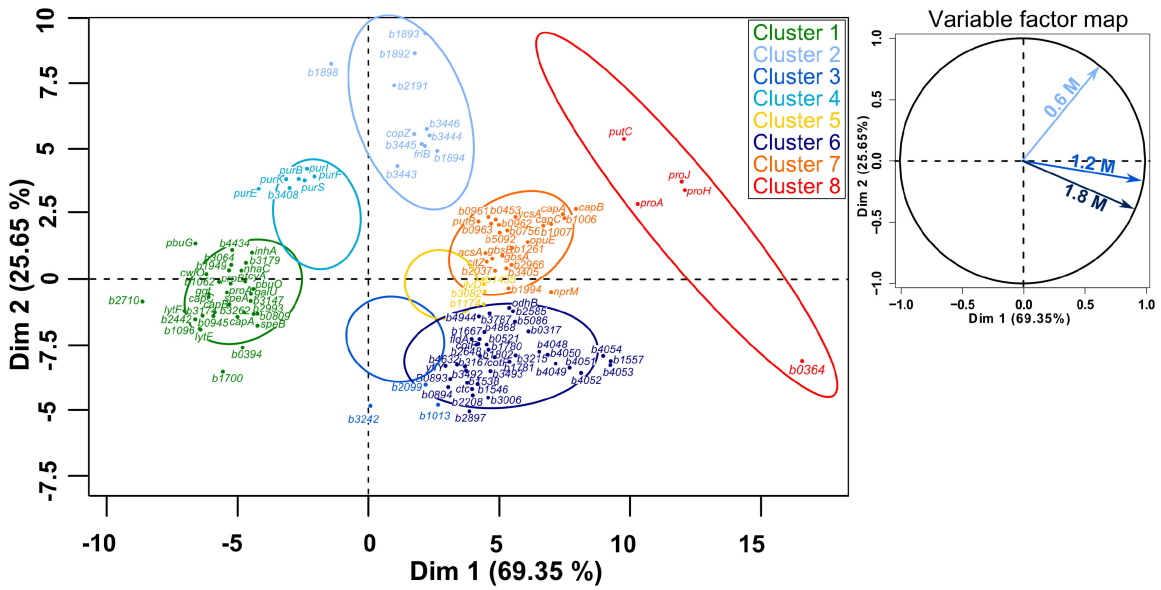

FIGURE 8 | Principal component analysis (PCA) followed by hierarchical clustering (HCPC) on gene expression ratios in *B. megaterium* DSM319 grown in M9 medium supplemented with 0.6, 1.2, and 1.8 M NaCl. For more clarity, *bmd* was replaced by b in gene names and only the 125 genes most relevant for the PCA construction are presented. **Cluster 1**: Genes whose expression is down-regulated under both mild (0.6 M NaCl) and severe salt stress (1.2 and 1.8 M NaCl), **Cluster 2**: Gene whose expression is only stronger under mild stress, **Cluster 3**: Genes whose expression is slightly reduced at 0.6 M NaCl and slightly increased under severe salt stress, **Cluster 4**: Genes whose expression is slightly up-regulated at 0.6 M NaCl and strongly down-regulated under severe salt stress, **Cluster 5**: Genes whose expression is slightly up-regulated under both mild and severe salt stress, **Cluster 6**: Genes whose expression is specifically up-regulated under severe salt stress, **Cluster 7**: Genes whose expression is up-regulated under both mild and severe salt stress, **Cluster 8**: Genes involved in proline synthesis.

proposed in *B. subtilis* (Hoffmann et al., 2002; Höper et al., 2006; Zurbriggen et al., 2007).

Additional Adaptation Process Caused by High Salt Conditions

Proteome data also revealed a progressive reduction of concentrations of several ribosomal proteins (RplW, RpsN, RpsO, RpsT, RpmA, RplT), translation factors (BipA, PrfC, PrfB) and proteins from the purine and pyrimidine metabolisms (PurEKBCSQLFMNHD, PyrK, PyrAA, PyrAB, PyrC, PyrB, PyrG) with increasing salt concentrations which denotes a significant downturn in RNA synthesis and processing activities consistent with the reduction of RNA content (**Supplementary Figure 3** and **Supplementary Table 1**). In this regard, decrease in concentrations of enzymes involved in the synthesis of purines and pyrimidines was supported by the up to a 2.5-fold reduced expression of genes encoding them and proteins from the connected histidine biosynthesis pathway (**Figure 8** – Cluster 4).

Besides proline, arginine and histidine metabolisms, synthesis and transport of several other amino acids were affected at NaCl concentrations above 0.6 M. Notably, genes encoding methionine and cystine ABC transporters (*met*, *metN*, *metQ*, *metP*, *tcyC*, *tcyB*, *tcyA*) or involved in methionine salvage (*mtnA*, *mtnK*, *mtnE*, *mtnW*, *mtnX*, *mtnB*, *mtnD*) had approximately 2-fold decreased expression levels while concentration of methionine synthase MetE and cystathionine beta-lyase PatB was up to 16.5- and 2.7-fold increased, respectively (**Supplementary Tables 1**, **2**). Similarly, concentration of enzymes involved in tryptophan (BMD_2992, TrpA, TrpB, TrpC) and cysteine (YtkP) synthesis were up to 2.5- and 4-fold increased under severe salt stress, respectively. Given the reactivity of reactive oxygen and nitrogen species toward methionine, cysteine and tryptophan residues, all these modifications might be related to the emergence of oxidative damages under severe salt stress (Levine et al., 1999; Yamakura and Ikeda, 2006; Hochgräfe et al., 2007; Peyrot and Ducrocq, 2008). The up to 5-fold higher concentrations of enzymes from the pantothenate pathway (PanB, PanC, PanD) could help prevent oxidative damages (**Supplementary Figure 4** and **Supplementary Table 2**) (Wojtczak and Slyshenkov, 2003).

The expression of several genes encoding proteins associated to the cell wall or involved in peptidoglycan, murein and polysaccharide synthesis (*bmd_0452*, *bmd_1096*, *ponA*, *cwlO*, *yocH*, *lytF*, *lytE*, *bmd_1114*, *bmd_1117* to *1120*, *bmd_3174*) was up to 5-fold reduced at concentration above 0.6 M NaCl. Most of the corresponding proteins also had reduced concentrations, with the exception of the binding protein YocH which was, despite the 3-fold reduction in abundance, present in 12- and 19-fold higher amounts at 1.2 and 1.8 M NaCl, respectively (**Supplementary Figure 4** and **Supplementary Tables 1**, **2**) (Steil et al., 2003; Kohlstedt et al., 2014). Another essential element determining cell morphology in bacteria is the cell division protein FtsZ (Chien et al., 2012), whose abundance was enhanced by more than 3-fold (**Supplementary Table 2**). The repression of this gene leads to longer cells displaying a filamentous shape (Margolin, 2005), and in contrast by overproducing FtsZ, a higher growth rate and wider bacterial cells (Zhao et al., 2019). **Figure 9** shows the morphology of *B. megaterium* cells, which swelled in the

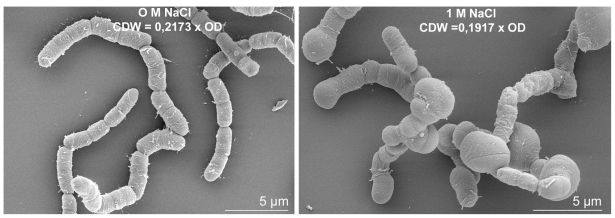

FIGURE 9 | Salt-induced modifications of cell morphology in *B. megaterium* DSM319. Scanning electron microscope picture of *B. megaterium* grown in the absence **(left)** and in the presence of 1 M NaCl **(right)**.

presence of sodium chloride. The cell wall indeed underwent an electrostatic contraction affecting its structure and properties as described by others (**Figure 9**) (Marquis, 1968; Koch, 1984). Moreover, the percentage of odd-numbered iso-fatty acids (iso C13:0 and iso C15:0) incorporated into the cell wall was gradually increased in cells exposed to higher NaCl-concentrations and probably responded to a reduction of membrane fluidity at higher osmolarities (data not shown) (Kaneda, 1991).

The PCA analyses further confirmed the existence of a physiological threshold at around 0.6 M NaCl and enabled the detection of four genes encoding unique two-component systems (*bmd_1892/1893* and *bmd_3442/3443*) which responded specifically to mild salt stress and might orchestrate an appropriate feedback response (**Figure 8** – Cluster 2). In particular, an elevated transcription of *copZ*, *copA*, and *bmd_1894*, whose product shares 40% homology with *B. subtilis*' CsoR regulator, may indicate an intensified scavenging of intracellular copper under these conditions (Banci et al., 2003; Radford et al., 2003; Corbett et al., 2011). Other induced genes encode an ABC transporter (*bmd_3446*) and two putative membrane proteins (*bmd_3444* and *3445*). Nevertheless, 55% of the 43 genes differently expressed under mild salt stress were shared with severe salt stress, and their regulation seems therefore crucial for adaptation. This core group naturally comprises genes with functions in proline synthesis (*putC*, *proH*, *proJ*, *proA**, see above) whose expression was up to 10.4-fold increased (**Figure 8** – Cluster 8) but also others involved in cell wall metabolism (*lytF*, *bmd_2442*, *bmd_1096*, *bmd_3174*) which were, on the contrary, up to 4.4-fold less expressed under osmotic stress (**Figure 8** – Cluster 1) (Steil et al., 2003). Besides, several NAD-dependent epimerases/hydratases (Bmd_0685, GalE, Mro, Bmd_2433, Bmd_2930 Bmd_3943) were found in response upon addition of NaCl whose concentrations increased up to 29-fold (**Supplementary Figure 4** and **Supplementary Table 2**). Finally, several oxidoreductases (BMD_0912, BMD_0989, BMD_1041, BMD_2681, BMD_3119, BMD_3139, BMD_3288, BMD_3473, BMD_3493), peptidases and proteases (BMD_0331, InhA, BMD_3039, PepQ, BMD_4817, CtpB, BMD_5202) were also part of this core group of proteins and their increased concentrations positively contributed to a reduction of damages resulting from the salt-induced perturbation of redox state and to the alteration of cell wall (**Supplementary Figure 4** and **Supplementary Table 2**) (Wang et al., 2006).

Osmotic Stress Triggers Polyhydroxybutyrate (PHB) Synthesis in *B. megaterium*

Determination of biomass composition under different NaCl concentrations revealed elevated levels of intracellular inclusion bodies under hypertonic conditions, most likely as a response mechanism to osmotic stress. Using gas chromatography mass spectrometry, we found that *B. megaterium* accumulated poly(3-hydroxybutyrate) (PHB). Under standard growth conditions, the PHB content was recorded at 6% of the CDW but increased to 14.4% at 0.6 M NaCl, and finally reached an accumulation of 29.5% of the CDW when cells grew with 1.2 M NaCl (**Figure 10**). As evidenced by fluxome analysis, a side effect of proline synthesis under salt stress was a stronger NADPH supply which was reflected in the increase of the global NADP(H) pool from 1180 to 1760 nmol $g_{CDW}{}^{-1}$ in cells cultivated with 1.2 M NaCl (**Figure 10**). However, NADPH supply already exceeded biosynthetic demand by more than 20% under normal conditions, and the increased PPP fluxes under salt stress only accentuated this discrepancy, generating an 87% NADPH excess at 1.2 M NaCl. The PHB biosynthetic pathway requires NADPH as a cofactor; thus, an increment in the NADPH pool has been reported to enhance the intracellular accumulation of the polyoxoester, while PHB synthesis might act as a redox regulator of the NADPH-to-$NADP^+$ ratio. Similarly, increased conversion of pyruvate to lactate is probably involved in the modulation of the NADH-to-NAD^+ ratio (Anderson and Dawes, 1990; Wang et al., 2005). Despite the higher PHB content at elevated salt concentrations, expression of genes and abundance of proteins involved in PHB synthesis showed no alteration in cells grown with 0.6 M NaCl. *B. megaterium* cells exposed to 1.2 M NaCl prompted the synthesis of the PhaR subunit of the polyhydroxyalkanoates (PHA) synthase and the phasin PhaP enzyme. The latter, a known stimulator of PHB production, showed a 2.2- and 1.8-fold increase at 0.6 and 1.2 M NaCl, respectively. These slight modifications cannot account alone for the sharply increased polymer content (York et al., 2001; Pötter and Steinbüchel, 2005) and suggest that other unknown underlying mechanisms trigger PHB accumulation when osmotic pressure becomes higher in *B. megaterium*.

DISCUSSION

As a soil bacterium, *B. megaterium* faces constant fluctuations of nutrient and water availability as a result of seasonal and daily weather variations. In this study, we aimed at unveiling the metabolic responses and regulatory mechanisms at the transcriptomic and proteomic level coping with the osmotic stress conditions (Schweder et al., 1999). In addition, metabolomics and *in vivo* flux analysis were integrated with the other molecular levels, thus delivering a more comprehensive and holistic explanation of the resulting phenotypes observed in *B. megaterium* cells challenged with hyperosmotic stress.

Firstly, at similar NaCl-concentrations, detrimental consequences on physiology were less pronounced in comparison

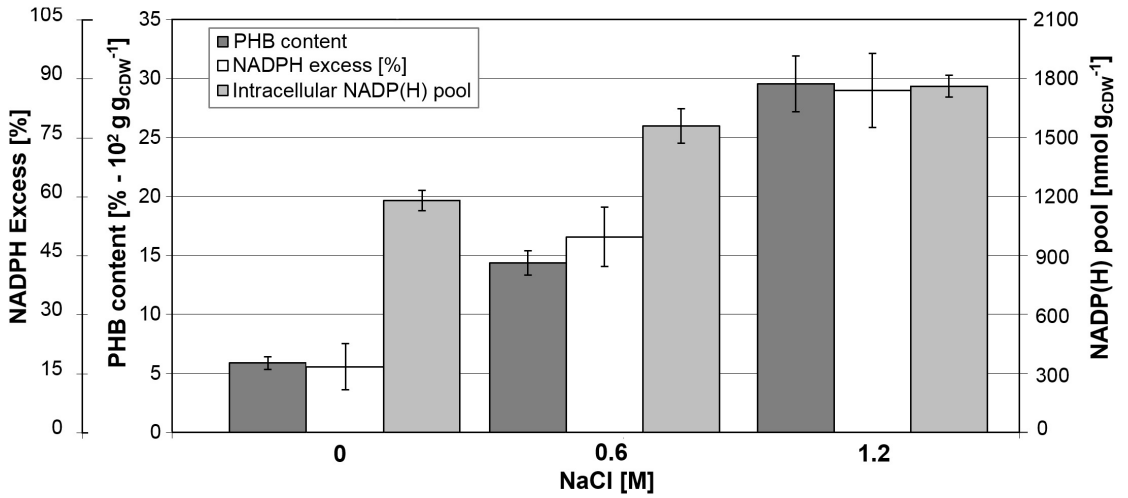

FIGURE 10 | Relationship between PHB content and NADPH production in *B. megaterium* DSM319 growing at 37°C in M9 minimal medium supplemented with up to 1.2 M NaCl. NADPH excess was calculated using the ratio between NADPH supply derived from flux analysis and biosynthetic NADPH demand estimated from biomass composition at the respective NaCl concentrations. Global NADP(H) pool represents the sum of NADP and NADPH pools as.

to other members of this genus (den Besten et al., 2009; Schroeter et al., 2013; Kohlstedt et al., 2014). This higher robustness of *B. megaterium* was further reflected in the up to 5-fold reduction of the number of genes whose expression was significantly altered at 1.2 M NaCl compared to *B. cereus, B. subtilis,* or *B. licheniformis* (den Besten et al., 2009; Hahne et al., 2010; Schroeter et al., 2013). With increasing NaCl amounts, the intracellular proline concentration drastically rose, reaching its maximum at 1.8 M NaCl. Since *B. megaterium* does not possess the genetic machinery for the *de novo* synthesis of other osmoprotectants such as ectoine, glycine betaine or trehalose, it seems that proline acts as the major osmoprotectant in this organism. Higher levels of intracellular proline were related to the upregulation of the expression of the genes *proJ-proA*-proH* encoding glutamate-5-kinase, glutamate-5-semialdehyde dehydrogenase and pyrroline-5-carboxylate reductase, respectively. The genes *proB*, *proA,* and *proI*, encoding the same proteins showed low expression under high salinity, obviously negatively influenced by proline, as previously reported in *B. subtilis* and *B. licheniformis* (Grundy and Henkin, 1993; Brill et al., 2011a,b). The existence of two distinctive ProA proteins indicates a strict separation between proline synthesis for anabolic and protective purposes similar to that in *B. licheniformis* and contrasting with the organization in *B. subtilis*, in which both routes are curiously interlinked by the unique ProA (BSU13130) (Brill et al., 2011a; Schroeter et al., 2013). Additionally, the upregulation of genes and proteins responsible for the last steps of the glycine betaine biosynthesis under high salt conditions suggest that, as observed in *B. subtilis*, synthesis of this compatible solute is only possible if its precursor choline is also present (Boch et al., 1996; Kappes et al., 1999; Nau-Wagner et al., 2012).

Another essential metabolic regulation occurs at the level of pyruvate where conversion to acetyl-CoA is modulated to fine-tune fluxes through the TCA cycle. In that case, the extra NADH supply resulting from the stronger production of malate dehydrogenase and 2-oxoglutarate oxidoreductase enzymes under salt stress has to be dissipated, and *B. megaterium* thus secretes higher amounts of lactate depleting NADH as cofactor. Under osmotic stress conditions, it seems clear that the pool of acetyl-CoA goes to the TCA cycle for 2-oxoglutarate synthesis, one of the main precursors for proline synthesis. The high operation of enzymes of the TCA cycle to process the carbon flux from acetyl-CoA, indeed, lead to an extreme synthesis of NADH. Hence, *B. megaterium* might partially release this burden by redirecting two molecules of acetyl-CoA to acetoacetyl-CoA (by B-ketothiolase PhaA), and subsequently to PHB synthesis (Madison and Huisman, 1999). This pathway also utilizes NADPH as cofactor, allowing balancing the entire redox state of the cell.

This enhanced intracellular accumulation of polyhydroxybutyrate (PHB) when NaCl concentration increases, surprisingly under non-limiting conditions of nutrients, was one of the most significant findings of this study. In fact, PHB is generally produced in bacteria when an inorganic nutrient, other than the C-source, becomes limiting, enabling the intracellular storage of excess carbon and reducing power under these conditions (Rehm, 2010). Under famine, the cell can then degrade the accumulated PHB to acetyl-CoA and (S)-3-hydroxybutyl-CoA, replenishing the TCA and β-oxidation cycles for energy production, respectively (Wang et al., 2009). Beneficial effects of PHB and related phasins on bacterial resistance against stressors such as heavy metals, temperature, phenol, ethanol, and peroxide stress have already been underlined in several studies, but a potential role against salt stress has only been advanced in nitrogen-fixing rhizobia so far (Natarajan et al., 1995; Ayub et al., 2004; Arora et al., 2006; Zhao et al., 2007; Nair et al., 2009; Wang et al., 2009; Woo et al., 2012). System-wide integration of all omics data explains this PHB build-up in *B. megaterium*. Indeed, increased mRNA and protein levels were observed within the

PPP and TCA cycle under ionic osmotic stress as compared to the control condition with no salt. Consequently, the carbon flux toward the former pathway increased and generated an NADPH surplus in cells grown in glucose and high NaCl concentrations. These findings were also confirmed by the *in vivo* flux analysis. This diversion of carbon flux toward the PPP pathway was furthermore fostered by a decreased concentration of the phosphofructokinase (PfkA) with increased NaCl concentrations that reduced efficiency of the upper part of the glycolysis. This cellular strategy has been proven to endow bacteria with the ability to cope with oxidative stress and guaranty production of cofactors for anabolic demands (Chavarria et al., 2013). However, in the case of *B. megaterium*, it also leads to an intracellular excess of NADPH and the observed accumulation of PHB.

In most PHB producing bacteria, nitrogen, or phosphorus are limited during the bioconversion of the supplied carbon source to trigger biopolymer synthesis in the cell (Mozejko-Ciesielska and Kiewisz, 2016). This nutrient-limited environment suppresses key enzymes of the TCA cycle such as the isocitrate dehydrogenase followed by the downregulation of genes encoding the succinate and malate dehydrogenase (Klonne et al., 1989; Poblete-Castro et al., 2012). Findings here were contrary to the usual mechanisms displayed by environmental bacteria for synthesizing polyhydroxyalkanoates (PHA), opening new avenues for the synthesis of this valuable biopolymer using varying salt concentrations under non-limiting nutrient conditions. The use of fatty acids as carbon substrates allows PHA synthesis in a growth-associated manner as demonstrated in *Bacillus* species (Sangkharak and Prasertsan, 2012), *Cupriavidus necator* (Verlinden et al., 2011), *and Pseudomonas putida* (Oliva-Arancibia et al., 2017) to name some, because of the generation of direct precursors, e.g., (*S*)-3-hydroxyacyl-CoA and 2-enoyl-CoA, from the B-oxidation route. One of only a few bacteria that does not require any nutrient limitation for PHA storage from glucose is *Azotobacter vinelandii*, a soil bacterium capable of nitrogen fixation (Hamilton et al., 2011). The biopolymer has been proposed to act as a protective agent to counteract oxidative stress during carbon deprivation as a result of the constant functioning of the nitrogenase enzyme (Page et al., 1992).

In the last decade, bacteria of the genus *Bacillus* have been exploited as efficient PHA producers using a wide variety of carbon substrates and wastes (Mohapatra et al., 2017) as well as a host for the creation of engineered and functionalized PHA beads (Grage et al., 2017). Halotolerant *Bacillus* strains are being utilized to develop unsterile bioprocesses for high-level PHB synthesis since they can rapidly grow with a NaCl concentration up to 2 M and accumulate approximately 50% of the CDW as PHB (Page et al., 1992). Fed-batch PHA processes using *Bacillus* species have already reached volumetric productivities similar to those obtained at industrial scale (Kulpreecha et al., 2009). Also, the biosynthesized polyoxoesters contain fewer endotoxins in comparison to Gram-negative bacteria, offering an advantage for medical applications. Based on the metabolic functioning of *B. megaterium* unveiled in this study, there is a lot of room for improvement for PHB production since the genes of the biopolymer biosynthetic pathway were almost not altered under hyperosmotic conditions. Genetic engineering of this route could enable a higher conversion of precursors of acetyl-CoA to acetoacetyl-CoA. Moreover, these genetic modifications toward the creation of novel biocatalysts can be coupled with unsterile bioprocessing development, making a cost-effective process for bacterial production of biopolymers from sugars.

CONCLUSION

Adaptation to ionic osmotic stress in *B. megaterium* was found to be initiated by the accumulation of synthesized glutamate and imported potassium within the cell. This step was followed by the massive *de novo* synthesis of the compatible solute proline and recruited an osmo-dependent pathway to fulfill this requirement. Here, higher mRNA and protein levels within these pathways were found and confirmed the reorganization of flux distribution toward proline production. Moreover, relative fluxes through the pentose phosphate pathway and tricarboxylic acid cycle were significantly increased to supply the cofactors NADPH and NADH, respectively. As a consequence, NADPH was present in significant excess in cells under sustained osmotic stress, triggering an accumulation of the storage compound PHB, a highly promising industrial biopolymer.

DATA AVAILABILITY STATEMENT

The datasets generated for this study can be found in the GEO database with the accession number GSE110712; ProteomeXchange Consortium with the dataset identifier PXD015605.

AUTHOR CONTRIBUTIONS

TG, RK, and RB conceived the idea. TG, DZ, GR, MW, and MR performed the experiments. TG, DZ, KR, IP-C, GR, RK, and RB analyzed the data. TG, IP-C, RK, and RB wrote the manuscript getting the input of all authors. All authors edited the manuscript and approved its final version.

ACKNOWLEDGMENTS

We are indebted to Dieter Jahn (BRICS, Braunschweig, Germany) for critically reading the manuscript and continuous support. We thank the Open Access Publication Funds of the Technische Universität Braunschweig. The funders had no role in study design, data collection and interpretation, or the decision to submit the work for publication.

SUPPLEMENTARY MATERIAL

The Supplementary Material for this article can be found online at: https://www.frontiersin.org/articles/10.3389/fbioe.2020.00047/full#supplementary-material

REFERENCES

Anderson, A. J., and Dawes, E. A. (1990). Occurrence, metabolism, metabolic role, and industrial uses of bacterial polyhydroxyalkanoates. *Microbiol. Rev.* 54, 450–472. doi: 10.1128/mmbr.54.4.450-472.1990

Antoniewicz, M. R., Kelleher, J. K., and Stephanopoulos, G. (2006). Determination of confidence intervals of metabolic fluxes estimated from stable isotope measurements. *Metab. Eng.* 8, 324–337. doi: 10.1016/j.ymben.2006.01.004

Arora, N., Singhal, V., and Maheshwari, D. (2006). Salinity-induced accumulation of poly-β-hydroxybutyrate in rhizobia indicating its role in cell protection. *World J. Microbiol. Biotechnol.* 22, 603–606. doi: 10.1007/s11274-005-9077-1

Ayub, N. D., Pettinari, M. J., Ruiz, J. A., and Lopez, N. I. (2004). A polyhydroxybutyrate-producing *Pseudomonas* sp. isolated from Antarctic environments with high stress resistance. *Curr. Microbiol.* 49, 170–174. doi: 10.1007/s00284-004-4254-2

Banci, L., Bertini, I., Ciofi-Baffoni, S., Del Conte, R., and Gonnelli, L. (2003). Understanding copper trafficking in bacteria: interaction between the copper transport protein CopZ and the N-terminal domain of the copper ATPase CopA from *Bacillus subtilis*. *Biochemistry* 42, 1939–1949. doi: 10.1021/bi027096p

Biedendieck, R. (2016). A *Bacillus megaterium* system for the production of recombinant proteins and protein complexes. *Adv. Exp. Med. Biol.* 896, 97–113. doi: 10.1007/978-3-319-27216-0_7

Biedendieck, R., Borgmeier, C., Bunk, B., Stammen, S., Scherling, C., Meinhardt, F., et al. (2011). Systems biology of recombinant protein production using *Bacillus megaterium*. *Methods Enzymol.* 500, 165–195. doi: 10.1016/B978-0-12-385118-5.00010-4

Biedendieck, R., Gamer, M., Jaensch, L., Meyer, S., Rohde, M., Deckwer, W. D., et al. (2007a). A sucrose-inducible promoter system for the intra- and extracellular protein production in *Bacillus megaterium*. *J. Biotechnol.* 132, 426–430. doi: 10.1016/j.jbiotec.2007.07.494

Biedendieck, R., Yang, Y., Deckwer, W. D., Malten, M., and Jahn, D. (2007b). Plasmid system for the intracellular production and purification of affinity-tagged proteins in *Bacillus megaterium*. *Biotechnol. Bioeng.* 96, 525–537. doi: 10.1002/bit.21145

Boch, J., Kempf, B., Schmid, R., and Bremer, E. (1996). Synthesis of the osmoprotectant glycine betaine in *Bacillus subtilis*: characterization of the *gbsAB* genes. *J. Bacteriol.* 178, 5121–5129. doi: 10.1128/jb.178.17.5121-5129.1996

Brill, J., Hoffmann, T., Bleisteiner, M., and Bremer, E. (2011a). Osmotically controlled synthesis of the compatible solute proline is critical for cellular defense of *Bacillus subtilis* against high osmolarity. *J. Bacteriol.* 193, 5335–5346. doi: 10.1128/JB.05490-11

Brill, J., Hoffmann, T., Putzer, H., and Bremer, E. (2011b). T-box-mediated control of the anabolic proline biosynthetic genes of *Bacillus subtilis*. *Microbiology* 157, 977–987. doi: 10.1099/mic.0.047357-0

Chavarria, M., Nikel, P. I., Perez-Pantoja, D., and de Lorenzo, V. (2013). The Entner-Doudoroff pathway empowers *Pseudomonas putida* KT2440 with a high tolerance to oxidative stress. *Environ. Microbiol.* 15, 1772–1785. doi: 10.1111/1462-2920.12069

Chien, A. C., Hill, N. S., and Levin, P. A. (2012). Cell size control in bacteria. *Curr. Biol.* 22, R340–R349. doi: 10.1016/j.cub.2012.02.032

Corbett, D., Schuler, S., Glenn, S., Andrew, P. W., Cavet, J. S., and Roberts, I. S. (2011). The combined actions of the copper-responsive repressor CsoR and copper-metallochaperone CopZ modulate CopA-mediated copper efflux in the intracellular pathogen *Listeria monocytogenes*. *Mol. Microbiol.* 81, 457–472. doi: 10.1111/j.1365-2958.2011.07705.x

Dejean, S., Gonzalez, I., Lê Cao, K.-A., and Monget, P. (2011). *mixOmics: Omics Data Integration Project. R package version, 2.9–4*.

den Besten, H. M., Mols, M., Moezelaar, R., Zwietering, M. H., and Abee, T. (2009). Phenotypic and transcriptomic analyses of mildly and severely salt-stressed *Bacillus cereus* ATCC 14579 cells. *Appl. Environ. Microbiol.* 75, 4111–4119. doi: 10.1128/AEM.02891-08

Eppinger, M., Bunk, B., Johns, M. A., Edirisinghe, J. N., Kutumbaka, K. K., Koenig, S. S., et al. (2011). Genome sequences of the biotechnologically important *Bacillus megaterium* strains QM B1551 and DSM319. *J. Bacteriol.* 193, 4199–4213. doi: 10.1128/JB.00449-11

Epstein, W. (2003). The roles and regulation of potassium in bacteria. *Prog. Nucleic Acid Res. Mol. Biol.* 75, 293–320. doi: 10.1016/s0079-6603(03)75008-9

Freedman, A. J. E., Peet, K. C., Boock, J. T., Penn, K., Prather, K. L. J., and Thompson, J. R. (2018). Isolation, development, and genomic analysis of *Bacillus megaterium* SR7 for growth and metabolite production under supercritical carbon dioxide. *Front. Microbiol.* 9:2152. doi: 10.3389/fmicb.2018.02152

Fürch, T., Wittmann, C., Wang, W., Franco-Lara, E., Jahn, D., and Deckwer, W. D. (2007). Effect of different carbon sources on central metabolic fluxes and the recombinant production of a hydrolase from *Thermobifida fusca* in *Bacillus megaterium*. *J. Biotechnol.* 132, 385–394. doi: 10.1016/j.jbiotec.2007.08.004

Galaris, D., and Pantopoulos, K. (2008). Oxidative stress and iron homeostasis: mechanistic and health aspects. *Crit. Rev. Clin. Lab. Sci.* 45, 1–23. doi: 10.1080/10408360701713104

Giro, M., Carrillo, N., and Krapp, A. R. (2006). Glucose-6-phosphate dehydrogenase and ferredoxin-NADP(H) reductase contribute to damage repair during the soxRS response of *Escherichia coli*. *Microbiology* 152(Pt 4), 1119–1128. doi: 10.1099/mic.0.28612-0

Graf, R., Anzali, S., Buenger, J., Pfluecker, F., and Driller, H. (2008). The multifunctional role of ectoine as a natural cell protectant. *Clin. Dermatol.* 26, 326–333. doi: 10.1016/j.clindermatol.2008.01.002

Grage, K., McDermott, P., and Rehm, B. H. A. (2017). Engineering *Bacillus megaterium* for production of functional intracellular materials. *Microb Cell Fact.* 16:211. doi: 10.1186/s12934-017-0823-5

Gröger, H., and Wilken, J. (2001). The application of l-proline as an enzyme mimic and further new asymmetric syntheses using small organic molecules as chiral catalysts. *Angew. Chem. Int. Ed.* 40, 529–532. doi: 10.1002/1521-3773(20010202)40:3<529::AID-ANIE529>3.0.CO;2-X

Grundy, F. J., and Henkin, T. M. (1993). tRNA as a positive regulator of transcription antitermination in *B. subtilis*. *Cell* 74, 475–482. doi: 10.1016/0092-8674(93)80049-k

Gunka, K., and Commichau, F. M. (2012). Control of glutamate homeostasis in *Bacillus subtilis*: a complex interplay between ammonium assimilation, glutamate biosynthesis and degradation. *Mol. Microbiol.* 85, 213–224. doi: 10.1111/j.1365-2958.2012.08105.x

Gyan, S., Shiohira, Y., Sato, I., Takeuchi, M., and Sato, T. (2006). Regulatory loop between redox sensing of the NADH/NAD(+) ratio by Rex (YdiH) and oxidation of NADH by NADH dehydrogenase Ndh in *Bacillus subtilis*. *J. Bacteriol.* 188, 7062–7071. doi: 10.1128/JB.00601-06

Hahne, H., Mader, U., Otto, A., Bonn, F., Steil, L., Bremer, E., et al. (2010). A comprehensive proteomics and transcriptomics analysis of *Bacillus subtilis* salt stress adaptation. *J. Bacteriol.* 192, 870–882. doi: 10.1128/JB.01106-09

Hamilton, T. L., Ludwig, M., Dixon, R., Boyd, E. S., Dos Santos, P. C., Setubal, J. C., et al. (2011). Transcriptional profiling of nitrogen fixation in *Azotobacter vinelandii*. *J. Bacteriol.* 193, 4477–4486. doi: 10.1128/JB.05099-11

Harwood, C. R., and Cutting, S. M. (1990). *Molecular Biological Methods for Bacillus*. New York, NY: Wiley.

Hecker, M., and Völker, U. (2001). General stress response of *Bacillus subtilis* and other bacteria. *Adv. Microb. Physiol.* 44, 35–91. doi: 10.1016/S0065-2911(01)44011-2

Hess, B., and Brand, K. (1965). "Enzyme and metabolite profiles," in *Control of Energy Metabolism*, eds E. R. Chance, and B. Williamson, Jr. (New York, NY: Academic Press), 111–122. doi: 10.1016/b978-1-4832-3161-7.50020-3

Hochgräfe, F., Mostertz, J., Pother, D. C., Becher, D., Helmann, J. D., and Hecker, M. (2007). S-cysteinylation is a general mechanism for thiol protection of *Bacillus subtilis* proteins after oxidative stress. *J. Biol. Chem.* 282, 25981–25985. doi: 10.1074/jbc.C700105200

Hoffmann, T., and Bremer, E. (2017). Guardians in a stressful world: the Opu family of compatible solute transporters from *Bacillus subtilis*. *Biol. Chem.* 398, 193–214. doi: 10.1515/hsz-2016-0265

Hoffmann, T., Schutz, A., Brosius, M., Volker, A., Volker, U., and Bremer, E. (2002). High-salinity-induced iron limitation in *Bacillus subtilis*. *J. Bacteriol.* 184, 718–727. doi: 10.1128/JB.184.3.718-727.2002

Hoffmann, T., Wensing, A., Brosius, M., Steil, L., Volker, U., and Bremer, E. (2013). Osmotic control of *opuA* expression in *Bacillus subtilis* and its modulation in response to intracellular glycine betaine and proline pools. *J. Bacteriol.* 195, 510–522. doi: 10.1128/JB.01505-12

Hollmann, R., and Deckwer, W. D. (2004). Pyruvate formation and suppression in recombinant *Bacillus megaterium* cultivation. *J. Biotechnol.* 111, 89–96. doi: 10.1016/j.jbiotec.2004.03.006

Holtmann, G., Bakker, E. P., Uozumi, N., and Bremer, E. (2003). KtrAB and KtrCD: two K+ uptake systems in *Bacillus subtilis* and their role in adaptation to hypertonicity. *J. Bacteriol.* 185, 1289–1298. doi: 10.1128/JB.185.4.1289-1298.2003

Höper, D., Bernhardt, J., and Hecker, M. (2006). Salt stress adaptation of *Bacillus subtilis*: a physiological proteomics approach. *Proteomics* 6, 1550–1562. doi: 10.1002/pmic.200500197

Huang, R., and Reusch, R. N. (1996). Poly (3-hydroxybutyrate) is associated with specific proteins in the cytoplasm and membranes of *Escherichia coli*. *J. Biol. Chem.* 271, 22196–22202. doi: 10.1074/jbc.271.36.22196

Ishikawa, T., Mizunoe, Y., Kawabata, S., Takade, A., Harada, M., Wai, S. N., et al. (2003). The iron-binding protein Dps confers hydrogen peroxide stress resistance to *Campylobacter jejuni*. *J. Bacteriol.* 185, 1010–1017. doi: 10.1128/JB.185.3.1010-1017.2003

Johnson, S. L., Daligault, H. E., Davenport, K. W., Jaissle, J., Frey, K. G., Ladner, J. T., et al. (2015). Complete genome sequences for 35 biothreat assay-relevant bacillus species. *Genome Announc.* 3:e00151-15. doi: 10.1128/genomeA.00151-15

Junker, B. H., Klukas, C., and Schreiber, F. (2006). VANTED: a system for advanced data analysis and visualization in the context of biological networks. *BMC Bioinformatics* 7:109. doi: 10.1186/1471-2105-7-109

Kaneda, T. (1991). Iso- and anteiso-fatty acids in bacteria: biosynthesis, function, and taxonomic significance. *Microbiol. Rev.* 55, 288–302. doi: 10.1128/mmbr.55.2.288-302.1991

Kappes, R. M., Kempf, B., Kneip, S., Boch, J., Gade, J., Meier-Wagner, J., et al. (1999). Two evolutionarily closely related ABC transporters mediate the uptake of choline for synthesis of the osmoprotectant glycine betaine in *Bacillus subtilis*. *Mol. Microbiol.* 32, 203–216. doi: 10.1046/j.1365-2958.1999.01354.x

Kempf, B., and Bremer, E. (1998). Uptake and synthesis of compatible solutes as microbial stress responses to high-osmolality environments. *Arch. Microbiol.* 170, 319–330. doi: 10.1007/s002030050649

Klonne, D. R., Dodd, D. E., Losco, P. E., Troup, C. M., and Tyler, T. R. (1989). Two-week aerosol inhalation study on polyethylene glycol (PEG) 3350 in F-344 rats. *Drug Chem. Toxicol.* 12, 39–48. doi: 10.3109/01480548908999141

Koch, A. L. (1984). Shrinkage of growing *Escherichia coli* cells by osmotic challenge. *J. Bacteriol.* 159, 919–924. doi: 10.1128/jb.159.3.919-924.1984

Kohlstedt, M., Sappa, P. K., Meyer, H., Maass, S., Zaprasis, A., Hoffmann, T., et al. (2014). Adaptation of *Bacillus subtilis* carbon core metabolism to simultaneous nutrient limitation and osmotic challenge: a multi-omics perspective. *Environ. Microbiol.* 16, 1898–1917. doi: 10.1111/1462-2920.12438

Korber, D. R., Choi, A., Wolfaardt, G. M., and Caldwell, D. E. (1996). Bacterial plasmolysis as a physical indicator of viability. *Appl. Environ. Microbiol.* 62, 3939–3947. doi: 10.1128/aem.62.11.3939-3947.1996

Korneli, C., Bolten, C. J., Godard, T., Franco-Lara, E., and Wittmann, C. (2012). Debottlenecking recombinant protein production in *Bacillus megaterium* under large-scale conditions–targeted precursor feeding designed from metabolomics. *Biotechnol. Bioeng.* 109, 1538–1550. doi: 10.1002/bit.24434

Korneli, C., David, F., Biedendieck, R., Jahn, D., and Wittmann, C. (2013). Getting the big beast to work—systems biotechnology of *Bacillus megaterium* for novel high-value proteins. *J. Biotechnol.* 163, 87–96. doi: 10.1016/j.jbiotec.2012.06.018

Kromer, J. O., Fritz, M., Heinzle, E., and Wittmann, C. (2005). In vivo quantification of intracellular amino acids and intermediates of the methionine pathway in *Corynebacterium glutamicum*. *Anal. Biochem.* 340, 171–173. doi: 10.1016/j.ab.2005.01.027

Kulpreecha, S., Boonruangthavorn, A., Meksiriporn, B., and Thongchul, N. (2009). Inexpensive fed-batch cultivation for high poly(3-hydroxybutyrate) production by a new isolate of *Bacillus megaterium*. *J. Biosci. Bioeng.* 107, 240–245. doi: 10.1016/j.jbiosc.2008.10.006

Lakowitz, A., Krull, R., and Biedendieck, R. (2017). Recombinant production of the antibody fragment D1.3 scFv with different *Bacillus strains*. *Microb Cell Fact.* 16:14. doi: 10.1186/s12934-017-0625-9

Lê, S., Josse, J., and Husson, F. (2008). FactoMineR: an R package for multivariate analysis. *J. Stat. Softw.* 25, 1–18. doi: 10.18637/jss.v025.i01

Levine, R. L., Berlett, B. S., Moskovitz, J., Mosoni, L., and Stadtman, E. R. (1999). Methionine residues may protect proteins from critical oxidative damage. *Mech. Ageing Dev.* 107, 323–332. doi: 10.1016/S0047-6374(98)00152-3

Lewis, D. F. V. (2002). Oxidative stress: the role of cytochromes P450 in oxygen activation. *J. Chem. Technol. Biotechnol.* 77, 1095–1100. doi: 10.1002/jctb.648

Li, M., Ho, P. Y., Yao, S., and Shimizu, K. (2006). Effect of *lpdA* gene knockout on the metabolism in *Escherichia coli* based on enzyme activities, intracellular metabolite concentrations and metabolic flux analysis by 13C-labeling experiments. *J. Biotechnol.* 122, 254–266. doi: 10.1016/j.jbiotec.2005.09.016

Liu, L., Li, Y., Zhang, J., Zou, W., Zhou, Z., Liu, J., et al. (2011). Complete genome sequence of the industrial strain *Bacillus megaterium* WSH-002. *J. Bacteriol.* 193, 6389–6390. doi: 10.1128/JB.06066-11

Mäder, U., Schmeisky, A. G., Flórez, L. A., and Stülke, J. (2012). SubtiWiki—a comprehensive community resource for the model organism *Bacillus subtilis*. *Nucleic Acids Res.* 40, D1278–D1287. doi: 10.1093/nar/gkr923

Madison, L. L., and Huisman, G. W. (1999). Metabolic engineering of poly(3-hydroxyalkanoates): from DNA to plastic. *Microbiol. Mol. Biol. Rev.* 63, 21–53. doi: 10.1128/mmbr.63.1.21-53.1999

Margolin, W. (2005). FtsZ and the division of prokaryotic cells and organelles. *Nat. Rev. Mol. Cell Biol.* 6, 862–871. doi: 10.1038/nrm1745

Marquis, R. E. (1968). Salt-induced contraction of bacterial cell walls. *J. Bacteriol.* 95, 775–781. doi: 10.1128/jb.95.3.775-781.1968

Mayer, J., Pippel, J., Gunther, G., Muller, C., Lauermann, A., Knuuti, T., et al. (2019). Crystal structures and protein engineering of three different penicillin G acylases from Gram-positive bacteria with different thermostability. *Appl. Microbiol. Biotechnol.* 103, 7537–7552. doi: 10.1007/s00253-019-09977-8

McLaggan, D., Naprstek, J., Buurman, E. T., and Epstein, W. (1994). Interdependence of K+ and glutamate accumulation during osmotic adaptation of *Escherichia coli*. *J. Biol. Chem.* 269, 1911–1917.

Misirli, G., Hallinan, J., Rottger, R., Baumbach, J., and Wipat, A. (2014). BacillusRegNet: a transcriptional regulation database and analysis platform for *Bacillus* species. *J. Integr. Bioinform.* 11:244. doi: 10.2390/biecoll-jib-2014-244

Mohapatra, S., Maity, S., Dash, H. R., Das, S., Pattnaik, S., Rath, C. C., et al. (2017). *Bacillus* and biopolymer: prospects and challenges. *Biochem. Biophys. Rep.* 12, 206–213. doi: 10.1016/j.bbrep.2017.10.001

Mozejko-Ciesielska, J., and Kiewisz, R. (2016). Bacterial polyhydroxyalkanoates: still fabulous? *Microbiol. Res.* 192, 271–282. doi: 10.1016/j.micres.2016.07.010

Muntel, J., Fromion, V., Goelzer, A., Maabeta, S., Mader, U., Buttner, K., et al. (2014). Comprehensive absolute quantification of the cytosolic proteome of *Bacillus subtilis* by data independent, parallel fragmentation in liquid chromatography/mass spectrometry (LC/MS(E)). *Mol. Cell. Proteomics* 13, 1008–1019. doi: 10.1074/mcp.M113.032631

Muntel, J., Hecker, M., and Becher, D. (2012). An exclusion list based label-free proteome quantification approach using an LTQ orbitrap. *Rapid Commun. Mass Spectrom.* 26, 701–709. doi: 10.1002/rcm.6147

Nair, I. C., Pradeep, S., Ajayan, M., Jayachandran, K., and Shashidhar, S. (2009). Accumulation of intracellular polyhydroxybutyrate in *Alcaligenes* sp. d2 under phenol stress. *Appl. Biochem. Biotechnol.* 159, 545–552. doi: 10.1007/s12010-008-8454-2

Natarajan, K., Kishore, L., and Babu, C. (1995). Sodium chloride stress results in increased poly-β-hydroxybutyrate production in Rhizobium DDSS 69. *Microbios* 82, 95–107.

Nau-Wagner, G., Opper, D., Rolbetzki, A., Boch, J., Kempf, B., Hoffmann, T., et al. (2012). Genetic control of osmoadaptive glycine betaine synthesis in *Bacillus subtilis* through the choline-sensing and glycine betaine-responsive GbsR repressor. *J. Bacteriol.* 194, 2703–2714. doi: 10.1128/JB.06642-11

Oliva-Arancibia, B., Ordenes-Aenishanslins, N., Bruna, N., Ibarra, P. S., Zacconi, F. C., Perez-Donoso, J. M., et al. (2017). Co-synthesis of medium-chain-length polyhydroxyalkanoates and CdS quantum dots nanoparticles in *Pseudomonas putida* KT2440. *J. Biotechnol.* 264, 29–37. doi: 10.1016/j.jbiotec.2017.10.013

Oren, A. (2010). Industrial and environmental applications of halophilic microorganisms. *Environ. Technol.* 31, 825–834. doi: 10.1080/09593330903370026

Pacheco, N., Orellana-Saez, M., Pepczynska, M., Enrione, J., Bassas-Galia, M., Borrero-de Acuna, J. M., et al. (2019). Exploiting the natural poly(3-hydroxyalkanoates) production capacity of Antarctic *Pseudomonas* strains:

from unique phenotypes to novel biopolymers. *J. Ind. Microbiol. Biotechnol.* 46, 1139–1153. doi: 10.1007/s10295-019-02186-2

Page, W. J., Manchak, J., and Rudy, B. (1992). Formation of poly(hydroxybutyrate-co-hydroxyvalerate) by *Azotobacter vinelandii* UWD. *Appl. Environ. Microbiol.* 58, 2866–2873. doi: 10.1128/aem.58.9.2866-2873.1992

Perez-Riverol, Y., Csordas, A., Bai, J., Bernal-Llinares, M., Hewapathirana, S., Kundu, D. J., et al. (2019). The PRIDE database and related tools and resources in 2019: improving support for quantification data. *Nucleic Acids Res.* 47, D442–D450. doi: 10.1093/nar/gky1106

Peyrot, F., and Ducrocq, C. (2008). Potential role of tryptophan derivatives in stress responses characterized by the generation of reactive oxygen and nitrogen species. *J. Pineal Res.* 45, 235–246. doi: 10.1111/j.1600-079X.2008.00580.x

Poblete-Castro, I., Escapa, I. F., Jäger, C., Puchalka, J., Lam, C. M. C., Schomburg, D., et al. (2012). The metabolic response of *P. putida* KT2442 producing high levels of polyhydroxyalkanoate under single-and multiple-nutrient-limited growth: highlights from a multi-level omics approach. *Microb Cell Fact.* 11:34. doi: 10.1186/1475-2859-11-34

Pomposiello, P. J., Bennik, M. H., and Demple, B. (2001). Genome-wide transcriptional profiling of the *Escherichia coli* responses to superoxide stress and sodium salicylate. *J. Bacteriol.* 183, 3890–3902. doi: 10.1128/JB.183.13.3890-3902.2001

Pötter, M., and Steinbüchel, A. (2005). Poly (3-hydroxybutyrate) granule-associated proteins: impacts on poly (3-hydroxybutyrate) synthesis and degradation. *Biomacromolecules* 6, 552–560. doi: 10.1021/bm049401n

Quek, L.-E., Wittmann, C., Nielsen, L. K., and Krömer, J. O. (2009). OpenFLUX: efficient modelling software for 13C-based metabolic flux analysis. *Microb Cell Fact.* 8:25. doi: 10.1186/1475-2859-8-25

Radford, D. S., Kihlken, M. A., Borrelly, G. P., Harwood, C. R., Le Brun, N. E., and Cavet, J. S. (2003). CopZ from *Bacillus subtilis* interacts in vivo with a copper exporting CPx-type ATPase CopA. *FEMS Microbiol. Lett.* 220, 105–112. doi: 10.1016/S0378-1097(03)00095-8

Rappsilber, J., Mann, M., and Ishihama, Y. (2007). Protocol for micro-purification, enrichment, pre-fractionation and storage of peptides for proteomics using StageTips. *Nat. Protoc.* 2, 1896–1906. doi: 10.1038/nprot.2007.261

Rehm, B. H. (2010). Bacterial polymers: biosynthesis, modifications and applications. *Nat. Rev. Microbiol.* 8, 578–592. doi: 10.1038/nrmicro2354

Rhee, S. G., Kang, S. W., Jeong, W., Chang, T. S., Yang, K. S., and Woo, H. A. (2005). Intracellular messenger function of hydrogen peroxide and its regulation by peroxiredoxins. *Curr. Opin. Cell Biol.* 17, 183–189. doi: 10.1016/j.ceb.2005.02.004

Rohn, H., Hartmann, A., Junker, A., Junker, B. H., and Schreiber, F. (2012). FluxMap: a VANTED add-on for the visual exploration of flux distributions in biological networks. *BMC Syst. Biol.* 6:33. doi: 10.1186/1752-0509-6-33

Rygus, T., and Hillen, W. (1991). Inducible high-level expression of heterologous genes in *Bacillus megaterium* using the regulatory elements of the xylose-utilization operon. *Appl. Microbiol. Biotechnol.* 35, 594–599.

Sangkharak, K., and Prasertsan, P. (2012). Screening and identification of polyhydroxyalkanoates producing bacteria and biochemical characterization of their possible application. *J. Gen. Appl. Microbiol.* 58, 173–182. doi: 10.2323/jgam.58.173

Sauer, U., and Eikmanns, B. J. (2005). The PEP-pyruvate-oxaloacetate node as the switch point for carbon flux distribution in bacteria. *FEMS Microbiol. Rev.* 29, 765–794. doi: 10.1016/j.femsre.2004.11.002

Schroeter, R., Hoffmann, T., Voigt, B., Meyer, H., Bleisteiner, M., Muntel, J., et al. (2013). Stress responses of the industrial workhorse *Bacillus licheniformis* to osmotic challenges. *PLoS One* 8:e80956. doi: 10.1371/journal.pone.0080956

Schweder, T., Kruger, E., Xu, B., Jurgen, B., Blomsten, G., Enfors, S. O., et al. (1999). Monitoring of genes that respond to process-related stress in large-scale bioprocesses. *Biotechnol. Bioeng.* 65, 151–159. doi: 10.1002/(sici)1097-0290(19991020)65:2<151::aid-bit4>3.0.co;2-v

Singh, K. P., Zaidi, A., Anwar, S., Bimal, S., Das, P., and Ali, V. (2014). Reactive oxygen species regulates expression of iron–sulfur cluster assembly protein IscS of *Leishmania donovani*. *Free Radic. Biol. Med.* 75, 195–209. doi: 10.1016/j.freeradbiomed.2014.07.017

Stammen, S., Muller, B. K., Korneli, C., Biedendieck, R., Gamer, M., Franco-Lara, E., et al. (2010). High-yield intra- and extracellular protein production using *Bacillus megaterium*. *Appl. Environ. Microbiol.* 76, 4037–4046. doi: 10.1128/AEM.00431-10

Steil, L., Hoffmann, T., Budde, I., Volker, U., and Bremer, E. (2003). Genome-wide transcriptional profiling analysis of adaptation of *Bacillus subtilis* to high salinity. *J. Bacteriol.* 185, 6358–6370. doi: 10.1128/JB.185.21.6358-6370.2003

Takagi, H. (2008). Proline as a stress protectant in yeast: physiological functions, metabolic regulations, and biotechnological applications. *Appl. Microbiol. Biotechnol.* 81, 211–223. doi: 10.1007/s00253-008-1698-5

Tognetti, V. B., Palatnik, J. F., Fillat, M. F., Melzer, M., Hajirezaei, M.-R., Valle, E. M., et al. (2006). Functional replacement of ferredoxin by a cyanobacterial flavodoxin in tobacco confers broad-range stress tolerance. *Plant Cell* 18, 2035–2050. doi: 10.1105/tpc.106.042424

van Winden, W. A., Wittmann, C., Heinzle, E., and Heijnen, J. J. (2002). Correcting mass isotopomer distributions for naturally occurring isotopes. *Biotechnol. Bioeng.* 80, 477–479. doi: 10.1002/bit.10393

Vary, P. S., Biedendieck, R., Fuerch, T., Meinhardt, F., Rohde, M., Deckwer, W. D., et al. (2007). *Bacillus megaterium*–from simple soil bacterium to industrial protein production host. *Appl. Microbiol. Biotechnol.* 76, 957–967. doi: 10.1007/s00253-007-1089-3

Verlinden, R. A., Hill, D. J., Kenward, M. A., Williams, C. D., Piotrowska-Seget, Z., and Radecka, I. K. (2011). Production of polyhydroxyalkanoates from waste frying oil by *Cupriavidus necator*. *AMB Express* 1:11. doi: 10.1186/2191-0855-1-11

Wang, Q., Yu, H., Xia, Y., Kang, Z., and Qi, Q. (2009). Complete PHB mobilization in *Escherichia coli* enhances the stress tolerance: a potential biotechnological application. *Microb Cell Fact.* 8:47. doi: 10.1186/1475-2859-8-47

Wang, W., Hollmann, R., Furch, T., Nimtz, M., Malten, M., Jahn, D., et al. (2005). Proteome analysis of a recombinant *Bacillus megaterium* strain during heterologous production of a glucosyltransferase. *Proteome Sci.* 3:4. doi: 10.1186/1477-5956-3-4

Wang, W., Sun, J., Hollmann, R., Zeng, A. P., and Deckwer, W. D. (2006). Proteomic characterization of transient expression and secretion of a stress-related metalloprotease in high cell density culture of *Bacillus megaterium*. *J. Biotechnol.* 126, 313–324. doi: 10.1016/j.jbiotec.2006.05.005

Warnes, G. R., Bolker, B., Bonebakker, L., Gentleman, R., Huber, W., Liaw, A., et al. (2014). *gplots: Various R Programming Tools for Plotting Data. 2013. R package version 2(1)*.

Whatmore, A. M., Chudek, J. A., and Reed, R. H. (1990). The effects of osmotic upshock on the intracellular solute pools of *Bacillus subtilis*. *J. Gen. Microbiol.* 136, 2527–2535. doi: 10.1099/00221287-136-12-2527

Wilkinson, L., and Urbanek, S. (2011). *Venneuler: Venn and Euler Diagrams. R package version 1(1)*.

Wittmann, C. (2002). Metabolic flux analysis using mass spectrometry. *Adv. Biochem. Eng. Biotechnol.* 74, 39–64. doi: 10.1007/3-540-45736-4_3

Wittmann, C., Hans, M., and Heinzle, E. (2002). *In vivo* analysis of intracellular amino acid labelings by GC/MS. *Anal. Biochem.* 307, 379–382. doi: 10.1016/S0003-2697(02)00030-1

Wojtczak, L., and Slyshenkov, V. S. (2003). Protection by pantothenic acid against apoptosis and cell damage by oxygen free radicals-the role of glutathione. *Biofactors* 17, 61–73. doi: 10.1002/biof.5520170107

Woo, S., Subramanian, P., Ramasamy, K., Joe, M. M., and Sa, T. (2012). EPS production, PHB accumulation and abiotic stress endurance of plant growth promoting *Methylobacterium* strains grown in a high carbon concentration. *Korean J. Soil Sci. Fert.* 45, 572–581. doi: 10.7745/KJSSF.2012.45.4.572

Yamakura, F., and Ikeda, K. (2006). Modification of tryptophan and tryptophan residues in proteins by reactive nitrogen species. *Nitric Oxide* 14, 152–161. doi: 10.1016/j.niox.2005.07.009

Yang, J., Wongsa, S., Kadirkamanathan, V., Billings, S., and Wright, P. (2005). Metabolic flux distribution analysis by 13C-tracer experiments using the Markov chain-Monte Carlo method. *Biochem. Soc. Trans.* 33, 1421–1422. doi: 10.1042/BST20051421

Ying, W. (2008). NAD+/NADH and NADP+/NADPH in cellular functions and cell death: regulation and biological consequences. *Antioxid. Redox Signal.* 10, 179–206. doi: 10.1089/ars.2007.1672

York, G. M., Stubbe, J., and Sinskey, A. J. (2001). New insight into the role of the PhaP phasin of *Ralstonia eutropha* in promoting synthesis of polyhydroxybutyrate. *J. Bacteriol.* 183, 2394–2397. doi: 10.1128/JB.183.7.2394-2397.2001

Zhao, F., Gong, T., Liu, X., Fan, X., Huang, R., Ma, T., et al. (2019). Morphology engineering for enhanced production of medium-chain-length polyhydroxyalkanoates in *Pseudomonas mendocina* NK-01. *Appl. Microbiol. Biotechnol.* 103, 1713–1724. doi: 10.1007/s00253-018-9546-8

Zhao, Y. H., Li, H. M., Qin, L. F., Wang, H. H., and Chen, G.-Q. (2007). Disruption of the polyhydroxyalkanoate synthase gene in *Aeromonas hydrophila* reduces its survival ability under stress conditions. *FEMS Microbiol. Lett.* 276, 34–41. doi: 10.1111/j.1574-6968.2007.00904.x

Zühlke, D., Dorries, K., Bernhardt, J., Maass, S., Muntel, J., Liebscher, V., et al. (2016). Costs of life - Dynamics of the protein inventory of *Staphylococcus aureus* during anaerobiosis. *Sci. Rep*. 6:28172. doi: 10.1038/srep28172

Zurbriggen, M. D., Tognetti, V. B., and Carrillo, N. (2007). Stress-inducible flavodoxin from photosynthetic microorganisms. The mystery of flavodoxin loss from the plant genome. *IUBMB Life* 59, 355–360. doi: 10.1080/15216540701258744

Conflict of Interest: The authors declare that the research was conducted in the absence of any commercial or financial relationships that could be construed as a potential conflict of interest.

frontiers in Bioengineering and Biotechnology

ORIGINAL RESEARCH
published: 05 March 2020
doi: 10.3389/fbioe.2020.00161

Engineering the Osmotic State of *Pseudomonas putida* KT2440 for Efficient Cell Disruption and Downstream Processing of Poly(3-Hydroxyalkanoates)

*Ignacio Poblete-Castro[1], Carla Aravena-Carrasco[1], Matias Orellana-Saez[1], Nicolás Pacheco[1], Alex Cabrera[2] and José Manuel Borrero-de Acuña[3,4]**

[1] Biosystems Engineering Laboratory, Center for Bioinformatics and Integrative Biology, Faculty of Life Sciences, Universidad Andres Bello, Santiago, Chile, [2] Unidad de Citometría de Flujo, Facultad de Ciencias Biológicas, Pontificia Universidad Católica de Chile, Santiago, Chile, [3] Institute of Microbiology, Technische Universität Braunschweig, Braunschweig, Germany, [4] Braunschweig Integrated Centre of Systems Biology, Technische Universität Braunschweig, Braunschweig, Germany

OPEN ACCESS

Edited by:
Susana Rodriguez-Couto,
Independent Researcher, Vigo, Spain

Reviewed by:
Vivek Sharma,
Chandigarh University, India
Bo Zhang,
Zhejiang University of Technology, China
Martin Koller,
University of Graz, Austria

***Correspondence:**
José Manuel Borrero-de Acuña
josborre@tu-bs.de

Specialty section:
This article was submitted to Industrial Biotechnology, a section of the journal Frontiers in Bioengineering and Biotechnology

Received: 04 December 2019
Accepted: 17 February 2020
Published: 05 March 2020

Citation:
Poblete-Castro I, Aravena-Carrasco C, Orellana-Saez M, Pacheco N, Cabrera A and Borrero-de Acuña JM (2020) Engineering the Osmotic State of Pseudomonas putida KT2440 for Efficient Cell Disruption and Downstream Processing of Poly(3-Hydroxyalkanoates). Front. Bioeng. Biotechnol. 8:161. doi: 10.3389/fbioe.2020.00161

In the last decade, the development of novel programmable cell lytic systems based on different inducible genetic constructs like the holin–endolysin and lysozyme appears as a promising alternative to circumvent the use of costly enzymes and mechanical disrupters for downstream processing of intracellular microbial products. Despite the advances, upon activation of these systems the cellular disruption of the biocatalyst occurs in an extended period, thus delaying the recovery of poly(3-hydroxyalkanoate) (PHA). Herein the osmotic state of *Pseudomonas putida* KT2440 was engineered by inactivating the inner-membrane residing rescue valve MscL, which is responsible mainly for circumventing low-osmolarity challenges. Then the major outer membrane porin OprF and the specific porin OprE were overproduced during PHA producing conditions on decanoate-grown cells. The engineered *P. putida* strains carrying each porin showed no impairment on growth rate and final biomass and PHA yield after 48 h cultivation. Expression of both porins in tandem in the mutant strain KTΔ*mscL-oprFE* led to a slight reduction of the biomass synthesis (∼10%) but higher PHA accumulation (%wt) relative to the cell dry mass. Each strain was then challenged to an osmotic upshift for 1 h and subsequently to a rapid passage to a hypotonic condition where the membrane stability of the KTΔ*mscL-oprFE* suffered damage, resulting in a rapid reduction of cell viability. Cell disruption accounted for >95% of the cell population within 3 h as reported by colony forming units (CFU), FACS analyses, and transmission electron microscopy. PHA recovery yielded 94.2% of the biosynthesized biopolymer displaying no significant alterations on the final monomer composition. This study can serve as an efficient genetic platform for the recovery of any microbial intracellular compound allowing less unit operation steps for cellular disruption.

Keywords: *Pseudomonas putida*, cell lysis, porins, MscL, osmotic stress, poly(3-hydroxyalkanoates), PHA recovery

INTRODUCTION

Bio-based plastics represent an attractive solution to circumvent the environmental burden posed by conventional plastics derived from fossil resources (Poblete-Castro et al., 2013). Many species of bacteria can synthesize a myriad of intracellular polymer forms ranging from polyphosphates (PolyP) (Varas et al., 2017) to sugar-containing monomers (Moradali et al., 2015). One of the most studied biopolymers in microbes is the family of poly(3-hydroxyalkanoate) (PHA), carbon inclusion bodies displaying similar physical properties to petroleum-based plastics such as polypropylene (PP). PHA diverge in the length of the monomer carbon chain comprising various polyesters such as short-chain-length (*scl*-PHA) and medium-chain-length PHA (*mcl*-PHA) (Volova et al., 2017). The PHA synthase (PhaC) catalyzes the polymerization process enabling the incorporation of different monomers in the polymeric chain of the polyoxoester, which finally results in distinct thermophysical attributes, thus expanding the number of products and application (Volova et al., 2017; Pacheco et al., 2019). *Pseudomonas putida* KT2440 is an archetype bacterium for the production of mcl-PHA (Poblete-Castro et al., 2017; Mozejko-Ciesielska et al., 2019), where their accumulation in the cell usually occurs under carbon excess accompanied by the limitation of inorganic compounds such as N, O_2, or P (Prieto et al., 2016).

The highly versatile metabolism *of P. putida* KT2440 endows the bacterium to harness a wide spectrum of substrates – waste oils, raw glycerol, lignin derivatives and further aromatics – which allows reducing the production costs (Poblete-Castro et al., 2014; Kohlstedt et al., 2018; Borrero-De Acuña et al., 2019; Poblete-Castro et al., 2019). Additionally, downstream processing procedures also contribute to increasing the overall production expenses due to the use of lytic enzymes, mechanical cell disruptors, high pressure, or temperature for recovery of the added-value products from the intracellular space of the cell. In the last decade, researchers have developed several programmable genetic systems to induce cell disruption upon command relying on holin–endolysin binary action (Liu and Curtiss, 2009; Martinez et al., 2011; Tamekou Lacmata et al., 2017) or lysozyme translocation into the periplasmic space to enable degradation of the peptidoglycan layer (Borrero-De Acuna et al., 2017).

These inducible tools find applications not only in the biopolymer manufacturer sector but also for intracellular protein release and fatty acid extraction. Despite the advances in autolysis cell technology, there are however still some pitfalls: (i) low titers of the final biopolymer, (ii) biopolymer-producing conditions harm the expression of the genetic circuits, and (iii) the cell disruption process is very slow (Borrero-De Acuna et al., 2017). With the aim of bypassing these drawbacks the construction of a programmable cell lysis system relying on the drastic shift of the osmotic state of *P. putida* cells was sought. It was hypothesized that rapid osmotic alteration of the cell milieu from hypertonic to hypotonic conditions and further depriving *P. putida* of specific response mechanisms designed to counteract osmotic stress would lead to extensive cell disruption in a shorter time.

In Gram-negative bacteria, different molecular elements localized to the inner and outer membranes maintain the cell turgor. Among them, porin proteins are water-filled channels residing in the outer membranes of Gram-negative bacteria that preserve the osmotic equilibrium in ever-changing environments as well as translocating a vast array of solutes (Hancock and Brinkman, 2002). So far, four categories of porins are known: non-specific porins, substrate-specific porins, gated porins (translocate ligands in an energy-dependent fashion), and efflux porins (Hancock and Brinkman, 2002). In pseudomonads, the major non-specific outer membrane porin is the OprF, which encloses a large N-terminal beta-barrel channel allowing the uptake of a broad range of solutes and a periplasmic C-terminal domain rich in alpha-helices (Sugawara et al., 2006). This pleiotropic trans-outer-membrane porin is to a large extent responsible for cell wall permeability and integrity and further contributes to the maintenance of the cell shape. Besides ion incorporation (weakly biased to cations), it is also responsible for the passage of low molecular mass sugars, toluene, and nitrate/nitrite (Chevalier et al., 2017).

Conversely to OprF, anaerobic condition induces the expression of the narrow channel and specific substrate-binding porin OprE (Jaouen et al., 2006). Although showing poor conductivity, the ionophore properties of OprE in *P. fluorescens* point toward a specific cation selectivity and allow diffusion of small ions (Obara and Nakae, 1992; Jaouen et al., 2006). As *P. putida* inefficiently thrives under oxygen-depleted environments the body of knowledge on how gene expression of the *oprE* remains still elusive. Moderate expression of *oprE* has been visualized by Microarray experiments when cells are grown on minimal medium with succinate as a carbon source (Hancock and Brinkman, 2002).

On the other hand, mechanosensitive channels (MscL) have proven essential in both prokaryotes and eukaryotes for regulating the cell turgor (Wang et al., 2014). The ubiquitous MscL of large conductance MscL is a conserved membrane-embedded valve, where mechanical stress cues mediate its response (Sukharev et al., 2001). In bacterial cells they act as safety valves opening their pores upon sudden hypo-osmotic shock to relieve the pressure (Colombo et al., 2003). Gating of the MscL is controlled by high external pressure (∼10 mN/m) that prompts the non-selective pore to open permitting permeabilization to various ions and small organic osmolytes (Najem et al., 2015). In bacteria, its inner membrane settlement represents the last barrier resort of the cell that prevents them from lysing.

In this study, it was hypothesized that the concomitant overproduction of the porins OprF and OprE in *P. putida* and addition of increasing amounts of salt would impose a severe osmotic stress consequently leading to outer membrane perturbation. It was found that aggravation of the osmotic distress endured by the cells via the drastic hypotonic shift in MscL devoid strains by adding distilled water. Our results show that this combined strategy provoked >95% cell lysis within 3 h as recorded by CFU counting and FACS analysis. Furthermore, the system functioned well under PHA-producing conditions, reaching a recovery of nearly 94% of the synthesized mcl-PHA.

RESULTS

Rational Approach and Assembly of the Auto-Inducible Cell Disruption System

The MscL is a relief valve that plays a crucial role during hypotonic shock in *Pseudomonas* species. Cell exposure to an external drop of osmolarity immediately triggers MscL channel production, which in consequence permits homeostatic ion release toward the outside counteracting thereby osmotic shock. It was presumed that disruption of the *mscL* gene of *P. putida* (PP_4645) would lead to deterioration of the inner membrane when cells endure hypotonic shock (**Figure 1**). Therefore, deletion of the ORF encoding for the MscL was addressed by homologous recombination leading to a scarless mutation as specified in the section "Materials and Methods." The resulting strain is hereafter named KTΔ*mscL*. Cell turgor also relies on an array of outer membrane porins, which incorporate ions into the bacterial periplasm upon demand. Altering the abundance of outer membrane-residing porins was speculated to result in drastic impairments on osmotic stress for *P. putida* and subsequently provoke cell wall damage (**Figure 1**). To utterly ensure imbalance of the cell wall osmolarity two porins were selected for overproduction. Firstly, the major outer membrane porin (OprF) encoded in the ORF PP_2089 was targeted (**Figure 1**). The second channel taken into analysis was the outer membrane integral porin OprE (PP_0234), which is normally produced under anoxygenic conditions in other *Pseudomonas* strains (**Figure 1**). In line with this, the *oprF* and *oprE* genes including Shine-Dalgarno sequences (**Table 1**) were PCR-amplified from single colonies and introduced separately into the Isopropyl β-d-1-thiogalactopyranoside (IPTG)-inducible vector pSEVA634. Each plasmid was further transferred into both KT2440 and KTΔ*mscL* strain giving rise to the following recombinant strains: KT-*oprF*, KT-*oprE*, KTΔ*mscL-oprF*, and KTΔ*mscL-oprE*. Finally, both porin-encoding genes *oprF* and *oprE* were spliced in the above given order and ligated into pSEVA634. Subsequently, this vector (pSEVA634-*oprFE*) was introduced by mating into KT2440 and KTΔ*mscL* originating the KT-*oprFE* and KTΔ*mscL-oprFE* strains, respectively.

Cell Growth and Membrane Assays of the Engineered and Wild-Type Strains

Firstly, it was evaluated whether inactivation of the *mscL* gene and overexpression of the porin genes exerted a detrimental effect on bacterial growth of all constructed strains. Frequently basal transcriptional leakage of plasmidial genes or gene suppression generates a diminished biomass synthesis that will lastly affect PHA accumulation (Guamán et al., 2018). The growth rate of the genetically modified KT2440 strains, namely KT-*oprF*, KT-*oprE*, and KT-*oprFE* did not vary significantly compared with KT2440 wild-type using decanoate (20 mM) as the sole carbon source in minimal salt medium (**Figure 2A**). Nor deletion of the *mscL* gene appears to influence biomass production negatively (**Figures 2A,B**), neither did the introduction of the porin genes into this knockout strain, before and after activation of the system via IPTG (1 mM) at 30 h cultivation (**Figure 2B**). The length of the cultivation was 48 h, as PHA synthesis reached maximal values. At this time point, the hydrophobicity and permeability of the cells were evaluated among strains. The porins locate in the outer membrane of bacteria comprise hydrophobic amino

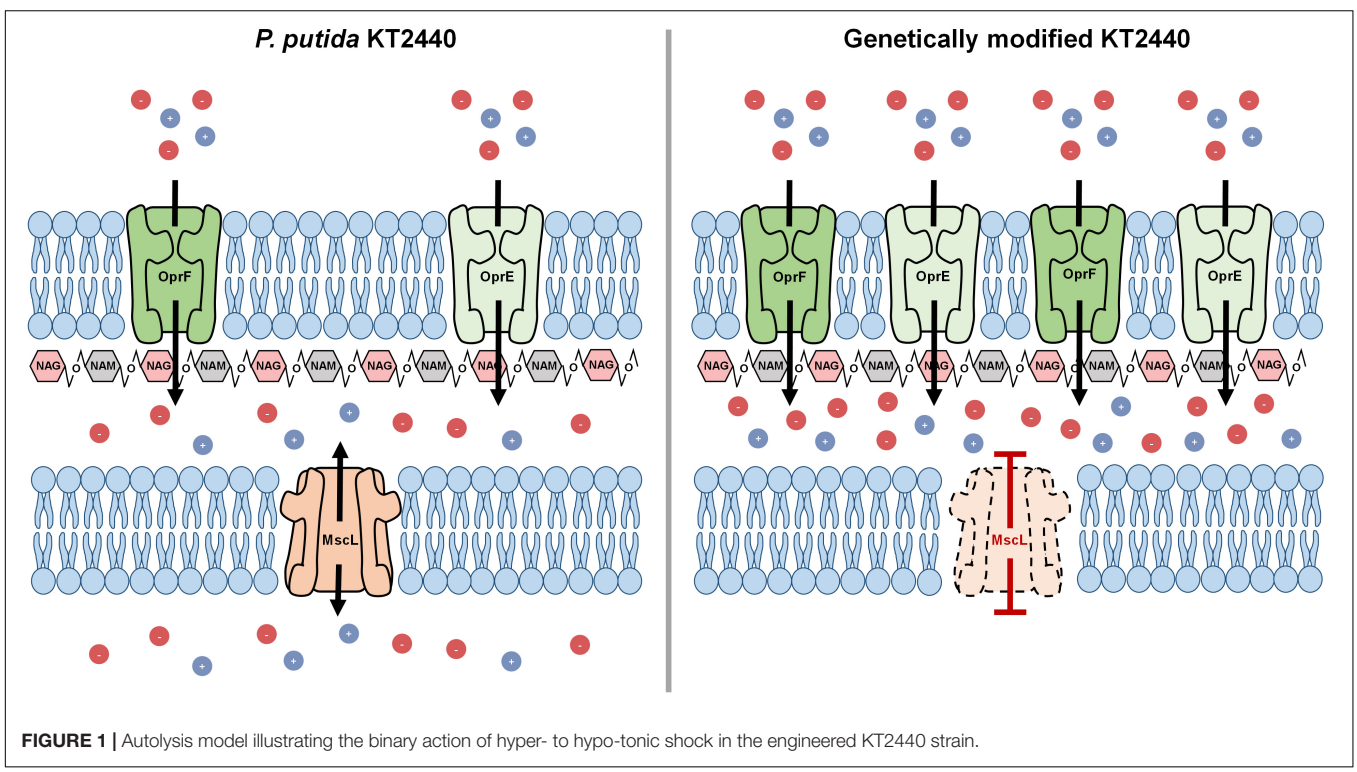

FIGURE 1 | Autolysis model illustrating the binary action of hyper- to hypo-tonic shock in the engineered KT2440 strain.

TABLE 1 | Strains, vectors, and oligos employed throughout this study.

Strain/vector	Features[a]	Source/Reference
Pseudomonas putida		
KT2440	Wild-type strain derived from *P. putida* mt-2, devoid of the pWW0 TOL plasmid	(DSMZ)
KTΔ*mscL*	KT2440 deletion mutant lacking the *mscL* gene	This study
KT-*oprF*	KT2440 strain bearing the pSEVA634-*oprF* plasmid	This study
KT-*oprE*	KT2440 strain bearing the pSEVA634-*oprE* plasmid	This study
KT-*oprFE*	KT2440 strain bearing the pSEVA634-*oprFE* plasmid	This study
KTΔ*mscL-oprF*	KT2440ΔmscL mutant strain bearing the pSEVA634-*oprF* plasmid	This study
KTΔ*mscL-oprE*	KT2440ΔmscL mutant strain bearing the pSEVA634-*oprE* plasmid	This study
KTΔ*mscL-oprFE*	KT2440ΔmscL mutant strain bearing the pSEVA634-*oprFE* plasmid	This study
Escherichia coli		
DH5α	F–Φ80*lacZ*ΔM15 Δ(*lacZYA-arg*F) U169 *rec*A1 *end*A1 *hsd*R17 (rK–, mK+) *pho*A *sup*E44 λ– *thi*-1 *gyr*A96 *rel*A1	ThermoFisher, Scientific, Darmstadt, Germany
DH5α(λpir	*sup* E44, Δ*lacU169* (Φ*lac*ZΔM15), *recA1*, *endA1*, *hsdR17*, *thi-1*, *gyrA96*, *relA1*, λpir phage lysogen	Biomedal, Seville, Spain
HB101	Helper strain; F– λ– *hsdS20*(rB– mB–) *recA13 leuB6*(Am) *araC14* Δ(gpt-proA)62 *lacY1 galK2*(Oc) *xyl*-5 *mtl*-1 *thiE1 rpsL20* (Sm^R) *glnX44*(AS)	Benedetti et al., 2016
Plasmids		
pJET1.2	Ap^R; *oriV* (pMB1) Plasmid employed for subcloning steps	ThermoFisher, Scientific, Darmstadt, Germany
pRK600	Cm^R; *oriV* (ColE1), tra+ mob+, RK2-based plasmid	Benedetti et al., 2016
pSEVA212	Km^R; *oriV* (R6K), Sce-I RS. *P. putida* non-replicative vector	Martinez-Garcia et al., 2015
pSEVA628	Gm^R; *oriV* (RK2), *xylS*-Pm → SceI	Martinez-Garcia et al., 2015
pSEVA634	Gm^R; *oriV* (RK2), *lacIq*-P*trc*	Martinez-Garcia et al., 2015
pJET1.2-*mscl*UPDW	Ap^R; pJET1.2 plasmid bearing the fused up- and downstream arms of the *mscL* gene	This study
pSEVA212-*mscl*UPDW	Km^R; pSEVA212 harboring the spliced up- and downstream flanks of the *mscL* gene	This study
pSEVA634-*oprF*	pSEVA634 plasmid enclosing the major outer membrane porin *oprF* gene	This study
pSEVA634-*oprE*	pSEVA634 plasmid harboring anaerobically induced outer membrane porin *oprE* gene	This study
pSEVA634-oprFE	pSEVA634 plasmid bearing both the *oprF* and *oprE* genes	This study
Oligos (5′ 3′)		
*mscl*UpFw	GAATTCGCAATGTTGCACAAGGTCTG	ThermoFisher, Scientific, Darmstadt, Germany
*mscl*UpRv	ACTGGACTCTTCGCCAGCTTTGGTTCCTTGTAACAAAAGGT	ThermoFisher, Scientific, Darmstadt, Germany
*mscl*DwFw	GCTGGCGAAGAGTCCAGT	ThermoFisher, Scientific, Darmstadt, Germany
*mscl*DwRv	GGATCCGGAGGTCGTGACCTGTGG	ThermoFisher, Scientific, Darmstadt, Germany
*mscl*KOFw	GCATGCTCAACGAGTTCAAG	ThermoFisher, Scientific, Darmstadt, Germany
*mscl*KORv	CGATTCTGGTTCTGCGTCTT	ThermoFisher, Scientific, Darmstadt, Germany
*oprF*Fw	GGATCC*AGGAGG*AAAAACATATGAAACTGAAAAACACCTTGG	ThermoFisher, Scientific, Darmstadt, Germany
*oprF*Rv	TCTAGATTACTTGGCCTGGGCTTCTA	ThermoFisher, Scientific, Darmstadt, Germany
*oprE*Fw	TCTAGA*AGGAGG*AAAAACATATGTACAAGTCCAGCCTGGCTC	ThermoFisher, Scientific, Darmstadt, Germany
*oprE*Rv	AAGCTTTTACAGGAAGTTGTAAGTGTAGT	ThermoFisher, Scientific, Darmstadt, Germany

[a]*Abbreviations shown in this table: Cm^R, chloramphenicol resistance cassette; Km^R, kanamycin resistance cassette; Gm^R, gentamycin resistance cassette; Ap^R, ampicillin resistance cassette; I-SceI, SceI endonuclease from Saccharomyces cerevisiae; xylS-Pm, genetic circuit inducible upon methyl benzoate addition; lacIq-Ptrc, genetic system governed by IPTG induction. Restriction sites are underlined. Shine-Dalgarno sequences are shown in italics.*

acids and hydrophilic residues. Thus, overexpression of the *oprF* and *oprE* might render the membrane more hydrophobic (Delcour, 2009). **Figures 2C,D** show that the KT2440 strains carrying the porin proteins boosted the hydrophobicity of the membrane by more than threefold in comparison to the parental and the mutant KTΔ*mscL* strain. The OprF protein contributed the most to this process, as this is the major water-filling porin in Pseudomonas (Chevalier et al., 2017). Consistent with the enhanced hydrophobicity of the cell's surface of the engineered KT2440 strains, changes in the uptake of *N*-phenyl-1-naphtylamina (NPN) were found, a suitable compound to assess the permeability barrier of the membrane (Helander and Mattila-Sandholm, 2000). This analysis confirms the key role that both porins play in the degree of permeability of the bacterial envelop since the fluorescence intensity is clearly higher for the recombinant strains than that of *P. putida* KT2440 (**Figures 2E,F**).

Triggering Cell Disruption in the Engineered *P. putida* KT2440 Strains Using a Coordinated Hypertonic and Hypotonic Treatment

Afterward, the osmolarity of cultures was increased by adding NaCl to attain a final concentration of 10 (g/L). After 1 h, CFU exhibited minor cell viability variations in all tested bacterial strains (**Figures 3A,B**). Later, the entire culture broth was centrifuged, the supernatant discarded, and finally the cell pellet resuspended in the same amount of volume using distilled water, causing thereby a hypoosmotic shock. Strikingly, while the hypotonic pressure did not seem to affect cell survival on most of the strains (**Figure 3C**), the KTΔ*mscL-oprFE* showed substantial cell death (**Figure 3D**). After imposing hypoosmotic shock cell population diminished by 20, 80, and 96% after 1, 2, and 3 h, respectively (**Figure 3D**). Thus, the concerted pressure of both OprF and OprE porins and the abolishment of the MscL safe valve are required to achieve the desired impact on cell viability. In contrast the individual action of each porin did not apply sufficient osmotic pressure on the engineered strains to account for enhanced cell mortality rates.

Assessment of Cellular Disruption by FACS Analysis

Although cell death in the engineered KTΔ*mscL-oprFE* strain by CFU counts was confirmed, this fact does not directly correlate with cell membrane disruption, which is essential for downstream PHA recovery. Therefore, cell death and membrane integrity were assessed by LIVE/DEATH cell discrimination analysis via FACS employing the non-permeable DNA intercalating agent propidium iodide. This reagent can dye the chromosome solely when the cell membrane is damaged. First, non-lysed cells taken in the middle of the exponential growth phase were recorded in order to establish a threshold for living cells. As depicted in **Figure 4A**, intact cells present almost no fluorescence. In a separate control experiment to set up a death gate of cells, KT2440 cells underwent rapid shifts of heat-cold shock as described in the section "Materials and Methods." After five cycles of heat-shock treatment, 99.6% of the cell population was estimated dead spanning the fluorescence range of 5×10^3 to 10^5 (**Figure 4A**). Cell viability analysis revealed no apparent changes in membrane permeability of intact cells between KT2440 and the mutant *mscL* strain as they were superimposed (**Figure 4B**). When the autolytic system was induced in the KT-*oprFE* strain a 21% of cell membrane disturbance was brought about (**Figure 4B**). Finally, the porin-MscL dual system was triggered in the KTΔ*mscL-oprFE* strain resulting in 96.3% cell disruption and death (**Figure 3B**). This outcome is practically comparable to the total amount of lysed cells after heat-cold shock treatment endurance.

PHA Yield, Composition, and Recovery

Once the efficiency of the lytic genetic system was verified, the biomass synthesis, PHA yields, and monomer composition was evaluated in the genetically modified *Pseudomonas* strains. The wild-type and the engineered strains displayed nearly equal biomass titers of about 2.5 (g/L) according to their CDM (**Figures 5A,B**). Hence, it appears that the genome editing and carriage of recombinant porin genes did not impact detrimentally cellular formation. The KTΔ*mscL* deletion mutant produced 2.3 (g/L) and amassed 31.5% of their CDM as PHA (**Figures 5A,B**), showing similar values to the ones already reported (Oliva-Arancibia et al., 2017). *P. putida* strains harboring the *oprF* or *oprE* constructs trigger a slight decline of about 2 and 11 PHA (%wt), respectively (**Figures 5A,B**). Interestingly, the KT-*oprFE* and KTΔ*mscL-oprFE* strains accumulated almost 10% more PHA (%wt) than their parental strains (**Figures 5A,B**). By inspecting the monomer composition of the biosynthesized PHA via GC–MS, no considerable variation among the *P. putida* strains was found, being 3-hydroxyhexanoate (C6) the minor monomer and 3-hydroxyoctanoate (C8) and 3-hydroxydecanoate (C10) almost equally distributed in the polymeric chain (**Table 2**).

Finally, to gain insights into the applicability of the procedure to recover proper amounts of PHA, the final cultures were resuspended (after hypotonic treatment) in non-harmful amounts of chloroform for the cell (5% v/v final concentration), and PHA was let to dissolve for 2 h. After complete chloroform evaporation, the recovered PHA was quantified as displayed in **Figures 5C,D**. Scarce PHA quantities, <5% over total PHA amounts, could be recovered from seven of the strains with the only exception of the KTΔ*mscL-oprFE* (**Figures 5C,D**). PHA recovery yielded 93.3% contrasted to the whole produced amounts in this strain (**Figure 5D**).

Examination of Cell Wall Damage by Transmission Electron Microscopy

To obtain visual evidence of the provoked membrane damage, osmotic shock treatment was carried out as previously specified on the KTΔ*mscL* and wild-type strains and each bacterium carrying the *oprFE* overexpression system grown on decanoate and analyzed the samples employing transmission electron microscopy (**Figure 6**). The KT2440 parental and KTΔ*mscL* strains displayed the distinctive PHA granules enclosed in

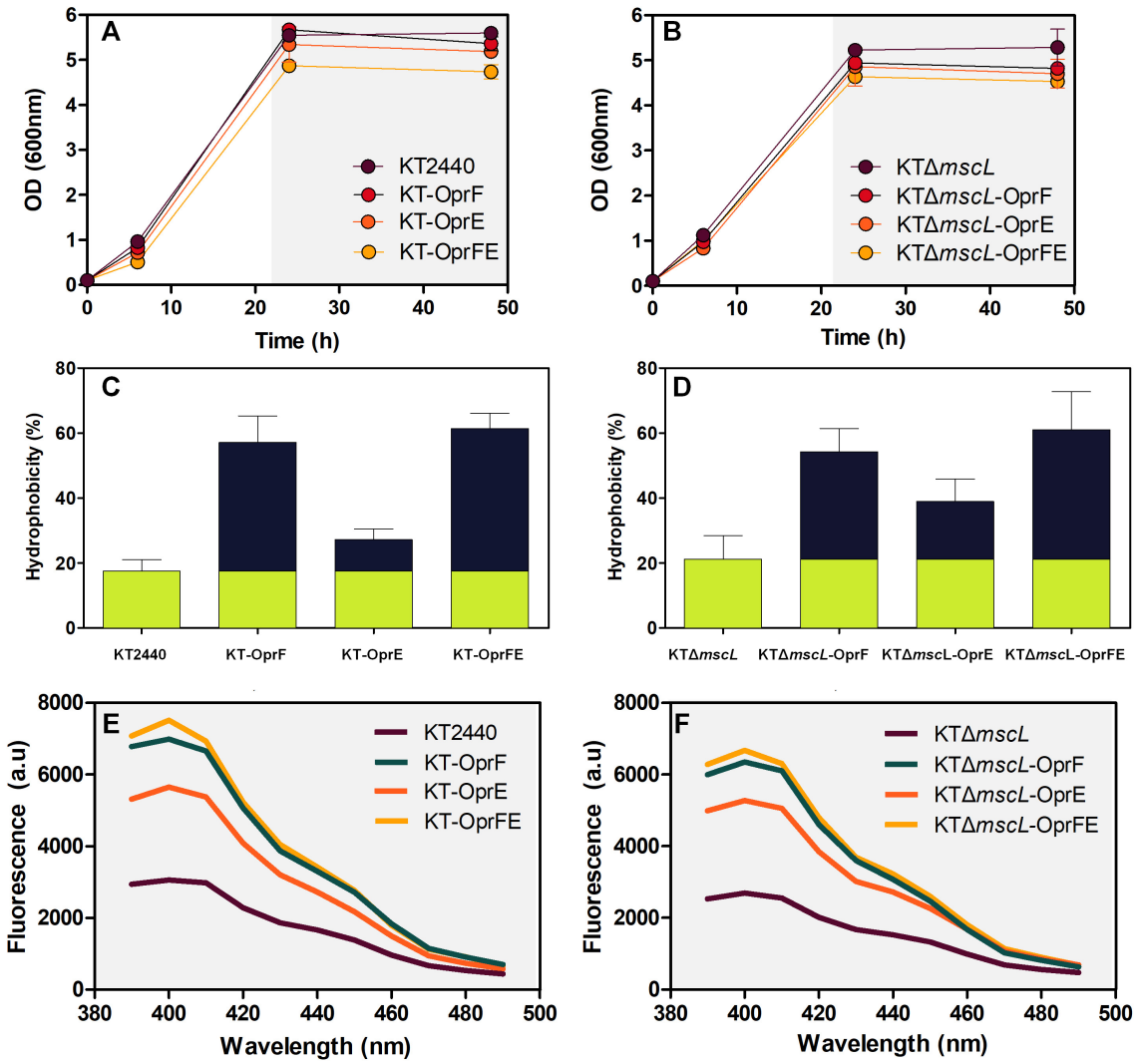

FIGURE 2 | Growth behavior under PHA-producing conditions on decanoate (20 mM) **(A,B)**, overall membrane hydrophobicity **(C,D)**, and permeability **(E,F)** of the engineered *P. putida* strains.

the cytoplasmic space, and additionally, no apparent cell wall breakage was observed in the overall bacterial population (**Figures 6A,B**). Overproduction of the OprFE enzymes in KT2440 did not trigger considerable wall disruption, but there is a slight alteration on the membrane (**Figure 6C**). Conversely, the KTΔ*mscL-oprFE* engineered strain clearly presented disrupted membranes in the vast majority of the cells (**Figure 6D**). This strain was able to produce the biopolymer similarly to the wild type, but these bacteria most likely failed to restrain it within the cellular barriers when treated with chloroform for PHA recovery (**Figure 5D**).

DISCUSSION

Here a novel system for bacterial cell lysis during biopolymer production is reported. The osmotic state of *P. putida* KT2440 in response to a combination of hypertonic and hypotonic treatments by perturbing the cell membrane was rationally engineered. First, the deletion of the *mscL* in KT2440 did not impair growth rate or total biomass yield on decanoate. Moreover, the introduction in *trans* of individual porin genes under the regulation of an inducible promoter had no restraint bacterial growth to a great extent. Both porins belong to the conserved OmpA family of proteins that constitute the major responsible players for cell turgor maintenance (Chevalier et al., 2017) and acting as non-specific transporters of ionic species (Nestorovich et al., 2006). These data confirm that the imposed challenge after salt treatment (10 g/L) did not impair significantly vital metabolic functions of the biocatalysts as recorded via cell viability (CFU) and visualization of the membrane integrity via electron microscopy (**Figure 6**). Most likely, this relies on the high capacity of *P. putida* to adapt itself and cope with the extracellular ever-changing osmotic state by modulating

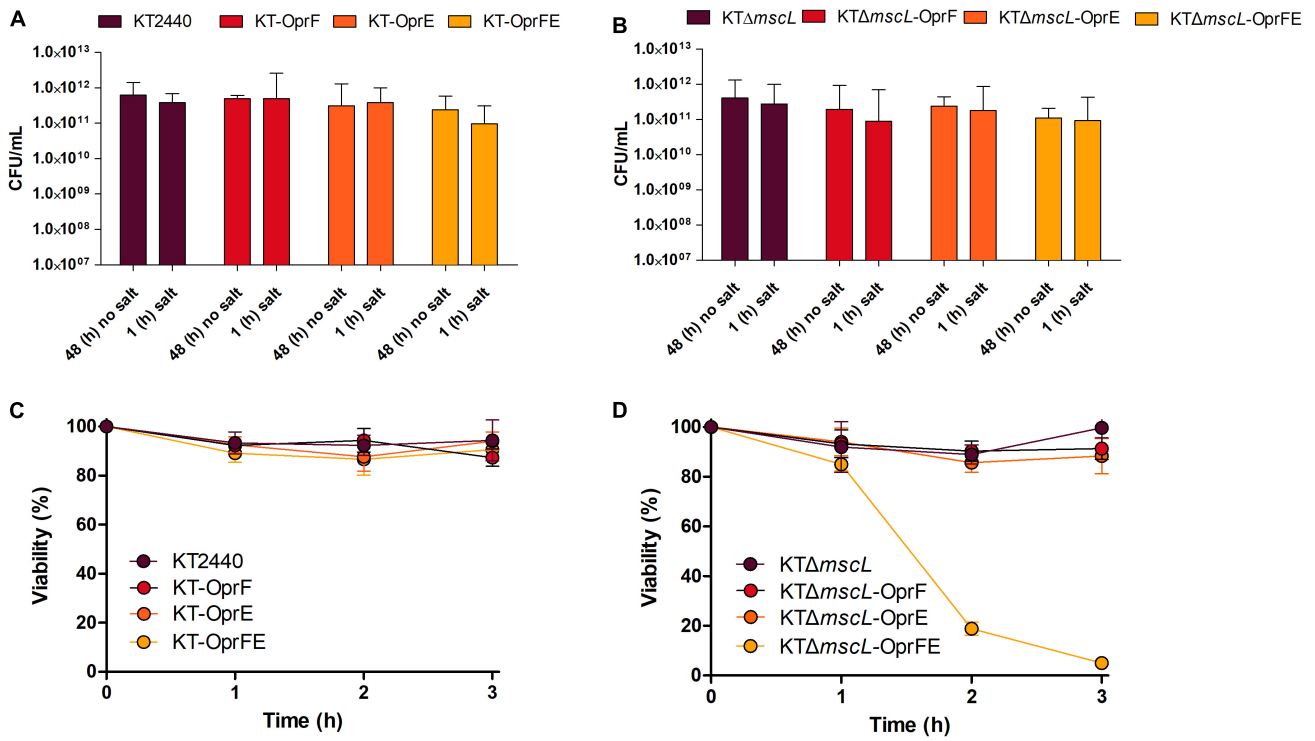

FIGURE 3 | Cell survival expressed as CFU counts per mL after osmotic upshift **(A,B)** and cell viability reflected in percentage (%) over the initial cell density over 3 h **(C,D)** of each genetically modified and parental strain.

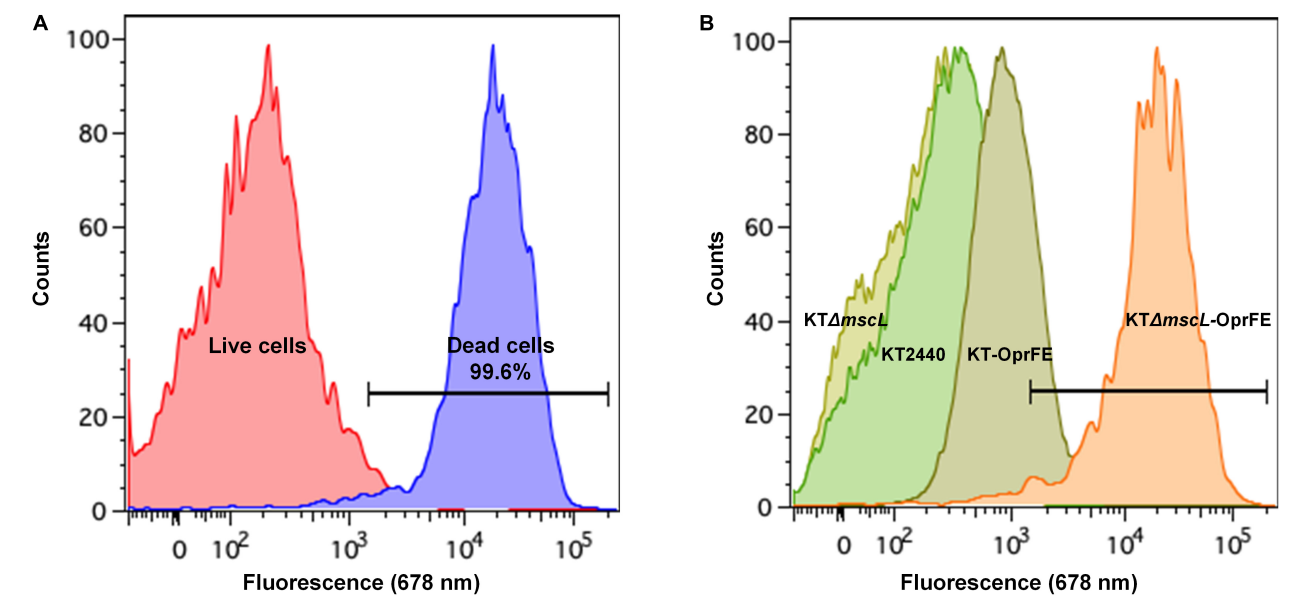

FIGURE 4 | FACS analysis by LIVE/DEATH staining. Cell death and live gates after heat-cold treatment are shown on the left side **(A)** while cell disruption of KT220 wild type, KTΔ*mscL*, KT-*oprFE*, and KTΔ*mscL*-*oprFE* strains is displayed on the right panel **(B)**.

the expression of alternative valves and porins (Hancock and Brinkman, 2002). In the genome of KT2440 there are at least other eight genes encoding for MscLs (PP_4533, PP_1353, PP_5067, PP_3360, PP_0707, PP_1728, PP_5256, and PP_2741) and a wide range of porin proteins (OprE, OprC, OprJ, OprI, OprG, OprH) (Nelson et al., 2002) that could regulate the osmotic response and counteract stress. This array of osmotic stress modulators might endow *P. putida* engineered strains with a

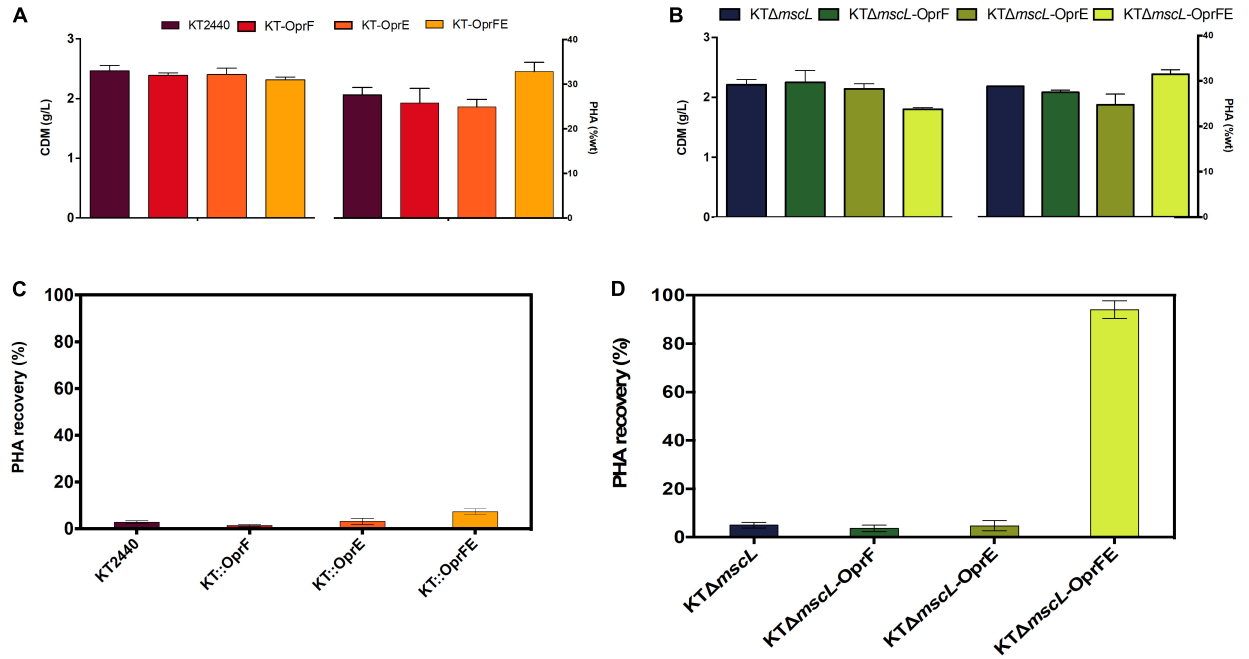

FIGURE 5 | Registration of cell dry mass (CDM) in g/L and PHA accumulation (%wt) of the employed strains **(A,B)** and PHA recovery **(C,D)** of the genetically modified and parental KT2440 strains.

toolbox to overcome high-salt osmotic challenges, and therefore, a downshift to hypotonic environments was required. Targeted manipulation of further osmotic stress modulators might be crucial to efficiently disrupt the cell membranes of *P. putida* without the need to drastically shifting its osmotic state and might also trigger to some extent biomass loss or premature decay of cell wall integrity.

By expressing both outer membrane porins in tandem, the strains KT-*oprFE* and KTΔ*mscL-oprFE* displayed a slight reduction in biomass synthesis (10%) and viability after salt treatments, pointing a higher sensitivity for those strains to hypertonic shock. Many studies have reported a decrease in biomass formation when overexpressing foreign and native enzymes in the cell due to multiple factors including high energy expenditure (Borkowski et al., 2018; Shah et al., 2013) and rearrangement of the assemble machinery for enzyme synthesis (Bolognesi and Lehner, 2018). It was also striking to record a boosted biopolymer accumulation relative to the cell dry mass of the engineered strain overproducing the OprFE enzymes (**Figure 5**). *P. putida* and *E. coli* bacteria mediate the transport of fatty acids into the cell utilizing the porins OprF and OmpF, respectively (Tan et al., 2017). A multi-omics study reported

TABLE 2 | Monomer composition of the biopolymers produced by the engineered *P. putida* strains.

Strain	Monomer composition (%)		
	C6	C8	C10
KT2440	6.1 ± 0.2	47.8 ± 1.4	46.1 ± 1.9
KT-*oprF*	7.2 ± 0.3	42.8 ± 1.6	50.0 ± 1.1
KT-*oprE*	4.2 ± 0.1	52.6 ± 0.9	43.2 ± 0.5
KT-*oprFE*	4.8 ± 0.6	46.7 ± 1.7	48.5 ± 1.2
KTΔ*mscL*	5.4 ± 0.1	50.6 ± 1.1	44.0 ± 1.8
KTΔ*mscL-oprF*	6.1 ± 0.3	43.7 ± 0.8	50.2 ± 1.9
KTΔ*mscL-oprE*	5.7 ± 0.4	46.9 ± 1.5	47.4 ± 2.1
KTΔ*mscL-oprFE*	3.8 ± 0.2	48.7 ± 1.3	47.5 ± 0.9

Values represent the mean and ±SD calculated from three independent replicates. C6, 3-hydroxyhexanoate; C8, 3-hydroxyocyanoate; C10, 3-hydroxydecanoate.

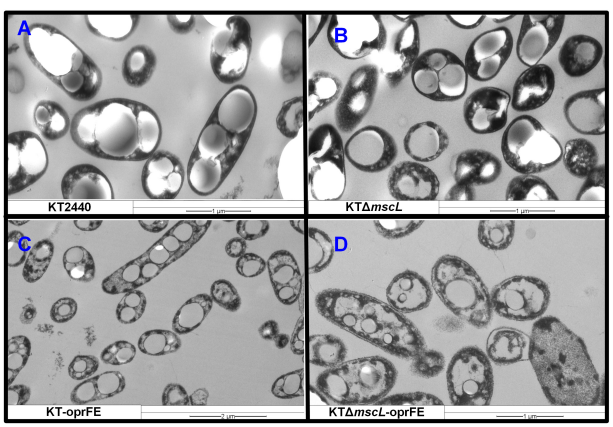

FIGURE 6 | Transmission electron microscopy pictures of *Pseudomonas putida* cells producing PHA on decanoate after osmotic treatments. **(A)** KT2440, **(B)** KTΔ*mscL*, **(C)** KT-oprFE, and **(D)** KTΔ*mscL-oprFE* strains.

a higher abundance of the porin OprF and OprE enzymes in *P. putida* cells when the cells produced elevated quantities of PHA (80 wt%) on decanoate in chemostat cultures (Poblete-Castro et al., 2012), which could explain to some extent the observed phenomena.

As environmental factors modulate the abundance of porins (OprF, OprC, OprD, OprH, and OprE) in bacteria of the genus *Pseudomonas* (Yamano et al., 1993), the higher production levels of these porin family proteins might turn the cell membrane more sensitive to osmotic shocks. For instance, anaerobiosis induces the expression of the *oprC* and *oprE* gene expression in *P. aeruginosa*, yet they showed no alteration to osmotic upshift (Yamano et al., 1993). As *P. putida* KT2440 is strictly aerobic, activation of the OprE in conjunction with OprF might concert a destabilization effect on the bacterial membrane. During the hypotonic shock to the salt-treated cells, a rapid loss of cell viability was only recorded in the KTΔ*mscL-oprFE* strain indicating that overexpression of both porins is effective in promoting cell death by abolishing the proper functioning of the MscL channel. More importantly, a biopolymer recovery of 94.2% of the biosynthesized PHA was attained. These results are consistent with our rational approach, proving that the inactivation of one of the main MscLs to relieve excessive turgor via solute secretion (Martinac et al., 1987) combined with the overproduction of the two key porin proteins (OprF and OprE) no longer sustained the physical integrity of the membrane of KT2440.

The cell lytic system developed in this study presents advantages over other self-disrupting genetic circuits implemented in the natural PHA producer *P. putida* strain. The phage holin–endolysin system has been the first strategy for biopolymer recovery with various outcomes (Hori et al., 2002; Martinez et al., 2011; Tamekou Lacmata et al., 2017). Implementation of this system in *P. putida* KT2440 have been reported to result in 16% PHA recovery of the produced biopolymer and 86% of disrupted cells, taking >15 h to complete this process (Martinez et al., 2011). Additionally, a lysozyme-based programmable lytic system had been previously devised in our group, which was very efficient in both cell disruption and PHA recuperation – 75% of the synthesized PHA – but also took >15 h to fully lysate the cell population (Borrero-De Acuna et al., 2017). The current system surpasses the available autolytic genetic systems since the cell counts diminished immediately upon hypotonic treatment leading to the complete release of the biopolymer after 3 h. This is of great importance in terms of the length of the biopolymer production process and the associated costs. Another key aspect is the similar product yields and monomer composition of the synthesized PHA between the engineered *P. putida* strain and the wild-type KT2440.

CONCLUSION

In summary, a novel genetic tool to deliver controllable cell disruption upon command suitable for PHA downstream processing was developed. Importantly, PHA titers that did not differ from the biopolymer synthesized by the KT2440 wild-type strain were attained. High rates of cell lysis under PHA-producing conditions and improved biopolymer recovery in comparison to previously reported systems were demonstrated. Follow up research endeavors should target the concurrent genetic manipulation of further outer or inner membrane channels, responding to either hyper- or hypo-osmosis, to achieve cell breakage after passage through only one osmotic state. By these means, the time for cell disruption might reduce as well as the process expenses. Scaling-up the current system to render cell lyses in industrial fed-batch processes may also pose a challenge due to the high cell densities reached in bioreactors.

MATERIALS AND METHODS

Bacterial Strain Generation

Pseudomonas putida KT2440 strain was employed as a reference/control strain and as background organism for genetic engineering of the designed system. All generated plasmids, primers, and strains employed throughout this work are shown in **Table 1**. A previously reported knockout strategy (Borrero-De Acuña et al., 2019) was used to eliminate the *mscL* gene of the KT2440 genome. The upstream flank of the *mscL* gene was amplified using the primers *mscl*UPFw and *mscl*UPRv, whereas the downstream arm was generated with the oligos *mscl*DWFw and *mscl*DWRv. Both flanking regions of the *mscL* ORF were fused by sewing PCR employing as DNA templates equal amounts of both PCR products and the oligos *mscl*UPFw and *mscl*DWRv. The spliced *mscL* upstream–downstream fragment was firstly introduced in a subcloning step into the toxin-encoding blunt end pJET1.2 commercial vector. Secondly, the *Eco*RI and *Bam*HI restriction sites present in the primer overhangs were profited for digestion and further insertion into the suicide vector pSEVA212 giving rise to pSEVA212-*mscl*UPDW. DH5αλpir cell was transformed with the constructed plasmid and kanamycin-resistant clones were browsed for proper plasmid introduction. Triparental mating was conducted using the *Escherichia coli* HB101 strain carrying the plasmid pRK600 to transfer the plasmid into KT2440 as previously specified (Benedetti et al., 2016). Kanamycin-tolerant KT2440 transconjugants were screened for genomic integration of the pSEVA212-*mscl*UPDW plasmid by PCR-amplification of the beforehand non-existing upstream–downstream spliced segment using the primers *mscl*UPFw and *mscl*DWRv. Subsequently, the I-SceI restriction enzyme-expressing plasmid pSEVA628 was introduced into the verified transconjugant and clones were selected on gentamicin plates. Expression of the I-SceI endonuclease was induced overnight by adding 15 mM m-toluic acid (Sigma-Aldrich, Darmstadt, Germany). A few resulting kanamycin-sensitive clones were PCR-assessed for proper deletion of the *mscL* gene using the combination of primers *mscl*UPFw/*mscl*DWRv and the gene aligning oligos *mscl*KOFw/*mscl*KORv. The raised strain was named KTΔ*mscL*. In parallel, the genes encoding for *oprF* and *oprE* porins were amplified from the genome of KT2440 by single-colony PCR with the oligo pairs *oprF*Fw/*oprF*Rv and *oprE*Fw/*oprE*Rv, respectively. Once again, the pJET1.2 vector was

employed for subcloning purposes and both ORF were further *Eco*RI–*Xba*I (for *oprF*) and *Xba*I–*Hin*dIII (for *oprE*) inserted into the IPTG-inducible plasmid pSEVA634, which harbors a gentamicin cassette. The resulting constructs, namely pSEVA634-*oprF* and pSEVA634-*oprE*, were introduced into KT2440 and KTΔ*mscL* by triparental mating originating the following strains: KT-*oprF*, KT-*oprE*, KTΔ*mscL*-*oprF*, and KTΔ*mscL*-*oprE*. Lastly the *oprE* gene was further cleaved off the pSEVA634 plasmid with *Xba*I and *Hin*dIII and packed downstream the *oprF* gene into pSEVA634 for tandem expression of both porins. This plasmid was also incorporated into the wild-type strain and KT2440Δ*mscL* by triparental mating leading to the generation of KT-*oprFE* and KTΔ*mscL*-*oprFE*.

Growth Conditions

Escherichia coli strains were incubated on Lysogeny Broth (LB) medium for sub- and cloning purposes as was *P. putida* for genetic engineering and strain construction at 37 and 30°C, respectively. The first preinoculum to carry out the bacterial PHA production started by picking one colony of the engineered and wild-type *P. putida* strains, which was suspended in 10 mL of M9 minimal medium (per liter): 12.8 g $Na_2HPO_4 \cdot 7H_2O$, 3 g KH_2PO_4, 1 g NH_4Cl, and 0.5 g NaCl. This mixture was sterilized and supplemented with 0.12 g of $MgSO_4 \cdot 7H_2O$, trace elements (6.0 $FeSO_4 \cdot 7H_2O$, 2.7 $CaCO_3$, 2.0 $ZnSO_4 \cdot H_2O$, 1.16 $MnSO_4 \cdot H_2O$, 0.37 $CoSO_4 \cdot 7H_2O$, 0.33 $CuSO_4 \cdot 5H_2O$, 0.08 H_3BO_3) (mg/L) (filter-sterilized), and 5 mM of decanoate as the sole carbon source. The OD_{600} values of the overnight cultures were recorded and *P. putida* cells were added to obtain an initial optical density of 0.1 in the shaking flasks. Each 500 mL Erlenmeyer flask contained 100 mL of M9 salt medium, antibiotics, trace elements, and magnesium sulfate supplemented with 20 mM of decanoate. The bacterial strains were grown in a rotary shaker set at 30°C and spinning at 180 rpm (Ecotron, INFORS HT, Switzerland). To induce porin expression IPTG (final concentration 1 mM) was added to the growing cultures at 30 h after starting the batch culture. Antibiotics were supplemented when demanded at the following final concentrations for *E. coli* (μg/mL): streptomycin 60, ampicillin 150, kanamycin 50, and gentamycin 15. For *P. putida* strains 50 mg/mL kanamycin and 50 μg/mL gentamicin were added.

Cell Surface Hydrophobicity Assay

The bacterial adhesion to hydrocarbon assay (BAHA) was performed as described by Reifsteck et al. (1987) with slight modifications. Briefly, after 48 h of starting the batch, 2 mL of cultures was centrifuged at 4,000 × *g* for 10 min at 4°C, the supernatant discarded, and the cells resuspended in the same volume with phosphate buffered saline (PBS). This step was repeated two more times, and finally resuspended in PBS to reach an OD_{600} of 0.4. To a 2.5 mL of cell suspension in a glass tube, 0.5 mL of *p*-xylene was added and vigorously stirred using a vortex for 1 min, and finally held for 30 min at room temperature to allow hydrocarbon separation. The absorbance (OD_{600}) of the aqueous phase was measured before (A_0) and after the treatment (A), and the BAHA calculated using the following formula (%): $100.[1-(A/A_0)]$.

Outer Membrane Permeability Assay

After culture for 48 h, 2 mL of the *P. putida* cells was washed three times with PBS buffer and resuspended with the same buffer to reach an optical density of (OD_{600}) of 0.2. Subsequently, 10 μL of *N*-phenyl-1-naphthylamine (NPN) stock solution 1 mM in 1 M Tris-HCl was mixed with 1 mL of the cell suspension. The mixture reacted for 2 min at room temperature and 0.1 mL of 1 M KH_2PO_4 was added to terminate the reaction. The florescence intensity (excitation at 355 nm) was recorded by inspecting the emission spectrum from 390 to 490 nm using a multiplate reader (Synergy H1, Biotek, United States).

Colony Forming Unit Counting

Pseudomonas putida KT2440, and recombinant strains were incubated in M9 medium supplemented with 20 mM decanoate in shaking flasks. After 30 h of growth, expression of the corresponding porins was induced by adding 1 mM IPTG. Gene over-expression was permitted for 18 h. Prior to salt treatment cell viability was monitored by conducting serial dilutions of each culture in PBS and plating 100 μL on LB with 2.5% w/v agar. CFU were counted on each dilution. Immediately after, 10 g/L of sterile NaCl was added to the growing cultures. The hyper-osmotic shock was allowed for 1 h and CFU counted as above specified. Subsequently, the entire cell culture was centrifuged at room temperature (5,000 × *g* for 5 min), the supernatant discarded, and cells resuspended in 100 mL of distilled water. Afterward, the CFU again numbered over 3 h period.

FACS Analysis

Flow cytometry analysis performed on a FACS ARIA FUSION cell sorter (BD Biosciences, San Jose, CA, United States) equipped with two lasers with excitation wavelengths of 488 and 633 nm. An instrument quality control was carried out by using FACS DIVA CS&T Research beads (BD Biosciences, San Jose, CA, United States) prior to bacteria introduction, following the manufacturer's instructions. Preliminary tests were conducted on the flow cytometer to rule out detection of cells debris or other components that might be present on the media culture or FACS Staining buffer (PBS, Tween 20 at 0.01%). Thereby, the noise effect, voltage, and threshold settings were determined. According to the provider's guidelines bacterial cultures were stained with BD Cell Viability Kit (CAT #349483 BD Biosciences, San Jose, CA, United States). In brief, approximately 5×10^6 bacteria/mL were transferred to a 12 × 75 mm polystyrene test tube and resuspended in 200 μL of FACS staining buffer. Two sorts of control samples were included in the assessment: non-lysed cells or bacterial culture lysates undergoing to heat-cold shock treatment (five cycles of freezing at −80°C for 3 min followed by 3 min of incubation at 90°C). By these means the instruments settings and dead cells gate/threshold were established. A staining mixture was set up by reverse pipetting by adding 5 μL of Thiazole Orange solution 17 μM and 5 μL of propidium iodide solution 19 mM. The samples were lastly acquired on the FACS Aria Fusion instrument after 5 min incubation time.

PHA Quantification and Characterization

Methanolysis of lyophilized cell dry mass (5–10 mg) was introduced in sealed tubes containing 2 mL chloroform, 2 mL methanol, 15% (v/v) H_2SO_4, and 0.5 (mg/mL) 3-methylbenzoic acid. The tubes were incubated for 4 h at 100°C in a thermoblock. After the tubes reached room temperature, 1 mL of miliQ water was mixed with the reaction solution, and vigorously agitated for 1 min. The mixture was then transferred to a Falcon tube (15 mL) and centrifuged for 10 min at 6,000 × *g*. The lower part of the biphasic solution, containing the methyl esters of the biopolymer, was separated and analyzed via gas chromatography coupled to mass spectrometry (YL6900, Young Instruments, South Korea) using the methodology previously described by Borrero-De Acuña et al. (2019). Briefly, a calibration curve was created using a purified medium-chain-length-PHA synthesized in a previous work (Oliva-Arancibia et al., 2017) to interpolate data samples. Once the retention time of the peaks was contrasted with the standards, their chemical structures were characterized based on the resulting mass compatibility (NIST 17 Mass Spectral library). The percentage of PHA in the cell was defined as the amount of the biopolymer divided by the total cell dry mass and multiplied by 100.

Biopolymer Recovery

In order to determine the PHA recovery of each *P. putida* strain, 36 mL culture was blended with 2 mL of high-grade chloroform at a final concentration of 5% (v/v). Subsequently, the mixture was stirred at room temperature for 2 h and further centrifuged at 3,400 × *g* for 10 min at 4°C. Thereby, PHA precipitation was avoided and a phase constituted of chloroform-PHA was generated. The aforesaid phase was retrieved with a Pasteur pipette and maintained at room temperature until the chloroform evaporated. The recovered PHA was transferred to 500 μL chloroform and quantified as described in the prior section.

Electron Microscopy Operation

Fixation of chilled cultures was driven by addition of glutaraldehyde and formaldehyde at 2 and 5%, respectively. Washing was carried out with cacodylate buffer (0.01 mol/L) 1 cacodylate (0.01 mol/L), 1 $CaCl_2$ (0.01 mol/L), 1 $MgCl_2$ $6H_2O$ (0.09 mol/L), 1 sucrose, pH 6/9) being the samples stained with aqueous osmium for 1 h at room temperature. Samples were subsequently dried out gradually with acetone at the increasing concentrations of 10, 30, 50, 70, 90, and 100%. Each dehydration step grade with acetone was performed for 30 min with the exception of the 70% acetone step that was conducted overnight mixed with 2% uranyl acetate. Exposy was the resin of choice being infiltrated following the Spurr method for hard resin for several days. Cells were sliced into 40 nm ultrathin sections with a diamond knife and further counterstained with uranyl acetate and lead citrate. The resulting samples were analyzed operating a TEM910 transmission electron microscope (Carl Zeiss, Oberkochen, Germany) at an acceleration voltage of 80 kV. Digital images were taken with Slow-Scan CCD-Camera (ProScan, 1024 × 1024, Scheuring, Germany) with ITEM-Software (Olympus Soft Imaging Solutions, Munster, Germany) and recorded onto a MO-disc. Adobe Photoshop was used to fine-tune contrast and brightness.

DATA AVAILABILITY STATEMENT

All datasets generated for this study are included in the article/supplementary material.

AUTHOR CONTRIBUTIONS

MO-S, AC, CA-C, and NP conducted the experimental work. JB-DA and IP-C designed the experiments, analyzed the data, and wrote the manuscript.

FUNDING

This work was funded by the Federal State of Lower Saxony, Niedersächsisches Vorab CDiff and CDInfect projects (VWZN2889/3215/3266), and the Deutsche Forschungsgemeinschaft (DFG, German Research Foundation) - 281361126/GRK2223, Protein Complex Assembly (PROCOMPAS). We acknowledge support by the German Research Foundation and the Open Access Publication Funds of the Technische Universität Braunschweig.

ACKNOWLEDGMENTS

JB-DA acknowledges the excellent technical work of the Sina Tiller. CA-C and NP acknowledge the scholarship provided by Doctorado en Biotecnología (UNAB).

REFERENCES

Benedetti, I., De Lorenzo, V., and Nikel, P. I. (2016). Genetic programming of catalytic *Pseudomonas putida* biofilms for boosting biodegradation of haloalkanes. *Metab. Eng.* 33, 109–118. doi: 10.1016/j.ymben.2015.11.004

Bolognesi, B., and Lehner, B. (2018). Protein overexpression: reaching the limit. *eLife* 7:e39804. doi: 10.7554/eLife.39804

Borkowski, O., Bricio, C., Murgiano, M., Rothschild-Mancinelli, B., Stan, G. B., Ellis, T. (2018). Cell-free prediction of protein expression costs for growing cells. *Nat. Commun.* 9, 1–11

Borrero-De Acuña, J. M., Aravena-Carrasco, C., Gutierrez-Urrutia, I., Duchens, D., and Poblete-Castro, I. (2019). Enhanced synthesis of medium-chain-length poly (3-hydroxyalkanoates) by inactivating the tricarboxylate transport system of *Pseudomonas putida* KT2440 and process development using waste vegetable oil. *Process. Biochem.* 77, 23–30. doi: 10.1016/j.procbio.2018.10.012

Borrero-De Acuna, J. M., Hidalgo-Dumont, C., Pacheco, N., Cabrera, A., and Poblete-Castro, I. (2017). A novel programmable lysozyme-based lysis system in *Pseudomonas putida* for biopolymer production. *Sci. Rep.* 7:4373. doi: 10.1038/s41598-017-04741-2

Chevalier, S., Bouffartigues, E., Bodilis, J., Maillot, O., Lesouhaitier, O., Feuilloley, M. G. J., et al. (2017). Structure, function and regulation of *Pseudomonas aeruginosa* porins. *FEMS Microbiol. Rev.* 41, 698–722. doi: 10.1093/femsre/fux020

Colombo, G., Marrink, S. J., and Mark, A. E. (2003). Simulation of MscL gating in a bilayer under stress. *Biophys. J.* 84, 2331–2337. doi: 10.1016/s0006-3495(03)75038-3

Delcour, A. H. (2009). Outer membrane permeability and antibiotic resistance. *Biochim. Biophys. Acta* 1794, 808–816. doi: 10.1016/j.bbapap.2008.11.005

Guamán, L. P., Barba-Ostria, C., Zhang, F., Oliveira-Filho, E. R., Gomez, J. G. C., and Silva, L. F. (2018). Engineering xylose metabolism for production of polyhydroxybutyrate in the non-model bacterium *Burkholderia sacchari*. *Microb. Cell Fact.* 17:74. doi: 10.1186/s12934-018-0924-9

Hancock, R. E., and Brinkman, F. S. (2002). Function of *Pseudomonas porins* in uptake and efflux. *Annu. Rev. Microbiol.* 56, 17–38.

Helander, I. M., and Mattila-Sandholm, T. (2000). Fluorometric assessment of gram-negative bacterial permeabilization. *J. Appl. Microbiol.* 88, 213–219. doi: 10.1046/j.1365-2672.2000.00971.x

Hori, K., Kaneko, M., Tanji, Y., Xing, X. -H., and Unno, H. (2002). Construction of self-disruptive *Bacillus megaterium* in response to substrate exhaustion for polyhydroxybutyrate production. *Appl. Microbiol. Biotechnol.* 59, 211–216. doi: 10.1007/s00253-002-0986-8

Jaouen, T., Coquet, L., Marvin-Guy, L., Orange, N., Chevalier, S., and De, E. (2006). Functional characterization of *Pseudomonas fluorescens* OprE and OprQ membrane proteins. *Biochem. Biophys. Res. Commun.* 346, 1048–1052. doi: 10.1016/j.bbrc.2006.06.013

Kohlstedt, M., Starck, S., Barton, N., Stolzenberger, J., Selzer, M., Mehlmann, K., et al. (2018). From lignin to nylon: cascaded chemical and biochemical conversion using metabolically engineered *Pseudomonas putida*. *Metab. Eng.* 47, 279–293. doi: 10.1016/j.ymben.2018.03.003

Liu, X., and Curtiss, R. III. (2009). Nickel-inducible lysis system in *Synechocystis* sp. PCC 6803. *Proc. Natl. Acad. Sci. U.S.A.* 106, 21550–21554. doi: 10.1073/pnas.0911953106

Martinac, B., Buechner, M., Delcour, A. H., Adler, J., and Kung, C. (1987). Pressure-sensitive ion channel in *Escherichia coli*. *Proc. Natl. Acad. Sci. U.S.A.* 84, 2297–2301. doi: 10.1073/pnas.84.8.2297

Martinez-Garcia, E., Aparicio, T., Goni-Moreno, A., Fraile, S., and De Lorenzo, V. (2015). SEVA 2.0: an update of the Standard European Vector Architecture for de-/re-construction of bacterial functionalities. *Nucleic Acids Res.* 43, D1183-D1189. doi: 10.1093/nar/gku1114

Martinez, V., Garcia, P., Garcia, J. L., and Prieto, M. A. (2011). Controlled autolysis facilitates the polyhydroxyalkanoate recovery in *Pseudomonas putida* KT2440. *Microb. Biotechnol.* 4, 533–547. doi: 10.1111/j.1751-7915.2011.00257.x

Moradali, M. F., Donati, I., Sims, I. M., Ghods, S., and Rehm, B. H. (2015). Alginate Polymerization and Modification Are Linked in *Pseudomonas aeruginosa*. *mBio* 6:e00453-15. doi: 10.1128/mBio.00453-15

Mozejko-Ciesielska, J., Szacherska, K., and Marciniak, P. (2019). *Pseudomonas* species as producers of eco-friendly polyhydroxyalkanoates. *J. Polym. Environ.* 27, 1151–1166. doi: 10.1007/s10924-019-01422-1

Najem, J. S., Dunlap, M. D., Rowe, I. D., Freeman, E. C., Grant, J. W., Sukharev, S., et al. (2015). Activation of bacterial channel MscL in mechanically stimulated droplet interface bilayers. *Sci. Rep.* 5:13726. doi: 10.1038/srep13726

Nelson, K. E., Weinel, C., Paulsen, I. T., Dodson, R. J., Hilbert, H., Martins Dos Santos, V. A., et al. (2002). Complete genome sequence and comparative analysis of the metabolically versatile *Pseudomonas putida* KT2440. *Environ. Microbiol.* 4, 799–808.

Nestorovich, E. M., Sugawara, E., Nikaido, H., and Bezrukov, S. M. (2006). *Pseudomonas aeruginosa* porin OprF: properties of the channel. *J. Biol. Chem.* 281, 16230–16237.

Obara, M., and Nakae, T. (1992). Porin of *Pseudomonas aeruginosa* forms low conductance ion channel in planar lipid bilayers. *Biochem. Biophys. Res. Commun.* 186, 645–651. doi: 10.1016/0006-291x(92)90795-m

Oliva-Arancibia, B., Ordenes-Aenishanslins, N., Bruna, N., Ibarra, P. S., Zacconi, F. C., Perez-Donoso, J. M., et al. (2017). Co-synthesis of medium-chain-length polyhydroxyalkanoates and CdS quantum dots nanoparticles in *Pseudomonas putida* KT2440. *J. Biotechnol.* 264, 29–37. doi: 10.1016/j.jbiotec.2017.10.013

Pacheco, N., Orellana-Saez, M., Pepczynska, M., Enrione, J., Bassas-Galia, M., Borrero-De Acuna, J. M., et al. (2019). Exploiting the natural poly(3-hydroxyalkanoates) production capacity of Antarctic *Pseudomonas* strains: from unique phenotypes to novel biopolymers. *J. Ind. Microbiol. Biotechnol.* 46, 1139–1153. doi: 10.1007/s10295-019-02186-2

Poblete-Castro, I., Escapa, I. F., Jager, C., Puchalka, J., Chi Lam, C., Schomburg, D., Prieto, M. A., Martins dos Santos, V. (2012). The metabolic response of *Pseudomonas putida* KT2442 producing high levels of polyhydroxyalkanoate under single- and multiple-nutrient-limited growth: highlights from a multi-level omics approach. *Microb. Cell Fact.* 11:34. doi: 10.1186/1475-2859-11-34

Poblete-Castro, I., Binger, D., Oehlert, R., and Rohde, M. (2014). Comparison of mcl-Poly(3-hydroxyalkanoates) synthesis by different *Pseudomonas putida* strains from crude glycerol: citrate accumulates at high titer under PHA-producing conditions. *BMC Biotechnol.* 14:962. doi: 10.1186/s12896-014-0110-z

Poblete-Castro, I., Binger, D., Rodrigues, A., Becker, J., Martins Dos Santos, V.A., and Wittmann, C. (2013). In-silico-driven metabolic engineering of *Pseudomonas putida* for enhanced production of poly-hydroxyalkanoates. *Metab. Eng.* 15, 113-123. doi: 10.1016/j.ymben.2012.10.004

Poblete-Castro, I., Borrero-De Acuña, J. M., Nikel, P. I., Kohlstedt, M., and Wittmann, C. (2017). Host organism: *Pseudomonas putida*. *Indus. Biotechnol.* 1, 299–326.

Poblete-Castro, I., Wittmann, C., and Nikel, P. I. (2019). Biochemistry, genetics and biotechnology of glycerol utilization in *Pseudomonas* species. *Microb. Biotechnol.* 13, 32–53 doi: 10.1111/1751-7915.13400

Prieto, A., Escapa, I. F., Martinez, V., Dinjaski, N., Herencias, C., De La Pena, F., et al. (2016). A holistic view of polyhydroxyalkanoate metabolism in *Pseudomonas putida*. *Environ. Microbiol.* 18, 341–357. doi: 10.1111/1462-2920.12760

Reifsteck, F., Wee, S., and Wilkinson, B. J. (1987). Hydrophobicity-hydrophilicity of *staphylococci*. *J. Med. Microbiol.* 24, 65–73. doi: 10.1099/00222615-24-1-65

Shah, P., Ding, Y., Niemczyk, M., Kudla, G., Plotkin, J. B. (2013). Rate-limiting steps in yeast protein translation. *Cell* 153, 1589–1601. doi: 10.1016/j.cell.2013.05.049

Sugawara, E., Nestorovich, E. M., Bezrukov, S. M., and Nikaido, H. (2006). *Pseudomonas aeruginosa* porin OprF exists in two different conformations. *J. Biol. Chem.* 281, 16220–16229. doi: 10.1074/jbc.m600680200

Sukharev, S., Betanzos, M., Chiang, C. S., and Guy, H. R. (2001). The gating mechanism of the large mechanosensitive channel MscL. *Nature* 409, 720–724. doi: 10.1038/35055559

Tamekou Lacmata, S., Yao, L., Xian, M., Liu, H., Kuiate, J. R., Liu, H., et al. (2017). A novel autolysis system controlled by magnesium and its application to poly (3-hydroxypropionate) production in engineered *Escherichia coli*. *Bioengineered* 8, 594–599. doi: 10.1080/21655979.2017.1286432

Tan, Z., Black, W., Yoon, J. M., Shanks, J. V., Jarboe, L. R. (2017). Improving *Escherichia coli* membrane integrity and fatty acid production by expression tuning of FadL and OmpF. *Microb. Cell Fact.* 16:38. doi: 10.1186/s12934-017-0650-8

Varas, M., Valdivieso, C., Mauriaca, C., Ortiz-Severin, J., Paradela, A., Poblete-Castro, I., et al. (2017). Multi-level evaluation of *Escherichia coli* polyphosphate related mutants using global transcriptomic, proteomic and phenomic analyses. *Biochim. Biophys. Acta Gen. Subj.* 1861, 871–883. doi: 10.1016/j.bbagen.2017.01.007

Volova, T. G., Prudnikova, S. V., Vinogradova, O. N., Syrvacheva, D. A., and Shishatskaya, E. I. (2017). Microbial degradation of polyhydroxyalkanoates with different chemical compositions and their biodegradability. *Microb. Ecol.* 73, 353–367. doi: 10.1007/s00248-016-0852-3

Wang, Y., Liu, Y., Deberg, H. A., Nomura, T., Hoffman, M. T., Rohde, P. R., et al. (2014). Single molecule FRET reveals pore size and opening mechanism of a mechano-sensitive ion channel. *eLife* 3:e01834. doi: 10.7554/eLife.01834

Yamano, Y., Nishikawa, T., and Komatsu, Y. (1993). Cloning and nucleotide sequence of anaerobically induced porin protein E1 (OprE) of *Pseudomonas aeruginosa* PAO1. *Mol. Microbiol.* 8, 993–1004. doi: 10.1111/j.1365-2958.1993.tb01643.x

Conflict of Interest: The authors declare that the research was conducted in the absence of any commercial or financial relationships that could be construed as a potential conflict of interest.

frontiers in Bioengineering and Biotechnology

REVIEW
published: 03 April 2020
doi: 10.3389/fbioe.2020.00248

Beyond Intracellular Accumulation of Polyhydroxyalkanoates: Chiral Hydroxyalkanoic Acids and Polymer Secretion

Luz Yañez[1], *Raúl Conejeros*[2], *Alberto Vergara-Fernández*[1] *and Felipe Scott*[1]*

[1] Green Technology Research Group, Facultad de Ingeniería y Ciencias Aplicadas, Universidad de los Andes, Santiago, Chile,
[2] Escuela de Ingeniería Bioquímica, Pontificia Universidad Católica de Valparaíso, Valparaíso, Chile

Polyhydroxyalkanoates (PHAs) are ubiquitous prokaryotic storage compounds of carbon and energy, acting as sinks for reducing power during periods of surplus of carbon source relative to other nutrients. With close to 150 different hydroxyalkanoate monomers identified, the structure and properties of these polyesters can be adjusted to serve applications ranging from food packaging to biomedical uses. Despite its versatility and the intensive research in the area over the last three decades, the market share of PHAs is still low. While considerable rich literature has accumulated concerning biochemical, physiological, and genetic aspects of PHAs intracellular accumulation, the costs of substrates and processing costs, including the extraction of the polymer accumulated in intracellular granules, still hampers a more widespread use of this family of polymers. This review presents a comprehensive survey and critical analysis of the process engineering and metabolic engineering strategies reported in literature aimed at the production of chiral (*R*)-hydroxycarboxylic acids (RHAs), either from the accumulated polymer or by bypassing the accumulation of PHAs using metabolically engineered bacteria, and the strategies developed to recover the accumulated polymer without using conventional downstream separations processes. Each of these topics, that have received less attention compared to PHAs accumulation, could potentially improve the economy of PHAs production and use. (*R*)-hydroxycarboxylic acids can be used as chiral precursors, thanks to its easily modifiable functional groups, and can be either produced *de-novo* or be obtained from recycled PHA products. On the other hand, efficient mechanisms of PHAs release from bacterial cells, including controlled cell lysis and PHA excretion, could reduce downstream costs and simplify the polymer recovery process.

Keywords: 3-hydroxyalkanaoic acids, polyhydroxyalkanoates, chiral compounds, biosynthesis, metabolic engineering

OPEN ACCESS

Edited by:
Ignacio Poblete-Castro, Andres Bello University, Chile

Reviewed by:
Prasun Kumar, Chungbuk National University, South Korea
Jose Manuel Borrero De Acuña, Technische Universitat Braunschweig, Germany

***Correspondence:**
Felipe Scott
fscott@miuandes.cl

Specialty section:
This article was submitted to Industrial Biotechnology, a section of the journal Frontiers in Bioengineering and Biotechnology

Received: *06 December 2019*
Accepted: *10 March 2020*
Published: *03 April 2020*

Citation:
Yañez L, Conejeros R, Vergara-Fernández A and Scott F (2020) Beyond Intracellular Accumulation of Polyhydroxyalkanoates: Chiral Hydroxyalkanoic Acids and Polymer Secretion. Front. Bioeng. Biotechnol. 8:248. doi: 10.3389/fbioe.2020.00248

INTRODUCTION

Synthetic plastics produced from petroleum-derived monomers, such as ethylene, propylene, styrene, and polyethylene terephthalate, are non-biodegradable polymers that undergo slow fragmentation to micron-size particles (Kubowicz and Booth, 2017). Nearly 60% of all plastics produced between 1950 and 2015, equivalent to 4,900 metric tons, can be found in landfills or

in the natural environment. Another 800 metric tons were incinerated and 600 MT recycled. Only 10% of the recycled plastics have been recycled more than once (Geyer et al., 2017).

The environmental burden imposed by the production of petroleum-derived polymers can be ascribed to its persistence in the environment and its impact on climate change. On the former, evidence suggests a complex toxicology of microplastics on marine life and in the food chain (Worm et al., 2017). Regarding the latter, each stage in the current plastic lifecycle generates greenhouse gases (GHGs): fossil fuel extraction and transport, monomer production, plastic refining and manufacturing, and plastic waste management. Estimations indicate that if plastic production grows at the current rate, by 2050 the cumulative emissions from plastic use could account for over 56 gigatons of carbon. This is equivalent to 10–13% of the remaining carbon budget (Hamilton et al., 2019).

The search for biodegradable polymers with a reduced emission of GHGs has led to the development of microbial-based processes using natural or genetically engineered microorganisms capable of producing polymers (e.g., polylactic acid and polyhydroxyalkanoates) or monomers (lactic acid, succinic acid, caproic acid, and hydroxyalkanoic acids) with the potential of replacing the current petroleum-based methods (Tsuge et al., 2016).

Renewable bio-based and biodegradable polymers are expected to play a key role in curbing the impacts of plastic production and use in the near future (Zheng and Suh, 2019). One of the most studied biopolymers is poly(R-3-hydroxybutyrate), PHB, an intracellular polyester accumulated in many bacteria. PHB is a member of a large family of renewable and biodegradable bio-polyesters collectively known as polyhydroxyalkanoates (PHAs). They are built by (*R*)-3-hydroxy fatty acid monomers varying from 3 to 5 carbon atoms (short-chain-length PHAs, scl-PHA) and from 6 to 14 carbons (medium-chain-length PHAs, mcl-PHA). Although as many as 150 different congeners of PHA are known with different monomers (Steinbüchel and Valentin, 1995), PHB is the most extensively studied and excellent reviews have been published regarding strategies to improve its production (Peña et al., 2014) and its process technology (Alves et al., 2017).

PHB has been studied for decades as a source of a renewable polymer for the substitution of fossil-derived plastics (Chen and Patel, 2012). However, its use as a substitute for thermoplastics has been hampered by high production costs, dominated by the cost of substrates for the fermentation stage and the costs of downstream extraction and purification. The costs of supplying the required carbon and energy source for microbial growth and PHB production are estimated to be between 30 and 50% of the product cost if sugars are used (Choi and Lee, 1999; Levett et al., 2016). On the other hand, the downstream processes rely on hypochlorite (Heinrich et al., 2012) and solvents (Jiang et al., 2018) for the extraction and precipitation of the polymers. Solvent recovery further adds to processing costs and energy use.

Finally, the large variety of monomers that can be incorporated into PHAs makes PHB only one member of a large family of polymers with different physical properties. Costs are further increased by the precursors required for the production of customized thermoplastics, such as poly(3-hydroxybutyrate-*co*-3-hydroxyvalerate) were valerate is used to change the polymer composition (Choi and Lee, 1999).

This review focuses on a simple but powerful concept, multiple carbon substrates can be funneled to poly(hydroxyalkanoates) and its enantiomerically pure monomers, 3-hydroxyalkanoic acids (3HAs). These monomers are a family of related compounds having at least two functional groups (a hydroxy group and a carboxyl group) that are amenable for chemical modification, they can play a role as building blocks for the synthesis of a large number of products, including diols, polyesters, and fine chemicals. These monomers can be produced either by *in-vivo* depolymerization of the accumulated PHAs, by fermentation for the direct production of 3HAs into the culture media and by conversion of purified PHAs. The advantage of the first two alternatives is that production does not require the extraction of the intracellular PHAs.

Here, we first introduce the potential uses of polyhydroxyalkanoates and its monomers (section Potential Uses of Polyhydroxyalkanoates and Its Monomers) followed by the substrates used for its production (section Substrates for the Production of Polyhydroxyalkanoates and Its Monomers). Section Accumulation and Mobilization of PHAs deals with the pathways and mechanisms of PHAs accumulation and mobilization in bacteria, with an emphasis on PHB. In section Production of R-3-Hydroxyalkanoic Acids From PHAs and Alternative Substrates and Microorganisms for 3HA Production, different strategies for the production of 3HAs are discussed, including *in-vivo* hydrolysis of PHAs and genetic modifications aimed at the direct production of these acids without a polymer accumulation step. Finally, section Secretion of PHAs discusses the research on alternative methods for PHAs liberation and recovery from bacteria to supply substrates for 3-hydroxy acids production.

POTENTIAL USES OF POLYHYDROXYALKANOATES AND ITS MONOMERS

Polyhydroxyalkanoates (PHAs) have been extensively investigated to identify possible applications. Homopolymers, random copolymers, and block copolymers can be produced depending on the structure of the polymer chain, this is dictated by the species of bacteria and the substrate used for the accumulation of PHA (Braunegg et al., 2004). The diversity of applications is wide, including production of biodegradable plastics that are environmentally friendly for use in packaging (Koller, 2014; Khosravi-Darani, 2015), fibers (Dietrich et al., 2016), biodegradable and biocompatible implants (Misra et al., 2006), drugs and fine chemical (Rathbone et al., 2010), and biofuels (Zhang et al., 2009).

PHAs have been traditionally used in the packaging of a series of products as shampoo bottles, shopping bags, containers and paper coatings, utensils, carpets, compostable bags, and thermoformed articles (Bugnicourt et al., 2014).

As biomedical materials, PHAs have been used in suture materials and repair patches, meniscus restoration devices, cardiovascular patches, orthopedic pins, and cartilage

regeneration aids, among others (Volova et al., 2003; Wang et al., 2005). Many of these uses are related to the customizable composition and properties of PHAs, which allow them to have favorable mechanical properties, biocompatibility, and to degrade in reasonable times under specific physiological conditions (Misra et al., 2006; Hazer et al., 2012). In particular, mcl-PHAs have potential applications in coatings and in medical temporary implants such as scaffoldings for the regeneration of arteries and nerve axons (Witholt and Kessler, 1999). On the other hand, the use of these polymers has been studied in controlled drug delivery (Shah et al., 2010). The kinetics of drug release can be engineered by altering the degradation rate of the PHA matrix coating. In this regard, mcl-PHA have been used as drug carriers since its low fusion point and low crystallinity makes them suitable for controlled drug release (Ueda and Tabata, 2003).

Finally, PHA derived compounds can be used as biofuels after the esterification of PHB and mcl-PHAs with methanol for its conversion to hydroxyalkanoate methyl esters (Zhang et al., 2009). These hydroxyalkanoate methyl esters can be mixed with gasoline and diesel in ratios of 10 to 30%. In particular, (*R*)-3-hydroxy-methyl-butyrate was reported to have similar or improved properties as a fuel additive (oxygen content, dynamic viscosity, flash point, and boiling point) compared to ethanol (Wang et al., 2010). Using PHA derivatives as biofuels can be viewed as a promising application since mixtures of PHA can be used without a costly separation step (Gao et al., 2011).

The most well-known (*R*)-3-hydroxyalkanoic acid, (*R*)-3-hydroxybutyric acid (R3HBA) can be used as a building block in the synthesis of fine chemicals and pharmaceuticals such as antibiotics (Ren et al., 2005), bulk chemicals for the polymer industry (such as hydrogenation to 1,3 butanediol), fragrances and insecticides (Matsuyama et al., 2001) (see **Figure 1**). 1,3 butanediol can be dehydrated to yield unsaturated alcohols which can be further dehydrated to form 1,3 butadiene (Nozawa et al., 2009), a building block for the production of styrene-butadiene rubber. The world consumption of butadiene reached 10 million metric tons in 2012 (Biddy et al., 2016). R3HBA can be esterified with butanol or ethanol or converted to ethers by reaction with alcohols using the catalytic Williamson ether synthesis (Fuhrmann and Talbiersky, 2005) or dehydrated to crotonic acid, which upon hydrogenation yields butyric acid and *n*-butanol (Schweitzer et al., 2015).

Similarly, 3-hydroxypropionic acid (3HPA), a non-chiral compound, can yield upon chemical modification access to acrylic acid, acrylamide and acrylonitrile, all with market sizes larger than 1 billion dollars, and other niche market compounds such as 1,3 propanodiol, methyl acrylate, and malonic acid (Jers et al., 2019).

More than three decades ago Seebach et al. (1986), reported the synthesis of the macrolide antibiotics pyrenophorin, colletodiol, garamycin A1, and elaiophylidene starting from (*R*)-3-hydroxybutyrate and malate. R3HBA and its derivatives have also been used as potential drugs. Cao et al. (2014) showed that R3HBA and its derivative 3-hydroxybutyrate methyl ester inhibit the development of osteoporosis in mice kept under simulated microgravity. Using *in-vivo* studies with mice suffering from Alzheimer's disease, Zhang et al. (2013) showed that intragastric administration of 3-hydroxybutyrate methyl ester reduced amyloid-β deposition in mouse brains and improved the performance of the treatment group in the Morris water maze (a standardized test in the study of spatial learning and memory) compared to the control group. In a related study in mice, Tieu et al. (2003) showed that the infusion of R3HBA led to improved mitochondrial respiration and ATP production in mice treated with the neurotoxin 1-methyl-4-phenyl-1,2,3,6-tetrahydropyridine causing a mitochondrial deficit reminiscent of Parkinson disease. Finally, Yamanashi et al. (2017) showed that R3HBA could act as a therapeutic candidate for the treatment of stress-related mood disorders (depression). The mechanism involves an anti-inflammatory effect mediated by a reduction in the levels of the inflammatory cytokines inter-leukine 1β and tumor necrosis factor α in the hippocampus of mice.

Other potential uses of R3HBA include its use as a chemical chaperone for heat-mediated denaturation and oxidative damage by Cu^{2+} and H_2O_2 produced on industrially relevant enzymes such as lipases and lysozymes (Obruca et al., 2016).

Finally, (*R*)-3-hydroxyalkanoic acids can be used as building blocks that can be biologically produced, excreted from cells and then polymerized or co-polymerized to yield PHAs with the desirable mechanical and thermal properties (Wang et al., 2018). Advantages of the *ex-situ* polymerization starting from biomonomers over the conventional approach of biopolymer accumulation inside cells include (Adkins et al., 2012): (i) simplified downstream product recovery of the extracellular biomonomers compared to the intracellular polymers, (ii) polymerization in controlled chemocatalytic environments allows for polymers with finely tuned properties and high purities, and (iii) higher diversity of plastics thanks to the ability to co-polymerize different monomers. Examples of *in-vitro* synthesis include the production of PHB from R3HBA by a three-enzyme system that only consumes ATP and the monomer (Jossek and Steinbüchel, 1998). The yield of this system was recently improved by using a thermostable acetyl-CoA synthetase, CoA transferase, and PHA synthase (Tajima et al., 2016). A polymer incorporating lactate and R3HBA residues was produced by Tajima et al. (2012) by using an engineered PHA synthase capable of lactate polymerization. An excellent revision of the chemosynthesis of copolymers containing different 3HAs monomers and lactate was recently published (Hiroe et al., 2019). However, a general drawback of these systems so far is the consumption of ATP, specifically to drive the activation of acetate to acetyl-CoA, a molecule that needs to be present on the reaction mixture to act as the CoA donor to yield the hydroxyacyl-CoAs required for the polymerization reaction.

SUBSTRATES FOR THE PRODUCTION OF POLYHYDROXYALKANOATES AND ITS MONOMERS

This section summarizes the carbon and energy substrates currently used for the production of PHA and the potential of moving to lignocellulosic substrates, agro-food wastes, and

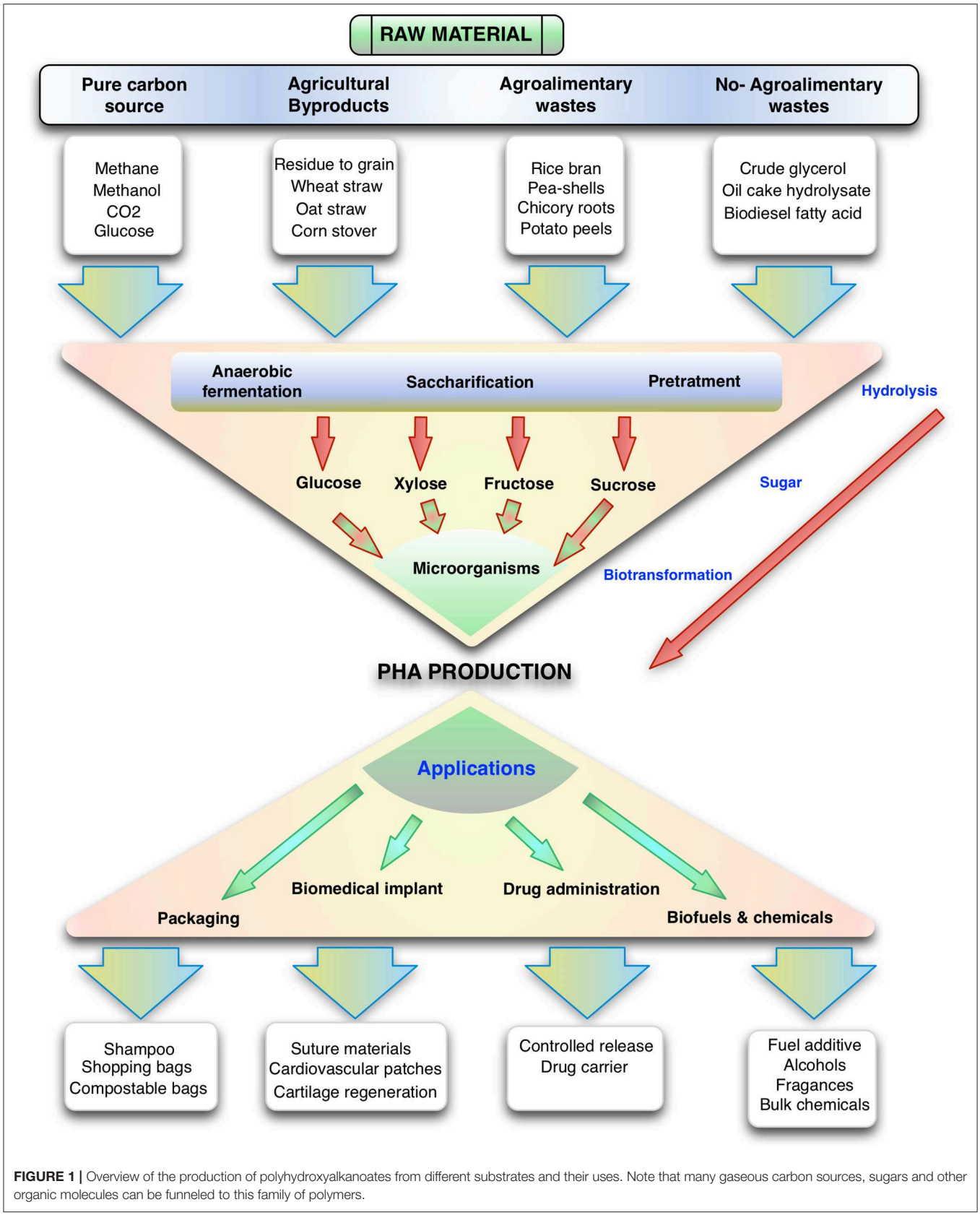

FIGURE 1 | Overview of the production of polyhydroxyalkanoates from different substrates and their uses. Note that many gaseous carbon sources, sugars and other organic molecules can be funneled to this family of polymers.

abundant gaseous substrates such as syngas, knallgas, or methane. For a comprehensive review regarding the many substrates for PHA production, the reader is referred to Jiang et al. (2016). The production of 3-hydroxyalkanoic acids from these unconventional sources is presented in section Alternative Substrates and Microorganisms for 3HA Production.

Substrates commonly used for industrial production of PHAs are represented by corn starch, sucrose obtained from sugar cane and vegetable oils, all edible feedstock requiring arable lands and agricultural practices that affect both its economy and sustainability (Levett et al., 2016). Commercial PHAs are produced using sucrose in *Azohydromonas lata* (Biomer Germany, with trade name Biomer^{TM}) and *Bacillus* sp. (PHB Industrial S.A. Brazil, Biocycle^{TM}); glucose from corn in *C. necator* (Metabolix, Mirela^{TM} and Tianan Biologic Material, Enmat^{TM}); or fatty acids using *Pseudomonas putida* (ETH, PHA^{TM}) or *C. necator* by Kaneka Corporation and marketed as Kaneka PHBH^{TM} (Chen, 2009; Bugnicourt et al., 2014; Mozejko-Ciesielska and Kiewisz, 2016).

Due to the high costs and sustainability concerns associated with raw materials traditionally used in the production of PHA, the use of agro-food waste, food industry waste, and other non-food industry residues, have been increasingly studied (Braunegg et al., 2004). For example, several solid residues have been examined such as rice bran (Oh et al., 2015), pea-shells (Kumar et al., 2016), chicory roots (Haas, 2015), potato peels, apple pomace, onion peels (Kumar et al., 2016), grape pomace (Follonier, 2015), animal farm waste, poultry litter (Bhati and Mallick, 2016), and palm oil (Loo et al., 2005). In the case of food wastes for PHAs production, literature report on the use of spent coffee grounds (Cruz et al., 2014), food waste composite (Amulya et al., 2015), and used cooking oil (Gómez Cardozo et al., 2016; Borrero-de Acuña et al., 2019).

Finally, non agro-alimentary residues are generated by biodiesel manufacturing: crude glycerol (de Paula et al., 2017), oil cake hydrolysate (Bera et al., 2015), and biodiesel fatty acid by-product from glycerol purification (Cruz et al., 2016). Glycerol can be used for the accumulation of mcl-PHAs and scl-PHAs in *Pseudomonas putida* strains (Poblete-Castro et al., 2014), *C. necator* (Mothes et al., 2007), and *Bacillus megaterium* (Naranjo et al., 2013), among others.

The availability and sustainability issues of conventional substrates have motivated the exploration of alternative feedstock as sources of carbon and energy for microbial production of chemicals, such as lignocellulose which can be obtained from the "residues" left after the harvest of agricultural products or from dedicated high yield cultivars (poplar, eucalyptus, miscanthus) (Loow et al., 2016), thus reducing the environmental burden associated with its production. Reducing even further the water and land usage, compounds containing one carbon atom, such as methanol and formate can be obtained from the reduction of CO_2 using electrons harnessed from solar energy (Agarwal et al., 2011; Pérez-Fortes et al., 2016; Yishai et al., 2016).

Regarding the use of monomeric sugars obtained from lignocellulose, these are always accompanied by non-sugar compounds like acetic acid, furfural, and other organic acids and aromatic compounds that are produced during pretreatment (Hodge et al., 2008). Biomass is pretreated to improve the action of carbohydrate hydrolases that break down cellulose and hemicellulose during saccharification. In dilute sulfuric acid hydrolysis of corn stover, a leading pretreatment technology, lignocellulosic biomass is deconstructed into pretreated corn stover: a solid fraction (or pulp), enriched in cellulose and lignin, and a liquid fraction (pretreatment liquor), containing oligomers and monomers of hemicellulose and acetic acid (Chen et al., 2012). To further break down cellulose and hemicellulose remaining in the pulp into fermentable sugars, an enzymatic hydrolysis step is necessary.

Regarding PHB production from sugars and acids present in lignocellulosic hydrolysates, albeit *A. lata* or *C. necator* are unable to use xylose, they are tolerant to acetic acid, furfural, and hydroxy-methyl-furfural (among other compounds found in lignocellulosic hydrolysates) (Dietrich et al., 2013). On the other hand, *Burkholderia sacchari* (Brämer et al., 2001) and *Burkholderia cepacia* can use xylose for growth and PHB production. In a fed-batch culture experiment using glucose and xylose to promote PHB accumulation in *B. cepacia*, 60 g L^{-1} of biomass were attained in 70 h with 58% PHB content. The yield of PHB was 0.46 g PHB per gram of substrate (Silva et al., 2004). *B. cepacia* was able to incorporate vanillin to PHB (Pan et al., 2012; Dietrich et al., 2013), while levulinic acid was incorporated as hydroxyvalerate (Keenan et al., 2006). Both vanillin and levulinic acid are compounds present in lignocellulosic hydrolyzates. Moreover, the minimum inhibitory concentrations of acetic acid, hydroxy-methyl-furfural and furfural reported for *B. cepacia* growth are 4.00, 6.00, and 6.00 g L^{-1} respectively (Dietrich et al., 2013). Raposo et al. (2017) recently showed that in fed-batch cultures of *B. sacchari* DSM 17165, the catabolite repression of glucose on xylose consumption can be avoided by maintaining glucose concentration below 10 g L^{-1}. Notably, they showed that when xylose concentration increases in the fermenter, xylitol appears as a second product (xylose concentration above 30–40 g L^{-1}).

Among inexpensive substrates that are readily available for reducing the total cost of PHA production, certain C1 carbon sources, e.g., methane, methanol, and CO_2 have received a great deal of attention due to their contribution to global warming (Khosravi-Darani et al., 2013). Production of PHB from waste methane may help reduce the impact on the greenhouse effect of this gas. Accumulation of PHB, but not other PHAs, has been studied in several *Methylocystis* species using methane and *Methylobacterium* from methanol [*cf.* Strong et al. (2016)]. In this regard, Listewnik et al. (2007) estimated a price of 6.35 UK pound/kg for produced PHB from natural gas in a two-stage plant producing 500 t PHB per year. Similarly, Levett et al. (2016) estimated a production cost range of 4.1 to 6.8 USD per kg of PHB, with a reduction in the share of the carbon source in the total product cost from 30% when sugar feedstocks are used to 22% for methane. However, these production costs are high when compared to the estimations made by Posada et al. (2011), who performed a techno-economic evaluation of PHB production from glycerol as energy and carbon source. They reported production costs between 1.9 and 2.5 USD per kg and a substrate share between 5 and 8%. The higher production cost

when methane is used as substrate is greatly influenced by the slow mass transfer of methane into the media. This leads to large reactors and, thereby high investment costs.

Knallgas bacteria, such as *C. necator* and *A. lata* can use mixtures of hydrogen, carbon dioxide and oxygen for the accumulation of PHB (Reinecke and Steinbüchel, 2008), biofuels (Brigham, 2019), or acetoin (Windhorst and Gescher, 2019). Albeit the production of PHB has been studied thoroughly, with cultures of *C. necator* or *Ideonella* sp. O-1 accumulating over 60 g L^{-1} of PHB (Tanaka et al., 1995, 2011), no reports of PHAs accumulation aside PHB are available (for a review on PHB production from C1 sources see Khosravi-Darani et al., 2013).

ACCUMULATION AND MOBILIZATION OF PHAs

The model organism for PHB production is *Cupriavidus necator* (formerly *Ralstonia eutropha* and *Alcaligenes eutrophus*), a gram-negative, obligate aerobe, capable of autotrophic growth in the presence of hydrogen, CO_2 and oxygen, and heterotrophic growth and PHB production from a wide variety of carbon sources including sugars (chiefly fructose in the wild type organism *C. necator* H16 ATCC 17699) and organic acids (Lu et al., 2016). For example, using glucose in a fed-batch culture of *C. necator* NCIMB 11599, a mutant of *C. necator* H16 capable of using glucose, a concentration of biomass of 164 g L^{-1} was obtained, with a PHB content of 74% (Kim et al., 1994).

In *C. necator*, synthesis of PHB occurs when excess carbon in the form of acetyl-CoA is condensed via a β-ketothiolase (EC 2.3.1.16) to generate acetoacetyl-CoA, which is then reduced to (R)-3-hydroxybutyryl-Coenzyme A by a NADPH-dependent acetoacetyl-CoA reductase (EC 1.1.1.36). Finally, the enzyme PHB synthase (EC 3.1.1.75) catalyzes the polymerization of (R)-3-hydroxybutyrl-CoA monomers. This pathway is the most widespread route in bacteria for providing 3-hydroxybutyryl-CoA monomers (Steinbüchel and Hein, 2001). Production of mcl-PHAs, such as the polymers accumulated in *Pseudomonas* spp., requires precursors derived from the dissociated fatty acid biosynthesis pathway unless these precursors are supplied through related carbon sources (such as octanoic acid for the synthesis of poly(3-hydroxyoctanoate). For details regarding this pathway, we point to the excellent reviews by Lu et al. (2009) and Suriyamongkol et al. (2007).

The regulation of PHB biosynthesis is tightly connected to the cellular levels of reduced nicotinamide nucleotides. Lee (1995) found that when *C. necator* was cultivated in nitrogen-limited media, the NADPH/NADP and NADH/NAD ratios and the intracellular concentrations of NADH and NADP were higher than those found under nitrogen sufficient conditions. Moreover, the rate of PHB accumulation was found to increase with both NADH/NAD and NADPH/NADP ratios. This effect was explained through the analysis of citrate synthase activity. Citrate synthase was inhibited by NADPH and NADH, thus funneling the carbon to PHB instead of being directed to the tricarboxylic acid cycle. Similar conclusions were reported by Henderson and Jones (1997).

Although PHB accumulation occurs under unfavorable conditions for growth induced by nutrient limitation of oxygen, nitrogen, or phosphorous, with excess carbon (Steinbüchel and Hein, 2001), these conditions impact the productivity of the PHB accumulation phase. Grousseau et al. (2013) showed that sustaining a controlled residual growth rate, by feeding a controlled amount of phosphate along with the carbon source (butyric acid), allows for an improved PHB specific productivity and high yield. Interestingly, using Metabolic Flux Balances they showed that the maximal specific PHB production rate is defined by the maximum specific rate of NADPH produced. When a low growth rate is allowed in the fed-batch fermentation (for example, feeding a nitrogen source), the NADPH is produced in the Entner-Doudoroff pathway; whereas without biomass production regeneration of NADPH is only possible via isocitrate dehydrogenase.

Another possibility to increase PHB volumetric productivities is to rely on microorganisms where growth and PHB production occur simultaneously. In this regard, *Azohydromonas lata* consumes glucose, sucrose and acetic acid (Chen et al., 1991), but it does not consume xylose, accumulating PHB during its growth (Yamane et al., 1996). In a fed-batch culture using sucrose as the carbon source and a continuous feeding of ammonia, controlled by the decrease in pH as the culture consumes the source of nitrogen (pH-stat), 143 g L^{-1} of cells with 50% PHB were attained with a PHB productivity of 3.97 g L^{-1} h^{-1}, one of the highest ever reported (Yamane et al., 1996). One year later, Wang and Lee (1997) reported even higher productivity (4.94 g L^{-1} h^{-1}) and PHB intracellular content in *A. lata* (88%) applying nitrogen limitation in a two-stage fed-batch culture (nitrogen sufficient followed by nitrogen-limited culture).

Assuming that PHAs act as a reserve compound of carbon and energy, without a source of carbon and energy, but in the presence of other growth factors (such as nitrogen or oxygen), PHAs should be depolymerized to its monomers and incorporated into the metabolism, using the degradation products for growth and survival, a process termed PHA mobilization. This behavior has been shown at least in *C. necator* H16 (Uchino et al., 2007; Juengert et al., 2017), *A. lata* (Lee et al., 1999), *Legionella pneumophila* (James et al., 1999), *Hydrogenophaga pseudoflava* (Choi et al., 1999), and *Halomonas* sp. KM-1 (Kawata et al., 2015).

Compared to PHB accumulation, depolymerization of PHB to R3HBA, and its transformation to acetyl-CoA, has been less studied as confirmed by fewer reports in the literature. However, evidence exists pointing that the granules of PHB and other PHAs are supramolecular complexes (called carbonosomes), constituted by a polymer core and a surface layer of at least a dozen proteins (Sznajder et al., 2015), but without a phospholipids membrane (Bresan et al., 2016). The proteins in the carbonosomes include the PHA synthase (PhaC) and PHB depolimerazes (PhaZs), which are thought to be constitutively expressed (Lawrence et al., 2005; Brigham et al., 2012).

It has been reported that PHB synthesis and its degradation can happen simultaneously in the model PHB accumulating organism *C. necator* (Doi, 1990; Taidi et al., 1995). Doi concluded this after cultivating *C. necator* in butyrate as

carbon source under nitrogen-free conditions, thus inducing the accumulation of PHB, and changing the carbon source to pentanoic acid. After the shift in the substrate, the accumulated PHB was gradually replaced by poly(3-hydroxyvalerate-co-3-hydroxybutirate) without a net increase of total polymer content in the cells. This indicates that PHB was degraded and replaced by PHV even in the absence of a nitrogen source. Similarly, Taidi et al. (1995) showed a turnover of PHB after the accumulation of the polymer ceased in a nitrogen-limited batch culture with glucose as the sole carbon and energy source. The turnover was evidenced by the incorporation of radioactivity into the accumulated polymer after feeding labeled glucose (D-[U-^{14}C] glucose). Interestingly, the high-molecular-weight polymer accumulated during the unlabeled glucose phase was replaced by a low-molecular-weight polymer during the labeled glucose experiment. These observations are in agreement with the evidence showing the constitutive expression of PHB synthase and PHB depolymerase in *C. necator* (Lawrence et al., 2005; Sznajder et al., 2015). Corroboration of constitutive expression of PHB synthase and depolymerase in other organisms is scarce, with the exception of the study of Kim et al. (1996) who found simultaneous activities of both enzymes during the batch culture of *Azohydromonas lata* under nitrogen-limited conditions.

Thereby, this leads to the intriguing question of how the synthesis and mobilization of PHAs are regulated, and particularly, how a cycle of simultaneous synthesis and degradation is avoided. Considering that the simultaneous polymerization and depolymerization of PHB and its conversion to acetyl-CoA trough 3-hydroxybutyrate, acetoacetate, and acetoacetyl-CoA requires one NADPH molecule and one ATP molecule and produces only one NADH molecule, the cycle would consume energy for the formation of thioester bonds, thus creating a futile cycle.

To tackle this unsolved issue, Uchino et al. (2007) isolated native PHB granules produced in *C. necator* by glycerol gradient centrifugation to preserve the proteins bounded to the granule, and discovered that in the presence of CoA, these granules produced 3HB-CoA and small amounts of acetyl-CoA. If NAD^+, but not NADH, is added to the initial reaction mixture, 3HB-CoA remains undetectable, but the concentration of acetyl-CoA increases 5-fold. The authors assumed that in the presence of NAD^+, the intermediately formed 3HB-CoA is rapidly transformed to acetyl-CoA in NAD^+ dependent reactions. The authors also found, as expected, that the native granules release R3HBA in pH-stat experiments using methods previously described (Gebauer and Jendrossek, 2006). Therefore, it remains unclear which depolymerization mechanism, hydrolysis or thiolysis, is used *in-vivo* for the mobilization of PHB.

In order to identify the enzymes responsible for the thiolytic cleavage, Uchino et al. (2007) incorporated the PHB synthesis genes *phaCAB* in *E. coli* S17-1 along with the phasin gene *phaP1*, the depolymerase gene *phaZa1* or *phaP1* + *phaZa1*. Interestingly, the recombinant strain only produced 3HB-CoA in the presence of CoA when both *phaP1* and *phaZa1* were present in a *phaCAB* background. Moreover, no significant amounts of acetyl-CoA were detected in this experiment, an indication that downstream enzymes for the use of 3HB-CoA were absent in *E. coli*.

The study of Uchino et al. (2007), suggests that *in-vivo* intracellular depolymerization of PHB does not represent a futile cycle and an energy waste in the form of thioester bonds. If the main product of PHB polymerization, at least in *C. necator*, is 3HB-CoA instead of 3HB, then there is no loss of energy for the formation of acetoacetyl-CoA from acetoacetate (see **Figure 2**).

Regarding the regulation of PHB synthesis and degradation, Juengert et al. (2017), found that the degradation of the accumulated PHB in *Ralstonia eutropha* was fast and efficient in the absence of the alarmone (p)ppGpp, and that when present, (p)ppGpp directly or indirectly inhibits PHB mobilization. (p)ppGpp is a key signaling molecule, which, when present at high concentrations induces the stringent response in *E. coli* and other bacterial species. This alarmone accumulates in amino acids starved cells, and inhibit the synthesis of ribosomal and transfer RNAs (Srivatsan and Wang, 2008). The results suggest that PHB accumulation under nitrogen-limited conditions is favored by the inhibition of PhaZ1 by (p)ppGpp as shown by the observed PHB accumulation in a triple knockout mutant (Δ*spoT*1 + Δ*spoT*2 + Δ*phaZa*1) that was unable to produce (p)ppGpp. In contrast, the double knockout mutant Δ*spoT*1 + Δ*spoT*2 accumulated negligible amounts of PHB. In a subsequent work, Juengert et al. (2018) identified that PhaC1 was phosphorylated in multiple phosphosites during the stationary growth phase in nutrient broth medium with gluconate as carbon source, but it was not modified during the exponential and PHB accumulation phases or when grown in a fructose-mineral medium. On the other hand, PhaZa1 was phosphorylated in Ser35 both during the exponential and stationary growth phases. Mutagenesis of the identified residues showed that PHB accumulation was unaffected for most mutants of PhaC1, except for a mutant with changes to four aminoacid residues. On the other hand, exchanging the phosphorylated residues in PhaZa1 to aspartate (a phosphomimetic residue) produced mutants with a strongly reduced ability to mobilize the accumulated PHB.

Little experimental evidence exists concerning the role of the stringent response in the accumulation of PHA in other organisms. In this regard, Mozejko-Ciesielska et al. (2017) obtained a *relA*/*spot* mutant of *P. putida* KT2440. This mutant, unable to induce the stringent response, was used to assess the accumulation of PHA under nitrogen deprived and optimal nitrogen conditions. Results show that this mutant is able to accumulate mcl-PHAs under both conditions.

Taken together, the works of Mozejko-Ciesielska et al. (2017) and Juengert et al. (2017; 2018) provide insights into the molecular basis of the regulation of PHB accumulation and mobilization. As it will be covered in section *in-vivo* Strategies these regulatory mechanisms play a key role in the production of R3HBA *in-vivo* from cells that accumulated PHB.

PRODUCTION OF R-3-HYDROXYALKANOIC ACIDS FROM PHAs

Several strategies based on operational changes or genetic modifications have been devised for the production of chiral

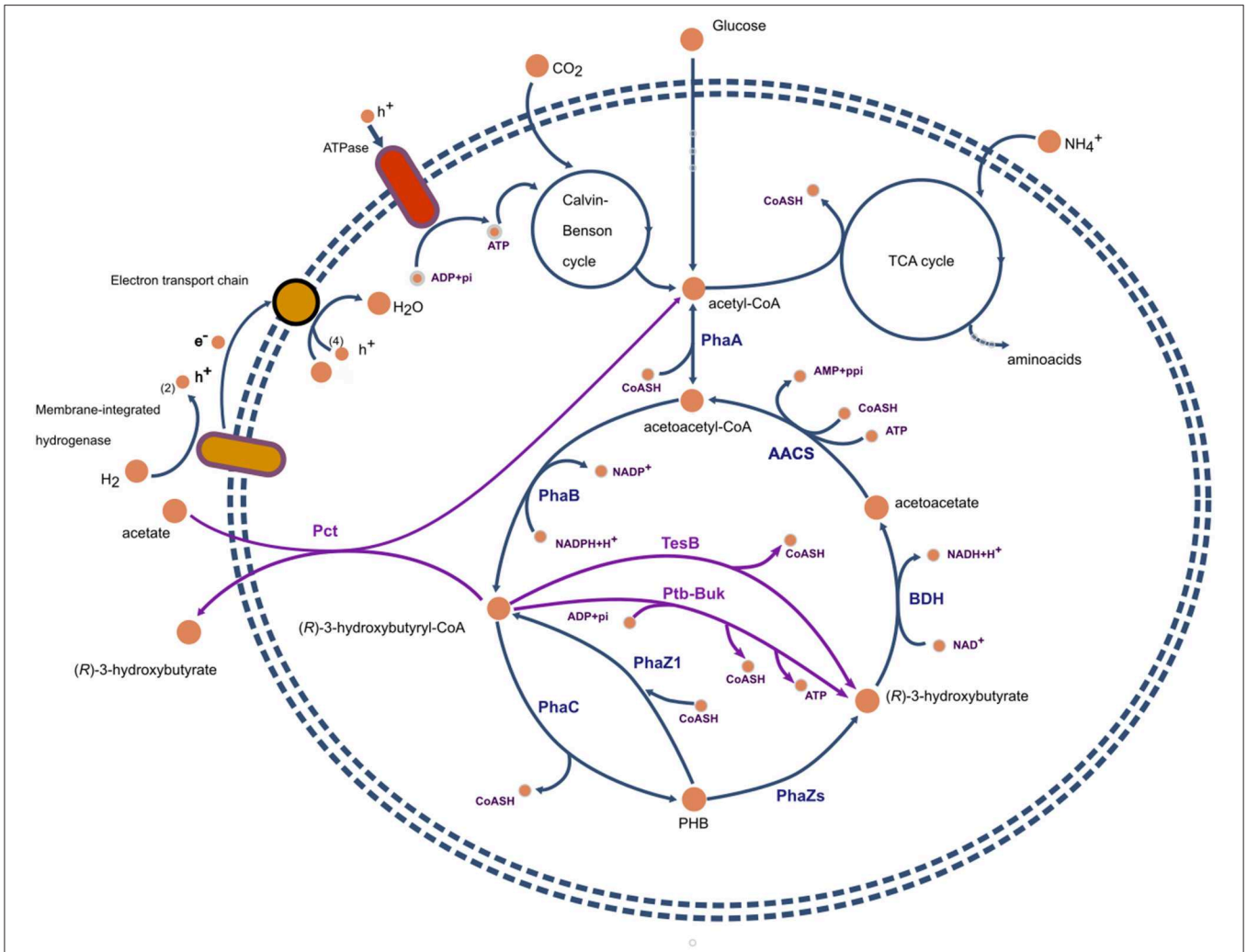

FIGURE 2 | Representation of metabolic pathways involved in the synthesis of polyhydroxybutyrate and (*R*)-3-hydroxybutyrate in *Cupriavidus necator*. Reactions and proteins present in the wild type are presented in blue. In magenta, recombinant proteins and reactions commonly expresed in host organisms such as *E. coli.* PhaA, β-ketoacyl-CoA thiolase; PhaB, acetoacetyl-CoA reductase; PhaZs, PHA depolymerases; BDH, (*R*)-3-hydroxybutyrate dehydrogenase; PhaC, PHA polymerase; TesB, acyl-CoA thioesterase II; Ptb-Buk, phosphor-transbutyrylase and butyrate kinase; AACS, acetoacetyl-CoA synthase.

hydroxyalkanoic acids. This section organizes such strategies in three categories, *ex-vivo* strategies, *in-vivo* strategies using non-genetically modified organisms and, finally, the construction of recombinant organisms. This material updates and complements the excellent review of Ren et al. (2010), that extensively covers the potential applications of hydroxyalkanoic acids and also focused on the chemical synthesis of these compounds and the review by Gao et al. (2011), dealing with a broader view, the synthesis of PHAs and its monomers.

In-vitro Strategies

Under this approach, the accumulated PHAs are extracted from cells and then subjected to a chemical or enzymatic depolymerization process. The PHA recovery process starts when cells are separated by centrifugation to increase product concentration and to remove the components of the culture media. The concentration step is followed by drying or lyophilization of the concentrated biomass. The extraction of PHAs from the dried biomass can be performed by solvent extraction, by dissolving the biomass using oxidizing agents or by disrupting cells to liberate the PHAs granules (Kosseva and Rusbandi, 2018). Mechanical cell disruption techniques, such as bead milling and high-pressure homogenization have been widely used to release intracellular protein, and have been adapted for PHAs recovery (Melih Tamer et al., 1998; Kunasundari and Sudesh, 2011). Melih Tamer et al. (1998) compared bead milling and high-pressure homogenization for the recovery of PHB accumulated in *Azohydromonas lata*. They recommended bead milling over high-pressure homogenization as the preferred method for recovering PHB from heat-shocked cells of *A. lata*. Interestingly, since PHB is recovered without solubilizing it, the native amorphous morphology of the polymer was conserved.

The common method for PHAs extraction is the use of solvents for its speed and simplicity. Solvents alter the cell membrane and then dissolve the polymers. PHAs are recovered by solvent evaporation or precipitation with an anti-solvent (Liddell, 1999; Hänggi, 2012). In the solvents category, the chlorinated hydrocarbons chloroform, 1,2-dichloroethane, and methylene chloride are used (Ramsay et al., 1994). Non-chlorinated solvents have been proposed such as ethylene carbonate and 1, 2-propylene (Lafferty and Heinzle, 1977) or solvent mixtures of acetone/ethanol/propylene carbonate (Fei et al., 2016). On the other hand, the precipitation of PHAs is generally induced by non-solvent agents such as water, ethanol, and methanol (Ramsay et al., 1994; Mikkili et al., 2014). In summary, solvent extraction is characterized by numerous advantages such as the elimination of endotoxins and low polymer degradation (Liddell, 1999). However, there are hurdles in the use of solvents, including their high cost (Poirier et al., 1995), high energy consumption for the separation of miscible solvents and anti-solvents, and risks both for the operator and for the environment that need to be considered during the process design stage (Gorenflo et al., 2001).

On the other hand, digestion with sodium hypochlorite decomposes the cells allowing high levels of PHA purity to be reached (Hahn et al., 1994; Kim et al., 2003), however, sodium hypochlorite degrades PHB, resulting in a polymer with low molecular weight (Ramsay et al., 1990; Mikkili et al., 2014).

Chemical and Enzymatic Hydrolysis of Recovered PHAs

After recovery, and possible purification, the extracted PHAs can be chemically or enzymatically converted into high-purity 3-hydroxyalkanoic acids. Chemical methods for modifying PHB have been reported for the production of (*R*)-methyl 3-hydroxybutanoate and (*R*)-3-hydroxybutanoic acid, these methods involve the use of methanol and sulfuric acid and methanol and *p*-toluenesulfonic acid monohydrate respectively (Seebach et al., 2003). Another approach, reported by Lee et al. (2000), considers the acidic alcoholysis of PHB, yielding methyl, ethyl, and *n*-propyl esters of (*R*)-3- hydroxybutyrate, using 1,2 dichloroethane as solvent with either sulfuric acid or hydrochloric acid as catalyst. de Roo et al. (2002) extended this method for the production of mcl-3HAs from the mcl-PHAs accumulated in *P. putida*. After a step of acid methanolysis, the obtained (*R*)-3HA methyl esters were distilled into fractions and saponified to yield the corresponding (*R*)-3-hydroxycarboxylic acids.

The multistep chemical processes outlined in the previous paragraph can be efficiently catalyzed by PHA depolymerases in a single step. This subject has been recently reviewed (Roohi and Kuddus, 2018). Thus, only some selected works will be covered. Several extracellular depolymerases have been identified and characterized (an excellent tool for its classification was presented by Knoll et al., 2009). Extracellular PHA depolymerases degrade denaturated PHA granules whose structure has been altered during the extraction process and are not covered by the native layer of proteins surrounding the granule. One exception is the PHB depolymerase from *Pseudomonas lemoignei* which is active against native PHB granules (Handrick et al., 2001).

PHB degradation studies by extracellular depolymerases are typically performed using PHB films as substrate, producing R3HBA as the hydrolysis product (Polyák et al., 2018), thus limiting the access of enzymes to its substrate. In order to achieve high R3HBA titers, a high initial concentration of PHB should be used. However, due to its water-insoluble nature, only low PHB concentrations can be suspended in water. For example, 24 g L^{-1} of 3RHBA were produced from 25 g L^{-1} of suspended PHB powder using an extracellular PHB depolymerase from *Pseudomonas* sp. DS1001a (Li et al., 2016). As with chemical hydrolysis methods, enzymatic hydrolysis requires the separation and partial purification of the PHA accumulated in cells and this contributes to the overall costs of 3HAs. These disadvantages could be eliminated in processes where 3HAs are produced directly from the PHAs accumulated by the cells using their own intracellular enzymes for the depolymerization process.

In-vivo Strategies

Hydroxy-Acids Production by *in-vivo* Depolymerization of PHAs

This section reviews the production of 3HAs obtained through the depolymerization of PHAs accumulated using sugars and fatty acids as carbon and energy sources. The analysis of 3HAs obtained from other carbon sources is deferred to section Alternative Substrates and Microorganisms for 3HA Production.

In-vivo depolymerization of accumulated PHAs to R3HAs has been reported to occur with high yields in *Azohydromonas lata* (Lee et al., 1999) and *Pseudomonas putida* GPo1 (Ren et al., 2005). The depolymerization process has been shown to be highly dependent on pH. Lee et al. (1999), in a pioneering work, achieved the depolymerization of PHB to R3HBA in *A. lata* cells grown in mineral medium with sucrose as the carbon and energy source. The depolymerization process was carried out at different initial pHs in water, after washing the cells, at 37°C and without shaking to minimize oxygen transfer. Exceedingly high R3HBA yields and productivities, as high as 96% in 30 min were found at pH 4.0, but not at higher pH values. This result was explained in terms of the effects of pH on PHB depolymerase and 3-hydroxybutyrate dehydrogenase activities. The highest activity of PHB depolymerase was achieved at pHs 3 and 4, at which the monomer production rate was also the highest. Interestingly, in *A. lata* no activity of (*R*)-3-hydroxybutyric acid dehydrogenase was detected at pH 4, therefore it was argued that no 3HBA was degraded to acetoacetate (see **Figure 2** for the degradation pathway).

At pH 5, the attained depolymerization yield was 31% and decreased toward neutral pHs. From the work of Lee et al. (1999), it is not possible to ascertain whether these lower yields are due to the consumption of the released R3HBA or a decrease in the amount of PHB depolymerized. Presumably the latter is true since the depolymerization assays were performed without shaking, thus restricting the ability of cells to regenerate NADH into NAD^+, a cofactor of 3-hydroxybutyrate dehydrogenase.

Following the high depolymerization yields obtained at low pHs, the authors assayed the *in-vivo* depolymerization in

Cupriavidus necator NCIMB 11599, *Pseudomonas oleovorans* ATCC 29347, and *Pseudomonas aeruginosa* PAO1 (DSM 1707) at pH values below 7.0. The depolymerization yields and productivities were close to 20% for *C. necator* and below 10% for *Pseudomonas* species (see **Table 1**).

Ren et al. (2005) showed that for *Pseudomonas putida* GPo1, the PHB depolymerization rate was higher at pH 11 in citrate buffer, which helps to control the pH drop caused by the accumulation of R3HAs. The released monomers corresponded to (*R*)-3-hydroxyoctanaoic (R3HO) acid and (*R*)-3-hydroxyhexanoic acid (R3HHx), in a proportion closely matching the ratio of monomers in the copolymer accumulated in continuous culture with octanoic acid as carbon and energy source. The depolymerization was performed for 6 h, thus decreasing the volumetric productivity compared to the work of Lee et al. (1999) (see **Table 1**). A second factor decreasing the volumetric productivity was the low initial PHA concentration used. However, this work showed that R3HAs different than R3HBA could be obtained with high yields by using the correct pH during the depolymerization process. This work was further extended by Ruth et al. (2007) showing that applying the same depolymerization process at pH 10 to PHAs accumulated in *P. putida* GPo1, grown in continuous culture with either octanoic, undecanoic or 10-undecenoic acid, led to the production of (*R*)-3-hydroxyoctanoic acid (R3HO), (*R*)-3-hydroxyhexanoic acid (R3HHx), (*R*)-3-hydroxy-10-undecenoic acid (R3C11-1), (*R*)-3-hydroxy-8-nonenoic acid (R3C9-1), (*R*)-3-hydroxy-6-heptenoic acid (R3-C7-1), (*R*)-3-hydroxyundecanoic acid (R3-C11-0), (*R*)-3-hydroxynonanoic acid (R3-C9-0), and (*R*)-3-hydroxyheptanoic acid (R3-C7-1).

Recently, Anis et al. (2018) studied the *in-vivo* depolymerization of PHAs accumulated in *P. putida* Bet001 after 48 h of batch culture with lauric acid as the carbon source and under nitrogen-limited conditions. The depolymerization was performed for 48 h in 0.2M Tris–HCl buffer, pH 9, and 30 °C. Unlike the report of Lee et al. (1999) using *Pseudomonas aeruginosa* PAO1 (DSM 1707), *P. putida* Bet001 produced R3HO, R3HHx, (*R*)-3-hydroxydecanoic acid (R3HD), and (*R*)-3-hydroxydodecanoic acid (R3HDD) with very different yields (see **Table 1**), being the highest depolymerization yield achieved for R3HD. It is not clear if this difference in yields is due to a channeling of R3HO, R3HHx, and R3HDD toward cell metabolism or if they have yet to be hydrolyzed from the granules and thus, reflects an affinity of the PHA depolymerases.

The experiments performed by Lee et al. (1999), Ren et al. (2005), and Ruth et al. (2007) used either water or phosphate buffer as depolymerization media at a pH initially set at a given value. However, the release of 3HAs leads to a decrease in the initial pH, potentially affecting process efficiency. This factor was recognized by Wang et al. (2007), leading to the design and application of a pH-stat process. In this system, the pH is controlled at a setpoint by the automatic addition of an alkaline solution (NaOH). Interestingly, the amount of NaOH added in time (the flow of the alkaline solution), if recorded, allows the estimation of the release rate of acids (hydroxy acids and protons). Using a pH-stat apparatus coupled to a dissolved oxygen meter, Wang et al. (2007) investigated the behavior of the wild type *P. putida* GPo1 strain and a PHA depolymerase negative mutant. Results showed that the rate of acid production (not necessarily hydroxy acids) of the mutant strain was only 27% of the rate obtained with the wild type. Analysis of the supernatants revealed that the acids released by the wild type were R3HO and R3HHx. On the other hand, no detectable amounts of these compounds were found in the supernatants of the depolymerase mutant. Moreover, oxygen consumption measurements indicated a low respiratory activity for the wild type and a high respiration rate for the mutant. Finally, they also found that the acid production rate of the mutant, but not of the wild type, could be enhanced by aeration. These results support the hypothesis that the high depolymerase activity allowed the wild type strain to compensate for the high external pH. On the other hand, in the PHA depolymerase deficient mutant this could only be performed by the production of protons in aerobic conditions.

Although the results obtained by Wang et al. (2007) support this hypothesis for the depolymerization of PHAs to 3HAs at high pHs, the compensatory mechanism of pH involved in it does not explain the behavior found for *A. lata* at low pH values. Thus, the only conclusion applicable for both species is that in *A. lata* and *P. putida* GPO1 the depolymerization process is enhanced at a certain pH and simultaneously the consumption of the released monomers is impaired.

Process engineering strategies for 3HAs production are nearly non-existent with the exception of the work of Ren et al. (2007) who coupled a chemostat culture of *P. putida* GPo1 (nitrogen-limited, dilution rate of 0.1 h^{-1}, octanoic acid as the sole carbon source) to a second continuous depolymerization stirred tank reactor. The depolymerization tank was operated as a pH-stat at a pH of 10.0 and its discharge was sent to a plug-flow reactor with a residence time of 6 h. This continuous system does not require the separation of cells or the exchange of the culture media to water or buffer. Only a simple pH shift was enough to achieve a depolymerization yield of 90%, however, the volumetric productivity was not different from previously reported works using batch depolymerization (Ren et al., 2005). Clearly, the volumetric productivity could be improved by increasing the concentration of PHA leaving the chemostat.

A different strategy for the *in-vivo* production of R3HBA has been reported using several strains of *Halomonas.* Using *Halomonas* sp. KM-1, 15.2 g L^{-1} of R3HBA could be obtained under microaerobic conditions from 16.4 g L^{-1} of PHB that were accumulated under aerobic conditions using glycerol as the sole carbon and energy source. The initial concentration of the nitrogen source was 12.5 g L^{-1} (sodium nitrate), hence the limiting nutrient was presumably different from nitrogen, although this was not clarified (Kawata et al., 2012). These conditions, when applied to cultures grown in glucose (Kawata et al., 2014) did not result in any 3HBA secretion. The glucose concentration decreased from 20 to 6% during the first 36 h of culture and then remained constant. Thus, in this experiment, a nitrogen shortage was suspected.

When extra nitrate was pulse fed at 24, 36, and 48 h to a culture of *Halomonas* sp. KM-1 with 20% (w/v) glucose, then 40.3 g L^{-1} R3HBA were secreted with a productivity of

TABLE 1 | Summary of studies reporting the production of 3HA in non-genetically modified organisms using several operational strategies.

Microorganism	Strategy	Hydroxy acid[d]	Yield [a](3HA Titer, gL^{-1})	HA Volumetric productivity (gL^{-1} h^{-1})		References
				Depolymerization[b]	Fermentation and depolymerization[c]	
Azohydromonas lata DSM 1123	Water, initial pH 4.0, 37°C	R3HBA	84% (117.8)	117.8	4.91	Lee et al., 1999
			96% (0.99)	1.98	0.0825	
Cupriavidus necator NCIMB 11599	Water, initial pH 7.0, 30°C	R3HBA	19% (5.8)	0.17	NA	Lee et al., 1999
		R3HVA	23% (0.6)	0.017	NA	
Pseudomonas oleovorans ATCC 29347	Water, initial pH 7.0, 30°C	R3HHx	9.2% (0.13)	0.0014	NA	Lee et al., 1999
		R3HO	9.7% (1.42)	0.015	NA	
Pseudomonas aeruginosa PAO1 (DSM 1707)	Water, initial pH 7.0, 30°C	R3HO	9.6% (0.34)	0.0035	NA	Lee et al., 1999
		R3HD	8.8% (1.02)	0.0106	NA	
		R3HDD	6.7% (0.08)	0.0008	NA	
P. putida GPo1	50 mM potassium phosphate buffer, pH 11, 30°C	R3HO	76%(0.356)	0.059	0.022	Ren et al., 2005
		R3HHx	21%(0.015)	0.003	0.001	
P. putida GPo1	50 mM potassium phosphate buffer, pH 10, 30°C	mcl-HAs	Average 70% (≈ 1.1)	0.14	0.058	Ruth et al., 2007
P. putida GPo1	Culture broth, pH-stat at pH 10, 30°C.	R3HOR3HHx	90% (0.63)	NA	0.042	Ren et al., 2007
P. putida Bet001	0.2MTris–HCl buffer, pH 9, I = 0.2M, 30 °C	R3HO	54% (0.06)	0.001	0.001	Anis et al., 2018
		R3HHx	69% (0.64)	0.013	0.007	
		R3HD	98% (0.73)	0.015	0.008	
		R3HDD	47% (0.18)	0.004	0.002	
Halomonas sp. KM-1	Shift to microaerobic conditions under nitrogen rich condition	R3HBA	55% (40.3)	1.68	0.48	Kawata et al., 2014
Halomonas sp. OITC1261	Aerobic culture, sucrose, sodium nitrate as limiting nutrient	R3HBA	58 g L^{-1} R3HBA +27 g L^{-1} PHB	NA	0.65	Yokaryo et al., 2018

[a] *Yield refers to the mass of 3-hydroxyalkanoic acid obtained over the initial mass of polyhydroxyalkanoates in cells mass. The titer of 3HA is shown in parenthesis.*
[b] *Volumetric productivity of the depolymerization process, not accounting for the time required for PHAs production.*
[c] *Volumetric productivity of the depolymerization and fermentation process, accounting for the time required for PHAs production.*
[d] *R3HBA, (R)-3-hydroxybutyric acid; R3HVA, (R)-3-hydroxyvaleric acid; R3HHx, (R)-3-hydroxyhexanoic acid; R3HO, (R)-3-hydroxyoctanoic acid; R3HD, (R)-3-hydroxydecanoic acid; R3HDD, (R)-3-hydroxydodecanoic acid.*

0.48 g L^{-1} h^{-1} after a shift from aerobic cultivation for 60 h to microaerobic cultivation for 24 h. No R3HBA was secreted when no extra nitrate was supplemented (Kawata et al., 2014) indicating that a regulatory mechanism was controlling the activity of the PHB depolymerase, presumably related to the stringent response (see section Accumulation and Mobilization of PHAs). Glucose concentration during the depolymerization phase under microaerobic conditions was zero and a decrease in total cell concentration was observed. This behavior is consistent with the depolymerization of the accumulated PHB with only partial use of the released R3HBA for growth (our calculations show that 79% of the depolymerized PHB was recovered as 3HBA, equivalent to 55% of the maximum recovery if all the accumulated PHB is transformed to 3HBA). This can be ascribed to the microaerobic conditions applied that limited the use of acetyl-CoA for growth and the regeneration of NAD^+ from NADH. Since NAD^+ is the cofactor used by 3-hydroxybutyrate dehydrogenase, this could explain the high titers of R3HBA. Unfortunately, no nitrate concentrations during the growth or depolymerization phase were reported to ascertain whether it is consumed or not during the microaerobic cultivation. Moreover, PHB was not completely mobilized. Since no information regarding the pH of the culture (or its control) was presented, presumably the lack of complete depolymerization was caused by a decrease in pH.

A new species of *Halomonas, Halomonas* sp. OITC1261 was isolated by Yokaryo et al. (2018). Unlike *Halomonas* sp. KM-1, *Halomonas* sp. OITC1261 produces R3HBA under

aerobic conditions and, apparently, without the need to supplement with extra nitrogen source once the carbon source is exhausted to promote PHB depolymerization. In fact, the data presented by Yokaryo et al. (2018) showed that R3HBA is produced concomitantly with PHB after ∼10 h of cell growth. Presumably, PHB and R3HBA started to accumulate after the exhaustion of the nitrogen source, which could also explain the increase in the dissolved oxygen concentration. It is not clear whether the production of R3HBA occurs through PHB *in-vivo* depolymerization or proceeds directly from (*R*)-3-hydroxybutyryl-CoA or acetoacetate.

Production of Hydroxyalkanoates in Genetically Modified Microorganisms

Mutants of native PHA producers

The exploration of alternative pathways for the production of R3HAs emerges from the recognition of two characteristics found in native PHA producers: (i) depolymerization products can be metabolized, for example, R3HBA is converted to acetoacetate by the 3-hydroxybutyrate dehydrogenase (HBD) enzyme (Tokiwa and Ugwu, 2007) and (ii) producing 3HA is a two-stage process where PHA is accumulated and then depolymerized in a subsequent step that often requires a change in media or process conditions. A process for the isolation of 3-hydroxybutyrate dehydrogenase null mutants was described more than 40 years ago (Lafferty, 1977), including UV mutagenesis, followed by the destruction using antibiotics of the bacteria capable of 3HBA assimilation and the selection of 3HBD null mutants by spread plating of the individuals surviving the treatment with bactericidal.

Ugwu et al. (2008), reported the production of R3HBA in *C. necator* through the acetoacetate pathway induced by random mutation using UV radiation. The mutants achieved a titer of 0.150 g L^{-1} of R3HBA in a 5 L fermenter after 48 h of cultivation using either glucose or sucrose as carbon source. The concentration of R3HBA was increased by feeding lithium acetoacetate to resting cells of the mutant strain, reaching 0.84 g L^{-1} of R3HBA. The results were interpreted as indicative of a disruption in the *phbB* gene (coding for acetoacetyl-CoA reductase), making this strain unable of PHB accumulation (see **Figure 2**). Ugwu et al. (2008) reasoned that the excess of acetoacetyl-CoA produced under conditions allowing for PHB accumulation was channeled toward R3HBA via acetoacetate.

Using UV mutagenesis, Ugwu et al. (2011) obtained an R3HBA-producing mutant of *Azohydromonas lata*. When cells of this mutant were resuspended in phosphate buffer containing glucose (1% v/w), ethylacetoacetate (2% v/v), or (R,S)-1,3-butanediol (3% v/v), the resting cells produced R3HBA at concentrations of 6.5, 7.3, and 8.7 g L^{-1}, respectively.

Production of 3HAs in recombinant E.coli strains

</H4>An alternative process for the production of R3HBA is the use of recombinant methods to express PHA related genes in well-characterized non-PHA producing and fast-growing microorganisms such as *Escherichia coli* (Chen et al., 2013). Lee et al. modified *E. coli* strains by inserting two plasmid systems containing the $phaA_{Re}$, $phbB_{Re,}$ and $phbC_{Re}$ genes) and the $phaZ1_{Re}$ depolymerase from *Ralstonia eutropha* (Lee and Lee, 2003). This design achieved an R3HBA concentration of 9.6 g L^{-1} in 51 h of fermentation using glucose as a carbon source.

Shiraki et al. (2006) engineered *E. coli* and *R. eutropha* to express the same enzymes leading to the production of PHB but different depolymerases. The strains compared were an *R. eutropha* null mutant for 3-hydroxybutyrate dehydrogenase and a recombinant *E. coli* strain harboring the synthetic PHB operon of *R. eutropha* and an extracellular depolymerase of *Paucimonas lemoignei*. The production of R3HBA by the 3-hydroxybutyrate dehydrogenase null mutant of *R. eutropha* was found to be dependent on the supply of oxygen, achieving an R3HBA concentration of 3.13 g L^{-1} under anaerobic conditions and concentrations in the 0.41–1.04 g L^{-1} range under aerobic culture conditions. The intracellular PHB content decreased concomitantly with the production of R3HBA, reaching almost zero for the experiment performed under anaerobic conditions after 50 h of depolymerization. Presumably, under aerobic conditions the accumulated PHB was depolymerized to a molecule different than R3HBA, such as 3-hydroxybutyryl-CoA, or the produced R3HBA was metabolized using pathways not using 3-hydroxybutyrate dehydrogenase (BDH). In fact, Shiraki et al. (2006) verified that no BDH was expressed and no BDH was found in the supernatant fraction of cells grown under PHB accumulation conditions, however, it was not verified whether the mutant could grow in R3HBA. On the other hand, the recombinant *E. coli* harboring the PHB operon and the *P. lemoignei* depolymerase reached a concentration of approximately 7.3 g L^{-1} of R3HBA after 100 h. Since *E. coli* is not a native PHB producer, presumably there were no alternative pathways for R3HBA production or consumption different from the inserted genes (Shiraki et al., 2006). Interestingly, the difference between the R3HBA production pathways used by Shiraki et al. (2006) and Lee and Lee (2003) is the PHB depolymerase gene. While Shiraki used the extracellular depolymerase of *Paucimonas lemoignei* capable of hydrolyzing both native PHB granules and denaturated ones (Handrick et al., 2001), Lee and Lee used a gene from *R. eutropha*. In particular, the depolymerase PhaZa1 used by Lee and Lee (2003) was found to secrete rather low concentrations of R3HBA when expressed in the same *E. coli* strain (Uchino et al., 2008).

Generally, the use of the *phaCAB* and *phaZ* genes requires a two-stage fermentation, accumulation of the polymer followed by depolymerization, thereby the required cultivation times are usually long. Hence, the interest in the last decades focused on the direct microbial production of extracellular 3HA monomer without going through these two stages and achieving a straightforward, less energy and time-consuming process.

The first alternative pathway was reported by Gao et al. (2002), by introducing the *phbA*, *phbB*, *buk* and *ptb* genes in recombinant *E. coli* DH5K. This pathway starts from glucose to yield acetyl-CoA, which is the key compound in glycolysis, PhbA catalyzes the formation of acetoacetyl-CoA from two acetyl-CoAs, which is then reduced to (*R*)-3-hydroxybutyryl-CoA under the action of PhbB. (*R*)-3-hydroxybutyryl-CoA is then transformed into (*R*)-3-hydroxybutyryl-P by Ptb (see **Figure 2**). Finally, Buk converts the (*R*)-3 hydroxybutyryl-P into R3HBA, resulting in

the production of 12 g L^{-1} in fed-batch cultures (Gao et al., 2002). The direct method presents some advantages: (i) glucose is transformed without accumulation and depolymerization of PHB, (ii) R3HBA production is not associated with cell growth, and (iii) immobilization of the recombinant strain may allow a continuous R3HBA production process to be established.

Similarly to the system presented by Gao et al. (2002), (*R*)-3HB-CoA can be directly hydrolyzed into R3HBA using TesB, a class II thioesterase enzyme that catalyzed the hydrolysis of the CoA moiety from acyl-CoAs (Naggert et al., 1991). For example, when TesB acts on 3 hydroxybutyryl-CoA, free R3HBA monomers are obtained by cleaving coenzyme A.

Liu et al. (2007) used *E. coli* BW25113 as host for the expression of *phbA* and *phbB* genes from *R. eutropha* and *tesB* from *E. coli*. This strain produced 3.98 g L^{-1} R3HBA in shake flask culture using 11.4 g L^{-1} of glucose. Using a fed-batch strategy, 12.2 g L^{-1} R3HBA were accumulated in 24 h. The feeding strategy consisted of pumping a solution containing glucose (20 g L^{-1}) and ammonium sulfate (2 g L^{-1}) each time glucose concentration in the broth was lower than 10 g L^{-1}. The productivity achieved by this system (0.51 g L^{-1} h^{-1}) is among the highest reported so far for the direct production of R3HBA (see **Table 2**). Previous to this work, it was well established that TesB was capable of releasing CoA from acyl CoA of C_6-C_{18} carbon length, as well as 3-hydroxyacyl-CoA esters, to their corresponding free fatty acids (Naggert et al., 1991), but not from short-chain length hydroxyacyl-CoA. In this regard, Zheng et al. (2004) reported the production of (*R*)-3-hydroxydecanoic acid (R3HD) from fructose by a recombinant *E. coli*. The recombinant strain contains the *phaG* gene from *P. putida* encoding for (*R*)-3-hydroxydecanoyl-acyl carrier protein-coenzyme A transacylase. PhaG links fatty acid *de novo* biosynthesis and PHA production by catalyzing the conversion between (*R*)-3-hydroxydecanoyl-acyl carrier protein and (*R*)-3-hydroxydecanoyl-CoA (Rehm et al., 1998). When the *E. coli* strain containing only PhaG was cultured in shake flasks with 20 g L^{-1} fructose, 0.64 g L^{-1} of R3HD, and 2.11 g L^{-1} of biomass were obtained. The R3HD titer was increased to 1.02 g L^{-1} when a plasmid expressing *tesB* was also inserted into the strain along with *phaG*, suggesting that the activity of TesB in the strain containing only *phaG* was insufficient for efficient hydrolysis of the produced (*R*)-3-hydroxydecanoyl-CoA.

In *E. coli*, acetate is often produced concomitantly with R3HBA (Gao et al., 2002; Tseng et al., 2009; Guevara-Martínez et al., 2015), decreasing product yield and lowering the growth rate at concentrations as low as 0.5 g L^{-1}; thus, difficulting the use of high-cell-density cultures with high volumetric productivities (Nakano et al., 1997; Roe et al., 2002). Perez-Zabaleta et al. (2019) studied the production of R3HBA using the native *E. coli* acyl-CoA thioesterases (*fadM*, *tesA*, *tesB*, *ybgC*, *ydiI*, and *yciA*). These enzymes are also active with acetyl-CoA as substrate (McMahon and Prather, 2014), and therefore could contribute to the production of acetate. In this work, the impact of deletion of genes involved in the production of acetic acid (*poxB*, *pta*, or *iclR*) on R3HBA producing fed-batch cultures was investigated using *E. coli* AF1000. Also, several *E. coli* strains were compared including *E. coli* AF1000 and BL21 as low acetate-forming R3HBA production platforms. All the strains carrying β-ketothiolase (*t3*) and acetoacetyl-CoA reductase (*rx*) from *Halomonas boliviensis* and overexpressing the glucose-6-phosphate dehydrogenase gene (*zwf*). No important reduction on acetic acid titers was found for the deletion of the aforementioned genes. The best results were obtained using strain BL21 achieving the highest R3HBA titer and volumetric productivity reported up to date (see **Table 2**). Interestingly, Guevara-Martínez et al. (2019) working with the same recombinant strain (*E. coli* AF1000-*t3-rx-zwf*) showed that the deletion of *tesA* or *fadM* resulted in minor decreases in R3HBA production, while deletion of *tesB* and *yciA* decreased the R3HBA titer by 11 and 33%, respectively. These results suggest that YciA, and not TesB, is the acyl-CoA thioesterase largely responsible for R3HBA production from (*R*)-3-hydroxybutyryl-CoA in *E. coli*.

The production of S3HBA from glucose in an engineered *E. coli* strain was reported by Lee et al. (2008). The genes coding for PhaA from *R. eutropha*, (*S*)-3-hydroxybutyryl-CoA dehydrogenase (HBD) from *Clostridium acetobutylicum* ATCC824, and 3-hydroxyisobutyryl-CoA hydrolase (BCH) from *Bacillus cereus* ATCC14579 were inserted in *E. coli* BL21. Under fed-batch cultivation with glucose as substrate, 10.3 g L^{-1} of S3HBA and 65 g L^{-1} of biomass were accumulated in 38 h. The yield of S3HBA production was low compared with that of R3HBA from glucose found by Gao et al. (2002). Lee et al. (2008) interpreted this low yield as a consequence of S3HBA-CoA being an intermediate of fatty-acid β-oxidation pathway; therefore, it can be degraded into acetyl-CoA. Similarly, Tseng et al. reported the production of S3HBA and R3HBA using an *E. coli* strain harboring plasmids containing genes for different thiolases (*phaA* and *bktB* from *R. eutropha* and *thl* from *C. acetobutylicum* ATCC 824), *hbd* and *phaB* genes for the production of (*R*) and (*S*) hydroxybutyryl-CoA and either *tesB* or *ptb-buk* genes to remove the CoA moiety. The impact of the thiolase in the titers of the hydroxy acids was found to be low. On the other the selection of the enzyme hydrolyzing the CoA was critical. In fact, when Ptb-Buk was used no S3HBA was detected. If TesB was included, then both R3HBA and S3HBA were produced.

Recently, (*R*)-3-hydroxyvalerate (R3HVA) and R3HBA were produced in a recombinant strain of *E. coli* capable of glycerol conversion (Miscevic et al., 2019). The engineered strain (P3HA31) harbors the *phaA* and *bktB* genes (from *Cupriavidus necator* ATCC 43291) to catalyze the condensation of two acetyl-CoA molecules or an acetyl-CoA and a propionyl-CoA molecule for the formation of acetoacetyl-CoA and 3-ketovaleryl-CoA, respectively. Two genes for the reduction of acetoacetyl-CoA were inserted, *phaB* from *C. necator* and *hdb* from *Clostridium acetobutylicum* ATCC 824 catalyzing the formation of (*R*)-3-hydroxybutyril-CoA and its *S* stereoisomer, respectively. Finally, *tesB* was introduced for the production of the corresponding hydroxycarboxylic acids. The strain was further optimized to increase the propionyl-CoA pool from succinyl-CoA by deregulating the glyoxylate shunt (mutating *iclR*) and by inactivating the oxidative TCA cycle gene *sdhA*, thus blocking the conversion of succinate to fumarate. The double mutant P3HA31Δ*sdhA*Δ*iclR* achieved a concentration

TABLE 2 | Summary of engineered strains for the production of 3-hydroxyalkanoic acids.

Strains	Carbon substrate	3HA titer (gL^{-1})[a]	3HA Volumetric productivity (gL^{-1} h^{-1})	References
E. coli DH5α(phbA-phbB-buk+ ptb)	Glucose	12.0 (R3HBA)	0.25	Gao et al., 2002
E. coli XLI-Blue (phaA-phaB-phaC-phaZi)	Glucose	9.6 (R3HBA)	0.19	Lee and Lee, 2003
E. coli DH5 (phbA-phbB-phaG)	Glucose + Acrylic acid	0.7 (R3HBA)	0.01	Zhao et al., 2003
E. coli JM 109 (pha CAB-phaZ7)	Glucose	7.3 (R3HBA)	0.073	Shiraki et al., 2006
UV radiation mutant *Cupriavidus necator*	Glucose or sucrose + Lithium acetoacetate	0.84 (R3HBA)	0.026	Ugwu et al., 2008
UV mutant radiation *Azohydromonas lata*	Sucrose +1,3 butanodiol	8.7 (R3HBA)	0.082	Ugwu et al., 2011
E. coli BW25113 (phbA- phbB - tesB)	Glucose	12.2 (R3HBA)	0.51	Liu et al., 2007
Pseudomonas putida KTOY07 (with pSPH09 plasmid)	Lauric acid	7.27 (96% R3HDD)	0.26	Chung et al., 2009
E. coli K-12 MG1655(DE3)	Glucose	2.92 (R3HBA)	0.06	Tseng et al., 2009
		2.08 (S3HBA)	0.04	
E. coli with the plasmid sets pET-PB-B, and pCDF-T-H (for (S)-3HV synthesis) or pCDF-T-P (for (R)-3HV synthesis)	Glucose	0.50 (R3HVA)	0.007	Tseng et al., 2010
		0.31 (S3HVA)	0.004	
	Glycerol	0.60 (R3HVA)	0.0084	
		0.19 (S3HVA)	0.003	
E. coli (phaAB-pct)	Glucose +acetate	5.2 (R3HBA)	0.22	Matsumoto et al., 2013
Mutant of *M. rhodesianum* (DlipA$^-$ Dhbd$^-$)	Methanol	2.81(R3HBA)	0.014	Hölscher et al., 2010
E. coli strain AF1000 pJBGT3RX	Glucose + phosphate-limited	2.85(R3HBA)	1.5	Guevara-Martínez et al., 2015
E. coli (phaA-HBD-BCH)	Glucose	10.3 (S3HBA)	0.12	Lee et al., 2008
Clostridium coskatii [p83_tcb]	Syngas, anaerobic culture	0.1 (R3HBA)	$1.4 \cdot 10^{-4}$	Flüchter et al., 2019
Clostridium coskatii [p83_tcb](thlA-ctfA/ctfB-bdhA)	Fructose, anaerobic culture	2.25 (R3HBA)	0.032	Flüchter et al., 2019
S. cerevisiae (ERG10- hbd-tesB)	Ethanol biotransformation under aerobic conditions	12 (S3HBA)	0.06	Yun et al., 2015
Arxula adeninivorans (thl-phaB)	Glucose fed-batch followed by ethanol feeding	3.78 (R3HBA)	0.043	Biernacki et al., 2017
E. coli BL21 (t3-rx- zwf)	Nitrogen limited fed-batch cultivation with glucose as substrate	16.3 (R3HBA)	1.52	Perez-Zabaleta et al., 2019
Synechocystis sp. (phaA-phaB1-TesB)	Photosynthetic cultivation	1.84 (R3HBA)	$7.7 \cdot 10^{-3}$	Wang et al., 2018
E. coli AF1000 (t3-rx)	Glucose, xylose and arabinose as substrate	0.54 (R3HBA)	0.029	Jarmander et al., 2015
E. coli (phaA -bktB-phaB-hdb-tesB-ΔsdhAΔiclR)	Glycerol as carbon and energy source, aerobic	2.0 (R3HBA)	0.042	Miscevic et al., 2019
		3.71 (R3HVA)	0.077	

[a] *R3HBA, (R)-3-hydroxybutyric acid; R3HDD, (R)-3-hydroxydodecanoic acid; S3HBA, (S)-3-hydroxybutyric acid; S3HVA, (S)-3-hydroxyvaleric acid.*

of 3.71 g L^{-1} of R3HVA, 2.97 g L^{-1} of propionate and nearly 2 g L^{-1} of R3HBA. Despite the fact that *hdb* was expressed, results suggest that PhaB was catalytically more active than Hbd since higher titers in (*R*)-3-HB/HV than (*S*)-3-HB/HV were found. Alternatively, this might be the consequence of a larger abundance of NAPDH compared to NADH, as PhaB and Hbd are NADPH-dependent and NADH-dependent, respectively. Tseng et al. (2010) previously reported that a similar *E. coli* engineered strain was able to produce R3HBAs and (*R*) and (*S*) 3HVAs. When glycerol was used as carbon source, 0.60 g L^{-1} R3HVA, 0.19 g L^{-1} S3HVA, 0.58 g L^{-1} R3HBA, and nearly 1.2 g L^{-1} acetate were produced.

Finally, a third alternative for the hydrolysis of CoA from (*R*)-3-hydroxybutyryl-CoA, besides TesB and Ptb-Buk, was designed based on the use of a propionyl CoA transferase (Pct). Pct works by transferring a CoA from (*R*)-3-hydroxybutyryl-CoA to another short-chain fatty acid. Matsumoto et al. (2013) engineered *E. coli* BW25113 by inserting a plasmid containing the *phaA* and *phaB* genes from *R. eutropha* and *pct* from *Clostridium propionicum*. This *pct* gene was selected since catalyzes the

transfer reaction of CoA between R3HBA and acetate (Jossek et al., 1998). Cells were cultured for 24 h in test tubes at 30°C with 10 g L^{-1} glucose and acetate concentrations in the 0–10 g L^{-1} range. Acetic acid enhances R3HBA production when Pct is expressed as will act as the molecule receiving the CoA moiety and will serve as substrate for the condensation reaction of two acetyl-CoAs catalyzed by PhaA. Results showed that the maximum concentration (9.0 g L^{-1}) and volumetric productivity (0.22 g L^{-1} h^{-1}) were attained at a concentration of 6.6 g L^{-1} of acetic acid. Unfortunately, no efforts were made to investigate the performance of the engineered strain using a fed-batch culture where acetic acid and glucose concentrations could be controlled independently, possibly increasing product titer and volumetric productivity.

ALTERNATIVE SUBSTRATES AND MICROORGANISMS FOR 3HA PRODUCTION

Decreasing the cost of industrial PHA production requires the use of abundant and low-cost carbon and energy substrates such as molasses, glucose, sucrose derived from sugar cane, sugars produced from lignocellulose, one-carbon compounds (formate and methanol) and gaseous substrates (syngas, knallgas, and methane). This is also true for the production of the monomers constituting PHAs.

Regarding the use of lignocellulosic hydrolyzates, Wang and Liu (2014) discovered that in batch cultures of *B. cepacia*, the concentration of R3HBA released during growth was stimulated by nitrate and chloride ions. The concentration of R3HBA reached 16.2 g L^{-1} in hydrolysates of *Paulownia elongate*, however, this concentration could not be achieved in model hydrolyzates. The production of 3HBA with *Halomonas* sp. KM-1 has also been shown with sugars obtained from lignocellulosic materials. Using saccharified Japanese cedar as carbon source, a concentration of 21.1 g L^{-1} R3HBA was obtained with a yield of 89% (based on initial PHB) after shifting from an aerobic accumulation phase to a microaerobic PHB depolymerization phase (Kawata et al., 2015). Interestingly in this microorganism, the R3HBA titer obtained without the addition of urea at the onset of the microaerobic phase was lower compared to adding 7.1 g L^{-1} of urea. Unfortunately, it is not clear whether the effect of urea is due to an increase in media pH or to its consumption.

Jarmander et al. (2015) reported the construction of an *E. coli* strain capable of producing R3HBA from xylose, glucose and arabinose harboring the acetoacetyl-CoA thiolase (*t3*) and acetoacetyl-CoA reductase (*rx*) genes from *H. boliviensis*. The conversion of 3-hydroxybutyryl-CoA to R3HBA was assumed to be catalyzed by the *E. coli* native TesB enzyme. Albeit this work represents an interesting achievement from a genetic manipulation perspective targeting the production of new compounds from lignocellulosic derived sugars, the highest R3HBA yield on mixed sugars was 0.23 g/g with a 3HBA titer of 0.54 g L^{-1} under nitrogen depleted conditions in batch culture. On the other hand, the highest concentration of R3HBA (1.87 g L^{-1}) was achieved in a nitrogen fed-batch culture with an overall yield of 0.05 g R3HBA g $sugars^{-1}$.

Although the accumulation of PHB from knallgas is well-documented (see section Substrates for the Production of Polyhydroxyalkanoates and Its Monomers), no evidence exists in the open literature regarding the production of 3HBA or 3HAs from knallgas, despite *A. lata* being one of the first bacteria where R3HBA production was demonstrated (Lee et al., 1999). Similarly, the accumulation of PHB in methanotrophs is well documented (for a recent review see Strong et al., 2016), however, no known organism has been reported to produce 3HBA or any other 3HA either from *in-vivo* depolymerization of the accumulated PHB, through an engineered pathway or from the *ex-vivo* depolymerization of the extracted PHB.

A notable exception regarding the use of C1 compounds for the production of 3HAs is the use of methanol for the obtention of R3HBA. *Methylobacterium rhodesianum* MB 126 was genetically modified by knocking-out the 3-hydroxybutyrate dehydrogenase gene. Since the mutant strain still exhibits growth in R3HBA, transposon mutagenesis was used to obtain a double mutant unable to grow on R3HBA. The double mutant was shown to have, along with a lack of 3-hydroxybutyrate dehydrogenase, an incomplete citric acid cycle due to a defective lipoic acid synthase (LipA). In fed-batch culture, using methanol as the sole carbon and energy substrate, 2.8 g L^{-1} of R3HBA were obtained after accumulating PHB under nitrogen limitation and inducing its degradation under a carbon limited and nitrogen-rich condition (Hölscher et al., 2010).

All the aforementioned genetic modifications lead to the production of 3HBA or 3HAs under aerobic conditions. Flüchter et al. (2019) constructed a genetically modified strain of *Clostridium coskatii* harboring the thiolase A gene (*thlA*; CA_C2873) and the acetoacetyl-CoA:acetate/butyrate CoA transferase genes (*ctfA/ctfB*; CA_P0163/ CA_P0164) from *C. acetobutylicum* ATCC 824 and the 3-hydroxybutyrate dehydrogenase gene (*bdhA*; CDIF630_02933) from *Clostridium difficile* DSM 27543. The engineered pathway directs acetyl-CoA to acetoacetyl-CoA using thiolase A, which is converted into acetoacetate using the acetoacetyl- CoA:acetate/butyrate CoA transferase and the final conversion of acetoacetate to 3-hydroxybutyrate by 3-hydroxybutyrate dehydrogenase. Under heterotrophic conditions with fructose as carbon and energy source and under anaerobic condition, 2.3 g L^{-1} of R3HBA accumulated in 60 h of batch culture and 3.9 g L^{-1} of acetate were concomitantly produced. Under autotrophic conditions using syngas (CO 40 mol %, H_2 40 mol %, CO_2 10 mol % and N_2 10 mol %) a concentration of 0.1 g L^{-1} of R3HBA was obtained along with 2.1 g L^{-1} of acetate. Although the achieved concentrations, especially under autotrophic conditions are low, this study represents an important proof of concept for the utilization of inexpensive and abundant gaseous substrates. Interestingly, although the production of acetate should be reduced, it cannot be completely eliminated as acetate is used in the reaction catalyzed by the acetoacetyl- CoA:acetate/butyrate CoA transferase to accept the CoA molecule in the step leading to the production of acetoacetate. In a previous report, Woolston et al. (2018) achieved comparable titers both under heterotrophic and

autotrophic growth. However, the product obtained by Woolston et al. was (S)-3-HBA instead of R-3-HBA due to an engineered pathway using the *phaA* gene from *C. necator,* the NADH-dependent (*S*)-3-hydroxybutyryl-CoA dehydrogenase from *C. acetobutylicum* and the thioesterase *tesB* from *E. coli.*

The production of (*S*)-3-HBA has been also demonstrated in metabolically engineered *Saccharomyces cerevisiae*, Yun et al. (2015) reported one of the few modifications in yeasts aimed at the production of hydroxyacids, where the following genes were introduced: acetyl-CoA C-acetyltransferase (*erg10p* from *S. cerevisiae* BY4741) for the condensation of two molecules of acetyl-CoA into acetoacetyl-CoA, NADH-dependent acetoacetyl-CoA reductase (*ACR*, hbd from *C. acetobutylicum* ATCC 824) converting acetoacetyl-CoA to (S)-3-hydroxybutyryl-CoA and 3-hydroxybutyryl-CoA thioesterase (*tesB* from *E. coli* K-12 MG1655) to remove the CoA molecule from (*S*)-3-hydroxybutyryl-CoA. Using ethanol as the substrate in fed-batch cultivation, 12 g L^{-1} of (*S*)-3-HBA were accumulated in 200 h. Small amounts of glycerol were accumulated during the first half of the culture (close to 6 g L^{-1}) but they were reduced to zero by the end of the culture. A similar strategy was used by Biernacki et al. (2017) for the production of R3HBA in *Arxula adeninivorans* after inserting the *thl* gene from *C. acetobutylicum* ATCC 824 and *phbB* from *C. necator* H16. In fed-batch cultures with glucose as the carbon source, ethanol is produced under hypoxic conditions during the first 50 h of culture. A shift to aerobic conditions promotes ethanol assimilation and R3HBA production reaching a maximum of 3.78 g L^{-1}.

Finally, the use of photosynthetic organisms for 3HA production has also been explored. Wang et al. (2018) modified the cyanobacteria *Synechocystis* sp. After inserting the genes *phaA*, *phaB1,* and *tesB* a concentration of 1.84 g L^{-1} of R3HBA was obtained at the end of 10 days of photoautotrophic cultivation.

Most of the available literature on the direct microbial production of HAs (without accumulation of PHAs) deals with the obtention of short-chain length hydroxy acids. Notable exceptions are the engineered systems based on *Pseudomonas putida* strains. Chung et al. (2009) constructed a novel pathway in *Pseudomonas putida* KTOY01, a mutant of *P. putida* KT2440 unable to accumulate PHA due to a PHA synthesis operon knockout, by expressing the *tesB* gene and knocking the genes *fadB* and *fadA* to create a β-oxidation-pathway-deficient mutant. This strain accumulated 7.27 g L^{-1} of R3HAs, with over 96% mol of (*R*)-3-hydroxydodecanoic acid when lauric acid was added into the culture broth. However, lauric acid is a related carbon source making this process closer to biotransformation rather than synthesis. Similar work was performed by Chung et al. using *Pseudomonas entomophila* as the host strain. When tetranoic acid and dodecanoic acid were used as related carbon sources in shake flask cultures, 6.65 g L^{-1} 3-hydroxytetradecanoic acid and 4.6 g L^{-1} 3-hydroxydodecanoic acid were obtained. No reports of the production of mcl-HAs are available in the literature, however, the work of Agnew et al. (2012) showing the production of C_{12} and C_{14} polyhydroxyalkanoates from glucose in *E. coli* could be a starting point for the introduction of a thioesterase such as TesB.

SECRETION OF PHAs

A possible approach to decrease the cost of PHAs and 3HAs production is to devise simplified methods for the recovery of the accumulated polymers. Although the production of 3HAs from recovered PHAs requires more steps than the direct fermentation strategies presented in the previous section, starting from pure or partially purified PHAs could lead to a simplified downstream processing. Moreover, the production 3HAs esters, as outlined in section Chemical and Enzymatic Hydrolysis of Recovered PHAs starts from PHAs, and thus it can benefit from simplified methods for the recovery of these polymers. A recurrent strategy is the induction of cell lysis to release the PHA granules.

Resch et al. (1998) expressed the *Alcaligenes eutrophus phbCAB* genes and the cloned lysis gene E of bacteriophage PhiX174 in *E.coli* cells, which allowed to perform PHB synthesis and at the same time generate the E-lysis tunnel structure that is characterized by a small opening with edges in the transmembrane envelope (Resch et al., 1998). E-lysis produces holes approximately of equal size to the diameter of the cells (producing lysis) and releases around 90% of the PHB. The PHB granules vary in size and have the tendency of self-aggregation. Based on these facts and the structural analysis of protein E it was postulated as a way to obtain free PHB granules in the extracellular medium. Similarly, a *P. putida* KT2440 mutant was constructed by expressing two proteins from the pneumococcal bacteriophage EJ-1, an endolysin (Ejl) and a holin (Ejh) and the mutation of the *tolB* gene to reduce the integrity of the membrane and promote a lysis sensitivity. After inducing the accumulation of PHAs and the lysis of cells, 0.28 g L^{-1} of PHAs were recovered using direct extraction of the wet biomass with ethyl acetate (Martínez et al., 2011). Using the endolysin (Ejl) and a holin (Ejh) system, but under the control of a promoter induced by xylose but inhibited by glucose, nearly two-thirds of the PHB accumulated in *Bacillus megaterium* using glucose as carbon source was released into the broth after 20 h of culture post glucose exhaustion. A fraction of the PHB remains associated with the cell debris, possible trough hydrophobic interactions (Hori et al., 2002).

A different but related approach was presented by Borrero-de Acuña et al. (2017). A programmable lysis system was built based on the expression of lysozyme and tested in *Pseudomonas putida* KT2440 under conditions promoting growth or PHA accumulation. The lytic system did not affect the biomass yield or growth rate of *P. putida* under balanced growth but did reduce the biomass production by 25% when conditions permissive of PHA accumulation were applied. Notwithstanding, the PHA content was kept and after the induction of the lytic system, nearly 75% of the accumulated polymer was recovered. The released polymer was recovered by mixing the fermentation broth with chloroform at a 18:1 (v/v) ratio followed by phase separation, representing an excellent reduction in solvent and energy use.

Another strategy for the recovery of PHAs is the use of external cell lytic agents such as the *Bdellovibrio bacteriovorus*

HD100 bacterium, an obligate predator of other gram-negative bacteria which acts as a lithic agent for the recovery of intracellular bioproducts of industrial interest (Martínez et al., 2016). *B. bacteriovorus* HD100 was genetically modified by eliminating the PHA depolymerase gene in order to prevent the breakdown of the recovered PHAs. After allowing the accumulation of PHAs in *P. putida*, *C. necator,* and a recombinant *E. coli* strain, each culture was infected with a suspension of *B. bacteriovorus* cells. Sixty-five percentage of the PHA accumulated in *P. putida* could be recovered at high cell densities using this method. The polymer was directly extractable from the wet biomass of the co-cultures, thus avoiding the need for biomass drying. When *C. necator* cells were used as prey in low concentration (PHB titer less than 1 g L^{-1}), the PHB recovery yield was 80%.

Currently, efforts are focused on the creation of "leaking" bacteria for an easy "export" of PHB, this is the implementation of secretion mechanisms in which a cell breakdown is not required in a chemical or mechanical way and the biomass could be recycled to implement a semi-continuous PHB production system. Protein secretion is the main route by which bacteria not only interact with the extracellular environment, but also secrete products that are essential for cells, which include adhesion, pathogenicity, adaptation, and in some cases enzymatic degradation. Hence, the gram-negative bacteria have developed a wide variety of pathways for the secretion of different products into the extracellular matrix while maintaining the integrity of the cellular structure (Henderson and He, 2009; Costa et al., 2015).

Type I secretion systems (T1SS) or ABC transporters (ATP-binding cassette) are heterotrimeric complexes that are composed of three segments that interact with each other (Nicaud et al., 1986). Type II secretion systems (T2SS) are one of the best-known secretion systems because they are conserved in most gram-negative bacteria. Type II systems are able to transport folded proteins from the periplasm to the extracellular environment (Green and Mecsas, 2016). T1SS and T2SS are the most used secretion systems in biological engineering and therefore the most studied in detail. These two systems stand out for the fact that each one of them recognizes a sequence through its peptide ends as an objective, that is, the signalized sequence can be fused with other proteins which causes the cell to target the new fusion protein for their respective secretion. Fusion proteins have been applied to indirectly secrete PHB molecules, this has been reported by Linton et al. (2012), who initially conducted a study to evaluate the efficacy and viability of the secretion systems used by *E. coli*. The signal peptides corresponded to HlyA (T1SS), TorA (T2SS, TAT), GeneIII (T2SS, Sec), and PelB (T2SS, Sec) (Linton et al., 2012). The results obtained show that the PelB system was not effective in the translocation of GFP, while the other two T2SSs successfully exported GFP to the periplasm and with respect to the HlyA system, also secrete the GFP protein to the extracellular medium (Linton et al., 2012). Based on these results, the HlyA signal peptide fusion protein and a fascine that associates with the PHB granules were used to bind the signaling sequence to the PHB granule, leading to the secretion of PHB to the extracellular medium (Rahman et al., 2013). Results indicate that after 48 h of culture 36% of the total PHB produced by the secretory strain was collected in the secreted fraction while the remaining 64% corresponded to the internal fraction. SEM images of the PHB accumulating *E. coli* strain with and without the secretory system show that PHB is not excreted as granules, but as an amorphous material. This evidence, combined with the low secretion found, suggest that the system cannot export the intact PHB granules. Sabirova et al. (2006) constructed an *Alcanivorax borkumensis* SK2 mutant capable of PHA hyperproduction. Interestingly, this mutant release part of the produced PHA to the extracellular medium when it was cultured in alkanes without cell lysis. The secretion mechanism remains unknown.

CONCLUSION AND PERSPECTIVES

As outlined in this review, after 20 years of the discovery of the *in-vivo* hydrolysis of PHB accumulated in *Azohydromonas lata*, and even though this system remains as the one showing the highest titer of (*R*)-3-hydroxybutyrate, a large body of knowledge have been accumulated regarding the production of other, potentially more industrially useful, 3-hydroxyalkanoic acids from diverse substrates including fatty acids and sugars derived from lignocellulosic materials. In this regard, the production of 3-hydroxyacids directly from its precursors, and without the accumulation of PHAs, in recombinant strains show the potential of transferring this production system into a wide range of hosts to expand the number of substrates that can be used for the production of these valuable compounds.

Thanks to the availability of techniques for genetic manipulation, *E. coli* served as the preferred host for the introduction of new pathways for the direct production of 3HAs. Since the first reports dealing with the production of R3HBA using the native *E. coli* thioesterases, significant efforts were performed to increase titer, yield, and productivities and to expand the range of 3HAs that can be obtained in *E. coli.*

However, more research is needed for bacterial production of these hydroxy acids to reach a level of industrial use. Research needs include increasing titer and productivities in *E. coli* from sugars and other readily available substrates, as well as achieving its production from inexpensive gaseous substrates such as methane, syngas, and knallgas. Up to date, only the production of 3-hydroxybutyrate has been demonstrated from syngas, remaining the production of this acid from knallgas and methane, as well as the production of mcl-hydroxy acids a completely unexplored area of research.

Finally, the secretion and lytic systems, mainly developed during the last two decades, open the possibility of a facile and inexpensive PHA recovery, combined with efficient chemical or enzymatic hydrolysis methods, they can constitute a powerful combination for gaining access to a wide range of 3-hydroxy acids.

AUTHOR CONTRIBUTIONS

All the authors performed literature search and drafted sections of the manuscript. LY, RC, and FS drafted most of the sections dealing with PHA accumulation, 3HA production and alternative PHA recovery strategies. AV-F drafted sections dealing with the different substrates used for PHA production and created **Figure 1**. All authors revised the manuscript and approved the final version.

FUNDING

FS gratefully acknowledges financial support from CONICYT – Chile (National Commission for Scientific and Technological Research), grants Fondecyt Iniciación 11170081 and Proyectos REDES ETAPA INICIAL, Convocatoria 2017, REDI170254. LY, AV-F, and FS acknowledge financial support from grant Apoyo a la Formación de Redes Internacionales entre Centros de Investigación REDES190137, CONICYT-PCI.

REFERENCES

Adkins, J., Pugh, S., McKenna, R., and Nielsen, D. R. (2012). Engineering microbial chemical factories to produce renewable "biomonomers." *Front. Microbiol.* 3:313. doi: 10.3389/fmicb.2012.00313

Agarwal, A. S., Zhai, Y., Hill, D., and Sridhar, N. (2011). The electrochemical reduction of carbon dioxide to formate/formic acid: engineering and economic feasibility. *ChemSusChem* 4, 1301–1310. doi: 10.1002/cssc.201100220

Agnew, D. E., Stevermer, A. K., Youngquist, J. T., and Pfleger, B. F. (2012). Engineering *Escherichia coli* for production of C12–C14 polyhydroxyalkanoate from glucose. *Metab. Eng.* 14, 705–713. doi: 10.1016/j.ymben.2012.08.003

Alves, M. I., Macagnan, K. L., Rodrigues, A. A., de Assis, D. A., Torres, M. M., de Oliveira, P. D., et al. (2017). Poly(3-hydroxybutyrate)-P(3HB): review of production process technology. *Ind. Biotechnol.* 13, 192–208. doi: 10.1089/ind.2017.0013

Amulya, K., Jukuri, S., and Venkata Mohan, S. (2015). Sustainable multistage process for enhanced productivity of bioplastics from waste remediation through aerobic dynamic feeding strategy: process integration for up-scaling. *Bioresour. Technol.* 188, 231–239. doi: 10.1016/j.biortech.2015.01.070

Anis, S. N. S., Annuar, M. S. M., and Simarani, K. (2018). Microbial biosynthesis and *in vivo* depolymerization of intracellular medium-chain-length poly-3-hydroxyalkanoates as potential route to platform chemicals. *Biotechnol. Appl. Biochem.* 65, 784–796. doi: 10.1002/bab.1666

Bera, A., Dubey, S., Bhayani, K., Mondal, D., Mishra, S., and Ghosh, P. K. (2015). Microbial synthesis of polyhydroxyalkanoate using seaweed-derived crude levulinic acid as co-nutrient. *Int. J. Biol. Macromol.* 72, 487–494. doi: 10.1016/j.ijbiomac.2014.08.037

Bhati, R., and Mallick, N. (2016). Carbon dioxide and poultry waste utilization for production of polyhydroxyalkanoate biopolymers by Nostoc muscorum Agardh: a sustainable approach. *J. Appl. Phycol.* 28, 161–168. doi: 10.1007/s10811-015-0573-x

Biddy, M. J., Scarlata, C. J., and Kinchin, C. M. (2016). *Chemicals From Biomass: A Market Assessment of Bioproducts With Near-Term Potential*. Golden, CO: NREL.

Biernacki, M., Riechen, J., Hähnel, U., Roick, T., Baronian, K., Bode, R., et al. (2017). Production of (R)-3-hydroxybutyric acid by Arxula adeninivorans. *AMB Express* 7, 1–12. doi: 10.1186/s13568-016-0303-z

Borrero-de Acuña, J. M., Aravena-Carrasco, C., Gutierrez-Urrutia, I., Duchens, D., and Poblete-Castro, I. (2019). Enhanced synthesis of medium-chain-length poly(3-hydroxyalkanoates) by inactivating the tricarboxylate transport system of *Pseudomonas putida* KT2440 and process development using waste vegetable oil. *Process Biochem.* 77, 23–30. doi: 10.1016/j.procbio.2018.10.012

Borrero-de Acuña, J. M., Hidalgo-Dumont, C., Pacheco, N., Cabrera, A., and Poblete-Castro, I. (2017). A novel programmable lysozyme-based lysis system in *Pseudomonas putida* for biopolymer production. *Sci. Rep.* 7:4373. doi: 10.1038/s41598-017-04741-2

Brämer, C. O., Vandamme, P., da Silva, L. F., Gomez, J. G., and Steinbüchel, A. (2001). Polyhydroxyalkanoate-accumulating bacterium isolated from soil of a sugar-cane plantation in Brazil. *Int. J. Syst. Evol. Microbiol.* 51, 1709–1713. doi: 10.1099/00207713-51-5-1709

Braunegg, G., Bona, R., and Koller, M. (2004). Sustainable polymer production. *Polym. Plast. Technol. Eng.* 43, 1779–1793. doi: 10.1081/PPT-200040130

Bresan, S., Sznajder, A., Hauf, W., Forchhammer, K., Pfeiffer, D., and Jendrossek, D. (2016). Polyhydroxyalkanoate (PHA) granules have no phospholipids. *Sci. Rep.* 6:26612. doi: 10.1038/srep26612

Brigham, C. (2019). Perspectives for the biotechnological production of biofuels from CO2 and H2 using Ralstonia eutropha and other 'Knallgas' bacteria. *Appl. Microbiol. Biotechnol.* 103, 2113–2120. doi: 10.1007/s00253-019-09636-y

Brigham, C. J., Speth, D. R., Rha, C., and Sinskey, A. J. (2012). Whole-genome microarray and gene deletion studies reveal regulation of the polyhydroxyalkanoate production cycle by the stringent response in Ralstonia eutropha H16. *Appl. Environ. Microbiol.* 78, 8033–8044. doi: 10.1128/AEM.01693-12

Bugnicourt, E., Cinelli, P., Lazzeri, A., and Alvarez, V. (2014). Polyhydroxyalkanoate (PHA): review of synthesis, characteristics, processing and potential applications in packaging. *Express Polym. Lett.* 8, 791–808. doi: 10.3144/expresspolymlett.2014.82

Cao, Q., Zhang, J., Liu, H., Wu, Q., Chen, J., and Chen, G.-Q. (2014). The mechanism of anti-osteoporosis effects of 3-hydroxybutyrate and derivatives under simulated microgravity. *Biomaterials* 35, 8273–8283. doi: 10.1016/j.biomaterials.2014.06.020

Chen, G.-Q. (2009). A microbial polyhydroxyalkanoates (PHA) based bio- and materials industry. *Chem. Soc. Rev.* 38:2434. doi: 10.1039/b812677c

Chen, G.-Q., König, K.-H., Lafferty, and R. M. (1991). Production of poly-D(-)-3-hydroxybutyrate and poly-D(-)-3-hydroxyvalerate by strains of Alcaligenes latus. *Anton. Leeuwen.* 60, 61–66. doi: 10.1007/BF00580443

Chen, G.-Q., and Patel, M. K. (2012). Plastics derived from biological sources: present and future: a technical and environmental review. *Chem. Rev.* 112, 2082–2099. doi: 10.1021/cr200162d

Chen, X., Tao, L., Shekiro, J., Mohaghaghi, A., Decker, S., Wang, W., et al. (2012). Improved ethanol yield and reduced Minimum Ethanol Selling Price (MESP) by modifying low severity dilute acid pretreatment with deacetylation and mechanical refining: 1) experimental. *Biotechnol. Biofuels* 5:60. doi: 10.1186/1754-6834-5-60

Chen, X., Zhou, L., Tian, K., Kumar, A., Singh, S., Prior, B. A., et al. (2013). Metabolic engineering of *Escherichia coli*: a sustainable industrial platform for bio-based chemical production. *Biotechnol. Adv.* 31, 1200–1223. doi: 10.1016/j.biotechadv.2013.02.009

Choi, J., and Lee, S. Y. (1999). Factors affecting the economics of polyhydroxyalkanoate production by bacterial fermentation. *Appl. Microbiol. Biotechnol.* 51, 13–21. doi: 10.1007/s002530051357

Choi, M. H., Yoon, S. C., and Lenz, R. W. (1999). Production of poly(3-hydroxybutyric acid-co-4-hydroxybutyric acid) and poly(4-hydroxybutyric acid) without subsequent degradation by *Hydrogenophaga pseudoflava*. *Appl. Environ. Microbiol.* 65, 1570–1577.

Chung, A., Liu, Q., Ouyang, S. P., Wu, Q., and Chen, G. Q. (2009). Microbial production of 3-hydroxydodecanoic acid by pha operon and fadBA knockout mutant of *Pseudomonas putida* KT2442 harboring tesB gene. *Appl. Microbiol. Biotechnol.* 83, 513–519. doi: 10.1007/s00253-009-1919-6

Costa, T. R. D., Felisberto-rodrigues, C., Meir, A., Prevost, M. S., Redzej, A., Trokter, M., et al. (2015). Secretion systems in Gram-negative insights. *Nat. Publ. Gr.* 13, 343–359. doi: 10.1038/nrmicro3456

Cruz, M. V., Freitas, F., Paiva, A., Mano, F., Dionísio, M., Ramos, A. M., et al. (2016). Valorization of fatty acids-containing wastes and byproducts into short- and medium-chain length polyhydroxyalkanoates. *N. Biotechnol.* 33, 206–215. doi: 10.1016/j.nbt.2015.05.005

Cruz, M. V., Paiva, A., Lisboa, P., Freitas, F., Alves, V. D., Simões, P., et al. (2014). Production of polyhydroxyalkanoates from spent coffee grounds oil obtained by supercritical fluid extraction technology. *Bioresour. Technol.* 157, 360–363. doi: 10.1016/j.biortech.2014.02.013

de Paula, F. C., Kakazu, S., de Paula, C. B. C., Gomez, J. G. C., and Contiero, J. (2017). Polyhydroxyalkanoate production from crude glycerol by newly isolated Pandoraea sp. *J. King Saud Univ. Sci.* 29, 166–173. doi: 10.1016/j.jksus.2016.07.002

de Roo, G., Kellerhals, M. B., Ren, Q., Witholt, B., and Kessler, B. (2002). Production of chiralR-3-hydroxyalkanoic acids andR-3-hydroxyalkanoic acid methylesters via hydrolytic degradation of polyhydroxyalkanoate synthesized by pseudomonads. *Biotechnol. Bioeng.* 77, 717–722. doi: 10.1002/bit.10139

Dietrich, D., Illman, B., and Crooks, C. (2013). Differential sensitivity of polyhydroxyalkanoate producing bacteria to fermentation inhibitors and comparison of polyhydroxybutyrate production from Burkholderia cepacia and Pseudomonas pseudoflava. *BMC Res. Notes* 6:219. doi: 10.1186/1756-0500-6-219

Dietrich, K., Dumont, M.-J. J., Del Rio, L. F., and Orsat, V. V. (2016). Producing PHAs in the bioeconomy - Towards a sustainable bioplastic. *Sustain. Prod. Consum.* 9, 58–70. doi: 10.1016/j.spc.2016.09.001

Doi, Y. (1990). Cyclic nature of poly(3-hydroxyalkanoate) metabolism in *Alcaligenes eutrophus*. *FEMS Microbiol. Lett.* 67, 165–169. doi: 10.1016/0378-1097(90)90188-V

Fei, T., Cazeneuve, S., Wen, Z., Wu, L., and Wang, T. (2016). Effective recovery of poly-β-hydroxybutyrate (PHB) biopolymer from C upriavidus necator using a novel and environmentally friendly solvent system. *Biotechnol. Prog.* 32, 678–685. doi: 10.1002/btpr.2247

Flüchter, S., Follonier, S., Schiel-Bengelsdorf, B., Bengelsdorf, F. R., Zinn, M., and Dürre, P. (2019). Anaerobic production of poly(3-hydroxybutyrate) and its precursor 3-hydroxybutyrate from synthesis gas by autotrophic clostridia. *Biomacromolecules* 20, 3271–3282. doi: 10.1021/acs.biomac.9b00342

Follonier, S. (2015). Pilot-scale production of functionalized mcl-PHA from grape pomace supplemented with fatty acids. *Chem. Biochem. Eng. Q.* 29, 113–121. doi: 10.15255/CABEQ.2014.2251

Fuhrmann, E., and Talbiersky, J. (2005). Synthesis of alkyl aryl ethers by catalytic williamson ether synthesis with weak alkylation agents. *Org. Process Res. Dev.* 9, 206–211. doi: 10.1021/op050001h

Gao, H. J., Wu, Q., and Chen, G. Q. (2002). Enhanced production of D-(-)-3-hydroxybutyric acid by recombinant *Escherichia coli*. *FEMS Microbiol. Lett.* 213, 59–65. doi: 10.1016/S0378-1097(02)00788-7

Gao, X., Chen, J.-C. C., Wu, Q., and Chen, G.-Q. Q. (2011). Polyhydroxyalkanoates as a source of chemicals, polymers, and biofuels. *Curr. Opin. Biotechnol.* 22, 768–774. doi: 10.1016/j.copbio.2011.06.005

Gebauer, B., and Jendrossek, D. (2006). Assay of poly(3-hydroxybutyrate) depolymerase activity and product determination. *Appl. Environ. Microbiol.* 72, 6094–6100. doi: 10.1128/AEM.01184-06

Geyer, R., Jambeck, J. R., and Law, K. L. (2017). Production, use, and fate of all plastics ever made. *Sci. Adv.* 3:e1700782. doi: 10.1126/sciadv.1700782

Gómez Cardozo, J. R., Mora Martínez, A. L., Yepes Pérez, M., and Correa Londoño, G. A. (2016). Production and characterization of polyhydroxyalkanoates and native microorganisms synthesized from fatty waste. *Int. J. Polym. Sci.* 2016, 1–12. doi: 10.1155/2016/6541718

Gorenflo, V., Schmack, G., Vogel, R., and Steinbüchel, A. (2001). Development of a process for the biotechnological large-scale production of 4-hydroxyvalerate-containing polyesters and characterization of their physical and mechanical properties. *Biomacromolecules* 2, 45–57. doi: 10.1021/bm0000992

Green, E. R., and Mecsas, J. (2016). Bacterial secretion systems: an overview. *Microbiol. Spectr.* 4, 215–239. doi: 10.1128/microbiolspec.vmbf-0012-2015

Grousseau, E., Blanchet, E., Déléris, S., Albuquerque, M. G. E., Paul, E., and Uribelarrea, J. L. (2013). Impact of sustaining a controlled residual growth on polyhydroxybutyrate yield and production kinetics in *Cupriavidus necator*. *Bioresour. Technol.* 148, 30–38. doi: 10.1016/j.biortech.2013.08.120

Guevara-Martínez, M., Gällnö, K. S., Sjöberg, G., Jarmander, J., Perez-Zabaleta, M., Quillaguamán, J., et al. (2015). Regulating the production of (R)-3-hydroxybutyrate in escherichia coli by N or P limitation. *Front. Microbiol.* 6, 844. doi: 10.3389/fmicb.2015.00844

Guevara-Martínez, M., Perez-Zabaleta, M., Gustavsson, M., Quillaguamán, J., Larsson, G., and van Maris, A. J. A. (2019). The role of the acyl-CoA thioesterase "YciA" in the production of (R)-3-hydroxybutyrate by recombinant *Escherichia coli*. *Appl. Microbiol. Biotechnol.* 103, 3693–3704. doi: 10.1007/s00253-019-09707-0

Haas, C. (2015). Production of PHB from chicory roots – Comparison of three cupriavidus necator strains. *Chem. Biochem. Eng. Q.* 29, 99–112. doi: 10.15255/CABEQ.2014.2250

Hahn, S. K., Chang, Y. K., Kim, B. S., and Chang, H. N. (1994). Optimization of microbial poly(3-hydroxybutyrate) recover using dispersions of sodium hypochlorite solution and chloroform. *Biotechnol. Bioeng.* 44, 256–261. doi: 10.1002/bit.260440215

Hamilton, L. A., Feilt, S., Muffett, C., Kelso, M., Rubright, S., Bernhardt, C., et al. (2019). *The Hidden Costs of a Plastic Planet*. Available online at: www.ciel.org/plasticandclimate

Handrick, R., Reinhardt, S., Focarete, M. L., Scandola, M., Adamus, G., Kowalczuk, M., et al. (2001). A new type of thermoalkalophilic hydrolase of *Paucimonas lemoignei* with high specificity for amorphous polyesters of short chain-length hydroxyalkanoic acids. *J. Biol. Chem.* 276, 36215–36224. doi: 10.1074/jbc.M101106200

Hänggi, U. J. (2012). Pilot scale production of PHB with *Alcaligenes latus*. *Nov. Biodegrad. Microb. Polym.* 65–70. doi: 10.1007/978-94-009-2129-0_6

Hazer, D. B., Kiliçay, E., and Hazer, B. (2012). Poly(3-hydroxyalkanoate)s: diversification and biomedical applications. *Mater. Sci. Eng. C* 32, 637–647. doi: 10.1016/j.msec.2012.01.021

Heinrich, D., Madkour, M. H., Al-Ghamdi, M. A., Shabbaj, I. I., and Steinbüchel, A. (2012). Large scale extraction of poly(3-hydroxybutyrate) from Ralstonia eutropha H16 using sodium hypochlorite. *AMB Express* 2, 1–6. doi: 10.1186/2191-0855-2-59

Henderson, I. R., and He, M. (2009). Secretion and subcellular localizations of bacterial proteins : a semantic awareness issue. *Trends Microbiol.* 17, 139–145. doi: 10.1016/j.tim.2009.01.004

Henderson, R. A., and Jones, C. W. (1997). Physiology of poly-3-hydroxybutyrate (PHB) production by *Alcaligenes eutrophus* growing in continuous culture. *Microbiology* 143, 2361–2371. doi: 10.1099/00221287-143-7-2361

Hiroe, A., Chek, M. F., Hakoshima, T., Sudesh, K., and Taguchi, S. (2019). "Synthesis of polyesters III: acyltransferase as catalyst," in *Enzymatic Polymerization towards Green Polymer Chemistry*, eds S. Kobayashi, H. Uyama, K.J. Singapore: Springer, 199–231. doi: 10.1007/978-981-13-3813-7_7

Hodge, D. B., Karim, M. N., Schell, D. J., McMillan, J. D. (2008). Soluble and insoluble solids contributions to high-solids enzymatic hydrolysis of lignocellulose. *Bioresour. Technol.* 99, 8940–8948. doi: 10.1016/j.biortech.2008.05.015

Hölscher, T., Breuer, U., Adrian, L., Harms, H., and Maskow, T. (2010). Production of the chiral compound (R)-3-hydroxybutyrate by a genetically engineered methylotrophic bacterium. *Appl. Environ. Microbiol.* 76, 5585–5591. doi: 10.1128/AEM.01065-10

Hori, K., Kaneko, M., Tanji, Y., Xing, X.-H., and Unno, H. (2002). Construction of self-disruptive Bacillus megaterium in response to substrate exhaustion for polyhydroxybutyrate production. *Appl. Microbiol. Biotechnol.* 59, 211–216. doi: 10.1007/s00253-002-0986-8

James, B. W., Mauchline, W. S., Dennis, P. J., Keevil, C. W., and Wait, R. (1999). Poly-3-hydroxybutyrate in *Legionella pneumophila*, an energy source for survival in low-nutrient environments. *Appl. Environ. Microbiol.* 65, 822–827.

Jarmander, J., Belotserkovsky, J., Sjöberg, G., Guevara-Martínez, M., Pérez-Zabaleta, M., Quillaguamán, J., et al. (2015). Cultivation strategies for production of (R)-3-hydroxybutyric acid from simultaneous consumption of glucose, xylose and arabinose by *Escherichia coli*. *Microb. Cell Fact.* 14:51. doi: 10.1186/s12934-015-0236-2

Jers, C., Kalantari, A., Garg, A., and Mijakovic, I. (2019). Production of 3-hydroxypropanoic acid from glycerol by metabolically engineered bacteria. *Front. Bioeng. Biotechnol.* 7:124. doi: 10.3389/fbioe.2019.00124

Jiang, G., Hill, D., Kowalczuk, M., Johnston, B., Adamus, G., Irorere, V., et al. (2016). Carbon sources for polyhydroxyalkanoates and an integrated biorefinery. *Int. J. Mol. Sci.* 17:1157. doi: 10.3390/ijms17071157

Jiang, G., Johnston, B., Townrow, D., Radecka, I., Koller, M., Chaber, P., et al. (2018). Biomass extraction using non-chlorinated solvents for

biocompatibility improvement of polyhydroxyalkanoates. *Polymers* 10:731. doi: 10.3390/polym10070731

Jossek, R., Reichelt, R., and Steinbüchel, A. (1998). *In vitro* biosynthesis of poly(3-hydroxybutyric acid) by using purified poly(hydroxyalkanoic acid) synthase of *Chromatium vinosum*. *Appl. Microbiol. Biotechnol.* 49, 258–266. doi: 10.1007/s002530051166

Jossek, R., and Steinbüchel, A. (1998). *In vitro* synthesis of poly(3-hydroxybutyric acid) by using an enzymatic coenzyme A recycling system. *FEMS Microbiol. Lett.* 168, 319–324. doi: 10.1111/j.1574-6968.1998.tb13290.x

Juengert, J. R., Borisova, M., Mayer, C., Wolz, C., Brigham, C. J., Sinskey, A. J., et al. (2017). Absence of ppGpp leads to increased mobilization of intermediately accumulated poly(3-hydroxybutyrate) in *Ralstonia eutropha* H16. *Appl. Environ. Microbiol.* 83:AEM.00755–00717. doi: 10.1128/AEM.00755-17

Juengert, J. R., Patterson, C., and Jendrossek, D. (2018). Poly(3-hydroxybutyrate) (PHB) polymerase PhaC1 and PHB depolymerase PhaZa1 of *Ralstonia eutropha* are phosphorylated *in vivo*. *Appl. Environ. Microbiol.* 84, 1–12. doi: 10.1128/AEM.00604-18

Kawata, Y., Ando, H., Matsushita, I., and Tsubota, J. (2014). Efficient secretion of (R)-3-hydroxybutyric acid from Halomonas sp. KM-1 by nitrate fed-batch cultivation with glucose under microaerobic conditions. *Bioresour. Technol.* 156, 400–403. doi: 10.1016/j.biortech.2014.01.073

Kawata, Y., Kawasaki, K., and Shigeri, Y. (2012). Efficient secreted production of (R)-3-hydroxybutyric acid from living Halomonas sp. KM-1 under successive aerobic and microaerobic conditions. *Appl. Microbiol. Biotechnol.* 96, 913–920. doi: 10.1007/s00253-012-4218-6

Kawata, Y., Nojiri, M., Matsushita, I., and Tsubota, J. (2015). Improvement of (R)-3-hydroxybutyric acid secretion during Halomonas sp. KM-1 cultivation with saccharified Japanese cedar by the addition of urea. *Lett. Appl. Microbiol.* 61, 397–402. doi: 10.1111/lam.12473

Keenan, T. M., Nakas, J. P., and Tanenbaum, S. W. (2006). Polyhydroxyalkanoate copolymers from forest biomass. *J. Ind. Microbiol. Biotechnol.* 33, 616–626. doi: 10.1007/s10295-006-0131-2

Khosravi-Darani, K. (2015). Application of Poly(hydroxyalkanoate) In food packaging: improvements by nanotechnology. *Chem. Biochem. Eng. Q.* 29, 275–285. doi: 10.15255/CABEQ.2014.2260

Khosravi-Darani, K., Mokhtari, Z. B., Amai, T., and Tanaka, K. (2013). Microbial production of poly(hydroxybutyrate) from C1 carbon sources. *Appl. Microbiol. Biotechnol.* 97, 1407–1424. doi: 10.1007/s00253-012-4649-0

Kim, B. S., Lee, S. C., Lee, S. Y., Chang, H. N., Chang, Y. K., and Woo, S. I. (1994). Production of poly(3-hydroxybutyric acid) by fed-batch culture ofAlcaligenes eutrophus with glucose concentration control. *Biotechnol. Bioeng.* 43, 892–898. doi: 10.1002/bit.260430908

Kim, M., Cho, K. S., Ryu, H. W., Lee, E. G., and Chang, Y. K. (2003). Recovery of poly(3-hydroxybutyrate) from high cell density culture of *Ralstonia eutropha* by direct addition of sodium dodecyl sulfate. *Biotechnol. Lett.* 25, 55–59. doi: 10.1023/A:1021734216612

Kim, T. W., Park, J. S., and Lee, Y. H. (1996). Enzymatic characteristics of biosynthesis and degradation of poly-β-hydroxybutyrate of *Alcaligenes latus*. *J. Microbiol. Biotechnol.* 6, 425–431.

Knoll, M., Hamm, T. M., Wagner, F., Martinez, V., and Pleiss, J. (2009). The PHA depolymerase engineering database: a systematic analysis tool for the diverse family of polyhydroxyalkanoate (PHA) depolymerases. *BMC Bioinformatics* 10:89. doi: 10.1186/1471-2105-10-89

Koller, M. (2014). Poly(hydroxyalkanoates) for food packaging: application and attempts towards implementation. *Appl. Food Biotecnol.* 1, 3–15.

Kosseva, M. R., and Rusbandi, E. (2018). Trends in the biomanufacture of polyhydroxyalkanoates with focus on downstream processing. *Int. J. Biol. Macromol.* 107, 762–778. doi: 10.1016/j.ijbiomac.2017.09.054

Kubowicz, S., and Booth, A. M. (2017). Biodegradability of plastics: challenges and misconceptions. *Environ. Sci. Technol.* 51, 12058–12060. doi: 10.1021/acs.est.7b04051

Kumar, P., Ray, S., and Kalia, V. C. (2016). Production of co-polymers of polyhydroxyalkanoates by regulating the hydrolysis of biowastes. *Bioresour. Technol.* 200, 413–419. doi: 10.1016/j.biortech.2015.10.045

Kunasundari, B., and Sudesh, K. (2011). Isolation and recovery of microbial polyhydroxyalkanoates. *Express Polym. Lett.* 5, 620–634. doi: 10.3144/expresspolymlett.2011.60

Lafferty, R. M. (1977). *Process for the Manufacture of D(-)-3-Hydroxybutyric Acid and D(-)-3-Hydroxybutyric Acid Producing Mutants.* US4211846A.

Lafferty, R. M., and Heinzle, E. (1977). *Cyclic Carbonic Acid Esters as Solvents for Poly-β-Hydroxybutyric Acid.* US4101533A.

Lawrence, A. G., Schoenheit, J., He, A., Tian, J., Liu, P., Stubbe, J., et al. (2005). Transcriptional analysis of *Ralstonia eutropha* genes related to poly-(R)-3-hydroxybutyrate homeostasis during batch fermentation. *Appl. Microbiol. Biotechnol.* 68, 663–672. doi: 10.1007/s00253-005-1969-3

Lee, I. (1995). Regulation of poly-β-hydroxybutyrate biosynthesis by nicotinamide nucleotide in *Alcaligenes eutrophus*. *FEMS Microbiol. Lett.* 131, 35–39. doi: 10.1016/0378-1097(95)00231-S

Lee, S.-H., Park, S. J., Lee, S. Y., and Hong, S. H. (2008). Biosynthesis of enantiopure (S)-3-hydroxybutyric acid in metabolically engineered *Escherichia coli*. *Appl. Microbiol. Biotechnol.* 79, 633–641. doi: 10.1007/s00253-008-1473-7

Lee, S. Y., and Lee, Y. (2003). Metabolic engineering of *Escherichia coli* for production of enantiomerically pure (R)-(–)-hydroxycarboxylic acids. *Appl. Environ. Microbiol.* 69, 3421–3426. doi: 10.1128/AEM.69.6.3421

Lee, S. Y., Lee, Y., and Wang, F. (1999). Chiral compounds from bacterial polyesters: sugars to plastics to fine chemicals. *Biotechnol. Bioeng.* 65, 363–368. doi: 10.1002/(SICI)1097-0290(19991105)65:3<363::AID-BIT15>3.0.CO;2-1

Lee, Y., Park, S. H., Lim, I. T., Han, K., and Lee, S. Y. (2000). Preparation of alkyl (R)-(-)-3-hydroxybutyrate by acidic alcoholysis of poly-(R)-(-)-3-hydroxybutyrate. *Enzyme Microb. Technol.* 27, 33–36. doi: 10.1016/S0141-0229(00)00146-0

Levett, I., Birkett, G., Davies, N., Bell, A., Langford, A., Laycock, B., et al. (2016). Techno-economic assessment of poly-3-hydroxybutyrate (PHB) production from methane—The case for thermophilic bioprocessing. *J. Environ. Chem. Eng.* 4, 3724–3733. doi: 10.1016/j.jece.2016.07.033

Li, F., Zhang, C., Liu, Y., Liu, D., Xia, H., and Chen, S. (2016). Efficient production of (R)-3-hydroxybutyric acid by Pseudomonas sp. DS1001a and its extracellular poly(3-hydroxybutyrate) depolymerase. *Process Biochem.* 51, 369–373. doi: 10.1016/j.procbio.2015.12.016

Liddell, J. M. (1999). Process for the recovery of Polyhydroxyalkanoic acid. *U.S. Pat.* 5, 12–14.

Linton, E., Walsh, M. K., Sims, R. C., and Miller, C. D. (2012). Translocation of green fluorescent protein by comparative analysis with multiple signal peptides. *Biotechnol. J.* 7, 667–676. doi: 10.1002/biot.201100158

Listewnik, H.-F., Wendlandt, K.-D., Jechorek, M., and Mirschel, G. (2007). Process design for the microbial synthesis of poly-β-hydroxybutyrate (PHB) from natural gas. *Eng. Life Sci.* 7, 278–282. doi: 10.1002/elsc.200620193

Liu, Q., Ouyang, S. P., Chung, A., Wu, Q., and Chen, G. Q. (2007). Microbial production of R-3-hydroxybutyric acid by recombinant *E. coli* harboring genes of phbA, phbB, and tesB. *Appl. Microbiol. Biotechnol.* 76, 811–818. doi: 10.1007/s00253-007-1063-0

Loo, C.-Y., Lee, W.-H., Tsuge, T., Doi, Y., and Sudesh, K. (2005). Biosynthesis and characterization of poly(3-hydroxybutyrate-co-3- hydroxyhexanoate) from palm oil products in a *Wautersia eutropha* mutant. *Biotechnol. Lett.* 27, 1405–1410. doi: 10.1007/s10529-005-0690-8

Loow, Y.-L., Wu, T. Y., Md. Jahim, J., Mohammad, A. W., and Teoh, W. H. (2016). Typical conversion of lignocellulosic biomass into reducing sugars using dilute acid hydrolysis and alkaline pretreatment. *Cellulose* 23, 1491–1520. doi: 10.1007/s10570-016-0936-8

Lu, J., Brigham, C. J., Li, S., and Sinskey, A. J. (2016). Ralstonia eutropha H16 as a platform for the production of biofuels, biodegradable plastics, and fine chemicals from diverse carbon resources. *Biotechnol. Biofuel Prod. Optim.* 2016, 325–351. doi: 10.1016/B978-0-444-63475-7.00012-1

Lu, J., Tappel, R. C., and Nomura, C. T. (2009). Mini-review: biosynthesis of poly(hydroxyalkanoates). *Polym. Rev.* 49, 226–248. doi: 10.1080/15583720903048243

Martínez, V., García, P., García, J. L., and Prieto, M. A. (2011). Controlled autolysis facilitates the polyhydroxyalkanoate recovery in Pseudomonas putida KT2440. *Microb. Biotechnol.* 4, 533–547. doi: 10.1111/j.1751-7915.2011.00257.x

Martínez, V., Herencias, C., Jurkevitch, E., and Prieto, M. A. (2016). Engineering a predatory bacterium as a proficient killer agent for intracellular bio-products recovery: the case of the polyhydroxyalkanoates. *Sci. Rep.* 6:24381. doi: 10.1038/srep24381

Matsumoto, K., Okei, T., Honma, I., Ooi, T., Aoki, H., and Taguchi, S. (2013). Efficient (R)-3-hydroxybutyrate production using acetyl CoA-regenerating pathway catalyzed by coenzyme A transferase. *Appl. Microbiol. Biotechnol.* 97, 205–210. doi: 10.1007/s00253-012-4104-2

Matsuyama, A., Yamamoto, H., Kawada, N., and Kobayashi, Y. (2001). Industrial production of (R)-1,3-butanediol by new biocatalysts. *J. Mol. Catal. B Enzym.* 11, 513–521. doi: 10.1016/S1381-1177(00)00032-1

McMahon, M. D., and Prather, K. L. J. (2014). Functional screening and *in vitro* analysis reveal thioesterases with enhanced substrate specificity profiles that improve short-chain fatty acid production in *Escherichia coli*. *Appl. Environ. Microbiol.* 80, 1042–1050. doi: 10.1128/AEM.03303-13

Melih Tamer, I., Moo-Young, M., and Chisti, Y. (1998). Disruption of *Alcaligenes latus* for recovery of poly(β-hydroxybutyric acid): comparison of high-pressure homogenization, bead milling, and chemically induced lysis. *Ind. Eng. Chem. Res.* 37, 1807–1814.

Mikkili, I., Karlapudi, A. P., Venkateswarulu, T. C., D, J. B., Nath, S. B., and Kodali, V. P. (2014). Isolation, screening and extraction of polyhydroxybutyrate (PHB) producing bacteria from Sewage sample. *Int. J. Pharm. Tech. Res.* 6, 850–857.

Miscevic, D., Srirangan, K., Kefale, T., Kilpatrick, S., Chung, D. A., Moo-Young, M., et al. (2019). Heterologous production of 3-hydroxyvalerate in engineered *Escherichia coli*. *Metab. Eng.* doi: 10.1016/j.ymben.2019.11.005. [Epub ahead of print].

Misra, S. K., Valappil, S. P., Roy, I., and Boccaccini, A. R. (2006). Polyhydroxyalkanoate (PHA)/inorganic phase composites for tissue engineering applications. *Biomacromolecules* 7, 2249–2258. doi: 10.1021/bm060317c

Mothes, G., Schnorpfeil, C., and Ackermann, J.-U. (2007). Production of PHB from crude glycerol. *Eng. Life Sci.* 7, 475–479. doi: 10.1002/elsc.200620210

Mozejko-Ciesielska, J., Dabrowska, D., Szalewska-Palasz, A., and Ciesielski, S. (2017). Medium-chain-length polyhydroxyalkanoates synthesis by *Pseudomonas putida* KT2440 relA/spoT mutant: bioprocess characterization and transcriptome analysis. *AMB Express* 7:92. doi: 10.1186/s13568-017-0396-z

Mozejko-Ciesielska, J., and Kiewisz, R. (2016). Bacterial polyhydroxyalkanoates: still fabulous? *Microbiol. Res.* 192, 271–282. doi: 10.1016/j.micres.2016.07.010

Naggert, J., Narasimhan, M. L., DeVeaux, L., Cho, H., Randhawa, Z. I., Cronan, J. E., et al. (1991). Cloning, sequencing, and characterization of *Escherichia coli* thioesterase II. *J. Biol. Chem.* 266, 11044–11050.

Nakano, K., Rischke, M., Sato, S., and Märkl, H. (1997). Influence of acetic acid on the growth of *Escherichia coli* K12 during high-cell-density cultivation in a dialysis reactor. *Appl. Microbiol. Biotechnol.* 48, 597–601. doi: 10.1007/s002530051101

Naranjo, J. M., Posada, J. A., Higuita, J. C., and Cardona, C. A. (2013). Valorization of glycerol through the production of biopolymers: the PHB case using *Bacillus megaterium*. *Bioresour. Technol.* 133, 38–44. doi: 10.1016/j.biortech.2013.01.129

Nicaud, J. M., Mackman, N., Gray, L., and Holland, I. B. (1986). The C-terminal, 23 kDa peptide of *E. coli* haemolysin 2001 contains all the information necessary for its secretion by the haemolysin (Hly) export machinery. *FEBS Lett.* 204, 331–335. doi: 10.1016/0014-5793(86)80838-9

Nozawa, T., Sato, S., and Takahashi, R. (2009). Vapor-phase dehydration of 1,3-butanediol over CeO2–ZrO2 catalysts. *Top. Catal.* 52, 609–617. doi: 10.1007/s11244-009-9198-0

Obruca, S., Sedlacek, P., Mravec, F., Samek, O., and Marova, I. (2016). Evaluation of 3-hydroxybutyrate as an enzyme-protective agent against heating and oxidative damage and its potential role in stress response of poly(3-hydroxybutyrate) accumulating cells. *Appl. Microbiol. Biotechnol.* 100, 1365–1376. doi: 10.1007/s00253-015-7162-4

Oh, Y. H., Lee, S. H., Jang, Y.-A., Choi, J. W., Hong, K. S., Yu, J. H., et al. (2015). Development of rice bran treatment process and its use for the synthesis of polyhydroxyalkanoates from rice bran hydrolysate solution. *Bioresour. Technol.* 181, 283–290. doi: 10.1016/j.biortech.2015.01.075

Pan, W., Nomura, C. T., and Nakas, J.P. (2012). Estimation of inhibitory effects of hemicellulosic wood hydrolysate inhibitors on PHA production by Burkholderia cepacia ATCC 17759 using response surface methodology. *Bioresour. Technol.* 125, 275–282. doi: 10.1016/j.biortech.2012.08.107

Peña, C., Castillo, T., García, A., Millán, M., and Segura, D. (2014). Biotechnological strategies to improve production of microbial poly-(3-hydroxybutyrate): a review of recent research work. *Microb. Biotechnol.* 7, 278–293. doi: 10.1111/1751-7915.12129

Pérez-Fortes, M., Schöneberger, J. C., Boulamanti, A., and Tzimas, E. (2016). Methanol synthesis using captured CO2 as raw material: techno-economic and environmental assessment. *Appl. Energy* 161, 718–732. doi: 10.1016/j.apenergy.2015.07.067

Perez-Zabaleta, M., Guevara-Martínez, M., Gustavsson, M., Quillaguamán, J., Larsson, G., and van Maris, A. J. A. (2019). Comparison of engineered Escherichia coli AF1000 and BL21 strains for (R)-3-hydroxybutyrate production in fed-batch cultivation. *Appl. Microbiol. Biotechnol.* 103, 5627–5639. doi: 10.1007/s00253-019-09876-y

Poblete-Castro, I., Binger, D., Oehlert, R., and Rohde, M. (2014). Comparison of mcl-Poly(3-hydroxyalkanoates) synthesis by different Pseudomonas putida strains from crude glycerol: citrate accumulates at high titer under PHA-producing conditions. *BMC Biotechnol.* 14:962. doi: 10.1186/s12896-014-0110-z

Poirier, Y., Nawrath, C., and Somerville, C. (1995). Production of polyhydroxyalkanoates, a family of biodegradable plastics and elastomers, in bacteria and plants. *Nat. Biotechnol.* 13, 142–150. doi: 10.1038/nbt0295-142

Polyák, P., Dohovits, E., Nagy, G. N., Vértessy, B. G., Vörös, G., and Pukánszky, B. (2018). Enzymatic degradation of poly-[(R)-3-hydroxybutyrate]: mechanism, kinetics, consequences. *Int. J. Biol. Macromol.* 112, 156–162. doi: 10.1016/j.ijbiomac.2018.01.104

Posada, J. A., Naranjo, J. M., López, J. A., Higuita, J. C., and Cardona, C. A. (2011). Design and analysis of poly-3-hydroxybutyrate production processes from crude glycerol. *Process Biochem.* 46, 310–317. doi: 10.1016/j.procbio.2010.09.003

Rahman, A., Linton, E., Hatch, A. D., Sims, R. C., and Miller, C. D. (2013). Secretion of polyhydroxybutyrate in Escherichia coli using a synthetic biological engineering approach. *J. Biol. Eng.* 7:24. doi: 10.1186/1754-1611-7-24

Ramsay, J. A., Berger, E., Ramsay, B., and Chavarie, C. (1990). Poly-3-hydroxyalpoic acid granules by a stjrfactant-hypochlorite treatment. *J. Biotechnol. Technol.* 4, 221–226.

Ramsay, J. A., Berger, E., Voyer, R., and Chavarie, C. (1994). Extraction of poly-3-hydroxybutyrate using chlorinated solvents. *Biotechnol. Techn.* 8, 589–594.

Raposo, R. S., de Almeida, M. C. M. D., de Oliveira, M., da, C. M. A., da Fonseca, M. M., and Cesário, M. T. (2017). A *Burkholderia sacchari* cell factory: production of poly-3-hydroxybutyrate, xylitol and xylonic acid from xylose-rich sugar mixtures. *N. Biotechnol.* 34, 12–22. doi: 10.1016/j.nbt.2016.10.001

Rathbone, S., Furrer, P., Lübben, J., Zinn, M., and Cartmell, S. (2010). Biocompatibility of polyhydroxyalkanoate as a potential material for ligament and tendon scaffold material. *J. Biomed. Mater. Res. Part A* 93A, 1391–1403. doi: 10.1002/jbm.a.32641

Rehm, B. H. A., Krüger, N., and Steinbüchel, A. (1998). A new metabolic link between fatty acid *de novo* synthesis and polyhydroxyalkanoic acid synthesis. *J. Biol. Chem.* 273, 24044–24051. doi: 10.1074/jbc.273.37.24044

Reinecke, F., and Steinbüchel, A. (2008). *Ralstonia eutropha* strain H16 as model organism for PHA metabolism and for biotechnological production of technically interesting biopolymers. *J. Mol. Microbiol. Biotechnol.* 16, 91–108. doi: 10.1159/000142897

Ren, Q., Grubelnik, A., Hoerler, M., Ruth, K., Hartmann, R., Felber, H., et al. (2005). Bacterial poly(hydroxyalkanoates) as a source of chiral hydroxyalkanoic acids. *Biomacromolecules* 6, 2290–2298. doi: 10.1021/bm050187s

Ren, Q., Ruth, K., Thöny-Meyer, L., and Zinn, M. (2007). Process engineering for production of chiral hydroxycarboxylic acids from bacterial polyhydroxyalkanoates. *Macromol. Rapid Commun.* 28, 2131–2136. doi: 10.1002/marc.200700389

Ren, Q., Ruth, K., Thöny-Meyer, L., and Zinn, M. (2010). Enatiomerically pure hydroxycarboxylic acids: current approaches and future perspectives. *Appl. Microbiol. Biotechnol.* 87, 41–52. doi: 10.1007/s00253-010-2530-6

Resch, S., Gruber, K., Wanner, G., Slater, S., Dennis, D., and Lubitz, W. (1998). Aqueous release and purification of poly (b -hydroxybutyrate) from *Escherichia coli*. 65, 173–182.

Roe, A. J., O'Byrne, C., McLaggan, D., and Booth, I. R. (2002). Inhibition of Escherichia coli growth by acetic acid: a problem with methionine biosynthesis and homocysteine toxicity. *Microbiology* 148, 2215–2222. doi: 10.1099/00221287-148-7-2215

Roohi, Z. M. R., and Kuddus, M. (2018). PHB (poly-β-hydroxybutyrate) and its enzymatic degradation. *Polym. Adv. Technol.* 29, 30–40. doi: 10.1002/pat.4126

Ruth, K., Grubelnik, A., Hartmann, R., Egli, T., Zinn, M., and Ren, Q. (2007). Efficient production of (R)-3-hydroxycarboxylic acids by biotechnological conversion of polyhydroxyalkonoates and their purification. *Biomacromolecules* 8, 279–286. doi: 10.1021/bm060585a

Sabirova, J. S., Ferrer, M., Lunsdorf, H., Wray, V., Kalscheuer, R., Steinbuchel, A., et al. (2006). Mutation in a "tesB-Like" hydroxyacyl-coenzyme A-specific thioesterase gene causes hyperproduction of extracellular polyhydroxyalkanoates by *Alcanivorax borkumensis* SK2. *J. Bacteriol.* 188, 8452–8459. doi: 10.1128/JB.01321-06

Schweitzer, D., Mullen, C. A., Boateng, A. A., and Snell, K. D. (2015). Biobased n -butanol prepared from poly-3-hydroxybutyrate: optimization of the reduction of n -butyl crotonate to n -butanol. *Org. Process Res. Dev.* 19, 710–714. doi: 10.1021/op500156b

Seebach, D., Beck, A. K., Breitschuh, R., and Job, K. (2003). "Direct degradation of the biopolymer poly[(R)-3-hydroxybutyric acid] to (R)-3-hydroxybutanoic acid and its methyl ester," in *Organic Syntheses* (Hoboken, NJ: John Wiley & Sons, Inc.), 39–39. doi: 10.1002/0471264180.os071.05

Seebach, D., Chow, H.-F., Jackson, R. F. W., Sutter, M. A., Thaisrivongs, S., and Zimmermann, J. (1986). (+)-11,11′-Di-O-methylelaiophylidene – preparation from elaiophylin and total synthesis from (R)-3-hydroxybutyrate and (S)-malate. *Liebigs Ann. der Chemie* 1986, 1281–1308. doi: 10.1002/jlac.198619860714

Shah, M., Naseer, M. I., Choi, M. H., Kim, M. O., and Yoon, S. C. (2010). Amphiphilic PHA–mPEG copolymeric nanocontainers for drug delivery: preparation, characterization and *in vitro* evaluation. *Int. J. Pharm.* 400, 165–175. doi: 10.1016/j.ijpharm.2010.08.008

Shiraki, M., Endo, T., and Saito, T. (2006). Fermentative production of (R)-(-)-3-hydroxybutyrate using 3-hydroxybutyrate dehydrogenase null mutant of *Ralstonia eutropha* and recombinant *Escherichia coli*. *J. Biosci. Bioeng.* 102, 529–534. doi: 10.1263/jbb.102.529

Silva, L. F., Taciro, M. K., Michelin Ramos, M. E., Carter, J. M., Pradella, J. G. C., and Gomez, J. G. C. (2004). Poly-3-hydroxybutyrate (P3HB) production by bacteria from xylose, glucose and sugarcane bagasse hydrolysate. *J. Ind. Microbiol. Biotechnol.* 31, 245–254. doi: 10.1007/s10295-004-0136-7

Srivatsan, A., and Wang, J. D. (2008). Control of bacterial transcription, translation and replication by (p)ppGpp. *Curr. Opin. Microbiol.* 11, 100–105. doi: 10.1016/j.mib.2008.02.001

Steinbüchel, A., Hein, S. (2001). "Biochemical and molecular basis of microbial synthesis of polyhydroxyalkanoates in microorganisms," in: *Byopolyesters. Advances in Biochemical Engineering/Biotechnology*, Vol. 71, eds W. Babel and A. Steinbüchel (Berlin; Heidelberg: Springer), 81–123. doi: 10.1007/3-540-40021-4_3

Steinbüchel, A., and Valentin, H. E. (1995). Diversity of bacterial polyhydroxyalkanoic acids. *FEMS Microbiol. Lett.* 128, 219–228. doi: 10.1111/j.1574-6968.1995.tb07528.x

Strong, P., Laycock, B., Mahamud, S., Jensen, P., Lant, P., Tyson, G., et al. (2016). The opportunity for high-performance biomaterials from methane. *Microorganisms* 4:11. doi: 10.3390/microorganisms4010011

Suriyamongkol, P., Weselake, R., Narine, S., Moloney, M., and Shah, S. (2007). Biotechnological approaches for the production of polyhydroxyalkanoates in microorganisms and plants — A review. *Biotechnol. Adv.* 25, 148–175. doi: 10.1016/j.biotechadv.2006.11.007

Sznajder, A., Pfeiffer, D., and Jendrossek, D. (2015). Comparative proteome analysis reveals four novel polyhydroxybutyrate (PHB) granule-associated proteins in *Ralstonia eutropha* H16. *Appl. Environ. Microbiol.* 81, 1847–1858. doi: 10.1128/AEM.03791-14

Taidi, B., Mansfield, D. A., and Anderson, A. J. (1995). Turnover of poly(3-hydroxybutyrate) (PHB) and its influence on the molecular mass of the polymer accumulated by *Alcaligenes eutrophus* during batch culture. *FEMS Microbiol. Lett.* 129, 201–205. doi: 10.1111/j.1574-6968.1995.tb07580.x

Tajima, K., Han, X., Hashimoto, Y., Satoh, Y., Satoh, T., and Taguchi, S. (2016). *In vitro* synthesis of polyhydroxyalkanoates using thermostable acetyl-CoA synthetase, CoA transferase, and PHA synthase from thermotorelant bacteria. *J. Biosci. Bioeng.* 122, 660–665. doi: 10.1016/j.jbiosc.2016.06.001

Tajima, K., Han, X., Satoh, Y., Ishii, A., Araki, Y., Munekata, M., et al. (2012). *In vitro* synthesis of polyhydroxyalkanoate (PHA) incorporating lactate (LA) with a block sequence by using a newly engineered thermostable PHA synthase from Pseudomonas sp. SG4502 with acquired LA-polymerizing activity. *Appl. Microbiol. Biotechnol.* 94, 365–376. doi: 10.1007/s00253-011-3840-z

Tanaka, K., Ishizaki, A., Kanamaru, T., and Kawano, T. (1995). Production of poly (D-3-hydroxybutyrate) from CO2, H2, and O2 by high cell density autotrophic cultivation of *Alcaligenes eutrophus*. *Biotechnol. Bioeng.* 45, 268–275.

Tanaka, K., Miyawaki, K., Yamaguchi, A., Khosravi-Darani, K., and Matsusaki, H. (2011). Cell growth and P(3HB) accumulation from CO2 of a carbon monoxide-tolerant hydrogen-oxidizing bacterium, Ideonella sp. O-1. *Appl. Microbiol. Biotechnol.* 92, 1161–1169. doi: 10.1007/s00253-011-3420-2

Tieu, K., Perier, C., Caspersen, C., Teismann, P., Wu, D.-C., Yan, S.-D., et al. (2003). D-β-Hydroxybutyrate rescues mitochondrial respiration and mitigates features of Parkinson disease. *J. Clin. Invest.* 112, 892–901. doi: 10.1172/JCI18797

Tokiwa, Y., and Ugwu, C. U. (2007). Biotechnological production of (R)-3-hydroxybutyric acid monomer. *J. Biotechnol.* 132, 264–272. doi: 10.1016/j.jbiotec.2007.03.015

Tseng, H.-C. C., Harwell, C. L., Martin, C. H., and Prather, K. L. J. L. (2010). Biosynthesis of chiral 3-hydroxyvalerate from single propionate-unrelated carbon sources in metabolically engineered *E. coli*. *Microb. Cell Fact.* 9:96. doi: 10.1186/1475-2859-9-96

Tseng, H. C., Martin, C. H., Nielsen, D. R., and Prather, K. L. J. (2009). Metabolic engineering of *Escherichia coli* for enhanced production of (R)- And (S)-3-hydroxybutyrate. *Appl. Environ. Microbiol.* 75, 3137–3145. doi: 10.1128/AEM.02667-08

Tsuge, Y., Kawaguchi, H., Sasaki, K., and Kondo, A. (2016). Engineering cell factories for producing building block chemicals for bio-polymer synthesis. *Microb. Cell Fact.* 15:19. doi: 10.1186/s12934-016-0411-0

Uchino, K., Saito, T., Gebauer, B., and Jendrossek, D. (2007). Isolated poly(3-hydroxybutyrate) (PHB) granules are complex bacterial organelles catalyzing formation of PHB from acetyl coenzyme A (CoA) and degradation of PHB to acetyl-CoA. *J. Bacteriol.* 189, 8250–8256. doi: 10.1128/JB.00752-07

Uchino, K., Saito, T., and Jendrossek, D. (2008). Poly(3-hydroxybutyrate) (PHB) depolymerase PhaZa1 is involved in mobilization of accumulated PHB in *Ralstonia eutropha* H16. *Appl. Environ. Microbiol.* 74, 1058–1063. doi: 10.1128/AEM.02342-07

Ueda, H., and Tabata, Y. (2003). Polyhydroxyalkanonate derivatives in current clinical applications and trials. *Adv. Drug Deliv. Rev.* 55, 501–518. doi: 10.1016/S0169-409X(03)00037-1

Ugwu, C. U., Tokiwa, Y., Aoyagi, H., Uchiyama, H., and Tanaka, H. (2008). UV mutagenesis of *Cupriavidus necator* for extracellular production of (R)-3-hydroxybutyric acid. *J. Appl. Microbiol.* 105, 236–242. doi: 10.1111/j.1365-2672.2008.03774.x

Ugwu, C. U., Tokiwa, Y., and Ichiba, T. (2011). Production of (R)-3-hydroxybutyric acid by fermentation and bioconversion processes with *Azohydromonas lata*. *Bioresour. Technol.* 102, 6766–6768. doi: 10.1016/j.biortech.2011.03.073

Volova, T., Shishatskaya, E., Sevastianov, V., Efremov, S., and Mogilnaya, O. (2003). Results of biomedical investigations of PHB and PHB/PHV fibers. *Biochem. Eng. J.* 16, 125–133. doi: 10.1016/S1369-703X(03)00038-X

Wang, B., Xiong, W., Yu, J., Maness, P.-C., and Meldrum, D. R. (2018). Unlocking the photobiological conversion of CO 2 to (R)-3-hydroxybutyrate in cyanobacteria. *Green Chem.* 20, 3772–3782. doi: 10.1039/C8GC01208C

Wang, F., and Lee, S. (1997). Poly(3-Hydroxybutyrate) production with high productivity and high polymer content by a fed-batch culture of Alcaligenes latus under nitrogen limitation. *Appl. Envir. Microbiol.* 63, 3703–3706.

Wang, L., Armbruster, W., and Jendrossek, D. (2007). Production of medium-chain-length hydroxyalkanoic acids from *Pseudomonas putida* in pH stat. *Appl. Microbiol. Biotechnol.* 75, 1047–1053. doi: 10.1007/s00253-007-0920-1

Wang, S. Y., Wang, Z., Liu, M. M., Xu, Y., Zhang, X. J., and Chen, G.-Q. (2010). Properties of a new gasoline oxygenate blend component: 3-Hydroxybutyrate methyl ester produced from bacterial poly-3-hydroxybutyrate. *Biomass Bioenergy* 34, 1216–1222. doi: 10.1016/j.biombioe.2010.03.020

Wang, Y., and Liu, S. (2014). Production of (R)-3-hydroxybutyric acid by *Burkholderia cepacia* from wood extract hydrolysates. *AMB Express* 4:28. doi: 10.1186/s13568-014-0028-9

Wang, Y.-W., Wu, Q., Chen, J., and Chen, G.-Q. (2005). Evaluation of three-dimensional scaffolds made of blends of hydroxyapatite and poly(3-hydroxybutyrate-co-3-hydroxyhexanoate) for bone

reconstruction. *Biomaterials* 26, 899–904. doi: 10.1016/j.biomaterials.2004.03.035

Windhorst, C., and Gescher, J. (2019). Efficient biochemical production of acetoin from carbon dioxide using *Cupriavidus necator* H16. *Biotechnol. Biofuels* 12:163. doi: 10.1186/s13068-019-1512-x

Witholt, B., and Kessler, B. (1999). Perspectives of medium chain length poly(hydroxyalkanoates), a versatile set of bacterial bioplastics. *Curr. Opin. Biotechnol.* 10, 279–285. doi: 10.1016/S0958-1669(99)80049-4

Woolston, B. M., Emerson, D. F., Currie, D. H., and Stephanopoulos, G. (2018). Rediverting carbon flux in *Clostridium ljungdahlii* using CRISPR interference (CRISPRi). *Metab. Eng.* 48, 243–253. doi: 10.1016/j.ymben.2018.06.006

Worm, B., Lotze, H. K., Jubinville, I., Wilcox, C., and Jambeck, J. (2017). Plastic as a persistent marine pollutant. *Annu. Rev. Environ. Resour.* 42, 1–26. doi: 10.1146/annurev-environ-102016-060700

Yamanashi, T., Iwata, M., Kamiya, N., Tsunetomi, K., Kajitani, N., Wada, N., et al. (2017). Beta-hydroxybutyrate, an endogenic NLRP3 inflammasome inhibitor, attenuates stress-induced behavioral and inflammatory responses. *Sci. Rep.* 7:7677. doi: 10.1038/s41598-017-08055-1

Yamane, T., Fukunaga, M., Lee, Y. W. (1996). Increased PHB productivity by high-cell-density fed-batch culture ofAlcaligenes latus, a growth-associated PHB producer. *Biotechnol. Bioeng.* 50, 197–202. doi: 10.1002/(SICI)1097-0290(19960420)50:2<197::AID-BIT8>3.0.CO;2-H

Yishai, O., Lindner, S. N., Gonzalez de la Cruz, J., Tenenboim, H., and Bar-Even, A. (2016). The formate bio-economy. *Curr. Opin. Chem. Biol.* 35, 1–9. doi: 10.1016/j.cbpa.2016.07.005

Yokaryo, H., Teruya, M., Hanashiro, R., Goda, M., and Tokiwa, Y. (2018). Direct production of (R)-3-hydroxybutyric acid of high optical purity by Halomonas sp. OITC1261 under aerobic conditions. *Biotechnol. J.* 13, 1–6. doi: 10.1002/biot.201700343

Yun, E. J., Kwak, S., Kim, S. R., Park, Y. C., Jin, Y. S., and Kim, K. H. (2015). Production of (S)-3-hydroxybutyrate by metabolically engineered *Saccharomyces cerevisiae*. *J. Biotechnol.* 209, 23–30. doi: 10.1016/j.jbiotec.2015.05.017

Zhang, J., Cao, Q., Li, S., Lu, X., Zhao, Y., Guan, J.-S., et al. (2013). 3-Hydroxybutyrate methyl ester as a potential drug against Alzheimer's disease via mitochondria protection mechanism. *Biomaterials* 34, 7552–7562. doi: 10.1016/j.biomaterials.2013.06.043

Zhang, X., Luo, R., Wang, Z., Deng, Y., and Chen, G.-Q. (2009). Application of (R)-3-hydroxyalkanoate methyl esters derived from microbial polyhydroxyalkanoates as novel biofuels. *Biomacromolecules* 10, 707–711. doi: 10.1021/bm801424e

Zhao, K., Tian, G., Zheng, Z., Chen, J. C., and Chen, G. Q. (2003). Production of D-(-)-3-hydroxyalkanoic acid by recombinant *Escherichia coli*. *FEMS Microbiol. Lett.* 218, 59–64. doi: 10.1016/S0378-1097(02)01108-4

Zheng, J., and Suh, S. (2019). Strategies to reduce the global carbon footprint of plastics. *Nat. Clim. Change* 9, 374–378. doi: 10.1038/s41558-019-0459-z

Zheng, Z., Gong, Q., and Chen, G. (2004). Novel method for production of 3-hydroxydecanoic acid by recombinant *Escherichia coli* and *Pseudomonas putida*. *Chinese J. Chem. Eng.* 12, 550–555.

Conflict of Interest: The authors declare that the research was conducted in the absence of any commercial or financial relationships that could be construed as a potential conflict of interest.

frontiers in Bioengineering and Biotechnology

REVIEW
published: 30 April 2020
doi: 10.3389/fbioe.2020.00386

The Modification of Regulatory Circuits Involved in the Control of Polyhydroxyalkanoates Metabolism to Improve Their Production

*Claudia Velázquez-Sánchez[1], Guadalupe Espín[1], Carlos Peña[2] and Daniel Segura[1]**

[1] Departamento de Microbiología Molecular, Instituto de Biotecnología, Universidad Nacional Autónoma de México, Cuernavaca, Mexico, [2] Departamento Ingeniería Celular y Biocatálisis, Instituto de Biotecnología, Universidad Nacional Autónoma de México, Cuernavaca, Mexico

Poly-(3-hydroxyalkanoates) (PHAs) are bacterial carbon and energy storage compounds. These polymers are synthesized under conditions of nutritional imbalance, where a nutrient is growth-limiting while there is still enough carbon source in the medium. On the other side, the accumulated polymer is mobilized under conditions of nutrient accessibility or by limitation of the carbon source. Thus, it is well known that the accumulation of PHAs is affected by the availability of nutritional resources and this knowledge has been used to establish culture conditions favoring high productivities. In addition to this effect of the metabolic status on PHAs accumulation, several genetic regulatory networks have been shown to drive PHAs metabolism, so the expression of the PHAs genes is under the influence of global or specific regulators. These regulators are thought to coordinate PHAs synthesis and mobilization with the rest of bacterial physiology. While the metabolic and biochemical knowledge related to the biosynthesis of these polymers has led to the development of processes in bioreactors for high-level production and also to the establishment of strategies for metabolic engineering for the synthesis of modified biopolymers, the use of knowledge related to the regulatory circuits controlling PHAs metabolism for strain improvement is scarce. A better understanding of the genetic control systems involved could serve as the foundation for new strategies for strain modification in order to increase PHAs production or to adjust the chemical structure of these biopolymers. In this review, the regulatory systems involved in the control of PHAs metabolism are examined, with emphasis on those acting at the level of expression of the enzymes involved and their potential modification for strain improvement, both for higher titers, or manipulation of polymer properties. The case of the PHAs producer *Azotobacter vinelandii* is taken as an example of the complexity and variety of systems controlling the accumulation of these interesting polymers in response to diverse situations, many of which could be engineered to improve PHAs production.

Keywords: polyhydroxyalkanoates, global regulation, *Azotobacter vinelandii*, gene regulation, biopolymers

OPEN ACCESS

Edited by:
Manuel Benedetti, University of L'Aquila, Italy

Reviewed by:
David Bernard Levin, University of Manitoba, Canada
Ignacio Poblete-Castro, Andres Bello University, Chile

***Correspondence:**
Daniel Segura
daniel@ibt.unam.mx

Specialty section:
This article was submitted to Industrial Biotechnology, a section of the journal Frontiers in Bioengineering and Biotechnology

Received: *07 December 2019*
Accepted: *07 April 2020*
Published: *30 April 2020*

Citation:
Velázquez-Sánchez C, Espín G, Peña C and Segura D (2020) The Modification of Regulatory Circuits Involved in the Control of Polyhydroxyalkanoates Metabolism to Improve Their Production. Front. Bioeng. Biotechnol. 8:386. doi: 10.3389/fbioe.2020.00386

INTRODUCTORY REMARKS

Petrochemical plastics are materials widely used in industry and daily life. The excessive use of such synthetic materials poses detrimental effects on the environment because they are non-biodegradable and accumulate in the ecosystems. To deal with this problem, biodegradable plastics have emerged as an alternative to replace petrochemical plastics.

Polyhydroxyalkanoates (PHAs) are among the natural biodegradable plastics under research. These are polyesters composed by (R)-hydroxyalkanoate monomers which are synthesized by a wide number of bacterial species as a carbon and energy reserve material. Besides biodegradable, PHAs are biocompatible and structurally diverse, with more than 150 different kinds of (R)-hydroxyalkanoate monomers composing them (Steinbüchel and Lütke-Eversloh, 2003). According to the number of carbon atoms in their monomeric units, PHAs have been classified as short chain length (C4 and C5; scl-PHAs) and medium chain length (≥C6; mcl-PHAs) (Aldor and Keasling, 2003).

This variety of monomers represents an advantage over other biopolymers because it allows having diverse material properties. PHAs have the most variable melting temperatures (Tm), glass-transition temperatures (Tg), and thermodegradation temperatures (Td), with mechanical properties including a very flexible Young's modulus, elongation at break and tensile strength (Chen, 2010; Volova et al., 2013).

The diversity of PHAs is possible because the polymerizing enzymes producing them, PHA synthases, have a broad substrate range (Stubbe et al., 2005). In addition, the substrate monomers can be synthesized from different metabolic routes, depending on the microbial species used and the carbon source provided (reviewed in Lu et al., 2009; Chen, 2010; Panchal et al., 2013).

In the case of PHB, the homopolymer composed of the C4 3-hydroxyalkanoic acid 3-hydroxybutyrate (an scl-PHA), the biosynthesis starts with two molecules of acetyl-CoA that condense, forming acetoacetyl-CoA due to the activity of 3-ketothiolase (*phbA* gene). Acetoacetyl-CoA is then reduced by an acetoacetyl-CoA reductase (encoded by *phbB*) using NADPH and producing 3-hydroxybutyryl-CoA. Finally, the 3-hydroxybutyryl-CoA monomers are polymerized by a PHA synthase (*phbC* gene) (Lenz and Marchessault, 2005).

Poly-(3-hydroxyalkanoates) composed of C6–C16 3-hydroxy-alkanoic acids or mcl-PHAs, are generally produced from carbon sources structurally related to these monomers. In this case, the (R)-3-hydroxyacyl-CoAs precursor monomers come from β-oxidation of alkanes, alkanols or alkanoic acids (Kniewel et al., 2019). This requires producing the (R)-hydroxyacyl-CoA isomer (substrate for polymerization by the PHA synthase), instead of the (S)-hydroxyacyl-CoA normally produced during β–oxidation, by the activity of enzymes like the alternative enoyl-CoA hydratase encoded by *phaJ* (Tsuge et al., 2003). mcl-PHAs can also be produced from acetyl-CoA in several *Pseudomonas* species. In this case, the (R)-3-hydroxyacyl-CoAs are generated from (R)-3-hydroxyacyl-ACP intermediates of the *de novo* fatty acid biosynthesis, by the activities of an (R)-3-hydroxyacyl-ACP thioesterase (encoded by *phaG*) and an (R)-3-hydroxyacyl-CoA ligase, allowing the synthesis of mcl-PHAs from non-related carbon sources, like carbohydrates (Wang et al., 2012; Hokamura et al., 2015).

Under certain conditions, the PHAs accumulated are degraded by poly(3-hydroxyalkanoate) depolymerase enzymes (gene *phaZ*) producing biosynthetic precursors and reducing equivalents (Sznajder and Jendrossek, 2011).

Because of their biodegradability and their manufacture from renewable resources, commercial production of PHAs started in the 1980s by Imperial Chemical Industries, and later by several companies (Chen, 2009; Dietrich et al., 2017). These are used for the production of everyday items like containers, packaging films, coatings, bottles and other disposable items like razors, diapers, cups, bags, lids, etc. (Chen, 2009). Due to their biocompatibility and ability to maintain human cell growth, PHAs are also under research for many biomedical applications such as medical devices (stents, sutures, cardiovascular devices, nerve repair devices and wound dressing), tissue engineering scaffolds, drug-delivery systems, dental materials, etc. (Panchal et al., 2013).

Although the use of PHAs as plastic materials for bulk applications represents a benefit for the environment, wide utilization of these polymers at the industrial level is still limited, mainly due to their high production costs that lead to a high price in comparison to conventional plastics. PHAs can cost between United States $2.25–2.75/lb, which is 3 to 4 times higher than polymers like PE and PP (Kourmentza et al., 2017). These costs are due in part to the high price of the substrates used, complex downstream processing, and the cultivation strategies using discontinuous batch or two-step cultivation and fed-batch cultivation modes, that impact productivity (Choi and Lee, 1997; Kourmentza et al., 2017). These cultivation strategies are needed because PHAs accumulation is usually promoted when there is excess carbon in the medium, but under limitation of a nutrient essential for growth (Koller et al., 2010); therefore, a cultivation phase favoring growth must be implemented first to reach high cell density (needed for an intracellular product), followed by a growth-limiting PHAs production phase. This requirement of nutrient limitation is, in many cases, controlled by genetic regulatory mechanisms that coordinate PHAs production with the rest of the metabolism; therefore, modification of these regulatory circuits could help modify this necessity, improving productivity and as a consequence, production costs.

The existence of some bacteria able to produce PHAs during growth, with little or no requirement of growth-limiting conditions (reported for *Azotobacter vinelandii, Alcaligenes latus, Pseudomonas putida* LS46, *Methylobacterium* sp. ZP24, *Bacillus mycoides* RLJ B-017 and recombinant *Escherichia coli*) (Choi and Lee, 1997; Koller et al., 2010; Blunt et al., 2019), shows that is possible to have growth-associated production, thus enabling the implementation of more efficient cultivation strategies. Therefore, a better understanding of physiological conditions and the genetic regulatory mechanisms restricting PHAs synthesis during optimal growth could be exploited to improve productivity. Also, the advances in the knowledge of PHAs biosynthesis have led to the development of improved strains for the more efficient production of PHAs and the production of novel polymers, and also will allow the engineering

of PHAs producers through the use of synthetic biology methods (Jung et al., 2010; Chen et al., 2016; Chen and Jiang, 2017, 2018). However, in these strategies, the modification of the regulatory circuits controlling PHAs synthesis is generally not considered. In the future of strain modification not only the metabolic networks but also the regulatory circuits controlling them can be optimized to achieve improved performance in PHAs production (Jung et al., 2010). For this, a better understanding of the regulatory mechanisms involved is needed.

REGULATORY MECHANISMS CONTROLLING PHAs METABOLISM

Control of Enzymatic Activity

Bacteria control PHAs metabolism in response to environmental or nutritional conditions. This is done through diverse regulatory mechanisms. In *Ralstonia eutropha*, the model organism for scl-PHAs metabolism (Reinecke and Steinbüchel, 2009), the main genes involved in PHB metabolism (*phaA, phaB, phaC, phaR,* and *phaZa1*) seem to be constitutive and do not show significant changes in their transcripts levels throughout the cell cycle (Lawrence et al., 2005; Brigham et al., 2012; Sharma et al., 2016). However, one possibility of regulation is the control of enzyme activity. In fact, the first mechanisms described for the control of PHB synthesis was the allosteric regulation of the β-ketothiolase biosynthetic enzyme and of enzymes of the tricarboxylic acid cycle. Both *R. eutropha* (Haywood et al., 1988; Oeding and Schlegel, 1973) and *Azotobacter beijerinckii* (Senior and Dawes, 1973), showed inhibitory action by free CoA (most of it produced in the TCA cycle) on the β-ketothiolase condensation reaction, and of NAD(P)H on enzymes of the TCA cycle, proving that PHB metabolism is in part controlled by the redox state of the cell and the availability of carbon (intracellular levels of acetyl-CoA and free CoA), showing a central role for oxygen limitation in the control of PHB metabolism.

More recently, allosteric regulation was also found to participate in the control of PHAs metabolism in the mcl-PHAs producer *P. putida* GPo1. In this bacterium, Ren et al. (2009) analyzed the granule-bound proteins and showed that PHA polymerase (PhaC), PHA depolymerase (PhaZ) and an acyl-CoA synthetase (ACS1) are present simultaneously, and this could constitute a futile cycle. By studying enzymatic activities of some of these proteins, they found that the PhaC synthase is sensitive to the ratio of [R-3-hydroxyacyl-CoA]/[CoA], and free CoA is a moderate competitive inhibitor. On the other hand, the fatty acid oxidation complex (which is a provider or consumer of the 3-hydroxyacyl-CoA precursors or products), is affected by the [acetyl-CoA]/[CoA] and [NADH]/[NAD] ratios, with high ratios resulting in accumulation, whereas low ratios lead to oxidation of 3-hydroxyacyl-CoA. These results led them to conclude that PHAs accumulation is regulated by the [acetyl-CoA]/[CoA] and [NADH]/[NAD] ratios (Ren et al., 2009). Other allosteric regulatory effects exerted by key metabolites have been documented in other bacteria (Trotsenko and Belova, 2000).

Another example showing control at the level of enzyme activity was found in *Synechococcus* sp. In this cyanobacterium, PHB accumulation responds to nitrogen limitation, even in the presence of acetyl-CoA flux; PHB rapidly accumulates when transferred to nitrogen limiting conditions under light. This synthesis correlates with the appearance of PHB synthase activity in cell extracts, due to a post-translational activation of this enzyme mediated by acetyl phosphate. Because acetyl-phosphate is synthesized from acetyl-CoA through the activity of phosphotransacetylase, which is present only under nitrogen limitation, this enzyme acts as a switch indicating acetyl-CoA flux and acting as a signal of C:N balance (Miyake et al., 1997).

In *Rhodospirillum rubrum* PHB degradation is controlled at the level of enzymatic activity by an activator compound present in the cells. The activator compound was identified as a granule associated protein (phasin) named ApdA (activator of polymer degradation), that interacts with the surface of the granule and the PHA depolymerase, activating PHB degradation (Handrick et al., 2004).

A different mechanism for the regulation of PHAs metabolism, also through the control of enzyme activity, was reported in *R. eutropha* by Juengert et al. (2018). The constitutive presence of PHB synthase and PHB depolymerase during the different stages of growth led these authors to hypothesize that in order to avoid a futile cycle, their activities should be somehow regulated. Because covalent modification of enzymes by phosphorylation is a known way to modify their activities, they looked for phosphorylated residues in the PhaC1 synthase and the PHB depolymerase PhaZa1 during PHB accumulation and PHB degradation. Several phosphosites were identified in both enzymes, and phosphorylation of PhbC was dependent on the growth phase. Mutagenesis of the phosphorylatable residues showed that these modifications can affect their activities, so phosphorylation of these enzymes could also be part of the regulation of PHAs metabolism.

Participation of Global Regulators in the Control of PHAs Metabolism

Coordination between PHAs metabolism with the rest of bacterial metabolism involves some global regulators. Examples have been described in diverse bacteria, and in some cases, interesting additional physiological changes have been reported to occur when altering these regulators. A brief summary of these regulators follows. The effects of modifications of these regulatory systems on PHA accumulation are summarized in **Table 1**.

Alternative Sigma Factors in the Control of PHAs Metabolism

For transcriptional regulation, the selectivity of RNA polymerase is controlled by interaction with two types of regulatory proteins: sigma factors and transcription factors (Ishihama, 2012). The utilization of sigma factors alternative to the housekeeping σ70 provides a mechanism for bacterial responses to many stresses, by redirecting transcription initiation to the simultaneous regulation of large numbers of genes. Among these alternative sigma factors, RpoS increases under conditions of nutrient stress, or during the stationary phase, leading to general stress resistance (Battesti et al., 2011). PHB accumulation and mobilization are related to the nutrient status of bacteria (López et al., 2015),

TABLE 1 | Regulatory systems controlling PHAs metabolism in diverse bacteria and the effect of their modification.

Type of regulator	Bacterial species	Regulatory element	Effect on PHAs production/ accumulation	Growth conditions	References
Alternative sigma factors	*R. eutropha* H16 *P. putida* KT2440	RpoS	Deletion of *rpoS* increased PHAs mobilization during stationary phase.	Shake flasks. *R. eutropha* H16: Minimal medium, N-replete, no C source (PHB utilization medium). *P. putida* KT2440: Minimal medium, sodium octanoate.	Raiger-Iustman and Ruiz, 2008; Brigham et al., 2012
	P. aeruginosa PA14 and PAO1 *A. vinelandii* UW *P. chlororaphis* PA23	RpoS	Inactivation of *rpoS* had a negative effect on PHAs accumulation.	Shake flaks. *P. aeruginosa* PA14 and PAO1: Minimal medium, fructose. *A. vinelandii* UW: Minimal medium, N-limiting, sucrose. *P. chlororaphis* PA23: Minimal medium N-replete, glucose or octanoic acid.	Choi et al., 2011; Hernández-Eligio et al., 2011; Sharma et al., 2018
	P. putida KT2440	RpoN	Inactivation of *rpoN* increased PHAs accumulation 40% on octanoate but not gluconate.	Shake flasks. Minimal medium, N-limiting, octanoate or oleate.	Hoffmann and Rehm, 2004; Mozejko-Ciesielska et al., 2017
	P. aeruginosa PAK-N1	RpoN	Inactivation of *rpoN* abrogated PHAs synthesis on all conditions tested.	Shake flasks. Minimal medium, N-limiting or N-replete, gluconate or octanoate.	Hoffmann and Rehm, 2004
	Synechocystis sp. PCC 6803	SigE	Overexpression of *sigE* increased 2.3 times PHB production.	Minimal medium, N-limiting, glucose.	Osanai et al., 2013
Two-component system	*Synechocystis* sp. PCC 6803	Rre37	Overexpression of *rre*37 doubled PHB production.	Minimal medium, N-limiting, glucose.	Osanai et al., 2014
	A. brasilense SP7 *H. seropedicae* SmR1 *P. denitrificans* PD1222	NtrB NtrC	The *ntrB, ntrC* and/or *ntrBC* mutants produced higher amounts of PHB continuously during growth on N-replete conditions.	Batch fermentation or shake flasks. *A. brasilense* SP7: minimal medium, different concentrations of N, malate as C source. *H. seropedicae* SmR1: minimal medium, different concentrations of N on malate, glucose, fructose or xylose. *P. denitrificans* PD1222: mineral-salt medium, N-replete, succinate.	Sun et al., 2000; Sacomboio et al., 2017; Olaya-Abril et al., 2018
	P. putida CA-3 *P. putida* KT2442 *P. chlororaphis* PA23 *A. vinelandii* ATCC 9046	GacS	Disruption of the GacS sensor kinase had a negative effect on PHAs accumulation.	*P. putida* CA-3 and KT2442: PHAs not quantified. *P. chlororaphis* PA23: Mineral salt medium, N-replete, glucose or octanoate. *A. vinelandii* UW: mineral-salt medium, N-limiting with sucrose.	Castañeda et al., 2000; Ryan et al., 2013; Prieto et al., 2016; Sharma et al., 2018
Small RNAs	*S. meliloti* 2011	MmgR	Inactivation of *mmgR* increased PHB production 20% during stationary phase.	Mineral salt medium, N-limiting and surplus of sucrose.	Lagares et al., 2017.
	A. vinelandii UW136	RsmA	Inactivation of *rsmA* increased 25% PHB accumulation.	Shake flasks. Mineral-salt medium, N fixing conditions on sucrose.	Hernández-Eligio et al., 2012.
	*A. vinelandii*UW136	ArrF	Disruption of *arrF* gene reduced accumulation of PHB 75%.	Shake flasks. Mineral-salt medium, N fixing conditions on sucrose.	Muriel-Millán et al., 2014.

(Continued)

TABLE 1 | Continued

Type of regulator	Bacterial species	Regulatory element	Effect on PHAs production/ accumulation	Growth conditions	References
	A. vinelandii KCTC 23243	ArrF	Deletion of *arrF* gene increased accumulation of PHB 300-fold.	Shake flasks. Mineral-salt medium, N-replete on sucrose.	Pyla et al., 2009.
Stringent response	*R. etli* CE3	Rsh	Bacteroids with *rsh* gene inactivated were unable to accumulate PHB.	In symbiosis with *Phaseolus vulgaris*.	Calderón-Flores et al., 2005.
	R. eutropha H16	SpoT1 SpoT2	Stains unable to synthesize (p)ppGpp accumulated minor amounts of PHB, whereas increasing (p)ppGpp levels caused a 40% higher PHB accumulation.	Shake flasks. Nutrient broth with sodium gluconate.	Juengert et al., 2017.
	P. putida KT2440	RelA SpoT	A *relA*/*spoT* mutant accumulated mcl-PHAs in both optimal and nitrogen limiting conditions.	Shake flasks. Mineral-salt medium, N-replete and N-limiting, oleate.	Mozejko-Ciesielska et al., 2017
	P. chlororaphis PA23	RelA SpoT	Inactivation of *relA*/*spoT* decreases PHAs accumulation and changes monomeric composition of PHAs.	Mineral salt medium, N-replete, glucose or octanoate.	Sharma et al., 2018
Quorum sensing	*R. sphaeroides* 2.4.1	CerR CerI	Inactivation of *cerR*/*cerI* QS circuit accumulates a 2-fold higher content of PHB throughout aerobic growth.	Shake flasks. Mineral salt medium, succinate.	Kho et al., 2003
	P. chlororaphis PA23	AHL-deficient strain	Disruption of QS regulatory circuit decreases PHAs accumulation and changes the monomer composition of PHAs synthesized.	Shake flasks. Mineral salt medium, glucose or octanoate.	Mohanan et al., 2019
Oxygen-sensitive regulation	*P. extremaustralis* DSM 17835 *P. chlororaphis* PA23	Anr	Inactivation of *anr* decreases PHB accumulation under aerobic and microaerobic conditions.	Batch cultures or shake flasks. *P. extremaustralis* DSM 17835: Mineral-salt medium, octanoate and nitrate, with or without casein amino acids (CAS). *P. chlororaphis* PA23: Mineral-salt medium, glucose or octanoate.	Tribelli et al., 2010; Mohanan et al., 2019
	H. seropedicae SmR1	Fnr	A triple Fnr mutant showed a 50% reduction on PHB accumulation under low oxygen tension.	Shake flasks. NFbHPN-Malate mineral-salt medium, N-replete.	Batista et al., 2018
	A. vinelandii UW136	CydR	Inactivation of *cydR* increases accumulation of PHB during exponential growth phase.	Shake flasks. Mineral-salt medium, N-replete, glucose.	Wu et al., 2001
Phosphotransferase system	*A. vinelandii* UW136 *P. putida* KT2440	PTS^{Ntr}	Mutations producing a non-phosphorylated form of $EIIA^{Ntr}$, reduced PHAs accumulation. Inactivation of *ptsN* increased PHAs accumulation.	Shake flasks. *A. vinelandii* UW136: Peptone-yeast extract sucrose medium or mineral-salt medium, nitrogen fixing, sucrose. *P. putida* KT2440: Minimal SALT medium, octanoate.	Segura and Espín, 1998; Velázquez et al., 2007; Noguez et al., 2008
	R. eutropha H16	PEP-PTS PTS^{Ntr}	Absence of EI and/or HPr decreased PHB content. Inactivation of *ptsN* increased PHB accumulation.	Batch cultures or shake flasks. Mineral-salts medium N-replete, gluconate or glycerol.	Pries et al., 1991; Kaddor and Steinbüchel, 2011; Kaddor et al., 2012

(Continued)

TABLE 1 | Continued

Type of regulator	Bacterial species	Regulatory element	Effect on PHAs production/ accumulation	Growth conditions	References
Other transcriptional regulators	*P. putida* KT2442	Crc	*crc* inactivation increased two times PHAs accumulation during exponential growth. Volumetric production increased 65%.	N-replete conditions. LB medium, octanoate as extra-carbon source.	La Rosa et al., 2014
	P. putida KT2442	PsrA	PsrA inactivation reduced PHAs accumulation 16 to 54%. More active β-oxidation. Higher content of shorter chain length monomers.	Mineral salt medium, N-limiting, octanoate, decanoate, glucose, fructose and succinate.	Fonseca et al., 2014
Direct PHAs-regulators	*Pseudomonas* sp. 61-3 *A. vinelandii*UW136	PhbR[a]	PhbR directly regulates *phbBAC* operon. Inactivation of *phbR* diminished PHB production. Overexpression of *phbR* in *Pseudomonas* sp. 61-3 enhanced PHB biosynthesis.	Shake flasks. *Pseudomonas* sp. 61-3: mineral-salt medium, N-limited, gluconate, octanoate, dodecanoate, or tetradecanoate. *A. vinelandii* UW136: Shake flasks. Mineral-salt medium nitrogen fixing, sucrose.	Matsusaki et al., 1998; Segura et al., 2000
	P. putida GPo1 *P. putida* U *P. putida* KT2442	PhaD	PhaD directly regulates *phaC* and *phaIF* operons. Inactivation of *phaD* reduced PHAs production and affected the number and the size of PHAs granules.	Shake flasks. NE2 mineral salt medium, octanoate. M63 mineral salt medium, N-limited, octanoate.	Klinke et al., 2000; Sandoval et al., 2007; de Eugenio et al., 2010b
Granule-associated regulators	*P. denitrificans* ATCC 17741 *R. eutropha* H16 *S. meliloti* *R. etli* CE3 *B. diazoefficiens* *R. sphaeroides* FJ1	PhaR (AniA) (rhizobia species)	PhaR is not a direct PHAs-synthesis regulator, although in *R. etli*, mutations in this gene decreased ≈40% the PHAs synthesis.	*R. etli* CE3: Shake flasks. Mineral salt medium, pyruvate.	Maehara et al., 1999; Povolo and Casella, 2000; York et al., 2002; Chou et al., 2009; Quelas et al., 2016
	P. putida KT2442	PhaF[b]	PhaF is not a direct PHAs-synthesis regulator, binds DNA in a non-specific manner. Involved in segregation of granules between daughter cells during cell division.	Shake flasks. M63 mineral salt medium N-limited, octanoate.	Galán et al., 2011

[a]: PhbR is a member of the AraC/XylS family, not related to PhaR (AniA). [b]: Although PhaF, like PhaR, is able to bind to DNA and granules, its amino acid sequence shows no similarity to PhaR.

so RpoS has a role in the regulation of PHAs metabolism in some bacteria (Brigham et al., 2012).

In *R. eutropha*, inactivation of *rpoS* induced no change during PHB production, however, it exhibited an increased PHB depolymerization when polymer utilization was induced, in comparison to the wild-type strain H16. Therefore, RpoS was proposed to have a role in PHB utilization (Brigham et al., 2012).

A similar role was found in *P. putida* (Raiger-Iustman and Ruiz, 2008). In this organism inactivation of *rpoS* had no effect in PHAs accumulation, however, when entering the stationary phase, the polymer content of the mutant diminished faster than in the wild type, resulting in a lower PHAs accumulation. The transcript containing *phaC*1 and *phaZ* (coding for one of the two PHA synthases present in this bacterium and the PHA depolymerase) was overexpressed in the stationary phase, probably causing a higher depolymerization activity. The authors concluded that RpoS participates in the negative regulation of the promoter of *phaC*1-*phaZ*, probably in an indirect manner and suggested that PhaD, a transcriptional regulator of the TetR family, could be an intermediary.

In *Pseudomonas aeruginosa,* Choi et al. (2011) reported that *rpoS* inactivation in PA14 and PAO1 strains showed a strong negative effect on PHAs accumulation when grown on fructose, however, on decanoic acid, only the PA14 mutant showed a similar negative effect. These results suggest RpoS sigma factor participates in the transcription of some PHAs biosynthetic genes with differences depending on the strain. It is interesting to note that, besides the observed effect on the amount of polymer accumulated, inactivation of *rpoS* shifted the monomeric composition of the PHAs to longer hydroxyalkanoates (Choi et al., 2011). PHAs depolymerization has also been linked to *rpoS* expression and to tolerance to oxidative and thermal stresses, through an unknown mechanism (Ruiz et al., 2004). This could be related to the reported need of PHB utilization for ATP and ppGpp synthesis (Ruiz et al., 2001), or as part of the role that PHAs metabolism has in stress resistance in several bacteria (López et al., 2015).

The role of sigma factor RpoS has also been elucidated in *A. vinelandii* UW136. In this bacterium, the synthesis of PHB occurs mainly during the stationary growth phase. Accordingly, RpoS was shown to participate in the transcription of the PHB biosynthetic operon *phbBAC* and of *phbR,* which codes for the transcriptional activator of the *phb* genes (Hernández-Eligio et al., 2011).

In *Pseudomonas chlororaphis* PA23, inactivation of *rpoS* negatively affected the amount of PHAs, due to down-regulation of *phaC*1, *phaC*2, and the two phasin genes *phaF* and *phaI* (Sharma et al., 2018).

Because the alternative sigma factor RpoN (sigma 54) is involved in the regulation of nitrogen metabolism and nitrogen limitation induces PHAs biosynthesis, the participation of this sigma factor on the accumulation of these polymers was evaluated in *P. putida* KT2440 and in *P. aeruginosa* PAK by Hoffmann and Rehm (2004, 2005). They studied PHAs accumulation in the wild type and *rpoN*-negative mutant strains of these bacteria under nitrogen excess or nitrogen limitation. In *P. aeruginosa*, inactivation of *rpoN* abrogated PHAs accumulation on gluconate and octanoate, suggesting that RpoN participates in the expression of a gene involved in PHAs metabolism. The expression of transacylase PhaG (now reclassified as a 3-hydroxyacyl-ACP tioesterase), needed for the biosynthesis of PHAs from carbohydrates, was found to be inducible under nitrogen limitation in both species and was dependent on RpoN in *P. aeruginosa,* but not in *P. putida* (Hoffmann and Rehm, 2004). It was also suggested that RpoN is a negative regulator of *phaF,* which was thought to be a negative regulator of *phaC*1 (Hoffmann and Rehm, 2005). In the case of *P. putida* KT2440 it is interesting to note that, although *rpoN* inactivation had no effect on PHAs accumulation on gluconate, it increased their accumulation 40% on octanoate, reaching the highest accumulation in these experiments (Hoffmann and Rehm, 2004). A similar result was obtained by Mozejko-Ciesielska et al. (2017) while analyzing the effect of *rpoN* inactivation in the same *P. putida* strain. They also found a significant increase in the accumulation of mcl-PHAs in the *rpoN* mutant when growing on octanoate under nitrogen limitation. Therefore, the inactivation of *rpoN* could be further studied as a candidate for strain improvement in *P. putida*, which is the model bacterium for mcl-PHA synthesis.

Another example illustrating the participation of an alternative sigma factor on the control of PHB metabolism is found in the non-nitrogen-fixing cyanobacterium *Synechocystis* sp. PCC 6803 (Osanai et al., 2013). In this microorganism, PHB accumulation increases under phosphorous or nitrogen starvation. Transcription levels of PHB biosynthetic genes increase after nitrogen depletion. Coincidentally, the expression of the sigma factor named SigE also increased under this condition. A strain overexpressing *sigE* showed higher mRNA levels of the *phb* biosynthetic genes, with respect to those of the wild type, during the nitrogen-replete stage. This overexpression of *sigE* also increased the levels of the PHB biosynthetic enzymes during nitrogen limitation. This strategy increased 2.4 times the accumulation of PHB (Osanai et al., 2013).

Also in *Synechocystis* sp. PCC 6803, the response regulator Rre37 of a two-component system, has been shown to participate in the control of PHB accumulation (Osanai et al., 2014). This protein plays a role in carbon metabolism because the overexpression of *rre*37 up-regulated genes related to sugar catabolism, under both nitrogen-replete and nitrogen-depleted conditions and decreased glycogen accumulation. The expression of the *phb* biosynthetic genes was also up-regulated by Rre37, mainly under nitrogen depletion, and almost doubled PHB accumulation. Interestingly, overexpression of both Rre37 and SigE further increased PHB accumulation to 2.9 times. The Mr and monomer composition of PHB were not altered by the double overexpression of SigE and Rre37. Thus, Rre37 is a regulatory protein that changes the metabolic flow from glycogen to polyhydroxybutyrate and is probably participating in the same regulatory circuit with SigE, through an unknown mechanism. Besides suggesting the participation of sigma factor SigE and Rre37 in the control of transcription of the *phb* biosynthetic genes, these are good examples of how changing the regulatory networks affecting PHB metabolism can be a powerful approach, because not only the genes participating in

PHB accumulation altered their expression when overexpressing *sigE* or *rre37*, but a whole set of genes related with carbon metabolism (glycogen catabolism), among other changes, so PHB production improvement was due to a higher expression of the *phb* genes, but also to a change in carbon distribution from glycogen to PHB (Osanai et al., 2013, 2014). It is noteworthy that increasing the enzymatic activities involved in the synthesis of PHAs by introducing the biosynthetic genes of *R. eutropha* into *Synechocystis* 6803 did not really enhance PHB accumulation, suggesting this is not the only rate-limiting point for PHB synthesis (Sudesh et al., 2002).

PsrA, a positive regulator of *rpoS* expression that also represses the fatty acid β-oxidation operon *fadBA*5 in *P. aeruginosa* (Kojic and Venturi, 2001; Kang et al., 2008), has been implicated in the fatty acid - PHA metabolic network in *P. putida* KT2440. In this bacterium, inactivation of *psrA* reduced PHAs accumulation between 16 and 54%, depending on the carbon source. This effect was explained as a consequence of a more active β-oxidation pathway induced by the *psrA* inactivation, although direct regulation of *pha* genes by PsrA or changes in their expression caused by a negative effect on *rpoS* expression, were not ruled out. In fact, overexpression of *phaC*2 gene was observed in the *psrA* mutant. Interestingly, a change in the composition of the polymers was also observed in this mutant, with a higher content of short chain length monomers (Fonseca et al., 2014).

Control by the Stringent Response

Because PHAs in many organisms are produced under conditions of nutritional limitation, and adaptation to nutrient deprivation is mediated in many bacteria by the so-called stringent response (Boutte and Crosson, 2013), the participation of this stress response regulatory mechanism in the control of PHAs metabolism has been analyzed in several bacteria (López et al., 2015). Stringent response mediates adaptation to changes in nutrient availability by reprograming transcription of a high percentage of genes. This response is mediated by the nucleotides guanosine tetraphosphate (ppGpp) and guanosine pentaphosphate (pppGpp), the so-called alarmone, whose levels are controlled by the enzymes RelA (ppGpp synthetase), and SpoT (ppGpp synthetase/hydrolase) (Boutte and Crosson, 2013).

The first report showing a possible connection between stringent response and PHAs metabolism was found in *P. aeruginosa* GPo1 through the analysis of a *phbZ* minus mutant (Ruiz et al., 2001). It was shown that utilization of the PHB reserve is needed for the proper synthesis of ppGpp, and this, in turn, has an effect on stress resistance to ethanol and high temperature, however, no regulatory relationships between stringent response and PHAs metabolism were demonstrated.

Later, the analysis of a *Rhizobium etli* mutant unable to accumulate (p)ppGpp, showed that it was affected in amino acids and nitrate utilization, nodulation, nitrogen fixation and also was unable to accumulate PHB (Calderón-Flores et al., 2005).

In *R. eutropha*, the role of stringent response was investigated by inactivating the (p)ppGpp synthetase/hydrolase and (p)ppGpp synthetase genes of this bacterium. Double mutants, unable to synthesize (p)ppGpp, accumulated a minor amount of PHB, whereas unusually high levels of this polymer were obtained in a strain with increased levels of (p)ppGpp, generated by overexpression of the (p)ppGpp synthase SpoT2 in the absence of (p)ppGpp hydrolase. The artificial induction of stringent response through the addition of the amino acid analogs norvaline or serine hydroxamate, increased the contents of PHB during the stationary phase. Therefore, a positive correlation between the amount of ppGpp and the accumulation of PHB was suggested. The composition of the polymer was not affected by the induction of the stringent response. The authors concluded that the concentrations of (p)ppGpp affect PHB accumulation by negatively regulating PHB depolymerization, and suggested this could be done through allosteric regulation and covalent modification of the enzymes involved. They identified the main PHB depolymerase PhaZa1 as the target for this control (Juengert et al., 2017).

In *P. putida* KT2440 accumulation of PHAs is also induced under nitrogen limiting conditions. Interestingly, disruption of strict response by the inactivation of *relA* and *spoT* genes eliminated the need for nitrogen limitation, so the polymers were accumulated to the same level under both conditions. The *relA/spoT* mutant was able to accumulate 2.8 times the PHAs produced by the wild-type strain under no nitrogen limitation (Mozejko-Ciesielska et al., 2017). However, lower accumulation of PHAs was observed under nitrogen limitation, in comparison to the wild-type strain. In this case, the expression of the PHA depolymerase gene (*phaZ*) was lower in the absence of (p)ppGpp and could explain in part the phenotype observed. This altered regulation could be further investigated in order to promote PHAs accumulation under culture conditions allowing growth to high cell densities, with no need for a change to nutritional limitation to start producing the polymers.

More recently, a report in *P. chlororaphis* PA23, a bacterium used for biocontrol, showed that mutations in the regulatory genes *relA/spoT* significantly decreased PHAs accumulation, and also resulted in altered PHAs gene expression. In this study, it was shown that the two PHA synthase genes *phaC*1, *phaC*2, and the two phasin genes *phaF*, and *phaI* were also significantly down-regulated in *gacS* and *rpoS* mutants, reducing the amount of PHAs (Sharma et al., 2018). Interestingly, this work illustrates that the modification of stringent response and of other regulatory circuits can also change the monomeric composition of PHAs. For the three regulatory mutants (*relA/spoT, gacS*, *rpoS*), the PHAs produced on glucose contained significantly higher amounts of 3-hydroxyhexanoate and/or 3-hydroxyoctanoate, and the content of 3-hydroxydecanoate was lower, as compared to the parental strain. For the PHAs synthesized on octanoate, only in the case of the *gacS* mutant the monomer composition changed (Sharma et al., 2018).

Regulation by Quorum Sensing

Bacterial quorum sensing (QS) is a communication process that involves self-produced extracellular signaling molecules, called autoinducers, which can accumulate into levels that are required to collectively alter global patterns of gene expression (Papenfort and Bassler, 2016). The bioluminescent marine bacterium *Vibrio harveyi* is a good example of a canonical QS circuit, with a LuxR-type receptor that detects autoinducers. This bacterium

is capable to synthesize PHB only at a high cell density and this production is positively controlled by the LuxR-autoinducers circuit (Sun et al., 1994; Miyamoto et al., 1998). Although the exact molecular mechanism is unknown, it is proposed that *V. harveyi* autoinducer leads to the increased expression of *luxR*; the LuxR activator in turn stimulates at high cell density the expression of PHB synthesis and luminescence (Miyamoto et al., 1998). Similarly, the physiological implication of PHB synthesis in relation to the luminescence is not clear, but it is possible that the polymer in *V. harveyi* serves as an energy source for maintaining cell viability in the stationary growth phase.

Interestingly, it has been found that the PHB synthesis of *Rhodobacter sphaeroides*, a facultative photosynthetic bacterium, is controlled in a manner analogous to the induction of cell luminescence. However, unlike the positive regulation of the PHB synthesis of *V. harveyi*, the PHB synthesis of *R. sphaeroides* is under negative regulation. In this bacterium, the *cerR/cerI* QS circuit codes for LuxR-type regulator and the enzyme that synthesize the autoinducer molecule, respectively (Ye et al., 2013). Under aerobic growth conditions, mutations in the *cerR/cerI* genes resulted in a 2-fold increase in the cellular PHB content, with respect to the wild type, and this increase is coincidental with a proportional increase of the PHB synthase enzymatic activity. Moreover, the transcriptional levels of *phaC* gene were also 2-fold higher than the corresponding values of the wild type (Kho et al., 2003). The potential of mutations in *cerR/cerI* genes has not been fully explored.

Another example illustrating the participation of QS in the control of PHA gene expression is found in *P. chlororaphis* PA23. There are three distinct QS regulatory circuits in this bacterium, PhzRI, CsaRI, and AurRI, but only the Phz system has been characterized. An AHL-deficient strain (comparable to a triple *phzI*/*csaI*/*aurI* QS mutant) resembles stringent response-defective *P. chlororaphis* PA23: it shows a significantly decreased PHAs accumulation, a radical change in PHAs composition, and down-regulation of *phaC*1, *phaZ*, *phaC*2, *phaD*, *phaF*, and *phaI*. The search for regulatory sequences in these genes revealed the presence of a region with 15/20 conserved nucleotides upstream of *phaZ* and *phzF*, named "*phz*-box"; nevertheless, direct QS regulation of *phaZ* and *phaF* has not been demonstrated (Mohanan et al., 2019).

Control by Oxygen Responsive Regulators

In addition to the previously described allosteric regulatory mechanism controlling PHB synthesis in response to oxygen limitation in *R. eutropha* (Oeding and Schlegel, 1973) and *A. beijerinckii* (Senior and Dawes, 1973), other mechanisms for the control by oxygen have been described, but operate at the level of transcription.

In *Pseudomonas extremaustralis* PHB production is induced under micro aerobic and anaerobic cultures. The redox transcriptional regulator Anr (Fnr-like), which regulates several genes during the transition from aerobic to anaerobic growth, is involved in this control. The Anr protein contains a [4Fe-4S]$^{+2}$ cluster that suffers oxidation, changing its DNA binding affinity, thus sensing the redox state of the cell. Inactivation of *anr* decreased expression of *phaC* and *phaR* (coding for the transcriptional regulator of *pha* biosynthetic genes) and PHB production under aerobic and micro aerobic conditions. The presence of two putative binding sites in the regulatory region of these genes suggested a direct regulation of transcription of these genes by Anr (Tribelli et al., 2010).

In *Herbaspirillum seropedicae* SmR1, a nitrogen-fixing endophyte, where PHB has an important role in the maintenance of the intracellular redox balance, it was found that two of the three Fnr regulators encoded in this bacterium control expression of the *phaC* synthase gene. A triple Fnr mutant showed a 50% reduction on PHB accumulation under low oxygen tension, with respect to the wild-type strain (Batista et al., 2018).

A role for Anr in the control of mcl-PHA metabolism has also been shown in *P. chlororaphis* PA23. Inactivation of *anr* significantly reduced PHAs accumulation, although their monomeric composition was not drastically changed. Although expression of *phaC*1, *phaZ*, *phaC*2, *phaD*, *phaF*, and *phaI* genes related to PHAs metabolism was analyzed, only *phaF* showed a significant reduction in the mutant; nevertheless, Anr-recognition sequences were not found upstream of *phaF* (Mohanan et al., 2019).

The participation of an Fnr homolog (CydR) in the control of PHB metabolism in response to oxygen has also been reported in *A. vinelandii*, where this transcriptional regulator seems to be a repressor of the biosynthetic genes (Wu et al., 2001). This regulation is further described in section "Regulation of PHB Synthesis in *Azotobacter*."

Control by Phosphate Limitation Through PhoB

In *Acinetobacter* sp. PHB accumulation is induced by phosphate starvation and a regulatory mechanism has been proposed. Schembri et al. (1995) showed that phosphate limitation induces transcription of the *pha* biosynthetic locus. The presence of two potential Pho-box consensus sequences, upstream of two transcription start points, and the requirement of PhoB (the *pho* regulon activator) and phosphate limitation for the expression of these transcripts, showed direct positive regulation of these genes by the transcriptional regulator PhoB under phosphate limitation.

The Carbon Catabolite Regulator Crc

Control by the global regulator Crc has been demonstrated in *P. putida* KT2442 (La Rosa et al., 2014). Crc is a protein that in *Pseudomonas* has a key role in carbon catabolite repression, a process that allows to first assimilate a preferred carbon source among a mixture of several compounds. Crc acts post-transcriptionally by binding to its target mRNAs on motifs close to their ribosome binding site, affecting translation (Rojo, 2010). In *P. putida*, La Rosa et al. (2014) showed that Crc links PHAs metabolism with the regulatory networks controlling carbon utilization. They identified a Crc binding motif on the PHA synthase gene *phaC*1 mRNA, and demonstrated that Crc inhibits *phaC*1 mRNA translation and not transcription. They also showed that the activity of this regulator is affected both by the carbon source present and by the C/N ratio of the medium. This is carried out by the antagonist small RNAs CrcZ and CrcY, which sequester Crc and the expression of

these RNAs is higher under conditions in which PHAs synthesis is high and Crc is strongly antagonized. They also reported that Crc negatively controls PHAs synthesis when growing in media with a balanced carbon/nitrogen ratio. Under unbalanced carbon/nitrogen conditions (where PHAs synthesis is allowed), Crc had no activity. Interestingly, in the *P. putida crc* negative mutant, the requirement for nitrogen limitation for polymer synthesis was lost, allowing to accumulate the same percentage of PHAs under nitrogen replete conditions. In LB medium with octanoate, the highest accumulation percentages and also the highest PHAs volumetric production were obtained with the *crc* mutant, eliminating the need to restrict growth by limiting nitrogen (La Rosa et al., 2014). Therefore, this is another example of the potential benefits of modifying the regulatory systems controlling PHAs metabolism for strain improvement.

The Two-Component System NtrB-NtrC

NtrB and NtrC proteins are the sensor kinase (NRII) and the response regulator (NRI) of a two-component regulatory system that in diverse bacteria is a key player in the control of expression of many genes of nitrogen metabolism (van Heeswijk et al., 2013). These regulators are also involved in the regulation of PHB in some bacteria.

In *Azospirillum brasilense* SP7, PHB production is inhibited by the presence of high ammonia concentration. Inactivation of *ntrB* or *ntrC* considerably increased PHB accumulation (up to 9-fold) on different C/N ratios. The *ntrB* or *ntrC* mutants couple PHB production and growth, producing PHB both during the growth phase and stationary phase. The absence of these regulators eliminates the inhibitory effect of ammonia, and interestingly, greatly diminished the respiration of *A. brasilense* (Sun et al., 2000). All these phenotypes show that NtrB and NtrC somehow regulate PHB metabolism; therefore, the corresponding mutants are interesting starting strains for future improvements.

In *H. seropedicae* SmR1, an *ntrC* mutant was also shown to accumulate higher levels of PHB than the wild type (up to 2-fold increase). The inactivation was found to increase the activity of glucose-6-phosphate dehydrogenase (a reaction producing NADPH), leading to a 2.1-fold increase in the NADPH/NADP + ratio. This increase in NADPH was proposed to cause the increased synthesis of the polymer (Sacomboio et al., 2017).

The NtrB regulator of *Paracoccus denitrificans* PD1222 was also shown to somehow regulate PHB accumulation. In this bacterium inactivation of *ntrB* induced the overproduction of the polymer (5-fold), when growing on nitrate, and also increased expression of the PHA synthase gene *phaC*. An interesting metabolic change was also observed. The acetyl-CoA concentration increased 4-fold in the *ntrB* mutant. Therefore, the increased accumulation of PHB in this mutant was a combination of the effect on *phb* gene expression with the induction of a metabolic change caused by altering the regulatory network (Olaya-Abril et al., 2018).

The Two-Component System GacS-GacA

Many other transcriptional regulatory systems have been reported to participate in the control of PHAs metabolism. One very interesting is the GacS-GacA two-component system, where GacS functions as a sensor histidine kinase protein that phosphorylates GacA, which is the response regulator that when phosphorylated activates transcription of its target genes. The GacS-GacA system is conserved in gram-negative bacteria. Its participation in the control of PHB metabolism was discovered in *A. vinelandii* while looking for regulators of alginate synthesis, because inactivation of *gacS* had a negative effect on the synthesis of this polysaccharide, but also on PHB accumulation (Castañeda et al., 2000). It was shown later that phosphorylated GacA is a positive regulator of PHB synthesis, *rpoS* expression (Castañeda et al., 2001), and for the expression of the small regulatory RNAs RsmZ/Y, that interact with the translational regulatory protein RsmA (Manzo et al., 2011). This regulation is further described in section "Regulation of PHB Synthesis in *Azotobacter*."

In *P. putida* CA-3 the participation of the GacS-GacA on the control of mcl-PHAs metabolism was found by random mini-Tn5 mutagenesis. A mutant unable to accumulate PHAs had disrupted the *gacS* gene. Transcription of the regulatory small RNAs RsmY and RsmZ, known to be regulated by GacS-GacA in other *Pseudomonas*, was not affected in the *gacS* mutant. Transcription of the PHA synthase *phaC*1 was also unaffected, but evidence of a lower content of the synthase enzyme suggested a post-transcriptional control (Ryan et al., 2013). In *P. putida* KT2442, inactivation of the sensor kinase GacS also reduced PHAs accumulation, but in this case, a reduction in the transcription rate of the PHAs gene cluster was observed and this was restored by expressing PhaD, an activator of the *pha* genes discussed in section "PhaD" (Prieto et al., 2016).

As previously mentioned, in *P. chlororaphis* PA23 inactivation of *gacS* strongly decreased PHAs accumulation and this correlated with a considerably diminished expression of genes *phaC*1, *phaC*2, *phaD, phaF, phaI* and *phaZ*. Interestingly, the *gacS* mutation also changed the monomeric composition of the mcl-PHAs produced by this bacterium (Sharma et al., 2018).

Regulatory Small RNAs

Small non-coding RNAs (sRNAs) play important regulatory roles in bacteria. Many of them act as antisense RNAs on multiple target mRNAs, other sRNAs act by binding to proteins, some of them regulatory, affecting their activity (Gottesman and Storz, 2011).

In the regulation of PHB metabolism, some examples of regulation by small RNAs have been documented. Free-living *Sinorhizobium meliloti* cells accumulate PHB under nitrogen-limiting conditions. For that reason, Lagares et al. (2017) studied a small RNA called MmgR (Makes more granules Regulator), whose expression is regulated by the amount of nitrogen source. They found that MmgR negatively regulates PHB accumulation under conditions of N starvation and C surplus. Inactivation of *mmgR* gene increased PHB production by 20% with respect to the wild type, without affecting growth. The increase in PHB was even higher when using higher C/N ratios. The overproduction occurred during the stationary phase, but not during the exponential growth, so PHB production was still affected by nutrient limitation. The *mmgR* mutation increased the number of granules and also resulted in the overexpression

of two phasin proteins. So, MmgR sRNA participates in the regulation of PHB accumulation in this bacterium, through an unknown mechanism. This mutation is another candidate for further studying its potential to improve PHB production.

A regulatory small RNA called ArrF has been implicated in the regulation of PHB accumulation in response to iron in *A. vinelandii* (Pyla et al., 2009; Muriel-Millán et al., 2014). Iron-limiting conditions increase PHB accumulation in this bacterium (Page, 1982). The ArrF RNA participates in this regulation by affecting translation of its target, the mRNA of *phbR,* through complementary binding, although the effects of this interaction probably differ between strains (Pyla et al., 2009; Muriel-Millán et al., 2014). This is further described in section "Regulation of PHB Synthesis in *Azotobacter*."

In *Pseudomonadaceae*, the non-coding small RNAs called RsmZ/Y/X regulate secondary metabolism and carbon storage (Lapouge et al., 2008). These RNAs, together with the RsmA protein, constitute a system of post-transcriptional regulation where RsmA acts as a translational repressor by binding to its mRNA targets, and the small RNAs counteract this repression through binding to RsmA. In *A. vinelandii*, inactivation of *rsmA* results in increased PHB production, because RsmA represses translation of the PHB biosynthetic operon *phbBAC* and of the *phbR* gene that codes for its transcriptional activator. At least two of the eight small RNAs present in this bacterium (RmZ1 and RsmZ2) have been shown to specifically bind RsmA and counteract this repression (Manzo et al., 2011; Hernández-Eligio et al., 2012). This regulation and its connection with the GacS/GacA two-component system will be described in section" Regulation of PHB Synthesis in *Azotobacter*."

The PTS^{Ntr} Regulatory System

Another regulatory mechanism controlling the synthesis of PHB is carried out by the nitrogen-related phosphotransferase system (PTS^{Ntr}). The participation of this system in the control of PHB synthesis was first reported in *A. vinelandii* (Segura and Espín, 1998). This system is homologous to the carbohydrate PTS used in many bacteria for uptake and phosphorylation of different sugar substrates. PTS^{Ntr} is present in most gram-negative bacteria and is composed of EI^{Ntr}, Npr and EIIA^{Ntr} proteins encoded by the *ptsP, ptsO* and *ptsN* genes, respectively. These proteins participate in a phosphorylation cascade where EIIA^{Ntr} seems to be the final phospho-acceptor. The PTS^{Ntr} seems to be exclusively involved in regulatory functions (Pflüger-Grau and Görke, 2010). In *P. putida,* inactivation of PTS^{Ntr} components reduced the synthesis of PHAs by increasing the level of unphosphorylated EIIA^{Ntr} (Velázquez et al., 2007). In a similar way, *A. vinelandii* mutants where EIIA^{Ntr} is present in an unphosphorylated form are unable to produce PHB (Segura and Espín, 1998; Noguez et al., 2008). The mechanism by which the PTS^{Ntr} system regulates the synthesis PHB has been widely investigated in *A. vinelandii* and is described in section "Regulation of PHB Synthesis in *Azotobacter*."

An interesting connection between PTS^{Ntr} and the stringent response was found in *R. eutropha* (Karstens et al., 2014). In an attempt to clarify the role of PTS^{Ntr} in the control of PHB metabolism in this bacterium, these authors screened for proteins able to interact with EIIA^{Ntr}. The bifunctional ppGpp synthase/hydrolase SpoT1 was shown to interact, but only with the unphosphorylated form of EIIA^{Ntr}. This could, in turn, alter the ppGpp levels, thus affecting PHB formation and the expression of genes responsive to this alarmone. A role for PTS^{Ntr} in the control of (p)ppGpp levels has also been described in *Caulobacter crescentus,* although its relation with PHAs metabolism was not investigated (Ronneau et al., 2016).

The participation in the control of PHB metabolism, not of the PTS^{Ntr} system, but of proteins of the sugar-specific-PTS system, has been documented in *R. eutropha* (Pries et al., 1991). Inactivation of *ptsH* or *ptsI* genes, coding for the components of the PTS, Enzyme I (EI) and the histidine phosphocarrier protein (HPr), respectively, caused a lower accumulation of PHB. These mutants showed a higher rate of PHB degradation, so the authors proposed that the PTS could be controlling, by phosphorylation, the activity of the PHB mobilizing enzymes or the affinity of a regulatory element controlling them (Pries et al., 1991). Later, Kaddor et al. (2012) reported a proteome analysis of a *ptsHI* double mutant of *R. eutropha* and showed that these mutations caused a down-regulation of the PHB biosynthetic acetoacetyl-CoA reductase and of two phasin proteins; also enzymes of central catabolism (Entner-Doudoroff pathway, the tricarboxylic acid cycle) were down-regulated in the mutant, whereas enzymes of gluconeogenesis showed enhanced expression in the mutant. Together, these changes explained the PHB-leaky phenotype observed.

It is interesting to point out that the permease components (EIIB and EIIC proteins/domains) that together with EI and Hpr proteins constitute a complete PTS for the transport of carbohydrates are not present in *R eutropha*, so EI and Hpr are likely to be involved in regulatory functions of carbon and PHB metabolism (Kaddor and Steinbüchel, 2011). Strikingly, this bacterium also lacks *ptsP* and *ptsO* genes of the PTS^{Ntr}, but has a homologous to *ptsN* (IIA^{Ntr}, H16_A0384) (Kaddor and Steinbüchel, 2011; Kaddor et al., 2012*)*. Inactivation of *ptsN* increased PHB accumulation, as in *A vinelandii*, and *P. putida* (Kaddor and Steinbüchel, 2011), and phosphorylation of EIIA^{Ntr} through EI and Hpr has been shown and it favors PHB accumulation (Krausse et al., 2009).

Specific Regulators of PHAs Metabolism

In different bacteria, some regulators specifically controlling the expression of *pha* genes, have been described. Here, we review the main transcriptional regulators reported.

PhbR

The genes encoding proteins involved in PHAs synthesis are often located in conserved PHAs gene clusters, depending if the bacteria are scl- or mcl-PHA producers. In some PHB-producing bacteria, like *A. vinelandii* (Peralta-Gil et al., 2002), *Azotobacter* FA8 (Pettinari et al., 2001), *Pseudomonas* sp. strain 61-3 (Matsusaki et al., 1998), and *Pseudomonas* sp. USM 4-55 (Tan et al., 2010), the *phbA*, *phbB* and *phbC* genes are clustered in the same *locus* and are organized in a single transcriptional unit. In all these cases, upstream of the *phbBAC* operon and in the opposite direction, the gene called *phbR* is located.

This gene codes for a member of the AraC/XylS family of transcriptional regulators, with a typical DNA binding domain helix-turn-helix (HTH). It is important to note that Matsusaki et al. (1998) reported for the first time the similarity between PhbR and other proteins belonging to the AraC family, such as OruR of *P. aeruginosa* and the virulence-associated regulator of *Mycobacterium tuberculosis*; thus, the ORF was referred to as *phbR*, and it is not related to other regulators also called PhaR, that are discussed later. In *A. vinelandii* and *Pseudomonas* sp. strain 61-3 it was demonstrated that PHB biosynthesis is positively regulated by PhbR, which activates transcription of the *phbBAC* biosynthetic operon (Matsusaki et al., 1998; Peralta-Gil et al., 2002; Hernández-Eligio et al., 2011).

Although the majority of bacteria accumulate either scl-PHAs or mcl-PHAs, some of them, like *Pseudomonas* sp. strain 61-3, are able to synthesize and accumulate a blend of PHB homopolymer and a random P(3HB-co-3HA) copolymer. This is possible because these bacteria possess two types of PHAs biosynthetic gene loci. Interestingly, when the activator *phbR* was overexpressed *in trans*, *Pseudomonas* sp. strain 61-3 increased its polymer content (51%). Furthermore, the overexpression of *phbR* enhanced PHB biosynthesis in this bacterium, resulting in an increase of the polymer content and enrichment of the 3HB fraction in the whole polymer (94 mol%) (Matsusaki et al., 1998).

PhaD

Most *Pseudomonas* species belonging to the ribosomal RNA-homology group I synthesize mcl-PHAs, whose synthesis requires the proteins encoded by the *pha*C1*ZC*2*DFI* cluster. This cluster contains two polymerases (PhaC1 and PhaC2), a depolymerase (PhaZ), and three proteins (PhaDFI) involved in granule formation and in the regulation of gene expression. PhaD is a TetR-family transcriptional regulator that in *P. aeruginosa* GPo1 (formerly *Pseudomonas oleovorans* GPo1; Klinke et al., 2000; Ramos et al., 2005), *P. putida U* (Sandoval et al., 2007) and *P. putida* KT2440 (de Eugenio et al., 2010b), positively regulates PHAs synthesis. Inactivation of *phaD* reduces not only the production of the polymers, but also affects the size and number of the PHAs granules (Klinke et al., 2000). This regulation is performed in a direct manner, since PhaD binds to the promoter region of synthase *pha*C1*ZC*2*D* and *phaIF* operons, auto activating its expression and that of the other *pha* genes. This phenomenon is carbon source dependent, with higher activation on the preferred carbon source octanoate and this, together with 3D modeling of PhaD, allowed the authors to suggest the participation of a β-oxidation metabolite as an effector (de Eugenio et al., 2010b).

The finding that PhaD simultaneously activates expression of the PhaZ depolymerase and the PHA synthases is in agreement with the conclusion that synthesis and mobilization in *Pseudomonas* is a cyclic process allowing PHAs turnover to achieve a metabolic balance (de Eugenio et al., 2010a). However, knowledge about how this potentially futile cycle is regulated or balanced is relatively limited. As discussed in section "Control of Enzymatic Activity," this could be accomplished through allosteric control of the enzymes involved. PHA synthase and the fatty acid oxidation complex, the provider or consumer of 3-hydroxyacyl-CoAs (precursors or depolymerization products), are affected by metabolites like R-3-hydroxyacyl-CoA, free CoA, acetyl-CoA, NADH and NAD; thus, the balance of this cycle could be determined by the metabolic status of the cell (Ren et al., 2009). In bacteria like *R. eutropha*, where a similar situation of constitutive *phb* gene expression and PHB turnover also occur (Doi et al., 1990; Brigham et al., 2012), the control of this cycle seems to be achieved also by controlling enzyme activities, through allosteric regulation by the intracellular levels of acetyl-CoA and free CoA and its redox state (Oeding and Schlegel, 1973; Haywood et al., 1988). As mentioned in sections "Control of Enzymatic Activity" and "Control by the Stringent Response," the activities of the PHB synthase or PhaZa1 depolymerase can also be controlled by (p)ppGpp levels or through phosphorylation (Juengert et al., 2017, 2018).

Granule-Associated Regulators

When PHAs are synthesized, they accumulate as granules, which are composed of 97.5% PHA, 2% proteins, and some lipids (Jendrossek and Pfeiffer, 2014). Four types of proteins are found associated to the granules: structural proteins called phasins, PHA metabolism enzymes, like PHA synthases and depolymerases, and regulatory proteins (Pötter and Steinbüchel, 2005).

PhaR (PhaF, AniA)

The accumulation of PHAs granules in the cytoplasm of producing bacteria is strongly influenced by phasins, which are amphipathic low-molecular-weight proteins that influence the number and size of granules (Pötter and Steinbüchel, 2005). In several scl-PHA producing bacteria, the major phasin, designated PhaP, is negatively regulated by PhaR (also designated PhbF, PhaF or AniA), a DNA-binding regulator. The regulatory circuit in which PhaR participates has been well studied in *R. eutropha* and *P. denitrificans*. In these bacterial species, PhaR is able to bind to three different targets: the promoter region of *phaP*, the promoter region of its own gene, and the surface of the granules, so this regulator is a granule associated protein. It is proposed that when bacteria are not accumulating PHAs, the expression of *phaP* and *phaR* remains at basal level. In this scenario, the presence of PhaP is not needed and its expression is repressed by direct binding of PhaR to the *phaP* promoter region. The excessive production of PhaR is also repressed by autoregulation. Under favorable PHA-synthesis conditions, the cells start to accumulate PHAs and PhaR dissociates from DNA and binds to the new polymer chains, allowing the expression of *phaP*. As the PHAs synthesis continues, the granules enlarge in size, and their surfaces become covered with PhaP. If PHAs synthesis stops or degradation occurs predominantly, PhaR molecules are freed and bind to the upstream elements of both *phaP* and *phaR,* repressing their expression (Maehara et al., 1999, 2002; York et al., 2002; Pötter et al., 2002, 2005).

PhaR is also a repressor of *phaP* gene in the purple, non-sulfur bacterium *R. sphaeroides* FJ1, although it is not known if the regulatory mechanism is the same. It is expected to be similar, because *R. sphaeroides* PhaR binds to the promoter regions of *phaP* and *phaR*, repressing their expression (Chou et al., 2009; Chou and Yang, 2010).

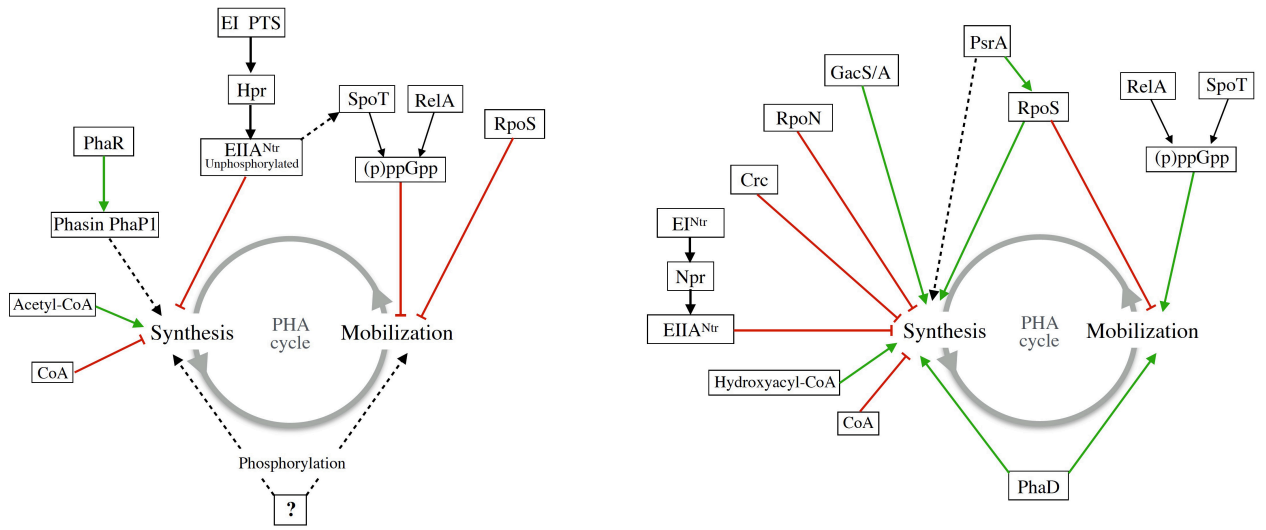

FIGURE 1 | Schematic diagram of the regulation of PHAs metabolism by global and specific regulatory systems in two model organisms: **(A)** the scl-PHA producer *Ralstonia eutropha* and **(B)** the mcl-PHA producer *Pseudomonas putida* KT2440. Green arrows indicate positive regulation and red lines negative regulation or effect. Dashed lines indicate unknown intermediates and unknown mechanism of regulation.

Homologs to PhaR (also known as *aniA* for anaerobically-induced gene A) were identified in rhizobia species, such as *S. meliloti* (Povolo and Casella, 2000); *R. etli* (Encarnación et al., 2002) and *Bradyrhizobium diazoefficiens* (Quelas et al., 2016). In *R. etli*, PhaR (AniA) is necessary for PHB synthesis, because a *phaR*:Tn5 mutant produced only around 40% the PHB level of the wild type; moreover, *phaR* inactivation caused a profound modification of global protein expression, which includes the disappearance of PhaB in proteome maps (Encarnación et al., 2002), suggesting that PhaR plays a more global regulatory role.

Even when in all these bacteria PhaR is not a direct PHA-synthesis regulator, knowledge about the regulation of expression of phasins might be important for establishing optimal conditions for PHAs production, both in natural PHA-producers or in recombinant bacteria. However, in *H. seropedicae* SmR1 PhaR has a wider role in the control of PHAs metabolism, because it binds to the regulatory regions of eleven genes, which include the phasin gene *phaP*1, but also the *pha* biosynthetic genes, acting on them as a repressor (Kadowaki et al., 2011). Surprisingly, the inactivation of *phaR* reduced PHB production 3.2-fold instead of increasing it, suggesting a role in the regulation of other genes important for PHB accumulation (Batista et al., 2016).

PhaF from Pseudomonas spp.

Two major granule-associated proteins, PhaF and PhaI, are found in the mcl-PHA producer *P. aeruginosa* GPo1 (Prieto et al., 1999). PhaF is a histone-H1-like protein, with two different domains, a DNA-binding domain at the C-terminus, and a phasin domain for PHA-binding, at the N-terminus. Although PhaF shares these bifunctional characteristics with PhaR from the scl-PHA producers (also named PhbF), the amino acid sequence of PhaF or PhaI showed no similarity to PhaR (Maehara et al., 2002); therefore, they are two different proteins with different functions. Early characterization of PhaF suggested that it represses the expression of *phaC*1 synthase, *phaI* and its own expression, because *phaF* mutants showed increased transcription of the *pha* cluster. The model proposed that PhaF could bind DNA, repressing the expression of *phaC*1 and *phaIF* operon, similarly to PhaR (Prieto et al., 1999). A more recent study showed that PhaF binds DNA in a non-specific manner and is involved in the segregation of granules between daughter cells during cell division (Galán et al., 2011).

As can be appreciated, the regulatory mechanisms implicated in the control of PHAs metabolism are diverse and can be different in different organisms. Most of them have not been fully characterized. In **Figure 1**, diagrams summarizing what is known in two different model organisms for PHAs production are shown.

REGULATION OF PHB SYNTHESIS IN *Azotobacter*

Azotobacter vinelandii is an scl-PHAs producing bacterium that synthesizes mainly PHB, although it can synthesize P(3HB-co-3HV) when valerate, heptanoate or nonanoate are added to the growth medium (Page et al., 1992). *A. vinelandii* can accumulate PHB up to 80% of the cell dry weight (Millán et al., 2017), and the polymer produced has a high molecular weight (6.6×10^6 Da) (Castillo et al., 2017). This bacterium can grow and produce PHB on several substrates, including organic acids, alcohols, sugars (Noar and Bruno-Bárcena, 2018) as well as low-cost substrates,

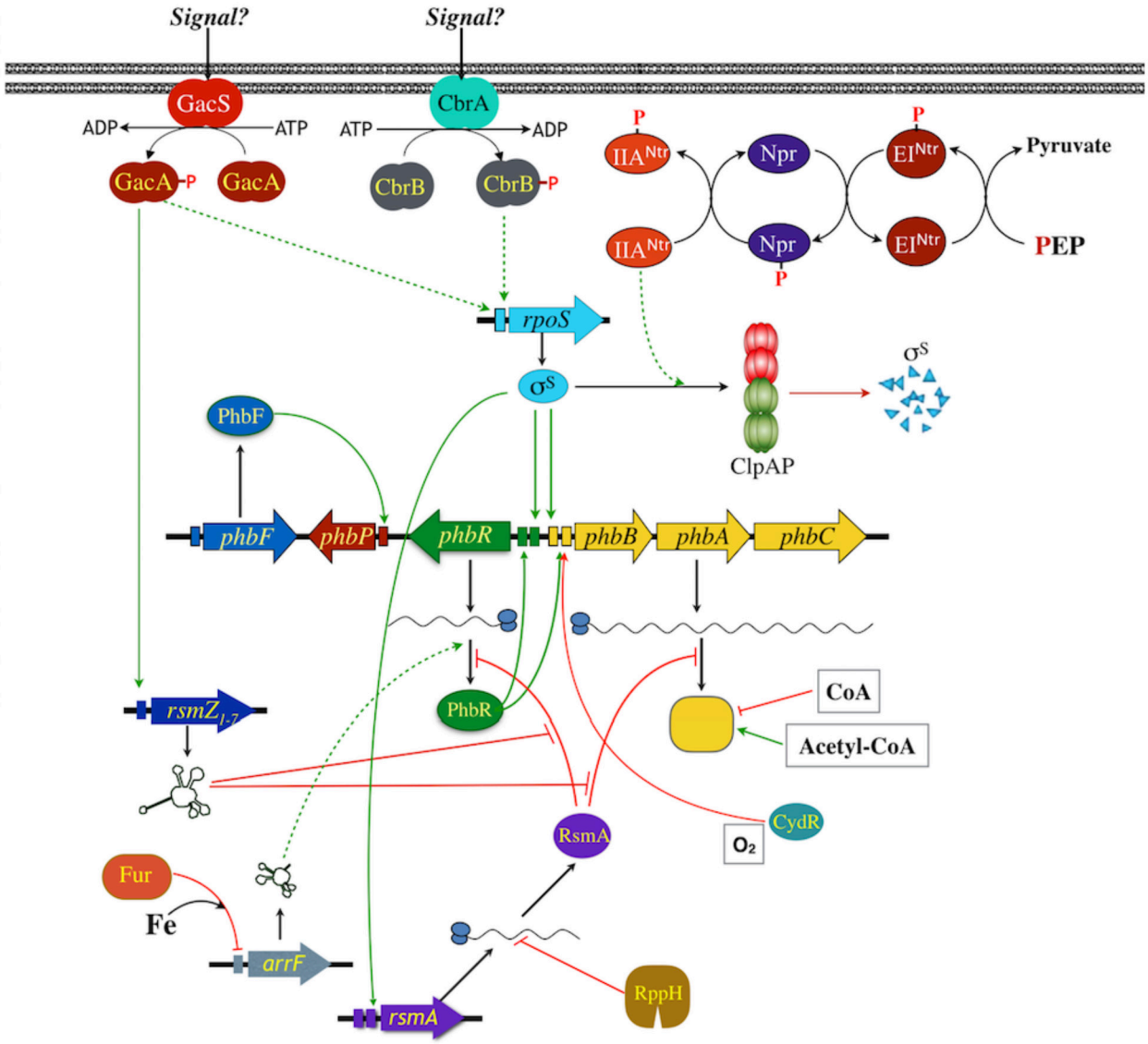

FIGURE 2 | Model for the regulation of *phbBAC* gene expression in *A. vinelandii*. Promoters are indicated as colored rectangles, two of them indicate two promoters identified. Positive regulation is indicated with green lines; red lines indicate negative regulation; dashed lines indicate unknown intermediates or mechanism.

like cane or beet molasses, corn syrup, malt extract, fish peptone and olive mill wastewater (Page, 1989, 1992a,b; Page et al., 1992; Page and Cornish, 1993; Chen and Page, 1994, 1997; Cho et al., 2001; Cerrone et al., 2010).

The allosteric regulation of the biosynthetic enzymes was reported in a species of this genus (*A. beijerinckii*) by Senior and Dawes (1973). This regulation was later confirmed to be similar in *A. vinelandii* UWD, where free CoA negatively regulated 3-ketothiolase, but this inhibition was overcome by acetyl-CoA (Manchak and Page, 1994).

Many details are known about the molecular genetics of PHAs production in *A. vinelandii* (**Figure 2**). The biosynthetic operon *phbBAC*, encoding the enzymes for PHAs synthesis has been characterized (Segura et al., 2000, 2003; Peralta-Gil et al., 2002). As was described previously, the *phbR* gene, encoding a transcriptional activator of the AraC family named PhbR, was identified upstream and in the opposite direction to the *phbBAC* operon. Inactivation of *phbR* reduced PHB accumulation and transcription of *phbBAC*. This operon is transcribed from two overlapping promoters (PB1 and PB2), where the −35 region of PB1 overlaps the −10 of PB2. PhbR was shown to bind specifically to a couple of almost identical 18 bp sites present in the *phbBAC* promoter region, and transcription from pB1 was shown to be activated by PhbR, whereas transcription from PB2 was shown to depend on RpoS sigma factor (Peralta-Gil et al., 2002; Hernández-Eligio et al., 2011).

With respect to transcription of *phbR*, it is also initiated from two promoters, pR1 and pR2 (Peralta-Gil et al., 2002).

Transcription from pR2 depends on RpoS (Hernández-Eligio et al., 2011). By using a *phbR:gusA* gene fusion it was shown that transcription of *phbR* is higher in the presence of a PhbR wild type copy, revealing a role for PhbR as auto-activator (Hernández-Eligio et al., 2011).

In addition to the regulation by PhbR and RpoS, the GacS-GacA two-component global regulatory system was shown to control PHB synthesis, as well as the production of other lipids and the polysaccharide alginate (Castañeda et al., 2000; Manzo et al., 2011; Romero et al., 2016; Trejo et al., 2017). The GacS-GacA system, formed by the GacS sensor kinase and the response regulator GacA, is conserved in gram-negative bacteria, and in the *Pseudomonadaceae* family, to which *Azotobacter* genus belongs, where it controls the expression of genes involved in secondary metabolism, phyto-pathogenesis and QS, among other processes. The regulation by GacS-GacA is mediated through a pathway known as Gac-Rsm (Lapouge et al., 2008), where GacA homologs activate the transcription of small regulatory RNAs named RsmZXY, that interact with a small protein named RsmA. The RsmA protein acts as a translational repressor through binding to its target mRNAs. Therefore, the interaction of RsmA with the RsmZXY RNAs counteracts its repressor activity.

Regarding the regulation of PHB synthesis in *A. vinelandii* by this system, it was first reported that mutations in either *gacS* or *gacA* genes impaired synthesis of this polymer (Castañeda et al., 2000, 2001), and later, that the Gac-Rsm pathway in *A. vinelandii* was composed by one RsmA protein and eight non-coding small RNAs, named RsmZ1–7 and RsmY (Manzo et al., 2011; Hernández-Eligio et al., 2012). Transcription of the *rsm* RNAs was shown to be dependent on GacA (Manzo et al., 2011; Hernández-Eligio et al., 2012) and at least two of these RNAs, RsmZ1, and RsmZ2, were shown to specifically bind RsmA (Manzo et al., 2011; Hernández-Eligio et al., 2012). Inactivation of *rsmA* increased PHB production and the RsmA protein was also demonstrated to bind to the predicted sites at the 5′ ends of the *phbR* and *phbBAC* mRNAs. Thus, RsmA binding to these transcripts represses their translation and also negatively affect their stability, and at least RsmZ1 and RsmZ2, counteract this repression (Hernández-Eligio et al., 2012).

Besides the control of RsmA activity through binding to the *rsm* RNAs, its expression is also regulated. RsmA expression in *A. vinelandii* is controlled both transcriptionally and post-transcriptionally. The CbrA/CbrB and Crc/Hfq regulatory systems participate in the phenomenon of carbon catabolite repression (CCR) in *Pseudomonas* spp. and *A. vinelandii* (Quiroz-Rocha et al., 2017b; Martínez-Valenzuela et al., 2018; for a recent review see Bharwad and Rajkumar, 2019). Inactivation of *cbrB* resulted in a reduction of the *rsmA* mRNA levels. The effect of CbrB on *rsmA* expression was proposed to be through the control of RpoS expression, because CbrA-CbrB is required for optimal levels of RpoS, and one of the promoters transcribing *rsmA* is RpoS dependent (Quiroz-Rocha et al., 2017a). However, the mechanism by which CbrB affects RpoS is still unknown.

With respect to the post-transcriptional control of RsmA expression, it was reported that its transcript is a substrate of an mRNA degradation pathway in which the pyrophosphohydrolase enzyme RppH participates (Bedoya-Pérez et al., 2018). Inactivation of *rppH* resulted in significantly lower levels of PHB, through a reduction in the expression of PhbR (at the translational level). This effect is through RsmA, because inactivation of its gene in the *rppH* mutant restored *phbR* expression and PHB synthesis, due to an increase in the level and stability of the *rsmA* transcript (Bedoya-Pérez et al., 2018). Thus, in summary, and as shown in **Figure 2**, GacA activates transcription of RsmZ RNAs, these RNAs bind to RsmA to prevent its binding to its target mRNAs that include the *phbR* and the *phbBAC* transcripts. The expression of RsmA, on the other hand, is controlled by an RNA degradation pathway with the participation of RppH.

As mentioned above, another regulatory mechanism controlling the synthesis of PHB in *A. vinelandii* is the nitrogen-related phosphotransferase system (PTS^{Ntr}; **Figure 2**). This is homologous to the carbohydrate PTS which in many bacteria transports and phosphorylates sugars and, in addition, participates in regulatory processes, such as carbon catabolite repression, chemotaxis, biofilm formation and virulence (Deutscher et al., 2014). PTS^{Ntr} is present in most gram-negative bacteria and is composed by EI^{Ntr}, Npr and $EIIA^{Ntr}$ proteins, encoded, respectively, by the *ptsP, ptsO* and *ptsN* genes. These components participate in a phosphorylation cascade starting from phosphoenolpyruvate, and ending with the final phospho-acceptor $EIIA^{Ntr}$. The PTS^{Ntr} seems to be exclusively involved in regulatory functions (Pflüger-Grau and Görke, 2010). Another difference between carbohydrate PTS and PTS^{Ntr} is the existence of a GAF domain in the N-terminal of EI^{Ntr} that can bind diverse ligands. In *E. coli,* binding of glutamine or α-ketoglutarate to this domain allows the sense the cellular nitrogen status to modulate the phosphorylation of PTS^{Ntr} (Lee et al., 2013). In *A. vinelandii,* strains carrying a non-phosphorylated form $EIIA^{Ntr}$, due to mutations in *ptsP*, *ptsO* or *ptsN*H56A (in which the phosphorylatable histidine residue was changed by an alanine), are unable to produce PHB and showed a reduction in transcription of *phbR* and *phbBAC* (Segura and Espín, 1998; Noguez et al., 2008).

When $EIIA^{Ntr}$ is unphosphorylated, the stability of the RpoS, necessary for transcription of both *phbR* and *phbBAC*, is reduced. It was found that the chaperone-protease ClpAP complex is involved, because inactivation of their genes in strains carrying unphosphorylated $EIIA^{Ntr}$, restored the levels and stability of RpoS, as well as the synthesis of PHB. Thus, in *A. vinelandii* the mechanism by which the unphosphorylated $EIIA^{Ntr}$ controls gene expression includes the induction of RpoS degradation by the proteolytic complex ClpAP (Muriel-Millán et al., 2017).

A relationship between GacA and the PTS^{Ntr} system was recently revealed. In the wild-type strain of *A. vinelandii*, both phosphorylated and unphosphorylated forms of $EIIA^{Ntr}$ are present. In contrast, in a *gacA* mutant only the unphosphorylated $EIIA^{Ntr}$ was detected (Trejo et al., 2017). Thus, GacA somehow regulates the PTS^{Ntr} phosphorylation cascade, which in turn controls PHB synthesis at the transcriptional level. The mechanism for this regulation is unknown; however, the hypothesis is that the expression of genes under *gacA* control could affect the nitrogen status, modulating phosphorylation of

PTS^{Ntr} through binding of glutamine and α-ketoglutarate to the EI^{Ntr} GAF domain.

PHB production in *A. vinelandii* is higher under oxygen limiting conditions, and the oxygen-responsive transcription factor CydR (Fnr-like), has been implicated in this control (Wu et al., 2001). Inactivation of the *cydR* gene, allowed a considerably higher accumulation of PHB than the wild type throughout the exponential growth phase. Proteomic analysis showed that the *cydR* mutant overexpressed the PHB biosynthetic enzymes β-ketothiolase and acetoacetyl-CoA reductase, and decreased expression of succinyl-CoA, an enzyme participating in PHB mobilization. Thus, CydR controls PHB metabolism, although the authors did not determine whether this control is direct or not. The behavior of this mutant strain under different oxygen conditions has not been tested, but it could be interesting to study for PHB production improvement.

Iron-limiting conditions also increase PHB accumulation in *A. vinelandii* (Page, 1982), and a regulatory small RNA ArrF has been found to participate (Pyla et al., 2009; Muriel-Millán et al., 2014), although the mechanism seems to differ depending on the strain. The Fur protein (ferric uptake repressor), a regulator of iron homeostasis, represses the expression of *arrF* in the presence of Fe(2+). In response to iron depletion, this repression is released and the expression of *arrF* is increased. ArrF, in turn, affects translation of its target mRNAs through the complementarity of its 5′-untranslated region, acting as antisense RNA (Jung and Kwon, 2008). In the *A. vinelandii* KCTC 23243, which produces small amounts of PHB, inactivation of *arrF* increased accumulation of the polymer 300-fold. Expression levels of the *phbBAC* biosynthetic genes and of their transcriptional activator *phbR* were also increased on this condition. ArrF was proposed to participate in the regulation by negatively controlling the expression of *phbR,* probably in an antisense manner (Pyla et al., 2009). In *A vinelandii* UW136, iron limitation also increases PHB accumulation and *phbBAC* transcription, through the post-transcriptional activation of *phbR* expression. However, in this strain, ArrF was shown to be required for full induction of the *phb* gene expression and PHB accumulation, both under iron-limited and non-lifted conditions. ArrF was concluded to act as a post-translational activator of *phbR*, thus activating transcription of *phbBAC* and production of PHB (Pyla et al., 2009; Muriel-Millán et al., 2014).

BIOPROCESS IN BIOREACTORS FOR HIGH-LEVEL PRODUCTION OF PHB AND MODIFICATION OF MOLECULAR MASS, USING *A. Vinelandii* REGULATORY MUTANTS

The main negative regulators identified in *A. vinelandii* so far are the small RsmA protein, that is a repressor of the translation of the *phbR* and *phbBAC* transcripts (Hernández-Eligio et al., 2012), and the Enzyme $EIIA^{Ntr}$, a protein that in its unphosphorylated form promotes degradation of RpoS by the ClpAP chaperone protease complex (Muriel-Millán et al., 2017).

As a result of the above knowledge, *A. vinelandii* strains carrying mutations in *rsmA* and *ptsN*, the genes coding for two negative regulators were constructed. Strain OPN, which carries a mutation inactivating *ptsN*, showed a PHB overproducing phenotype when cultured on PY sucrose agar plates, reaching a 70% higher accumulation than the value reached using the OP strain under that condition. On the other hand, when grown in shake flasks with PY sucrose medium a slightly higher volumetric amount of PHB was obtained with strain OPN, reaching 4.1 g L^{-1} at 60 h of cultivation; whereas, in the case of the wild-type OP strain, the PHB content was of 3.5 g L^{-1}. However, the specific production was considerably higher in the OPN mutant that reached 2.69 g PHB g $protein^{-1}$, which was almost 80% higher than that observed for the OP wild-type strain (1.52 g PHB g $protein^{-1}$) (Peña et al., 2013). This work also demonstrated that the molecular mass (MM) of the PHB was significantly influenced by *ptsN* mutation in addition to the aeration conditions. A higher MM was obtained under low-aeration conditions in both strains; however, a maximal molecular mass of 2,026 kDa was obtained with strain OPN, a value 2-fold higher than that obtained from the parental strain OP (MM = 1,013 kDa) under the same condition (Peña et al., 2013). From a technological point of view, the manipulation of the molecular weight of PHB by means of changes in the aeration conditions and the use of regulatory mutants is a convenient method that could considerably improve the properties of PHB.

Later, García et al. (2014) reported the use of *A. vinelandii* OPNA, a double mutant that carries inactivations on both PTS^{Ntr} and RsmA-RsmZ/Y regulatory systems. By using a strategy of exponential feeding coupled with nutrient pulses the production of PHB increased 7-fold (with respect to the batch culture) to reach a maximal PHB concentration of 27.3 ± 3.2 g L^{-1} at 60 h of growth.

With the use of strain OPNA, both in fed-batch and batch cultures, in addition to over-producing PHB, the synthesis of the polymer is growth associated and therefore it is not necessary to limit the culture (nutrients or oxygen) to promote the accumulation of PHB. This mutant is able to accumulate PHB up to 83% of its dry weight, even when grown under non-oxygen-limited conditions (4% of DOT). This behavior was clearly different from those reported for other *A. vinelandii* strains. For example, Flores et al. (2013) reported that in batch cultures of *A. vinelandii* ATCC 9046 at 5% of DOT, the cells accumulated only 20% of PHB (based on dry weight). In addition, Senior et al. (1972) reported PHB accumulation in *Azotobacter* under conditions of oxygen limitation, due to the increase of the ratios of NADPH + /NADP and acetyl-CoA/CoA, which promote PHB biosynthesis. Finally, an additional point to highlight is that the rates of oxygen consumption are 20% lower in the mutant than those observed with the parental strain. This offers advantages, from the operational point of view, because the commercial use of these strains would significantly reduce the aeration needs in large fermenters and therefore would decrease the production costs of the polymer, improving the balance of the economy of the process.

More recently, Castillo et al. (2017) and García et al. (2019) evaluated the use of OPNA mutant strain for PHB production

at different scales. In both reports, the authors showed that by using this strain in batch and fed-batch cultures it is possible to obtain a polymer of ultra-high molecular weight. It should be highlighted that a polymer having a very high molecular mass considerably improves its mechanical properties, expanding its potential applications. Castillo et al. (2017) found that in 3.0 L batch and fed-batch cultures in a fermenter, using different carbon/nitrogen molar ratios (10, 14, and 18), the OPNA strain produced PHB of high and ultra-high weight average molecular weight, with values between 2.3 and 6.6 MDa. This was highly dependent on the initial carbon/nitrogen ratio, reaching the highest value (6.6 MDa) in cultures conducted with a ratio of 18 and the lowest (2.3) with a ratio of 10. In fed-batch cultures, using a two-pulse feeding strategy, it was possible to obtain a global PHB volumetric productivity of 0.56 g L^{-1} h^{-1} and polymer concentration of 27.6 g L^{-1}.

García et al. (2019) scaled the process to fed-batch systems in 30 L fermenter using low-cost raw materials and found that the OPNA strain was able to reach good growth and PHB production, decreasing significantly the production cost of the polymer. When using the power input (P/V) as a criterion, it was possible to scale-up the process from 3 to 30 L bioreactors, confirming that the use of power input is an appropriate engineering parameter to scale-up the production process. In the 30 L bioreactor, both the polymer concentration and productivity were similar or even better than the values obtained in the fermenter of 3.0 L.

CONCLUDING REMARKS AND FUTURE PROSPECTS

In this article, the regulatory mechanisms that control PHAs metabolism are reviewed. PHAs accumulate in response to nutritional or environmental conditions. This is mediated by diverse regulatory mechanisms that may vary between different PHAs producing species.

The regulators of PHAs metabolism operate at different levels. The first one described was the control of the activity of the enzymes involved. This can be accomplished by allosterism, interaction with some metabolites, or through covalent modification of the biosynthetic or mobilizing enzymes. Also, many examples of transcriptional regulation by proteins like alternative sigma factors and transcription factors have been reported. Likewise, the control of transcription or translation of *pha* genes by small regulatory RNAs has been reported.

The phenotypes of mutants affected in these regulatory mechanisms have also been revised. Some of these regulatory mutants show PHAs overproducing phenotypes and even show modifications in the composition or molecular weight of the PHAs produced. Thus, knowledge of the regulatory mechanisms controlling PHAs metabolism can be used to design strains with better capabilities for the production of bioplastics. However, in many cases, the details of the mechanisms controlling *pha* gene expression are missing. In several examples, not even the targets of the regulation have been identified and only the final effect on PHAs accumulation is reported. Therefore, a deeper characterization of the regulatory systems reported would be useful.

Among the regulators participating in the control of PHAs metabolism, there are global regulators and also PHAs specific regulators. In many of the examples here reviewed it is shown that the need for nutrient deprivation to accumulate PHAs is mediated by some of these global regulators because their inactivation eliminates this limitation and the polymers can be accumulated during exponential growth under nutrient replete conditions. Some of these mutants even show other metabolic changes favorable for PHA production, contributing to the improved production phenotypes observed.

A better understanding of the fine details of the specific regulatory mechanisms that control PHAs accumulation could help identify targets for modification to improve polymer productivity, but a wider comprehension of the global regulatory networks connecting PHAs metabolism with the rest of the metabolism would also be important for this purpose. This can be achieved through whole-transcriptome or proteome studies of regulatory mutants because these are powerful tools for the study of wide responses. For example, deep RNA-sequencing analysis of these mutants would reveal not only the *pha* genes regulated, but other metabolic pathways which are co-regulated and probably related with PHAs metabolism, helping in the identification of genetic modifications for strain improvement.

The case of *A. vinelandii,* an organism whose PHB regulatory network has been extensively studied, illustrates how the modification of some regulatory elements (inactivation of two negative regulators), can be useful for the improvement of polymer production. Similar strategies could be used to explore the production capacities of other PHAs producing bacteria.

With respect to the control of the balance between PHAs synthesis and degradation, more research is needed to understand what conditions or effectors determine if the polymer is accumulated or mobilized, especially considering that the simultaneous expression of PHA synthase and depolymerases has been reported in some organisms (Doi et al., 1990; Ren et al., 2009; Brigham et al., 2012). From a practical point of view, this balance between PHA synthesis and depolymerization is relevant because it affects the amount and characteristics of the polymers produced. Low depolymerizing activities allow to increase PHA production and also favor the synthesis of ultra-high molecular weight PHAs, which in turn affects the properties of the polymer (Arikawa et al., 2016; Adaya et al., 2018).

AUTHOR CONTRIBUTIONS

DS contributed conception of the study. All authors wrote the sections of the manuscript, contributed to manuscript revision, read and approved the submitted version.

FUNDING

This work was supported in part by grants 255158 to DS and 255212 to GE from CONACyT.

REFERENCES

Adaya, L., Millán, M., Peña, C., Jendrossek, D., Espín, G., Tinoco-Valencia, R., et al. (2018). Inactivation of an intracellular poly-3-hydroxybutyrate depolymerase of *Azotobacter vinelandii* allows to obtain a polymer of uniform high molecular mass. *Appl. Microbiol. Biotechnol.* 102, 2693–2707. doi: 10.1007/s00253-018-8806-y

Aldor, I. S., and Keasling, J. D. (2003). Process design for microbial plastic factories: metabolic engineering of polyhydroxyalkanoates. *Curr. Opin. Biotechnol.* 14, 475–483. doi: 10.1016/j.copbio.2003.09.002

Arikawa, H., Sato, S., Fujiki, T., and Matsumoto, K. (2016). A study on the relationbetween poly(3-hydroxybutyrate) depolymerases or oligomer hydrolases and molecular weight of polyhydroxyalkanoates accumulatingin *Cupriavidus necator* H16. *J. Biotechnol.* 227, 94–102. doi: 10.1016/j.jbiotec.2016.04.004

Batista, M. B., Müller-Santos, M., Pedrosa, F. O., and de Souza, E. M. (2016). "Potentiality of *Herbaspirillum seropedicae* as a Platform for Bioplastic Production," in *Microbial Models: From Environmental to Industrial Sustainability. Microorganisms for Sustainability*, Vol. 1, ed. S. Castro-Sowinski (Singapore: Springer). doi: 10.1007/978-981-10-2555-6_2

Batista, M. B., Teixeira, C. S., Sfeir, M. Z. T., Alves, L. P. S., Valdameri, G., Pedrosa, F. D. O., et al. (2018). PHB biosynthesis counteracts redox stress in *Herbaspirillum seropedicae*. *Front. Microbiol.* 9:472. doi: 10.3389/fmicb.2018.00472

Battesti, A., Majdalani, N., and Gottesman, S. (2011). The RpoS-mediated general stress response in *Escherichia coli*. *Annu. Rev. Microbiol.* 65, 189–213. doi: 10.1146/annurev-micro-090110-102946

Bedoya-Pérez, L. P., Muriel-Millán, L. F., Moreno, S., Quiroz-Rocha, E., Rivera-Gómez, N., and Espín, G. (2018). The pyrophosphohydrolase RppH is involved in the control of RsmA/CsrA expression in *Azotobacter vinelandii* and *Escherichia coli*. *Microbiol. Res.* 214, 91–100. doi: 10.1016/j.micres.2018.05.013

Bharwad, K., and Rajkumar, S. (2019). Rewiring the functional complexity between Crc, Hfq and sRNAs to regulate carbon catabolite repression in *Pseudomonas*. *World J. Microbiol. Biotechnol.* 35:140. doi: 10.1007/s11274-019-2717-7

Blunt, W., Dartiailh, C., Sparling, R., Gapes, D. J., Levin, D. B., and Cicek, N. (2019). Development of high cell density cultivation strategies for improved medium chain length Polyhydroxyalkanoate productivity using *Pseudomonas putida* LS46. *Bioengineering* 6:E89. doi: 10.3390/bioengineering6040089

Boutte, C. C., and Crosson, S. (2013). Bacterial lifestyle shapes stringent response activation. *Trends Microbiol.* 21, 174–180. doi: 10.1016/j.tim.2013.01.002

Brigham, C. J., Speth, D. R., Rha, C. K., and Sinskey, A. J. (2012). Whole-genome microarray and gene deletion studies reveal regulation of the polyhydroxyalkanoate production cycle by the stringent response in *Ralstonia eutropha* H16. *Appl. Environ. Microbiol.* 78, 8033–8044. doi: 10.1128/AEM.01693-12

Calderón-Flores, A., Du Pont, G., Huerta-Saquero, A., Merchant-Larios, H., Servín-González, L., and Durán, S. (2005). The stringent response is required for amino acid and nitrate utilization, nod factor regulation, nodulation, and nitrogen fixation in *Rhizobium etli*. *J. Bacteriol.* 187, 5075–5083. doi: 10.1128/JB.187.15.5075-5083.2005

Castañeda, M., Guzmán, J., Moreno, S., and Espín, G. (2000). The GacS sensor kinase regulates alginate and poly-β-hydroxybutyrate production in *Azotobacter vinelandii*. *J. Bacteriol.* 182, 2624–2628. doi: 10.1128/JB.182.9.2624-2628.2000

Castañeda, M., Sánchez, J., Moreno, S., Núñez, C., and Espín, G. (2001). The global regulators GacA and σS form part of a cascade that controls alginate production in *Azotobacter vinelandii*. *J. Bacteriol.* 183, 6787–6793. doi: 10.1128/JB.183.23.6787-6793.2001

Castillo, T., Flores, C., Segura, D., Espín, G., Sanguino, J., Cabrera, E., et al. (2017). Production of polyhydroxybutyrate (PHB) of high and ultra-high molecular weight by *Azotobacter vinelandii* in batch and fed-batch cultures. *J. Chem. Technol. Biotechnol.* 92, 1809–1816. doi: 10.1002/jctb.5182

Cerrone, F., Sánchez-Peinado, M. M., Juárez-Jimenez, B., González-López, J., and Pozo, C. (2010). Biological treatment of two-phase olive mill wastewater (TPOMW, alpeorujo): polyhydroxyalkanoates (PHAs) production by *Azotobacter* strains. *J. Microbiol. Biotechnol.* 20, 594–601. doi: 10.4014/jmb.0906.06037

Chen, G. Q. (2009). A microbial polyhydroxyalkanoates (PHA) based bio-and materials industry. *Chem. Soc. Rev.* 38, 2434–2446. doi: 10.1039/b812677c

Chen, G. Q. (ed.) (2010). "Introduction of bacterial plastics PHA, PLA, PBS, PE, PTT, and PPP," in *Plastics from Bacteria, Natural Functions and Applications*, Vol. 14 (Berlin: Springer), 1–16. doi: 10.1007/978-3-642-03287_5_3

Chen, G. Q., and Jiang, X. R. (2017). Engineering bacteria for enhanced polyhydroxyalkanoates (PHA) biosynthesis. *Synth. Syst. Biotechnol.* 2, 192–197. doi: 10.1016/j.synbio.2017.09.001

Chen, G. Q., and Jiang, X. R. (2018). Engineering microorganisms for improving polyhydroxyalkanoate biosynthesis. *Curr. Opin. Biotechnol.* 53, 20–25. doi: 10.1016/j.copbio.2017.10.008

Chen, G. Q., Jiang, X. R., and Guo, Y. (2016). Synthetic biology of microbes synthesizing polyhydroxyalkanoates (PHA). *Synth. Syst. Biotechnol.* 1, 236–242. doi: 10.1016/j.synbio.2016.09.006

Chen, G. Q., and Page, W. J. (1994). The effect of substrate on the molecular weight of poly-β-hydroxybutyrate produced by *Azotobacter vinelandii* UWD. *Biotechnol. Lett.* 16, 155–160. doi: 10.1007/BF01021663

Chen, G. Q., and Page, W. J. (1997). Production of poly- β-hydroxybutyrate by *Azotobacter vinelandii* in a two-stage fermentation process. *Biotechnol Tech.* 108, 55–61. doi: 10.1023/A:1018435815864

Cho, K. S., Ryu, H. W., Park, C., and Goodrich, P. R. (2001). Utilization of swine wastewater as a feedstock for the production of polyhydroxyalkanoates by *Azotobacter vinelandii* UWD. *J. Biosci. Bioeng.* 91, 129–133. doi: 10.1016/S1389-1723(01)80054-2

Choi, J. I. L., and Lee, S. Y. (1997). Process analysis and economic evaluation for poly(3-hydroxybutyrate) production by fermentation. *Bioprocess Eng.* 17, 335–342. doi: 10.1007/s004490050394

Choi, M. H., Xu, J., Gutierrez, M., Yoo, T., Cho, Y. H., and Yoon, S. C. (2011). Metabolic relationship between polyhydroxyalkanoic acid and rhamnolipid synthesis in *Pseudomonas aeruginosa*: comparative 13C NMR analysis of the products in wild-type and mutants. *J. Biotechnol.* 151, 30–42. doi: 10.1016/j.jbiotec.2010.10.072

Chou, M. E., Chang, W. T., Chang, Y. C., and Yang, M. K. (2009). Expression of four PHAs genes involved in poly-β-hydroxybutyrate production and accumulation in *Rhodobacter sphaeroides* FJ1. *Mol. Genet. Genomics* 282, 97–106. doi: 10.1007/s00438-009-0448-4

Chou, M. E., and Yang, M. K. (2010). Analyses of binding sequences of the PhaR protein of *Rhodobacter sphaeroides* FJ1. *FEMS Microbiol. Lett.* 302, 138–143. doi: 10.1111/j.1574-6968.2009.01836.x

de Eugenio, L. I., Escapa, I., Morales, V., Dinjaski, N., Galan, B., Garcia, J., et al. (2010a). The turnover of medium-chain-length polyhydroxyalkanoates in *Pseudomonas putida* KT2442 and the fundamental role of PhaZ depolymerase for the metabolic balance. *Environ. Microbiol.* 12, 207–221. doi: 10.1111/j.1462-2920.2009.02061.x

de Eugenio, L. I., Galán, B., Escapa, I. F., Maestro, B., Sanz, J. M., García, J. L., et al. (2010b). The PhaD regulator controls the simultaneous expression of the PHAs genes involved in polyhydroxyalkanoate metabolism and turnover in *Pseudomonas putida* KT2442. *Environ. Microbiol.* 12, 1591–1603. doi: 10.1111/j.1462-2920.2010.02199.x

Deutscher, J., Aké, F. M. D., Derkaoui, M., Zébré, A. C., Cao, T. N., Bouraoui, H., et al. (2014). The bacterial phosphoenolpyruvate:carbohydrate phosphotransferase system: regulation by protein phosphorylation and phosphorylation-dependent protein-protein interactions. *Microbiol. Mol. Biol. Rev.* 78, 231–256. doi: 10.1128/mmbr.00001-14

Dietrich, K., Dumont, M. J., Del Rio, L. F., and Orsat, V. (2017). Producing PHAs in the bioeconomy - Towards a sustainable bioplastic. *Sustain. Prod. Consum.* 9, 58–70. doi: 10.1016/j.spc.2016.09.001

Doi, Y., Segawa, A., Kawaguchi, Y., and Kunioka, M. (1990). Cyclic nature of poly(3-hydroxyalkanoate) metabolism in *Alcaligenes eutrophus*. *FEMS Microbiol. Lett.* 67, 165–169. doi: 10.1111/j.1574-6968.1990.tb13856.x

Encarnación, S., Vargas, M. C., Dunn, M. F., Dávalos, A., Mendoza, G., Mora, Y., et al. (2002). AniA regulates reserve polymer accumulation and global protein expression in *Rhizobium etli*. *J. Bacteriol.* 184, 2287–2295. doi: 10.1128/JB.184.8.2287-2295.2002

Flores, C., Moreno, S., Espín, G., Peña, C., and Galindo, E. (2013). Expression of alginases and alginate polymerase genes in response to oxygen, and their relationship with the alginate molecular weight in *Azotobacter vinelandii*. *Enzyme Microb. Technol.* 53, 85–91. doi: 10.1016/j.enzmictec.2013.04.010

Fonseca, P., de la Peña, F., and Prieto, M. A. (2014). A role for the regulator PsrA in the polyhydroxyalkanoatemetabolism of *Pseudomonas putida* KT2440. *Int. J. Biol. Macromol.* 71, 14–20. doi: 10.1016/j.ijbiomac.2014.04.014

Galán, B., Dinjaski, N., Maestro, B., De Eugenio, L. I., Escapa, I. F., Sanz, J. M., et al. (2011). Nucleoid-associated PhaF phasin drives intracellular location and segregation of polyhydroxyalkanoate granules in *Pseudomonas putida* KT2442. *Mol. Microbiol.* 79, 402–418. doi: 10.1111/j.1365-2958.2010.07450.x

García, A., Pérez, D., Castro, M., Urtuvia, V., Castillo, T., Díaz-Barrera, A., et al. (2019). Production and recovery of poly-3-hydroxybutyrate [P(3HB)] of ultra-high molecular weight using fed-batch cultures of *Azotobacter vinelandii* OPNA strain. *J. Chem. Technol. Biotechnol.* 94, 1853–1860. doi: 10.1002/jctb.5959

García, A., Segura, D., Espín, G., Galindo, E., Castillo, T., and Peña, C. (2014). High production of poly-β-hydroxybutyrate (PHB) by an *Azotobacter vinelandii* mutant altered in PHB regulation using a fed-batch fermentation process. *Biochem. Eng. J.* 82, 117–123. doi: 10.1016/j.bej.2013.10.020

Gottesman, S., and Storz, G. (2011). Bacterial small RNA regulators: versatile roles and rapidly evolving variations. *Cold Spring Harb. Perspect. Biol.* 3:a003798. doi: 10.1101/cshperspect.a003798

Handrick, R., Reinhardt, S., Kimmig, P., and Jendrossek, D. (2004). The "intracellular" poly(3-hydroxybutyrate) (PHB) depolymerase of *Rhodospirillum rubrum* is a periplasm-located protein with specificity for native PHB and with structural similarity to extracellular PHB depolymerases. *J. Bacteriol.* 186, 7243–7253. doi: 10.1128/JB.186.21.7243-7253.2004

Haywood, G. W., Anderson, A. J., Chu, L., and Dawes, E. A. (1988). The role of NADH- and NADPH-linked acetoacetyl-CoA reductases in the poly-3-hydroxybutyrate synthesizing organism *Alcaligenes eutrophus*. *FEMS Microbiol. Lett.* 52, 259–264. doi: 10.1111/j.1574-6968.1988.tb02607.x

Hernández-Eligio, A., Castellanos, M., Moreno, S., and Espín, G. (2011). Transcriptional activation of the *Azotobacter vinelandii* polyhydroxybutyrate biosynthetic genes *phbBAC* by PhbR and RpoS. *Microbiology* 157, 3014–3023. doi: 10.1099/mic.0.051649-0

Hernández-Eligio, A., Moreno, S., Castellanos, M., Castañeda, M., Nuñez, C., Muriel-Millán, L. F., et al. (2012). RsmA post-transcriptionally controls PhbR expression and polyhydroxybutyrate biosynthesis in *Azotobacter vinelandii*. *Microbiology* 158, 1953–1963. doi: 10.1099/mic.0.059329-0

Hoffmann, N., and Rehm, B. H. A. (2004). Regulation of polyhydroxyalkanoate biosynthesis in *Pseudomonas putida* and *Pseudomonas aeruginosa*. *FEMS Microbiol. Lett.* 237, 1–7. doi: 10.1016/j.femsle.2004.06.029

Hoffmann, N., and Rehm, B. H. A. (2005). Nitrogen-dependent regulation of medium-chain length polyhydroxyalkanoate biosynthesis genes in pseudomonads. *Biotechnol. Lett.* 27, 279–282. doi: 10.1007/s10529-004-8353-8

Hokamura, A., Wakida, I., Miyahara, Y., Tsuge, T., Shiratsuchi, H., Tanaka, K., et al. (2015). Biosynthesis of poly(3-hydroxybutyrate-co-3-hydroxyalkanoates) by recombinant *Escherichia coli* from glucose. *J. Biosci. Bioeng.* 120, 305–310. doi: 10.1016/j.jbiosc.2015.01.022

Ishihama, A. (2012). Prokaryotic genome regulation: a revolutionary paradigm. *Proc. Jpn. Acad. Ser. B Phys. Biol. Sci.* 88, 485–508. doi: 10.2183/pjab.88.485

Jendrossek, D., and Pfeiffer, D. (2014). New insights in the formation of polyhydroxyalkanoate granules (carbonosomes) and novel functions of poly(3-hydroxybutyrate). *Environ. Microbiol.* 16, 2357–2373. doi: 10.1111/1462-2920.12356

Juengert, J. R., Borisova, M., Mayer, C., Wolz, C., Brigham, C. J., Sinskey, A. J., et al. (2017). Absence of ppGpp leads to increased mobilization of intermediately accumulated poly(3-hydroxybutyrate) in *Ralstonia eutropha* H16. *Appl. Environ. Microbiol.* 83:e00755-17. doi: 10.1128/AEM.00755-17

Juengert, J. R., Patterson, C., and Jendrossek, D. (2018). Poly(3-hydroxybutyrate) (PHB) polymerase PhaC1 and PHB depolymerase PhaZa1 of *Ralstonia eutropha* are phosphorylated *in vivo*. *Appl. Environ. Microbiol.* 84:e00604-18. doi: 10.1128/AEM.00604-18

Jung, Y. K., Lee, S. Y., and Tam, T. T. (2010). Towards systems metabolic engineering of PHAs producers. *Microbiol. Monogr.* 14, 63–84. doi: 10.1007/978-3-642-03287-5_4

Jung, Y. S., and Kwon, Y. M. (2008). Small RNA ArrF regulates the expression of sodB and feSII genes in *Azotobacter vinelandii*. *Curr. Microbiol.* 57, 593–597. doi: 10.1007/s00284-008-9248-z

Kaddor, C., and Steinbüchel, A. (2011). Effects of homologous phosphoenolpyruvate-carbohydrate phosphotransferase system proteins on carbohydrate uptake and poly(3-Hydroxybutyrate) accumulation in *Ralstonia eutropha* H16. *Appl. Environ. Microbiol.* 77, 3582–3590. doi: 10.1128/AEM.00218-11

Kaddor, C., Voigt, B., Hecker, M., and Steinbüchel, A. (2012). Impact of the core components of the phosphoenolpyruvate-carbohydrate phosphotransferase system, HPr and EI, on differential protein expression in Ralstonia eutropha H16. *J. Proteome Res.* 11, 3624–3636. doi: 10.1021/pr300042f

Kadowaki, M. A., Müller-Santos, M., Rego, F. G., Souza, E. M., Yates, M. G., Monteiro, R. A., et al. (2011). Identification and characterization of PhbF: A DNA binding protein with regulatory role in the PHB metabolism of *Herbaspirillum seropedicae* SmR1. *BMC Microbiol.* 11:230. doi: 10.1186/1471-2180-11-230

Kang, Y., Nguyen, D. T., Son, M. S., and Hoang, T. T. (2008). The *Pseudomonas aeruginosa* PsrAresponds to long-chain fatty acid signals to regulate the *fadBA5* beta-oxidationoperon. *Microbiology* 154, 1584–1598. doi: 10.1099/mic.0.2008/018135-0

Karstens, K., Zschiedrich, C. P., Bowien, B., Stülke, J., and Görke, B. (2014). Phosphotransferase protein EIIANtr interacts with SpoT, a key enzyme of the stringent response, in *Ralstonia eutropha* H16. *Microbiology* 160, 711–722. doi: 10.1099/mic.0.0752260

Kho, D. H., Jang, J. H., Kim, H. S., Kim, K. S., and Lee, J. K. (2003). Quorum sensing of *Rhodobacter sphaeroides* negatively regulates cellular poly-β-Hydroxybutyrate content under aerobic growth conditions. *J. Microbiol. Biotechnol.* 13, 477–481.

Klinke, S., De Roo, G., Witholt, B., and Kessler, B. (2000). Role of *phaD* in accumulation of medium-chain-length poly(3-hydroxyalkanoates) in *Pseudomonas oleovorans*. *Appl. Environ. Microbiol.* 66, 3705–3710. doi: 10.1128/AEM.66.9.3705-3710.2000

Kniewel, R., Lopez, O. R., and Prieto, M. A. (2019). "Biogenesis of medium-chain-length Polyhydroxyalkanoates," in *Biogenesis of Fatty Acids, Lipids and Membrane: Handbook of Hydrocarbon and Lipid Microbiology*, ed. O. Geiger (Cham: Springer). doi: 10.1007/978-3-319-50430-8_29

Kojic, M., and Venturi, V. (2001). Regulation of *rpoS* gene expression in *Pseudomonas*:involvement of a TetR family regulator. *J. Bacteriol.* 183, 3712–3720. doi: 10.1128/JB.183.12.3712-3720.2001

Koller, M., Atliæ, A., Dias, M., Reiterer, A., and Braunegg, G. (2010). "Microbial PHAs production from waste raw materials," in *Plastics from Bacteria Microbiology Monographs*, Vol. 14, ed. G. Q. Chen (Berlin: Springer). doi: 10.1007/978-3-642-03287-5_5

Kourmentza, C., Plácido, J., Venetsaneas, N., Burniol-Figols, A., Varrone, C., Gavala, H. N., et al. (2017). Recent advances and challenges towards sustainable polyhydroxyalkanoate (PHA) production. *Bioengineering* 4:E55. doi: 10.3390/bioengineering4020055

Krausse, D., Hunold, K., Kusian, B., Lenz, O., Stülke, J., Bowien, B., et al. (2009).). Essential role of the *hprK* gene in *Ralstonia eutropha* H16. *J. Mol. Microbiol. Biotechnol.* 17, 146–152. doi: 10.1159/000233505

La Rosa, R., de la Peña, F., Prieto, M. A., and Rojo, F. (2014). The Crc protein inhibits the production of polyhydroxyalkanoates in *Pseudomonas putida* under balanced carbon/nitrogen growth conditions. *Environ. Microbiol.* 16, 278–290. doi: 10.1111/1462-2920.12303

Lagares, A., Borella, G. C., Linne, U., Becker, A., and Valverde, C. (2017). Regulation of polyhydroxybutyrate accumulation in *Sinorhizobium meliloti* by the trans-encoded small RNA MmgR. *J. Bacteriol.* 199:e00776-16. doi: 10.1128/JB.00776-16

Lapouge, K., Schubert, M., Allain, F. H. T., and Haas, D. (2008). Gac/Rsm signal transduction pathway of gamma-*proteobacteria*: from RNA recognition to regulation of social behaviour. *Mol. Microbiol.* 67, 241–253. doi: 10.1111/j.1365-2958.2007.06042.x

Lawrence, A. G., Schoenheit, J., He, A., Tian, J., Liu, P., Stubbe, J., et al. (2005). Transcriptional analysis of *Ralstonia eutropha* genes related to poly-(R)-3-hydroxybutyrate homeostasis during batch fermentation. *Appl. Microbiol. Biotechnol.* 68, 663–672. doi: 10.1007/s00253-005-1969-3

Lee, C. R., Park, Y. H., Kim, M., Kim, Y. R., Park, S., Peterkofsky, A., et al. (2013). Reciprocal regulation of the autophosphorylation of enzyme INtr by glutamine and α-ketoglutarate in *Escherichia coli*. *Mol. Microbiol.* 88, 473–485. doi: 10.1111/mmi.12196

Lenz, R. W., and Marchessault, R. H. (2005). Bacterial polyesters: Biosynthesis, biodegradable plastics and biotechnology. *Biomacromolecules* 6, 1–8. doi: 10.1021/bm049700c

López, N. I., Pettinari, M. J., Nikel, P. I., and Méndez, B. S. (2015). Polyhydroxyalkanoates: much more than biodegradable plastics. *Adv. Appl. Microbiol.* 93, 73–106. doi: 10.1016/bs.aambs.2015.06.001

Lu, J., Tappel, R. C., and Nomura, C. T. (2009). Mini-review: Biosynthesis of poly(hydroxyalkanoates). *Polym. Rev.* 49, 226–248. doi: 10.1080/15583720903048243

Maehara, A., Taguchi, S., Nishiyama, T., Yamane, T., and Doi, Y. (2002). A repressor protein, PhaR, regulates polyhydroxyalkanoate (PHA) synthesis via its direct interaction with PHA. *J. Bacteriol.* 184, 3992–4002. doi: 10.1128/JB.184.14.3992-4002.2002

Maehara, A., Ueda, S., Nakano, H., and Yamane, T. (1999). Analyses of a polyhydroxyalkanoic acid granule-associated 16-kilodalton protein and its putative regulator in the PHAs locus of *Paracoccus denitrificans*. *J. Bacteriol.* 181, 2914–2921.

Manchak, J., and Page, W. J. (1994). Control of polyhydroxyalkanoate synthesis in *Azotobacter vinelandii* strain UWD. *Microbiology* 140, 953–963. doi: 10.1099/00221287-140-4-953

Manzo, J., Cocotl-Yañez, M., Tzontecomani, T., Martínez, V. M., Bustillos, R., Velásquez, C., et al. (2011). Post-transcriptional regulation of the alginate biosynthetic gene algD by the Gac/Rsm system in *Azotobacter vinelandii*. *J. Mol. Microbiol. Biotechnol.* 21, 147–159. doi: 10.1159/000334244

Martínez-Valenzuela, M., Guzmán, J., Moreno, S., Ahumada-Manuel, C. L., Espín, G., and Núñez, C. (2018). Expression of the sRNAs CrcZ and CrcY modulate the strength of carbon catabolite repression under diazotrophic or non-diazotrophic growing conditions in *Azotobacter vinelandii*. *PLoS One* 13:e0208975. doi: 10.1371/journal.pone.0208975

Matsusaki, H., Manji, S., Taguchi, K., Kato, M., Fukui, T., and Doi, Y. (1998). Cloning and molecular analysis of the poly(3-hydroxybutyrate) and poly(3-hydroxybutyrate-co-3-hydroxyalkanoate) biosynthesis genes in *Pseudomonas sp*. strain 61-3. *J. Bacteriol.* 180, 6459–6467.

Millán, M., Salazar, M., Segura, D., Castillo, T., Díaz-Barrera, Á., and Peña, C. (2017). Molecular mass of Poly-3-hydroxybutyrate (P3HB) produced by *Azotobacter vinelandii* is influenced by the polymer content in the inoculum. *J. Biotechnol.* 259, 50–55. doi: 10.1016/j.jbiotec.2017.08.016

Miyake, M., Kataoka, K., Shirai, M., and Asada, Y. (1997). Control of poly-β-hydroxybutyrate synthase mediated by acetyl phosphate in cyanobacteria. *J. Bacteriol.* 179, 5009–5013. doi: 10.1128/jb.179.16.5009-5013.1997

Miyamoto, C. M., Sun, W., and Meighen, E. A. (1998). The LuxR regulator protein controls synthesis of polyhydroxybutyrate in *Vibrio harveyi*. *Biochim. Biophys. Acta* 1384, 356–364. doi: 10.1016/S0167-4838(98)00028-4

Mohanan, N., Gislason, A., Sharma, P. K., Ghergab, A., Plouffe, J., Levin, D. B., et al. (2019). Quorum sensing and the anaerobic regulator (ANR) control polyhydroxyalkanoate (PHA) production in *Pseudomonas chlororaphis*PA23. *FEMS Microbiol. Lett.* 366:fnz223. doi: 10.1093/femsle/fnz223

Mozejko-Ciesielska, J., Dabrowska, D., Szalewska-Palasz, A., and Ciesielski, S. (2017). Medium-chain-length polyhydroxyalkanoates synthesis by *Pseudomonas putida* KT2440 *relA/spoT* mutant: bioprocess characterization and transcriptome analysis. *AMB Express* 7:92. doi: 10.1186/s13568-017-0396-z

Muriel-Millán, L. F., Castellanos, M., Hernandez-Eligio, J. A., Moreno, S., and Espín, G. (2014). Posttranscriptional regulation of PhbR, the transcriptional activator of polyhydroxybutyrate synthesis, by iron and the sRNA ArrF in *Azotobacter vinelandii*. *Appl. Microbiol. Biotechnol.* 98, 2173–2182. doi: 10.1007/s00253-013-5407-7

Muriel-Millán, L. F., Moreno, S., Gallegos-Monterrosa, R., and Espín, G. (2017). Unphosphorylated EIIANtr induces ClpAP-mediated degradation of RpoS in *Azotobacter vinelandii*. *Mol. Microbiol.* 104, 197–211. doi: 10.1111/mmi.13621

Noar, J. D., and Bruno-Bárcena, J. M. (2018). *Azotobacter vinelandii*: the source of 100 years of discoveries and many more to come. *Microbiology* 164, 421–436. doi: 10.1099/mic.0.000643

Noguez, R., Segura, D., Moreno, S., Hernández, A., Juárez, K., and Espín, G. (2008). Enzyme INtr, NPr and IIANtr are involved in regulation of the poly-β-hydroxybutyrate biosynthetic genes in *Azotobacter vinelandii*. *J. Mol. Microbiol. Biotechnol.* 15, 244–254. doi: 10.1159/000108658

Oeding, V., and Schlegel, H. G. (1973). β-Ketothiolase from *Hydrogenomonas eutropha* H16 and its significance in the regulation of poly β hydroxybutyrate metabolism. *Biochem. J.* 134, 239–248. doi: 10.1042/bj1340239

Olaya-Abril, A., Luque-Almagro, V. M., Manso, I., Gates, A. J., Conrado Moreno-Vivián, Richardson, D. J., et al. (2018). Poly(3-hydroxybutyrate) hyperproduction by a global nitrogen regulator NtrB mutant strain of *Paracoccus denitrificans* PD1222. *FEMS Microbiol. Lett.* 365:fnx251. doi: 10.1093/femsle/fnx251

Osanai, T., Numata, K., Oikawa, A., Kuwahara, A., Iijima, H., Doi, Y., et al. (2013). Increased bioplastic production with an RNA polymerase sigma factor SigE during nitrogen starvation in *Synechocystis* sp. PCC 6803. *DNA Res.* 20, 525–535. doi: 10.1093/dnares/dst028

Osanai, T., Oikawa, A., Numata, K., Kuwahara, A., Iijima, H., Doi, Y., et al. (2014). Pathway-level acceleration of glycogen catabolism by a response regulator in the cyanobacterium *Synechocystis* species PCC 6803. *Plant Physiol.* 164, 1831–1841. doi: 10.1104/pp.113.232025

Page, W. J. (1982). Optimal conditions for induction of competence in nitrogen-fixing *Azotobacter vinelandii*. *Can. J. Microbiol.* 28, 389–397. doi: 10.1139/m82-059

Page, W. J. (1989). Production of poly-β-hydroxybutyrate by *Azotobacter vinelandii* strain UWD during growth on molasses and other complex carbon sources. *Appl. Microbiol. Biotechnol.* 31, 329–333. doi: 10.1007/BF00257598

Page, W. J. (1992a). Production of poly-β-hydroxybutyrate by *Azotobacter vinelandii* UWD in media containing sugars and complex nitrogen sources. *Appl. Microbiol. Biotechnol.* 38, 117–121. doi: 10.1007/BF00169430

Page, W. J. (1992b). Suitability of commercial beet molasses fractions as substrates for polyhydroxyalkanoate production by *Azotobacter vinelandii* UWD. *Biotechnol. Lett.* 14, 385–390. doi: 10.1007/BF01021252

Page, W. J., and Cornish, A. (1993). Growth of *Azotobacter vinelandii* UWD in fish peptone medium and simplified extraction of poly-β-hydroxybutyrate. *Appl. Environ. Microbiol.* 59, 4236–4244.

Page, W. J., Manchak, J., and Rudy, B. (1992). Formation of poly(hydroxybutyrate-co-hydroxyvalerate) by *Azotobacter vinelandii* UWD. *Appl. Environ. Microbiol.* 58, 2866–2873.

Panchal, B., Bagdadi, A., and Roy, I. (2013). "Polyhydroxyalkanoates: The natural polymers produced by Bacterial Fermentation," in *Advances in Natural Polymers. Adv. Struct. Mater*, Vol. 18, eds S. Thomas, P. Visakh, and A. Mathew (Berlin: Springer). doi: 10.1007/978-3-642-20940-6_12

Papenfort, K., and Bassler, B. L. (2016). Quorum sensing signal-response systems in Gram-negative bacteria. *Nat. Rev. Microbiol.* 14, 576–588. doi: 10.1038/nrmicro.2016.89

Peña, C., López, S., García, A., Espín, G., Romo-Uribe, A., and Segura, D. (2013).). Biosynthesis of poly-β-hydroxybutyrate (PHB) with a high molecular mass by a mutant strain of *Azotobacter vinelandii* (OPN). *Ann. Microbiol.* 64, 39–47. doi: 10.1007/ s13213-013-0630-0

Peralta-Gil, M., Segura, D., Guzmán, J., Servín-González, L., and Espín, G. (2002). Expression of the *Azotobacter vinelandii* poly-β-hydroxybutyrate biosynthetic *phbBAC* operon is driven by two overlapping promoters and is dependent on the transcriptional activator PhbR. *J. Bacteriol.* 184, 5672–5677. doi: 10.1128/JB.184.20.5672-5677.2002

Pettinari, M. J., Vázquez, G. J., Silberschmidt, D., Rehm, B., Steibüchel, A., and Méndez, B. S. (2001). Poly(3-Hydroxybutyrate) synthesis genes in *Azotobacter* sp. strain FA8. *Appl. Environ. Microbiol.* 67, 5331–5334. doi: 10.1128/aem.67.11.5331-5334.2001

Pflüger-Grau, K., and Görke, B. (2010). Regulatory roles of the bacterial nitrogen-related phosphotransferase system. *Trends Microbiol.* 18, 205–214. doi: 10.1016/j.tim.2010.02.003

Pötter, M., and Steinbüchel, A. (2005). Poly(3-hydroxybutyrate) granule-associated proteins: impacts on poly(3-hydroxybutyrate) synthesis and degradation. *Biomacromolecules* 6, 552–560. doi: 10.1021/bm049401n

Pötter, M., Madkour, M. H., Mayer, F., and Steinbüchel, A. (2002). Regulation of phasin expression and polyhydroxylkanoate (PHA) granule formation in *Ralstonia eutropha* H16. *Microbiology* 148, 2413–2426. doi: 10.1099/00221287-148-8-2413

Pötter, M., Müller, H., and Steinbüchel, A. (2005). Influence of homologous phasins (PhaP) on PHAs accumulation and regulation of their expression by the transcriptional repressor PhaR in *Ralstonia eutropha* H16. *Microbiology* 151, 825–833. doi: 10.1099/mic.0.27613-0

Povolo, S., and Casella, S. (2000). A critical role for *aniA* in energy-carbon flux and symbiotic nitrogen fixation in *Sinorhizobium meliloti*. *Arch. Microbiol.* 174, 42–49. doi: 10.1007/s002030000171

Pries, A., Priefert, H., Kruger, N., and Steinbuchel, A. (1991). Identification and characterization of two *Alcaligenes eutrophus* gene loci relevant to the poly(β-hydroxybutyric acid)-leaky phenotype which exhibit homology to ptsH and ptsI of *Escherichia coli*. *J. Bacteriol.* 173, 5843–5853. doi: 10.1128/jb.173.18.5843-5853.1991

Prieto, A., Escapa, I. F., Martínez, V., Dinjaski, N., Herencias, C., de la Peña, F., et al. (2016). A holistic view of polyhydroxyalkanoate metabolism in *Pseudomonas putida*. *Environ. Microbiol.* 18, 341–357. doi: 10.1111/1462-2920.12760

Prieto, M. A., Bühler, B., Jung, K., Witholt, B., and Kessler, B. (1999). PhaF, a polyhydroxyalkanoate-granule-associated protein of *Pseudomonas oleovorans* GPo1 involved in the regulatory expression system for PHAs genes. *J. Bacteriol.* 181, 858–886.

Pyla, R., Kim, T. J., Silva, J. L., and Jung, Y. S. (2009). Overproduction of poly-β-hydroxybutyrate in the *Azotobacter vinelandii* mutant that does not express small RNA ArrF. *Appl. Microbiol. Biotechnol.* 84, 717–724. doi: 10.1007/s00253-009-2002-z

Quelas, J. I., Mesa, S., Mongiardini, E. J., Jendrossek, D., and Lodeiro, A. R. (2016). Regulation of polyhydroxybutyrate synthesis in the soil bacterium *Bradyrhizobium diazoefficiens*. *Appl. Environ. Microbiol.* 82, 4299–4308. doi: 10.1128/AEM.00757-16

Quiroz-Rocha, E., Bonilla-Badía, F., García-Aguilar, V., López-Pliego, L., Serrano-Román, J., Cocotl-Yañez, M., et al. (2017a). Two-component system CbrA/CbrB controls alginate production in *Azotobacter vinelandii*. *Microbiology* 163, 1105–1115. doi: 10.1099/mic.0.000457

Quiroz-Rocha, E., Moreno, R., Hernández-Ortíz, A., Fragoso-Jiménez, J. C., Muriel-Millán, L. F., Guzmán, J., et al. (2017b). Glucose uptake in *Azotobacter vinelandii* occurs through a GluP transporter that is under the control of the CbrA/CbrB and Hfq-Crc systems. *Sci. Rep.* 7:858. doi: 10.1038/s41598-017-00980-5

Raiger-Iustman, L. J., and Ruiz, J. A. (2008). The alternative sigma factor, σS, affects polyhydroxyalkanoate metabolism in *Pseudomonas putida*. *FEMS Microbiol. Lett.* 284, 218–224. doi: 10.1111/j.1574-6968.2008.01203.x

Ramos, J. L., Martinez-Bueno, M., Molina-Henares, A. J., Teran, W., Watanabe, K., Zhang, X., et al. (2005). The TetR family of transcriptional repressors. *Microbiol. Mol. Biol. Rev.* 69, 326–356. doi: 10.1128/mmbr.69.2.326-356.2005

Reinecke, F., and Steinbüchel, A. (2009). *Ralstonia eutropha* strain H16 as model organism for PHAs metabolism and for biotechnological production of technically interesting biopolymers. *J. Mol. Microbiol. Biotechnol.* 16, 91–108. doi: 10.1159/000142897

Ren, Q., de Roo, G., Ruth, K., Witholt, B., Zinn, M., and Thöny-Meyer, L. (2009). Simultaneous accumulationand degradation of polyhydroxyalkanoates: futile cycle or clever regulation? *Biomacromolecules* 10, 916–922. doi: 10.1021/bm801431c

Rojo, F. (2010). Carbon catabolite repression in *Pseudomonas*: Optimizing metabolic versatility and interactions with the environment. *FEMS Microbiol. Rev.* 34, 658–684. doi: 10.1111/j.1574-6976.2010.00218.x

Romero, Y., Guzmán, J., Moreno, S., Cocotl-Yañez, M., Vences-Guzmán, M. Á., Castañeda, M., et al. (2016). The GacS/A-RsmA signal transduction pathway controls the synthesis of alkylresorcinol lipids that replace membrane phospholipids during encystment of *Azotobacter vinelandii* SW136. *PLoS One* 11:e0153266. doi: 10.1371/journalpone.0153266

Ronneau, S., Petit, K., De Bolle, X., et al. (2016). Phosphotransferase-dependent accumulation of (p)ppGpp in response to glutamine deprivation in *Caulobacter crescentus*. *Nat. Commun.* 7:11423. doi: 10.1038/ncomms11423

Ruiz, J. A., López, N. I., Fernández, R. O., and Méndez, B. S. (2001). Polyhydroxyalkanoate degradation is associated with nucleotide accumulation and enhances stress resistance and survival of *Pseudomonas oleovorans* in natural water microcosms. *Appl. Environ. Microbiol.* 67, 225–230. doi: 10.1128/AEM.67.1.225-230.2001

Ruiz, J. A., López, N. I., and Méndez, B. S. (2004). rpoS gene expression in carbon-starved cultures of the polyhydroxyalkanoate-accumulating species *Pseudomonas oleovorans*. *Curr. Microbiol.* 48, 396–400. doi: 10.1007/s00284-003-4183-5

Ryan, W. J., O'Leary, N. D., O'Mahony, M., and Dobson, A. D. W. (2013). GacS-dependent regulation of polyhydroxyalkanoate synthesis in *Pseudomonas putida* CA-3. *Appl. Environ. Microbiol.* 79, 1795-1802. doi: 10.1128/AEM.02962-12

Sacomboio, E. N. M., Kim, E. Y. S., Correa, H. L. R., Bonato, P., Pedrosa, F. D. O., De Souza, E. M., et al. (2017). The transcriptional regulator NtrC controls glucose-6-phosphate dehydrogenase expression and polyhydroxybutyrate synthesis through NADPH availability in *Herbaspirillum seropedicae*. *Sci. Rep.* 7:13546. doi: 10.1038/s41598-017-12649-0

Sandoval, Á, Arias-Barrau, E., Arcos, M., Naharro, G., Olivera, E. R., and Luengo, J. M. (2007). Genetic and ultrastructural analysis of different mutants of *Pseudomonas putida* affected in the poly-3-hydroxy-n-alkanoate gene cluster. *Environ. Microbiol.* 9, 737-751. doi: 10.1111/j.1462-2920.2006.01196.x

Schembri, M. A., Bayly, R. C., and Davies, J. K. (1995). Phosphate concentration regulates transcription of the *Acinetobacter* polyhydroxyalkanoic acid biosynthetic genes. *J. Bacteriol.* 177, 4501–4507. doi: 10.1128/jb.177.15.4501-4507.1995

Segura, D., Cruz, T., and Espín, G. (2003). Encystment and alkylresorcinol production by *Azotobacter vinelandii* strains impaired in poly-β-hydroxybutyrate synthesis. *Arch. Microbiol.* 179, 437-443. doi: 10.1007/s00203-003-0553-4

Segura, D., and Espín, G. (1998). Mutational inactivation of a gene homologous to *Escherichia coli ptsP* affects poly-β-hydroxybutyrate accumulation and nitrogen fixation in *Azotobacter vinelandii*. *J. Bacteriol.* 180, 4790–4798.

Segura, D., Vargas, E., and Espín, G. (2000). β-Ketothiolase genes in *Azotobacter vinelandii*. *Gene* 260, 113–120. doi: 10.1016/S0378-1119(00)00462-5

Senior, P. J., Beech, G. A., Ritchie, G. A., and Dawes, E. A. (1972). The role of oxygen limitation in the formation of poly-β-hydroxybutyrate during batch and continuous culture of *Azotobacter beijerinckii*. *Biochem. J.* 128, 1193–1201. doi: 10.1042/bj1281193

Senior, P. J., and Dawes, E. A. (1973). The regulation of poly β hydroxybutyrate metabolism in *Azotobacter beijerinckii*. *Biochem. J.* 134, 225–238. doi: 10.1042/bj1340225

Sharma, P. K., Fu, J., Spicer, V., Krokhin, O. V., Cicek, N., Sparling, R., et al. (2016). Global changes in the proteome of *Cupriavidus necator* H16 during poly-(3-hydroxybutyrate) synthesis from various biodiesel by-product substrates. *AMB Express* 6:36. doi: 10.1186/s13568-016-0206-z

Sharma, P. K., Munir, R. I., Plouffe, J., Shah, N., de Kievit, T., and Levin, D. B. (2018). Polyhydroxyalkanoate (PHA) polymer accumulation and PHAs gene expression in phenazine (*phz*-) and pyrrolnitrin (*prn*-) defective mutants of *Pseudomonas chlororaphis* PA23. *Polymers* 10:E1203. doi: 10.3390/polym10111203

Steinbüchel, A., and Lütke-Eversloh, T. (2003). Metabolic engineering and pathway construction for biotechnological production of relevant polyhydroxyalkanoates in microorganisms. *Biochem. Eng. J.* 16, 81–96. doi: 10.1016/S1369-703X(03)00036-6

Stubbe, J., Tian, J., He, A., Sinskey, A. J., Lawrence, A. G., and Liu, P. (2005). Nontemplate-dependent polymerization processes: polyhydroxyalkanoate synthases as a paradigm. *Annu. Rev. Biochem.* 74, 433–480. doi: 10.1146/annurev.biochem.74.082803.133013

Sudesh, K., Taguchi, K., and Doi, Y. (2002). Effect of increased PHAs synthase activity on polyhydroxyalkanoates biosynthesis in *Synechocystis* sp. PCC6803. *Int. J. Biol. Macromol.* 30, 97–104. doi: 10.1016/S0141-8130(02)00010-7

Sun, J., Peng, X., Van Impe, J., and Vanderleyden, J. (2000). The *ntrB* and *ntrC* genes are involved in the regulation of poly-3-hydroxybutyrate biosynthesis by ammonia in *Azospirillum brasilense* Sp7. *Appl. Environ. Microbiol.* 66, 113–117. doi: 10.1128/AEM.66.1.113-117.2000

Sun, W., Cao, J. G., Teng, K., and Meighen, E. A. (1994). Biosynthesis of poly-3-hydroxybutyrate in the luminescent bacterium, *Vibrio harveyi*, and regulation by the lux autoinducer, N-(3- hydroxybutanoyl)homoserine lactone. *J. Biol. Chem.* 269, 20785–20790.

Sznajder, A., and Jendrossek, D. (2011). Biochemical characterization of a new type of intracellular PHB depolymerase from *Rhodospirillum rubrum* with high hydrolytic activity on native PHB granules. *Appl. Microbiol. Biotechnol.* 89, 1487–1495. doi: 10.1007/s00253-011-30967

Tan, Y., Neo, P. C., Najimudin, N., Sudesh, K., Muhammad, T. S. T., Othman, A. S., et al. (2010). Cloning and characterization of poly(3-hydroxybutyrate) biosynthesis genes from *Pseudomonas* sp. USM 4-55. *J. Basic Microbiol.* 50, 179–189. doi: 10.1002/jobm.200900138

Trejo, A., Moreno, S., Cocotl-Yañez, M., and Espín, G. (2017). GacA regulates the PTSNtr-dependent control of cyst formation in *Azotobacter vinelandii*. *FEMS Microbiol. Lett.* 364:fnw278. doi: 10.1093/femsle/fnw278

Tribelli, P. M., Méndez, B. S., and López, N. I. (2010). Oxygen-sensitive global regulator, *anr*, is involved in the biosynthesis of poly(3-Hydroxybutyrate) in

Pseudomonas extremaustralis. *J. Mol. Microbiol. Biotechnol.* 19, 180–188. doi: 10.1159/000320261

Trotsenko, Y. A., and Belova, L. L. (2000). Biosynthesis of poly(3-Hydroxybutyrate) and poly(3-hydroxybutyrate-co-3-hydroxyvalerate) and its regulation in bacteria. *Microbiology* 69, 635–645. doi: 10.1023/A:1026641821583

Tsuge, T., Taguchi, K., Taguchi, S., and Doi, Y. (2003). Molecular characterization and properties of (R)-specific enoyl-CoA hydratases from *Pseudomonas aeruginosa*: Metabolic tools for synthesis of polyhydroxyalkanoates via fatty acid β-oxidation. *Int. J. Biol. Macromol.* 31, 195–205. doi: 10.1016/S0141-8130(02)00082-X

van Heeswijk, W. C., Westerhoff, H. V., and Boogerd, F. C. (2013). Nitrogen assimilation in *Escherichia coli*: putting molecular data into a systems perspective. *Microbiol. Mol. Biol. Rev.* 77, 628–695. doi: 10.1128/mmbr.00025-13

Velázquez, F., Pflüger, K., Cases, I., De Eugenio, L. I., and De Lorenzo, V. (2007). The phosphotransferase system formed by PtsP, PtsO, and PtsN proteins controls production of polyhydroxyalkanoates in *Pseudomonas putida*. *J. Bacteriol.* 189, 4529–4533. doi: 10.1128/JB.00033

Volova, T. G., Zhila, N. O., Shishatskaya, E. I., Mironov, P. V., Vasil'Ev, A. D., Sukovatyi, A. G., et al. (2013). The physicochemical properties of polyhydroxyalkanoates with different chemical structures. *Polym. Sci. Ser. A.* 55, 427–437. doi: 10.1134/S0965545X13070080

Wang, Q., Tappel, R. C., Zhu, C., and Nomura, C. T. (2012). Development of a new strategy for production of medium-chain-length polyhydroxyalkanoates by recombinant *Escherichia coli* via inexpensive non-fatty acid feedstocks. *Appl. Environ. Microbiol.* 78, 519–527. doi: 10.1128/AEM.07020-11

Wu, G., Moir, A. J. G., Sawers, G., Hill, S., and Poole, R. K. (2001). Biosynthesis of poly-β-hydroxybutyrate (PHB) is controlled by CydR (Fnr) in the obligate aerobe *Azotobacter vinelandii*. *FEMS Microbiol. Lett.* 194, 215–220. doi: 10.1016/S0378-1097(00)00533-4

Ye, J. Y., Liu, T., Chen, Y., Liao, Q., Wang, Z. K., and Chen, G. C. (2013). Effect of AI crude extract on PHB accumulation and hydrogen photoproduction in *Rhodobacter sphaeroides*. *Int. J. Hydrogen Energy* 38, 15770–15776. doi: 10.1016/j.ijhydene.2013.03.141

York, G. M., Junker, B. H., Stubbe, J., and Sinskey, A. J. (2002). The *Ralstonia eutropha* PhaR protein couples synthesis of the PhaP phasin to the presence of polyhydroxybutyrate in cells and promotes polyhydroxybutyrate production. *J. Bacteriol.* 183, 59–66. doi: 10.1128/JB.184.1.59-66.2002

Conflict of Interest: The authors declare that the research was conducted in the absence of any commercial or financial relationships that could be construed as a potential conflict of interest.

frontiers in Bioengineering and Biotechnology

ORIGINAL RESEARCH
published: 05 May 2020
doi: 10.3389/fbioe.2020.00329

Catabolic Division of Labor Enhances Production of D-Lactate and Succinate From Glucose-Xylose Mixtures in Engineered *Escherichia coli* Co-culture Systems

Andrew D. Flores[1], Hyun G. Choi[2], Rodrigo Martinez[2], Moses Onyeabor[2], E. Zeynep Ayla[1], Amanda Godar[2], Michael Machas[1], David R. Nielsen[1] and Xuan Wang[2]**

[1] Chemical Engineering, School for Engineering of Matter, Transport, and Energy, Arizona State University, Tempe, AZ, United States, [2] School of Life Sciences, Arizona State University, Tempe, AZ, United States

OPEN ACCESS

Edited by:
Ignacio Poblete-Castro,
Andres Bello University, Chile

Reviewed by:
Rongming Liu,
University of Colorado Boulder, United States
Tsutomu Tanaka,
Kobe University, Japan
Patrick C. Cirino,
University of Houston, United States

***Correspondence:**
David R. Nielsen
david.r.nielsen@asu.edu
Xuan Wang
wangxuan@asu.edu

Specialty section:
This article was submitted to Industrial Biotechnology, a section of the journal Frontiers in Bioengineering and Biotechnology

Received: 29 January 2020
Accepted: 25 March 2020
Published: 05 May 2020

Citation:
Flores AD, Choi HG, Martinez R, Onyeabor M, Ayla EZ, Godar A, Machas M, Nielsen DR and Wang X (2020) Catabolic Division of Labor Enhances Production of D-Lactate and Succinate From Glucose-Xylose Mixtures in Engineered Escherichia coli Co-culture Systems. Front. Bioeng. Biotechnol. 8:329. doi: 10.3389/fbioe.2020.00329

Although biological upgrading of lignocellulosic sugars represents a promising and sustainable route to bioplastics, diverse and variable feedstock compositions (e.g., glucose from the cellulose fraction and xylose from the hemicellulose fraction) present several complex challenges. Specifically, sugar mixtures are often incompletely metabolized due to carbon catabolite repression while composition variability further complicates the optimization of co-utilization rates. Benefiting from several unique features including division of labor, increased metabolic diversity, and modularity, synthetic microbial communities represent a promising platform with the potential to address persistent bioconversion challenges. In this work, two unique and catabolically orthogonal *Escherichia coli* co-cultures systems were developed and used to enhance the production of D-lactate and succinate (two bioplastic monomers) from glucose–xylose mixtures (100 g L^{-1} total sugars, 2:1 by mass). In both cases, glucose specialist strains were engineered by deleting *xylR* (encoding the xylose-specific transcriptional activator, XylR) to disable xylose catabolism, whereas xylose specialist strains were engineered by deleting several key components involved with glucose transport and phosphorylation systems (i.e., *ptsI*, *ptsG*, *galP*, *glk*) while also increasing xylose utilization by introducing specific *xylR* mutations. Optimization of initial population ratios between complementary sugar specialists proved a key design variable for each pair of strains. In both cases, ∼91% utilization of total sugars was achieved in mineral salt media by

simple batch fermentation. High product titer (88 g L^{-1} D-lactate, 84 g L^{-1} succinate) and maximum productivity (2.5 g L^{-1} h^{-1} D-lactate, 1.3 g L^{-1} h^{-1} succinate) and product yield (0.97 g g-total $sugar^{-1}$ for D-lactate, 0.95 g g-total $sugar^{-1}$ for succinate) were also achieved.

Keywords: division of labor, co-culture, biomass conversion, lactate, succinate

INTRODUCTION

Production of D-lactate (LA) and succinate (SA) from renewable carbohydrate feedstocks provides a sustainable and greener alternative to their petroleum-based production (Abdel-Rahman et al., 2013; Ahn et al., 2016; Es et al., 2018). LA and SA serve as two important monomers in the production of biodegradable plastics, including poly(butylene succinate) (PBS) and poly(lactic acid) (PLA), respectively. SA is largely produced via petroleum-derived maleic anhydride, and only a handful of plants producing bio-based SA currently exists (Jansen and van Gulik, 2014). Meanwhile, ∼95% of global LA production occurs via fermentation, being derived almost entirely from costly raw materials such as grain starch or sucrose from sugar cane, feedstocks that compete with the food chain (Okano et al., 2010; Abdel-Rahman et al., 2011). Alternatively, lignocellulose-derived sugars from non-food carbohydrates such as agricultural residues, forest products, or energy crops represent an attractive feedstock for producing bio-based plastics due to their increased abundance and sustainability, as well as lower cost (Lynd, 2017). The two most abundant sugars in most lignocellulosic biomass is glucose (a hexose, accounting for ∼30–50% dry weight) from the cellulose fraction and xylose (a pentose, constituting ∼20–35% dry weight) from the hemicellulose fraction (Nieves et al., 2015). Minute quantities of other fermentable sugars (i.e., arabinose, galactose, mannose) are additionally found in lignocellulosic biomass (Nieves et al., 2015).

For many native and engineered bacteria, the inability to efficiently co-utilize sugar mixtures in mineral salts medium at high catabolic rates (e.g., > 2 g L^{-1} h^{-1} for each sugar) is due to a complex, global regulatory phenomenon known as carbon catabolite repression (CCR), which often results in incomplete and/or sequential sugar utilization. For instance, in *Escherichia coli*, this sequential sugar preference is controlled via the coordinated action of the global transcriptional regulator cyclic AMP (cAMP) receptor protein (CRP) along with a second regulator specific to the secondary sugars of interest, such as xylose. Activation of the requisite xylose catabolism operons (i.e., *xylFGH* and *xylAB*) requires both activated CRP (active when bound by cAMP) and XylR (regulator specific for xylose catabolism, active when bound by xylose) (Song and Park, 1997; **Figure 1**). When wild-type *E. coli* ferments glucose–xylose mixtures, for example, cAMP levels are low because abundant extracellular glucose leads to the active mode of the phosphotransferase system (PTS), increasing the abundance of unphosphorylated PTS components (IIA protein) and inhibiting the activity of adenylyl cyclase (AC; catalyzing cAMP synthesis). Xylose catabolism thus does not occur due to the lack of activated CRP and, as a result, initiates only after glucose is mostly utilized and phosphorylated IIA protein activates AC, leading to high cAMP levels (**Figure 1**).

To date, several engineered microorganisms producing LA [e.g., lactic-acid bacteria (LAB), *Saccharomyces cerevisiae, E. coli*] and SA (e.g., *Mannheimia succiniciproducens, Corynebacterium glutamicum, Bacillus* strains) have been reported using various substrates (Grabar et al., 2006; Ishida et al., 2006; Wang et al., 2011; Litsanov et al., 2012; Awasthi et al., 2018). While different strains have their own unique advantages/disadvantages (e.g., ease of genetic manipulation, product tolerance, and other physiological benefits), from a bioprocessing perspective, it is desirable that it should also be capable of rapidly and simultaneously utilizing the substrate at high initial loadings (e.g., ≥ 100 g L^{-1} total sugar). Under such conditions, *E. coli* has proven to be a particularly promising biocatalyst for the production of both LA and SA. In particular, via a combination of engineering strategies, *E. coli* strains have been developed to produce both LA and SA at high yields (>90%) and titers (>90 g L^{-1}) and maximum productivities (>1.0 g L^{-1} h^{-1}) (Sawisit et al., 2015; Utrilla et al., 2016; Sievert et al., 2017). Despite these achievements, however, challenges still remain with respect to the efficient conversion of glucose–xylose mixtures.

Owing to unique features such as strain-specific specialization and metabolic modularity, the engineering and use of synthetic microbial communities represent a promising bioprocessing strategy (Zhang et al., 2015; Zhou et al., 2015; Camacho-Zaragoza et al., 2016; Jones et al., 2017), with the potential to surmount many limitations faced by traditional monocultures (Lu et al., 2019; Roell et al., 2019). Through catabolic division of labor, for example, engineered co-cultures have specifically emerged as an effective strategy for achieving efficient co-utilization of different mixtures of lignocellulose-derived sugars (Eiteman et al., 2008; Zhang et al., 2015; Chappell and Nair, 2017; Wang et al., 2019). Eiteman et al. (2008) first demonstrated the utility of this approach, engineering a co-culture composed of *E. coli* sugar specialist strains to co-utilize glucose–xylose mixtures (∼14 g L^{-1} total sugars). This general strategy was later expanded upon by others to develop a three-member community of *E. coli* specialists to co-utilize a mixture of glucose, galactose, and mannose (∼7.5 g L^{-1} total sugars) (Chappell and Nair, 2017). Most recently, meanwhile, our group engineered two different catabolically orthogonal co-culture systems (derived from wild-type *E. coli* W or ethanologenic *E. coli* LY180), each capable of co-utilizing 100 g L^{-1} of a glucose–xylose mixture (2:1 by weight) in mineral salt media by simple batch fermentation (Flores et al., 2019). In this work, we further explore the utility of this strategy by applying analogous principles to engineer two unique co-culture systems composed of catabolically orthogonal *E. coli* strains for the production of LA and SA from glucose–xylose mixtures. In

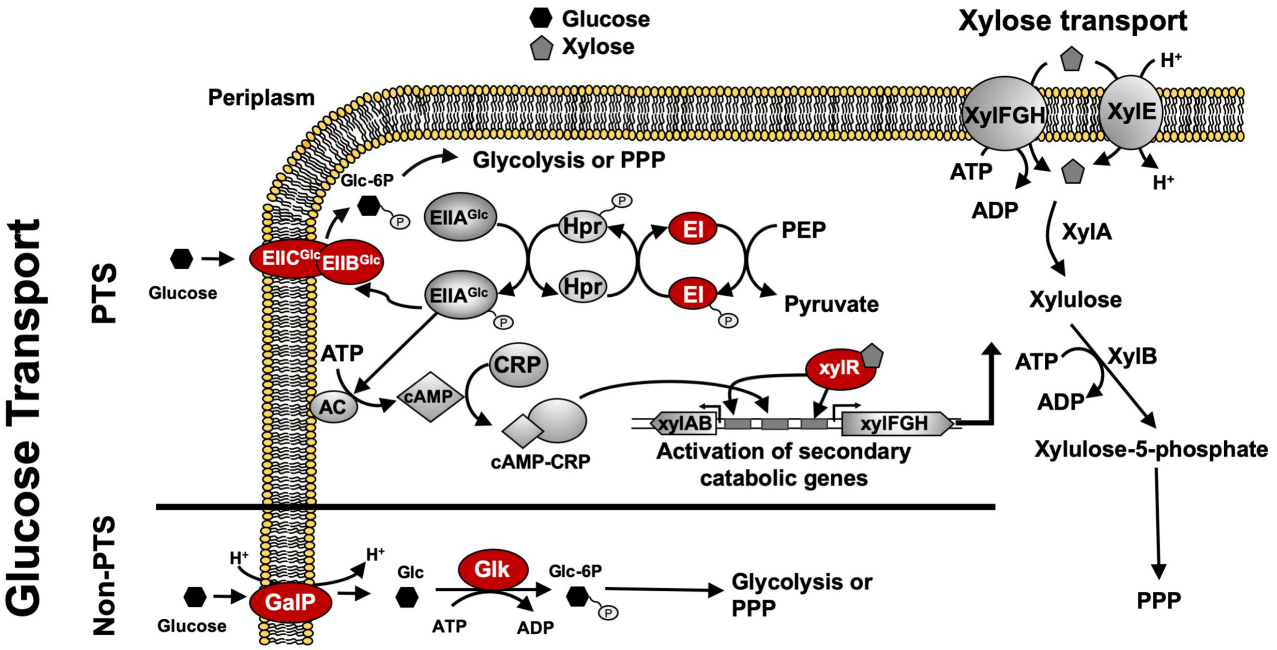

FIGURE 1 | Regulatory and catabolic pathways for glucose and xylose metabolism in *E. coli*. The primary mechanism for glucose transport in *E. coli* is through the phosphoenolpyruvate: sugar phosphotransferase system (PTS), including components $EIIBC^{Glc}$, $EIIA^{Glc}$, Hpr, and EI (encoded by *ptsG*, *crr*, *ptsH*, and *ptsI*, respectively). Under high glucose concentrations, glucose is transported via $EIICB^{Glc}$, leading to more abundant unphosphorylated $EIICA^{Glc}$ that inhibits adenylate cyclase (AC) and lowers cAMP levels. Glucose-induced catabolite repression is mainly caused by low levels of cAMP which leads to non-functional CRP. Without CRP activation, the transcriptional activation of xylose catabolism pathways cannot be achieved. Under low glucose concentrations, AC is active due to the decreased amount of unphosphorylated $EIICA^{Glc}$, thus leading to increased cAMP levels and activated CRP. Both activated CRP and XylR (activated when bound by xylose) are required to activate the xylose catabolic operons, *xylAB* and *xylFGH*. Phosphorylated sugar intermediates enter glycolysis or PPP pathways for full degradation. GalP functions as an alternative non-PTS glucose transporter and *glk* encodes cytoplasmic glucokinase to phosphorylate glucose for further glycolysis. Glucose uptake systems including both PTS components and GalP as well as Glk and XylR indicated in red ovals are genetic engineering targets to construct sugar specialists. Abbreviation: AC, adenylate cyclase; CRP, cAMP receptor protein; PPP, pentose phosphate pathway; Glc, glucose; Glc-6P, glucose 6-phosphate; Xyl; xylose.

both cases, optimization of initial population ratios between each strain pair proved a key design variable toward achieving efficient conversion of the feedstock mixture along with high production metrics. This strategy of "population-level" tuning helps to alleviate biosynthetic burden while circumventing technical difficulties that would otherwise accompany the more traditional optimization of multiple catabolic pathways in a single strain.

RESULTS AND DISCCUSION

Construction of Catabolically Orthogonal Sugar Specialists for D-Lactate Production

TG114 (a derivative of *E. coli* KO11 and based on *E. coli* W) has previously been shown to produce LA at maximum volumetric productivity (2.88 g L^{-1} h^{-1}), titer (118 g L^{-1}), yield (98%), and chiral purity (>99.9%) in mineral salts medium containing 120 g L^{-1} glucose (Grabar et al., 2006). In spite of this, however, poor performance is apparent in sugar mixtures as a result of CCR (**Supplementary Figures S1A–D**). Specifically, when cultured using a 100 g L^{-1} glucose–xylose mixture (2:1 by mass), TG114 utilized 88% of the provided glucose within the first 24 h and 100% by 48 h, but only 38% of the supplied xylose by 96 h, corresponding to only ∼80% total sugar utilization. LA was produced, meanwhile, at overall and maximum volumetric productivities (Q_{LA}) of 0.80 ± 0.01 and 2.6 ± 0.4 g L^{-1} h^{-1}, a final titer of 77 ± 1 g L^{-1}, and yield ($Y_{p/s}$) of 0.96 ± 0.02 g g-total sugars^{-1} (note: all reported yields based on total sugars consumed). To overcome the sugar co-utilization bottleneck experienced by TG114, a division of labor approach was used to construct a pair of complementary, catabolically orthogonal specialist strains, each capable of catabolizing either glucose or xylose but not both sugars (**Supplementary Figure S2A**). Specifically, a glucose specialist strain, TGglc, was constructed by deleting the xylose-specific transcriptional activator XylR (encoded by *xylR*) to inactivate xylose catabolism. A xylose specialist strain, TGxyl, was constructed by deleting the major components of glucose transport and its initial catabolism (i.e., *ptsI*, *ptsG*, *galP*, *glk*) (**Figure 1** and **Table 1**). To further enhance xylose utilization of this specialist strain, wild-type XylR was also replaced with a mutant copy [P363S and R121C; denoted as XylR* and reported to enable a stronger activation of the D-xylose catabolic genes (Sievert et al., 2017)].

TABLE 1 | List of strains and plasmids used in this study.

Strains and plasmids	Relevant characteristics	Source
Strains		
TG114	ATCC 9637 Δ*pflB frdBC*:FRT *adhE*:FRT *ackA*:FRT *mgsA*:FRT evolved for converting glucose to D-lactate	Grabar et al., 2006
TGglc	TG114 Δ*xylR*	This study
TGxyl	TG114 Δ*ptsI*Δ*ptsG*Δ*galP glk*:*kan*^{R} (Kan^R) *xylR*:*xylR**	This study
KJ122	ATCC 8739 *pck**^{A} *ptsI**^{B} Δ*ldhA* Δ*adhE* Δ*ackA*, Δ(*focA-pflB*) Δ*mgsA* Δ*poxB* Δ*tdcDE* Δ*citF* Δ*aspC* Δ*sfcA*	Jantama et al., 2008
KJglc	KJ122 *xylR*:*tetA-sacB* (Tet^R)	This study
KJxyl	KJ122 Δ*galP*Δ*ptsI glk*:*kan*^{R} (Kan^R) *xylR*:*xylR** quickly adapted in glucose-xylose mixture	This study
T-SACK	W3110 *ara*D < > *tetA-sacB-amp flic* < > *cat argG:Tn*5	Li et al., 2013
Plasmids		
pXW001	The *cat-sacB* cassette with the *sacB* native terminator cloned into a modified vector pLOI4162	Sievert et al., 2017
pKD46	Red recombinase, temperature-conditional, *bla*	Datsenko and Wanner, 2000

^{A}pck denotes a mutated form of pck (G to A at position -64 relative to the ATG start codon). ^{B}ptsI* denotes a mutated form of ptsI (single-base deletion at position 1,673 causing a frameshift mutation in the carboxyl-terminal region.*

Consistent with their respective genotypes, TGglc and TGxyl each preferentially utilized only one sugar when fermented in mineral salt media supplemented with 66 g L^{-1} glucose and 33 g L^{-1} xylose (**Figures 2A,B** and **Table 2**). TGglc utilized 100% of the supplied glucose within 48 h (77% within the first 24 h, similar to TG114) and virtually no xylose. This resulted in a maximum Q_{LA} of 2.0 ± 0.1 g L^{-1} h^{-1} (overall, Q_{LA} was 0.68 ± 0.01 g L^{-1} h^{-1}), final LA titer of 66 ± 1 g L^{-1}, and $Y_{p/s}$ of 0.96 g g-total sugars $^{-1}$ (**Figures 2C,D** and **Table 2**). In contrast, under the same conditions, TGxyl consumed just ∼80% of supplied xylose by 96 h and no glucose (**Figures 2A,B**). Growth of TGxyl, meanwhile, was significantly less than that of TGglc and TG114 [1.1 ± 0.1 g-dry cell weight (DCW) L^{-1} compared to 2.7 ± 0.1 and 2.9 ± 0.2 gDCW L^{-1}, respectively]. While this difference is at least in part due to the lower energy yield of xylose relative to glucose, it is also possible that, since TG114 was originally engineered for and adapted in mineral salt media containing only glucose as carbon source (Grabar et al., 2006), it may have only gained mutations specifically tailored for glucose catabolism. Despite its slower growth rate and reduced biomass accumulation, TGxyl still produced LA at a final titer of 25 ± 1 g L^{-1}, $Y_{p/s}$ of ∼0.99 g g-total sugars $^{-1}$, and maximum Q_{LA} of 0.50 ± 0.08 g L^{-1} h^{-1} (**Figures 2C,D** and **Table 2**).

Engineering and Optimizing a Synthetic Co-culture for Efficient Conversion of Glucose–Xylose Mixtures to D-Lactate

Given their promising performance metrics with respect to LA production and minimal cross-catabolic activities, TGglc and TGxyl were next used as complementary specialist strains with which to engineer a synthetic co-culture. To balance catabolic rates, simple titration of the initial inoculum ratio between TGglc and TGxyl (e.g., 1:1, 1:50, 1:100) while maintaining a constant total initial OD_{550nm} of 0.05 (the same initial OD_{550nm} as in monoculture fermentations) was performed. As shown in **Figure 3A** and **Table 2**, glucose was completely utilized within 48 h for all ratios (similar to TG144 and TGglc monocultures). However, as a result of tuning the initial population, initial volumetric rates of glucose utilization (Q_{Glc}) were subsequently reduced over the first 24 h in a manner proportional to the relative abundance of TGglc (2.4 ± 0.1, 0.82 ± 0.40, and 0.13 ± 0.02 g L^{-1} h^{-1} for ratios 1:1, 1:50, and 1:100, respectively), along with initial rates of biomass accumulation (**Figure 3D** and **Table 2**). The corresponding profiles of xylose fermentation (**Figure 3B**), meanwhile, revealed the opposite and expected effect with respect to xylose catabolism; increasing abundance of TGxyl in the initial inoculum improves xylose utilization. More specifically, at equal abundance (i.e., 1:1), total xylose utilization reached merely 22% by 96 h. This corresponded to 5% less total sugar utilization than by TG114 monocultures (75 vs. 80% total sugar utilization, respectively; **Table 2**). However, by tuning the initial inoculum ratio to 1:50, 2.6-, and 1.5-fold increases in xylose utilization (58% total xylose used) were realized relative to co-cultures with a 1:1 initial inoculum ratio and TG114 monocultures, respectively (**Table 2**). Owing to this significant increase in xylose co-utilization, final LA titers achieved by 1:50 co-cultures reached 84 ± 2 g L^{-1} (∼11% higher than the 1:1 co-culture; **Figure 3C**), while still maintaining high overall performance metrics ($Y_{p/s}$ of 0.96 g g-total sugars^{-1}, maximum Q_{LA} of 3.7 ± 1.1 g L^{-1} h^{-1}; **Table 2**). Further increasing the relative initial abundance of TGxyl, 1:100 co-cultures then enabled further increased utilization of supplied xylose, in this case reaching ∼71% (**Figure 3B**). Moreover, total sugar utilized reached 91% by the end of the 96 h fermentation, achieving a final LA titer of 88 ± 1 g L^{-1}, $Y_{p/s}$ of ∼0.97 g g-total sugars^{-1}, and maximum Q_{LA} of 2.5 ± 0.2 g L^{-1} h^{-1} (**Table 2**). Based on the promising trends observed with 1:50 and 1:100 co-cultures, additional tuning of the inoculum ratio to further increase the initial abundance of TGxyl was subsequently performed, in this case at both 1:500 and 1:1,000 (data not shown). However, no further performance enhancements were realized in terms of either total sugar utilization or LA production in such co-cultures, suggesting that the optimal initial inoculum ratio for TGglc:TGxyl exists at least close to 1:100. Thus, further improvement of this co-culture should next focus on enhancing the inherent properties of each individual strain; for example, increasing rates of xylose

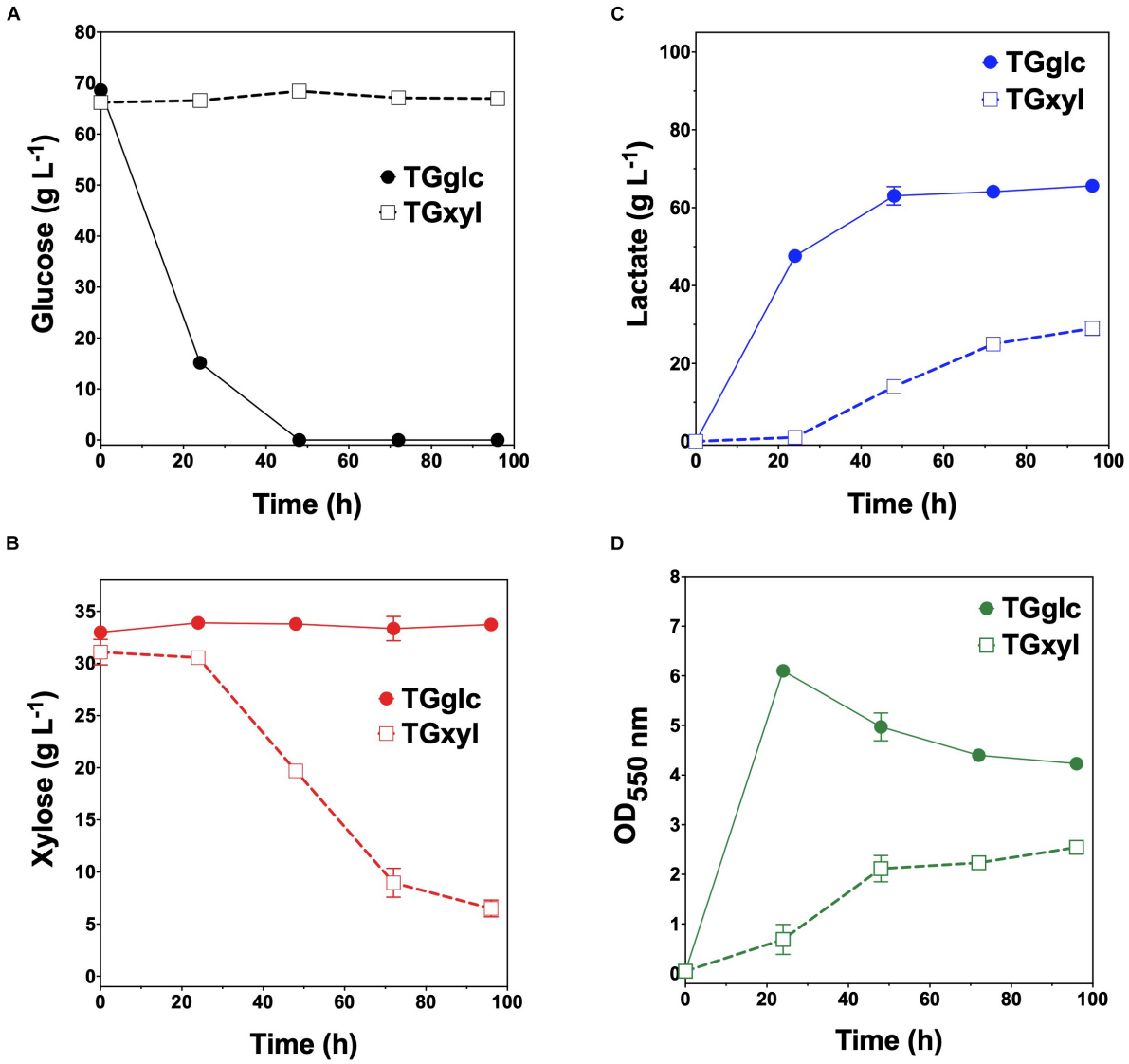

FIGURE 2 | Fermentation of glucose–xylose mixtures (2:1 by mass) by lactate-producing sugar specialist strains. Concentrations of **(A)** glucose, **(B)** xylose, **(C)** D-lactate, and **(D)** OD_{550nm} measured in the fermentation broth for TGglc (closed circles) and TGxyl (open squares). All fermentations were performed in batch mode and in mineral salts media. Data points represent the arithmetic mean of three replicates, and the error bars represent one standard deviation.

catabolism in sugar mixtures by TGxyl through adaptation and/or genetic engineering.

LA production performance demonstrated by the 1:100 co-culture compares well to that of other co-cultures previously engineered for the same purpose, as well as those developed to produce other related fermentation products (**Table 3**). In particular, Eiteman et al. (2009) developed an *E. coli* co-culture composed of glucose and xylose specialists capable of co-utilizing and converting a sugar mixture (~47 g L^{-1} total sugar, ratio of glucose to xylose is 1.5:1 by mass) to LA (final titer of 32 g L^{-1}, $Y_{p/s}$ of 0.68 g g-total sugars^{-1}) in a two-stage, aerobic–anaerobic process (**Table 3**). In this case, rather than tuning the initial population ratio, a sequential inoculation strategy was instead employed to balance the contribution of each specialist to the net catabolic activity, allowing more time initially for the xylose specialist strain to accumulate under aerobic conditions. Upon reaching the anaerobic phase, the population ratio in their co-culture was estimated as 2:3 glucose:xylose specialists, which similarly illustrates a need for increased abundance of the xylose specialist in this fermentation. In comparison to LA-producing monocultures, Sievert et al. (2017) demonstrated that substituting wild-type *xylR* with *xylR** (R121C and P363S; the same mutations used to develop TGxyl in this study) in TG114 enabled co-utilization of 50 g L^{-1} glucose and 43 g L^{-1} xylose (from 100 g L^{-1} glucose–xylose mixture, initially 1:1 by mass) to 86 g L^{-1} LA in mineral salt medium. While minor improvement in terms of sugar utilization was achieved using the present co-culture system, a unique advantage of this approach is the

TABLE 2 | Comparing the performance of individual *E. coli* sugar specialists and co-cultures during D-lactate (LA) and succinate (SA) fermentation.

Strains(s)	Sugar utilized (%)			Biomass[B]	Q (g L^{-1} h^{-1})[C]			$Y_{p/s}$	Titer
Fermented	**Glucose**	**Xylose**	**Total[A]**	**gDCW L^{-1}**	**Glucose**	**Xylose**	**Product**	**g g^{-1}[D]**	**g L^{-1}**
Lactate									
TGglc	100 ± 0	NC	68 ± 1	2.7 ± 0.1	2.2 ± 0.1	NR	2.0 ± 0.1	0.96 ± 0.01	65 ± 1
TGxyl	NC	80 ± 2	25 ± 1	1.1 ± 0.1	NR	0.44 ± 0.01	0.50 ± 0.08	0.99 ± 0.1	25 ± 1
TGglc:TGxyl Ratio 1:1	100 ± 0	22 ± 1	75 ± 1	2.8 ± 0.1	5.5 ± 0.4	0.35 ± 0.04	5.8 ± 0.5	0.99 ± 0.04	73 ± 2
TGglc:TGxyl Ratio 1:50	100 ± 0	58 ± 2	86 ± 1	2.7 ± 0.1	3.2 ± 0.6	0.44 ± 0.04	3.7 ± 1.1	0.95 ± 0.02	84 ± 2
TGglc:TGxyl Ratio 1:100	100 ± 0	71 ± 3	91 ± 1	2.7 ± 0.3	2.4 ± 0.2	0.52 ± 0.05	2.5 ± 0.2	0.97 ± 0.01	88 ± 1
Succinate									
KJglc	100 ± 0	NC	71 ± 1	2.9 ± 0.1	2.1 ± 0.1	NR	1.9 ± 0.1	0.88 ± 0.01	65 ± 1
KJxyl	NC	87 ± 2	28 ± 2	2.7 ± 0.2	NR	0.60 ± 0.06	0.69 ± 0.20	1.21 ± 0.05	33 ± 1
KJglc:KJxyl Ratio 1:1	93 ± 5	89 ± 2	91 ± 4	3.1 ± 0.2	0.84 ± 0.1	0.72 ± 0.04	1.3 ± 0.1	0.95 ± 0.01	84 ± 1
KJglc:KJxyl Ratio 1:50	19 ± 14	86 ± 2	39 ± 9	2.8 ± 0.2	0.49 ± 0.2	0.73 ± 0.1	0.82 ± 0.1	0.97 ± 0.1	37 ± 4
KJglc:KJxyl Ratio 1:100	6 ± 4	88 ± 1	31 ± 3	2.9 ± 0.1	0.2 ± 0.1	0.66 ± 0.06	0.69 ± 0.02	0.94 ± 0.1	29 ± 1
KJglc:KJxyl Ratio 2:1	100 ± 0	46 ± 4	83 ± 1	3.4 ± 0.1	1.4 ± 0.1	0.30 ± 0.09	2.1 ± 0.1	0.84 ± 0.08	76 ± 6

All cultures were initially supplied with ∼100 g L^{-1} of glucose–xylose mixtures (ratio 2:1 by mass). No Consumption (NC) < 1% sugar utilized; No Rate (NR) < 0.1 g L^{-1} h^{-1}. [A]Total sugar utilized per sugar supplied. [B]Dry cell weight (DCW) values are calculated from maximum OD_{550nm} (0.44 gDCW L^{-1} with an optical density of 1.0 at 550 nm). [C]Maximum volumetric rates (Q) are calculated when the slope of substrate utilization or product formation is most linear. [D]$Y_{p/s}$ denotes the product yield coefficient and is calculated as gram product per gram total sugar utilized.

facile tunability that it provides. In this case, catabolic rates can be titrated to achieve optimal fermentation performance by altering initial inoculum ratios between the two specialists. This ability will likely be beneficial when utilizing feedstocks of varying compositions and can be extended beyond simply binary sugar mixtures.

Finally, one intriguing observation associated with the developed LA co-culture system was that the volumetric rate of xylose utilization (Q_{Xyl}) was found to consistently and abruptly decrease in all co-cultures upon exhaustion of available glucose. For instance, as seen in **Figures 3A,B**, prior to glucose exhaustion, maximum Q_{Xyl} values were ∼0.35 ± 0.04, 0.44 ± 0.04, and 0.52 ± 0.05 g L^{-1} h^{-1} for 1:1, 1:50, and 1:100 co-cultures, respectively. However, following glucose exhaustion, Q_{Xyl} in the same co-cultures then dropped to just 0.034 ± 0.009, 0.062 ± 0.004, and 0.12 ± 0.02 g L^{-1} h^{-1}. It is unlikely that LA or by-product toxicity is responsible for this behavior since the parent strain (TG114) has been shown to achieve LA titers up to 120 g L^{-1}, and almost no other side products are detected during its fermentation (Grabar et al., 2006). This observation possibly suggests that, although the two strains were engineered to be catabolically orthogonal, interstrain interactions certainly do occur throughout these synthetic co-cultures. The exact nature and extent of this behavior remain unknown, however, and warrant further investigation.

Construction of Catabolically Orthogonal Sugar Specialists for Succinic Acid Production

To further investigate the generalizable nature of this co-culture strategy along with sets of specific genetic modifications used to create each sugar specialist, the same methodologies were next analogously applied to SA production from glucose–xylose mixtures. In this case, the succinogenic strain KJ122 (a derivative of *E. coli* ATCC 8739) was used as the common parent for constructing the two sugar specialist strains: KJglc and KJxyl (**Table 1** and **Supplementary Figure S2**). KJ122 was previously engineered and shown to ferment 100 g L^{-1} glucose to SA (final titer of 82 g L^{-1}, overall Q_{SA} of 0.88 g L^{-1} h^{-1}, $Y_{p/s}$ of 0.90 g g-total sugars^{-1}) in mineral salts media (Jantama et al., 2008). Similar to TGglc, batch fermentation of KJglc also revealed virtually no xylose utilization (**Figure 4B**). In this case, glucose was completely utilized within 42 h at a maximum Q_{Glc} of 2.1 ± 0.1 g L^{-1} h^{-1}, while SA was produced at a maximum Q_{SA} of 1.9 ± 0.1 g L^{-1} h^{-1}. At this output, the performance of KJglc was similar to that of its parent strain, KJ122 (**Figure 4A**, **Table 2**, and **Supplementary Figures S1A–D**). Likewise, and as expected, KJxyl was unable to utilize glucose throughout the 120 h fermentation (**Figure 4A**), but utilized 87% of supplied xylose, leaving just 5 g L^{-1} unused (**Figure 4B** and **Table 2**). With maximum Q_{Xyl} and Q_{SA} of 0.60 ± 0.06 and 0.69 ± 0.20 g L^{-1} h^{-1}, respectively, overall performance of KJxyl was also similar to that of KJ122 (**Supplementary Figure S1A**).

Engineering and Optimizing a Synthetic Co-culture for Efficient Conversion of Glucose– Xylose Mixtures to Succinic Acid

KJglc and KJxyl were next combined to develop a synthetic co-culture for producing SA from glucose–xylose mixtures, again employing the same population-level tuning strategy in order to optimize sugar co-utilization. Based on the outcomes revealed for LA production, initial inoculation ratios of 1:1, 1:50, and

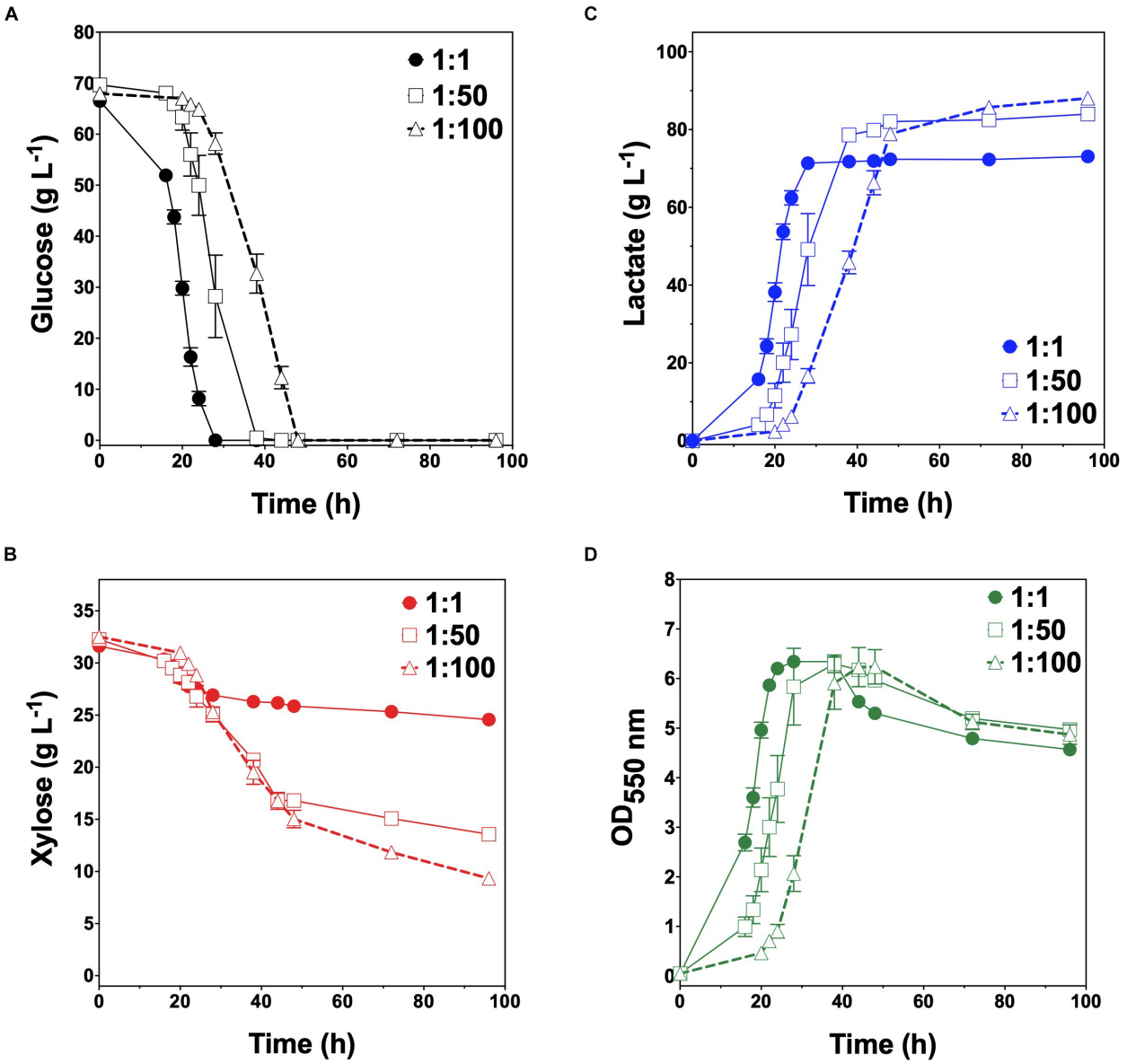

FIGURE 3 | Fermentation of glucose–xylose mixtures (2:1 by mass) co-cultures composed of catabolically orthogonal lactate-producing specialist strains. Concentrations of **(A)** glucose, **(B)** xylose, **(C)** D-lactate, and **(D)** OD_{550nm} measured in the fermentation broth for TGglc:TGxyl co-cultures using an initial inoculum ratio of 1:1 (closed circles), 1:50 (open squares) and 1:100 (open triangles). All fermentations were performed in batch mode and in mineral salts media. Data points represent the arithmetic mean of three replicates, and the error bars represent one standard deviation.

1:100 KJglc:KJxyl were first explored. As shown in **Figure 5B** and **Table 2**, total xylose utilization and Q_{Xyl} were similar for each of the 1:1, 1:50, and 1:100 co-cultures (each ∼87% and ∼0.67 g L^{-1} h^{-1}, respectively) and close to that of the KJxyl monoculture. Meanwhile, however, total glucose utilization unexpectedly declined across this initial series of co-cultures (**Figure 5A**). For instance, compared to 1:1 co-cultures, total glucose utilization dropped by 80 and 94% in the 1:50 and 1:100, respectively; while all three co-cultures displayed reduced maximum Q_{Glc} relative to KJglc monoculture (**Figure 5B** and **Table 2**). Overall, total sugar utilization was 91, 39, and 31% for the 1:1, 1:50, and 1:100 co-cultures, respectively (compared to 71% for KJglc monocultures; **Table 2**), with the highest final SA titers reaching 84 g L^{-1} ± 1 at the 1:1 ratio (at least two-fold greater than by 1:50 or 1:100) along with a maximum Q_{SA} of 1.3 ± 0.1 g L^{-1} h^{-1} (**Figure 5C** and **Table 2**). Interestingly, in contrast to the above LA co-cultures as well as our previous work (Flores et al., 2019), increased initial relative abundance of the xylose specialist did not result in enhanced xylose utilization or, in this case, improved production of SA (**Figures 5B,C**). This is likely because, in contrast to TGxyl, KJxyl displays much greater fitness, as demonstrated, for

TABLE 3 | Comparing the performance of different *E. coli* co-cultures engineered to convert glucose and xylose to fermentative products.

Media and fermentation condition(s)	Base strain and key mutations[A]	Product(s)	Performance metric(s)[B]	References
Modified AM1 6.6% Glucose 3.4% Xylose	**Glucose**: TG114 (an *E. coli* W derivative engineered for lactate production) Δ*xylR*	D-Lactate	$Q_{Glc} \approx 2.4$ g L^{-1} h^{-1} $q_{Glc} \approx 886$ mg $gDCW^{-1}$ h^{-1} $Q_{Xyl} \approx 0.5$ g L^{-1} h^{-1} $q_{Xyl} \approx 223$ mg $gDCW^{-1}$ h^{-1} Total Sugar Utilized ≈ 91g L^{-1} Titer ≈ 88g L^{-1} Productivity ≈ 2.5 g L^{-1} h^{-1} $Y_{p/s} \approx 0.97$	This study
Batch Microaerobic	**Xylose:** TG114 Δ*ptsI* Δ*ptsG* Δ*galP* Δ*glk xylR*:*xylR**			
Basal 3.1% Glucose 2.0% Xylose	**Glucose**: *E. coli* MG1655 *xylA748*:FRT *pflB*:Cam	D-Lactate	$q_{Glc} \approx 540$ mg $gDCW^{-1}$ h^{-1} $q_{Xyl} \approx 325$ mg $gDCW^{-1}$ h^{-1} Total Sugar Utilized ≈ 47 g L^{-1} Titer ≈ 32 g L^{-1} $Y_{p/s} \approx 0.68$	Eiteman et al., 2009
Batch Aerobic–anaerobic[C]	**Xylose:** *E. coli* MG1655 *pflB*:Cam *ptsG763*:FRT *manZ743*:FRT *glk-726*:FRT			
Modified AM1 6.6% Glucose 3.4% Xylose	**Glucose:** KJ122 (an *E. coli* C derivative engineered for succinate production) *xylR*:*tetA-sacB*	Succinate	$Q_{Glc} \approx 0.84$ g L^{-1} h^{-1} $q_{Glc} \approx 188$ mg	This study
Batch Microaerobic	**Xylose:** KJ122 Δ*galP* Δ*ptsI* *glk*:*Kan*^{R} *xylR*:*xylR**		$gDCW^{-1}$ h^{-1} $Q_{Xyl} \approx 0.72$ g L^{-1} h^{-1} $q_{Xyl} \approx 276$ mg $gDCW^{-1}$ h^{-1} Total Sugar Utilized ≈ 91 g L^{-1} Titer ≈ 84 g L^{-1} Productivity ≈ 1.3 g L^{-1} h^{-1} $Y_{p/s} \approx 0.95$ g g^{-1}	
Basal Initial Sugar: 3% Glucose 1% Xylose	**Glucose:** *E. coli* ATCC8739 *ptsG*:FRT *xylA*:FRT *pflB*:FRT *ldhA*:Kan^R	Succinate	Titer ≈ 45 g L^{-1} Productivity ≈ 1.7 g L^{-1} h^{-1} $Y_{p/s} \approx 0.97$ g g^{-1}	Xia et al., 2015
Fed: 1.5% Glucose 0.5% Xylose Fed-Batch Aerobic–Anaerobic[D]	**Xylose:** *E. coli* ATCC8739 *ptsG*:FRT *glk*:FRT *manZ*:FRT *crr*:FRT *ldhA*:FRT *pflB*:FRT *ppc*:Kan^R			
Basal 1.5% Glucose 1.5% Xylose 0.2% Acetate Batch and Fed-Batch Aerobic	**Glucose:** *E. coli* C *xylA748*:FRT *ace732*:FRT *ldhA744*:FRT *poxB772*:FRT *pps-776*: Kan^R	Pyruvate	**Batch:** Titer ≈ 19 g L^{-1} Yield ≈ 61% Productivity ≈ 1.44 g L^{-1} h^{-1} **Fed-Batch:** Titer ≈ 39 g L^{-1} Productivity ≈ 1.65 g L^{-1} h^{-1}	Maleki et al., 2018
	Xylose: *E. coli* C *ptsG763*:FRT *glk-726*:FRT *manZ743*:FRT *aceE732*:FRT *ldhA744*:FRT *poxB772*:FRT *pps-776*: Kan^R			
Modified AM1 6.6% Glucose 3.4% Xylose	**Glucose:** LY180 (an *E. coli* W derivative engineered for ethanol production) Δ*xylR* adapted in glucose-xylose	Ethanol	$q_{Glc-Max} \approx 620$ mg DCW^{-1} h^{-1} $q_{Xyl-Max} \approx 300$ mg DCW–1 h^{-1} Total Sugar Utilized ≈ 98 g L^{-1} Titer ≈ 46 g L^{-1} Productivity ≈ 488 mg L^{-1} h^{-1} $Y_{p/s} \approx 0.45$ g g^{-1}	(Flores et al., 2019)
Batch Microaerobic	**Xylose:** LY180 Δ*ptsI* Δ*ptsG* Δ*galP glk*:Kan^R *xylR*:*xylR**			

[A]Gene deletion, disruption, or modification. [B]q_{Glc}, specific rate of glucose utilization; Q_{Glc}, volumetric rate of glucose utilization; q_{Xyl}, specific rate of xylose utilization; Q_{Xyl}, volumetric rate of xylose utilization (each calculated when the rate of utilization was approximately constant); Dry cell weight (DCW) calculated from maximum OD_{550nm} (0.44 gDCW L^{-1} with an optical density of 1.0 at 550 nm). [C]Fermentation consisted of two stages: initial aerobic growth followed by an anaerobic phase. [D]Minor amounts of succinate, acetate, and ethanol were also detected.

example, by its ability to accumulate twice as much biomass during monoculture fermentations [2.7 ± 0.2 gDCW L^{-1} vs. 1.1 ± 0.1 gDCW L^{-1} for TGxyl and 1.7 ± 0.1 gDCW L^{-1} for LYglc1, a previously engineered ethanologenic xylose specialist (Flores et al., 2019)]. To test if it was in fact the relative activity of the glucose specialist that instead limited the overall performance of this SA-producing co-culture, an initial inoculum ratio of 2:1 KJglc:KJxyl was at last explored. While the 2:1 co-culture utilized glucose at a faster rate and consumed 100% of provided glucose by 96 h (compared to 44 h for KJglc monoculture and KJ122), total xylose utilization, on the other hand, dropped to just 46% overall (about half of that consumed by the 1:1 co-culture; **Figure 5B** and **Table 2**). Based on this outcome, it was determined that the optimal initial inoculum

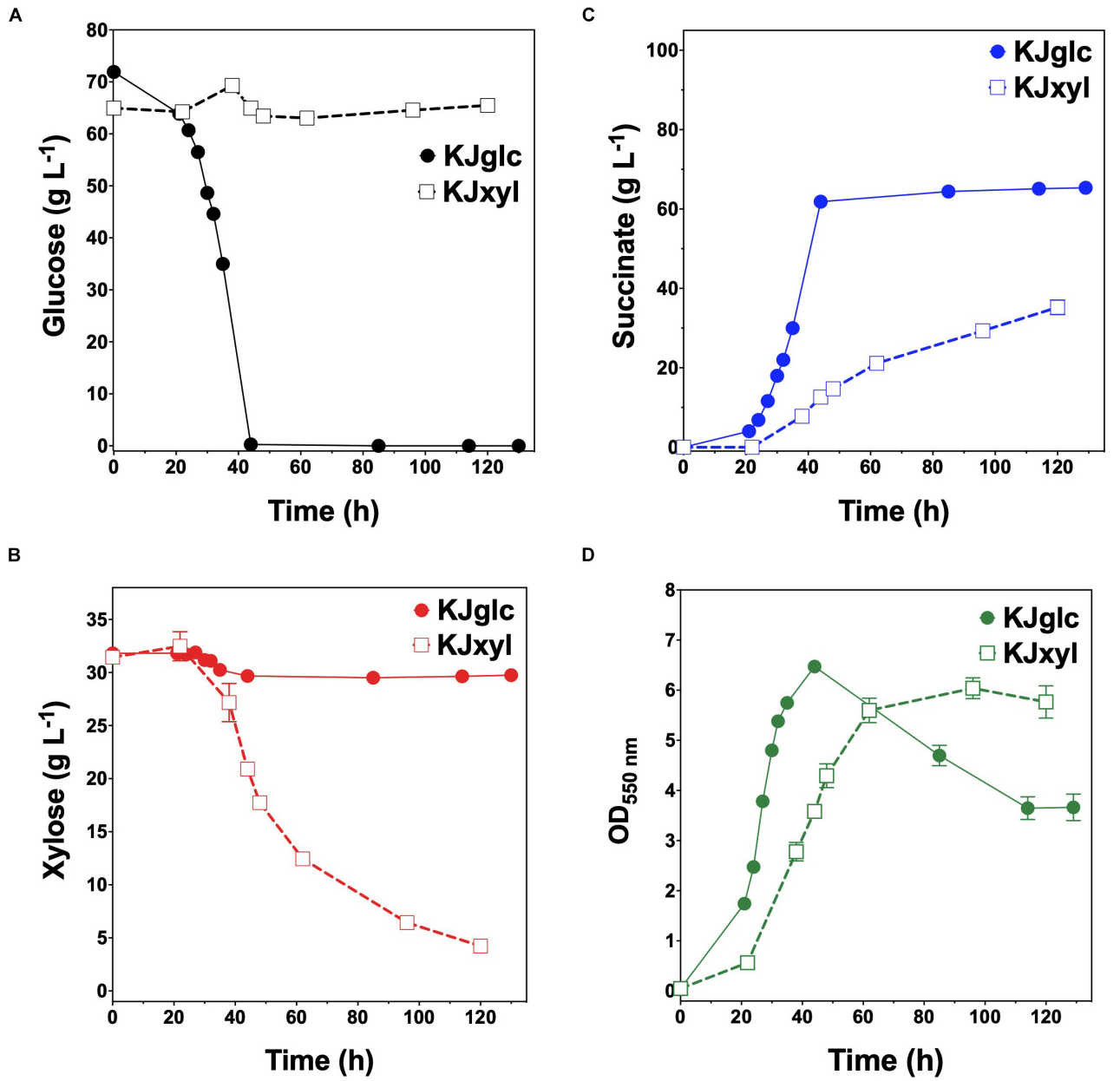

FIGURE 4 | Fermentation of glucose–xylose mixtures (2:1 by mass) by succinogenic sugar specialist strains. Concentrations of **(A)** glucose, **(B)** xylose, **(C)** succinate, and **(D)** OD_{550nm} measured in the fermentation broth for KJglc (closed circles) and KJxyl (open squares). All fermentations were performed in batch mode and in mineral salts media. Data points represent the arithmetic mean of three replicates, and the error bars represent one standard deviation.

ratio for this specific co-culture was close to 1:1. Meanwhile, the finding that a unique optimum initial population ratio was required for the developed LA- and SA-producing co-cultures is not altogether surprising and likely reflects the fact that the relative fitness levels differ between the two strains that make up each pair.

For comparison, Xia et al. (2015) previously developed an *E. coli* co-culture to convert glucose and xylose to SA via a two-stage, aerobic–anaerobic fed-batch process. Specifically, a mixture composed of ∼30 g L^{-1} glucose and ∼10 g L^{-1} xylose were first utilized aerobically for growth (producing no succinate), before then switching to anaerobic conditions to produce SA (∼15 g L^{-1} glucose and ∼5 g L^{-1} xylose were provided initially and then periodically added over 80 h; **Table 3**). Total sugar addition to this process over its 115 h duration was ∼100 g L^{-1} (3:1 glucose:xylose by mass), and final SA titers reached ∼45 g L^{-1}. From a bioprocessing perspective, while this two-stage approach has proven to be effective, use of a process that can operate simple batch mode, such as the co-culture

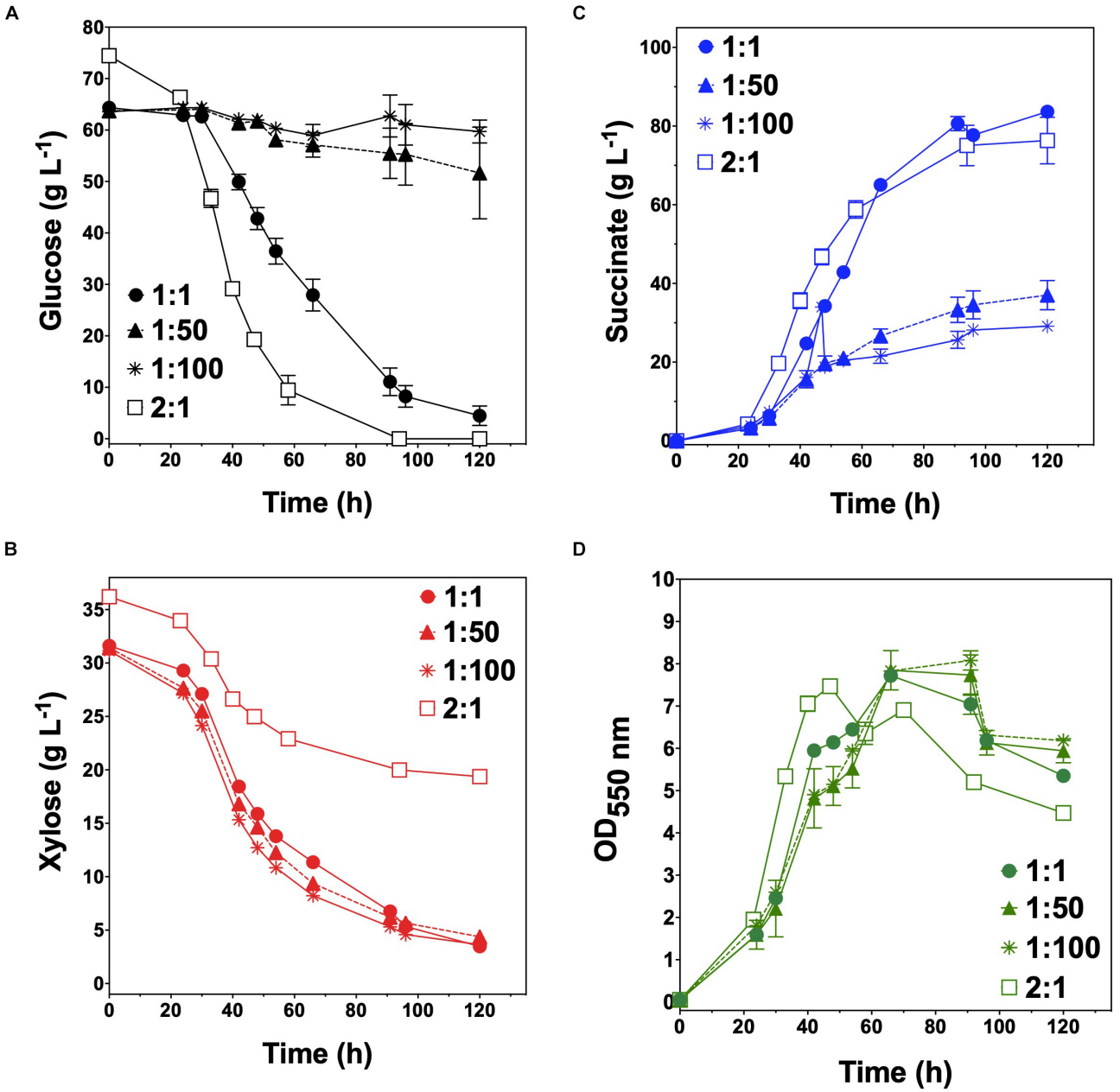

FIGURE 5 | Fermentation of glucose–xylose mixtures (2:1 by mass) co-cultures composed of catabolically orthogonal succinogenic specialist strains. Concentrations of **(A)** glucose, **(B)** xylose, **(C)** succinate, and **(D)** OD_{550nm} measured in the fermentation broth for KJglc:KJxyl co-cultures using an initial inoculum ratio of 1:1 (closed circles), 1:50 (closed dashed triangle), 1:100 (asterisk), and 2:1 (open squares). All fermentations were performed in batch mode and in mineral salts media. Data points represent the arithmetic mean of three replicates, and the error bars represent one standard deviation.

systems presented here, simplifies operation and control of the process. Similar to LA production, researchers have also engineered generalist strains to produce SA efficiently from sugar mixtures. For example, KJ122 further engineered to enhance conversion of a series of glucose–xylose mixtures (each 100 g L^{-1} total with 1:1, 2:1, or 3:1 glucose:xylose by mass) to up to ∼84 g L^{-1} SA using a combination of genetic engineering and adaptive laboratory evolution (Khunnonkwao et al., 2018). As discussed above, however, the current co-culture strategy is appealing due to its ability to facilitate effective catabolism of sugar mixtures through population tuning.

Overall, we have demonstrated the broad utility of engineering co-cultures composed of catabolically orthogonal *E. coli* strains for efficiently converting sugar mixtures into LA and SA, two important bioplastic monomers. Initial inoculum ratio was

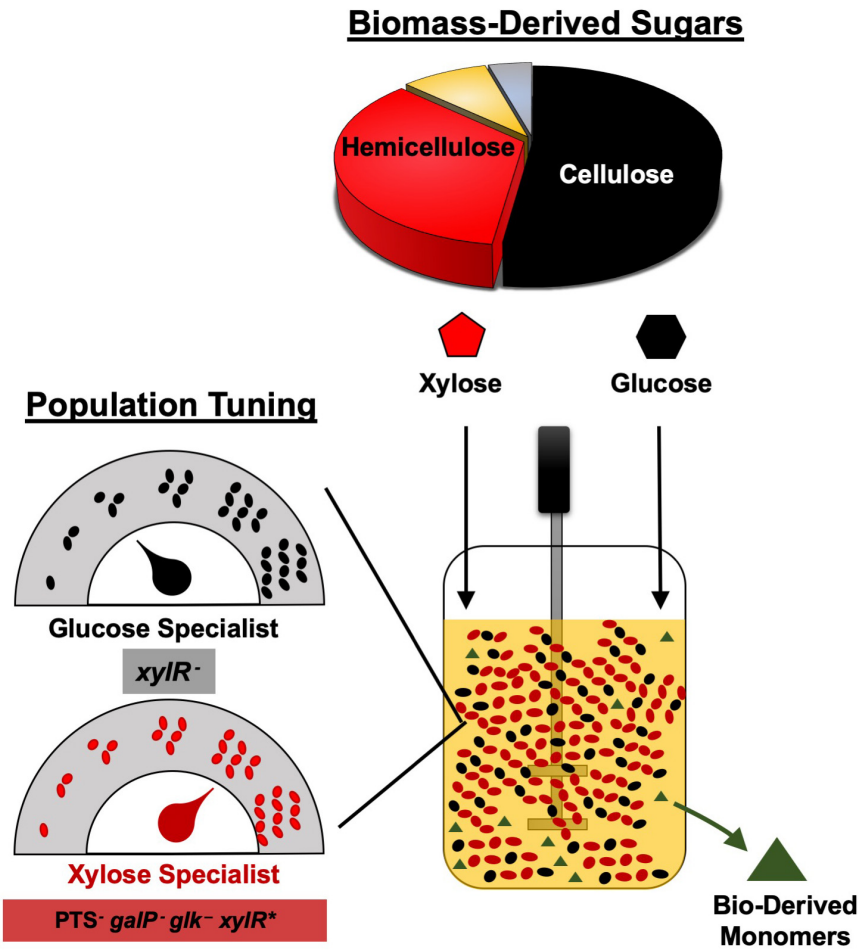

FIGURE 6 | Tuning the initial inoculum ratio enables enhanced bioplastic monomer production from glucose-xylose mixtures by co-cultures of catabolically-orthogonal specialist strains.

revealed to be an important design parameter for maximizing co-culture performance, the optimum value of which is unique to each specialist pair and can vary by even several orders of magnitude depending on relative phenotypic differences between member strains (**Figure 6**). Ultimately, by applying a population-level tuning strategy to balance rates of glucose and xylose co-utilization, both co-culture systems developed here were capable of fermenting a 100 g L^{-1} glucose–xylose mixture at ∼91% conversion to either LA or SA at high rates and yields. This population-level tuning strategy was simple to implement experimentally and should similarly prove useful in other co-culture applications. Holistically, this work contributes to an improved understanding of the behaviors of synthetic microbial consortia as enhanced bioproduction platforms for renewable fuels and chemicals from non-food carbohydrates. Ultimately, however, the ability to elucidate and understand the nature and potential importance of interstrain interactions and/or metabolite exchanges (Herre et al., 1999; Ponomarova and Patil, 2015; Scott and Hasty, 2016) will likely be important to further optimize these and other co-culture systems.

MATERIALS AND METHODS

Strain Construction

All *E. coli* strains and plasmids used in this study are presented in **Table 1**. A list of primers used is presented in **Supplementary Table S1**. The xylose specialist strain (Δ*galP* Δ*ptsI glk:kan*^{R} *xylR:xylR**) derived from KJ122 was initially found to grow poorly in media containing glucose–xylose and was accordingly adapted for improved growth under the conditions of interest. Growth was found to be significantly improved after performing just a single transfer, after which one clone, designated as KJxyl, was isolated. All chromosomal modifications were conducted using one- or two-step integration processes (Datsenko and Wanner, 2000; Sievert et al., 2017). Plasmid pXW001, containing a *cat-sacB* cassette, or strain T-SACK, containing a *tetA-sacB* cassette, were used as the PCR template to generate DNA fragments for primary integration into chromosomal sites of interest (Li et al., 2013; Sievert et al., 2017). Primary integration fragments contained the *cat-sacB* or *tetA-sacB* cassette flanked by 50-bp homology sequences from both upstream and

downstream regions of the gene of interest. To eliminate the integrated *cat-sacB* or *tetA-sacB* cassette, providing markerless gene deletions, secondary integration fragments were generated containing 500-bp homology sequences from both upstream and downstream regions of the gene of interest, as generated via fusion PCR. Plasmid pKD46, expressing λ-red recombinase, was used to facilitate all chromosomal integrations via double-crossover recombination, as previously described (Datsenko and Wanner, 2000). During both primary and secondary chromosomal integrations, cultures were inoculated in a 250 ml flask containing 25 ml Luria Broth (LB), 50 g L^{-1} arabinose, and 50 mg L^{-1} ampicillin and incubated at 30°C with shaking at 150 rpm until the optical density at 550 nm (OD_{550}) of the cultures reached ˜0.5. To prepare competent cells, cultures were subsequently centrifuged (5 min, 6,750 × g, 4°C), the supernatant was discarded, and the remaining cell pellet was resuspended in 20 ml of 4°C water. The described spin-wash cycle was repeated three times. On the last wash, all the supernatant was discarded except ˜150–200 µl of the remaining supernatant which was used to resuspend pelleted cells. For electroporation, 40 µl of competent cells were combined with 100–200 ng of DNA. Following electroporation, cells were transferred to a sterile test tube containing 1 ml LB and incubated at 30°C for 4 h. Cells were then plated on LB plates containing the appropriate antibiotic. Colony PCR and Sanger sequencing were used to verify positive clones after selecting for appropriate antibiotic resistance during primary integration and sucrose insensitivity (10% w/v) and loss of antibiotic resistance during secondary integration.

Cultivation Conditions

Monoculture and co-culture batch fermentations were conducted in a pH (7.0)- and temperature (37°C)-controlled vessel containing 300 ml of modified AM1 mineral salt medium (Martinez et al., 2007; Yomano et al., 2009) containing twice the ammonium phosphate [38.8 mM $(NH_4)_2H_2PO_4$ and 15.1 mM $(NH_4)H_2PO_4$] and 67 g L^{-1} glucose and 33 g L^{-1} xylose (Flores et al., 2019; Martinez et al., 2019). pH was maintained by automatic addition of 6 M KOH for LA-producing cultures and a mixture of 6 M KOH and 3 M K_2CO_3 (1:4 ratio by volume) for SA-producing cultures, as previously described (Grabar et al., 2006; Jantama et al., 2008). From –80°C frozen stocks, strains were streaked onto AM1 agar plates supplemented with 100 mM MOPS and 20 g L^{-1} glucose or 20 g L^{-1} xylose. Agar plates were placed inside a sealed canister filled with argon gas and incubated at 37°C for 16–24 h. Seed cultures were grown in AM1 medium containing 100 mM MOPS, 10 g L^{-1} glucose, and 10 g L^{-1} xylose and incubated at 37°C with shaking at 120 rpm for ∼12–16 h. Cells were harvested by centrifugation (5 min, 6,750 × g, 4°C) and resuspended in 300 ml fresh media. All monoculture and co-culture fermentations were seeded using a total initial OD_{550mn} of 0.05 (∼0.022 gDCW L^{-1}).

Analytical Methods

Cell growth was quantified using a UV/Vis spectrophotometer (Beckman Coulter DU-730, Indianapolis, IN, United States). Sugar and product concentrations were determined by high-performance liquid chromatography (HPLC; Thermo Fisher Scientific and UltiMate 3000, Waltham, MA, United States) equipped with a refractive index detector. Analyte separation was performed using an Aminex HPX-87H column (Bio-Rad Laboratories, Hercules, CA, United States) maintained at 45°C and a mobile phase consisting of 5 mM H_2SO_4 flowing at a constant rate of 0.4 ml min^{-1}. External standards prepared in house were used to quantify substrate and product concentrations. All experiments were performed in at least triplicates, and the average and standard deviation are shown in figures and tables.

DATA AVAILABILITY STATEMENT

The datasets generated for this study are available on request to the corresponding author.

AUTHOR CONTRIBUTIONS

AF, DN, and XW designed the experiments, analyzed the data, and wrote the manuscript. AF constructed all strains and performed all experiments with the assistance of HC, RM, MO, EA, AG, and MM.

FUNDING

This work was supported by the start-up fund from Arizona State University (ASU) and ASU LightWorks. AF was supported by an IGERT-SUN fellowship funded by the National Science Foundation (Award 1144616). HC was supported by a Research Experience for Undergraduate (REU) grant (Award 1511637). RM was supported by WAESO LSAMP Bridge to Doctorate Fellowship.

ACKNOWLEDGMENTS

We thank Prof. Lonnie Ingram, formerly of the University of Florida, for providing strains TG114 and KJ122. We also thank Dr. Donald Court (National Cancer Institute, Center for Cancer Research) for the generous gift of *E. coli* W3110 variant T-SACK.

SUPPLEMENTARY MATERIAL

The Supplementary Material for this article can be found online at: https://www.frontiersin.org/articles/10.3389/fbioe.2020.00329/full#supplementary-material

REFERENCES

Abdel-Rahman, M. A., Tashiro, Y., and Sonomoto, K. (2011). Lactic acid production from lignocellulose-derived sugars using lactic acid bacteria: overview and limits. *J. Biotechnol.* 156, 286–301. doi: 10.1016/j.jbiotec.2011.06.017

Abdel-Rahman, M. A., Tashiro, Y., and Sonomoto, K. (2013). Recent advances in lactic acid production by microbial fermentation processes. *Biotechnol. Adv.* 31, 877–902. doi: 10.1016/j.biotechadv.2013.04.002

Ahn, J. H., Jang, Y. S., and Lee, S. Y. (2016). Production of succinic acid by metabolically engineered microorganisms. *Curr. Opin. Biotechnol.* 42, 54–66. doi: 10.1016/j.copbio.2016.02.034

Awasthi, D., Wang, L., Rhee, M. S., Wang, Q., Chauliac, D., Ingram, L. O., et al. (2018). Metabolic engineering of *Bacillus subtilis* for production of D-lactic acid. *Biotechnol. Bioeng.* 115, 453–463. doi: 10.1002/bit.26472

Camacho-Zaragoza, J. M., Hernandez-Chavez, G., Moreno-Avitia, F., Ramirez-Iniguez, R., Martinez, A., Bolivar, F., et al. (2016). Engineering of a microbial coculture of *Escherichia coli* strains for the biosynthesis of resveratrol. *Microb. Cell Fact.* 15:163.

Chappell, T. C., and Nair, N. U. (2017). Co-utilization of hexoses by a microconsortium of sugar-specific *E. coli strains*. *Biotechnol. Bioeng.* 114, 2309–2318. doi: 10.1002/bit.26351

Datsenko, K. A., and Wanner, B. L. (2000). One-step inactivation of chromosomal genes in *Escherichia coli* K-12 using PCR products. *Proc. Natl. Acad. Sci. U.S.A.* 97, 6640–6645. doi: 10.1073/pnas.120163297

Eiteman, M. A., Lee, S. A., and Altman, E. (2008). A co-fermentation strategy to consume sugar mixtures effectively. *J. Biol. Eng.* 2:3. doi: 10.1186/1754-1611-2-3

Eiteman, M. A., Lee, S. A., Altman, R., and Altman, E. (2009). A substrate-selective co-fermentation strategy with *Escherichia coli* produces lactate by simultaneously consuming xylose and glucose. *Biotechnol. Bioeng.* 102, 822–827. doi: 10.1002/bit.22103

Es, I., Mousavi Khaneghah, A., Barba, F. J., Saraiva, J. A., Sant'Ana, A. S., and Hashemi, S. M. B. (2018). Recent advancements in lactic acid production - a review. *Food Res. Int.* 107, 763–770. doi: 10.1016/j.foodres.2018.01.001

Flores, A. D., Ayla, E. Z., Nielsen, D. R., and Wang, X. (2019). Engineering a synthetic, catabolically orthogonal coculture system for enhanced conversion of lignocellulose-derived sugars to ethanol. *ACS Synth. Biol.* 8, 1089–1099. doi: 10.1021/acssynbio.9b00007

Grabar, T. B., Zhou, S., Shanmugam, K. T., Yomano, L. P., and Ingram, L. O. (2006). Methylglyoxal bypass identified as source of chiral contamination in l(+) and d(-)-lactate fermentations by recombinant *Escherichia coli*. *Biotechnol. Lett.* 28, 1527–1535. doi: 10.1007/s10529-006-9122-7

Herre, E. A., Knowlton, N., Mueller, U. G., and Rehner, S. A. (1999). The evolution of mutualisms: exploring the paths between conflict and cooperation. *Trends Ecol. Evol.* 14, 49–53. doi: 10.1016/s0169-5347(98)01529-8

Ishida, N., Suzuki, T., Tokuhiro, K., Nagamori, E., Onishi, T., Saitoh, S., et al. (2006). D-lactic acid production by metabolically engineered *Saccharomyces cerevisiae*. *J. Biosci. Bioeng.* 101, 172–177. doi: 10.1263/jbb.101.172

Jansen, M. L., and van Gulik, W. M. (2014). Towards large scale fermentative production of succinic acid. *Curr. Opin. Biotechnol.* 30, 190–197. doi: 10.1016/j.copbio.2014.07.003

Jantama, K., Zhang, X., Moore, J. C., Shanmugam, K. T., Svoronos, S. A., and Ingram, L. O. (2008). Eliminating side products and increasing succinate yields in engineered strains of *Escherichia coli* C. *Biotechnol. Bioeng.* 101, 881–893. doi: 10.1002/bit.22005

Jones, J. A., Vernacchio, V. R., Collins, S. M., Shirke, A. N., Xiu, Y., Englaender, J. A., et al. (2017). Complete biosynthesis of anthocyanins using *E. coli Polycultures*. *mBio* 8:e00621-17. doi: 10.1128/mBio.00621-17

Khunnonkwao, P., Jantama, S. S., Kanchanatawee, S., and Jantama, K. (2018). Re-engineering *Escherichia coli* KJ122 to enhance the utilization of xylose and xylose/glucose mixture for efficient succinate production in mineral salt medium. *Appl. Microbiol. Biotechnol.* 102, 127–141. doi: 10.1007/s00253-017-8580-2

Li, X. T., Thomason, L. C., Sawitzke, J. A., Costantino, N., and Court, D. L. (2013). Positive and negative selection using the tetA-sacB cassette: recombineering and P1 transduction in *Escherichia coli*. *Nucleic Acids Res.* 41:e204. doi: 10.1093/nar/gkt1075

Litsanov, B., Kabus, A., Brocker, M., and Bott, M. (2012). Efficient aerobic succinate production from glucose in minimal medium with *Corynebacterium glutamicum*. *Microb. Biotechnol.* 5, 116–128. doi: 10.1111/j.1751-7915.2011.00310.x

Lu, H., Villada, J. C., and Lee, P. K. H. (2019). Modular metabolic engineering for biobased chemical production. *Trends Biotechnol.* 37, 152–166. doi: 10.1016/j.tibtech.2018.07.003

Lynd, L. R. (2017). The grand challenge of cellulosic biofuels. *Nat. Biotechnol.* 35, 912–915. doi: 10.1038/nbt.3976

Maleki, N., Safari, M., and Eiteman, M. A. (2018). Conversion of glucose-xylose mixtures to pyruvate using a consortium of metabolically engineered *Escherichia coli*. *Eng. Life Sci.* 18, 40–47. doi: 10.1002/elsc.201700109

Martinez, A., Grabar, T. B., Shanmugam, K. T., Yomano, L. P., York, S. W., and Ingram, L. O. (2007). Low salt medium for lactate and ethanol production by recombinant *Escherichia coli* B. *Biotechnol. Lett.* 29, 397–404. doi: 10.1007/s10529-006-9252-y

Martinez, R., Flores, A. D., Dufault, M. E., and Wang, X. (2019). The XylR variant (R121C and P363S) releases arabinose-induced catabolite repression on xylose fermentation and enhances coutilization of lignocellulosic sugar mixtures. *Biotechnol. Bioeng.* 116, 3476–3481. doi: 10.1002/bit.27144

Nieves, L. M., Panyon, L. A., and Wang, X. (2015). Engineering sugar utilization and microbial tolerance toward lignocellulose conversion. *Front. Bioeng. Biotechnol.* 3:17. doi: 10.3389/fbioe.2015.00017

Okano, K., Tanaka, T., Ogino, C., Fukuda, H., and Kondo, A. (2010). Biotechnological production of enantiomeric pure lactic acid from renewable resources: recent achievements, perspectives, and limits. *Appl. Microbiol. Biotechnol.* 85, 413–423. doi: 10.1007/s00253-009-2280-5

Ponomarova, O., and Patil, K. R. (2015). Metabolic interactions in microbial communities: untangling the Gordian knot. *Curr. Opin. Microbiol.* 27, 37–44. doi: 10.1016/j.mib.2015.06.014

Roell, G. W., Zha, J., Carr, R. R., Koffas, M. A., Fong, S. S., and Tang, Y. J. (2019). Engineering microbial consortia by division of labor. *Microb. Cell Fact.* 18:35. doi: 10.1186/s12934-019-1083-3

Sawisit, A., Jantama, K., Zheng, H., Yomano, L. P., York, S. W., Shanmugam, K. T., et al. (2015). Mutation in *galP* improved fermentation of mixed sugars to succinate using engineered *Escherichia coli* AS1600a and AM1 mineral salts medium. *Bioresour. Technol.* 193, 433–441. doi: 10.1016/j.biortech.2015.06.108

Scott, S. R., and Hasty, J. (2016). Quorum sensing communication modules for microbial consortia. *ACS Synth. Biol.* 5, 969–977. doi: 10.1021/acssynbio.5b00286

Sievert, C., Nieves, L. M., Panyon, L. A., Loeffler, T., Morris, C., Cartwright, R. A., et al. (2017). Experimental evolution reveals an effective avenue to release catabolite repression via mutations in XylR. *Proc. Natl. Acad. Sci. U.S.A.* 114, 7349–7354. doi: 10.1073/pnas.1700345114

Song, S., and Park, C. (1997). Organization and regulation of the D-xylose operons in *Escherichia coli* K-12: XylR acts as a transcriptional activator. *J. Bacteriol.* 179, 7025–7032. doi: 10.1128/jb.179.22.7025-7032.1997

Utrilla, J., Vargas-Tah, A., Trujillo-Martinez, B., Gosset, G., and Martinez, A. (2016). Production of D-lactate from sugarcane bagasse and corn stover hydrolysates using metabolic engineered *Escherichia coli* strains. *Bioresour. Technol.* 220, 208–214. doi: 10.1016/j.biortech.2016.08.067

Wang, L., York, S. W., Ingram, L. O., and Shanmugam, K. T. (2019). Simultaneous fermentation of biomass-derived sugars to ethanol by a co-culture of an engineered *Escherichia coli* and *Saccharomyces cerevisiae*. *Bioresour. Technol.* 273, 269–276. doi: 10.1016/j.biortech.2018.11.016

Wang, Q., Ingram, L. O., and Shanmugam, K. T. (2011). Evolution of D-lactate dehydrogenase activity from glycerol dehydrogenase and its utility for D-lactate production from lignocellulose. *Proc. Natl. Acad. Sci. U.S.A.* 108, 18920–18925. doi: 10.1073/pnas.1111085108

Xia, T., Altman, E., and Eiteman, M. A. (2015). Succinate production from xylose-glucose mixtures using a consortium of engineered *Escherichia coli*. *Eng. Life Sci.* 15, 65–72. doi: 10.1002/elsc.201400113

Yomano, L. P., York, S. W., Shanmugam, K. T., and Ingram, L. O. (2009). Deletion of methylglyoxal synthase gene (*mgsA*) increased sugar co-metabolism in ethanol-producing *Escherichia coli*. *Biotechnol. Lett.* 31, 1389–1398. doi: 10.1007/s10529-009-0011-8

Zhang, H., Pereira, B., Li, Z., and Stephanopoulos, G. (2015). Engineering *Escherichia coli* coculture systems for the production of biochemical products. *Proc. Natl. Acad. Sci. U.S.A.* 112, 8266–8271. doi: 10.1073/pnas.1506781112

Zhou, K., Qiao, K. J., Edgar, S., and Stephanopoulos, G. (2015). Distributing a metabolic pathway among a microbial consortium enhances production of natural products. *Nat. Biotechnol.* 33, 377–383. doi: 10.1038/nbt.3095

Conflict of Interest: The authors declare that the research was conducted in the absence of any commercial or financial relationships that could be construed as a potential conflict of interest.

frontiers in Bioengineering and Biotechnology

ORIGINAL RESEARCH
published: 25 May 2020
doi: 10.3389/fbioe.2020.00486

A Nitrate-Blind *P. putida* Strain Boosts PHA Production in a Synthetic Mixed Culture

*Karina Hobmeier, Hannes Löwe, Stephan Liefeldt, Andreas Kremling and Katharina Pflüger-Grau**

Systems Biotechnology, Technical University of Munich, Garching, Germany

One of the major challenges for the present and future generations is to find suitable substitutes for the fossil resources we rely on today. In this context, cyanobacterial carbohydrates have been discussed as an emerging renewable feedstock in industrial biotechnology for the production of fuels and chemicals. Based on this, we recently presented a synthetic bacterial co-culture for the production of medium-chain-length polyhydroxyalkanoates (PHAs) from CO_2. This co-cultivation system is composed of two partner strains: *Synechococcus elongatus cscB* which fixes CO_2, converts it to sucrose and exports it into the culture supernatant, and a *Pseudomonas putida* strain that metabolizes this sugar and accumulates PHAs in the cytoplasm. However, these biopolymers are preferably accumulated under conditions of nitrogen limitation, a situation difficult to achieve in a co-culture as the other partner, at best, should not perceive any limitation. In this article, we will present an approach to overcome this dilemma by uncoupling the PHA production from the presence of nitrate in the medium. This is achieved by the construction of a *P. putida* strain that is no longer able to grow with nitrate as nitrogen source -is thus nitrate blind, and able to grow with sucrose as carbon source. The deletion of the *nasT* gene encoding the response regulator of the NasS/NasT two-component system resulted in such a strain that has lost the ability use nitrate, but growth with ammonium was not affected. Subsequently, the *nasT* deletion was implemented in *P. putida cscRABY*, an efficient sucrose consuming strain. This genetic engineering approach introduced an artificial unilateral nitrogen limitation in the co-cultivation process, and the amount of PHA produced from light and CO_2 was 8.8 fold increased to 14.8% of its CDW compared to the nitrate consuming reference strain. This nitrate blind strain, *P. putida* Δ*nasT attTn7:cscRABY*, is not only a valuable partner in the co-cultivation but additionally enables the use of other nitrate containing substrates for medium-chain-length PHA production, like for example waste-water.

Keywords: *Pseudomonas putida*, genetic engineering, polyhydroxyalkanoates, co-cultivation, artificial nitrogen limitation

OPEN ACCESS

Edited by:
Ignacio Poblete-Castro, Andres Bello University, Chile

Reviewed by:
Tanja Narancic, University College Dublin, Ireland
Leonardo Rios Solis, The University of Edinburgh, United Kingdom

****Correspondence:***
Katharina Pflüger-Grau
k.pflueger-grau@tum.de

Specialty section:
This article was submitted to Industrial Biotechnology, a section of the journal Frontiers in Bioengineering and Biotechnology

Received: *06 December 2019*
Accepted: *27 April 2020*
Published: *25 May 2020*

Citation:
Hobmeier K, Löwe H, Liefeldt S, Kremling A and Pflüger-Grau K (2020) A Nitrate-Blind P. putida Strain Boosts PHA Production in a Synthetic Mixed Culture. Front. Bioeng. Biotechnol. 8:486. doi: 10.3389/fbioe.2020.00486

INTRODUCTION

In times of global warming, extreme weather conditions, and a growing world population, it is mandatory to dedicate arable land to food production and not "waste" it for energy formation or feedstock production for biotechnology. Along that line, efforts are directed toward replacing traditional, crop-based feedstocks like sugarcane, corn, and wheat by carbohydrates derived from ecologically more friendly sources, for example eukaryotic algae or cyanobacteria. These sources of feedstock can be produced on non-arable land with salty or brackish water. Moreover, global warming is combatted at the same time as CO_2 is captured in bio-chemical compounds. Unfortunately, the intrinsic capacities of photosynthetic microbes to produce interesting and tailored compounds are limited and efficiencies are low.

One approach to overcome this problem is to combine the phototrophic traits of the cyanobacteria with the biotechnological abilities of a heterotrophic organism. This can be done in a synthetic mixed culture, in which the cyanobacterium produces a substrate that is simultaneously metabolized by a heterotrophic co-culture partner (Ortiz-Marquez et al., 2013; Smith and Francis, 2016; Hays et al., 2017; Löwe et al., 2017). Along that line, a number of studies were published recently, that employed a genetically engineered *Synechococcus elongatus* PCC7942 strain in a functional mixed culture (Hays and Ducat, 2015; Smith and Francis, 2016; Li et al., 2017; Löwe et al., 2017; Weiss et al., 2017). This strain, *S. elongatus cscB* carries the sucrose/H^+-symporter CscB from *Escherichia coli* integrated into the chromosome (Ducat et al., 2012). *S. elongatus* naturally responds to elevated salt concentrations in the environment with the accumulation of sucrose as compatible solute to counteract the osmotic pressure. Thus, when the engineered strain is grown at elevated salt concentrations, sucrose is produced and exported into the medium by the activity of CscB (Ducat et al., 2012). This sugar is then taken up and converted into a valuable product by the co-culture partner, which likewise needs to be able to grow with elevated salt concentrations. Many of the defined mixed cultures were set up to produce polyhydroxybutyrate (PHB) by the heterotrophic host (Hays and Ducat, 2015; Smith and Francis, 2016; Weiss et al., 2017). The highest productivity of 28.3 mg L^{-1} d^{-1} was reached in a mixed culture between *S. elongatus* PCC7942 *cscB* and *Halomonas boliviensis*, which compares well with PHB production by genetically engineered cyanobacteria strains (Weiss et al., 2017). We recently set up a co-cultivation for the production of polyhydroxyalkanoates (PHA) with S. *elongatus* PCC7942 *cscB* and the genetically engineered strain *P. putida*:mini-Tn*5*(*cscAB*), capable of metabolizing sucrose (Löwe et al., 2017). With this mixed culture approach a production rate of PHA of around 23.8 mg L^{-1} d^{-1} was reached under nitrogen limiting conditions. However, at the end of the process a major fraction of sucrose was left untouched by *P. putida cscAB*. To face this problem, we recently engineered a more efficient sucrose consuming strain, *P. putida EM178 attTn7*:*cscRABY,* by the introduction of the gene cluster for sucrose metabolism from *Pseudomonas protegens* Pf-5 (Löwe et al., 2020). This strain was able to grow on sucrose with growth rates comparable to the ones obtained with the monomers glucose and fructose. *P. putida* is a very suitable partner for co-cultivations as it combines various traits, including its genetic tractability and its general stress resistance (Nikel et al., 2016), which is of great importance when grown in the non-optimal environment of the photobioreactor with elevated salt concentrations.

Natural polymers like PHA that show thermoplastic, polypropylene-like properties, could be a valuable substitute for conventional petroleum-based plastic. Depending on the chain-length of the 3-hydroxyalkanoic acids, the polymers have different mechanical properties: Most bacteria produce short chain-length PHA (scl-PHA) which consist mainly of 3-hydroxybutyrate monomers and have limited mechanical properties (Wecker et al., 2015) as they tend to be brittle when not combined with other 3-hydroxyalkanoic acids (Muhammadi et al., 2015). Only a few genera can produce longer chain-length PHAs that are more interesting for applications due to their superior and more flexible properties (Jiang et al., 2012; Wecker et al., 2015; Fontaine et al., 2017). *P. putida* is one of these native producers of medium chain-length PHA (mcl-PHA), either from lipid based substrates or carbohydrates (Huijberts et al., 1992) in conditions of one or multiple nutrient starvation (Poblete-Castro et al., 2012). *P. putida* can accumulate around 20% of its cellular dry weight as PHAs in conditions of carbon surplus and nitrogen limitation (Huijberts et al., 1992; Poblete-Castro et al., 2014). However, this is a situation difficult to achieve in a co-culture, as the other partner –at best, should not perceive any limitation.

The common growth medium for *S. elongatus* is the BG-11 medium (ATCC Medium 616) for blue-green algae (Stanier et al., 1971), which provides nitrate as nitrogen source. The modified BG-11$^+$ medium we adapted for the co-cultivation of *S. elongatus* and *P. putida* consequently also has nitrate as nitrogen source (Löwe et al., 2017). In bacteria the assimilation of nitrate takes place by the reduction of nitrate to nitrite and in a second step to ammonium by the activity of nitrate reductase and nitrite reductase. In *P. putida* the availability of nitrate or nitrite is detected by a two-component sensory system consisting of the sensor NasS and the response regulator NasT (Caballero et al., 2005; Luque-Almagro et al., 2013; **Supplementary Figure S1**). In the presence of nitrate or nitrite the sensory protein NasS (encoded by PP_2093) binds the substrate, dissociates from the stable complex with NasS and NasT (encoded by PP_2094) is released. The unbound NasT protein then activates transcription of the assimilating nitrate and nitrite reductases encoded by PP_1703 and *nirBD* (PP_1705, PP_1706), responsible for the reduction of nitrate to ammonium. Furthermore, it was shown that the transcription of *nasT* is highly induced right at the beginning of NH_4^+ deficiencies, suggesting that it forms part of the early response to ammonium depletion and helps the cell in preparing for the immediate consumption of the alternative nitrogen source nitrate (Mozejko-Ciesielska et al., 2017).

In this work, we will present a metabolic engineering approach to uncouple the PHA production by *P. putida* from the presence of nitrate in the medium. This is achieved by the development a "nitrate blind" mutant, which allows the introduction of an artificial unilateral nitrogen limitation in the co-cultivation process. This enabled us not only to increase the PHA produced

from CO_2 and light to 14.8% of the CDW compared to <1% in the reference strain, but additionally opens up the use of other nitrate containing substrates, like waste-water, for medium-chain-length PHA production with *P. putida*.

RESULTS AND DISCUSSION

NasT Is Essential for the Metabolism of Nitrate by *P. putida*

In order to uncouple the accumulation of PHA by *P. putida* from the presence of nitrate, we aimed to construct a nitrate-blind strain. As a target system we chose the nitrate/nitrite sensing two-component system NasS/NasT (**Supplementary Figure S1**). To this end, a clean deletion of *nasT* was introduced into *P. putida EM178*, a prophage free derivative of *P. putida* KT2440 by I-SceI aided double homologous recombination (Martínez-García and de Lorenzo, 2011). The resulting strain *P. putida* EM178 Δ*nasT* was no longer able to grow with nitrate as sole nitrogen source (**Supplementary Figure S2**). However, the growth with ammonium was not affected (**Figure 1**). Both strains showed a similar growth behavior in the presence of ammonium as sole nitrogen source and reached final cellular dry weights of around 1.3 g/L. To test whether the addition of nitrate, a situation found in the co-cultivation, has an effect on the recombinant strain *P. putida EM178* Δ*nasT*, both strains were grown with ammonium and nitrate (see **Supplementary Table S1**). The recombinant strain *P. putida* EM178 Δ*nasT* showed a growth behavior comparable to the one observed in the absence of nitrate, indicating that the additional presence of nitrate had no negative effect on *P. putida* EM178 Δ*nasT*. The parental strain *P. putida* EM178, however, grew best in the presence of both nitrogen sources up to around 1.75 g/L CDW. The overall amount of nitrogen was increased 1.3 fold by the addition of nitrate, which generates a 1.35 fold increase in the final CDW reached by *P. putida* EM178. The growth rates were similar in all cases, ranging between 0.52 and 0.55 h^{-1} (**Table 1**). Thus, the Δ*nasT* strain grew comparably to the parental strain with ammonium as nitrogen source and was not influenced by the presence of nitrate, as it is unable to induce the nitrate assimilatory pathways. This effect of *nasT* disruption was already observed in the close relative *Pseudomonas aeruginosa* PAO1 (Romeo et al., 2012).

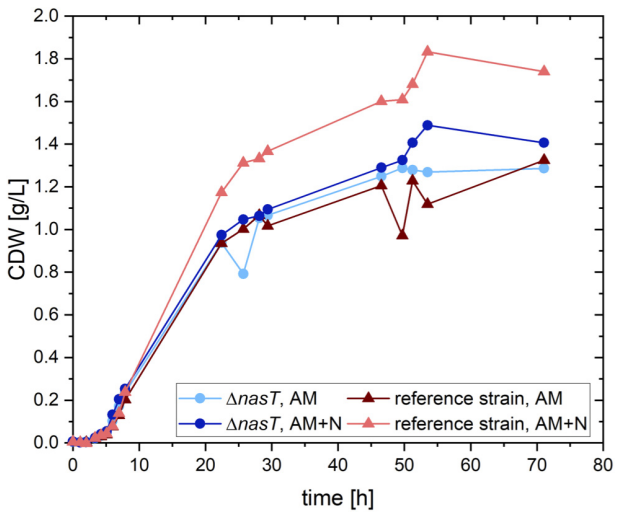

FIGURE 1 | Growth of *P. putida* EM178 Δ*nasT* with NH_4Cl is not affected. Shown is the calculated cellular dry weight (CDW) for *P. putida* EM178 (red triangles) and *P. putida* EM178 Δ*nasT* (blue circles) grown on glucose in M9 minimal medium with either ammonium as sole nitrogen source (NH_4Cl 0.22 g/L) or with a mixture of ammonium and nitrate (NH_4Cl 0.22 g/L + $NaNO_3$ 0.10 g/L). The additional growth of *P. putida* EM178 compared to the other strains can be attributed to the nitrate in the medium available as nitrogen source for this strain, but not for *P. putida* EM178 Δ*nasT*. Shown are the results of one representative experiment.

Construction of a Nitrate-Blind Sucrose Metabolizing *P. putida* Suited for the Co-culture

However, to employ the nitrate-blind mutant strain in the co-cultivation, it has to be able to metabolize sucrose, a trait not intrinsically present in *P. putida* (Nogales et al., 2019). Therefore, the deletion of *nasT* was next introduced into the genetically engineered *P. putida EM178 attTn7:cscRABY,* which is capable to grow on sucrose as sole carbon source (Löwe et al., 2020), yielding *P. putida EM178 attTn7:cscRABY* Δ*nasT*. For the sake of simplicity, the strain *P. putida EM178 attTn7:cscRABY* will from here on be referred to as "*P. putida cscRABY*" and *P. putida EM178 attTn7:cscRABY* Δ*nasT* as "*P. putida cscRABY* Δ*nasT*" (see **Supplementary Table S2** for more detail).

First, we analyzed the growth of both strains on sucrose with low ammonium concentrations and an excess of nitrate, to simulate the conditions in the co-cultivation. As control for the situation as it should be perceived by *P. putida cscRABY* Δ*nasT,* which can only grow on the ammonium present in the medium, *P. putida cscRABY* was grown solely with the low ammonium concentration. The growth rate, the biomass produced, and the nitrate consumed were compared (**Figure 2**). *P. putida cscRABY* grew to a CDW of 2.04 ± 0.313 g/L in the medium containing both

TABLE 1 | Growth rates of *P. putida EM178* and *P. putida EM178 ΔnasT on glucose*.

	Growth rates [h^{-1}] ± SD[a]	
	AM	**AM + N**
P. putida EM178	0.517 ± 0.015	0.528 ± 0.017
P. putida EM178 ΔnasT	0.54 ± 0.03	0.55 ± 0.03

P. putida strains were grown in M9 medium with ammonium (AM) (0.22 g/L NH_4Cl) and with or without the addition of nitrate (N) (0.1 g/L $NaNO_3$). Shown are the means of biological duplicates and the standard deviation. [a]Standard deviations were determined by propagation of error of the uncertainties of two independent biological replicates.

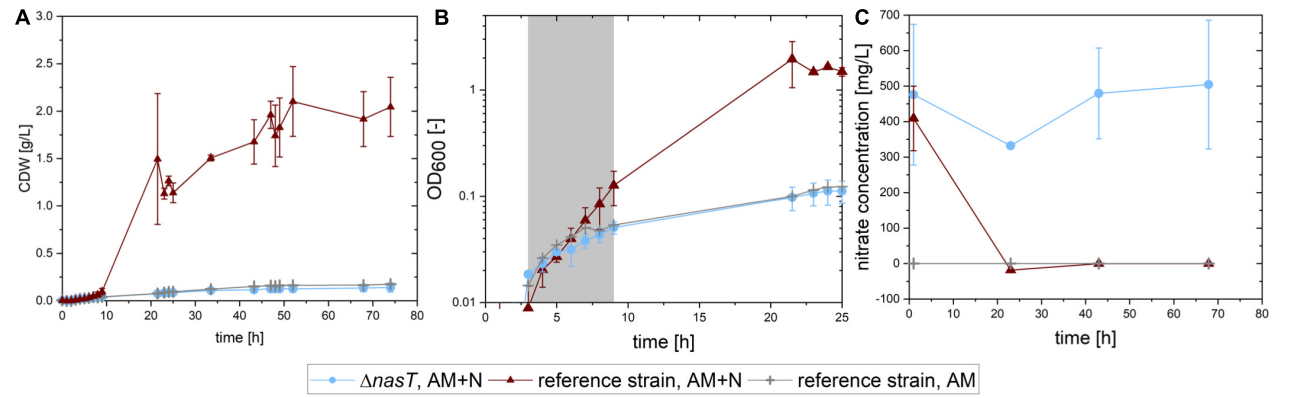

FIGURE 2 | Growth of *P. putida cscRABY and P. putida cscRABY ΔnasT* on sucrose. *P. putida cscRABY* (red triangles) and *P. putida cscRABY ΔnasT* (blue circles) were grown in M9 medium with low ammonium concentrations (AM = 0.03 g/L NH_4Cl) and with or without the addition of nitrate (N = 1 g/L $NaNO_3$) to simulate the conditions of the co-cultivation. **(A)** The development of the cellular dry weight (CDW) during the cultivation. CDW was calculated using an OD/CDW correlation (see **Supplementary Figure S3**). **(B)** The optical density measured at 600 nm along growth. The growth rate μ (see **Table 2**) was determined in the exponential growth phase (gray shaded area). **(C)** The nitrate concentration in the supernatant of the cultures.

nitrogen sources, whereas the *nasT* mutant, reached a biomass concentration of only about 0.14 g/L, even though nitrate was readily available (**Figure 2C**), corroborating the results from above. In fact, in the control experiment with *P. putida cscRABY* with ammonium only a similar CDW of about 0.18 g/L was reached.

This is also reflected in the growth rates (**Figure 2B** and **Table 2**): A similar growth rate was reached by the Δ*nasT* strain with both nitrogen sources and *P. putida cscRABY* grown on ammonium only. When *P. putida cscRABY* is grown with ammonium and nitrate, a higher growth rate is reached, a consequence of a simultaneous consumption of both nitrogen sources by the culture.

To confirm that *P. putida cscRABY ΔnasT* was no longer able to take up nitrate, the nitrate concentration was measured along growth (**Figure 2C**). *P. putida cscRABY* depleted nitrate in the first 20 h, whereas in the culture with *P. putida cscRABY ΔnasT* nitrate remained detectable for the time measured. Thus, the disruption of the two-component sensing system NasT/NasS by deletion of *nasT* in the sucrose consuming *P. putida cscRABY* generated a strain which is blind to nitrate in conditions resembling the situation found in the co-cultivation.

TABLE 2 | Growth rates of *P. putida cscRABY* and *P. putida cscRABY ΔnasT* on sucrose.

	Growth rates [h^{-1}] ± SD	
	AM	**AM + N**
P. putida cscRABY	0.20 ± 0.04[b]	0.39 ± 0.08[c]
P. putida cscRABY ΔnasT	n.d.[a]	0.162 ± 0.008[c]

P. putida strains were grown in M9 medium with low ammonium (AM) concentrations (0.03 g/L NH_4CL) and with or without an excess of nitrate (N) (1 g/L $NaNO_3$). Shown are the means of biological duplicates and the standard deviation. [a]Not determined. [b]The standard deviation was derived from the error of regression. [c]The standard deviation was derived from two independent biological replicates.

Co-cultivation of *P. putida* Δ*nasT* and *S. elongatus cscB* for PHA Production

The next step was to test the potential of *P. putida cscRABY ΔnasT* in the co-culture with *S. elongatus cscB* to produce PHA from light and CO_2. To provide proof of concept and to allow for parallel cultivations under comparable conditions, we performed the co-cultivation experiments in shaking flasks under constant illumination. All co-cultivations started with an exclusively auxotrophic growth phase of *S. elongatus cscB* for 3 days with solely nitrate as nitrogen source. Then the inoculation with *P. putida cscRABY ΔnasT* and simultaneous addition of ammonium took place. IPTG and elevated salt concentration were present from the beginning to induce sucrose production and excretion.

In a first round of experiments, we aimed to find the optimal ammonium concentration to allow for sufficient initial biomass formation of *P. putida cscRABY ΔnasT*. The availability of ammonium for *P. putida* cannot be predicted as it is likewise metabolized by *S. elongatus cscB*. An overview of the experimental setup is given in **Supplementary Figure S4** and the results are depicted in **Figure 3A**. Three different ammonium concentrations were tested in the co-cultivation of *S. elongatus cscB* with both, *P. putida cscRABY ΔnasT* and as control with *P. putida cscRABY*. To get an estimation of the biomass and sucrose produced by *S. elongatus cscB*, this strain was also grown in mono-culture. In the first auxotrophic phase before the inoculation with the heterotrophic co-culture partner and the addition of different ammonium concentrations, all eight replicates of *S. elongatus cscB* showed a uniform behavior (**Figure 3A**). After inoculation with *P. putida* a clear difference in the optical density (OD) can be observed in the different setups. In every case, the addition of *P. putida cscRABY ΔnasT* and ammonium led to higher optical densities compared to the mono-cultures of *S. elongatus cscB* without ammonium. This can be explained by the introduction of additional cells, but also by the addition of ammonium, which promotes growth

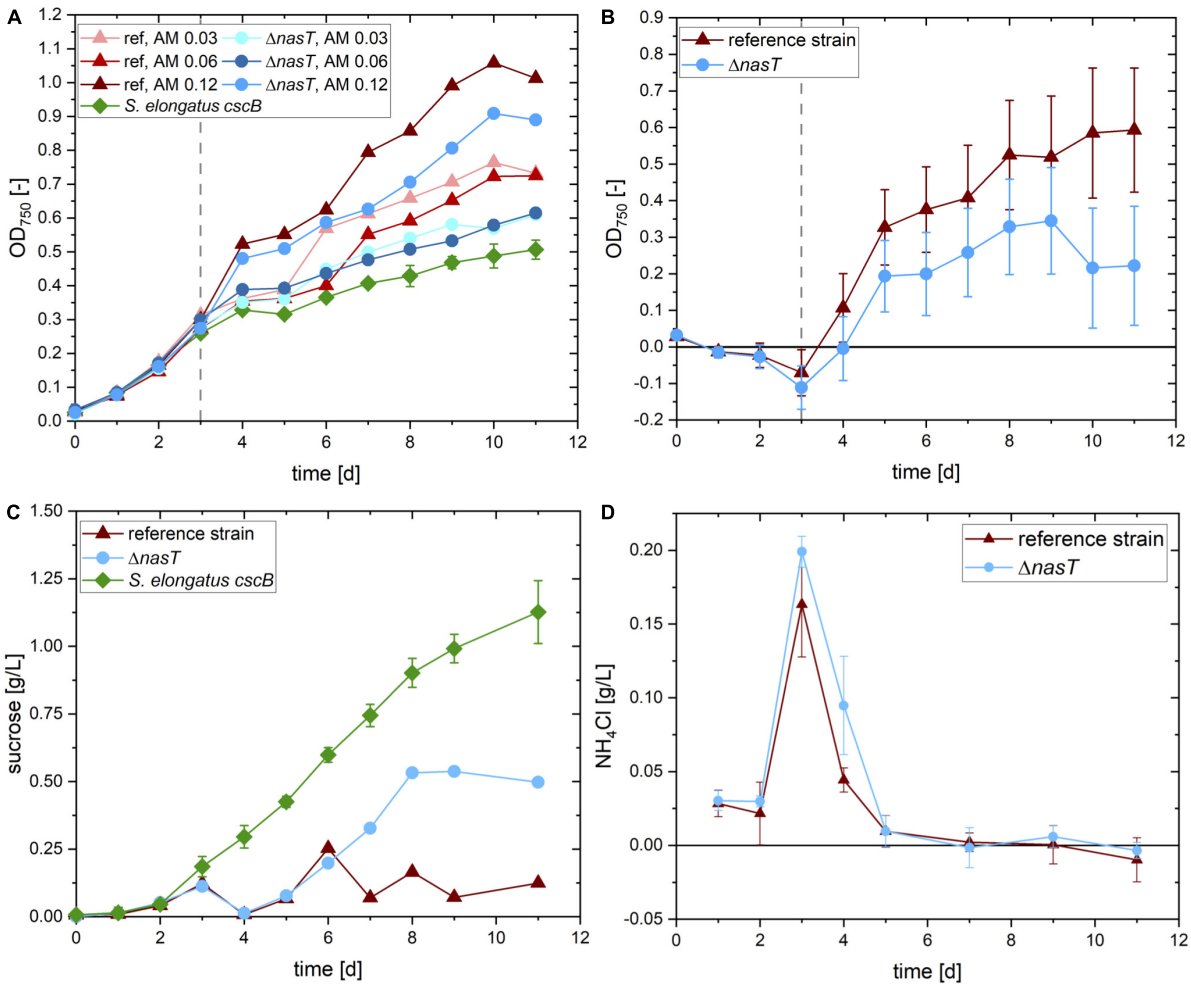

FIGURE 3 | Co-cultivation of *S. elongatus cscB* and *P. putida cscRABY* Δ*nasT*. **(A)** Total OD at 750 nm of the cultures with different ammonium concentrations. *S. elongatus cscB* (green diamonds) was grown in mono-culture as control. Co-cultivations were done with *P. putida cscRABY* (ref; triangles) or with *P. putida cscRABY* Δ*nasT* (Δ*nasT*; circles), AM 0.03: 0.03 g/L NH_4Cl; AM 0.06: 0.06 g/L NH_4Cl; AM 0.12: 0.12 g/L NH_4Cl. **(B)** Estimated optical density of the *P. putida* fraction of the co-cultivations with 0.12 g/L ammonium of *P. putida cscRABY* (red triangles) and *P. putida cscRABY* Δ*nasT* (blue circles). **(C)** Sucrose present in the control cultivation with *S. elongatus cscB* alone (green squares), or the co-cultivations with 0.12 g/L ammonium with *P. putida cscRABY* reference strain (red triangles), or *P. putida cscRABY* Δ*nasT* (blue circles). **(D)** Development of the NH_4Cl concentrations in the co-cultivations with 0.12 g/L ammonium with *P. putida cscRABY* reference strain (red triangles) or *P. putida cscRABY* Δ*nasT* (blue circles).

of the cyanobacterium as well. Comparing the co-cultivations with the Δ*nasT* mutant to the ones with *P. putida cscRABY* reveals, that in all cases a better overall growth is observed with *P. putida cscRABY*. As for this strain nitrate is available as nitrogen source, it reached higher optical densities that contribute to the total OD of the co-culture. A comparison of the development of the total OD with different ammonium concentrations in each of the co-cultivations revealed that no clear difference was observed with 0.03 g/L or 0.06 g/L NH_4Cl, i.e., that although the ammonium concentration was doubled the total OD did not increase correspondingly. Therefore, it was assumed that theses concentrations were too low to allow for substantial growth of *P. putida*. The addition of 0.12 g/L NH_4Cl, however, led to an increase in the overall OD, compared to the lower NH_4Cl concentrations, suggesting that ammonium was available for growth of *P. putida*. Thus, this co-culture was analyzed in more detail.

To get a rough estimation of the proportion of the OD achieved by *P. putida* cells, the signal stemming from *P. putida* was traced back using its different absorption characteristics (for details see Experimental Procedures and **Supplementary Material**). Therefore, a technique was applied similar to the fluorescence based "spectral unmixing" method described by Lichten et al. (2014). Instead of using variations in fluorescence intensity, here we used the different absorption characteristics of both bacteria. In particular, *S. elongatus* absorbs light via some pigments involved in photosynthesis, like chlorophyll and carotenoids, in a very different way than *P. putida*. By measuring at wavelengths that are specific and unspecific for each of the co-culture partners, information on the quantity of both

can be obtained. This allowed us to calculate the proportion of *P. putida* of the total OD. The estimated optical densities reached by *P. putida cscRABY* or *P. putida cscRABY* Δ*nasT* are shown in **Figure 3B**. At all time points, the estimated OD of *P. putida cscRABY* exceeds the one estimated for the Δ*nasT* mutant. Furthermore, according to these estimations, *P. putida cscRABY* makes up a higher proportion of the overall OD than the Δ*nasT* strain, which can be explained by the competition with *S. elongatus cscB* for nitrate.

Every day the sucrose content of these cultivations was determined by means of HPLC (**Figure 3C**). *S. elongatus cscB* excreted sucrose into the medium at a rate of 0.14 ± 0.014 g/L d and a titer of 1.13 ± 0.117 g/L was reached after 11 days. To bring this into context, this is roughly half of what was obtained in the bioreactor, where the cells are optimally supplied with light and CO_2 (Löwe et al., 2017). In both co-cultivations sucrose concentration decreased to the detection limit 1 h after the inoculation with the *P. putida* partner. However, whereas in the co-cultivation with *P. putida cscRABY* the sucrose concentration stayed on a low level throughout the experiment, it increased in the co-cultivation with the Δ*nasT* mutant strain to around 0.5 g/L of sucrose at the end of the experiment. This suggests that in the co-cultivation with *P. putida cscRABY* the sucrose produced by *S. elongatus cscB* is simultaneously taken up and metabolized by the heterotroph. In the co-cultivation with the Δ*nasT* mutant in contrast, the sucrose consumption pattern diverged from the one obtained with *P. putida cscRABY* from day six on. Measuring the NH_4Cl concentration revealed that this is the time when NH_4Cl becomes scarce and was no longer detectable from day seven on (**Figure 3D**). This suggests that the Δ*nasT* mutant stopped growing when ammonium was depleted. As a consequence, the Δ*nasT* mutant reduced the uptake of sucrose, whereas *P. putida cscRABY* continued to grow with nitrate as nitrogen source.

The plateau in the sucrose concentration reached at day eight might have different explanations on which only can be speculated. It could reflect the moment when cells switched to increased PHA accumulation which comes along with increased uptake of sucrose. However, it can also not be excluded that sucrose production by the cyanobacterium ceased for another reason. Nevertheless, the conditions from day seven on in the co-cultivation with *P. putida cscRABY* Δ*nasT*, where no nitrogen source is available for the heterotroph, but the carbon source is still present, should resemble a situation in which PHA accumulation is promoted.

The amount of PHA produced by the respective strain at the end of the co-cultivation experiment was determined. Indeed, *P. putida cscRABY* Δ*nasT* accumulated 25.24 mg/L PHA, which make up 14.8% of its calculated dry weight. In contrast, in *P. putida cscRABY* less than 1% of its calculated dry weight corresponded to PHAs (2.86 mg/L). Thus, deletion of *nasT* led to a 8.8 fold increase in the PHA accumulation in conditions in which nitrate is present. The distribution pattern of 3-hydroxyalkanoic acids is typical for *P. putida* (**Supplementary Table S3**), with 3-hydroxydecanoic acid being the most abundant monomer and does not differ substantially from the one usually obtained in *P. putida* and also reported in earlier co-cultivations in a photobioreactor (Poblete-Castro et al., 2014; Löwe et al., 2017).

Thus, by disruption of the nitrate sensing TCS, the PHA accumulation is uncoupled from the presence of nitrate in the medium. As a result, this strain experiences nitrogen limitation considerably earlier during the co-cultivation than *P. putida cscRABY* as it cannot sense nitrate and in consequence does not induce the assimilatory proteins. The lack of nitrogen assimilation should result in an internal decrease of glutamine, which triggers accumulation of the storage compound PHA. This strain is a promising candidate for PHA production from CO_2 and light not only at larger scale, but also opens up the use of other nitrate containing substrates, like waste-water, for PHA production.

This co-culture setup combined two novel elements on the side of the heterotroph compared to the published co-cultivations: (i) the blindness to nitrate, which uncouples PHA accumulation from the availability of nitrate and allows us to run the fermentation under normal nitrogen conditions, and (ii) the higher efficiency of sucrose consumption of *P. putida cscRABY* (Löwe et al., 2020), which represents a clear advance in the co-culture platform for PHA production with *P. putida*.

Stabilizing Effect of Co-cultivation of *P. putida* and *S. elongatus cscB*

At the end of the co-cultivation experiment described above, we observed that the two *S. elongatus* monocultures started

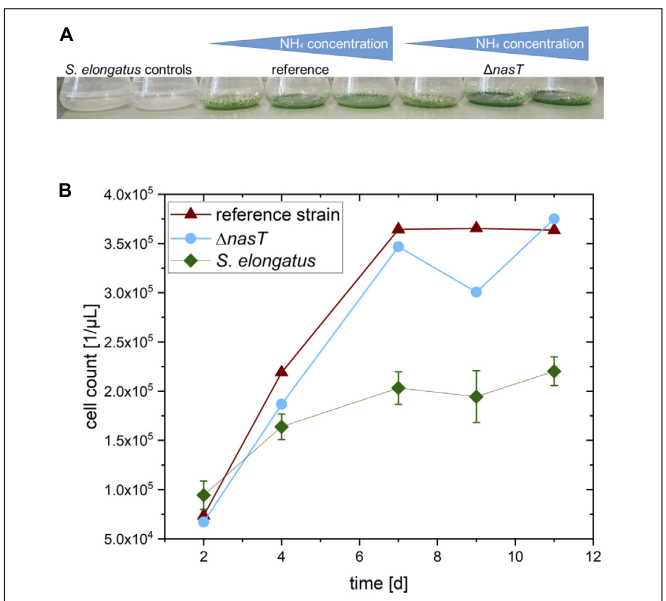

FIGURE 4 | Stabilizing effect of the co-cultivation. **(A)** Color of the cultures 4 weeks after the end of the experiment. Note that the mono-cultures have experienced complete chlorosis, whereas the co-cultures are still green. **(B)** Number of *S. elongatus cscB* cells in the different setups: *S. elongatus*, control: *S. elongatus cscB* in mono-culture; reference strain: Co-cultivation of *S. elongatus cscB* with *P. putida cscRABY* reference strain; Δ*nasT*: Co-cultivation of *S. elongatus cscB* with *P. putida* Δ*nasT*.

to lose the green pigmentation, whereas the co-cultures did not. This was even more pronounced 4 weeks after inoculation (**Figure 4A**). Furthermore, the intensity of the green color of the cultures increased with increasing ammonium concentration. The loss of pigmentation in cyanobacteria is known as chlorosis, a process that describes the depigmentation of cyanobacteria due to degradation of chlorophyll (Forchhammer and Schwarz, 2019). The fitness and viability of a cyanobacterial culture can be estimated from their chlorophyll content, which is reflected by the characteristic green color. When they are stressed or starved, they respond with chlorosis.

This observation that the presence of *P. putida* seems to have a stabilizing effect on the cyanobacterium was strengthened by the development of the cyanobacterial cell number in the co-cultivation (**Figure 4B**). In the mono-cultures of *S. elongatus cscB* a final cell count of around 2.2×10^5 cells/μL was determined, whereas in the co-cultivation setups *S. elongatus cscB* reached over 3.6×10^5 cells/μL. This effect was independent of the specific *P. putida* strain. However, the exact reason for the chlorosis cannot be determined from the experiment. It might be the consequence of the presence of *P. putida* cells. Thus, it can be speculated that the depletion of oxygen by respiration of *P. putida* provides an advantage for the cyanobacteria. On the other hand, the effect can also be attributed to the addition of ammonium together with the inoculation of *P. putida,* which might provide an additional advantage for the cyanobacteria. Another possible positive effect on *S. elongatus cscB* might be the depletion of sucrose in the culture medium by the activity of *P. putida.* Nevertheless, any combination thereof is also possible and will be in the focus of another study in out laboratory.

The stabilizing effect of co-cultivations on one of the co-culture partners was not only observed by us, but has been previously reported also by other (Hays et al., 2017). Thus, co-cultivations do not only provide an advantage over mono-cultures due to the division of labor allowing for functions that are difficult to program in individual cells, but also might have an effect on the stability of the system.

CONCLUSION

Biopolymers like PHA are often accumulated in conditions of nutrient depletion, a situation which sometimes is difficult to achieve in a biotechnological application, or at least requires considerable efforts. Genetic engineering and process engineering open up ways to mimic limitations for the specific microbe, without interfering with the rest of the system. This allows not only to improve existing microbes in terms of their productivity, but may also lay the basis for the usage of novel, or less processed substrates.

Here, we reported that deletion of the *nasT* gene encoding the response regulator of the NasS/NasT two component system resulted in a strain insensitive to the presence of nitrate and unable to grow with nitrate as nitrogen source. Nevertheless, growth but with other nitrogen sources, like ammonium, remained unaffected. The introduction of this deletion into the sucrose consuming *P. putida cscRABY* created a strain very well suited as PHA producer strain in the co-cultivation with *S. elongatus cscB*. As in this strain the PHA accumulation was uncoupled from the presence of nitrate it was not necessary to apply a nitrate limitation on the co-cultivation to induce a regime in *P. putida* that allowed for accumulation of the polymer. The final PHA titer reached by this recombinant strain was about 9-fold higher than in *P. putida cscRABY*. However, these numbers are based on the snapshot at the end of the experiment. To quantify the improvement of this tailored strain, next we will determine the PHA production rate in an optimal environment, i.e., the photobioreactor, where controlled conditions can be ensured. Apart from being used as co-cultivation partner, this strain can also be used for mcl-PHA production from other feedstocks as nitrate containing waste and surplus material. The engineering strategy applied in this work represents an important step toward mcl-PHA production from carbohydrates, which have great potential as a source of sustainable bioplastics and for medical applications (Kniewel et al., 2019) as well as for the production of chiral 3-hydroxy fatty acids that themselves can serve as precursors for various high-value products (Lee et al., 1999).

MATERIALS AND METHODS

Bacterial Strains and Plasmids

Escherichia coli DH5α λ-pir was used for the extraction of plasmids, transformation and as the plasmid donor in conjugation. *E. coli* HB101 (pRK600) and *E. coli* DH5α (pTnS1) served as helpers in conjugation and Tn7 transposition, respectively. All *P. putida* strains used in this work are derived from *P. putida* EM178, a prophage-free derivative of *P. putida* KT2440 (created at Victor de Lorenzo's lab at CNB, Madrid). An overview on the *P. putida* strains used in this work and how they are designated in the text is given in **Supplementary Table S2**. The organisms employed in the mixed culture are the autotrophic host, *S. elongatus cscB* (Ducat et al., 2012) and *P. putida* EM178 *att*Tn7:*cscRABY* Δ*nasT*, a derivative of *P. putida* EM178 *att*Tn7:*cscRABY* (Löwe et al., 2020), was constructed as described below.

Bacterial Growth Conditions, Growth Experiments, and Data Analysis

Pseudomonas putida and *E. coli* strains were cultivated at 30°C or 37°C, respectively, in either LB or M9 mineral medium (Miller, 1974) with 2% [w/v] of either glucose for *P. putida* EM178 and *P. putida* EM178 Δ*nasT,* or sucrose for *P. putida* EM178 *att*Tn7:*cscRABY* and *P. putida* EM178 *att*Tn7:*cscRABY* Δ*nasT* as carbon source.

Growth experiments with *P. putida* EM178 and *P. putida* EM178 Δ*nasT* in the presence or absence of nitrate were conducted in an ammonium-reduced M9 medium: 6.77 g/L Na_2PO_4, 2.99 g/L KH_2PO_4, 0.5 g/L NaCl, and 0.22 g/L NH_4Cl with or without the addition of 0.01 g/L $NaNO_3$.

Each experiment was performed in biological duplicates. The mean growth rates were calculated by performing a

linear regression in the exponential phase (first 10 h frame) and averaging the slopes for both biological replicates. The given standard deviation refers to the error between biological replicates only since the error of the linear fit was found to be negligible.

For the characterization of the sucrose-metabolizing strain (*P. putida* EM178 *att*Tn7:*cscRABY*Δ*nasT*) the ratio between ammonium and nitrate was shifted toward a higher nitrate proportion to allow only for very little growth with ammonium (0.03 g/L NH_4CL and 1 g/L mM $NaNO_3$) and 10 μg/mL Gentamicin was added to select for the integrated sucrose operon. Additionally, the trace element solution A5 originally found in BG11 medium (ATCC Medium 616) was supplemented to avoid deficiency of inorganic cations during growth on nitrate. All cultivations were carried out in 250 mL shaking flasks with 10% filling volume in a shaking incubator at 220 rpm. The precultures were initially grown in LB medium followed by a M9 medium intermediate culture (0.5 g/L NH_4Cl). Before inoculation of the main culture the inoculum was washed once in the cultivation medium to avoid transfer of ammonium from the preculture medium.

Co-cultivation

The co-cultivation was performed in the modified $BG11^+$ medium described previously (Löwe et al., 2017) at 30°C and 120 min^{-1} rpm with 10% filling volume of 250 mL shaking flasks in the Multitron Pro incubator equipped with CO_2 gassing and LED lighting (Infors). A photon flux density of 24 μmol m^{-2} s^{-1} was applied and air was used as the sole source of CO_2. After inoculation with *S. elongatus cscB* an initial adaptation and auxotrophic growth phase of 3 days was allowed. Upon inoculation with *P. putida* various concentrations of NH_4Cl were supplied in parallel: 0.03 g/L, 0.06 g/L, and 0.12 g/L to allow for initial growth of *P. putida* EM178 *att*Tn7:*cscRABY*Δ*nasT* before the PHA production phase begins. To the two control flasks without heterotrophic partner no ammonium was added. The *S. elongatus cscB* pre-cultures were grown in 100 mL shaking flasks with 40 mL $BG11^+$ medium in the Multitron Pro incubator. The *P. putida* pre-cultures were initially grown in LB medium followed by a M9 medium intermediate culture. The main culture was inoculated with washed cells to eliminate carry over of nitrogen and carbon from the intermediate culture.

Construction of *P. putida* EM178 *attTn7:cscRABY* Δ*nasT*

The gene deletion was carried out as described in Martínez-García and de Lorenzo (2011). All enzymes used were obtained from New England Biolabs (United States). The flanking regions upstream and downstream of *nasT* of 709 bp, respectively, were amplified by PCR (Q5 Polymerase). The primers used (**Supplementary Table S4**) for amplification introduced complementary overhangs allowing to join both fragments by overlap extension PCR (Q5 Polymerase), as well as restriction sites for the enzymes *Eco*RI and *Hin*dIII. Thus, after joining, the gene fragment was inserted into the suicide vector pSEVA212S (Silva-Rocha et al., 2013) by restriction digest and ligation (T4 DNA Ligase) to create the integration vector pSEVA212S-Δ*nasT*. This suicide vector was transferred to *P. putida* EM178 *att*Tn:*cscRABY* by triparental mating with *E. coli* HB101 (pRK600) as helper and co-integrates were selected by plating on LB with 50 mg/ml Kanamycin (de Lorenzo and Timmis, 1994). The integration was confirmed by PCR (oneTaq Polymerase) with the primers fwP_nasT_orient and rvP_nasT_seq (**Supplementary Table S4**), which also allowed to determine the site of the homologous recombination. Subsequently, the helper plasmid pSW-I was transferred by triparental mating with *E. coli* DH5α (pTnS1) as donor and one clone with the integrated pSEVA212S-Δ*nasT* as receptor. Expression of the *I-Sce*I endonuclease was induced with 1 mM 3-methylbenzoic acid for 4 h in a stationary culture (Martínez-García and de Lorenzo, 2011). Subsequently, different dilutions were plated on M9 solid medium with citrate as C-source (0.2% w/v), incubated at 30°C and single-colonies were examined by PCR (oneTaq Polymerase) and the correct deletion was confirmed by complete sequencing (Eurofins Genomics, Ebersberg) of the flanking regions.

Determination of Growth, Nitrate Concentration, Ammonium Concentration, Sucrose Concentration and PHA Content

Growth of the *P. putida* cultures was followed by measuring the OD at 600 nm in a 96-well plate in the Infinite 2000 TECAN plate reader. In the case of co-cultivation with *S. elongatus cscB*, growth was followed likewise, but at 750 nm. The dry weight was approximated using an OD to dry weight correlation determined previously for the common parental strain *P. putida* EM178 (see **Supplementary Figure S3**).

The nitrate/nitrite concentration of culture supernatants was determined using a colorimetric assay (Nitrite/Nitrate colorimetric method, Roche Diagnostics GmbH, Penzberg, Germany) in a microplate reader based on the enzymatic reduction of nitrate to nitrite.

The ammonium concentration was determined with the Ammonia Assay (Cat. No. 11 112 732 035, Boehringer Manheim/R-Biopharm) according to the supplier's manual.

The sucrose concentrations were measured using high performance liquid chromatography (HPLC) via a Shodex SH1011 column and the PHA content was determined by gas chromatography (GC) from 2 ml of the culture, exactly as described in Löwe et al. (2017).

Flow Cytometry

For the cell count measurements, a 400 μL sample of the co-culture was centrifuged for 5 min at 12000 *g*. The cell pellet was then resuspended in 400 μL PBS and Nile-red resuspended in DMSO was added to a final concentration of 3.1 μg/mL. After an incubation period of 30 min at room temperature the sample was centrifuged and washed in PBS again and a 1:100 dilution was measured in the Cytoflow Flow Cytometer (Beckman Coulter). Cells were excited by a 488 nm laser and *S. elongatus cscB* could be identified by red fluorescence that is lacking in *P. putida*.

Estimation of the Contribution of *P. putida* Cells to the OD750

The OD at 750 nm measured during the experiments is a sum of the ODs of both species.

$$OD_{750} = OD_{750,\ P.\ putida} + OD_{750,\ S.\ elongatus}$$

For the differentiation between the OD of *S. elongatus* and *P. putida*, a technique was applied similar to the fluorescence based "spectral unmixing" method described by Lichten et al. (2014). Instead of using variations in fluorescence intensity, here we used the different absorption characteristics of both bacteria. As a photosynthetic organism, *S. elongatus* has a variety of fluorescent pigments like chlorophylls and carotenoids that strongly absorb in certain wavelength regions. In particular, we used the absorption at the wavelengths at 442 nm and 632 nm, both of which should be highly influenced by chlorophyll absorption. Control experiments with pure cultures indicated that the absorption at both wavelengths show a constant linear correlation with different correlation factors (see **Supplementary Figure S5**):

$$OD_{632} = m_{632/442}\ OD_{442}$$

where $m_{632/442}$ is the correlation factor of the two absorption-values which depends on the bacterial strain.

This can be used to estimate the proportions of different bacterial species which will be shown in the following equations. First, both *P. putida* and *S. elongatus* contribute to OD_{632}:

$$OD_{632} = OD_{632,\ P.\ putida} + OD_{632,\ S.\ elongatus} =$$

$$= m_{632/442,\ P.\ putida}\ OD_{442,\ P.\ putida} +$$

$$m_{632/442,\ S.\ elongatus}\ OD_{442,\ S.\ elongatus}$$

Likewise, $OD_{442}$is also the sum of individual absorptions of the two species:

$$OD_{442} = OD_{442,\ P.\ putida} + OD_{442,\ S.\ elongatus}$$

Having two equations with two variables ($OD_{442,\ P.\ putida}$and $OD_{442,\ S.\ elongatus}$), we can solve for the single variables:

$$OD_{442,\ P.\ putida} = \frac{OD_{632} - m_{632/442,\ S.\ elongatus} OD_{442}}{m_{632/442,\ P.\ putida} - m_{632/442,\ S.\ elongatus}}$$

Since $OD_{442,\ P.\ putida}$ also correlates linearly with $OD_{750,\ P.\ putida}$ (see **Supplementary Figure S6**), the proportion of *P. putida* can easily be calculated from the OD at 442 nm:

$$OD_{750,\ P.\ putida} = m_{750/442}\ OD_{442,\ P.\ putida}$$

$$OD_{750,\ S.\ elongatus} = OD_{750} - OD_{750,\ P.\ putida}$$

In total, absorption measurements at three different wavelengths are necessary to calculate these values when the correlation-factors $m_{i/j}$ are known. The errors of the calculated, final OD_{750}-values are therefore influenced not only by the errors of the correlation-factor $m_{i/j}$, but also by the error of measurement of three ODs. We calculated the errors accordingly with Gaussian propagation of uncertainty, assuming a combined handling and instrument error of 2%.

DATA AVAILABILITY STATEMENT

All datasets generated for this study are included in the article/**Supplementary Material**.

AUTHOR CONTRIBUTIONS

KH and HL conceived and planned the experiments. KH, SL, and HL carried out the experiments. KP-G wrote the manuscript with the help of HL and KH. KP-G and AK supervised the project with the help of HL. All authors discussed the results and commented on the manuscript.

ACKNOWLEDGMENTS

We gratefully thank Victor de Lorenzo, CNB, Spain, and his laboratory for access to the pSEVA plasmid collection and the genetically streamlined versions of *P. putida* KT2440 and the group of Thomas Bruück, Technical University of Munich, especially Martina Haack for help with the GC analytics.

SUPPLEMENTARY MATERIAL

The Supplementary Material for this article can be found online at: https://www.frontiersin.org/articles/10.3389/fbioe.2020.00486/full#supplementary-material

REFERENCES

Caballero, A., Esteve-Núñez, A., Zylstra, G. J., and Ramos, J. L. (2005). Assimilation of nitrogen from nitrite and trinitrotoluene in *Pseudomonas putida* JLR11. *J. Bacteriol.* 187, 396–399. doi: 10.1128/JB.187.1.396-399.2005

de Lorenzo, V., and Timmis, K. (1994). Analysis and construction of stable phenotypes in gram-negative bacteria with Tn5- and Tn10-derived minitransposons. *Methods Enzymol.* 235, 386–405. doi: 10.1016/0076-6879(94)35157-0

Ducat, D. C., Avelar-Rivas, J. A., Way, J. C., and Silver, P. A. (2012). Rerouting carbon flux to enhance photosynthetic productivity. *Appl. Environ. Microbiol.* 78, 2660–2668. doi: 10.1128/AEM.07901-11

Fontaine, P., Mosrati, R., and Corroler, D. (2017). Medium chain length polyhydroxyalkanoates biosynthesis in *Pseudomonas putida* mt-2 is enhanced by co-metabolism of glycerol/octanoate or fatty acids mixtures. *Int. J. Biol. Macromol.* 98, 430–435. doi: 10.1016/j.ijbiomac.2017.01.115

Forchhammer, K., and Schwarz, R. (2019). Nitrogen chlorosis in unicellular cyanobacteria – a developmental program for surviving nitrogen deprivation. *Environ. Microbiol.* 21, 1173–1184. doi: 10.1111/1462-2920.14447

Hays, S. G., and Ducat, D. C. (2015). Engineering cyanobacteria as photosynthetic feedstock factories. *Photosyn. Res.* 123, 285–295. doi: 10.1007/s11120-014-9980-0

Hays, S. G., Yan, L. L. W., Silver, P. A., and Ducat, D. C. (2017). Synthetic photosynthetic consortia define interactions leading to robustness and photoproduction. *J. Biol. Eng.* 11:4. doi: 10.1186/s13036-017-0048-5

Huijberts, G. N., Eggink, G., de Waard, P., Huisman, G. W., and Witholt, B. (1992). *Pseudomonas putida* KT2442 cultivated on glucose accumulates poly(3-hydroxyalkanoates) consisting of saturated and unsaturated monomers. *Appl. Environ. Microbiol.* 58, 536–544.

Jiang, X., Sun, Z., Marchessault, R. H., Ramsay, J. A., and Ramsay, B. A. (2012). Biosynthesis and properties of medium-chain-length polyhydroxyalkanoates with enriched content of the dominant monomer. *Biomacromolecules* 13, 2926–2932. doi: 10.1021/bm3009507

Kniewel, R., Lopez, O. R., and Prieto, M. A. (2019). "Biogenesis of Medium-Chain-Length Polyhydroxyalkanoates," in *Biogenesis of Fatty Acids, Lipids and Membranes. Handbook of Hydrocarbon and Lipid Microbiology*, ed. O. Geiger (Cham: Springer).

Lee, S. Y., Lee, Y., and Wang, F. (1999). Chiral compounds from bacterial polyesters: sugars to plastics to fine chemicals. *Biotechnol. Bioeng.* 65, 363–368. doi: 10.1002/(sici)1097-0290(19991105)65:3<363::aid-bit15>3.0.co;2-1

Li, T., Li, C.-T., Butler, K., Hays, S. G., Guarnieri, M. T., Oyler, G. A., et al. (2017). Mimicking lichens: incorporation of yeast strains together with sucrose-secreting cyanobacteria improves survival, growth, ROS removal, and lipid production in a stable mutualistic co-culture production platform. *Biotechnol. Biofuels* 10:55. doi: 10.1186/s13068-017-0736-x

Lichten, C. A., White, R., Clark, I. B. N., and Swain, P. S. (2014). Unmixing of fluorescence spectra to resolve quantitative time-series measurements of gene expression in plate readers. *BMC Biotechnol.* 14:11. doi: 10.1186/1472-6750-14-11

Löwe, H., Hobmeier, K., Moos, M., Kremling, A., and Pflüger-Grau, K. (2017). Photoautotrophic production of polyhydroxyalkanoates in a synthetic mixed culture of *Synechococcus elongatus* cscB and *Pseudomonas putida* cscAB. *Biotechnol. Biofuels* 10:190. doi: 10.1186/s13068-017-0875-0

Löwe, H., Sinner, P., Kremling, A., and Pflüger-Grau, K. (2020). Engineering sucrose metabolism in *Pseudomonas putida* highlights the importance of porins. *Microb. Biotechnol.* 13, 97–106. doi: 10.1111/1751-7915.13283

Luque-Almagro, V. M., Lyall, V. J., Ferguson, S. J., Roldán, M. D., Richardson, D. J., and Gates, A. J. (2013). Nitrogen oxyanion-dependent dissociation of a two-component complex that regulates bacterial nitrate assimilation. *J. Biol. Chem.* 288, 29692–29702. doi: 10.1074/jbc.M113.459032

Martínez-García, E., and de Lorenzo, V. (2011). Engineering multiple genomic deletions in Gram-negative bacteria: analysis of the multi-resistant antibiotic profile of *Pseudomonas putida* KT2440. *Environ. Microbiol.* 13, 2702–2716. doi: 10.1111/j.1462-2920.2011.02538.x

Miller, J. H. (1974). *Experiments in Molecular Genetics*. Cold Spring Harbor, NY: CHS Laboratory Press.

Mozejko-Ciesielska, J., Dabrowska, D., Szalewska-Palasz, A., and Ciesielski, S. (2017). Medium-chain-length polyhydroxyalkanoates synthesis by *Pseudomonas putida* KT2440 relA/spoT mutant: bioprocess characterization and transcriptome analysis. *AMB Express* 7:92. doi: 10.1186/s13568-017-0396-z

Muhammadi, Shabina, Afzal, M., and Hameed, S. (2015). Bacterial polyhydroxyalkanoates-eco-friendly next generation plastic: production, biocompatibility, biodegradation, physical properties and applications. *Green Chem. Lett. Rev.* 8, 56–77. doi: 10.1080/17518253.2015.1109715

Nikel, P. I., Chavarría, M., Danchin, A., and de Lorenzo, V. (2016). From dirt to industrial applications: *Pseudomonas putida* as a synthetic biology chassis for hosting harsh biochemical reactions. *Curr. Opin. Chem. Biol.* 34, 20–29. doi: 10.1016/j.cbpa.2016.05.011

Nogales, J., Mueller, J., Gudmundsson, S., Canalejo, F. J., Duque, E., Monk, J., et al. (2019). High-quality genome-scale metabolic modelling of *Pseudomonas putida* highlights its broad metabolic capabilities. *Environ. Microbiol.* 22, 255–269. doi: 10.1111/1462-2920.14843

Ortiz-Marquez, J. C. F., Do Nascimento, M., Zehr, J. P., and Curatti, L. (2013). Genetic engineering of multispecies microbial cell factories as an alternative for bioenergy production. *Trends Biotechnol.* 31, 521–529. doi: 10.1016/j.tibtech.2013.05.006

Poblete-Castro, I., Escapa, I. F., Jäger, C., Puchalka, J., Lam, C. M. C., Schomburg, D., et al. (2012). The metabolic response of *P. putida* KT2442 producing high levels of polyhydroxyalkanoate under single- and multiple-nutrient-limited growth: highlights from a multi-level omics approach. *Microb. Cell Fact.* 11:34. doi: 10.1186/1475-2859-11-34

Poblete-Castro, I., Rodriguez, A. L., Lam, C. M. C., and Kessler, W. (2014). Improved production of medium-chain-length polyhydroxyalkanoates in glucose-based fed-batch cultivations of metabolically engineered *Pseudomonas putida* strains. *J. Microbiol. Biotechnol.* 24, 59–69. doi: 10.4014/jmb.1308.08052

Romeo, A., Sonnleitner, E., Sorger-Domenigg, T., Nakano, M., Eisenhaber, B., and Bläsi, U. (2012). Transcriptional regulation of nitrate assimilation in *Pseudomonas aeruginosa* occurs via transcriptional antitermination within the nirBD-PA1779-cobA operon. *Microbiology* 158, 1543–1552. doi: 10.1099/mic.0.053850-0

Silva-Rocha, R., Martínez-García, E., Calles, B., Chavarría, M., Arce-Rodríguez, A., Las Heras de, A., et al. (2013). The Standard European Vector Architecture (SEVA): a coherent platform for the analysis and deployment of complex prokaryotic phenotypes. *Nucleic Acids Res.* 41, D666–D675. doi: 10.1093/nar/gks1119

Smith, M. J., and Francis, M. B. (2016). A designed A. vinelandii–*S. elongatus* coculture for chemical photoproduction from air, water, phosphate, and trace metals. *ACS Synth. Biol.* 5, 955–961. doi: 10.1021/acssynbio.6b00107

Stanier, R. Y., Kunisawa, R., Mandel, M., and Cohen-Bazire, G. (1971). Purification and properties of unicellular blue-green algae (order Chroococcales). *Bacteriol. Rev.* 35, 171–205.

Wecker, P., Moppert, X., Simon-Colin, C., Costa, B., and Berteaux-Lecellier, V. (2015). Discovery of a mcl-PHA with unexpected biotechnical properties: the marine environment of French Polynesia as a source for PHA-producing bacteria. *AMB Express* 5:74. doi: 10.1186/s13568-015-0163-y

Weiss, T. L., Young, E. J., and Ducat, D. C. (2017). A synthetic, light-driven consortium of cyanobacteria and heterotrophic bacteria enables stable polyhydroxybutyrate production. *Metab. Eng.* 44, 236–245. doi: 10.1016/j.ymben.2017.10.009

Conflict of Interest: The authors declare that the research was conducted in the absence of any commercial or financial relationships that could be construed as a potential conflict of interest.

frontiers in Bioengineering and Biotechnology

ORIGINAL RESEARCH
published: 09 July 2020
doi: 10.3389/fbioe.2020.00728

Engineering Expression Cassette of *pgdS* for Efficient Production of Poly-γ-Glutamic Acids With Specific Molecular Weights in *Bacillus licheniformis*

Dong Wang[1†], Huan Wang[1†], Yangyang Zhan[1], Yong Xu[1], Jie Deng[1], Jiangang Chen[2], Dongbo Cai[1], Qin Wang[1], Feng Sheng[1] and Shouwen Chen[1*]*

[1] State Key Laboratory of Biocatalysis and Enzyme Engineering, Environmental Microbial Technology Center of Hubei Province, College of Life Science, Hubei University, Wuhan, China, [2] Wuhan Junan Biotechnology Co., Ltd., Wuhan, China

OPEN ACCESS

Edited by:
Bernd Rehm, Griffith University, Australia

Reviewed by:
Jin-Song Gong, Jiangnan University, China
Samarthya Bhagia, Biosciences Division (BSD), Oak Ridge National Laboratory, United States

***Correspondence:**
Feng Sheng
shengfsk@163.com
Shouwen Chen
mel212@126.com

[†] These authors have contributed equally to this work

Specialty section:
This article was submitted to Industrial Biotechnology, a section of the journal Frontiers in Bioengineering and Biotechnology

Received: *03 October 2019*
Accepted: *09 June 2020*
Published: *09 July 2020*

Citation:
Wang D, Wang H, Zhan Y, Xu Y, Deng J, Chen J, Cai D, Wang Q, Sheng F and Chen S (2020) Engineering Expression Cassette of pgdS for Efficient Production of Poly-γ-Glutamic Acids With Specific Molecular Weights in Bacillus licheniformis. Front. Bioeng. Biotechnol. 8:728. doi: 10.3389/fbioe.2020.00728

Poly-γ-glutamic acid (γ-PGA) is an emerging biopolymer with various applications and γ-PGAs with different molecular weights exhibit distinctive properties. However, studies on the controllable molecular weights of biopolymers are limited. The purpose of this study is to achieve production of γ-PGAs with a wide range of molecular weights through manipulating the expression of γ-PGA depolymerase (PgdS) in *Bacillus licheniformis* WX-02. Firstly, the expression and secretion of PgdS were regulated through engineering its expression elements (four promoters and eight signal peptides), which generated γ-PGAs with molecular weights ranging from 6.82×10^4 to 1.78×10^6 Da. Subsequently, through combination of promoters with signal peptides, the production of γ-PGAs with a specific molecular weight could be efficiently obtained. Interestingly, the γ-PGA yield increased with the reduced molecular weight in flask cultures (Pearson correlation coefficient of −0.968, $P < 0.01$). Finally, in batch fermentation, the highest yield of γ-PGA with a weight-average molecular weight of 7.80×10^4 Da reached 39.13 g/L under glutamate-free medium. Collectively, we developed an efficient strategy for one-step production of γ-PGAs with specific molecular weights, which have potential application for industrial production of desirable γ-PGAs.

Keywords: *Bacillus licheniformis*, Poly-γ-glutamic acid, molecular weight, PgdS depolymerase, controllable degradation

INTRODUCTION

Poly-γ-glutamic acid (γ-PGA), an anionic polymer composed of repeated D- and L-glutamic acid units via γ-amide linkages, is mainly produced by *Bacillus* species (e.g., *B. licheniformis*, *B. subtilis*, *B. amyloliquefaciens*) (Sirisansaneeyakul et al., 2017). Due to its versatile physical properties, γ-PGA has been used in various fields, including agriculture, food, cosmetics, and pharmaceutical industries (Cao et al., 2018). Notably, depending on the producers, the molecular weight (Mw) of γ-PGA varied with a range from 1.0×10^4 to over 2.0×10^6 Da (Sirisansaneeyakul et al., 2017). The γ-PGAs with different Mws are exploited in different applications (Ogunleye et al., 2015). For example, γ-PGAs with high-Mws are used as superior flocculants in the wastewater treatment

(Yokoi et al., 1996). The medium-Mw γ-PGAs (∼9.9 × 10^5 Da) can efficiently remove basic dyes from solution (Inbaraj et al., 2006). Low-Mw γ-PGAs (2.0 × 10^4–2.7 × 10^5 Da) can be used as the drug carrier and tissue engineering nanocomposite in the biomedical industry (Shu et al., 2014). Thus, the controlled Mw is critical for the development and application of γ-PGA.

Previously, efforts have been made to change the Mws of γ-PGAs through changing fermentation conditions (Zeng et al., 2016; Feng et al., 2017). Also, several physical methods such as ultrasonication and heating (Pérez−Camero et al., 1999), as well as chemical methods like acidic and alkaline hydrolysis (Kubota et al., 1996), have been applied to depolymerize γ-PGA. However, since those methods lack precise control of Mws, the increasing polydispersity leads to a complicated purification process, which in turn limits the application of γ-PGA. By contrast, the enzymatic depolymerization via γ-PGA depolymerase is an alternative way to produce γ-PGA with desirable Mws with several superiorities, including mild reaction conditions and non-pollution (Yao et al., 2009). However, the extraction and purification of the depolymerase PgdS and subsequent hydrolysis processes are time-consuming and comparatively tedious, hampering the application of the enzymatic method for tailor-made γ-PGA production.

Recently, one-step fermentation is becoming an attractive method for biorefinery. For example, γ-PGA with a wider range of Mws (4.0 × 10^4–8.5 × 10^6 Da) were achieved in *B. subtilis* via expression of different γ-PGA synthetases (Halmschlag et al., 2019). Several endo-type PgdS depolymerases have been characterized (Suzuki and Tahara, 2003; Tian et al., 2014; Sha et al., 2018). Tian et al. (2014) characterized the PgdS hydrolase from *B. licheniformis* WX-02 and expressed this enzyme to achieve efficient production of low-Mw γ-PGAs. Moreover, Sha et al. (2018) achieved production of γ-PGA with different Mws through expressing four PgdS hydrolases with different hydrolytic activity. These results indicate that Mws of γ-PGA are correlated with PgdS hydrolase activity.

In this study, we develop a simple system for one-step production of γ-PGA through regulating the expression of PgdS depolymerase in *B. licheniformis* WX-02, a glutamate independent producer. The promoter and signal peptide are the vital factors for expression and secretion of proteins (Zhang et al., 2016). The Mws of γ-PGA was systematically modified by manipulating the promoters and signal peptides independently and in combination. By generating PgdS with different hydrolytic activities, γ-PGAs with a broad range of Mws were efficiently produced. Therefore, the strategy of engineering PgdS expression cassette is feasible to produce γ-PGAs with specific Mws.

MATERIALS AND METHODS

Strains, Plasmids and Culture Conditions

All strains and plasmids employed in this work were listed in **Table 1**. The pHY-300PLK plasmid and temperature-sensitive plasmid T_2(2)-ori were used to construct the expression and deletion vectors, respectively. All strains were generally cultivated at 37°C in Luria Bertani (LB) medium. When necessary, antibiotics (20 μg/L kanamycin, or 20 μg/L tetracycline) were supplemented into the media.

For the seed cultures, *B. licheniformis* cells were precultured in LB medium and incubated at 37°C for 12 h. For γ-PGA fermentation, 250 mL flasks containing 50 mL medium (glucose 80.00 g/L, sodium citrate 30.00 g/L, NH_4Cl 8.00 g/L, $NaNO_3$ 15.00 g/L, $K_2HPO_4{\cdot}3H_2O$ 1.00 g/L, $MgSO_4{\cdot}7H_2O$ 1.00 g/L, $ZnSO_4{\cdot}7H_2O$ 1.00 g/L, $CaCl_2$ 1.00 g/L, $MnSO_4{\cdot}H_2O$ 0.15 g/L, pH7.2) were inoculated with 3% (v/v) seed cultures and cultivated at 37°C.

The *B. licheniformis* cells grow in 1-L bioreactor (T&J Bio-engineering Co., Ltd., Shanghai, China) with 0.60 L of media for 10 h. The aeration rate was 1.0 vvm, and the stirring speed was 300 rpm. The volume fractions of exhausted O_2 and CO_2 were measured by exhaust gas analyzer, and the volumetric mass transfer coefficient were calculated by the exhaust gas analysis system (T&J Bio−engineering Co., Ltd., Shanghai, China) (Cai et al., 2018).

Batch fermentation was carried out in the 3-L bioreactor (T&J Bio-engineering Co., Ltd., Shanghai, China) containing 1.8 L media with an aeration rate of 1.0 vvm. The agitation speed was starting to set at 300 rpm and increased to 600 rpm after 12 h. Samples were collected periodically to analyze the cell growth, glucose, and γ-PGA concentrations. Δ*pgdS* was further verified by diagnostic PCR and DNA sequencing.

Construction of Gene Expression Strains

As an example, the construction procedure of the plasmid pHYP43-SPsacB (containing P43 promoter and SPsacB) was described. Briefly, P43 promoter of *B. subtilis* 168, signal peptide of levansucrase SacB (SPsacB), gene *pgdS* (without its own signal peptide) and *amyL* terminator of *B. licheniformis* WX-02 were amplified and fused by overlapping PCR to obtain the expression cassettes (**Figure 1**). The expression cassettes were inserted into *Eco*RI/*Xba*I-cut pHY-300PLK, and the resulting plasmids were transformed into WX-02Δ*pgdS* to obtain recombinant strain SP18. Other PgdS expression strains were constructed by the similar method. Notably, all the recombinant vectors were verified by DNA sequencing. Moreover, the empty plasmid pHY300PLK was transformed into WX-02Δ*pgdS* to generate the control strain SP01.

Enzymatic Assay for PgdS

Crude enzyme solution of PgdS was attained by removing the cells via centrifugation (13 700 × *g*, 20 min). Enzyme activity was measured as described by Ashiuchi et al. (2006). Briefly, the reaction contains 20 μM f potassium phosphate buffer (pH 6.0), 0.2 nM 1.0 × 10^6 Da γ-PGA substrate, 2 μM dithiothreitol and 10 μL of crude enzyme solution, and was incubated at 37°C for 4 h. After stopped, 100 μL of reaction solution was withdrawn and mixed with 100 μL of 0.2 M borate buffer (pH 8.5) and 20 μL of 10 mmol/L fluorodinitrobenzene (FDNB, in acetone). The hydrolysis of FDNB-modified fragments and the assay of dinitrophenyl glutamate monomers (DNPGlu) were performed as described previously (Ashiuchi et al., 2006). One unit of PgdS was defined as the amount of enzyme that generated 1 nmol of terminal glutamate group per minute.

TABLE 1 | Strains and plasmids in this study.

Strains or plasmids	Relevant properties	References
Escherichia coli		
DH5α	F^-, φ80d*lacZ*ΔM1, Δ(*lacZYA-argF*)U169, *deoR*, *recA*1, *endA*1, *hsdR*17 (rk^-, mk^+), *phoA*, *supE*44, λ^-*thi*-1, *gyrA*96, *relA*1	Stored in lab
Bacillus licheniformis		
WX-02	Wide-type (CCTCC M208065)	Wei et al., 2010
WX-02Δ*pgdS*	deletion of *pgdS* in WX-02	This study
Control		
SP01	WX-02Δ*pgdS* derivative with expression plasmid pHY300PLK	This study
Signal peptide		
SP11	WX-02Δ*pgdS* derivative with expression plasmid pHYP43-SPsacC	This study
SP12	WX-02Δ*pgdS* derivative with expression plasmid pHYP43-SPvpr	This study
SP13	WX-02Δ*pgdS* derivative with expression plasmid pHYP43- SPbprA	This study
SP14	WX-02Δ*pgdS* derivative with expression plasmid pHYP43-SPggt	This study
SP15	WX-02Δ*pgdS* derivative with expression plasmid pHYP43-SPaprE	This study
SP16	WX-02Δ*pgdS* derivative with expression plasmid pHYP43-SPpgdS	This study
SP17	WX-02Δ*pgdS* derivative with expression plasmid pHYP43-SPyvpA	This study
SP18	WX-02Δ*pgdS* derivative with expression plasmid pHYP43-SPsacB	This study
Promoter		
SP23	WX-02Δ*pgdS* derivative with expression plasmid pHYPpgdS-SPbprA	This study
SP33	WX-02Δ*pgdS* derivative with expression plasmid pHYPbacA-SPbprA	This study
SP43	WX-02Δ*pgdS* derivative with expression plasmid pHYPbprA-SPbprA	This study
Combination		
SP21	WX-02Δ*pgdS* derivative with expression plasmid pHYPpgdS-SPsacC	This study
SP25	WX-02Δ*pgdS* derivative with expression plasmid pHYPpgdS-SPaprE	This study
SP28	WX-02Δ*pgdS* derivative with expression plasmid pHYPpgdS-SPsacB	This study
SP31	WX-02Δ*pgdS* derivative with expression plasmid pHYPbacA-SPsacC	This study
SP35	WX-02Δ*pgdS* derivative with expression plasmid pHYPbacA-SPaprE	This study
SP38	WX-02Δ*pgdS* derivative with expression plasmid pHYPbacA-SPsacB	This study
SP41	WX-02Δ*pgdS* derivative with expression plasmid pHYPbprA-SPsacC	This study
SP45	WX-02Δ*pgdS* derivative with expression plasmid pHYPbprA-SPaprE	This study
SP48	WX-02Δ*pgdS* derivative with expression plasmid pHYPbprA-SPsacB	This study
Plasmids		
T_2(2)-ori	*E. coli* and *B. subtilis* shuttle vector; Ori_{pUC}/Ori_{ts}, Kan^r	Qiu et al., 2014
T_2-*pgdS*	T_2 derivation with deletion fragment of *pgdS*	This study
pHY300PLK	*E. coli-Bacillus* shuttle vector; Amp^r in *E. coli*,Tc^r in both *E. coli* and *B. subtilis*	Purchased from Takara
pHYP43-SPsacB	pHY300PLK derivative carrying P43 promoter, SP *sacB*, *pgdS* gene	This study
pHYP43-SPyvpA	pHY300PLK derivative carrying P43 promoter, SP*yvpA*, *pgdS* gene	This study
pHYP43-SPbprA	pHY300PLK derivative carrying P43 promoter, SP*bprA*, *pgdS* gene	This study
pHYP43-SPaprE	pHY300PLK derivative carrying P43 promoter, SP*aprE*, *pgdS* gene	This study
pHYP43-SPvpr	pHY300PLK derivative carrying P43 promoter, SP*vpr*, *pgdS* gene	This study
pHYP43-SPsacC	pHY300PLK derivative carrying P43 promoter, SP*sacC*, *pgdS* gene	This study
pHYP43-SPggt	pHY300PLK derivative carrying P43 promoter, SP*ggt*, *pgdS* gene	This study
pHYP43-SPpgdS	pHY300PLK derivative carrying P43 promoter, SP*pgdS*, *pgdS* gene	This study
pHYPpgdS-SPbprA	pHY300PLK derivative carrying PpgdS promoter, SP*bprA*, *pgdS* gene	This study
pHYPbprA-SPbprA	pHY300PLK derivative carrying PbprA promoter, SP*bprA*, *pgdS* gene	This study
pHYPbacA-SPbprA	pHY300PLK derivative carrying PbacA promoter, SP*bprA*, *pgdS* gene	This study
pHYPbprA-SPsacB	pHY300PLK derivative carrying PbprA promoter, SP*sacB*, *pgdS* gene	This study
pHYPbprA-SPaprE	pHY300PLK derivative carrying PbprA promoter, SP*aprE*, *pgdS* gene	This study
pHYPbprA-SPsacC	pHY300PLK derivative carrying PbprA promoter, SP*sacC*, *pgdS* gene	This study
pHYPpgdS-SPsacB	pHY300PLK derivative carrying PpgdS promoter, SP*sacB*, *pgdS* gene	This study
pHYPpgdS-SPaprE	pHY300PLK derivative carrying PpgdS promoter, SP*aprE*, *pgdS* gene	This study
pHYPpgdS-SPsacC	pHY300PLK derivative carrying PpgdS promoter, SP*sacC*, *pgdS* gene	This study
pHYPbacA-SPsacB	pHY300PLK derivative carrying PbacA promoter, SP*sacB*, *pgdS* gene	This study
pHYPbacA-SPaprE	pHY300PLK derivative carrying PbacA promoter, SP*aprE*, *pgdS* gene	This study
pHYPbacA-SPsacC	pHY300PLK derivative carrying PbacA promoter, SP*sacC*, *pgdS* gene	This study

Ori_{ts} thermosensitive replication origin, Kan^r kanamycin resistance gene, Amp^r ampicillin resistance gene, Tc^r tetracycline resistance gene.

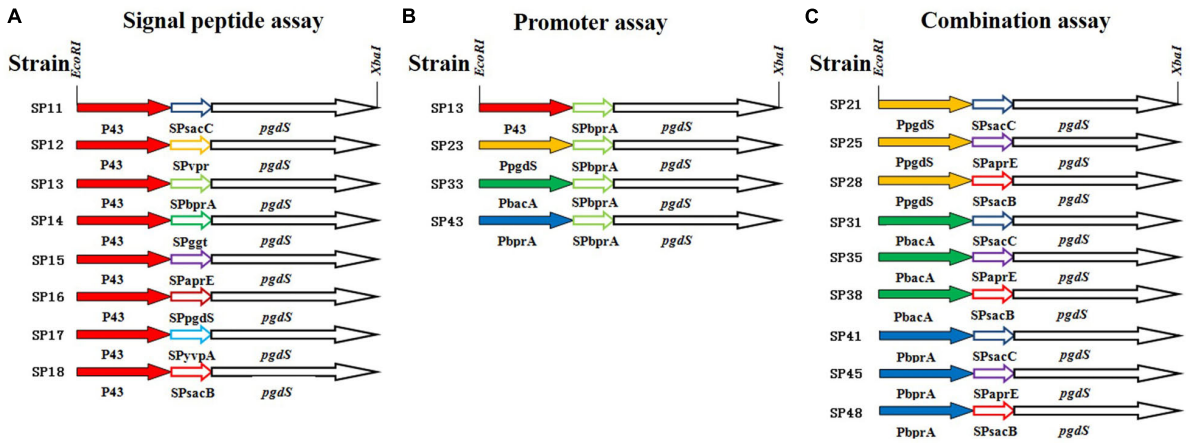

FIGURE 1 | The details of PgdS expression cassettes constructed by manipulating its promoter and signal peptide independently and in combination. **(A)** Signal peptide assay containing SPsacB, SPaprE, SPggt, SPvpr, SPbprA, SPyvpA, SPpgdS, and SPsacC using P43 promoter; **(B)** promoter assay containing P43, PbacA, PpgdS, and PbprA using BprA signal peptide; **(C)** combination assay containing three promoters (PpgdS, PbacA, and PbprA) and three signal peptides (SPsacB, SPpgdS, and SPsacC). Different colors indicate different promoters or signal peptides, and the named rule of strains: first number means promoter, second number means signal peptide.

SDS-PAGE Analysis

SDS-PAGE analysis was applied to determine the extracellular contents of PgdS in recombinant strains and the BSA (bovine serum albumin) was used as a protein standard. Briefly, 1 mL fermentation broth was centrifuged at 10000 × *g* for 10 min, and the supernatant was precipitated by 6.12 mol/L trichloroacetic acid (TCA). The precipitate was washed with absolute alcohol, and re-dissolved in a 100 uL solution which containing 2 mol/L thiourea and 8 mol/L urea. Protein concentrations were quantitated by Bradford assay (Hammond and Kruger, 1988) and BSA was used as a protein standard. Protein samples as while as BSA solution were mixed with 2 × SDS–PAGE loading buffer containing β-mercaptoethanol in 1:1 ratio, then boiling water bath for 5 min and then samples contain loading buffer were analyzed by the 15% (w/v) gel (Cai et al., 2016). The gels were then imaged with a Bio-Rad's Gel Doc XR + system (Bio-Rad, United States). The target bands in the gels were visualized and quantified with ImageJ software (Rasband, W.S., ImageJ, United States National Institutes of Health, Bethesda, MD, United States) (Gallagher, 2014), and the BSA proteins were used as standards.

Quantitative PCR Analysis

When the cells grew into the mid-logarithmic growth phase, the cells were collected for RNA extraction according to Shi's method (Shi et al., 2019), The HiScript®II Q RT SuperMix for qPCR (+gDNA wiper) (Vazyme, China) was employed for cDNA synthesis. The real-time PCR was performed using iTaqTM Universal SYBR® Green Supermix (Bio-Rad, United States). The experiments were performed in three replicates, and *16S rRNA* was used as the reference gene (Rocha et al., 2015). The relative transcriptional level of *pgdS* gene was calculated using the $2^{-\Delta\Delta Ct}$ method.

Analytical Methods

The cell density (OD_{600}) was measured using the 752N spectrophotometer (Shanghai Opler Instrument Co., Ltd., Shanghai, China). The glucose concentration was determined by SBA-40C bioanalyzer (Academy of Sciences, Shandong, China).

The purification of γ –PGA was carried out by the method reported previously (Tian et al., 2014). Number average molecular weight (Mn), weight average molecular weight (Mw), and polydispersity index (Mw/Mn) of γ-PGA were measured using gel permeation chromatography (GPC) with a refractive index (RI) detector and a Shodex OHpak SB-806 HQ column (8.0 mm ID × 300 mm, 13 μm) (Birrer et al., 1994). Pullulan standards of narrow polydispersity (SHANGHAI ZZBIO CO., Ltd., Shanghai, China) were employed to establish a calibration curve. The concentration of γ-PGA was calculated from the peak area of the GPC measurements, with purified γ-PGA as a standard (Birrer et al., 1994; Xu et al., 2019).

Statistical Analysis

All data are represented as the means of three replicates and bars represent the standard deviations. Data were analyzed by SPSS Statistics software v. 19.0. Pearson correlation coefficient, *t*-test, and ANOVA test were carried out to compare means values and $p < 0.05$ were considered statistically significant.

RESULTS

To systematically study the influence of PgdS expression level on the Mws of γ-PGAs, the native *pgdS* gene was deleted from the genome of *B. licheniformis* WX-02. PgdS depolymerase was expressed episomally and controlled by the promoter and signal peptide independently and in combination. We employed the strategy to construct twenty recombinant strains with different PgdS hydrolytic activities to generate γ-PGA with different Mws.

In our previous study, the nattokinase was used as a reporter to test the effects of signal peptide on protein expression (Cai et al., 2016). According to the data, nattokinase protein with the eight signal peptides (SPsacB, SPaprE, SPpgdS, SPbprA, SPggt, SPsacC, SPyvpA, and SPvpr) expressed in various levels (nearly ten times between the highest level and the lowest level, due to the high copy number of plasmid harboring pgdS gene, we tend to choose the signal peptides with low expression level to avoid over expression of PgdS) (**Supplementary Table S2**). In order to get multiple expression levels of PgdS, those eight signal peptides and four promoters (P43, PpgdS, PbprA, and PbacA) were employed to construct *pgdS* expression vectors (**Figure 1**). According to the result of pre-experiment (**Supplementary Figure S1A**), the PGA titers of each strain were highest at 36 h. The molecular weight of PGA was decreased with the prolonged fermentation (**Supplementary Figure S1B**), while, at the later period of fermentation (30–42 h), the γ-PGA molecular weight values for the recombinants SP12, SP14, and SP18 were maintained. So the time of fermentation of all the strains were set as 36 h.

Modulating PgdS Secretion to Tune γ-PGA Molecular Weight

All PgdS expression vectors were transferred into the *pgdS* deletion strain WX-02Δ*pgdS*, and the resultant strains were designated *B. licheniformis* SP11–SP18, respectively (**Table 1**).

In our previous study, we have construct SP library in *B. licheniformis* using nattokinase as reporter (Cai et al., 2016). We choose eight different SP from *B. licheniformis* to expression PgdS. The SDS-PAGE analysis of the culture supernatants (**Supplementary Figure S2**) showed a band of the predicted molecular mass (4.2×10^4 Da) among the SP12–SP18 strains, except the control strain SP01 and SP11 (carrying cassette with the combination of P43-SPsacC). Among these strains, the secretion efficiency ratios were SPsacB > SPyvpA > SPpgdS > SPaprE > SPggt > SPbprA > SPvpr > SPsacC (**Table 2**). As indicated in **Figure 2**, overexpression of PgdS enabled efficient reduction of Mws, which was consistent with the results reported by Tian et al. (2014) and Sha et al. (2018). The PgdS overexpression strains also produced γ-PGA with lower Mns values and polydispersity index (**Table 2**). The Mws of γ-PGAs produced by recombinant strains were ranged from $(6.82 \pm 0.51) \times 10^4$ to $(1.71 \pm 0.08) \times 10^6$ Da, compared with the control strain $(1.99 \pm 0.11) \times 10^6$ Da. Interestingly, cell growth showed no significant differences between the recombinant strains and control strain SP01. Therefore, our results indicated that γ-PGA with a wide range of Mws (6.82×10^4–1.71×10^6 Da) could be achieved via modulating the secretory capability of PgdS.

TABLE 2 | The γ-PGA yields of recombinant strains and the PgdS concentrations of culture supernatants.

Strain	Mw ($\times 10^5$ Da)	Mn ($\times 10^5$ Da)	Polydispersity index	γ-PGA yields (g/L)	PgdS protein concentrations of culture supernatant (mg/L)	Total protein concentrations of culture supernatant (mg/L)	PgdS activity (U/mL)
SP01	19.96 ± 1.16	13.49 ± 0.89	1.48 ± 0.07	25.65 ± 0.56	ND	83.4 ± 4.2	0
SP41	19.10 ± 0.75	13.08 ± 0.78	1.46 ± 0.04	26.86 ± 0.94	2.4	112.4 ± 11.3	0.72 ± 0.23
SP43	17.80 ± 0.87	12.11 ± 0.86	1.47 ± 0.06	27.36 ± 0.73	ND	103.7 ± 17.3	0.54 ± 0.33
SP31	17.43 ± 0.56	12.10 ± 0.54	1.44 ± 0.03	27.88 ± 0.61	3.3	115.1 ± 12.3	1.25 ± 0.21
SP21	17.40 ± 0.11	12.03 ± 0.77	1.45 ± 0.03	27.14 ± 1.14	4.2	127.3 ± 17.8	1.22 ± 0.17
SP11	17.13 ± 0.84	12.06 ± 0.61	1.42 ± 0.05	27.09 ± 0.99	ND	121.9 ± 11.5	1.09 ± 0.37
SP45	16.72 ± 0.88	11.77 ± 0.92	1.42 ± 0.06	27.87 ± 0.62	7.7	121.3 ± 7.6	6.37 ± 0.42
SP33	14.41 ± 0.67	10.44 ± 1.02	1.38 ± 0.07	28.19 ± 0.48	7.7	112.7 ± 9.5	6.71 ± 0.21
SP48	13.40 ± 0.73	9.64 ± 0.55	1.39 ± 0.04	28.75 ± 0.38	8.6	128.8 ± 14.7	7.22 ± 0.33
SP12	10.21 ± 0.73	7.51 ± 0.43	1.36 ± 0.05	28.32 ± 0.56	9.1	115.1 ± 7.2	8.17 ± 0.54
SP23	9.55 ± 0.46	7.07 ± 0.50	1.35 ± 0.01	28.68 ± 0.71	9.9	124.1 ± 8.1	8.68 ± 0.38
SP13	7.78 ± 0.42	5.72 ± 0.67	1.36 ± 0.03	29.27 ± 1.28	12.5	127.5 ± 17.9	10.05 ± 0.21
SP14	5.06 ± 0.32	3.80 ± 0.31	1.33 ± 0.01	31.58 ± 1.49	13.3	122.3 ± 15.5	12.12 ± 0.26
SP35	3.19 ± 0.16	2.40 ± 0.27	1.33 ± 0.03	32.67 ± 0.59	14.5	128.0 ± 16.2	13.22 ± 0.38
SP15	1.21 ± 0.08	0.92 ± 0.13	1.31 ± 0.01	31.45 ± 1.39	25.1	124.3 ± 10.3	22.18 ± 0.51
SP25	1.18 ± 0.10	0.90 ± 0.15	1.31 ± 0.01	33.30 ± 1.06	28.6	146.6 ± 15.0	25.26 ± 0.40
SP38	1.12 ± 0.10	0.85 ± 0.07	1.32 ± 0.02	33.80 ± 0.97	28.4	143.2 ± 18.5	25.13 ± 0.37
SP16	0.97 ± 0.05	0.76 ± 0.07	1.27 ± 0.01	34.00 ± 0.12	40.7	165.6 ± 14.7	26.18 ± 0.62
SP17	0.78 ± 0.06	0.63 ± 0.05	1.24 ± 0.01	34.46 ± 0.75	41.4	161.8 ± 11.4	26.38 ± 0.49
SP28	0.77 ± 0.08	0.62 ± 0.06	1.25 ± 0.01	34.33 ± 1.21	40.9	155.6 ± 18.1	26.12 ± 0.45
SP18	0.68 ± 0.05	0.56 ± 0.05	1.22 ± 0.01	34.60 ± 0.65	42.7	158.9 ± 16.6	32.22 ± 0.39

The assays of molecular weights, γ-PGA yields were performed in triplicate. The total protein concentrations of fermentation supernatant were converting from the concentrations of re-dissolved precipitate and the errors are shown as standard deviations. Mw emphasizes the influence of the part with the highest molecular weight to the average molecular weight, while Mn emphasizes the influence of the part with the largest molecular number in a certain range to the average molecular weight. The value of polydispersity index (Mw/Mn) reflects the uniformity of particle size, the lower the value, the more uniform of the grain size.

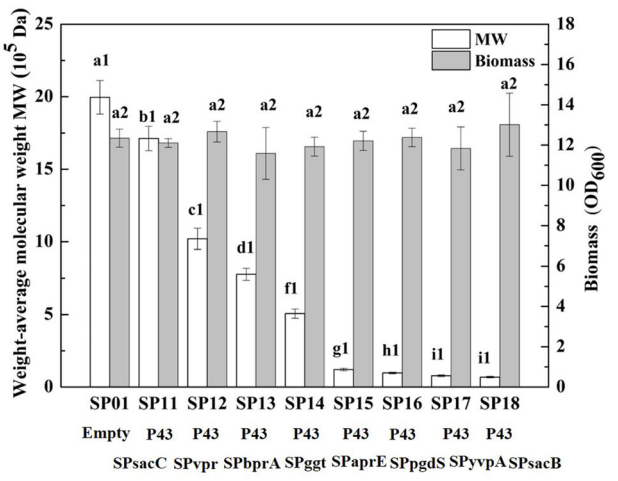

FIGURE 2 | Comparison of Mws and biomass in *B. licheniformis* under different signal peptides. The data are presented as the mean ± SD of three replications. Different lowercase letters indicate significant differences among strains at 0.05 level ($p < 0.05$).

Modification of γ-PGA Molecular Weight by Regulating *pgdS* Transcriptional Level

According to the above results, the Mws of γ-PGAs could be tuned by PgdS secretion. We then evaluated the effect of the transcriptional levels of *pgdS* on Mws by using promoters with different strength. Four promoters P43, PpgdS, PbacA, and PbprA were applied to drive the transcription of *pgdS*. The four recombinant vectors harboring the signal peptide BprA were constructed and transformed into the WX-02Δ*pgdS*, generated four recombinant strains SP13, SP23, SP33, and SP43, respectively (**Table 1**).

To examine the expression efficiency of the four promoters, the transcriptional levels of *pgdS* driven by these promoters were determined by real-time PCR. The results showed that the transcription levels from P43, PpgdS, and PbacA were increased in different degrees compared with the PbprA, and P43 exhibited the highest transcription level ($p < 0.05$) (**Figure 3A**). The expression strength of different promoters was also determined by SDS-PAGE assay (**Supplementary Figure S3**), and the concentrations of PgdS were quantified (**Table 2**), the results confirmed that the expression strength of these four promoters was in a descending order of P43 > PpgdS > PbacA > PbprA.

After 36 h cultivation, we measured the Mws and yields of γ-PGA produced by these recombinant strains. The Mws of the polymer produced by SP13, SP23, SP33, and SP43 were $(7.78 \pm 0.23) \times 10^5$, $(9.55 \pm 0.46) \times 10^5$, $(14.41 \pm 0.67) \times 10^5$, and $(17.80 \pm 0.87) \times 10^5$ Da, respectively (**Figure 3B**), which decreased by 61.02, 52.15, 27.81, and 10.82%, respectively, compared to the control strain SP01 (19.96×10^5 Da). However, the cell growth of these four recombinant strains were approximately the same as that of SP01. Collectively, our results showed that an apparent reduction of Mws along with the enhanced promoter strength.

Varying Levels of PgdS Expression Enable Controlling the Molecular Weights of γ-PGAs

In order to further boost the performance, the promoter and signal peptide were combined to regulate PgdS expression. Three promoters [PpgdS(H), PbacA(M) and PbprA(L)] and signal peptides [SPsacB(H), SPpgdS(M), SPsacC(L)] were selected and combined to form nine expression cassettes (**Figure 1**). Every expression cassette was cloned in pHY300PLK, and the resultant vectors were transformed into WX-02Δ*pgdS*. The transformed strains were designated as *B. licheniformis* SP21, SP25, SP28, SP31, SP35, SP38, SP41, SP45, and SP48, respectively.

As shown in **Table 2**, the activities of PgdS in strains SP28, SP25, and SP38 (26.12 ± 0.45, 25.26 ± 0.4, and 25.13 ± 0.37 U/mL) were significantly greater among all strains, and SP35 (13.22 ± 0.38 U/mL) and SP48 (7.22 ± 0.33 U/mL) exhibited moderate activity. In contrast, weak enzyme activities were detected in strains SP21, SP31, SP41, and SP45. The results of SDS-PAGE assay (**Supplementary Figures S4, S5**) and the concentrations of PgdS protein of each strains (**Table 2**) were consistent with PgdS activity assay. The Mws of γ-PGA produced by these combinations were measured at 36 h (**Figure 4**). The Mws of γ-PGA mediated by the nine combinations varied greatly from $(7.74 \pm 0.80) \times 10^4$ to $(1.91 \pm 0.08) \times 10^6$ Da. To assess the relationship between PgdS expression and γ-PGA Mws, the Pearson correlation coefficients were calculated (Weaver and Wuensch, 2013). A correlation coefficient of −0.945 indicated a strong inverse relation between extracellular PgdS activity and γ-PGA Mws ($P < 0.01$) (**Supplementary Figure S6A**). Taken together, engineering PgdS expression cassette was an efficient approach to produce γ-PGAs with specific Mws.

Increasing γ-PGA Yield Along With Reduced Molecular Weights

In this study, we achieved the production of low-, medium-, and high-Mw γ-PGA in the same microbial chassis. The effect of PgdS expression levels on γ-PGA yield was further studied (**Table 2**). We found that the γ-PGA yield in recombinant strains was obviously increased compared to the control strain when the Mws of γ-PGA decreased by over 50%. A dispersion diagram was obtained with the PgdS yields and logarithms of γ-PGA molecular weight (**Supplementary Figure S6B**), showing the increasing γ-PGA yield along with the reduction of molecular weights (Pearson correlation coefficient = −0.958). Furthermore, the strain SP18 produced 34.60 g/L γ-PGAs, which increased by 34.89% compared with the control strain (25.65 g/L).

The viscosity of fermentation broth affects the oxygen transfer rate (OTR), which is proportional to the volumetric mass transfer coefficient and substrate utilization. The OTR plays vital roles in the growth of strains and the production of target metabolites (Damiani et al., 2014). We hypothesized that improvement of γ-PGA yield in engineered strains may be due to the higher OTR. To prove this hypothesis, the OTRs of fermentation broths from the *B. licheniformis* SP01 (Mw, 1.99×10^6 Da), SP12 (Mw, 1.02×10^6 Da), SP14 (Mw, 5.06×10^5 Da), and SP18 (Mw, 6.82×10^4 Da) were compared in 1-L fermenter (**Figure 5**).

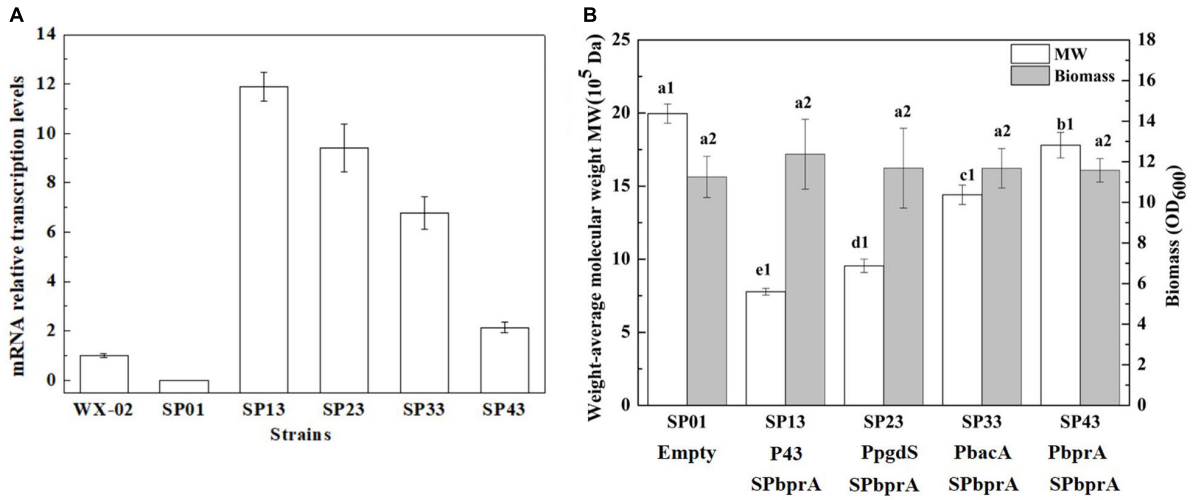

FIGURE 3 | The transcriptional levels of gene *pgdS* among strains with different promoters **(A)**. Data are expressed as mean ± SD of three replications. Comparison of Mws and biomass in *B. licheniformis* under different promoters **(B)**. The data are presented as the mean ± SD of three replications. Different lowercase letters indicate significant differences among strains at 0.05 level ($p < 0.05$).

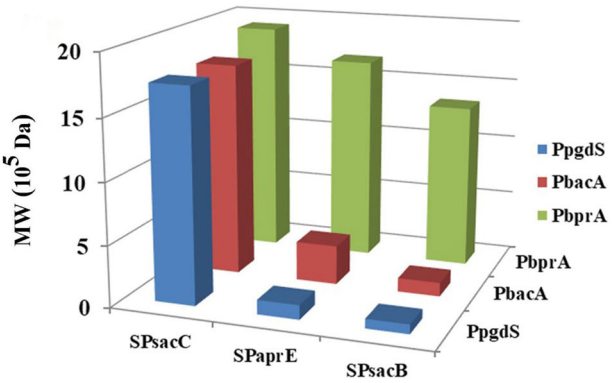

FIGURE 4 | The Mws of γ-PGA in recombinant strains (SP01, SP41, SP45, SP48, SP31, SP35, SP38, SP21, SP25, and SP28). Data are expressed as mean ± SD of three replications, *M*: protein marker.

All recombinant strains showed improved k_La compared to the control strain SP01 throughout the fermentation process. Among them, k_La and DO were consistent with the trend of values negatively correlated with the γ-PGA Mws in these recombinant strains (**Figures 5A,B**). These results confirmed that low viscosity of fermentation broth could improve γ-PGA yield by increasing the oxygen transfer rate.

Large-Scale Fermentation of Recombinant *B. licheniformis* in 3-L Fermenter

Based on the above results, an efficient system for one-step synthesis of γ-PGA with a wide range of Mws (6.82×10^4–1.99×10^6 Da) was developed by regulating PgdS expression. Therefore, in order to further explored the applicability of this system in large-scale γ-PGA production, the engineered strains SP01, SP12, SP14, and SP18 were carried out in a 3-L bioreactor, respectively (**Figure 6**). Compared to the control strain SP01, the DO values in cultures of SP12, SP14, and SP18 were maintained at higher levels, resulting in higher cell growth rates and biomass (**Figure 6**). The highest yield of γ-PGAs produced by the SP01 was 29.00 g/L at 30 h (**Figure 5A**). In contrast, the maximal γ-PGA yields in strains SP12, SP14, and SP18 reached 33.05, 35.91, and 39.13 g/L, respectively, increasing by 12.25, 23.83, and 34.93% (**Figures 5B–D**), and the Mws of γ-PGAs in corresponding strains were 1.42×10^6, 5.56×10^5, and 7.83×10^4 Da, respectively. Therefore, our results demonstrated that it was feasible and efficient to produce specific γ-PGAs using glutamate-free medium by the controllable expression of PgdS.

DISCUSSION

Since γ-PGAs with different Mws show specific applications, the Mws must be precisely controlled. γ-PGAs produced by a single strain was often difficult to meet the requirements of molecular weight differentiation (**Supplementary Table S4**). In this work, we aimed to develop a convenient system for one-step production of regulated-molecular-weight γ-PGAs through the controlled expression of PgdS depolymerase by manipulating the promoters and signal peptides independently and in combination.

Currently, many endo-type γ-PGA hydrolases (PgdS) has been characterized from various strains (Suzuki and Tahara, 2003; Tian et al., 2014) and used as a target to improve the yields of γ-PGAs (Scoffone et al., 2013; Sha et al., 2018). It has been proved that PgdS degraded γ-PGA in the extracellular region (Yao et al., 2009). The optimization of signal peptides is an efficient method to increase the secretion of desirable proteins (Zhang et al., 2016). According to Cai et al., 81

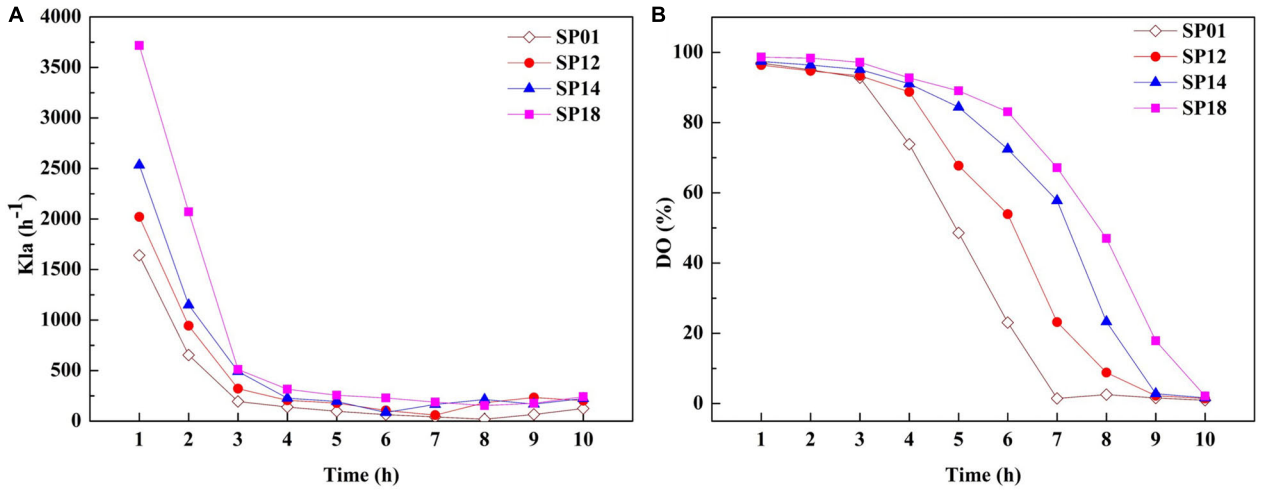

FIGURE 5 | Comparison of k_La **(A)** and dissolved oxygen (DO) **(B)** between control strain SP01 and recombinant strains in a 1-L fermenter. Time courses of recombinant strains SP01, SP12, SP14, and SP18 in batch culture. The k_La and DO were measured and calculated at regular intervals.

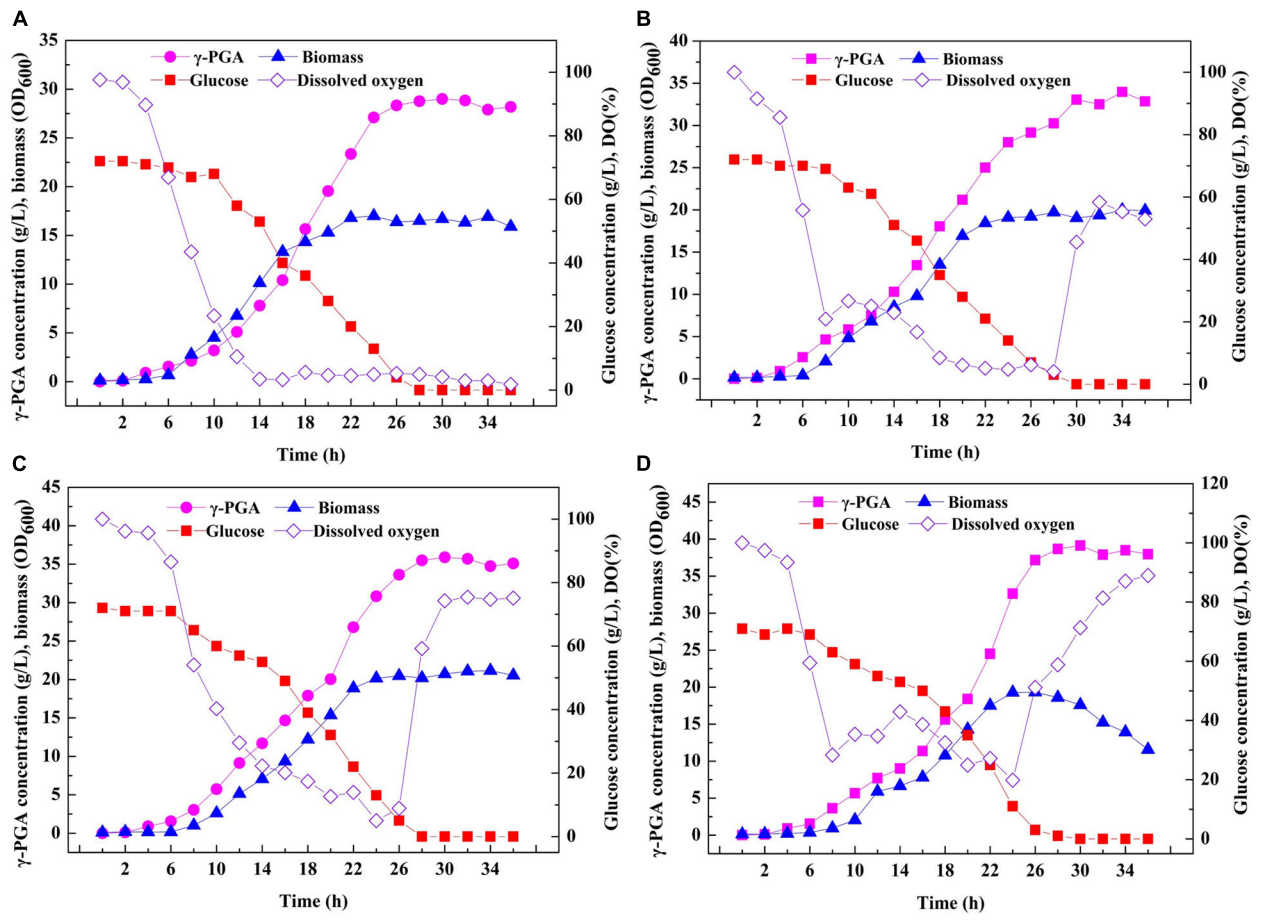

FIGURE 6 | Large-scale fermentation of recombinant *B. licheniformis* strains in 3-L fermenter. Time courses of recombinant strains SP01 **(A)**, SP12 **(B)**, SP14 **(C)**, and SP18 **(D)** in batch culture. γ-PGA concentration, biomass (OD_{600}), glucose concentration and DO were measured and calculated at regular intervals.

signal peptides were identified in *B. licheniformis* WX-02 by the SignalP tool[1] (Cai et al., 2016). The effects of all signal peptides on the secretion of nattokinase from *B. subtilis* MBS 04-6 were investigated, and the strains with different signal peptides showed different activities ranging from 0 to 31.99 FU/mL (Cai et al., 2016). In this study, we investigated the effects of eight proteases signal peptides (SacC, Vpr, BprA, GGT, AprE, PgdS, YvpA, and SacB) on PgdS secretion and γ-PGA Mws. Our results showed that higher γ-PGA degradation capability was achieved with the increased PgdS secretion, which was consistent with the previous reports (Yuan et al., 2015; Jin et al., 2016). Besides, the optimal signal peptides varied for different proteins (Degering et al., 2010). In this study, the maximum activity of PgdS being obtained under the signal peptide of SPsacB in *B. licheniformis* among the selected signal peptides (**Table 2**), which is different with the optimal signal peptide (SPaprE) for nattokinase secretion (Cai et al., 2016).

The promoter is another critical element for controlling the protein expression (Wang et al., 2014). There are many classes of promoters that could be employed to dynamically regulate the expression of protein, such as inducible promoters, constitutive promoters of different strengths, condition-responsive promoters, and growth phase responsive promoters (Fontana et al., 2018; Maury et al., 2018; Tekel et al., 2019). In this work, we explore the effects of *pgdS* transcriptional levels on γ-PGA Mws using promoters with different strengths (P43, PbacA, PbprA, and PpgdS). P43 is considered as a strong promoter for protein expression (Zhang et al., 2007). PpgdS is the native promoter of PgdS depolymerase and regulated by sigma D factor from *B. licheniformis* (Mitsunaga et al., 2016). PbacA is the promoter of *bacABC* operon involved in bacitracin synthesis from *B. licheniformis* DW2 (Shu et al., 2018). PbprA, the promoter of bacillopeptidase F (BprA), is a weak promoter according to our transcriptome data (data not shown) and used as a control. Among the four promoters, P43 promoter is the most effective one to drive the expression of *pgdS*.

In order to further evaluate the effect of regulated PgdS expression on the Mws of γ-PGAs, we explored various levels of PgdS expression by combining promoters and signal peptides. Through this strategy, the combined strains provided γ-PGA with a wide range of Mws [$(7.74 \pm 0.80) \times 10^4$–$(1.91 \pm 0.08) \times 10^6$ Da]. Based on these results, regulating PgdS expression was an efficient and simple method to obtain γ-PGAs with specific Mws. Compared to other methods, we could achieve broader range of Mws of γ-PGAs, which is beneficial to broaden the industrial application of γ-PGAs. Previous studies have mainly focused on increasing the production of high-Mw γ-PGAs (Birrer et al., 1994; Scoffone et al., 2013), limiting the applications of γ-PGAs in other fields. However, one limitation of this study is that the determination of the correlations between the PgdS expression and γ-PGA Mws is based on small dataset (n = 9). We will achieve precise control of Mws via the titratable regulation of PgdS expression using the further development of tools.

Specially, all recombinant strains containing *pgdS* gene produced higher γ-PGA yields compared with the control strain SP01, which confirmed that overexpression of PgdS is an efficient approach to enhance γ-PGA production. Due to the high viscosity of high-Mw γ-PGAs, it severely decreases oxygen transfer in the fermentation process, resulting in inhibition of cell growth and limit of γ-PGA production (Su et al., 2010). In this paper, the k_La and DO of fermentation broths in recombinant strains were improved compared to the control strain SP01 with high-Mw γ-PGA. One possible explanation for the increased DO was that the reduced Mws decreased the viscosity of the fermentation broth, enabling higher oxygen transfer rate, further improving cell growth, substrate utilization and γ-PGA yields.

Ultimately, we investigated the applicability of the system in the large-scale production of specific-molecular-weight γ-PGAs. Our results indicated that the γ-PGA could be efficiently produced on a high level (29.00–39.13 g/L) without additional glutamic acid using the recombinant strains in 3-L fermenter. The results from this work and related studies were summarized in **Table 3**. In particular, the highest yield of γ-PGA (39.13 g/L) with molecular-weight value of 7.83×10^4 Da was obtained in SP18 strain, which was 34.93% higher than that of control strain SP01, and the yield was higher than those produced by most γ-PGA producers (**Table 3**). Moreover, the γ-PGA productivity was 1.30 g/L/h, which was the highest from glutamate-free medium to date. One possible explanation for the increased DO was that the reduced Mws decreased the viscosity of the fermentation broth, enabling higher oxygen transfer rate, further improving cell growth, substrate utilization and γ-PGA yields.

[1]http://www.cbs.dtu.dk/services/SignalP/

TABLE 3 | Comparison of γ-PGA production from glutamic acid independent stains.

Strains	Key nutrients (g/L)	Yield g/g	Titer (g/L)	Productivity (g/L/h)	References
B. subtilis C1	Glycerol, citric acid, NH_4Cl	144	21.4	0.15	Shih et al., 2005
B. licheniformis A13	Glucose, NH_4Cl, yeast extract	72	28.2	0.39	Mabrouk et al., 2012
B. subtilis C10	Glucose, NH_4Cl	32	27.7	0.87	Zhang et al., 2012
B. licheniformis TISTR 1010	Glucose, citric acid, NH_4Cl	77	27.5	0.29	Kongklom et al., 2015
B. licheniformis TISTR 1010	Glucose, citric acid, NH_4Cl	43	39.9	0.93	Kongklom et al., 2017
B. amyloliquefaciens NB (pNX01-*pgdS*1)	Raw inulin extract, glutamate, $(NH_4)_2SO_4$	72	17.62		Sha et al., 2018
B. licheniformis BC4	Glycerol, sodium citrate, $NaNO_3$, NH_4Cl	48	19.20	0.40	Zhan et al., 2018
B. licheniformis SP18	Glucose, sodium citrate, $NaNO_3$, NH_4Cl	30	39.13	1.30	This study

Collectively, it is more applicable to industrially produce specific-molecular-weight γ-PGAs using our strategies than previously reported studies.

In conclusion, we developed an efficient system for one-step production of specific Mws γ-PGA through regulating the PgdS expression in *B. licheniformis* for the first time. The ability to produce γ-PGA with low, medium, and high Mws ranging between 6.82×10^4 Da and 1.99×10^6 Da was demonstrated by manipulating the promoter and signal peptide independently and in combination. The maximum production of γ-PGA (Mw, 7.83×10^4 Da) reached 39.13 g/L from glutamate-free medium in batch fermentation. Our study presented a potential method for commercial production of specific-molecular-weight γ-PGA, and this strategy could also be used to produce other biopolymers by precisely controlling corresponding depolymerase expression.

DATA AVAILABILITY STATEMENT

All datasets generated for this study are included in the article/**Supplementary Material**.

AUTHOR CONTRIBUTIONS

SC and FS designed and supervised the study. HW, DW, YX, JD, and JC performed the experiments. DW and HW analyzed the data and wrote the manuscript. YZ, QW, DC, SC, and FS revised the manuscript. All authors read and approved the final manuscript.

FUNDING

This work was supported by the National Natural Science Foundation of China (No. 31972849), the National Key Research and Development Program of China (2018YFA090039), and the Technical Innovation Special Fund of Hubei Province (No. 2018ACA149).

SUPPLEMENTARY MATERIAL

The Supplementary Material for this article can be found online at: https://www.frontiersin.org/articles/10.3389/fbioe.2020.00728/full#supplementary-material

REFERENCES

Ashiuchi, M., Nakamura, H., Yamamoto, M., and Misono, H. (2006). Novel poly -γ-glutamate-processing enzyme catalyzing γ-glutamyl DD-amidohydrolysis. *J. Biosci. Bioeng.* 102, 60–65. doi: 10.1263/jbb.102.60

Birrer, G. A., Cromwick, A. M., and Gross, R. A. (1994). Gamma-poly(glutamic acid) formation by *Bacillus licheniformis* 9945a: physiological and biochemical studies. *Int. J. Biol. Macromol.* 16, 265–275. doi: 10.1016/0141-8130(94)90032-9

Cai, D., Chen, Y., He, P., Wang, S., Mo, F., Li, X., et al. (2018). Enhanced production of poly−γ−glutamic acid by improving ATP supply in metabolically engineered *Bacillus licheniformis*. *Biotechnol. Bioeng.* 115, 2541–2553. doi: 10.1002/bit.26774

Cai, D., Wei, X., Qiu, Y., Chen, Y., Chen, J., Wen, Z., et al. (2016). High-level expression of nattokinase in *Bacillus licheniformis* by manipulating signal peptide and signal peptidase. *J. Appl. Microbiol.* 121, 704–712. doi: 10.1111/jam.13175

Cao, M., Feng, J., Sirisansaneeyakul, S., Song, C., and Chisti, Y. (2018). Genetic and metabolic engineering for microbial production of poly-gamma-glutamic acid. *Biotechnol. Adv.* 36, 1424–1433. doi: 10.1016/j.biotechadv.2018.05.006

Damiani, A. L., Kim, M. H., and Wang, J. (2014). An improved dynamic method to measure kLa in bioreactors. *Biotechnol. Bioeng.* 111, 2120–2125. doi: 10.1002/bit.25258

Degering, C., Eggert, T., Puls, M., Bongaerts, J., Evers, S., Maurer, K. H., et al. (2010). Optimization of protease secretion in *Bacillus subtilis* and *Bacillus licheniformis* by screening of homologous and heterologous signal peptides. *Appl. Environ. Microbiol.* 76, 6370–6376. doi: 10.1128/AEM.01146-10

Feng, J., Shi, Q., Zhou, G., Wang, L., Chen, A., Xie, X., et al. (2017). Improved production of poly-γ-glutamic acid with low molecular weight under high ferric ion concentration stress in *Bacillus licheniformis* ATCC 9945a. *Process. Biochem.* 56, 30–36. doi: 10.1016/j.procbio.2017.02.017

Fontana, J., Dong, C., Ham, J. Y., Zalatan, J. G., and Carothers, J. M. (2018). Regulated expression of sgRNAs tunes CRISPRi in *E. coli*. *Biotechnol. J.* 13:e1800069. doi: 10.1002/biot.201800069

Gallagher, S. R. (2014). Digital image processing and analysis with ImageJ. *Curr Protoc. Essent Lab. Techni.* 3, 36–42. doi: 10.1002/9780470089941.eta03cs9

Halmschlag, B., Steurer, X., Putri, S. P., Fukusaki, E., and Blank, L. M. (2019). Tailor-made poly-γ-glutamic acid production. *Metab. Eng.* 55, 239–248. doi: 10.1016/j.ymben.2019.07.009

Hammond, J. B. W., and Kruger, N. J. (1988). The Bradford method for protein quantitation. *Methods Mol. Biol.* 3, 25–32. doi: 10.1385/0-89603-126-8:25

Inbaraj, B. S., Chiu, C. P., Ho, G. H., Yang, J., and Chen, B. H. (2006). Removal of cationic dyes from aqueous solution using an anionic poly-gamma-glutamic acid-based adsorbent. *J. Hazard. Mater.* 137, 226–234. doi: 10.1016/j.jhazmat.2006.01.057

Jin, P., Kang, Z., Yuan, P., Du, G., and Chen, J. (2016). Production of specific-molecular-weight hyaluronan by metabolically engineered *Bacillus subtilis* 168. *Metab. Eng.* 35, 21–30. doi: 10.1016/j.ymben.2016.01.008

Kongklom, N., Luo, H., Shi, Z., Pechyen, C., Chisti, Y., and Sirisansaneeyakul, S. (2015). Production of poly-γ-glutamic acid by glutamic acid-independent *Bacillus licheniformis* TISTR 1010 using different feeding strategies. *Biochem. Eng. J.* 100, 67–75. doi: 10.1016/j.bej.2015.04.007

Kongklom, N., Shi, Z., Chisti, Y., and Sirisansaneeyakul, S. (2017). Enhanced production of Poly-gamma-glutamic Acid by *Bacillus licheniformis* TISTR 1010 with environmental controls. *Appl. Biochem. Biotechno.l* 182, 990–999. doi: 10.1007/s12010-016-2376-1

Kubota, H., Nambu, Y., and Endo, T. (1996). Alkaline hydrolysis of poly (γ−glutamic acid) produced by microorganism. *J. Polym. Sci. Pol. Chem.* 34, 1347–1351. doi: 10.1002/(SICI)1099-0518(199605)34:7<1347::AID-POLA24<3.0.CO;2-8

Mabrouk, M., Abou-Zeid, D., and Sabra, W. (2012). Application of Plackett–Burman experimental design to evaluate nutritional requirements for poly (γ-glutamic acid) production in batch fermentation by *Bacillus licheniformis* A13. *Afr. J. Appl. Microbiol. Res* 1, 6–18.

Maury, J., Kannan, S., Jensen, N. B., Oberg, F. K., Kildegaard, K. R., Forster, J., et al. (2018). Glucose-dependent promoters for dynamic regulation of metabolic pathways. *Front. Bioeng. Biotechnol.* 6:63. doi: 10.3389/fbioe.2018.00063

Mitsunaga, H., Meissner, L., Buchs, J., and Fukusaki, E. (2016). Branched chain amino acids maintain the molecular weight of poly(gamma-glutamic acid) of *Bacillus licheniformis* ATCC 9945 during the fermentation. *J. Biosci. Bioeng.* 122, 400–405. doi: 10.1016/j.jbiosc.2016.03.007

Ogunleye, A., Bhat, A., Irorere, V. U., Hill, D., Williams, C., and Radecka, I. (2015). Poly-gamma-glutamic acid: production, properties and applications. *Microbiology.* 161(Pt 1), 1–17. doi: 10.1099/mic.0.081448-0

Pérez−Camero, G., Congregado, F., Bou, J. J., and Muñoz−Guerra, S. (1999). Biosynthesis and ultrasonic degradation of bacterial poly (γ−glutamic acid). *Biotechnol. Bioeng.* 63, 110–115. doi: 10.1002/(sici)1097-0290(19990405)63:1<110::aid-bit11>3.0.co;2-t

Qiu, Y., Xiao, F., Wei, X., Wen, Z., and Chen, S. (2014). Improvement of lichenysin production in *Bacillus licheniformis* by replacement of native promoter of lichenysin biosynthesis operon and medium optimization. *Appl. Microbiol. Biotechnol.* 98, 8895–8903. doi: 10.1007/s00253-014-5978-y

Rocha, J., Santos, S., and Pacheco, G. (2015). Bacterial reference genes for gene expression studies by RT-qPCR: survey and analysis. *Anton Van Leeuw.* 108, 685–693. doi: 10.1007/s10482-015-0524-1

Scoffone, V., Dondi, D., Biino, G., Borghese, G., Pasini, D., Galizzi, A., et al. (2013). Knockout of *pgdS* and *ggt* genes improves gamma-PGA yield in *B. subtilis*. *Biotechnol. Bioeng.* 110, 2006–2012. doi: 10.1002/bit.24846

Sha, Y., Zhang, Y., Qiu, Y., Xu, Z., Li, S., Feng, X., et al. (2018). Efficient biosynthesis of low-molecular-weight poly-gamma-glutamic acid by stable overexpression of PgdS hydrolase in *Bacillus amyloliquefaciens* NB. *J Agric. Food. Chem.* 67, 282–290. doi: 10.1021/acs.jafc.8b05485

Shi, J., Zhan, Y., Zhou, M., He, M., Wang, Q., Li, X., et al. (2019). High-level production of short branched-chain fatty acids from waste materials by genetically modified *Bacillus licheniformis*. *Bioresour. Technol.* 271, 325–331. doi: 10.1016/j.biortech.2018.08.134

Shih, L., Wu, P. J., and Shieh, C. J. (2005). Microbial production of a poly (γ-glutamic acid) derivative by *Bacillus subtilis*. *Process. Biochem.* 40, 2827–2832. doi: 10.1016/j.procbio.2004.12.009

Shu, C., Wang, D., Guo, J., Song, J., Chen, S., Chen, L., et al. (2018). Analyzing AbrB-knockout effects through genome and transcriptome sequencing of *Bacillus licheniformis* DW2. *Front. Microbiol.* 9:307. doi: 10.3389/fmicb.2018.00307

Shu, X., Shi, Q., Feng, J., Xie, X., and Chen, Y. (2014). Design and in vitro evaluation of novel γ-PGA/hydroxyapatite nanocomposites for bone tissue engineering. *J. Mater. Sci.* 49, 7742–7749. doi: 10.1007/s10853-014-8484-9

Sirisansaneeyakul, S., Cao, M., Kongklom, N., Chuensangjun, C., Shi, Z., and Chisti, Y. (2017). Microbial production of poly-gamma-glutamic acid. *World. J. Microbiol. Biotechnol.* 33:173. doi: 10.1007/s11274-017-2338-y

Su, Y., Li, X., Liu, Q., Hou, Z., Zhu, X., Guo, X., et al. (2010). Improved poly-γ-glutamic acid production by chromosomal integration of the *Vitreoscilla* hemoglobin gene (*vgb*) in *Bacillus subtilis*. *Bioresour. Technol.* 101, 4733–4736. doi: 10.1016/j.biortech.2010.01.128

Suzuki, T., and Tahara, Y. (2003). Characterization of the *Bacillus subtilis ywtD* gene, whose product is involved in gamma-polyglutamic acid degradation. *J. Bacteriol.* 185, 2379–2382. doi: 10.1128/JB.185.7.2379-2382.2003

Tekel, S. J., Smith, C. L., Lopez, B., Mani, A., Connot, C., Livingstone, X., et al. (2019). Engineered orthogonal quorum sensing systems for synthetic gene regulation in *Escherichia coli*. *Front. Bioeng. Biotechnol.* 7:80. doi: 10.3389/fbioe.2019.00080

Tian, G., Fu, J., Wei, X., Ji, Z., Ma, X., Qi, G., et al. (2014). Enhanced expression of *pgdS* gene for high production of poly−γ−glutamic aicd with lower molecular weight in *Bacillus licheniformis* WX−02. *J. Chem. Technol. Biotechnol.* 89, 1825–1832. doi: 10.1002/jctb.4261

Wang, Y., Liu, Y., Wang, Z., and Lu, F. (2014). Influence of promoter and signal peptide on the expression of pullulanase in *Bacillus subtilis*. *Biotechnol. Lett.* 36, 1783–1789. doi: 10.1007/s10529-014-1538-x

Weaver, B., and Wuensch, K. L. (2013). SPSS and SAS programs for comparing Pearson correlations and OLS regression coefficients. *Behav. Res. Methods.* 45, 880–895. doi: 10.3758/s13428-012-0289-7

Wei, X., Ji, Z., and Chen, S. (2010). Isolation of halotolerant *Bacillus licheniformis* WX-02 and regulatory effects of sodium chloride on yield and molecular sizes of poly-gamma-glutamic acid. *Appl. Biochem. Biotechnol.* 160, 1332–1340. doi: 10.1007/s12010-009-8681-1

Xu, G., Zha, J., Cheng, H., Ibrahim, M. H. A., Yang, F., Dalton, H., et al. (2019). Engineering *Corynebacterium glutamicum* for the de novo biosynthesis of tailored poly-gamma-glutamic acid. *Metab. Eng.* 56, 39–49. doi: 10.1016/j.ymben.2019.08.011

Yao, J., Jing, J., Xu, H., Liang, J., Wu, Q., Feng, X., et al. (2009). Investigation on enzymatic degradation of γ-polyglutamic acid from *Bacillus subtilis* NX-2. *J. Mol. Catal. B Enzym.* 56, 158–164. doi: 10.1016/j.molcatb.2007.12.027

Yokoi, H., Arima, T., Hirose, J., Hayashi, S., and Takasaki, Y. (1996). Flocculation properties of poly (γ-glutamic acid) produced by *Bacillus subtilis*. *J. Ferment. Bioeng.* 82, 84–87. doi: 10.1016/0922-338X(96)89461-X

Yuan, P., Lv, M., Jin, P., Wang, M., Du, G., Chen, J., et al. (2015). Enzymatic production of specifically distributed hyaluronan oligosaccharides. *Carbohydr. Polym.* 129, 194–200. doi: 10.1016/j.carbpol.2015.04.068

Zeng, W., Liang, Z., Li, Z., Bian, Y., Li, Z., Tang, Z., et al. (2016). Regulation of poly-γ-glutamic acid production in *Bacillus subtilis* GXA-28 by potassium. *J. Taiwan. Inst. Chem. E.* 61, 83–89. doi: 10.1016/j.jtice.2015.12.026

Zhan, Y., Sheng, B., Wang, H., Shi, J., Cai, D., Yi, L., et al. (2018). Rewiring glycerol metabolism for enhanced production of poly-γ-glutamic acid in *Bacillus licheniformis*. *Biotechnol. Biofuels.* 11:306. doi: 10.1186/s13068-018-1311-9

Zhang, A. L., Liu, H., Yang, M. M., Gong, Y. S., and Chen, H. (2007). Assay and characterization of a strong promoter element from *B. subtilis*. *Biochem. Biophys. Res. Commun.* 354, 90–95. doi: 10.1016/j.bbrc.2006.12.137

Zhang, H., Zhu, J., Zhu, X., Cai, J., Zhang, A., Hong, Y., et al. (2012). High-level exogenous glutamic acid-independent production of poly-(γ-glutamic acid) with organic acid addition in a new isolated *Bacillus subtilis* C10. *Bioresour. Technol.* 116, 241–246. doi: 10.1016/j.biortech.2011.11.085

Zhang, W., Yang, M., Yang, Y., Zhan, J., Zhou, Y., and Zhao, X. (2016). Optimal secretion of alkali-tolerant xylanase in *Bacillus subtilis* by signal peptide screening. *Appl. Microbiol. Biotechnol.* 100, 8745–8756. doi: 10.1007/s00253-016-7615-4

Conflict of Interest: The authors declare that the research was conducted in the absence of any commercial or financial relationships that could be construed as a potential conflict of interest.

frontiers in Bioengineering and Biotechnology

ORIGINAL RESEARCH
published: 27 August 2020
doi: 10.3389/fbioe.2020.517336

Enhancing the Glucose Flux of an Engineered EP-Bifido Pathway for High Poly(Hydroxybutyrate) Yield Production

*Ying Li[1†], Zhijie Sun[2†], Ya Xu[1], Yaqi Luan[1], Jiasheng Xu[1], Quanfeng Liang[1], Qingsheng Qi[1,3] and Qian Wang[1]**

[1] National Glycoengineering Research Center, State Key Laboratory of Microbial Technology, Shandong University, Qingdao, China, [2] Marine Biology Institute, Shantou University, Shantou, China, [3] CAS Key Lab of Biobased Materials, Qingdao Institute of Bioenergy and Bioprocess Technology, Chinese Academy of Sciences, Qingdao, China

OPEN ACCESS

Edited by:
Bernd Rehm,
Griffith University, Australia

Reviewed by:
Takeharu Tsuge,
Tokyo Institute of Technology, Japan
Christopher John Brigham,
Wentworth Institute of Technology, United States
Ignacio Poblete-Castro,
Andres Bello University, Chile

***Correspondence:**
Qian Wang
qiqi20011983@gmail.com

† These authors have contributed equally to this work

Specialty section:
This article was submitted to Industrial Biotechnology, a section of the journal Frontiers in Bioengineering and Biotechnology

Received: 04 December 2019
Accepted: 12 August 2020
Published: 27 August 2020

Citation:
Li Y, Sun Z, Xu Y, Luan Y, Xu J, Liang Q, Qi Q and Wang Q (2020) Enhancing the Glucose Flux of an Engineered EP-Bifido Pathway for High Poly(Hydroxybutyrate) Yield Production. Front. Bioeng. Biotechnol. 8:517336. doi: 10.3389/fbioe.2020.517336

Background: As the greenhouse effect becomes more serious and carbon dioxide emissions continue rise, the application prospects of carbon sequestration or carbon-saving pathways increase. Previously, we constructed an EP-bifido pathway in *Escherichia coli* by combining Embden-Meyerhof-Parnas pathway, pentose phosphate pathway and "bifid shunt" for high acetyl-CoA production. There is much room for improvement in the EP-bifido pathway, including in production of target compounds such as poly(hydroxybutyrate) (PHB).

Result: To optimize the EP-bifido pathway and obtain higher PHB yields, we knocked out the specific phosphoenolpyruvate phosphate transferase system (PTS) component II Cglc, encoded by *ptsG*. This severely inhibited the growth and sugar consumption of the bacterial cells. Subsequently, we used multiple automated genome engineering (MAGE) to optimize the ribosome binding site (RBS) sequences of *galP* (galactose: H (+) symporter) and *glk* (glucokinase gene bank: NC_017262.1), encoding galactose permease and glucokinase, respectively. Growth and glucose uptake were partially restored in the bacteria. Finally, we introduced the glf (UDP-galactopyranose) from *Zymomonas mobilis* mutase sugar transport vector into the host strain genome.

Conclusion: After optimizing RBS of *galP*, the resulting strain L-6 obtained a PHB yield of 71.9% (mol/mol) and a 76 wt% PHB content using glucose as the carbon source. Then when *glf* was integrated into the genome strain L-6, the resulting strain M-6 reached a 5.81 g/L PHB titer and 85.1 wt% PHB content.

Keywords: poly(hydroxybutyrate) yield, glucose flux, EP-bifido pathway, MAGE, *Escherichia coli*

INTRODUCTION

In 2018, global carbon dioxide emissions increased 1.7% over the previous year, hitting a record high of 33.143 billion tons. Accelerating the adoption of renewable energy and improving energy efficiency in response to global warming are urgent priorities (International Energy Agency, 2019). Bio-manufacturing, which uses food crops as raw materials, has wide application prospects.

Through biological manufacturing, biomass resources can be converted to ethanol, polylactic acid, 1, 3-propanediol, and other bulk chemicals (Ragauskas et al., 2006; Lee et al., 2012). A key barrier to this process is the CO_2 emissions that occur during natural aerobic fermentation. Many carbon dioxide fixation pathways have been exploited using the six carbon fixation pathways discovered in nature (Gong et al., 2016). However, complex reaction steps and enzyme requirements limit the broad application of these carbon sequestration pathways (Erb et al., 2007; Schwander et al., 2016).

In natural microorganism fermentation, glucose can be transformed through the Embden-Meyerhof-Parnas (EMP) pathway to pyruvate. Pyruvate metabolism leads to the production of two molecules of acetyl-CoA (AcCoA), the key precursor of ethanol, butanol, fatty acids, amino acids, and pharmaceuticals. This process produces two molecules of CO_2 from one mol of glucose, making it an uneconomical way to biosynthesize products using AcCoA as precursor. Other glycol metabolism pathways, such as the phosphoketolase pathway, employ a pentose phosphate specific transketolase to produce a mixture of ethanol, lactic acid, and CO_2. Additionally, the bifido bacteria exclusive bifid shunt pathway can generate 1 mol of lactic acid and 1.5 mol of acetate from 1 mol of glucose (Meile et al., 2001; Posthuma et al., 2002). However, all of these glucose metabolic pathways lose carbon in the form of CO_2 during the decarboxylation process. Therefore, several carbon-saving pathways, including the non-oxidative glycolytic (NOG) and EP-bifido pathways, have been engineered. The NOG pathway can transform all six carbon atoms of glucose into three AcCoA molecules without CO_2 loss (Bogorad et al., 2013). However, it cannot provide the reducing power NADPH that is needed for PHB and other chemicals biosynthesis. The EP-bifido pathway employs EMP, pentose phosphate pathway (PPP) and the Bifido shunt for high-yield of AcCoA generation. As a reducing power sponsor, the oxidation part of the PPP consumes 1 mol of glucose, and provides 2 mol of NADPH and 1mol of xylulose-5-phosphate (X5P). The enzyme encoded by the *f/xpk* gene of the EP-bifido pathway has both fructose-6-phosphate (F6P) and X5P activity. It is able to catalyze X5P to form acetyl phosphate (AcP) and glyceraldehyde 3-phosphate (G3P) or split F6P to form erythrose 4-phosphate and AcP. The former G3P can generate AcP through carbon rearrangement, each of these processes releases only 1 mol of CO_2, thus saving the carbon source to a certain extent (**Figure 1**). This carbon-saving pathway has been applied to the production of several compounds that use AcCoA as the precursor (Wang et al., 2019). Previously, we achieved a relatively high level of production and yield, but there remains room to improve carbon conversion in our system.

In *Escherichia coli*, glucose is transported through the phosphate transferase system (PTS). This system is involved in phosphoenolpyruvate (PEP)-dependent sugar transport and its activity has an important impact on carbon flux redistribution in the PEP and pyruvate nodes (Gosset, 2005). Glucose was phosphorylated to G6P by the phosphoryl generated from PEP, which was dephosphorylated to form pyruvate. Then pyruvate further decarboxylated to AcCoA and released 1 mol of CO_2, leading to the loss of the carbon source. In addition, PEP is a key intermediate metabolite of the EMP pathway. Therefore, an increase in the EMP pathway reduces the carbon conversion efficiency of the EP-bifido pathway.

Poly(hydroxybutyrate) (PHB) is the most common poly(hydroxyalkanoate) (PHA). PHB can be synthesized and accumulated by more than 300 microorganisms as both an energy and carbon store (Lee and Choi, 2001; van der Walle et al., 2001). The *in vivo* biosynthesis of PHB requires three steps using AcCoA as the precursor, and PHB production has been intensively studied (Lee et al., 1994; Wang Q. et al., 2009). Many strategies have been applied to engineer *E. coli* to improve PHB production, however, the yield still has much room to progress. By overexpressing NAD kinase, recombinant *E. coli* produced 14 g/L PHB and the yield based on glucose reached 0.31 mol/mol (0.15 g PHB/g glucose) (Li et al., 2009). By applying fed-batch strategy, *E. coli* could accumulate 125 g/L PHB, but the yield based on glucose was only 0.46 mol/mol (0.22 g PHB/g glucose) (Mozumder et al., 2014). Previously, we have achieved relatively high level of PHB content and PHB yield (68.4 wt% and 63.7% mol/mol, respectively) (Wang et al., 2019). In this study, we optimized the EP-bifido pathway for improved PHB production in *E. coli*. The non-PTS glucose transport pathway genes *glk*, *galP* and heterogeneous *glf* were enhanced and introduced into EP-bifido strains through multiple automated genome engineering (MAGE) and conditional-replication, integration, excision, and retrieval (CRIM) plasmids. The improved PHB production indicates that our modification increased the efficiency of artificial carbon-saving pathways for high carbon conversion rate from glucose.

MATERIALS AND METHODS

Culture Media and Conditions

For plasmid preparation, *E. coli* strains were cultured at 37°C on a rotary shaker (220 rpm) in test. For plasmid preparation, *E. coli* strains were cultured at 37°C on a rotary shaker (220 rpm) in test tubes containing 5 mL Lysogeny broth (LB) medium. For PHB biosynthesis, 50-mL shake flask cultures were started by 2% inoculation from the 5-mL LB culture. The 50-mL cultures contained M9 minimal medium with 0.2% yeast extract containing 20 g/L glucose and shaken at 37°C in a rotary shaker (120 rpm) for 48 h. Overnight cultures were shaken at 37°C in a rotary shaker (220 rpm). Antibiotics were added as follows: ampicillin (Amp) 100 μg/mL, spectinomycin (Spc) 50 μg/mL, and chloromycetin (Cm) 25 μg/mL. For MAGE procedure, strains were cultivated in SOB medium.

Lysogeny broth medium contains (g/L): tryptone (10), yeast extract (5), and NaCl (10). M9 medium contains (g/L): $Na_2HPO_4{\cdot}12H_2O$ (15.138), KH_2PO_4 (3), NaCl (0.5), and NH_4Cl (1). SOB medium contains (g/L): tryptone (20), yeast extract (5), and NaCl (5).

Strains and Plasmids

All *E. coli* strains and plasmids used are listed in **Table 1**. DH-EP was used as the starting strain for further genetic

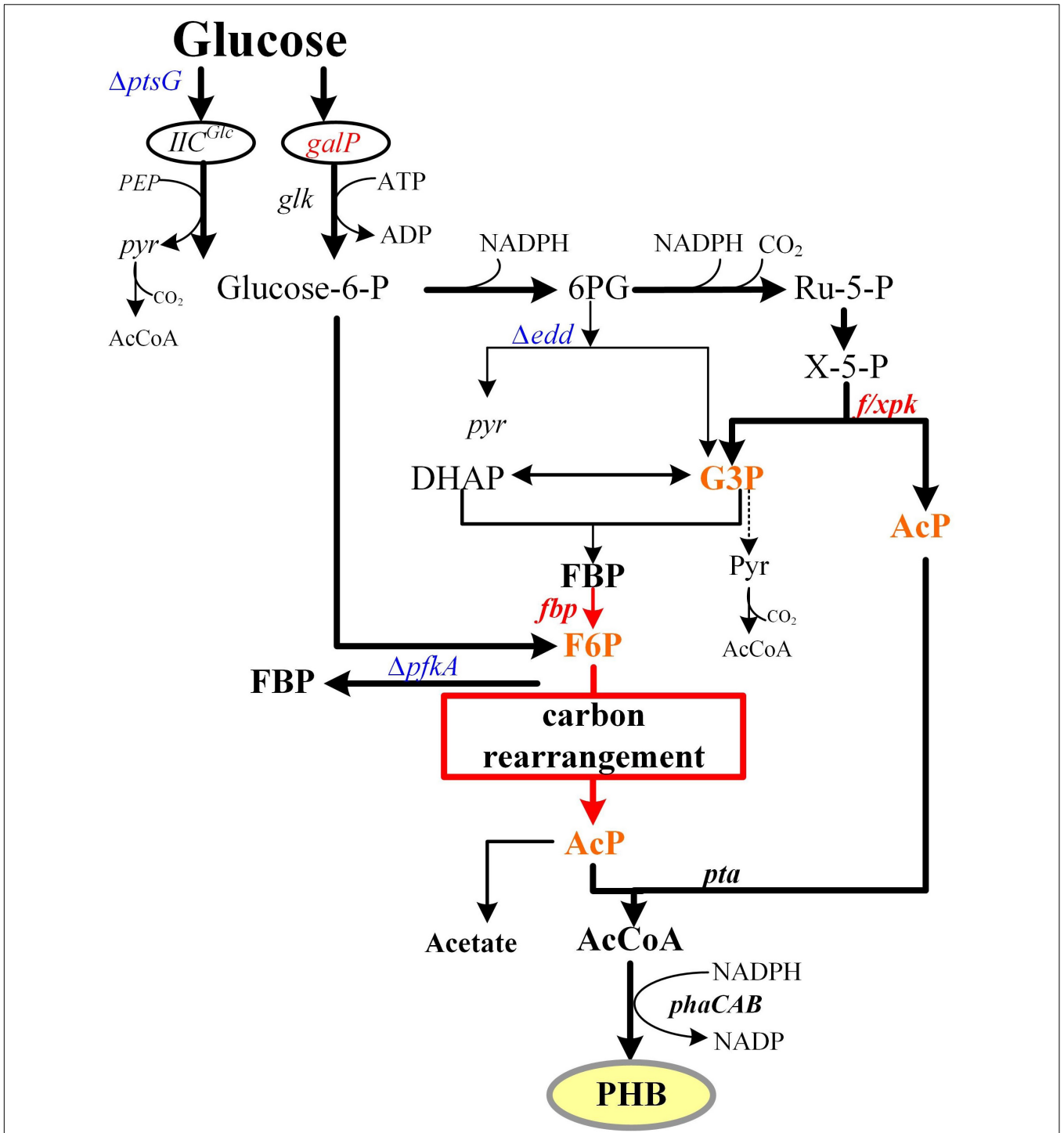

FIGURE 1 | EP-bifido pathway and theory carbon flux distribution. Metabolic optimization of EP-bifido pathway. The red box referred to the carbon rearrangement procedure. Overexpressed genes are shown in red. Deleted genes are shown in blue. Intermediate metabolites participated in carbon rearrangement are shown in orange.

manipulation. All primers used for molecular manipulations are listed in **Table 2**.

The Red homologous recombination method was employed for gene deletion. The pTKRED complementary plasmid was transformed into the target strain. Deletion fragments of *ptsG* gene were amplified from the JW1087-2 single-gene knockout mutant (Baba et al., 2006) (bought from Coli Genetic Stock Center, CGSC) using primers Q-ptsG-F/Q-ptsG-R.

TABLE 1 | Bacterial strains and plasmids used in this study.

Strain and plasmids	Relevant properties	Sources
Strains		
JW1087-2	JW25113 derivative, Δ*ptsG:kan*	Baba et al. (2006)
DH-EP	DH5α derivative, Δ*edd*Δ*pfkA*	Wang et al. (2019)
DH-EPP	DH5α derivative, Δ*edd*Δ*pfkA*Δ*ptsG*	This study
L-6	DH-EPP derivative, Δ*edd*Δ*pfkA*Δ*ptsG galP* RBS:TGAAAGGGAAA	This study
M-6	L-6 derivative, Δ*edd*Δ*pfkA*Δ*ptsG:trc-rbs-glf*$_{zm}$	This study
Plasmids		
pCAB	pBluescriptII SK, phbC and phbAB gene from *Ralstonia eutropha*	Wang et al. (2019)
pCDFtrc	Cloning vector, Spe^R	Wang et al. (2019)
pFF	pCDFtrc, *fxpk* gene from *B. adolescentis* and *fbp* gene from *E. coli*	Wang et al. (2019)
pKD3	Template plasmid with Cm^R gene and FLP recognition target	Datsenko and Wanner (2000)
pTKRED	P_{BAD} promoter containing plasmid, Spe^R	Kuhlman and Cox (2010)
pCP20	Helper plasmid expressing FLP recombinase, ts-rep, Amp^R, Cm^R	Datsenko and Wanner (2000)
pAH69	Helper plasmid expressing HK022 integrase, Amp^R	Haldimann and Wanner (2001)

TABLE 2 | Key oligonucleotide primers used in this study for DNA manipulation.

Primers	Sequence (5′-3′)
Q-ptsG-F	5′-GGCTGTGTTGAAAGGTGTTGC-3′
Q-ptsG-R	5′-AACGCGCTATATTGCAGAGG-3′
Glf-F	5′-GGTCGGTAAATCGCTGCTTGACAATTAATCATCCGGC TCGTATAATGTCTAGAGAAAGAGGAGAAATACTAGATGAG TTCTGAAAGTAGTCAGGGTC-3′
Glf-R	5′-GCCTACCCGGATATTATCGTGAGGATGCGAATTGTG TAGGCTGGAGCTGCTTC-3′
R6K-F	5′-TCGCATCCTCACGATAATATCCGGGTAGGC-3′
R6K-R	5′-TTGTCAAGCAGCATCAGCGATTTACCGACCGATCC GGCCACGATGCGTCC-3′

Measurement of Extracellular Metabolites

A spectrophotometer was used to measure the optical density at 600 nm (OD_{600}) of the bacterial culture. PHB was quantified using gas chromatography (GC). Cells were harvested by centrifugation at 6,000 × *g* for 10 min, 4°C. The cell pellets were washed twice with distilled water and lyophilized for 7 h. Before GC analysis, 1 mL chloroform, 850 μL methanol, and 150 μL sulfuric acid (98%, w/w) were added to the weighed cells in vials. The vials were incubated at 100°C for 1 h. Then, 1 mL water was added for stratification and cooling vials. After standing for 1 h, the mixture separated into layers and the heavier chloroform phase was transferred to new vial for GC analysis. The GC detection process was performed using a Shimadzu GC2010 gas chromatograph (Kyoto, Japan) equipped with an AOC-20i auto injector and a Restek Rtx-5 column. PHB standard samples of methyl-(R)-3-hydroxybutyrate (Sigma-Aldrich) were dissolved in chloroform and analyzed by GC. The temperature program used was: 80°C for 1 min, ramped to 120°C at 10°C/min, then ramped to 160°C at 45°C/min for 5 min, and the total time was 10.89 min.

For extracellular metabolite analysis, 1 mL of culture was centrifuged at12,000 × *g* for 2 min. The supernatant was filtered through a 0.22-μm syringe filter for high-performance liquid chromatography analysis. Glucose, acetate, and pyruvate were measured on an ion exchange column (HPX-87H; Bio-Rad Labs) with a differential refractive index detector (Shimadzu RID-10A). A 0.5-mL/min mobile phase using a 5-mM H_2SO_4 solution was applied to the column. The column was operated at 65°C.

MAGE Procedure

The ribosome binding sites (RBSs) designed for the modulation of *GalP* and *glk* transcription rates were 5′-GTCGTACTC ACCTATCTTAATTCACAATAAAAAATAACCADDRRRRRD DDDATCATGCCTGACGCTAAAAAACAGGGGCGGTCAAA CAAG-3′ (D = A, G, T; and R = A, G) and 5′-GCCGCCCACA TCACCGACTAATGCATACTTTGTCATTCTHHHHYYYYYH HGCTAAAGTCAAAATAATTCTTTCTCACACTGTAAATAC CT-3′ (H = T, C, A; and Y = T, C), respectively, with four phosphorothioated bases at the 5′ terminus. The initiation of MAGE requires that pTKRED was transformed into the target strain. The MAGE cycles were performed by growing DH-EPP in 5 mL SOB medium at 30°C and shaking at 220 rpm for 12 h. For the first MAGE round, 5-mL shake flask cultures using SOB broth were started with a 1% inoculation from the overnight culture. Isopropyl-β-D-thiogalactopyranoside (IPTG) was added to a final concentration of 0.5 mM to induce λ-prophage (*bet*, *gam*, and *exo*) gene expression. Cells were then incubated at 30°C and shaking at 220 rpm until reaching an OD_{600} of 0.5 to 0.6. Cells were collected (2 mL), pelleted, and washed three times with cold sterile water to make them electrocompetent. ssDNA mixture (1 μM) was added to electrocompetent cells and electroporated at 2.5 kV. To start the second MAGE round, cells were recovered in 5 mL SOC with IPTG until their OD_{600} reached 0.5 to 0.6, after which cells underwent pelleting, washing, and electroporation. Three to four MAGE rounds were performed per day and 16 cycles were performed in total. The resulting pool of variants were then characterized using the Nile red assay.

Screening of PHB Competent Cells by Nile Red Assay

When PHB is combined with Nile red dye a red color is produced. We transformed the pCAB plasmid into these variants and added 100 μL Amp, 50 μL IPTG, 20 g/L glucose, and 200 μL Nile red dye to the solid M9 medium supplemented with 0.2% yeast extract. The MAGE variants were diluted 200-fold and spread onto several plates. After incubation at 37°C for 16 h, the plates were placed at 4°C for 3 days to allow the color reaction to develop. Based on the color difference, we picked single red colonies for sequencing. For all the sequenced colonies with mutations identified, the pTKRED plasmid was removed and the strains were transformed with the pFF and pCAB plasmids for further verification of the PHB competent cells.

Integration of glf

For glf integration, the *trc-rbs-glf* module was amplified from *Zymomonas mobilis* genomic DNA by PCR using primers GLF-F and GLF-R. The PCR product (*trc-rbs-glf*) was cloned into a vector that carries R6K replicon and phage attachment sites (attP). This plasmid was named R6K-glf and was confirmed by DNA sequencing. The pAH69 helper plasmid was transformed into the L-6 strain. The target strain carrying pAH69 was incubated overnight at 30°C and transferred to 37°C for 1 h before transfection. Then the pR6K-glf plasmid was introduced into L-6 by electroporation. The centrifuged bacteria were plated onto plates containing 25 μg/mL kanamycin for overnight incubation at 37°C. R6K-glf positive transformants were selected by their kan^R phenotype and were verified by PCR.

Determination of CO_2 Emissions

CO_2 emission was determined using a thermostatic oscillation incubator with a CO_2 detector (BCP-CO_2, Bluesens, Germany) that monitored CO_2 volume every 20 s and transmitted the data to a computer. Cultures were grown at 37°C with shaking at 150 rpm.

RESULTS

Inhibiting PTS to Reduce PEP Consumption

In *E. coli*, glucose is transported through the PTS system. This system is involved in PEP-dependent sugar transport and its activity has an important impact on carbon flux redistribution in the PEP and pyruvate nodes (Gosset, 2005). Glucose transport into the cytoplasm by $EIICB^{Glc}$ (encoded by *ptsG*) is coupled to its phosphorylation. The phosphate group is derived from PEP and is transferred via a cascade of proteins, enzyme I (EI), HPr, EIIA, and EIIB. This procedure consumes almost half of the PEP (Valle et al., 1996; Wang et al., 2012). Glucose was phosphorylated to G6P by phosphoryl generated from PEP dephosphorylated to pyruvate, the formed pyruvate is further decarboxylated to AcCoA and releases 1 mol CO_2, leading to carbon source loss. While PEP is not the precursor in our study, PEP consumption would convert carbon flux to the EMP pathway, which is not desirable in our EP-bifido pathway. Therefore, modulation of the PEP-independent uptake and phosphorylation system is required. Knocking out *ptsG* and replacing it with other glucose transport pathways is a common method used in the production of PEP-precursor products (Gosset, 2005; Lee et al., 2005; Li et al., 2013; Kyselova et al., 2018). Therefore, we knocked out *ptsG* in strain DH-EP and named the strain DH-EPP. But found that *ptsG* deletion severely impaired the growth capacity of the resulting strain. Compared with DH-EP (pFFpCAB) strain, PHB yield of DH-EPP strain decreased from 63.7 to 26.3% (mol/mol) (**Figure 2**).

For glucose uptake recovery, replacing PTS with an alternative PEP-independent uptake and phosphorylation system could be an efficient solution to this problem.

Improving Glucose Flux Through Non-PTS Pathway

When *E. coli* strains lack PTS, the low affinity galactose: H^+ symporter, GalP, encoded by *galP*, is induced. Glucose

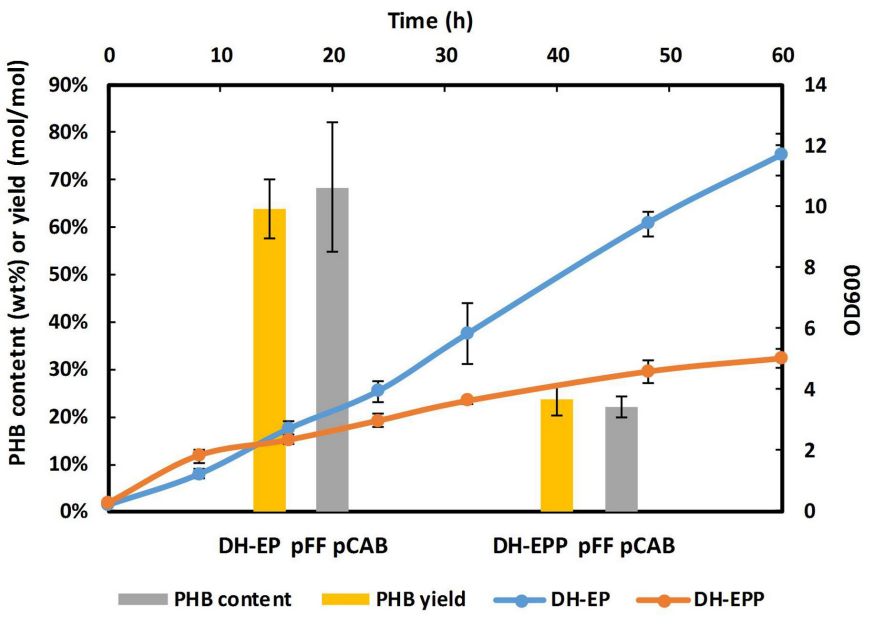

FIGURE 2 | Fermentation result of *ptsG* knockout strain. The date of PHB yield and content of both strains were calculated based on fermentation samples at 60 h. The time axis at the top was used to depict growth curve. The growth carve was showed in orange red. The experiments were performed in duplicate and error bars indicate s.d. Strains were cultivated with M9 at 37°C, 150 rpm.

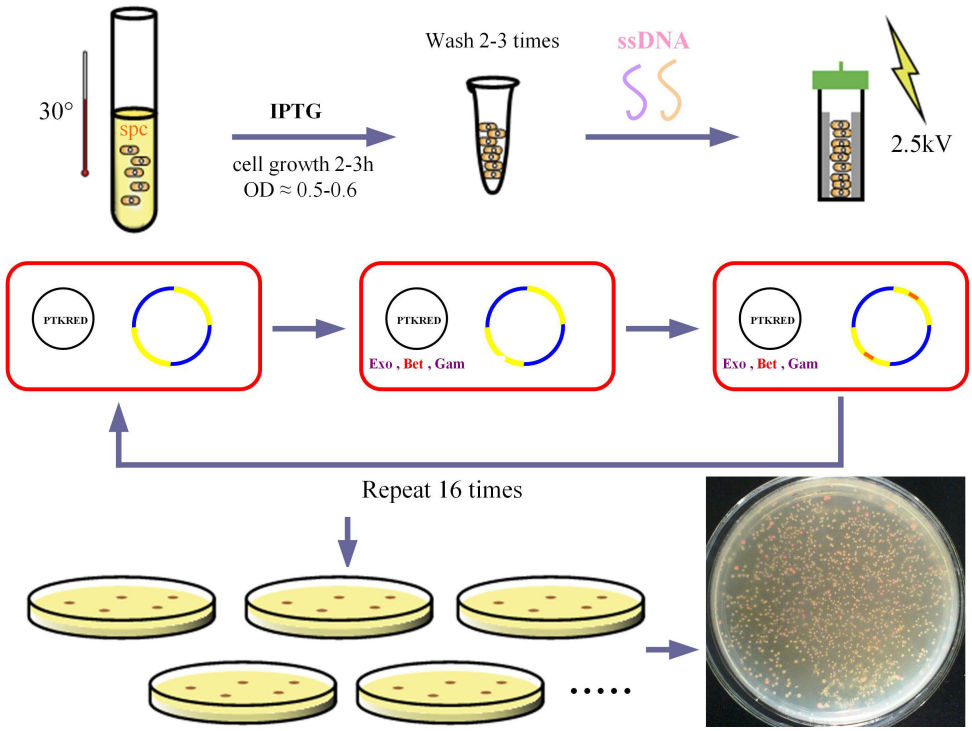

FIGURE 3 | MAGE procedure. The red squares represent the cells, the black circles represent the ptkRED plasmid, and Exo, Bet and gam are the gene sequences of the enzymes on the plasmid. The yellow and blue circles represent the bacterial genome, with the red portion representing the target engineered gene sequence. Exo, exonuclease; Bet, phage recombination protein Bet; gam, host-nuclease inhibitor protein Gam.

internalized by GalP must be phosphorylated by glucokinase (encoded by *glk*), which catalyzes the ATP-dependent phosphorylation of glucose to generate G6P in the cytoplasm without CO_2 emission, thus saving the carbon source (Gosset, 2005). Therefore, we modified *galP* and *glk* expression levels to improve the glucose utilization rate. While increasing *galP* and *glk* transcriptional levels through plasmid overexpression is a pervasive strategy (Hernandez-Montalvo et al., 2003; Wang et al., 2006), it has several disadvantages, including metabolic burden and unexpected lateral effects. Modulation of *galP* and *glk* expression levels through plasmid overexpression or high strength promoter substitution cannot provide multiple combination of expression intensity for screening. Discovering a way to effectively modulate the transcription of the two genes to an optimal strength in combination is a pressing problem. We adopted MAGE to simultaneously regulate *galP* and *glk* expression levels (Wang H.H. et al., 2009). Using this approach, colonies with high PHB yields can be identified using Nile red dye staining.

After 16 rounds of MAGE modulation (**Figure 3**), recombinant strains were screened by Nile red staining. Recombinant strains with higher PHB production showed redder color. Screening and sequencing results are shown in **Table 3**. Using single colony color screening, we found that the RBS of both *glk* and *galP* genes were changed, and the amount of ssDNA (single string DNA) recombination of *glk* exceeded that of *galP*. This may be because the location of the *glk* gene is more susceptible to ssDNA recombination during genome replication. However, no recombinant was screened out in which the two genes were simultaneously mutated.

TABLE 3 | Screening result of MAGE recombination strains.

Strain number	Gene	Origin RBS sequence	Mutated RBS sequence
1	*glk*	GGAGCAGTTGA	GAAGGGAGAGG
2	*glk*	GGAGCAGTTGA	GAAAGAAATGA
6	*galP*	TATTGGAGGGC	TGAAAGGGAAA
9	*glk*	GGAGCAGTTGA	GGAGGGATGGA
16	*glk*	GGAGCAGTTGA	TAGGAGGAGTT
18	*glk*	GGAGCAGTTGA	AAAAAGGGTTA
19	*glk*	GGAGCAGTTGA	GAAGGAGGGGT
20	*galP*	TATTGGAGGGC	GGAGAGGGTTA
21	*glk*	GGAGCAGTTGA	TGGGGGGAGGG
22	*glk*	GGAGCAGTTGA	AAAGGGGTTTG
23	*glk*	GGAGCAGTTGA	GAAGGGGTTTG
24	*glk*	GGAGCAGTTGA	AGAGGAAGAGA
27	*glk*	GGAGCAGTTGA	AAAAGGGATAG
28	*glk*	GGAGCAGTTGA	TTGGAAGATAT
30	*glk*	GGAGCAGTTGA	TGAGGAATGAA
32	*glk*	GGAGCAGTTGA	GTGGAAATAGA
36	*glk*	GGAGCAGTTGA	TTAGGGGGAGT
51	*glk*	GGAGCAGTTGA	TTAAGGGATAT
62	*glk*	GGAGCAGTTGA	GGAAGGAGAAT

Nineteen mutant strains were selected and transformed with pFF and pCAB, subsequently. Three batches fermentation of these 19 strains lead to the selection of strains in consideration of glucose consumption and PHB content, named EPPG-6, EPPG-16, EPPG-51, and EPPG-62 (**Figure 4D**). Then, we repeated fermentation using the four selected strains (**Figure 4E**). Fermentation results showed that after glucose transport system modulation, the DH-EPPG-6 strain had a recovered growth rate.

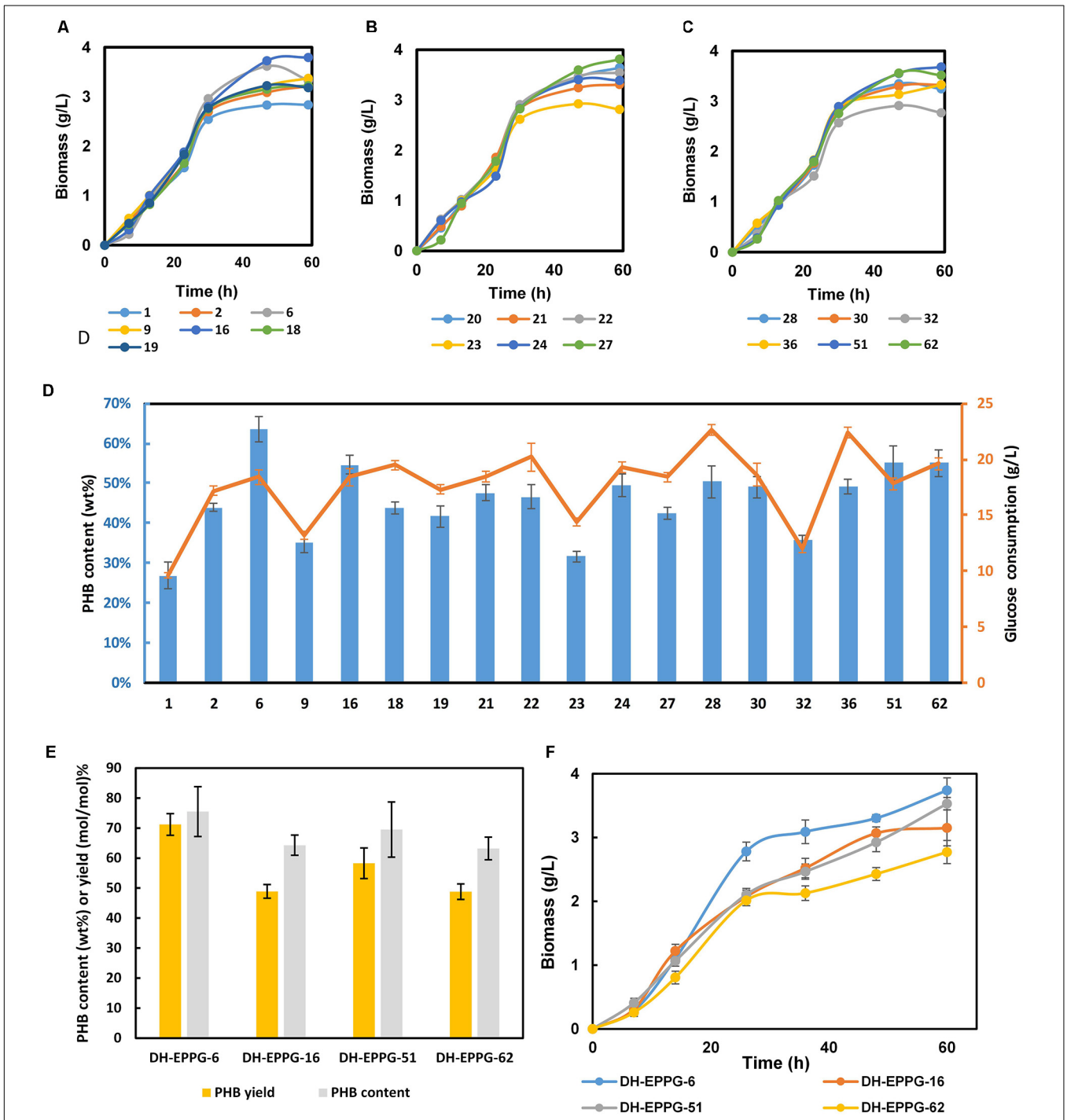

FIGURE 4 | Fermentation result of the engineered EP-bifido strains. **(A)** Growth curve of first batch selection. **(B)** Growth curve of second batch selection. **(C)** Growth curve of third batch selection. **(D)** PHB content and glucose consumption of these three batches selection. The blue columns represent PHB content and orange red broken line represents glucose consumption. **(E)** PHB content and yield of selected recombinants. The experiments were performed in triplicate and error bars indicate s.d. For mutant fermentation selection, strains were cultivated with M9 at 37°C, 150 rpm. **(F)** Growth curve of selected recombinants.

The PHB yield reached 71.2% (mol/mol), which was 63.7% higher than that of the strain DH-EP. Then DH-EPPG-6 strain was renamed L-6, in which the wild type RBS sequence of *galP* was mutated to TGAAAGGGAAA.

Expressing Heterogeneous Sugar Transporter to Reinforce Glucose Uptake

To further enhance the consumption of glucose, we compared the kinetic parameters of several transporters with their glucose transport capacity and energy consumption during glucose internalization and phosphorylation (Gosset, 2005). Because the transmembrane proton potential is a form of energy, the energy consumption of the *glf* sugar transporter from *Zymomonas mobilis* is comparable to that of the *E. coli* glucose-specific PTS (PTS^{Glc}). Compared with *galP*, the glf_{zm} transporter used less energy to produce a higher maximum velocity. Therefore, the high-rate, low-energy sugar transporter glf_{zm} was chosen to improve the glucose absorption capacity of engineered bacteria. Then glf_{zm} was inserted at the attP genomic site of strain L-6 using the CRIM plasmid system (Haldimann and Wanner, 2001), resulting the strain M-6. We deduced that *glf* integration was conducive to growth recovery in later growth stages. In **Figure 5B**, M-6 (pFFpCAB) showed a better growth

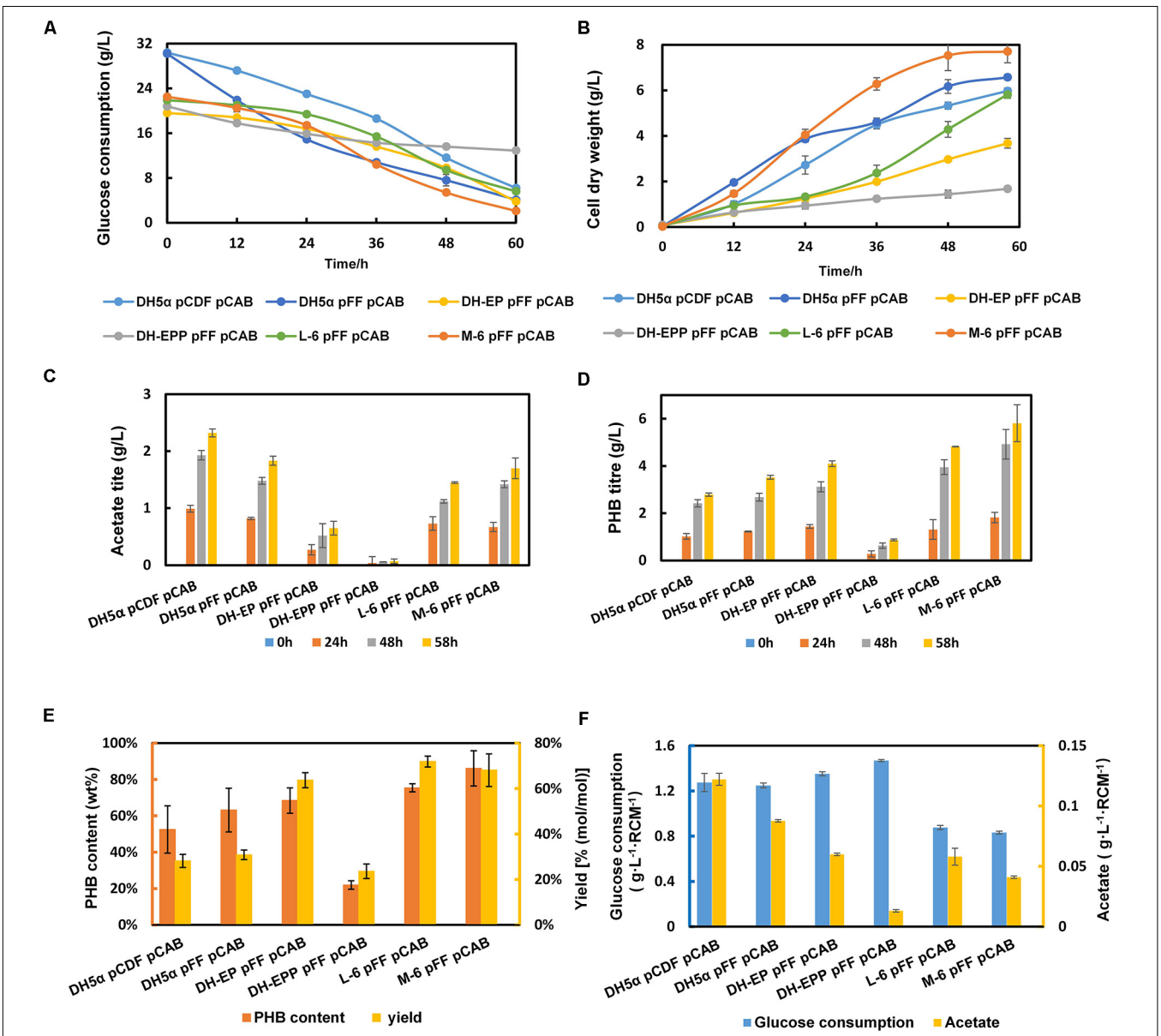

FIGURE 5 | The fermentation profile and PHB yield of all the engineered EP-bifido strains. **(A)** Glucose consumption. **(B)** Cell dry weight. **(C)** Acetate production. **(D)** PHB production. **(E)** PHB content and PHB yield. **(F)** Glucose consumption and acetate normalized by residual cell mass. The experiments were performed in triplicate and error bars indicate s.d. Strains were cultivated in M9 with glucose at 37°C, 150 rpm.

TABLE 4 | Specific growth rates and glucose utilization rates of DH5α, DH-EP (pFFpCAB), DH-EPP (pFFpCAB), L-6 (pFFpCAB), and M-6 (pFFpCAB).

Strains	Specific growth rate (h^{-1})	Specific glucose utilization rate ($g \cdot L^{-1} \cdot h^{-1}$)
DH5α (pFFpCAB)	0.35 ± 0.011	0.78 ± 0.02
DH-EP (pFFpCAB)	0.20 ± 0.020	0.41 ± 0.03
DH-EPP (pFFpCAB)	0.09 ± 0.002	0.23 ± 0.01
L-6 (pFFpCAB)	0.28 ± 0.018	0.52 ± 0.01
M-6 (pFFpCAB)	0.50 ± 0.026	0.71 ± 0.03

Specific growth rates and glucose utilization rates were calculated based on the 0–48 h data.

TABLE 5 | PHB productivity of the engineered PHB-producing strains.

Strains	PHB titer ($g \cdot L^{-1} \cdot h^{-1}$)
DH5α (pCDF pCAB)	0.048 ± 0.07
DH5α (pFF pCAB)	0.061 ± 0.08
DH-EP (pFF pCAB)	0.071 ± 0.012
DH-EPP (pFF pCAB)	0.015 ± 0.04
L-6 (pFF pCAB)	0.083 ± 0.015
M-6 (pFF pCAB)	0.100 ± 0.078

curve than the control DH5α (pCDFpCAB). Simultaneously, as we expected, gross glucose consumption improved compared with L-6, increased from 16.2 to 20.4 g/L (**Figure 5A**). The glucose consumption of all engineered strains changed obviously after every modification step. PHB titer of M-6 improved significantly, from 4.82 to 5.81 g/L in comparison with that of L-6 (**Figure 5D**), and PHB content in M-6 strain reached 85.1 wt% (**Figure 5E**). The only drawback was that PHB yield of M-6 reached 68.1% (mol/mol) slightly decreased compared with L-6 (**Figure 5E**). In general, compared with parental strain DH-EP (pFFpCAB), the PHB titer and content improved 41.71 and 24.41% in M-6, respectively. And compared with the control DH5α (pCDFpCAB), the PHB content and yield of M-6 improved 61.9 and 141.7% in M-6, respectively (**Figure 5**). All the engineered strains produced some amount of acetate, M-6 and L-6 produced less acetate than DH-EP strain. We also calculated the acetate formation and glucose consumption normalized by residual cell mass (RCM).

In order to confirm that the glucose consumption rates in our engineered strains are indeed improved, we calculated the specific growth rate and glucose utilization rates of DH-EP (pFFpCAB), DH5α-EPP (pFFpCAB), L-6 (pFFpCAB), and M-6 (pFFpCAB). After *ptsG* gene was deleted, the specific growth rate of DH-EPP decreased from 0.20 to 0.09 h^{-1}, and the glucose utilization rate decreased from 0.78 to 0.41 g L^{-1} h^{-1} (**Table 4**). After glf_{zm} integration based on L-6, the specific growth rate of M-6 (pFFpCAB) increased obviously from 0.28 to 0.50 h^{-1}, improved 42.8% compared to that of DH5α (pFFpCAB). The growth consumption rate recovered to 0.71 g L^{-1} h^{-1}, 73% higher than DH-EP (pFFpCAB). M-6 and L-6 showed lower normalized glucose consumption. Thus M-6 and L-6 had improved PHB biosynthesis and PHB productivity since they produced less by-product acetate and consumed less glucose per residual cell mass (**Figure 5F** and **Table 5**).

We further examined the CO_2 release from the constructed EP-bifido strains. The total CO_2 release of DH5α-EPP (pFFpCAB) decreased to 32.5% compared to DH-EP (pFFpCAB) (**Figure 6A**). And the CO_2 emission of L-6 (pFFpCAB), M-6 (pFFpCAB) improved 177 and 332% compared to that of DH5α-EPP (pFFpCAB). We believe that the restoring growth contributed to the increased CO_2 release. The CO_2 yield of DH5α-EPP (pFFpCAB), L-6 (pFFpCAB), and M-6 (pFFpCAB) decreased to 16.9% (mol/mol), 74.4% (mol/mol) and 92.4% (mol/mol) compared to their controls, respectively (**Figure 6B**). The above data confirmed the recovery of growth after PTS system deficiency and the decreased CO_2 emission from the L-6 (pFFpCAB) and M-6 (pFFpCAB) strains.

DISCUSSION

As environmental problems intensify, carbon saving or carbon sequestration pathways have become a new focus for bio-manufacturing. Previously, we successfully constructed an efficient carbon-saving pathway in *E. coli* called the EP-bifido

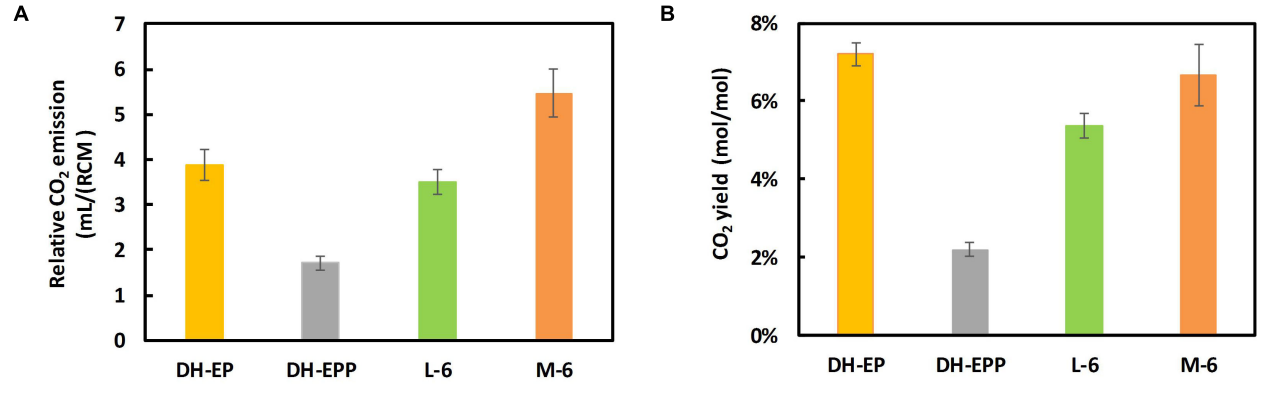

FIGURE 6 | Determination of CO_2 release. **(A)** Relative CO_2 emission and **(B)** CO_2 yield. Strains were cultivated in modified M9 medium containing 20 g/L glucose at 37°C and 150 rpm. CO_2 yield were calculated as mol/mol glucose × 100%. The experiments were performed in triplicate and error bars indicate s.d.

pathway. This pathway has been applied to the production of several compounds that use acetyl-CoA as a precursor. As a degradable material, PHB has great application prospects. While we believe that there is potential for further optimization of PHB production by the EP-bifido pathway. In this study, we knocked out the *ptsG* gene, a key glucose transporter of the PTS system that employs PEP as phosphate donor. The glucose consumption rate and cell growth were significantly reduced in the *ptsG* mutant under aerobic fermentation conditions. The deficiency in the PTS system dramatically impairs glucose uptake and causes growth restriction. It is speculated that the reason for growth restriction is not insufficient glucose uptake, but the subsequent decrease in glucose phosphorylation efficiency due to limited glucokinase activity (Steinsiek and Bettenbrock, 2012).

To overcome this growth hindrance, we optimized the RBS sequences of *galP* and *glk* genes, encoding glucose permease and glucokinase, respectively. Subsequently, we introduced the *Z. mobilis* glucose transporter, glf_{zm}, into the L-6 high-yield strain, and observed cell growth recovery. After optimization, PHB yield reached 71.9% (mol/mol) in L-6 strain. In the resulting strain M-6, the intracellular PHB content reached 85.1 wt%, and the titer reached 5.81 g/L. Previously, most studies have compensated for PTS knockout-induced inhibition of glucose uptake by overexpression of *glk*, and *galP* or by heterologous expression of *glf* (Snoep et al., 1994; Gosset, 2005; Lin et al., 2018). Instead, we applied MAGE technology to directly alter genomic *glk* and *galP* to optimize their expression (Gallagher et al., 2014). Meanwhile, the RBS library constructed using MAGE provided rich genotypes for subsequent screening of high-yield PHB strains. After glf_{zm} integration, recovered growth rate and glucose consumption was evident in strain M-6. Compared with parent strain DH-EP (pFFpCAB), the glucose consumption of M-6 increased 4.6 g/L, 29.1% higher than that of parent strain in **Figure 5A**. The PHB content and yield of strain M-6 improved compared with that of DH-EP(pFFpCAB). M-6 and L-6 showed lower normalized glucose consumption. Thus M-6 and L-6 had improved PHB production since they produced less by-product acetate and consumed less glucose per residual cell mass. We inferred that increased glucose uptake enhanced flux through EMP, which is supported by increased cell growth. The growth of DH-EP strain improved with decreased acetate formation in M-6 strain. The specific growth rate and CO_2 release data of constructed strains further confirmed our inference. Our study provided an efficient way for improving glucose absorption and total carbon conversion rate in artificial carbon-saving pathways by replacing PTS with other glucose transporters. It also describes an efficient screening strategy for MAGE ssDNA recombineering technology. The efficient utilization of carbon sources has been one of the determinant for high productivity in microbial fermentation. In the future, the effective allocation of carbon resources and the construction of effective strategies for balancing cell growth and product biosynthesis will still be the direction of metabolic engineering.

DATA AVAILABILITY STATEMENT

All datasets generated for this study are included in the article/supplementary material.

AUTHOR CONTRIBUTIONS

QW and QQ designed the work. YLi, YLu, and JX performed the experiments. ZS and YLi analyzed the ^{13}C-MFA data. QQ and QL encouraged this project. YLi and QW wrote the manuscript. All authors read and approved the final manuscript. All authors contributed to the article and approved the submitted version.

FUNDING

This work was supported by grants from the National Key R&D Program of China (2019YFA0904900), the National Natural Science Foundation of China (31730003, 31670047, and 31770095), and Young Scholars Program of Shandong University and State Key Laboratory of Microbial Technology Open Projects Fund (M2019-11).

REFERENCES

Baba, T., Ara, T., Hasegawa, M., Takai, Y., Okumura, Y., Baba, M., et al. (2006). Construction of *Escherichia coli* K-12 in-frame, single-gene knockout mutants: the Keio collection. *Mol. Syst. Biol.* 2:2006.0008.

Bogorad, I. W., Lin, T. S., and Liao, J. C. (2013). Synthetic non-oxidative glycolysis enables complete carbon conservation. *Nature* 502, 693–697. doi: 10.1038/nature12575

Datsenko, K. A., and Wanner, B. L. (2000). One-step inactivation of chromosomal genes in *Escherichia coli* K-12 using PCR products. *Proc. Natl. Acad. Sci. U.S.A.* 97, 6640–6645. doi: 10.1073/pnas.120163297

Erb, T. J., Berg, I. A., Brecht, V., Muller, M., Fuchs, G., and Alber, B. E. (2007). Synthesis of C5-dicarboxylic acids from C2-units involving crotonyl-CoA carboxylase/reductase: the ethylmalonyl-CoA pathway. *Proc. Natl. Acad. Sci. U.S.A.* 104, 10631–10636. doi: 10.1073/pnas.0702791104

Gallagher, R. R., Li, Z., Lewis, A. O., and Isaacs, F. J. (2014). Rapid editing and evolution of bacterial genomes using libraries of synthetic DNA. *Nat. Protoc.* 9, 2301–2316. doi: 10.1038/nprot.2014.082

Gong, F., Cai, Z., and Li, Y. (2016). Synthetic biology for CO2 fixation. *Sci. China Life Sci.* 59, 1106–1114. doi: 10.1007/s11427-016-0304-2

Gosset, G. (2005). Improvement of *Escherichia coli* production strains by modification of the phosphoenolpyruvate:sugar phosphotransferase system. *Microb. Cell Fact* 4:14.

Haldimann, A., and Wanner, B. L. (2001). Conditional-replication, integration, excision, and retrieval plasmid-host systems for gene structure-function studies of bacteria. *J. Bacteriol.* 183, 6384–6393. doi: 10.1128/jb.183.21.6384-6393.2001

Hernandez-Montalvo, V., Martinez, A., Hernandez-Chavez, G., Bolivar, F., Valle, F., and Gosset, G. (2003). Expression of galP and glk in a *Escherichia coli* PTS mutant restores glucose transport and increases glycolytic flux to fermentation products. *Biotechnol. Bioeng.* 83, 687–694. doi: 10.1002/bit.10702

International Energy Agency (2019). *Data From: Global Energy and CO_2_Status Report*. Paris: International Energy Agency.

Kuhlman, T. E., and Cox, E. C. (2010). Site-specific chromosomal integration of large synthetic constructs. *Nucleic Acids Res.* 38:e92. doi: 10.1093/nar/gkp1193

Kyselova, L., Kreitmayer, D., Kremling, A., and Bettenbrock, K. (2018). Type and capacity of glucose transport influences succinate yield in two-stage cultivations. *Microb. Cell Factor.* 17:132.

Lee, J. W., Na, D., Park, J. M., Lee, J., Choi, S., and Lee, S. Y. (2012). Systems metabolic engineering of microorganisms for natural and non-natural chemicals. *Nat. Chem. Biol.* 8, 536–546. doi: 10.1038/nchembio.970

Lee, S. J., Lee, D. Y., Kim, T. Y., Kim, B. H., Lee, J. W., and Lee, S. Y. (2005). Metabolic engineering of *Escherichia coli* for enhanced production of succinic acid, based on genome comparison and in silico gene knockout simulation. *Appl. Environ. Microbiol.* 71, 7880–7887. doi: 10.1128/aem.71.12.7880-7887.2005

Lee, S. Y., and Choi, J. I. (2001). Production of microbial polyester by fermentation of recombinant microorganisms. *Adv. Biochem. Eng. Biotechnol.* 71, 183–207. doi: 10.1007/3-540-40021-4_6

Lee, S. Y., Lee, K. M., Chang, H. N., and Steinbuchel, A. (1994). Comparison of recombinant *Escherichia-Coli* strains for synthesis and accumulation of poly-(3-hydroxybutyric acid) and morphological-changes. *Biotechnol. Bioeng.* 44, 1337–1347. doi: 10.1002/bit.260441110

Li, Y., Li, M., Zhang, X., Yang, P., Liang, Q., and Qi, Q. (2013). A novel whole-phase succinate fermentation strategy with high volumetric productivity in engineered *Escherichia coli*. *Bioresour. Technol.* 149, 333–340. doi: 10.1016/j.biortech.2013.09.077

Li, Z. J., Cai, L., Wu, Q., and Chen, G. Q. (2009). Overexpression of NAD kinase in recombinant *Escherichia coli* harboring the phbCAB operon improves poly(3-hydroxybutyrate) production. *Appl. Microbiol. Biotechnol.* 83, 939–947. doi: 10.1007/s00253-009-1943-6

Lin, P. P., Jaeger, A. J., Wu, T. Y., Xu, S. C., Lee, A. S., Gao, F. K., et al. (2018). Construction and evolution of an *Escherichia coli* strain relying on nonoxidative glycolysis for sugar catabolism. *Proc. Natl. Acad. Sci. U.S.A.* 115, 3538–3546. doi: 10.1073/pnas.1802191115

Meile, L., Rohr, L. M., Geissmann, T. A., Herensperger, M., and Teuber, M. (2001). Characterization of the D-xylulose 5-phosphate/D-fructose 6-phosphate phosphoketolase gene (xfp) from *Bifidobacterium lactis*. *J. Bacteriol.* 183, 2929–2936. doi: 10.1128/jb.183.9.2929-2936.2001

Mozumder, M. S. I., De Wever, H., Volcke, E. I. P., and Garcia-Gonzalez, L. (2014). A robust fed-batch feeding strategy independent of the carbon source for optimal polyhydroxybutyrate production. *Process Biochem.* 49, 365–373. doi: 10.1016/j.procbio.2013.12.004

Posthuma, C. C., Bader, R., Engelmann, R., Postma, P. W., Hengstenberg, W., and Pouwels, P. H. (2002). Expression of the xylulose 5-phosphate phosphoketolase gene, xpkA, from Lactobacillus pentosus MD363 is induced by sugars that are fermented via the phosphoketolase pathway and is repressed by glucose mediated by CcpA and the mannose phosphoenolpyruvate phosphotransferase system. *Appl. Environ. Microbiol.* 68, 831–837. doi: 10.1128/aem.68.2.831-837.2002

Ragauskas, A. J., Williams, C. K., Davison, B. H., Britovsek, G., Cairney, J., Eckert, C. A., et al. (2006). The path forward for biofuels and biomaterials. *Science* 311, 484–489. doi: 10.1126/science.1114736

Schwander, T., Schada Von Borzyskowski, L., Burgener, S., Cortina, N. S., and Erb, T. J. (2016). A synthetic pathway for the fixation of carbon dioxide in vitro. *Science* 354, 900–904. doi: 10.1126/science.aah5237

Snoep, J. L., Arfman, N., Yomano, L. P., Fliege, R. K., Conway, T., and Ingram, L. O. (1994). Reconstruction of glucose uptake and phosphorylation in a glucose-negative mutant of *Escherichia coli* by using Zymomonas mobilis genes encoding the glucose facilitator protein and glucokinase. *J. Bacteriol.* 176, 2133–2135. doi: 10.1128/jb.176.7.2133-2135.1994

Steinsiek, S., and Bettenbrock, K. (2012). Glucose transport in *Escherichia coli* mutant strains with defects in sugar transport systems. *J. Bacteriol.* 194, 5897–5908. doi: 10.1128/jb.01502-12

Valle, F., Munoz, E., Ponce, E., Flores, N., and Bolivar, F. (1996). Basic and applied aspects of metabolic diversity: the phosphoenolpyruvate node. *J. Industr. Microbiol. Biotechnol.* 17, 458–462. doi: 10.1007/bf01574776

van der Walle, G. A., De Koning, G. J., Weusthuis, R. A., and Eggink, G. (2001). Properties, modifications and applications of biopolyesters. *Adv. Biochem. Eng. Biotechnol.* 71, 263–291. doi: 10.1007/3-540-40021-4_9

Wang, H. H., Isaacs, F. J., Carr, P. A., Sun, Z. Z., Xu, G., Forest, C. R., et al. (2009). Programming cells by multiplex genome engineering and accelerated evolution. *Nature* 460, 894–898. doi: 10.1038/nature08187

Wang, Q., Yu, H. M., Xia, Y. Z., Kang, Z., and Qi, Q. S. (2009). Complete PHB mobilization in *Escherichia coli* enhances the stress tolerance: a potential biotechnological application. *Microb. Cell Factor.* 8:47. doi: 10.1186/1475-2859-8-47

Wang, Q., Wu, C., Chen, T., Chen, X., and Zhao, X. (2006). Expression of galactose permease and pyruvate carboxylase in *Escherichia coli* ptsG mutant increases the growth rate and succinate yield under anaerobic conditions. *Biotechnol. Lett.* 28, 89–93. doi: 10.1007/s10529-005-4952-2

Wang, Q., Xia, Y. Z., Chen, Q., and Qi, Q. S. (2012). Incremental truncation of PHA synthases results in altered product specificity. *Enzyme Microb. Technol.* 50, 293–297. doi: 10.1016/j.enzmictec.2012.02.003

Wang, Q., Xu, J., Sun, Z., Luan, Y., Li, Y., Wang, J., et al. (2019). Engineering an in vivo EP-bifido pathway in *Escherichia coli* for high-yield acetyl-CoA generation with low CO_2 emission. *Metab. Eng.* 51, 79–87. doi: 10.1016/j.ymben.2018.08.003

Conflict of Interest: The authors declare that the research was conducted in the absence of any commercial or financial relationships that could be construed as a potential conflict of interest.

Advantages of publishing in Frontiers

OPEN ACCESS
Articles are free to read for greatest visibility and readership

FAST PUBLICATION
Around 90 days from submission to decision

HIGH QUALITY PEER-REVIEW
Rigorous, collaborative, and constructive peer-review

TRANSPARENT PEER-REVIEW
Editors and reviewers acknowledged by name on published articles

Frontiers
Avenue du Tribunal-Fédéral 34
1005 Lausanne | Switzerland

Visit us: www.frontiersin.org
Contact us: frontiersin.org/about/contact

REPRODUCIBILITY OF RESEARCH
Support open data and methods to enhance research reproducibility

DIGITAL PUBLISHING
Articles designed for optimal readership across devices

FOLLOW US
@frontiersin

IMPACT METRICS
Advanced article metrics track visibility across digital media

EXTENSIVE PROMOTION
Marketing and promotion of impactful research

LOOP RESEARCH NETWORK
Our network increases your article's readership